NS — SECTION I

# 77-NI...

**PROVEN** HIGH CHROMIUM ALLOY GRATE BARS
PRODUCED BY **CARONDELET'S** MELTING *and* CASTING METHODS
*...and* **NOW** FURTHER CONTROLLED BY
SPECTROGRAPHIC ANALYSIS . . . . . .

**...MEANS GRATE BARS FOR FERROUS *and* NON-FERROUS SINTERING WITH AN INCREASED SERVICE LIFE OF FROM 6 TO 10 TIMES . . . . . .**

77-NI alloy Grate Bars are receiving more and more recognition as a means of cutting sintering costs. CARONDELET'S engineering, metal melting procedures and now spectrographic analysis of "pre-pouring" Test Bars, as shown, are reasons for the superiority of 77-NI.

Heat, wear and shock resistance are dependent upon close metal analysis control. The Spectrograph gives us the opportunity to analyze Test Bars from each heat quickly and adjust before pouring, thus assuring the best chemical properties in the final sintering grate bar castings. 77-NI grate bars cost less because they last longer.

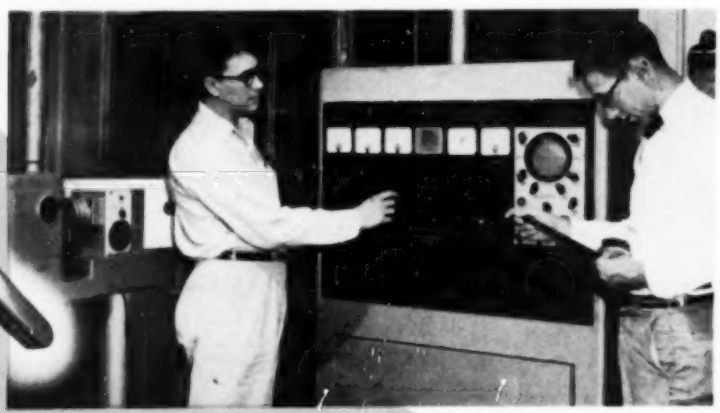

CARONDELET FOUNDRY COMPANY
SINCE 1890 CASTINGS
ST LOUIS MO

*SEND TODAY FOR SPECIAL BOOKLET . . . . . ON 77-NI* ▶▶▶

**CARONDELET FOUNDRY CO.**

2101 S. KINGSHIGHWAY BLVD. • ST. LOUIS 10, MISSOURI

JOURNAL OF

# METALS

Published to provide a continuing, authoritative, and up-to-date record of technological, engineering, and economic progress in all branches of the metals industry by the
Metals Branch
American Institute of Mining and Metallurgical Engineers, Inc.
29 West 39th Street, New York 18

ALVIN S. COHAN
Manager of Publications
Editor, JOURNAL OF METALS
EDWIN M. WEISS
Associate Editor

M. A. MATZKIN M. SNEDEKER
G. M. ZILL
Assistant Editors
GRACE PUGSLEY Production Manager
W. J. SEWING Asst. Prod. Mgr.

METALS BRANCH COUNCIL
R. R. McNaughton Chairman
E. O. Kirkendall Secretary
J. H. Scaff IMD Chairman
J. S. Marsh ISD Chairman
P. T. Stroup EMD Chairman
M. Cohen R. D. Parks
T. J. McLoughlin D. S. Eppelsheimer

EDITORIAL ADVISORY COMMITTEE
J. S. Smart, Jr. Chairman
W. A. Dean Evan Just
J. C. Kinnear, Jr. John Marsh
T. D. Jones M. Tenenbaum

TECHNICAL PUBLICATIONS COMMITTEES
Robert Aborn AIME Chairman
M. A. Jones ISD Chairman
S. J. Dickinson EMD Chairman
W. R. Hibbard, Jr. IMD Chairman
E. J. Kennedy, Jr. Secretary

FRED STANLEY
Eastern Advertising Manager
BOB WILSON
Western Advertising Manager
84 E. Randolph St., Chicago

**The AIME Publishes:**
Journal of Metals
Mining Engineering
Journal of Petroleum Technology

VOL. 6, NO. 11 NOVEMBER, 1954

## COVER

No one can help but be impressed with the current tempo of construction. Harry Brocke reflects this influence on the cover which illustrates the preliminary step to all building work—the scaffolding.

## NEWS


| | | | |
|---|---|---|---|
| Employment Service | 1174 | Trends | 1182 |
| Meet the Authors | 1176 | Drift of Things | 1184 |
| Industrial Notes | 1179 | Journal of Metals Reporter | 1187 |
| Coming Events | 1179 | AIME News | 1232 |
| Books for Engineers | 1180 | Personals | 1236 |

Preliminary Program for Electric Furnace Steel Conference 1231


## TECHNICAL FEATURES


**French Patent Solves Fume Problem in Oxygen Steelmaking** P. J. Leroy, L. Septier 1189

**Power Equipment Increases Open Hearth Productivity** G. E. Cooper 1192

**Furnace Operation and Casting Improved at Copper Cliff** J. C. Bischoff 1194

**Borehole Camera Is Milestone in Subsurface Exploration** E. B. Burwell, R. H. Nesbitt 1197


## TRANSACTIONS


**Fundamentals of Mixing and Agitation with Applications to Extractive Metallurgy** J. H. Rushton, L. H. Mahony 1199

**Thoughts on Lead Blast-Furnace Smelting, With Discussion** L. B. Haney, R. J. Hopkins 1208

**Applicability of Powder Metallurgy to Problems of High Temperature Materials, With Discussion** G. M. Ault, G. C. Deutsch 1214


## TECHNICAL NOTE


**Effect of Subcritical Rate on the Brittle-Fracture Characteristics of Structural Steel** L. Mair 1206


**This issue of JOURNAL OF METALS is in two Sections:**
**Section 1—Magazine Section 2—Transactions Section**

Published the first day of each month by the American Institute of Mining and Metallurgical Engineers, Inc., 29 West 39th Street, New York 18, N. Y. Telephone: PEnnsylvania 6-9220. Subscription $8 per year for non-AIME members in United States and North, South and Central America; $10, foreign; $6 for AIME members, or $4 additional in combination with a subscription to "Mining Engineering" or "Journal of Petroleum Technology." Single copies, 75 cents; single copies foreign, $1.00; special issues, $.50 . . . The AIME is not responsible for any statement made or opinion expressed in its publications . . . Copyright 1954 by the American Institute of Mining and Metallurgical Engineers, Inc. . . . Registered cable address, AIME New York . . . Indexed in Engineering Index, Industrial Arts Index and Chemical Abstracts . . . Reentered as second-class matter Sept. 21, 1949, at the post office at New York, N. Y., under the Act of March 3, 1879. Additional entry established at Manchester, N. H.

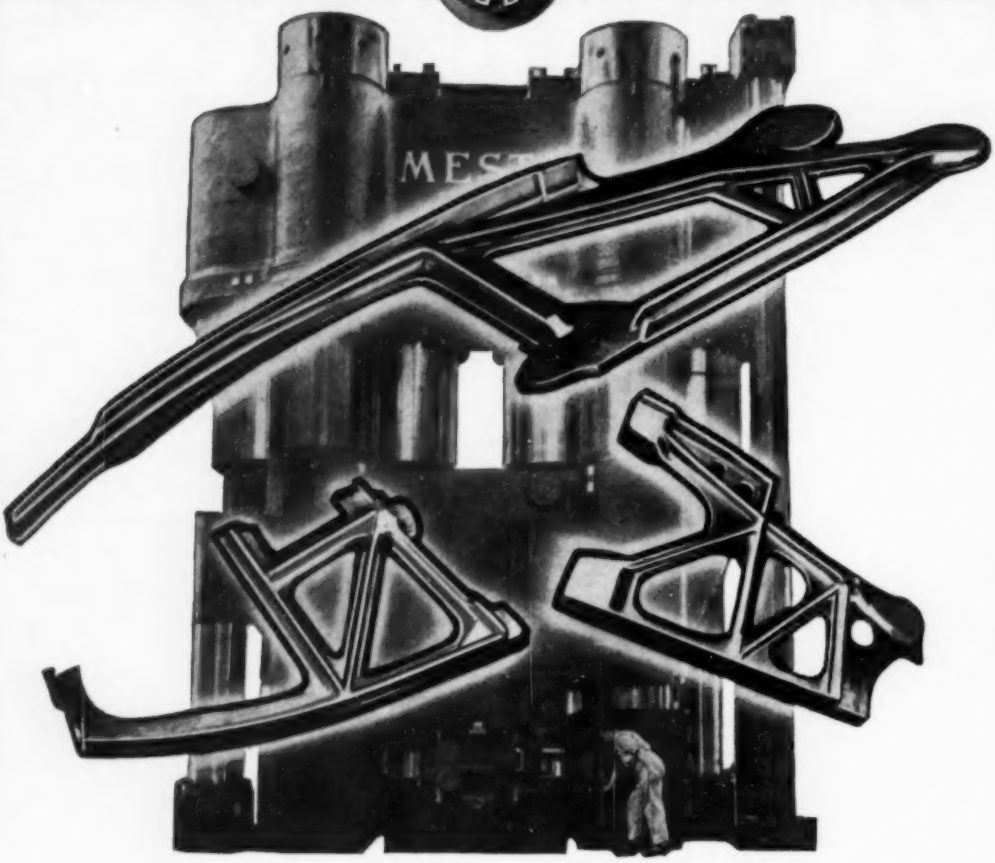

***Greater Size and Speed in Aircraft*** have created engineering problems, the solution of which has required larger and larger forgings of high-strength aluminum alloy. *Examples* shown above are forged structural members used in a modern military bomber, the largest more than seven feet over all. These are forged on an 18,000 ton press, the biggest ever built in this country.

***Wyman-Gordon Experience***—the most extensive in the industry—is keeping abreast of new forging demands involving the use of Steel, Aluminum, Magnesium, High Density Alloys and Titanium.

• • •

***Standard of the Industry for More than Seventy Years***

# WYMAN-GORDON

FORGINGS OF ALUMINUM • MAGNESIUM • STEEL • TITANIUM

WORCESTER, MASSACHUSETTS

HARVEY, ILLINOIS DETROIT, MICHIGAN

# Heroult
## ELECTRIC MELTING FURNACES

TOPS FOR PRODUCTION OF HIGH GRADE STAINLESS, ALLOY AND RIMMING STEELS

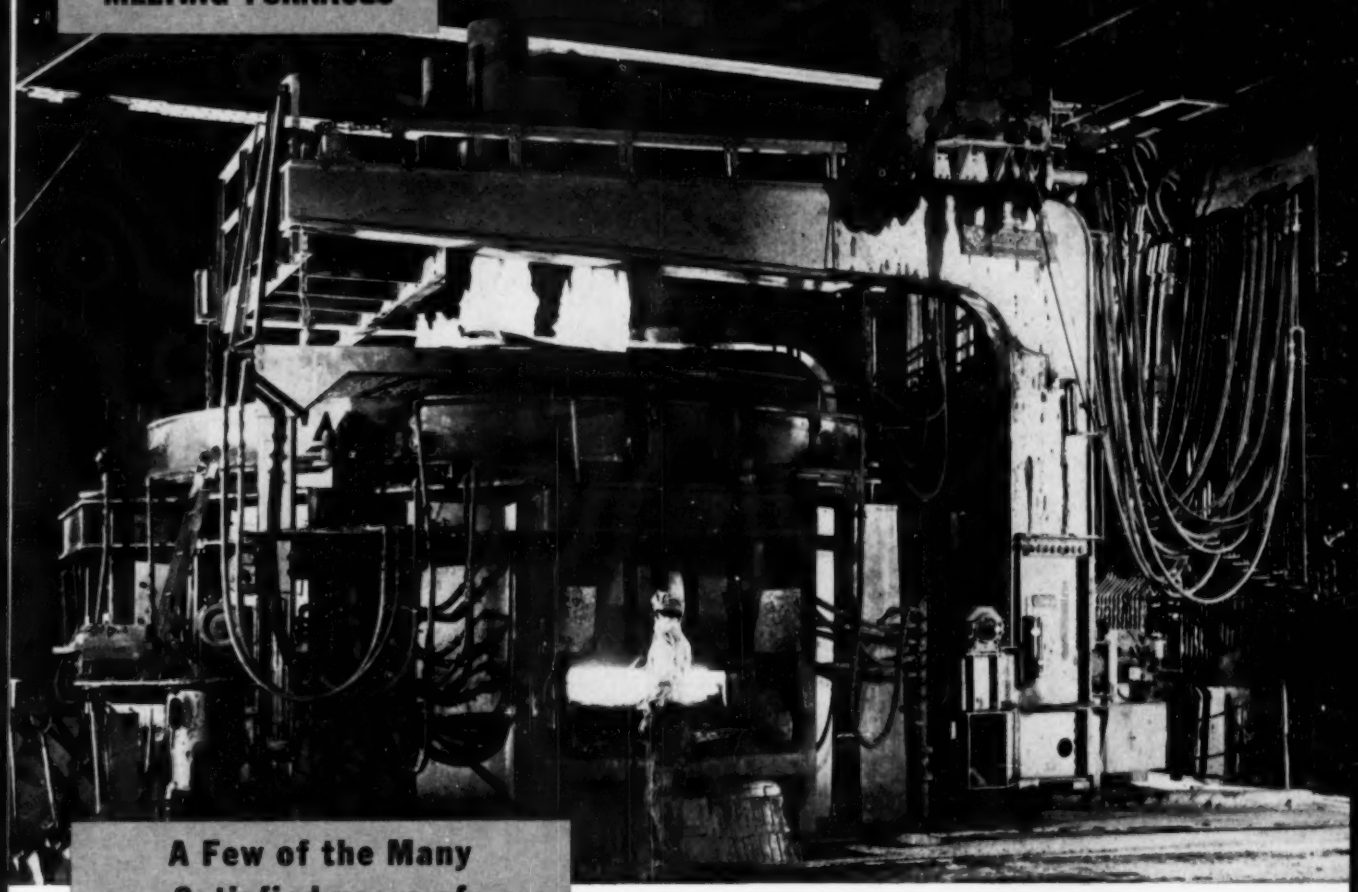

## A Few of the Many Satisfied users of HEROULT FURNACES

A. M. Byers Company
Allegheny Ludlum Steel Corporation
American Steel Foundries
Crucible Steel Co. of America
Ingersoll Steel Division, Borg-Warner Corp.
McLouth Steel Corporation
Ohio Steel Foundry Company
Republic Steel Corporation
Rotary Electric Steel Company
The Timken Roller Bearing Company
Vanadium-Alloys Steel Company

## NEW CATALOGUE NOW READY

Contains up-to-date information on Heroult Electric Melting Furnaces — types, sizes, capacities, ratings, etc. Write Pittsburgh Office for free copy.

# Heroult
# the standard of efficiency and safety!

Embodying the latest in mechanical and electrical equipment, these widely used furnaces are noted for their efficient performance, safety, and low operating cost and maintenance.

We welcome an opportunity to help you select and install the furnace best suited to your particular requirements.

**AMERICAN BRIDGE DIVISION, UNITED STATES STEEL CORPORATION**
**GENERAL OFFICES: 525 WILLIAM PENN PLACE, PITTSBURGH, PA.**

Contracting Offices in New York, Philadelphia, Chicago, San Francisco and other principal cities.
United States Steel Export Company, New York

USS

4-288

UNITED STATES STEEL

# —Personnel Service—

THE following employment items are made available to AIME members on a non-profit basis by the Engineering Societies Personnel Service Inc., operating in cooperation with the Four Founder Societies. Local offices of the Personnel Service are at 8 W. 40th St., **New York 18;** 100 Farnsworth Ave., **Detroit;** 57 Post St., **San Francisco;** 84 E. Randolph St., **Chicago 1.** Applicants should address all mail to the proper key numbers in care of the New York office and include 6c in stamps for forwarding and returning application. The applicant agrees, if placed in a position by means of the Service, to pay the placement fee listed by the Service. AIME members may secure a weekly bulletin of positions available for $3.50 a quarter, $12 a year.

## MEN AVAILABLE

**Metallurgical Engineer,** 29, family. Eight years responsible experience production metallurgist in Swiss and British nonferrous metal industry. Specialized experience hot and cold working of metals, machining. Some experience in consultancy. Desires interesting position with American firm. Swiss citizen, presently resident Great Britain. Fluent English, German, Swedish, and French; some Spanish. Willing to go anywhere. M-129.

**Mining and Metallurgical Engineer,** Dutch, equivalent M.Sc., 30, family. Now employed South America. Three years experience test and operational work large American company. Speaks and writes English, French, Spanish, German. Desires job in mill; go anywhere. M-130.

**Technical Sales or Process Metallurgist,** 10 years technical sales of nonferrous mill products in eastern areas. Ten years processing and research on brass mill products. Age 44. Desires to apply contacts and experience to sale of mill products or production. M-131.

**Mechanical Metallurgist,** 34, SM, mechanical; Sc.D., metallurgy; seven years' college teaching both fields. Two years' design; three years' industrial research light metals. Author technical papers. Registered Pennsylvania. Desires research and development. M-132.

## POSITIONS OPEN

**Physical Metallurgist,** graduate, with up to three years experience. Junior category will be working in conjunction with Ph.D. and research work. Will also work on development problems, equipment specifications and determine failure of various pieces of equipment that are going into the plant; chemical corrosion problems, etc. Will also do research and development of new products. Salary, one year's experience $4800 to $5000, two years experience $5000 to $5500, three years experience $5500 to $6000 a year. Location, New Jersey. W551.

**Field Engineer,** young, graduate, with equipment experience in chemical, metallurgical or process industry, for service work covering equipment improvements. Considerable traveling. Salary, $4500 to $5400 a year. Location, eastern states. W532.

**Physical Chemist,** Chemical engineer or metallurgist, whose experience and work preference are inclined toward precision optical, electrical or electromechanical equipment and or components might be suitable. Salary, $6500 to $6760 a year. W497(a).

**Sales Engineer,** 25 to 30, metallurgical engineering degree. Must have three to five years experience selling industrial equipment, for the application and sale of industrial burned systems by direct personal solicitation. Field travel away from home frequently required, but never exceeding 25 pct of time. Salary, $5400 to $6000 a year. Location, Indiana. W302.

**Production Shift Engineer,** graduate metallurgical or chemical engineer, to take complete charge of shift of lead smelter. Salary, $5400 to $6000 a year. Location, Midwest. W299(b).

**Sales Engineer,** 30 to 45, metallurgical engineering degree, with industrial sales experience. Will sell electrical contacts, thermometals, powder metals and special purpose alloys. Salary, $5200 to $7200 a year. Location, Newark, N. J. area, and later assignment in East or Midwest. W213.

**Metallurgical Engineer,** to take charge of the metallurgical problems of a mining operation. Should have a thorough knowledge of flotation, cyanidation, lixiviation and if possible, have some knowledge of running a sulphuric acid plant. Accommodations for man and wife only. Salary open. Location, Chile. F172.

**Metallurgists** (a) Metallurgists, recent graduates, for research laboratory, for work involving routine analysis and research assistance until sufficiently developed to handle product development work. Location, Ohio. (b) Metallurgists, recent graduates, for plant metallurgy departments. Will be placed in a training program that would sufficiently inform them of products, processes and metallurgical problems so that they can handle metallurgical control work in these operating divisions. Locations, Pennsylvania and Maryland. Y9518.

**Chief Engineer,** 40 to 50, thoroughly experienced in the processing of nonmetallic ore; should have at least 20 years experience in engineering, including design, plant layout, etc. Must be familiar with mining equipment, flotation, jigs, ball mills, centrifuges, conveyor systems, etc. Some travel. Salary about $10,000 a year. Location, Southwest. W287.


**RESEARCH METALLURGIST:** Sound, resourceful, physical metallurgist with experience in the Optical Metallography of Metals. To develop and supervise the optical examination of titanium and its alloys. Challenging, interesting work with excellent growth prospects. Liberal benefits. Send complete resume of education and experience to:

Box K-22M AIME
29 W. 39th St., New York 18

**SALES-PRODUCTION METALLURGIST**

20 years experience in processing and technical sales of brass mill products. Desires to apply contacts to sales or production. Resume upon request.

**Box K-23M AIME**
**29 W. 39th St., New York 18**

**DEVELOPMENT ENGINEER**

To develop techniques for non-destructive inspection of reactor components. An unusual opportunity to set up laboratory and direct experimental programs. Two years of applicable experience required. Laboratories located in suburban Pittsburgh near excellent housing of all types. Your application will be handled promptly and confidentially. Please write in detail giving complete information concerning training, experience and salary requirements to Mr. C. F. Stewart, Supervisor of Industrial Relations, P.O. Box 1468, Pittsburgh 30, Pennsylvania.

**WESTINGHOUSE**
**ATOMIC POWER DIVISION**

**METALLURGIST-PHYSICIST**
**PERMANENT MAGNETS**

Experienced in Alnico production and control with practical and theoretical background for developing magnetic material. Must be U. S. citizen. Location New Jersey.

Box J-20M AIME
29 West 39th St., New York

**PHYSICAL METALLURGIST**

Unusual opportunity for personal and professional growth in association with important research programs. Desire strong interest in research pursuits, with ability to approach objectives in a diversity of fields. Liberal benefits including tuition free graduate study. Call Calumet 5-9600 or write:

Mr. John F. Collins

**Armour Research Foundation**

of Illinois Institute of Technology
10 W. 35th Street
Chicago 16, Illinois

# *The Furnace that Stirs Itself!*

## ELECTROMAGNETIC PRESSURE CIRCULATES MOLTEN METAL

*— In this 60 Cycle —*

**AJAX** TAMA-WYATT *Induction Furnace*

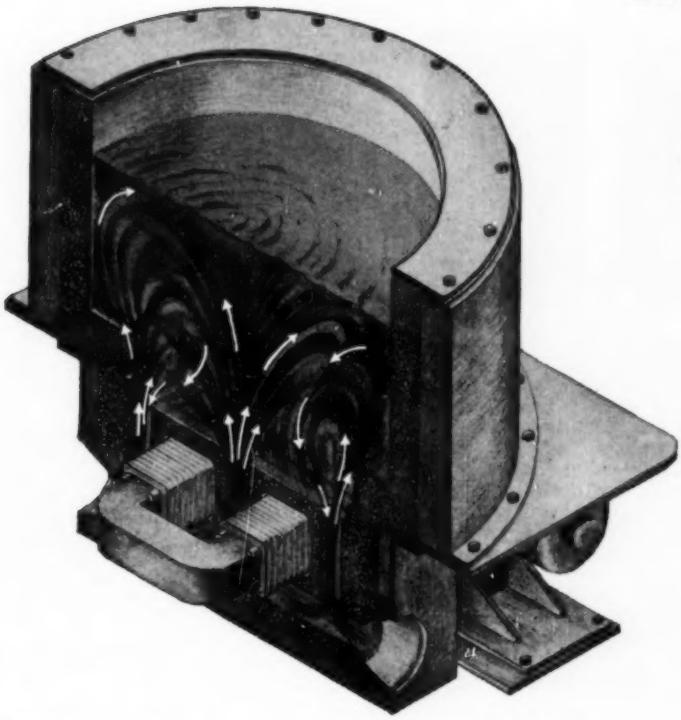

Heat is generated only in the melting channels. Controlled stirring *(neither too much nor too little)* guarantees uniformity of metal temperature and alloy composition and also leads to efficient melting of light scrap. Tiresome puddling is eliminated. The metal is held entirely in an inert refractory lining. The atmosphere is cool and free from contaminating gases.

### *No Other Method Enables such Completely* CONTROLLED MELTING

Today, AJAX builds a complete line of these time-tested furnaces in standard sizes up to 333 kW for the dependable melting of aluminum, brass, copper and zinc. Units for special applications are carefully engineered to specifications.

### TWIN COIL INDUCTORS *Lead Non-Ferrous Melting*

The sectional view above shows the twin coil stirring action of the 100 kW Ajax-Tama Wyatt 60 cycle induction furnace. Heat induced in the secondary channels below is conveyed throughout the melt by electromagnetic circulation as shown by the arrows. The 100 kW furnace shown here, which will be on display at the 1954 Metal Show, is one of a family of twin coil furnaces available today for melting rates from 300 to 10,000 lbs. per hour.

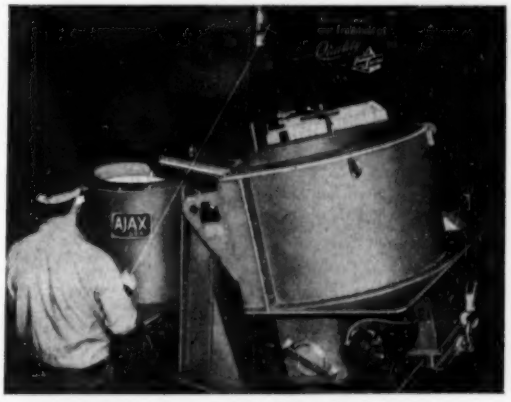


*We cordially invite you to inspect the 100 kW AJAX furnace exhibited at the NATIONAL METAL SHOW, Chicago, Nov. 1-5, 1954, Booth #752.*

**AJAX ENGINEERING CORP., TRENTON 7, N. J.**

**AJAX** TAMA-WYATT

# INDUCTION MELTING FURNACE

**AJAX ELECTRO METALLURGICAL CORP.**, and Associated Companies
**AJAX ELECTROTHERMIC CORP.**, Ajax Northrup High Frequency Induction Furnaces
**AJAX ELECTRIC CO., INC.**, The Ajax Hultgren Electric Salt Bath Furnace
**AJAX ELECTRIC FURNACE CORP.**, Ajax Wyatt Induction Furnaces for Melting

# Meet The Authors

**J. H. Rushton** (p. 1199) is professor of chemical engineering at the Illinois Institute of Technology, Chicago. Dr. Rushton was born at New London, Pa., and holds degrees from the University of Pennsylvania. He has held positions as a chemical engineer in industry, teaching, and consulting. Dr. Rushton taught at Drexel Institute of Technology, and the Universities of Michigan and Virginia. During World War II, he served with the Office of Scientific Research and Development as a technical aide and was section chief in charge of the oxygen program for the National Defense Research Committee. At present he is an expert consultant for the Dept. of Defense. Dr. Rushton has written more than 40 technical articles. He is the recipient of the William H. Walker Award from the AIChE for outstanding contributions to the literature of chemical engineering. Dr. Rushton is a member of various professional organizations and is past chairman of the industrial and engineering chemistry div. of the American Chemical Society. He is also a director of the AIChE.

J. H. RUSHTON

G. F. TISINAI

**G. F. Tisinai** (p. 1259) is a native Chicagoan and a graduate of University of Illinois and Illinois Institute of Technology. Mr. Tisinai joined the engineering research dept. of Standard Oil Co. of Ind. in 1948 and is now a research engineer for the company. A Member of the Chicago Local Section of AIME, he enjoys golf, bowling, and reading in his spare time.

**C. H. Samans** (p. 1259) has been associate director, materials engineering research dept., Standard Oil Co. of Ind., since 1949. Mr. Samans was born at Greenville, Pa., and is a graduate of Rensselaer Polytechnic Institute and Yale University. In 1929 he joined the research dept. of the Chase Brass & Copper Co., Waterbury, Conn. He was an instructor in metallurgy at Lehigh University for one year and for two years was an instructor in metallurgical engineering at Rensselaer. While at Pennsylvania State University he was assistant and associate professor of metallurgy, respectively. Dr. Samans joined the American Optical Co. in 1941 and remained with them until 1949. He is a Member of AIME, as well as several other professional societies.

C. H. SAMANS

J. K. STANLEY

**J. K. Stanley** (p. 1259) was an assistant metallurgist for the National Smelting Co., Cleveland from 1934 to 1937. He then joined Westinghouse Electric Co. and remained with that firm until 1950. Dr. Stanley has been section head of the materials div., engineering research dept., Standard Oil Co. of Ind. since 1950. Born in Cleveland, he attended Case Institute of Technology, Western Reserve University, and University of Pittsburgh. He is a Member of the AIME Chicago Local Section and has presented five articles before AIME. When his work permits, he likes to swim and go camping.

**L. H. Mahony** (p. 1199) is a graduate of the University of Denver and Illinois Institute of Technology (B.S., M.S.). Mr. Mahony is presently assistant to the vice president in charge of sales with Mixing Equipment Co., Inc., Rochester, N. Y. He has been with the firm since 1945 and has been successively application engineer and manager application engineering. Prior to joining Mixing Equipment, Mr. Mahony had been a field service engineer with NDRC. His varied hobbies include skiing and folk dancing.

L. H. MAHONY

J. C. BISCHOFF

**Joseph C. Bischoff** (p. 1194) who was born at Bridgeport, Conn., is presently residing at Sudbury, Ont., Canada. Mr. Bischoff is works metallurgist of the copper refining div., International Nickel Co. of Canada. From 1927 to 1930 he had been employed as a research engineer with the U. S. Metals Refining Co., Carteret, N. J. He then went to Canada and joined the staff of the Ontario Refining Co., which later became the copper refining div. of Inco. Mr. Bischoff is a Member of AIME, CIM, and Electrochemical Society. In his free time he enjoys fishing, hunting, and photography.

**R. J. Hopkins** (p. 1208) was born at Victoria, Australia. Since 1926 he has been associated with the Broken Hill Associated Smelters Pty. Ltd. In 1937 he was a technical sales engineer at Melbourne. Mr. Hopkins was named chief chemist in 1937 and in 1943 became technical superintendent. In 1947 Mr. Hopkins was named works research superintendent at Port Pirie. He visited the United States and Europe in 1948 and is presently abroad.

**L. B. Haney** (p. 1208) is a graduate of Hobart Technical College, 1922. Mr. Haney was associated with the Electrolytic Zinc Co., Australia from 1922 to 1926. For three years he worked on development of concentrate roasting. He joined the Broken Hill Associated Smelters Pty. Ltd. in 1929. He has held the positions of shift superintendent, assistant smelter superintendent, smelter superintendent and to date is assistant research superintendent at Port Pirie, South Australia. Mr. Haney visited the United States in 1949.

**G. C. Deutsch** (p. 1214) is a native of Hungary, but graduated from the Case Institute of Technology. From 1942 to 1944 Mr. Deutsch was with the Copperweld Steel Co., metallurgy dept. During the war he was in the U. S. Navy as a deck officer. Following his discharge he joined the National Advisory Committee for Aeronautics where he is now a research metallurgist at the Lewis Flight Propulsion Laboratory, Cleveland.

**G. M. Ault** (p. 1214) is head of the materials research section, NACA, Lewis Flight Propulsion Laboratory. Mr. Ault has been employed at NACA since his graduation from Iowa State College in 1943.

**Pierre J. Leroy** (p. 1189) is assistant to the chief of the steelmaking dept., Institut de Recherches de la Siderurgie Française, St. Germain-en-laye, France. Born in Paris, Mr. Leroy received his degree in metallurgy from the Ecole Superieure des Mines de Nancy in 1943. Prior to joining IRS, he had been with the Societe Metallurgique de Senelle-Maubeuge engaged in work on Bessemer converters and open hearth furnaces.

*Announcing...*

# ELECTROLYTIC MANGANESE

## 99.9% PURE

**Now available from ELECTROMET in tonnage quantities. For all uses where a high purity manganese is required, including:**

. *Low-Carbon Stainless Steels*
. *High-Temperature Alloys*
. *Non-Ferrous Alloys*
. *Electrical Resistance Alloys*

Electrolytic manganese is now being produced in tonnage quantities at ELECTROMET's new Marietta, Ohio, plant. ELECTROMET's new manufacturing process produces manganese of very high purity with 99.9 per cent minimum manganese.

Additional information about electrolytic manganese and other ELECTROMET ferro-alloys and metals will be gladly furnished on request. The ELECTROMET office in your area will be pleased to answer your inquiry.

The term "Electromet" is a registered trade-mark of Union Carbide and Carbon Corporation.

**ELECTRO METALLURGICAL COMPANY**
A Division of Union Carbide and Carbon Corporation
30 East 42nd Street UCC New York 17, N. Y.
OFFICES: Birmingham • Chicago • Cleveland • Detroit
Houston • Los Angeles • New York • Pittsburgh • San Francisco
In Canada: Electro Metallurgical Company, Division of Union Carbide Canada Limited, Welland, Ontario

**Electromet**
TRADE MARK
Ferro-Alloys and Metals

# a **ton** of **clean** steel for a **dime**...

Approximately one pound of High Carbon Ferro Titanium added to a ton of semi-killed or killed steel can yield one ton of clean steel.

Titanium dioxide ($TiO_2$), formed from the addition, has excellent fluxing action with non-metallic inclusions such as silicates and aluminates. Low melting point oxides formed are carried up to the slag in the ladle.

Most effective scavenging action results when the amount of the alloy used is small—generally not more than 1 lb. per ton—and it is added in the ladle *after* such deoxidizers as aluminum, ferro silicon, etc.

Get complete facts by writing our New York City Office.

**TAM**
**PRODUCTS**
Registered U. S. Pat. Off.

**TITANIUM ALLOY MFG. DIVISION**
**NATIONAL LEAD COMPANY**

*Executive and Sales Offices:*
111 Broadway, New York City

*General Offices, Works and Research Laboratories:*
Niagara Falls, New York

# Industrial Notes

**• First large scale production of Chlorothene (inhibited 1,1,1-Trichloroethane), new nonflammable solvent for use in metal and metalworking industries has been announced by Dow Chemical Co. According to Dow the product is a nonflammable, low toxicity solvent to be used in cold cleaning and cold degreasing operations. Although, 1,1,1-Trichloroethane by itself may corrode aluminum and aluminum alloys, Chlorothene, the new inhibited grade, virtually eliminates such corrosion except under the most drastic conditions, according to Dow.**

• *Sutton Engineering Co., Bellefonte, Pa., announced completion of a new 750-ton horizontal, direct-powered extrusion press for aluminum, brass or copper shapes, bars, and tubes. Features of the press include extra fast cycling; positive billet loading, easy die change; heavy duty shear or extra high capacity; sensitive control of the main ram; and other similar aids to the user. The press will take preheated aluminum, brass, copper, or magnesium billet 4 7/16 in. diam and will extrude solid strips, rods, and hollow or semi-hollow sections.*

• Pennsalt Chemicals of Canada has been established, according to Albert H. Clem, president of the chemical specialties div. of the Pennsylvania Salt Mfg. Co. Under agreement with Canadian Industries Ltd., who for the past 15 years have handled Pennsalt metal cleaner sales in Canada, this new component will serve the Canadian market through sales offices and warehouse facilities at Hamilton, Ont.

• A new cold draw section, which extends length limitations on rods and tubes and triples capacity for producing heat exchanger tubes, is now in operation at the Huntington Works of the International Nickel Co., Inc., Huntington, W. Va. The unit comprises a building extension 350 ft long x 108 ft wide, a draw bench capable of drawing some tubes and rods up to 85 ft, and a gas-fired annealing furnace 220 ft in overall length. A magazine loading device consisting of a revolving cylinder in which six mandrels in sets of three each are placed one above the other, is one of the features of the draw bench. While tubing is drawn from the lower part of the cylinder, the upper three can be loaded in preparation for the next draw. At the end of a drawing operation, while the *mule* is being returned to start position, the cylinder rotates and brings three mandrels with tubes on them into position before the dies.

**• Olin Mathieson Chemical Corp. has acquired a substantial interest in Hunter Engineering Co. of Riverside, Calif., a firm engaged in research and development of methods for fabrication of nonferrous metals. Joseph L. Hunter will continue as chief executive officer of the firm.**

• Plans are underway for major improvements at U. S. Steel Corp.'s Homestead Works for improving finishing facilities for structural shapes. Improvements will be designed to meet increased demand for light wide-flange structural sections for which the mill has a limited capacity. Work will start when engineering plans are completed.

• *Edward A. Livingstone, vice president in charge of tubular products div. of Babcock & Wilcox Co. predicts that annual shipments of alloy steel tubing will reach 1 million tons in 1960. Mr. Livingstone noted that shipments increased from 276,217 tons in 1946 to 576,068 tons in 1953. The division has completed a four-year expansion program providing a capacity of about 230,000 ingot tons per year. Two electric arc furnaces, one with a 75-ton capacity and the other with 50 tons recently added brings the total to four in service.*

**• Major plant expansion at Aluminum Co. of America's Vernon, Calif. Works will bring two large hydraulic forging presses, one 8000 ton and the other 1500 ton capacity, to the West Coast. The entire expansion project is expected to involve about $4 million.**

• *United Engineering & Foundry Co., Pittsburgh, Pa., has been awarded a contract to modernize a 16 stand rod mill in the Buffalo, N. Y. plant of the Wickwire Spencer Div. of Colorado Fuel & Iron Corp. The rebuilt mill will be a 20 stand installation rolling 3 strands with a maximum delivery speed of 4400 fpm. United will supply new roll stands; complete new drive mechanism and coiling equipment.*

**• Ledoux & Co., Teaneck, N. J., has adopted a bromination technique for the determination of oxygen in various materials. The costs are less than one half those incurred in making similar analyses by the vacuum-fusion method, while the results are comparable in accuracy. Ledoux & Co., has been particularly successful in adapting the new technique to oxygen determinations in titanium metal and alloys.**

# Coming Events

**Nov. 1, AIME**, Boston Local Section, M.I.T., Faculty Club, Cambridge, Mass.

**Nov. 1-3, AIME**, Institute of Metals Div., fall meeting, Hotel Morrison, Chicago, Ill.

**Nov. 1-5, American Welding Society**, Hotel Sherman, Chicago, Ill.

**Nov. 1-5, American Society for Metals**, National Metal Congress, Palmer House, exposition, International Amphitheatre, Chicago, Ill.

**Nov. 3-4, AIME**, Columbia Local Section, President-elect's visit, Kellogg and Spokane.

**Nov. 3-5, Steel Founders' Society of America**, technical and operating conference, Carter Hotel, Cleveland, Ohio.

**Nov. 4-5, AIME**, National Open Hearth Conference, Southern Ohio Section, Deshler-Hilton Hotel, Columbus, Ohio.

**Nov. 8-11, American Petroleum Institute**, annual meeting, Conrad Hilton Hotel and Palmer House, Chicago, Ill.

**Nov. 10, AIME**, Connecticut Local Section, Hammond Metallurgical Laboratory, Yale University, New Haven, Conn.

**Nov. 12, Illinois Mining Institute**, Hotel Abraham Lincoln, Springfield, Ill.

**Nov. 18, AIME**, Cleveland Local Section, Manger (Allerton) Hotel, American Room, Cleveland, Ohio.

**Nov. 18, AIME**, Utah Local Section, joint meeting with Intermountain Assn. of Petroleum Geologists, Newhouse Hotel, Salt Lake City, Utah.

**Nov. 18-19, National Assn. of Corrosion Engineers**, 4th annual conference of western region, Hotel Biltmore, Los Angeles, Calif.

**Nov. 18-19, American Zinc Institute, Inc.**, Galvanizers' Committee, William Penn Hotel, Pittsburgh, Pa.

**Nov. 23, Society for Applied Spectroscopy**, dinner, Lido Restaurant; meeting, Philadelphia College of Pharmacy and Science, Philadelphia, Pa.

**Nov. 28-Dec. 3, ASME**, annual meeting, Hotel Statler, New York, N. Y.

**Nov. 30, ASTM**, Northern California District Meeting, Engineers' Club, San Francisco, Calif.

**Dec. 1-3, AIME**, Electric Furnace Steel Conference, William Penn Hotel, Pittsburgh, Pa.

**Dec. 3-4, AIME**, Columbia Local Section, joint session with North West Mining Assn.

**Dec. 12-15, American Institute of Chemical Engineers**, annual meeting, Statler Hotel, New York, N. Y.

**Dec. 26-31, American Assn. for the Advancement of Science**, national meeting, University of California, Berkeley, Calif.

**Jan. 12, 1955, AIME**, Connecticut Local Section, Bridgeport, Conn.

**Jan. 13, AIME**, Cleveland Local Section, annual dinner meeting, Manger Hotel, Cleveland, Ohio.

**Jan. 23-25, 1955, Indian Institute of Metals**, annual general meeting, United Club, Jamshedpur, India.

**Feb. 14-17, AIME**, annual meeting, Hotel Conrad Hilton, Chicago, Ill.

**Mar. 14-15, Steel Founders' Society of America**, annual meeting, Drake Hotel, Chicago, Ill.

**Mar. 16, AIME**, Connecticut Local Section, annual meeting, Statler Hotel, Hartford, Conn.

# Books for Engineers

ORDER YOUR BOOKS THROUGH AIME—Address Irene K. Sharp, Book Department. Ten per cent discount given whenever possible. Order Government publications direct from the agency concerned.

**Statistical Yearbook of the World Power Conference, No. 7,** available through the ASME, $5.85, edited by Frederick Brown. *Lund Humphries & Co. Ltd.* $5.85, approx, 160 pp., 1954. —The Yearbook has come to be regarded as an authoritative reference on world power resources. In some ways the current issue is more comprehensive than its predecessor. It brings most of the annual statistics forward to 1952 and in a few instances to 1953, and includes a number of additional and revised data on fuel and power resources.

**The Light Metals Handbook,** two volumes, by George A. Pagonis. *D. Van Nostrand Co., Inc.* $8.50, 383 pp., 1954.—The book is aimed at relieving the scarcity of data for men working in the fields of research and industry using aluminum and magnesium cast parts and wrought products, and alloys of better structural stability for internal combustion, jet, and turbo-jet engines. The book simplifies the task of gathering facts and information on aluminum and magnesium-base alloys. Volume I covers the text and Volume II consists of the tables to be used simultaneously with the text. Each volume is divided into two parts: Part 1, Magnesium and Magnesium-Base Alloys; and Part 2, Aluminum and Aluminum-Base Alloys.

**Strength and Resistance of Metals,** by John M. Lessells. *John Wiley & Sons, Inc.* $10.00, 450 pp., 1954.—The book attempts to give the senior and graduate student as well as the design engineer the information on behavior of metals under stress as revealed by numerous workers in the field. Most of the discussion centers around behavior of steel. However, mention is made of nonferrous alloys and cast iron in those instances where behavior differs from steel.

**Progress in Metal Physics,** Vol. V edited by Bruce Chalmers and R. King. *Interscience Publishers.* $9.50, 324 pp., 1954.—This is the fifth volume in a series whose purpose is to provide a review of the papers in the general area of the physics of metals. Papers cover such topics as: the fracture of metals; geometric aspects of the plastic deformation of metal single crystals; the structure of liquid metals; precipitation; and solidification of metals.

**Chromium Plating,** by P. Morisset, J. W. Oswald, C. R. Draper, and R. Pinner. *Robert Draper Ltd.* 611 pp., 1954.—Purpose of the book is to supply useful information to the plater who wishes to learn the practical details involved in any of the many different chromium plating processes and sequences, as well as to the chemist engaged in routine testing and solution analysis, the foreman, the manager or superintendent, the student, research worker, and the engineer and designer. The text has been arranged for easy reference and extensive use has been made of graphic presentation.

**Monomeric Acrylic Esters,** by Edward H. Riddle. *Reinhold Publishing Corp.* $5.00, 221 pp., 1954.—The book provides up-to-date information on commercially available acrylate and methacrylate esters. It begins with a brief history of acrylic monomers and polymers, including the processes formerly and now in use in preparation of monomeric acrylic esters. Physical properties of both the technical grades and purified materials are then presented, with methods of removing inhibitors, explosive limits, toxicity, and facilities for unloading and storage of monomers.

**Dielectric Materials and Applications,** edited by Arthur R. von Hippel. *The Technology Press and John Wiley & Sons, Inc.* $17.50, 438 pp., 1954.—Lectures delivered at the Summer Session course at the Massachusetts Institute of Technology in September 1952 have been edited and revised for this book. Twenty-two authors contributed to the work. Fundamental and practical knowledge for the engineer, scientist, and manufacturer who uses dielectrics is presented. The book opens with a section on theory, followed by description of methods and techniques for measuring permittivity. Properties and applications are treated in a third section. Armed forces requirements are also presented. The Tables of Dielectric Materials of the Laboratory for Insulation Research at MIT are reproduced in full.

**Materials of Construction,** by M. O. Withey and G. W. Washa. *John Wiley & Sons, Inc.* $9.00, 1954.—Book covers sources, manufacture, and fabrication of the principal construction materials. It also presents carefully selected information covering more important mechanical and physical properties, and influence of various factors on these properties. A full chapter is devoted to concrete aggregates and another section deals with nondestructive testing.

**Dielectrics and Waves,** by Arthur von Hippel. *John Wiley & Sons, Inc.* $16.00, 284 pp., 1954.—The subject matter, dielectrics, refers not to a narrow class of so-called insulators but embraces any nonmetal—and even metals as a boundary case—where their interaction with electromagnetic fields is under consideration. The book shows that dielectric analysis has gone far enough to permit the beginnings of dielectric synthesis, in which the properties of materials are tailored to order. Part I introduces the complex permittivity and permeability as the basic parameters and derives the macroscopic theory in a unified manner for the electrical and optical frequency spectrum from the field and circuit aspect. Part II gives the molecular reinterpretation by considering the action of induced and permanent moments and of mobile charge carriers in gases, liquids, and solids.

**Minerals for Atomic Energy,** by Robert D. Nininger. *D. Van Nostrand Co., Inc.* $7.50, 367 pp., 1954.—This is a complete handbook to prospecting for atomic energy minerals written by the deputy assistant director for exploration of the Atomic Energy Commission. It describes what and where to look, tools and methods to use, and how to make a reliable evaluation of findings. Organization of the book is designed to make it useful to the untrained and professional geologist or prospector. Part I describes the minerals and mineral deposits that are sources and potential sources of uranium, thorium, and beryllium. Part II is a comprehensive survey of the various areas of the world with respect to their favorability for new deposits of atomic energy minerals, with particular attention to the U. S.

**Modern Physics for the Engineer,** edited by Louis N. Ridenour. *McGraw-Hill Book Co.* $7.50, 499 pp., 1954.—This volume comprises a collection of lectures delivered to an extension course at the University of California, Los Angeles, during the year 1952-53. The editor collected the lectures under three categories. Part I, The Laws of Nature, covers physics in its narrow definition. Part II, Man's Physical Environment, discusses the application of physical laws and techniques of investigation, to the study of the universe, of the earth, and of the air. Part III deals with the application of physics to that branch of engineering known as modern electronics.

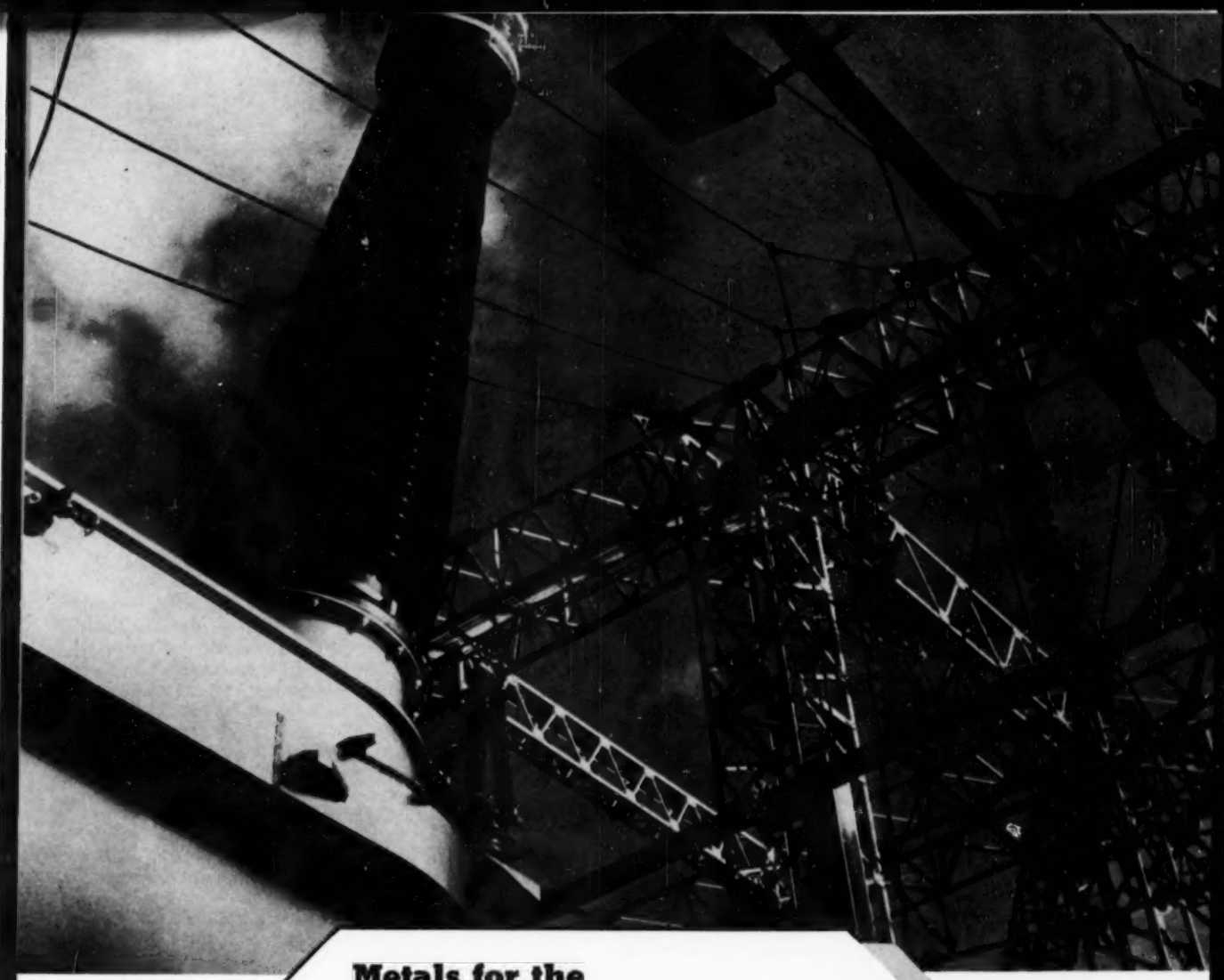

## Metals for the *Electrical Industry*

GLC GRAPHITE ELECTRODES help make many of the metals essential to the production, transmission and utilization of electricity.

The performance of GLC GRAPHITE ELECTRODES is unsurpassed in the manufacture of electric steels, foundry metals, ferroalloys and magnesium.

ELECTRODE DIVISION

**Great Lakes Carbon Corporation**

Niagara Falls, N.Y. GLC Morganton, N. C.

**Graphite Electrodes, Anodes, Molds and Specialties**

**Sales office:** Niagara Falls, N.Y. **Other offices:** New York, N.Y., Oak Park, Ill., Pittsburgh, Pa.

Sales Agents: J. B. Hayes, Birmingham, Ala.; George O'Hara, Long Beach, Cal.; Great Northern Carbon & Chemical Co., Ltd., Montreal, Canada; Overseas Carbon & Coke Company, Inc., Geneva, Switzerland; Great Eastern Carbon & Chemical Co., Inc., Chiyoda-Ku, Tokyo, Japan.

FOUR weeks after President Eisenhower signed the 1954 atomic energy bill members of the Atomic Industry Forum gathered in New York City to discuss "The New Atomic Energy Law—What it Means to Industry." Sitting in on discussions, attending sessions, and just eavesdropping near hallway conversations left one impression. The people attending the meeting—representing that segment of U. S. industry presently interested in atomic energy—indicate that private enterprise in entering into the new partnership with Government is conscious of its responsibilities.

One speaker, T. Keith Glennan, president of Case Institute of Technology and former U. S. Atomic Energy Commissioner, emphasised that the new law meant new problems in the relationship of business and government. "As I see it, the central problem for the government is to recognize that there is not only a new letter to the law; there is also now a new spirit to the law. I have some misgivings that this new spirit may not immediately be appreciated in all parts of the government, particularly among those who during the past 12 years of Manhattan District and Atomic Energy Commission operation have become accustomed to administering a government monopoly."

Mr. Glennan continued, "There should be no misunderstanding of the fact that the government retains enormous powers under the new atomic energy law. Although its ownership monopoly is gone, its authority to control remains. And with this position, for the present, I find myself in agreement." He also pointed out that "The power to withhold information is the power to make meaningless the licensing and leasing provisions of the new Atomic Energy Act." Mr. Glennan noted that of course the old rules must continue to apply to weapons. He warned industry not to "act as though a grab-bag labeled atomic energy" had just been opened.

Precise meaning of the law is still to be discovered. "One of the first questions will be definitions of 'production facility,' and important component parts of each," according to William Mitchell, general counsel, U. S. Atomic Energy Commission. Temporarily, to prevent a lapse in the licensing regulations the AEC has determined that the term 'production facility' has the same meaning as the term 'facilities for the production of fissionable material' under previous regulations for the control of facilities for production of fissionable material. New regulations will be forthcoming for "production facility" and "utilization facility."

George L. Weil drew a word picture of what might happen if a major accident took place in a nuclear plant. "In the absence of realistic information based upon experience, those concerned with the design and responsible for the operation of nuclear power plants must make the most pessimistic assumptions with regard to potential accidents and their consequences." He emphasized that the most foolproof system can go wrong in the hands of a 'great enough fool.' Tied in with Mr. Weil's discussion was one on atomic insurance problems. Stuart MacMacken, counsel, Atomic Energy Products Div., General Electric Co., told his audience that the magnitude of the job insurance companies in the atomic energy field would be asked to perform was much too large for them to handle alone. He urged that Government step in and help. The possible damage arising from atomic energy accidents is so great that no insurance company, or even group of companies could cope with the situation.

Generally, the feeling at the meeting was that the old relationship whereby industry was treated by Government as mere employee had changed. The new setup is more like the senior partner and junior partner arrangement.

◆◆◆◆◆◆

SINCE the end of World War II it has become increasingly obvious that the future of the Pacific Northwest as a significant industrial area depends upon the ability to get more power. Droughts have seriously hampered the firm power supply, causing particular hardships to the aluminum industry. Now Kaiser Aluminum & Chemical Corp. has taken a preliminary step that may help to ward off that danger. An agreement has been reached between the Government of British Columbia and Kaiser permitting the company to carry out engineering and geological investigations of sites for the construction of a storage dam in Castlegar Narrows at the foot of Arrow Lakes on the Columbia River.

If the project continues to the building stage, the dam will be of the low-head type, making it uneconomical and impractical to generate electricity at the site. Electric power will be generated at downstream facilities in the U. S. Should preliminary investigations prove the project worthwhile a dam with a reservoir capacity of about 3 million acre ft will be constructed at a cost of approximately $25 million. Kaiser plans to form a Canadian company before Mar. 1, 1955 to apply for the necessary conditional water license to permit construction. After completion a final license will be issued for 50 years with provision for renewal according to agreement reached by the B. C. Government and the Canadian company at that time.

Water rental to be collected by the province will be in terms of electrical energy and will equal 20 pct of the kilowatt hours which could be generated at downstream plants of the Federal Government of the U. S. from the net storage created by the dam.

◆◆◆◆◆◆

SOME 175 large fire losses between 1942 and 1953 cost U. S. metals plants about $150 million, contrasted with the period 1931 to 1942 when the loss was approximately $8.5 million. Large fire losses are considered to be those where damage is more than $250,000. According to a survey on *Fire Hazards and Safeguards For Metalworking Industries*,

issued by the National Board of Fire Underwriters, part of the increase in loss can be traced to the higher concentration of values in buildings, equipment, and products. New factors have entered the fire safety picture. More important is the presence of old causes in new forms.

With the increased use of plastics in the metals industry flammable liquid fires have continued to predominate. The report states that automatic sprinkler systems are uncommon in many phases of the metals industry. Twenty six out of twenty seven large-loss fires in 1951 were in plants without sprinklers. Fires have spread uncontrollably in some cases because of lack of water supplies and "ineffective fire-fighting units in some of the smaller communities." Delays in detection and calling the fire dept. have also taken a large toll.

Causes of fire that continue to prevail in the industry are the careless uses of welding torches and sawdust for removal of oil from operating floor areas in machine shops. Some of the most severe losses of life are caused by metal dust explosions. Control problems in recent years have enlarged to include fires from hydraulic fluids, molten salt baths, and quench tanks, as well as electroplating and electropolishing.

The report states that some of the new processing methods that may become significant in the fire-loss statistics of the future include: use of oil fogs as cooling and lubricating media in machine tool operations; higher speed machine tools which may bring an increase in the presence of hot metal chips; potential increase in use of titanium, zirconium, magnesium, and other combustible metals; trends in die casting with light metals requiring sodium as a coolant; increased use of hydraulic equipment near hot metalworking processes with the possibility of fires and explosions; fire and explosion hazards inherent in some of the new controlled atmosphere heat treating furnaces; use of hot paint sprays in metal finishing operations; application of rubberized sealing material compounded with flammable solvents as undercoatings, and the use of the various flammable adhesives and waterproofing plastics for automotive equipment; increased use of oxygen and compressed fuel gases for flame hardening, surface cleaning, and similar operations; and introduction of large quantities of plastics in the form of automotive bodies, bringing a mixed production into facilities originally designed solely for metalworking.

◆◆◆◆◆◆

SIZABLE price reductions for titanium that were to materialize as large tonnage production appeared have not been entirely in evidence. That's one of the arguments advanced by Loren W. Smith, head of Cornell Aeronautical Laboratory's metallurgical section, in attempting to take some of the shine off the "wonder metal."

He says that "Some small reductions have been effected recently but, for other than special purposes, titanium cannot compete at present with other materials on a cost basis."

He compares the price of less than $1 for mill shapes and sheet stocks of steel and aluminum with the $10 to $15 a lb for titanium mill shapes and $20 to $25 a lb for titanium sheet stock. Mr. Smith states that the nonuniformity of properties in delivered titanium has resulted in rejection rates many times that of steel and aluminum, thus pushing overall cost even higher.

Titanium melting, because of the particular properties of the metal, has been extremely expensive. Mr. Smith also brings up the matter of supply—a rather paradoxical situation. One year ago titanium was in short supply. Today, producers seem to be having trouble finding outlets for a supply seemingly exceeding demand. Mr. Smith, modifies his stand by predicting a bright future for titanium in the aircraft industry. "It is much too early to write off the very solid virtues that titanium definitely possesses simply because these virtues cannot be had merely for the asking."

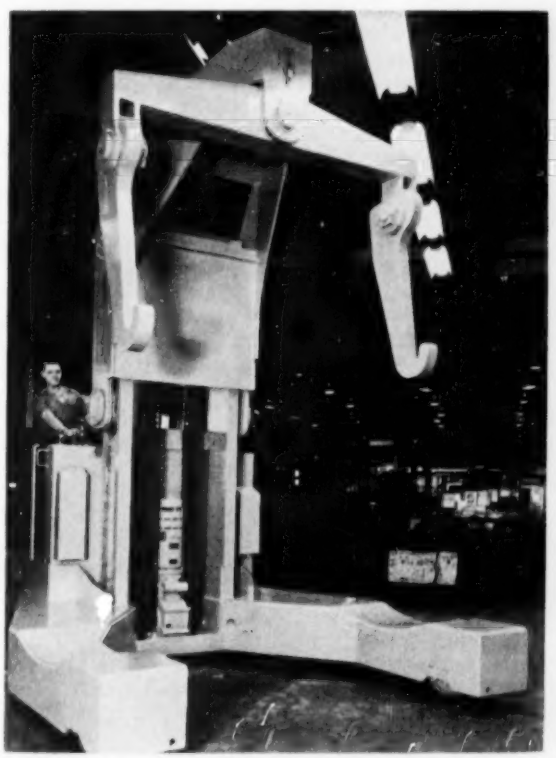

**Aluminum Co. of America has solved the problem of transporting molten aluminum from furnace to pouring stations with this special Yale 20,000 lb capacity high lift crucible handling electric straddle truck. Built by Yale & Town Mfg. Co., Philadelphia, the truck has an overall height of 154 in. with a maximum lifting hook height of 103 in. A diesel electric unit provides electric power for drive and hoist operations.**

# Drift of Things

WHAT happened to 50,000 flasks of mercury that seems to have just upped and disappeared? Along with the mystery of who's got the quicksilver is the rather unusual behavior of mercury in the market place. The flask price has been acting like a thermometer in mid-August—right now sellers are asking and getting around $330 per flask. One government contractor is almost certain to fall down on his end of the bargain because he can't buy mercury in the quantity he needs for his product, even though he's offering fantastic sums.

What would anyone do with 50,000 flasks? The immediate reaction to such a question is conditioned by the times. Atomic energy leaps forward as a logical place for the use of so much of the metal. Yet, consider this—the most obvious place would be in a reactor plant utilizing vacuum pumps or mercury as a heat transfer device. But, despite the magnitude of a vacuum pump setup, little or no mercury is lost in the operation of such a plant. In the case of mercury's use as a heat transfer medium, it is not the best available, ranking fifth in importance. Mercury has a tendency to pick up radioactivity and thus becomes rather *hot* to handle.

Newspapers throughout the U.S. carried headlines several months ago concerning the U. S. Government's intention to encourage mercury mining in this country. General Services Administration was going to buy 200,000 flasks of domestic and Mexican quicksilver during the next three and a half years at a price no higher than $225 per flask. Even then, the going price for mercury was much steeper. Some exploration contracts have been offered in line with mercury's position on the critical minerals list. A few small mines have announced or are going ahead with plans to reopen. The New Idria mine in California is planning to start up operations. However, one large mercury mining outfit has announced that it has no intentions of reopening West Coast mines unless something more concrete is forthcoming. This in the face of a skyrocketing market.

A financial reporter for one of the nation's most respected newspapers says that he was told about the coming mercury boom last April. He didn't believe the story. Now he's wondering about the rest of the tale. His informant stated that the boom would be shortlived, reaching its peak somewhere around this winter and then quietly folding up.

There is one strong possibility in the search for an answer. Two countries, Italy and Spain, produce the greatest part of the world's mercury. Two others, the U.S. and Soviet Russia, may for the sake of argument be considered the biggest buyers. The mercury market place is confined to a relatively small space—with well defined buyers and sellers. Suppose for the moment that Russia and the U. S., for vaguely defined reasons, have been going about buying mercury just so the other can't get its hands on as much as it wants. This would involve a certain amount of bidding. Could it be that the U. S. and the Russians are running the price up? Could it also be that they are both involved in a fantastic but shortlived shopping spree? If true, the answer to the skyhooked mercury price is apparent. M.A.M. and R.A.B.

ENGINEERS Joint Council, of which AIME is an active member, has organized a General Committee on Nuclear Engineering and Science to "meet the pressing problems of nuclear engineering and the related sciences," with emphasis on the "industrial usefulness" of atomic power. For some time, various individuals have talked about forming a new professional society to cover nuclear engineering, and one or more societies of this type are in the process of formation. We heartily support the EJC principle that inasmuch as the nuclear field cuts across all organized branches of engineering, the needs of this group could best be served by a joint effort of the organized societies.

Tentative plans call for a Nuclear Congress to be held July 11 to 16, 1955. However, if the United Nations acts on the proposal of Secretary of State Dulles to hold an international conference on the creation of a world bank of fissionable material for peaceful productivity, the general committee will cooperate fully with this program. If the United Nations conference is held in a city in North America, EJC would be willing to forego its own conference and assume the civilian aspects of the meeting. In the event the EJC Nuclear Congress is not held in 1955, the committees and divisions of the societies constituting the General Committee will be urged to hold their own sessions on nuclear matters at their regularly scheduled meetings. If the Nuclear Congress is held, technical papers scheduled for the Congress will be prepared by the individual societies through their divisions or committees concerned with nuclear power.

The organization of the Committee on Nuclear Engineering and Science is a further development of the Nuclear Congress sponsored by the American Institute of Chemical Engineers which was held in Ann Arbor last June. In addition to the 170,000 engineers and scientists represented by the eight members of EJC (American Institute of Mining & Metallurgical Engineers, American Society of Civil Engineers, American Society of Mechanical Engineers, American Water Works Assn., American Institute of Electrical Engineers, Society of Naval Architects and Marine Engineers, American Society for Engineering Education, American Institute of Chemical Engineers) the American Chemical Society has put the weight of its 70,000 members behind the new committee. The committee has also invited the participation, as members, of organizations of physicists and others concerned with nuclear development.

John R. Dunning, Dean of Engineering at Columbia University, has been elected Chairman of the General Committee, with Donald L. Katz, University of Michigan, Secretary and Program Chairman. A. B. Kinzel, Union Carbide & Carbon Co., is the AIME representative on the General Committee. Other committee members are Alex D. Bailey, past president of ASME; Manson Benedict, MIT; Raymond J. Faust, AWWA; Jewell M. Garrelts, Columbia University; D. C. MacMillan, George C. Sharpe, Inc.; Philip N. Powers, Monsanto Chemical Co.; J. C. Warner, Carnegie Institute of Technology; Julian D. Tebo, Bell Telephone Laboratories.

*A. S. Cohan*

# 5 Morgan Ejectors
## at The Fairless Works
OF THE UNITED STATES STEEL CORPORATION

***Four*** Morgan Ejectors are on the Rust Slab Heating Furnaces on the Hot Strip Mill.

***One,*** shown here, is on the 10′ Morgan Continuous Bar Mill Billet Heating Furnace. This Rust Furnace has a greater capacity in tons per hour than any billet furnace previously built.

*We like to think Morgan Ejectors help.*

CCC-44G

**MORGAN CONSTRUCTION CO.**
**WORCESTER, MASSACHUSETTS**
ROLLING MILLS • MORGOIL BEARINGS • REGENERATIVE FURNACE CONTROL • EJECTORS • WIRE MILLS • GAS PRODUCERS

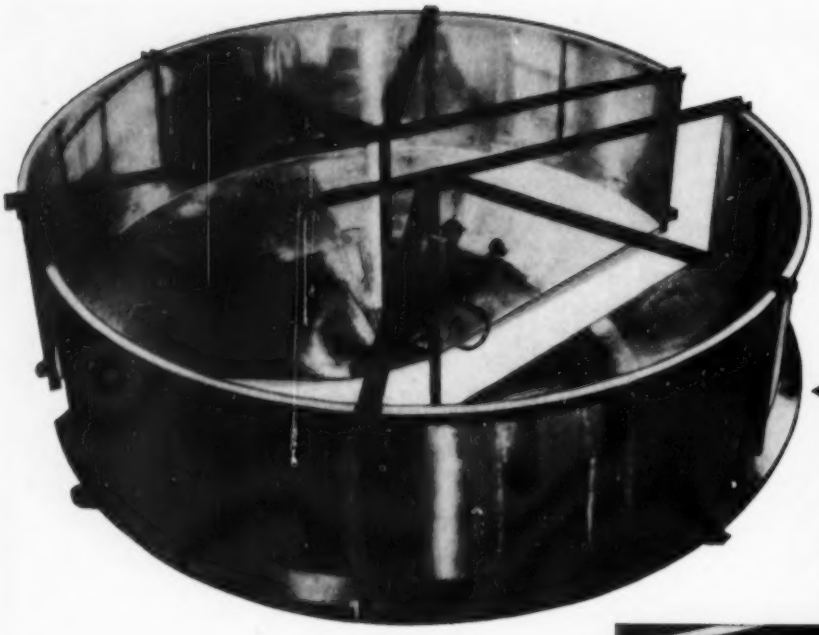

**75 Tons of Type 304 Stainless Steel** were fabricated for the new Anheuser-Busch West Coast brewhall. Note size of this starting tank, by comparison with workman polishing it at plant of Nooter Corp., St. Louis, Mo.

**New Method of Supporting Brewing Tanks,** devised by Nooter engineers, provides superior stability and performance. Eliminating usual costly complicated under framing. Nooter suspended three from floor beams of the plant itself, and rested others on steel legs sunk deep into concrete beams in the floor.

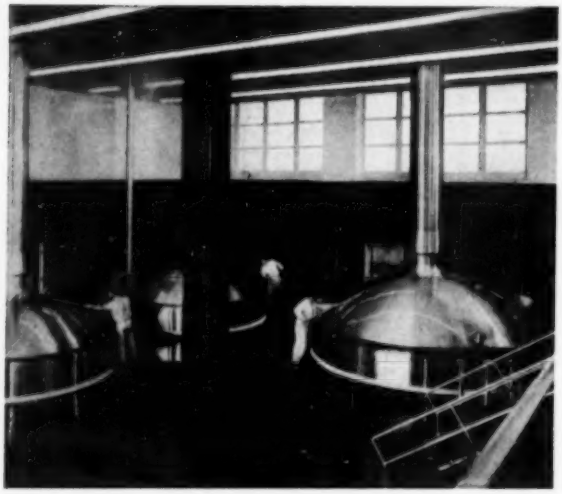

# All Stainless Steel

## Brewhall of Anheuser-Busch Cuts Maintenance and Promotes Product Purity

The new Anheuser-Busch brewery in California's San Fernando Valley is a man-made beauty . . .

It's the nation's first brewhall built to an integrated design, with all equipment of lustrous chromium-nickel stainless steel.

Easy to clean and keep clean, it helps assure product purity in all divisions of the food and beverage industries. That is why Anheuser-Busch selected chromium-nickel stainless with its invaluable protection against corrosion, year-after-year. The smooth, silvery-white surface of the Type 304 stainless steel allows no harbor for contaminants, no chance for product impurity.

For other industries with different demands, it provides unusual strength at elevated temperatures, yet, in sub-zero service it possesses enviable toughness. It resists wear and has other useful properties. And, of course, it readily responds to all usual forms of fabrication, including welding.

Use chromium-nickel stainless to *improve your products.* Leading steel companies produce these austenitic alloys in all commercial forms. A list of sources of supply will be furnished on request.

EMBLEM OF INCO SERVICE

**THE INTERNATIONAL NICKEL COMPANY, INC.** 67 WALL STREET NEW YORK 5, N.Y.

Capacity of the Kitimat aluminum smelter in British Columbia is to be expanded by 60,000 tons to meet market requirements. The smelter started operations a short time ago with an initial capacity of 91,500 tons. Approximately $45 million will be spent between 1955 and 1956 for the increased capacity.

Government stockpile copper will be distributed on a limited basis to those companies facing shutdowns for lack of the metal. In detailing the Government's aid in the copper shortage, Commerce Secretary Weeks said that tighter restrictions would be placed on exports of refined copper, copper scrap, and copper base alloy scrap in the current quarter.

Increased amounts of Spanish mercury can be expected on the market soon, according to reports. Minas de Almaden, only Spanish producer, is said to have solved difficulties which arose at the beginning of the year. Production blocks kept output at about 3000 flasks per month.

An atomic power pilot plant is scheduled for construction by Allis-Chalmers Mfg. Co. in Lemont Dupage County, Ill. Sargent & Lundy Co. of Chicago will design the boiling water reactor. Construction is slated to begin next year for completion in 1956. The Atomic Energy Commission hopes to determine the future of nuclear fuels as a competitor or replacement for conventional fuels in electric power generation.

Productinn of electrolytic cobalt has been started at the Port Colborne refinery of International Nickel Co. of Canada, Ltd. Until recently Inco's entire cobalt output has been marketed as oxides and salts from the Clydach, Wales refinery.

Torrential rains bombarding Chicago forced curtailment of steel production. U. S. Steel Corp. closed down two electric furnaces while Republic shut down five. Flood damage to power installations forced Commonwealth Edison to curtail by almost 100 pct, electric power to 17 of its largest customers. U. S. Steel's American Steel & Wire Div., was forced to shut down completely.

Total steel production for the first nine months of 1954 reached 64,197,136 tons, equal to 69 pct of capacity. During a similar period last year output totaled 85,510,617 tons.

The sodium reduction method is being used by Imperial Chemical Industries in its British titanium reduction plant. Most of the plants in Great Britain use the Kroll process. Operations are presently in the pilot plant stage. Production plans call for 1500 tons of sponge titanium annually.

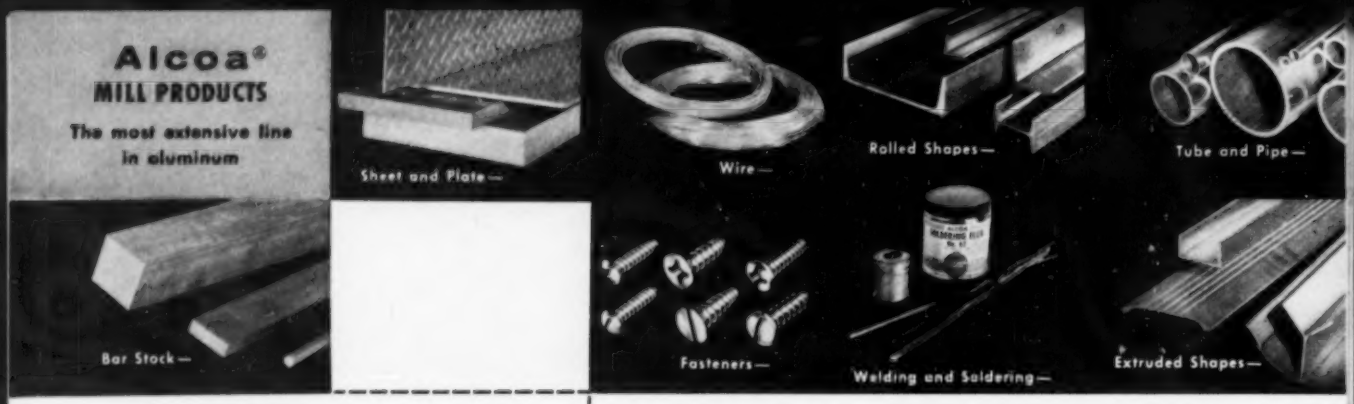


Alcoa manufactures a wide variety of standard rolled and extruded shapes for structural and architectural applications. With them, building costs are lower, construction time reduced.

There are extruded shapes for window sills, threshold, railings, copings and gravel stops; sheet for roofing and siding; pattern sheet for doors, partitions and siding; trim and moldings for glass-setting members, door accessories and interior moldings—and many more.

All these architectural products are available to you through Alcoa's 54 distributor outlets. They act as your warehouse, thus minimizing your stocking and handling problems; and they can readily supply your needs either in small lots for special jobs or in large quantities for continuous production runs.

To find out more about Alcoa's Architectural Products, call your local Alcoa Distributor. He is listed under "Aluminum" in the classified section of your telephone directory. Or write ALUMINUM COMPANY OF AMERICA, 878-L Alcoa Building, Pittsburgh 19, Pennsylvania.

# Alcoa
## Architectural Products

For Low-Cost, Modern Construction

YOUR ALCOA DISTRIBUTOR HAS ALCOA STANDARD WAREHOUSE ITEMS IN STOCK

ALCOA ALUMINUM

ALUMINUM COMPANY OF AMERICA

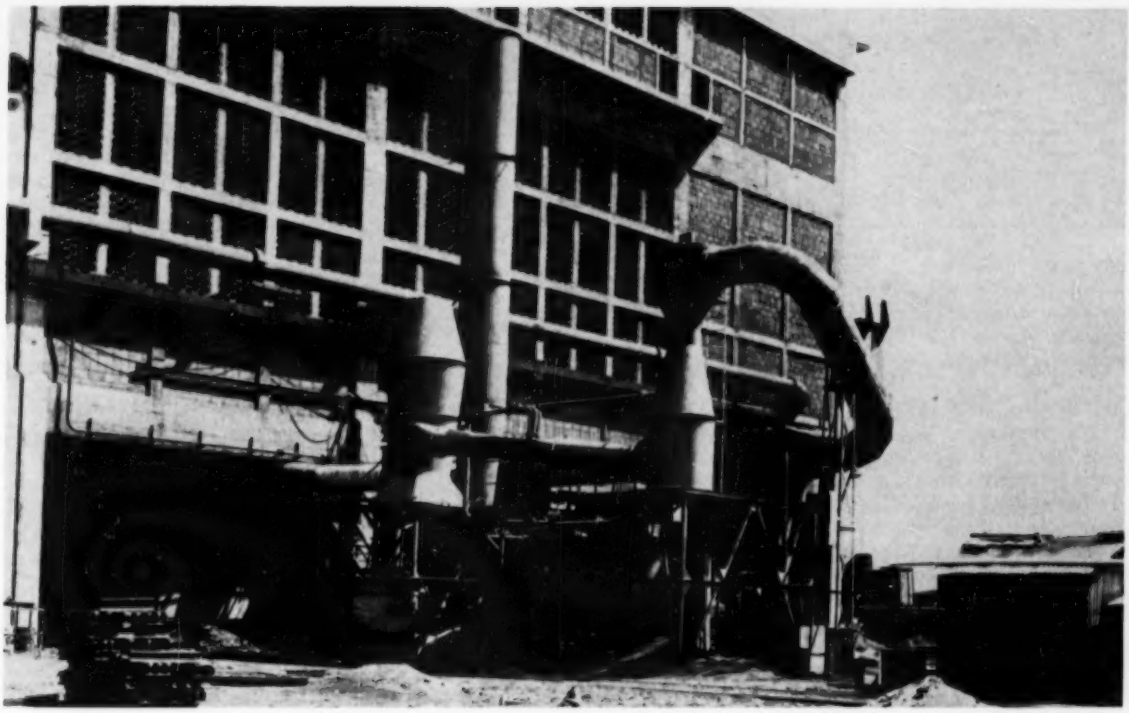

General view of pilot unit set up at the Mondeville plant of the Societe Metallurgique de Normandie for the recovery of red fumes resulting from oxygen lancing. The operation utilizes the French patent of M. de la Fourniere.

# French Patent Solves Fume Problem in Oxygen Steelmaking

by Pierre J. Leroy and L. Septier

RED fumes boiling up out of the bath in the oxygen lance injection method for prerefining of iron is the principal nuisance accompanying an otherwise valuable process. The red oxide dust billows out to cover the shop, workers, and countryside with a layer of fine dust.

The IRSID (Institut de Recherches de la Sidérurgie Française) has set up a pilot plant using the French patent of M. de la Fournière for separating the oxide particles. Working on a semi-industrial scale at the Mondeville plant of the Société Métallurgique de Normandie, the unit was the first to be operated in France.

A recovery of 99 pct or better of the free dust is possible based upon the performance of the pilot plant. Experience has shown that the yield is dependent on dust concentration at the inlet, temperature, moisture content, and the power of the installation (blowers, duct diameter, etc.).

P. J. LEROY and L. SEPTIER are Metallurgical Engineers, Institut de Recherches de la Siderugie Francaise (IRSID), St. Germaine-en-laye, France.

While work has been based mainly on the recovery of fumes generated in the prerefining of Thomas iron,[1] other possible applications would be on: A—The Austrian technique of surface blowing with oxygen gas in solid bottom converters,[2] B—the basic Thomas converter of Western Europe using air containing up to 40 pct $O_2$,[3] and C—the open hearth and electric furnace.

Among the oxides present in the red fumes other than iron are $SiO_2$, MnO, and $P_2O_5$. Iron itself is found in two states of oxidation, $Fe^{++}$ and $Fe^{+++}$, in various proportions depending on operating and

Table I. Water Consumption for Purification at Oxygen Flow of 40 Cfm

| Stage | Pressure Psi | Gal Per Min | Avg Gal Per Min |
|---|---|---|---|
| Under Hood | 140 | 10 to 30 | 20 |
| Wet Purification (scrubber, venturi, and cyclone) | 28.5 | 130 | — |

Table II. Typical Circulating Volume of Gas

| Water Psi | Flow of Gas Cfh |
|---|---|
| 0 (no water) | 810,000 |
| 21.3 | 635,000 |
| 25.6 | 600,000 |
| 28.4 | 565,000 |

sampling procedures. The IRSID installation has not only mitigated the fume nuisance but also has demonstrated that the cheap recovery of large quantities of fine powered iron oxide may improve the economic feasibility of the oxygen process.

## Description of Installation

The prerefining installation shown in Fig. 1 consists of: A—Lance for oxygen injection made of copper tubing either protected by a refractory coating or cooled by a water jacket, B—hood provided with a vent where the ladle is placed for the operation. A patented high pressure water sprinkler forms a mist for cooling the hot gases, C—trailer or truck for carrying ladle under the hood, and D—platform to control the handling of lance and ladle.

The red fumes which are formed mainly in the reaction zone are drawn up under the hood. Before dry purification, they enter a large diameter conduit, the first few yards of which are made of stainless steel and jacketed for water cooling.

A preliminary dry purification separates the larger particles and starts cooling the fumes. The dry separator contains 49 honeycomb cells with baffled inlets which cause a centrifugal whirl of the gas stream. The larger particles hit the cell walls and are collected in a bin. The cell outlets are baffled in the opposite direction. Safety clappets are provided on both sides to minimize explosion hazards.

Wet purification to collect the bulk of the remaining dust, utilizing the French patents of de la Fournière (Nos. 136, 128-620, 429-50, 479) is the essence of the whole process. Purification is made in three consecutive stages:

A—The scrubbing tower which is 15 ft high contains a spray nozzle. The fumes travel from the bottom to the top counter-current to the water spray.

B—The venturi tube has a rectangular section where three vertical spray nozzles are placed at the constriction. The side sprays have one nozzle and the central spray has two. This enables the production of a continuous water mist at the constriction.

C—The cyclone collector is a 15-ft tower with a vertical water sprinkler midway up which spurts water vertically to finish the dust precipitation and to wash the tower walls. The incoming and outgoing fumes enter and leave the tower tangentially to the wall in a screw-like fashion throwing the sludge to the outside.

For the different stages of purification, the water consumption for an oxygen flow of 420 cfm is given in Table I. Water pressure in the Venturi can be regulated. Values in Table I are maximums used when dust intensity is high. A large part of the water is recycled from the decantation tank. Total consumption averages 3000 gal per hr and is regulated by a 7 *cv* (cheval vapeur) centrifugal pump. (One *cv* is equivalent to 0.986 hp.)

After purification, the fumes are exhausted into a 50-ft high chimney with a blower driven by a 75 *cv* motor. Total circulating volume of gas varies with operating conditions. Typical examples of gas volume are given in Table II.

Capacity of the decanting tank is 7000 gal. It is

Table III. Typical Dust Concentrations Under Certain Conditions

| Conditions | Dust Concentration | |
|---|---|---|
| | Lb Per Cu Ft | Lb Per Cu Ft of $O_2$ |
| Oxygen alone at 215 psi | 0.0015 to 0.0075 | 0.03 to 0.15 |
| Oxygen at 215 and Steam at 155 psi | 0.0009 to 0.0045* | 0.018 to 0.072 |

* Although dust produced is small, oxygen and steam method is not used because iron is cooled.

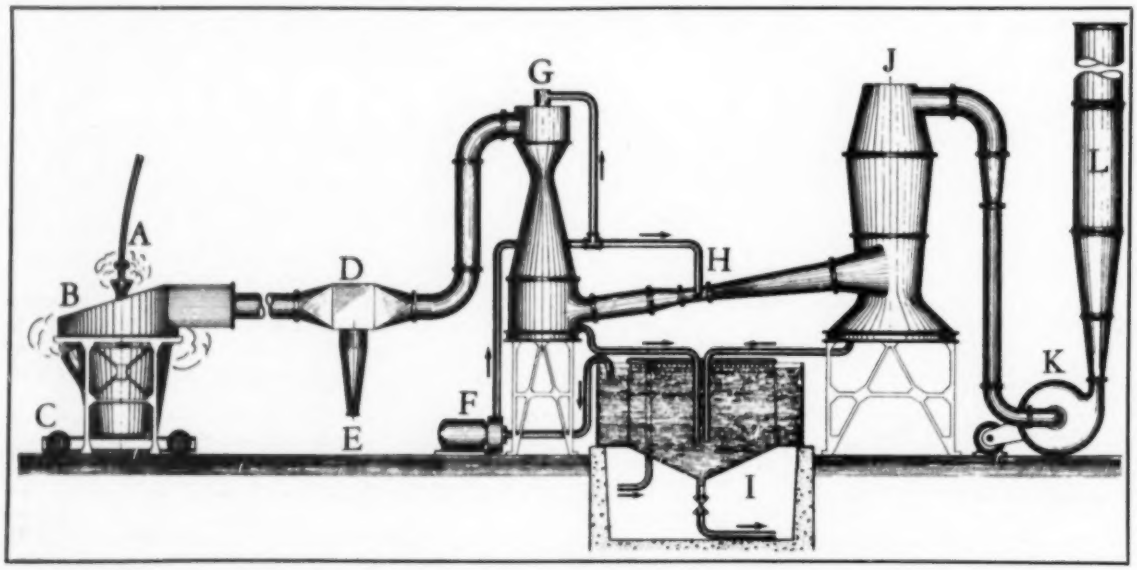


Fig. 1—Schematic view of pilot plant shows: A—tubing for oxygen injection, B—hood and vent, C—trailor and ladle, D—dry separator, E—bin for dry collection, F—Centrifugal pump, G—scrubbing tower, H—venturi tube, I—decantation tank, J— cyclone collector, K—blower, and L—50 ft chimney.

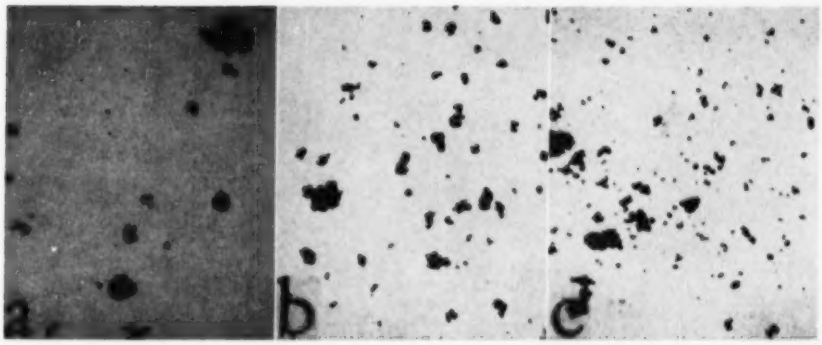

Fig. 2—Electron micrographs show: a—elementary particles (10,000X), b—dry separation particles (2000X), and c—wet separation particles (2000X).

fed by a rectangular trough capable of filling the tank at 80 gal per min. Flow during the operation is 11 gal per min. This is sufficient to maintain the recycled water below 86°F. Higher temperature would be detrimental to precipitation.

After each prerefining operation, part of the sludge is removed and replaced by fresh water to prevent a high sludge build up. Generally, the solid content of the water in the tank is never more than 10 lb per 100 gal. Decantation is rapid; at least 80 pct of the solid particles are deposited after an hour. Sludge is removed by an underground pump operated by a 3 *cv* motor.

### Operating Procedure

The following is a resumé of the operations during prerefining:

A—After the ladle is placed under the hood, and before lancing the oxygen, the blower and water circulations are started.

B—When lancing begins the stainless steel section of the conduit is watered and the sprinklers of the hood, the water-jacket circuit, and the lance are opened.

C—Water pressure at the sprinklers is regulated according to the appearance of the fumes.

D—Sprinklers are stopped immediately after lancing.

E—Fifteen min later, ventilators and pumps are switched off; 15 min are enough to cool hot parts of the installation.

F—Between prerefining operations 20 pct of the tank is evacuated and refilled.

G—Sprinklers are cleaned after ten operations.

H—Water inlet of the scrubbing tower is cleaned after 30 operations.

### Dust Characteristics

The dust concentration varies with the condition of the iron and with the flow rate of oxygen gas. It increases with temperature of the hot metal, and decreases with increasing silicon content. It increases with the flow of oxygen and decreases with the injection of steam under the hood. A typical example of variations obtained with injection of oxygen gas only and of oxygen gas with steam is given in Table III.

Table IV. Dust Composition for Various Purification Stages, Pct

| Stage | Analyses | | | | |
|---|---|---|---|---|---|
| | $Fe_2O_3$ | FeO | $P_2O_5$ | $SiO_2$ | MnO |
| Wet Purification | | | | | |
| Oxygen | 77 | 10 | 6.5 | 1.5 | 0.2 |
| Oxygen and Steam | 82 | 6 | 9.5 | 0.8 | 0.4 |
| Dry Purification | 83 | 14 | 2.2 | 0.4 | 0.1 |

Fumes at the dry separator can be at a temperature ranging from 212° to 1650°F, depending on the presence or the absence of the decarbonizing flames. The latter temperature occurs with irons having a silicon content lower than 0.3 pct. The initial iron temperature has an influence on the rate of increasing temperature, for example, a change from 2250° to 2450°F corresponds to a raise from 1200° to 1300°F for the fumes.

Injection of steam with oxygen has a cooling effect of about 400°F, while high silicon content results in a lower fume temperature. For instance, 0.95 pct instead of 0.35 pct Si decreases the fume temperature by 275°F.

Moisture content varies depending on the operation regulations, steam injection, and water sprinkling. This content is usually between 0 to 0.011 lb per cu ft.

Dust composition is relatively constant, regardless of the operating condition, if no addition is made to the ladle. Table IV gives analyses for various stages. Several oxidation stages, characterized by the ratio $Fe_2O_3/FeO$, have been noted for the iron. In the sludge, with pure oxygen injection, the ratio is seven. It is 12 when oxygen and steam are injected. At the dry purification where the oxidation is less, the ratio is six.

Elementary particles are small. The electron microscope reveals a spheroidal shape with a diameter of approximately 1/20th of a micron. The particles agglomerate in various proportions to about 0.1 to 5 microns with an average dimension of one micron.

Fig. 2 shows the elementary particles and the particles of the dry and wet purification. Dust, because of small particle composition, can be recovered in the form of pebbles when treated with 5 pct water in a revolving horizontal cylindrical mill.

Quality of the compacts is even better when 5 pct water is added to the dried dust, although agglomeration is easier when using sludge from the wet purification.

### References


[1] P. J. Leroy: Silicon Content of Blast Furnace Iron Lowered by Oxygen Injection in the Ladle. JOURNAL OF METALS (March 1953) p. 396.

[2] O. Cuscoleca: The Development of Oxygen Steelmaking. *Trans.* AIME (1954) **200**, p. 817; JOURNAL OF METALS (July 1954).

[3] P. Coheur and H. Kosmider: On the Basic Bessemer Process. *Trans.* AIME (1954) **200**, p. 829; JOURNAL OF METALS (July 1954).

# Power Equipment Increases Open Hearth Productivity

by G. E. Cooper

MONUMENTAL demands on the steel industry, first felt during World War II have added momentum to the drive for better use of manpower. Greater use of available manpower resources implies less physical force and greater utilization of man's ability to think. Thus, intelligent application of machines and new methods is the key to increased productivity. Steel management has been in the forefront of those seeking new ways to boost production. World War II and post war production is testimony to the industry's efforts.

Typical of what is happening today is No. 3 open hearth of the Steel Co. of Canada Ltd. Optimum use of truck and railtransportation, and highly mobile materials handling equipment has been designed *into* the shop. These pictures show some of the things that Steel Co. of Canada Ltd. did.

G. E. COOPER is Assistant Superintendent, Open Hearths, The Steel Co. of Canada Ltd., Hamilton, Ont., Canada. This paper was presented at the AIME National Open Hearth Conference, Chicago, Apr. 5 to 7, 1954.

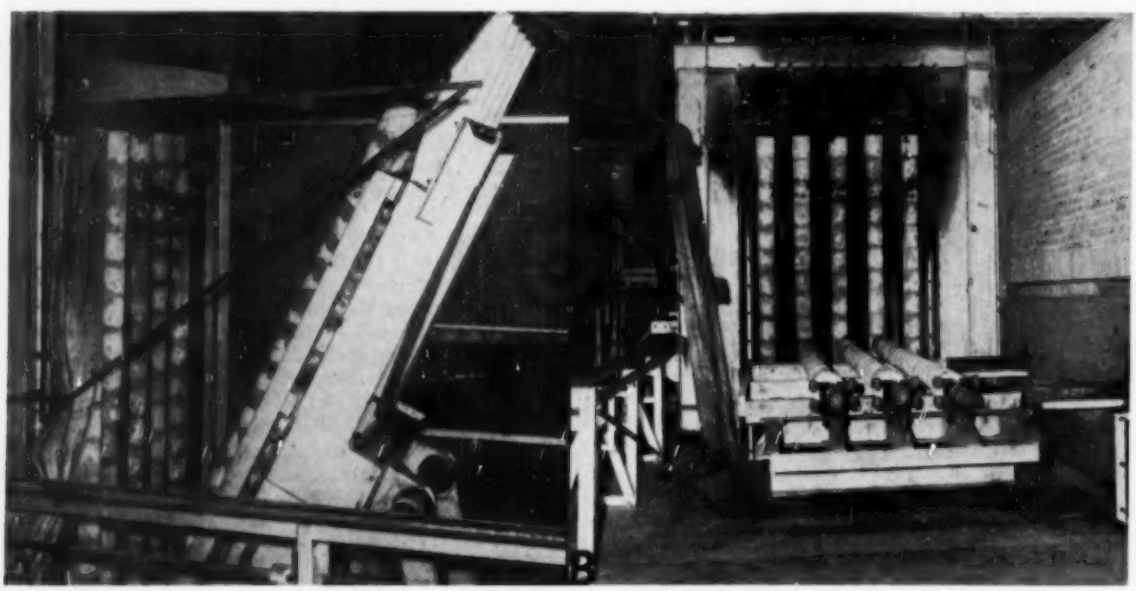

Handling of stopper rods from the makeup rack to the drying oven is facilitated by a motor operated bed which swings up and places the rods on the oven runways. Pictures show: A—stopper rods being placed in furnace, and B—stopper rods on bed.

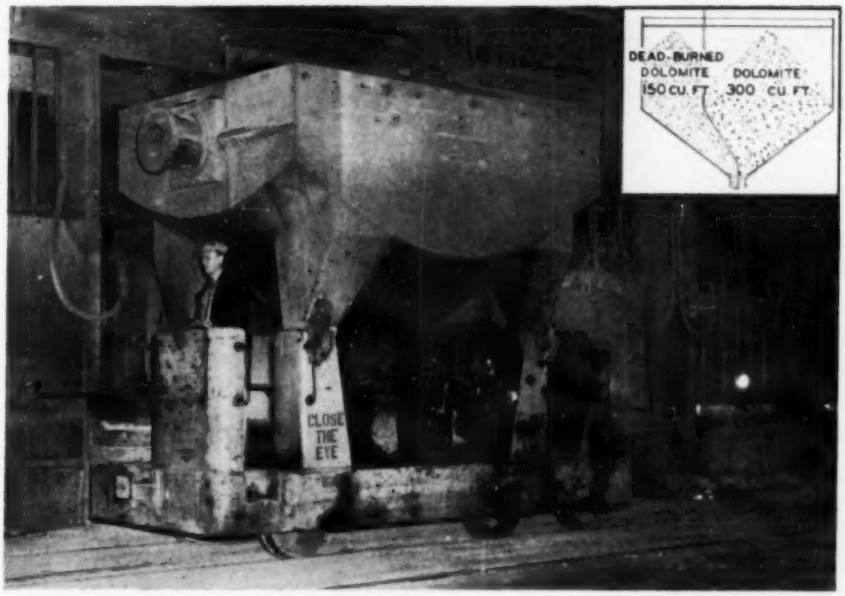


Use of dolomite slinger was made more practical by dividing the hopper and gate mechanism so that two materials can be carried and used at any time.

Improved crane service to floor operations is obtained by a 10-ton mobile crane on wheels which can operate at any place on the floor without interfering with hot metal handling or scrap charging.

Dumping dolomite on door sills is one of the many applications of payloaders. Floor areas and layouts are such that this type of mobile equipment can work with a minimum of interference.

Use of power equipment has not been neglected in furnace rebuilding and repair operations. A charging machine hoe has been developed to knock in and rake out roof debris. Debris is then handled by front end loader to dump trucks or to the slag pot.

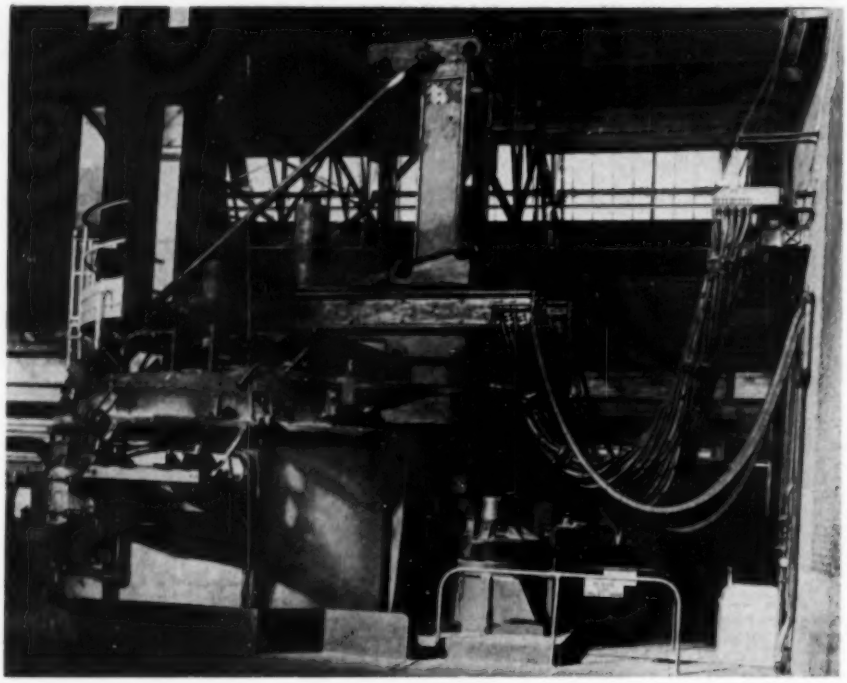

Electric furnace roofs are dome shaped and built of 9-in. refractory brick. The electrodes are 18 in. in diam x 60 to 72 in. in length.

# Furnace Operation and Casting Improved at Copper Cliff

by Joseph C. Bischoff

THE International Nickel Co. of Canada Ltd. pioneered in the continuous melting of copper in three-phase direct arc furnaces. The two electric furnaces installed at Copper Cliff are of similar design, differing principally in that No. 2 unit is equipped with a swing roof to permit top charging.

The furnace shells are fabricated 1⅛-in. steel plate, cylindrical with spheroidal bottoms. Each is 15 ft in diam and 9 ft 7⅛ in. in height. The furnaces are of the nose-tilt type—a forward tilt of 25° and a back tilt of 10° can be obtained. The normal operating position is horizontal, metal flowing from the tapping channel by the displacing effect of the continuous charge. The weight of each furnace with lining and charge is approximately 207 tons.[1, 2]

Since the installation of these first large scale electric furnaces for melting electrolytic cathode copper, a few basic changes have been made along with improvements in operation or casting techniques.

## Bottoms

The monolithic magnesitic bottoms have remained in service in No. 1 and No. 2 furnaces since burning-in in 1936 and 1938, respectively. Total copper melted on the two bottoms to the end of 1953 was in excess of 1,800,000 tons. While more recent installations at other plants have been of basic brick construction, the evident stability of the monolith precludes any thought of change at the present.

Areas of localized erosion do occur, generally under the charge slot and electrodes. The condition is more prevalent in the No. 1 furnace which melts croppings from the cast shapes and castings rejected for physical reasons in addition to the regular cathode feed. The average operating temperature of this furnace, which is dictated by the type of shape cast, is also higher than that of No. 2 furnace which handles cathodes only as the solid feed.

The problem of erosion is effectively controlled by patching with a low iron cor.tent ground magnesite clinker to which are added silicious materials to facilitate fusion. In this regard, the trend has been away from the use of alkali silicates and towards reduction in the quantity of free silica. The main diluent used is crushed calcium silicate slag (a synthetic Wollastonite) having the nominal composition given in Table I. A typical fusion batch is composed of 50 parts of the ground magnesite clinker and 7 parts of calcium silicate slag. In areas where fusion

J. C. BISCHOFF is Works Metallurgist, Copper Refining Div., The International Nickel Co. of Canada, Ltd., Copper Cliff, Ont., Canada.

may be difficult 1½ parts of pulverized silica sand are added.

During 1953 consumption of magnesitic material amounted to 0.389 lb per ton of copper melted in No. 1 furnace, and 0.021 lb per ton in No. 2 furnace.

### Sidewalls

Furnace sidewall construction has been modified by the substitution of clay brick for the 4½ in. of insulating brick adjacent to the steel shell and by the replacement of chemically bonded brick above the metal line with low iron content, high MgO burned periclase brick. Backing-up brick are two 4½ in. courses of hard burned clay.

While the use of periclase brick for this purpose is regarded as of an experimental nature, it may be of interest to mention that initially the sidewalls were constructed of white magnesite, a burned brick. In 1939 to 1940 the change was to chemically bonded brick of somewhat higher iron and chrome content. More recently, burned periclase brick have been introduced to this service.

The brick exhibit excellent resistance to slag or erosive attack but unfortunately show some tendency towards spalling. They are laid up with a thick buttered 3/16-in. joint of proprietary hydrated magnesite cement which provides for expansion and results in minimizing pinch spalling.

One such lining has now been in service for more than two years. The chemically bonded brick linings have an average life of about two years except where protected by build-up on the banks which, of course, results in increased life.

### Roofs

Sillimanite brick roofs were used mainly during bottom burning-in operations. Burned white magnesite brick roofs were then used intermittently during the first two years of regular melting operation, but chemically bonded brick were soon adopted as standard for this installation. From 1940 to 1946 experience with the latter was quite satisfactory; some of the installations were under heat for 750 days without brick replacements and others, with one maintenance repair, for 900 to 1100 days. Starting in mid-1947 and continuing for about two years, there were a number of premature failures due to softening and sagging of the roof structure. Burned brick were again tried, but in general it was found that serious spalling occurred with the low iron periclase type and excessive growth was encountered with the higher iron chrome-magnesite brick. Use was reverted back to the chemically bonded brick, and one roof of this type has now been in service for 527 days.

A typical roof is constructed of 9-in. brick. The skew brick are usually sillimanite, but at present a few high grade fire-clay brick are being used experimentally. The radius of the pallet, on which the roof contour is formed, is 12 ft 7¾ in. and the rise is 20 11/32 in. Expansion is provided for by means of ⅛-in. paper at every 10th brick in the header course and at every 18th brick in the rowlock course. The joints are made with a thin coating of No. 60 Hi-Temp cement. Every 4th brick in the header course and every 8th brick in the rowlock course are left up 1 in. for driving.

Clay brick rings are used on the roof around electrode openings and the structure is insulated with 2 in. of Vermiculite granules and 1 in. of Vermiculite coating.

### Charge Slot and Skim Bay Opening

A double arch supports the charge slot opening, the upper arch is 15x9 in. unburned low chrome, high magnesia brick and the lower arch is 12x9 in. burned high chrome, low magnesia brick. The sill over which the cathodes slide is laid up with specially designed carbofrax shapes. The skim bay door arch is of 12-in. sillimanite brick, and jambs for both openings are chemically bonded magnesite brick.

A water cooled charge slot is being tried out in No. 1 furnace. The first unit was of boiler plate construction and failed due to leakage and burnout.

**Table I. Nominal Composition of Crushed Silicate Slag**

| Material | Pct |
|---|---|
| CaO | 46.5 |
| $SiO_2$ | 44.0 |
| Fe | 0.1 |
| $Al_2O_3$ | 2.5 |
| $CaF_2$ | 6.2 |

A lot of stainless steel construction of improved design is now in service. This is fabricated of ½-in. type 304 and type 321 plate and has cooling water channels in the top and bottom sections only. These sections were tapered so that the leading edges within the furnace wall presented a minimum of surface for conduction, the objective being the prevention of skulling up from metal splash. This objective has not been entirely achieved and considerable buildup occurs. The use of this slot, however, has facilitated the charging of croppings and miscellaneous electro revert materials because of the greater clearance provided. This is 7 in. as against 5½ in. for No. 2 furnace.

### Dust and Fume Recovery System

The furnace vents from both furnaces are served by individual dust recovery systems. A separate

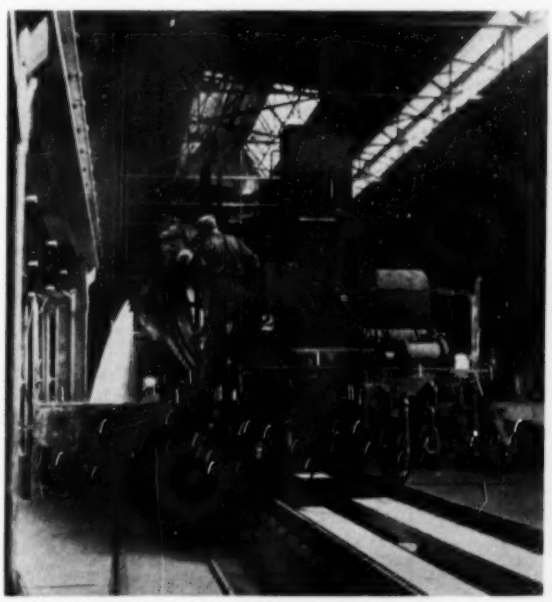

Hot metal car is shown discharging molten copper into anode furnace at the copper refinery of the International Nickel Co. of Canada Ltd.

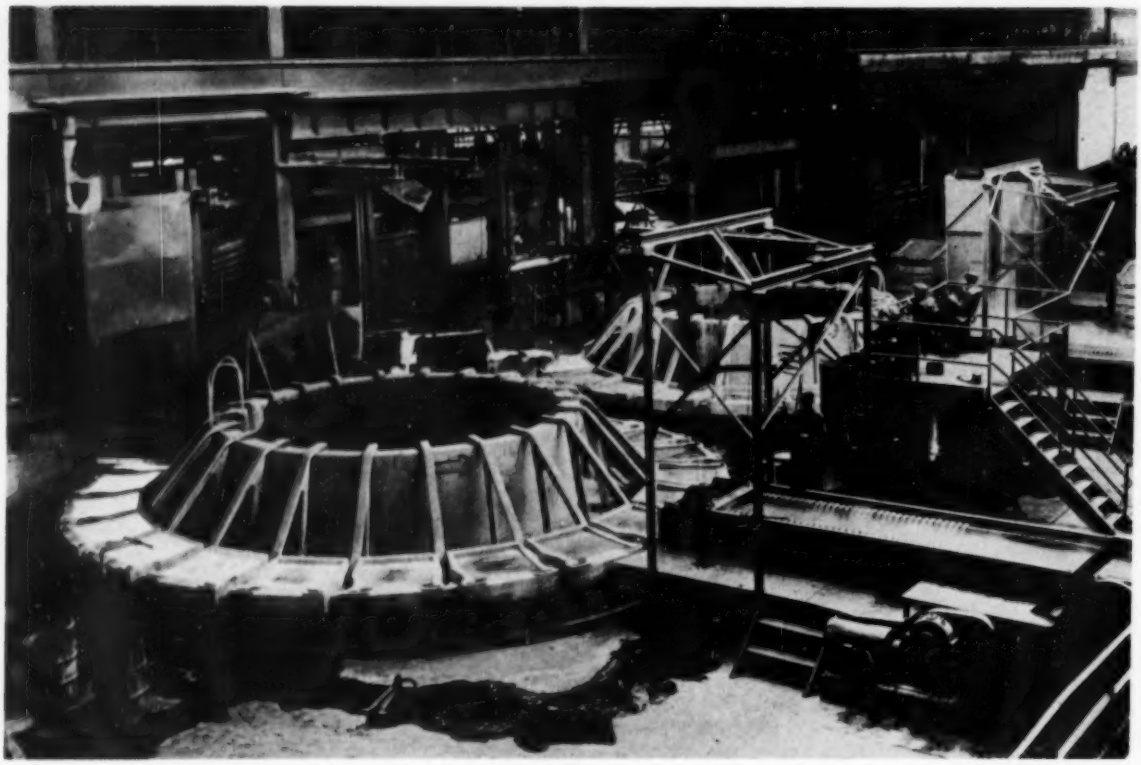

Throughout the anode casting process, the furnace operator is constantly concerned with melting rate, temperature, oxygen content, and general electrical operation. Melting rate is normally determined by the particular casting operation involved. In the case of horizontally-cast wire bars, for example, the melting rate will be 15 tons per hr. This necessitates the charging of about two cathodes per min; the melting of which requires the power input of 3300 kw.

unit is also provided for the hoods over the charge slot and working door on No. 1 furnace.

The original installation consisted of two recovery systems, but a third unit was found to be necessary when cold charging heavy shapes in order to prevent fume loss to the building.

Each dust recovery unit is constructed of type 304 stainless steel plate and consists of a 24-in. diam wet scrubber followed by a 20-in. diam cyclone. The wet sludge is collected in a central receiving tank, where it is slurried and pumped to a plate and frame press for de-watering.

Overall recovery of metallic and oxide dust is 95 pct. Production amounts to 4.1 to 4.3 lb of copper per ton melted, or 51 to 54 lb per hour casting. Loss is 0.2 lb of copper per ton melted.

## Heated Ladles

Electrically heated ladle lips are used during the casting of horizontal wire bars which are poured at relatively low temperatures. Their use minimizes skulling-up of the lips, which otherwise would cause distortion of the metal stream and result in surface defects on the castings.

The ladle itself is of the usual spoon shape and is superimposed between the pour-hearth and the molds. The shell is fabricated of ½-in. steel plate and is lined with high grade fire-clay brick. Holding capacity is about 1800 lb of molten copper. The ladle throat is also lined with fire-clay brick backed-up, as dimensional considerations permit, with insulating brick. The lips are of preformed silicon carbide 3x2¾ in. also set on insulating material. Channel sections leading to the lips are of similar material and are 9 in. in length.

External heat is provided by means of metallic resistors bent in inverted U form, placed over the lip and channel portion of the ladle. The resistors are composed of two 27 ft elements of ⅜-in. diam Chromel A, connected in series. Power requirement is 170 amp at 50 v.

The throat and lip sections of the ladle are protected by fire-clay brick and a heavy coating of refractory insulating material.

## Other Changes

The low frequency induction heated pour hearth for No. 1 furnace was shortened 18 in. and the normal holding capacity of 5 tons reduced by about 20 pct. The change was made on this unit in order to accommodate an intermediate pouring ladle when producing phosphorus deoxidized and other shapes.

Initial induction unit rammed linings were of Battersea material, an alumina-silicate material containing titanium oxide. More recently blocks have been formed of mullite and other sillimanite mixes. The basic refractory structure of the shell remains unchanged.

## References

[1] R. H. Waddington and J. C. Bischoff: *Trans.* Canadian Institute of Mining and Metallurgy (1946) **49**, p. 199.

[2] R. H. Waddington: *Journal* Institute of Metals (1949) **75**, Part 5, p. 311.

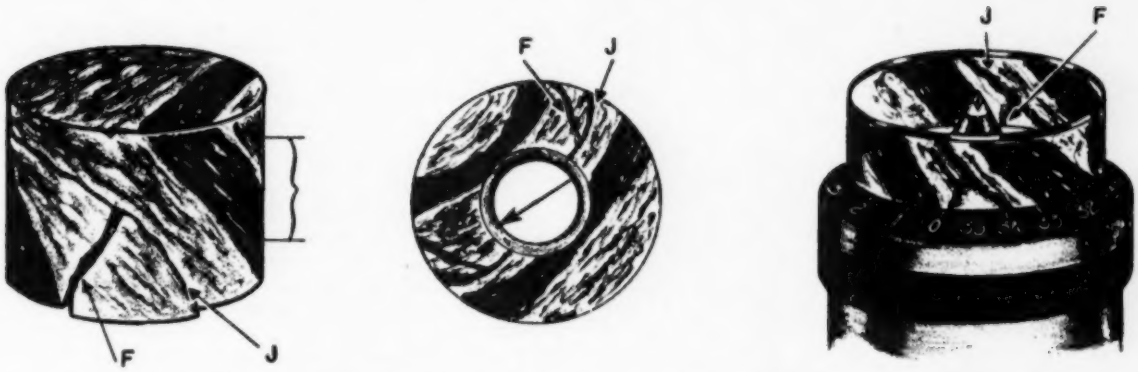


Fig. 1—The relationship between plane and cylindrical images as taken by the borehole camera is illustrated above. On the left is a core specimen of granite gneiss. The center illustration is the borehole camera film image of the section of the boring which is bracketed. On the right is the cylindrical projection of the plane image. In all three J and F are rock fractures.

# Borehole Camera Is Milestone In Subsurface Exploration

**The NX borehole camera is simple in concept yet so obviously efficient that the principles it employs may have even wider application than those intended by the army engineers who designed it. Here is a device for peering into openings which defy other means of investigation. The JOURNAL OF METALS is publishing this article in the belief that it may have an appeal to those seeking new ways to meet the challenge of other problems.**

by E. B. Burwell, Jr. and R. H. Nesbitt

A NEW milestone in the progress of photography and subsurface exploration was reached when the Chief of Army Engineers announced the development of the NX borehole camera. In obtaining continuous undistorted cylindrical color pictures of dry or water-filled borings the device surpasses all other cameras designed for photographing interior surfaces of pipes, wells, and conduits.

The usefulness of the camera and the unique projector that comes with it are at once apparent. To the geological, mining, and civil engineer alike it signifies the end of guesswork with respect to underground conditions that have eluded identification by conventional core-drilling methods. To the medical profession it may well signal new progress in photo optics which could result in cylindrical color photographs supplementing the X-ray and existing photographic methods used in exploratory surgery.

The pilot model of the camera has more than paid for itself as a result of its success in bringing to the surface at two dams information previously obtainable only by costly drilling of mansized boreholes for subsurface on-the-spot examination. Such bores cost as much as $200 per lineal ft as against $10 per ft for the conventional 3-in. or NX exploratory core borings from which the present invention derives its name. The NX camera can now photograph completely the interior surface of these borings.

Research and development for the first camera and projection equipment were conducted by Engineering Research Associates, Div. of Remington Rand, Inc., under the technical supervision of the Geology and Geophysics Branch, Office of the Chief of Army Engineers in Washington, in accordance with plans and specifications furnished by this branch. Subsequent modifications of the camera-lowering device, transporting equipment, and special field tools were made in the Corps of Engineers' Ohio River Div. Laboratories in Cincinnati. The background of this development is interesting.

Among the more difficult foundation problems involved in construction of concrete dams are those resulting from bedrock imperfections that escape disclosure by conventional exploration methods. Often these imperfections are of sufficient magnitude to introduce costly changes, especially when their presence is discovered only after foundation excavation is well in progress. Bedrock flaws most frequently camouflaged may be ruptures resulting from the enormous stresses to which rocks have been subjected, or they may be planes or zones of weakness

E. B. BURWELL, JR., and R. H. NESBITT are Chief Geologist and Assistant Chief Geologist respectively, Office of the Chief of Engineers, Dept. of the Army, Washington, D. C. This article is abstracted from MINING ENGINEERING, August 1954.

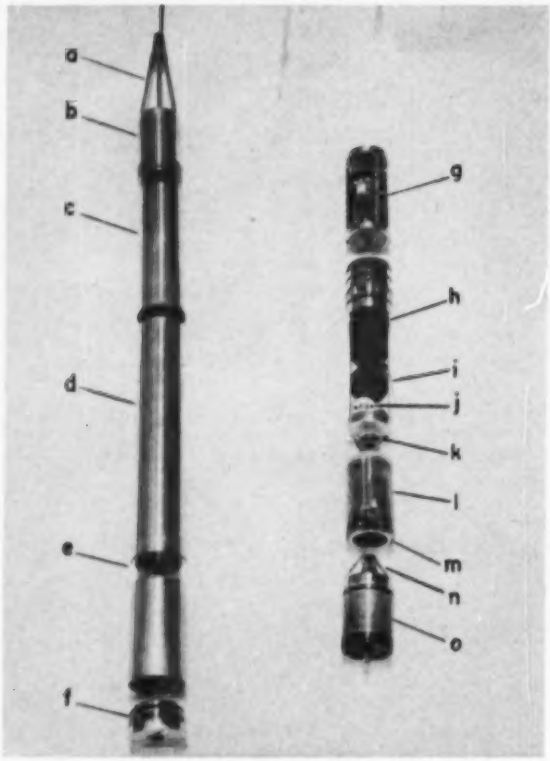


Fig. 2—A view of the NX borehole camera showing external elements of camera tubing on left, internal elements on right. (Tapering of lefthand figure is due to off-center position of photographer's camera.) Reference letters are covered in the text.

related to chemical alteration and underground erosion. Obviously, detailed information on their location, dimensions, and structure is important, as these factors can affect the stability of a dam and the security of life and property downstream. Their discovery and appraisal entail extensive subsurface exploration.

At present the most economical exploratory tool available to geologists and engineers is the small-diameter diamond core drill by means of which cores of the foundation bedrock are recovered for examination and testing. All too often, however, these samples fail to disclose minor foundation flaws that may be of major importance before a structure is completed. As a result, the small-diameter drillings are supplemented generally by more reliable but much more costly shafts, tunnels, or large-diameter calyx drill holes that permit the investigator to examine the foundation rocks in place. It was to reduce the number and cost of these expensive and time-consuming investigations, as well as to obtain more complete information on rock structure from the smaller borings, that the NX borehole camera was developed. That it has been eminently satisfactory in accomplishing that purpose is demonstrated by its success most recently at the Folsom Dam, under construction on the American River, 23 miles upstream from Sacramento, Calif. Here some seventeen 3-in. boreholes, drilled to penetrate a fault zone in the granite at depths of 50 to 75 ft below the foundation, were completely photographed in kodachrome.

In addition to locating and photographing the fault zone precisely, the pictures recorded delicate changes in rock coloring, fractures as small as 1/100 in., and the surface of the groundwater table. A compass, visible in each picture, permitted orientation of all these features on a unique cylindrical projection screen. Since the materials in the fault zone were too soft to be recovered completely by the small-diameter core drill, their investigation and the extent of the fault as a whole could be accomplished only by tunnels, shafts, and costly mansized calyx borings. The camera came to the rescue in time to eliminate the proposed calyx borings by producing faithful color-picture records of all 17 small-diameter holes. Previously the camera had been used successfully in locating cracks in the spillway of a high concrete dam and in photographing bedrock texture and structure in dam foundations in Virginia and Pennsylvania. Fig. 1 illustrates the relationship between plane and cylindrical images as taken with the borehole camera

Externally the camera unit, shown in Fig. 2, is a simple stainless-steel tube, length 31½ in. and diam 2¾ in., with a circular quartz window *(e)*, not unlike a miniature lighthouse window, located 5 in. above the lower end. Internally the principal elements include an oil-damped compass *(o)* which supports a hollow and truncated conical mirror *(n)*. The mirror is situated inside and directly opposite the quartz window and thus comprises the eye of the camera. The hollow and truncated construction of the conical mirror makes the underlying compass visible to the 15-mm camera lens *(k)* located a short distance above the mirror. A high-voltage circular flash tube *(m)*, midway between the cone mirror and camera lens and actuated by a current pulsing device on the camera lowering rig, simultaneously illuminates the boring and exposes the film to the bright mirror image. Directly above the lens is a conventional 16-mm motion picture camera *(h, i, j)*, with motor and spool drive synchronized by the same pulsing circuit which actuates the flash tube. A power condenser and relay unit *(g)* contacts the top of the camera unit. The camera is designed to make 16 flash exposures per ft of boring. Thus with a 1-in. section of drillhole exposed at each flash and with 16 exposures per ft of boring, sufficient overlap from picture to picture is obtained.

Suspending the camera from the ground control mechanism is a three-conductor cable, armored externally by reverse-lay preformed steel wire which prevents cable twisting. The tensile strength of this cable is 2700 lb.

Pictures are taken during the ascent or retrieving of the camera, in as much as cable tension is more constant and the motion of the camera steadier. A dummy camera of the same weight and dimensions is lowered and retrieved before the real camera is risked in the boring. Since the camera pulsing wheel is geared into the crank and gear-drive of the cable reel and guide reel, the time interval between picture exposures is controlled by the speed at which the hand crank is turned. Best results are obtained when the exposure interval is 2/3 sec. With a capacity for 25 ft of 16-mm film, 75 ft of boring may be photographed continuously before reloading is needed.

The camera is designed to withstand a hydrostatic head of 500 ft. Pictures obtained in dry and water-filled borings are equally good. When a film is completely exposed, the individual pictures are projected and studied as a series of separate still photoflash images and not as a moving picture film.

# Fundamentals of Mixing and Agitation

## With Applications to Extractive Metallurgy

by J. H. Rushton and L. H. Mahony

**Principles of fluid motion and turbulence which have been found to be of use in mixing and agitation problems are discussed, as well as suggested applications in extractive-metallurgy processes. Various types of impellers are described, together with other conditions that affect flow pattern and turbulence. The choice of equipment for particular requirements is considered, and equations for power input are given. Modern heavy-duty mixing and agitation equipment can take an increasingly important part in such extractive-metallurgy processes as solids handling, crystallizing and leaching, chemical operations, and flotation. Application of mixing and fluid-mechanics principles to extraction methods can lead to greater process rates and a resultant saving in time and money.**

MIXERS are being applied with increasing frequency to problems in the metallurgical industries. The increase represents in part the modernization of mechanical equipment used through the application of unitized drives, modern electric motors and speed reducers, and recently developed materials of construction. Some applications have resulted from process changes and the use of techniques for operations similar to those that have been demonstrated and proven in the chemical industry. Still more applications are being developed through the use of fluid-dynamics principles not previously recognized as applicable to these operations.

It is the purpose of this paper to describe those principles of fluid motion and turbulence which have been found to be of use in mixing and agitation problems, and to suggest applications for them in the extractive-metallurgy processes.

Modern mixing equipment has been designed to provide the fluid motion consistent with that best suited to different operations.[1] When properly applied, these more efficient fluid-handling mixers result in lower process-production costs.

Metallurgical operations usually involve large amounts of solids. The characteristics of the ore control the process and only enough liquid is added to provide sufficient fluidity for handling and processing. The reactive part of the ore, the mineral value to be extracted, is likely to be low in percentage, and the quantity of reagent required is similarly low, but excessive dilution makes additional reagent necessary and therefore is undesirable. Thus, the primary problems in minerals processing are to handle as high a concentration of solids as possible and to distribute reagents uniformly. These pulps, or slurries, are in a range of solids concentration where hindered settling rates apply, and care must be taken to agitate and mix sufficiently to maintain suspension and flow throughout the equipment. Such slurries have high densities which are the weighted average of the components and viscosities that are spoken of as "effective viscosities" but are difficult to evaluate.

It is convenient to separate metallurgical operations involving mixers and agitators into three categories: solids handling, mechanical or physical operations, and chemical operations. In each of these categories fluid motion is required to maintain suspension, to distribute surface-active agents, to blend components and reactants, and to induce high rates of chemical reaction. After a discussion of some basic principles of mixing and agitation, examples of application to the three categories will follow.

### Fluid Motion

The fundamental problems of mixing and agitation of liquids have to do with the mechanics of fluid streams and the means by which they are

J. H. RUSHTON is Professor of Chemical Engineering, Illinois Institute of Technology, Chicago, and L. H. MAHONY is associated with the Mixing Equipment Co., Inc., Rochester, N. Y.

Discussion on this paper, TP 3865D, may be sent, 2 copies, to AIME by Jan. 1, 1955. Manuscript, Feb. 10, 1954. New York Meeting, February 1954.



*The Transactions papers appearing in the Journal of Metals during 1954 will subsequently appear in AIME Transactions Volume 200, and may be permanently referenced to that volume.*

Fig. 1—Marine-type propeller with stabilizing fins.

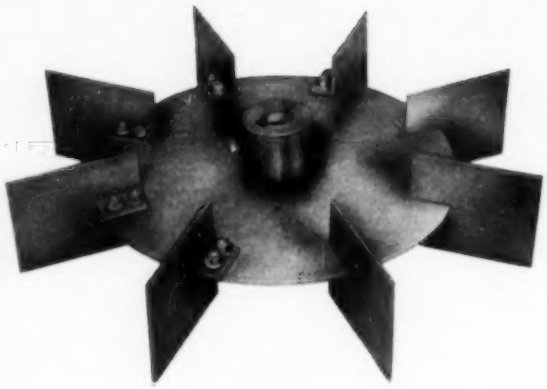

Fig. 2—Flat-blade turbine.

moved. Mixing is accomplished by material transfer through momentum transfer and turbulence. Agitation is the result of turbulent fluid motion. In most large-scale mixing operations, a rotating impeller is used to produce liquid flow. Turbulence may be generated in four ways: by the action of the impeller blade on the liquid; by the rubbing of liquid on the walls of the tank; by the passage of the liquid around an obstruction; or by high velocity streams moving adjacent to low velocity streams. This latter mechanism involves a flow-velocity discontinuity and plays the largest single role in the creation of turbulence and agitation by propeller and turbine-type mixers. The high velocity streams emerging from rotating-mixing impellers set up fluid shear stresses with adjacent slower moving fluid; and, when these stresses overcome viscosity, a disturbance is created, and eddy currents and agitation are initiated. Thus, whenever a fluid stream moves at relatively high velocity compared to the fluid around it, turbulence and agitation are produced and carried along with the flowing stream. Adjacent fluid is entrained in the stream by turbulence, and the pattern of agitation spreads along the path of flow.[1]

Most commercial liquid-agitation and mixing operations are carried out by rotating impellers. They move the fluid, and the flow path, velocity, and quantity of flow are dependent upon the shape and position of the impeller, the shape of the container and its fittings, and on the physical properties and boundary positions of the liquid. As a result of operating experience and compromise among the many practical and economic considerations, the best practice may be generalized as follows:

The mixing tank should be cylindrical with axis vertical, the bottom may be flat, dished out, or a shallow cone. Liquid depth equal to the tank diameter is good practice, but may be as deep as two diameters. In large tanks the liquid depth may be less, but good mixing cannot be obtained if the depth is too low. Square or rectangular tanks are to be avoided because it is often difficult to secure adequate fluid motion in the corners.

Mixing impellers used to produce flow and agitation are rotating impellers such as the marine-type propeller (Fig. 1), the turbine (Fig. 2), and the flat paddle (a flat rectangular solid plate with a hub at the middle for attaching to a rotating shaft). There are many variations in design from these common impellers. The answer to most agitation problems, however, it is not to be found in some unusual impeller form, but rather in the knowledge of the type of fluid flow and turbulence resulting from different impellers, fluids, and the containers, and of the flow pattern best suited to the particular agitation problem. Impellers are usually made to be about ¼ to ½ the tank diameter, and if only one is on a shaft, it is placed no more than one impeller diameter from

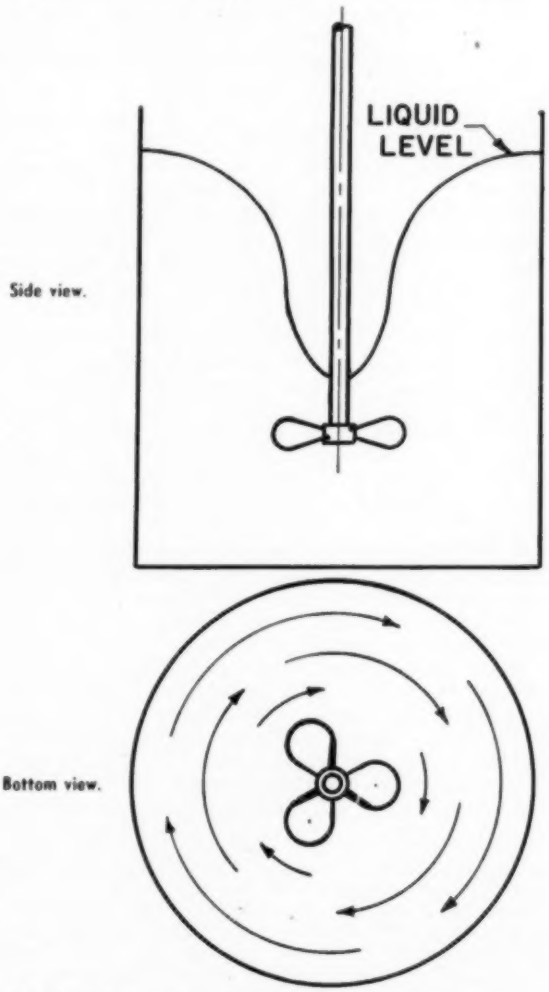


Fig. 3—Flow pattern for impeller of any shape without baffles.

the bottom. Two or more impellers on a shaft are placed at least one impeller diameter apart. Impellers are rarely placed closer than one diameter to the liquid surface unless gas is to be drawn in through the surface. Vertical shafts with impellers are placed on the center line of the tank and baffles are used at the tank walls or, sometimes, near the impeller. Occasionally a baffle is used across the bottom of the tank or horizontally across the liquid surface. Propellers are often used in an off-centered position (Figs. 6 and 7) without baffles, and the shaft may enter through the top of liquid or through the side wall. When rectangular tanks must be used, propellers are placed so as to promote flow in corners; they are placed in position as dictated by experience. When the solids' content is greater than 50 pct by weight, the impeller diameter is usually increased, but it depends in all instances on the operation to be carried out and its particular requirements.

### Flow Patterns for Mixing

The impeller causes fluid motion and generates, together with the wall, the principal lines of flow through the liquid. When a single impeller of any shape or size is rotated on the center line of a smooth-wall cylindrical tank, the flow motion which is set up is a rotary swirling or vortex motion, Fig. 3. The flow is circular and there is practically no vertical motion. The liquid moves as in a merry-go-round, and there is little chance for mixing because liquid is not forced sideways or vertically. If, however, there are obstructions on the wall of the tank or elswhere, different impellers will give either of two different principal types of flow patterns. The marine-type propeller produces axial flow: the flow leaves the impeller in the direction of the axis of rotation. The flow pattern is illustrated in Fig. 4. It should be noted that there are vertical and lateral-flow lines: liquid is moved up, down, and horizontally, providing good top-to-bottom turnover, and this motion is conducive to good mixing. Note that propellers are almost always operated to discharge downward, and, when two are used on one shaft, they both discharge downward.

When flat paddles or turbines are rotated with obstruction in the liquid, the liquid moves from the turbines in a plane perpendicular to the axis of rotation. Such motion has been called radial motion, and any impeller which generates this type of flow is classed as a radial-flow impeller. The flow pattern is shown in Fig. 5. Here, as in the case of the propeller with baffles, there are vertical and lateral flow currents resulting in motion conducive to good mixing. The liquid motion from the impeller, therefore, is dependent upon the impeller shape and also upon the obstructions present or the physical boundaries of the liquid. Ordinarily, the obstructions used to prevent rotary motion and swirl are baffles which are placed at or near the tank wall. Usually, baffles extend to 1/12 the tank diameter from the wall. They may extend vertically the full liquid depth or only part of the liquid depth. If some rotary motion and swirl is desired at the surface of the liquid, baffles can be used in the lower part of the liquid but cut off below the surface. This will result in some swirl and vortex around the shaft, a condition sometimes desired in cases where solids are to be introduced into the liquid, for, if the solids are hard to wet, they can be poured into the vortex. Sometimes it is desirable to separate heavy objects at the bottom of a tank by cutting off baffles at the bottom, thus allowing some rotary motion to be developed there.

Ordinarily, impeller shafts enter through the top surface of the liquid, centered, and baffles are used. However, propellers can be used to give axial flow, top-entering without baffles, or side-entering without baffles, in off-centered positions. Fig. 6 shows the off-centered position for a top-entering mixer (either portable or fixed) with the propeller turning counterclockwise looking down the shaft. In this case the shaft is to the left of the center line looking down the shaft and the angle of the shaft is approximately 15° from the vertical. The position is a very critical one and depends upon the tank diameter, liquid depth, and height of impeller above the tank bottom. The proper location can be found readily by moving the shaft to various angles and to the proper side of the tank until all swirl and vortex disappears from the top of the liquid. The discharge of liquid from the propeller is axial in direction. Sometimes this position is referred to as equivalent to the use of the baffles, since a propeller will only give axial flow when swirling motion is eliminated. Also, the power required by a propeller in the off-centered position is equal to that required when four baffles, each 1/12 of the tank diameter, are used at the tank wall.

Impellers are important items for mixing but they alone do not control flow motion. It should be em-

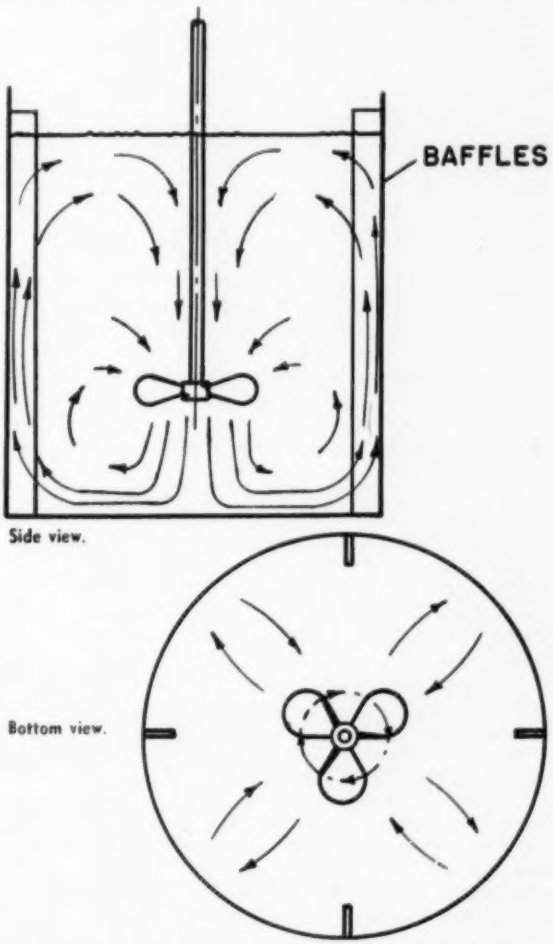


Fig. 4—Flow pattern for propeller with baffles at tank wall.

Table I. Data for Power Consumption of Mixing Impellers*

| | Values of K | |
|---|---|---|
| | Eq. 3, Viscous | Eq. 2, Turbulent |
| Propeller 3-blade, pitch = diam | 41.0 | 0.32 |
| Propeller 3-blade, pitch = 2 diam | 43.5 | 1.00 |
| Turbine, flat-blade (Fig. 2), 4 blades | 70.0 | 4.50 |
| Turbine, flat-blade, 6 blades | 71.0 | 6.30 |
| Turbine, flat-blade, 8 blades | 72.0 | 7.80 |
| Fan turbine, blades at 45°, 6 blades | 70.0 | 1.65 |
| Shrouded turbine, stator ring | 172.5 | 1.12 |
| Flat paddles, 2 blades (single paddle), $D/W = 4$ | 43.0 | 2.25 |
| Flat paddles, 2 blades, $D/W = 6$ | 36.5 | 1.60 |
| Flat paddles, 2 blades, $D/W = 8$ | 33.0 | 1.15 |
| Flat paddles, 4 blades, $D/W = 6$ | 49.0 | 2.75 |
| Flat paddles, 6 blades, $D/W = 6$ | 71.0 | 3.82 |

* In a cylindrical tank, four baffles each 1/12 tank diameter; impeller one diameter above flat bottom, liquid depth equal to tank diameter, impeller shaft vertical and at centerline of tank.

phasized that the configuration of the tank, the nature of the liquid, and the location of the impeller are just as important as tank fittings and impeller design in determining a flow pattern, and these factors all must be considered for proper mixing and agitation. Figs. 4 and 5 show the preferred use of tank fittings in mixing operations. The three common forms of mixing impellers—marine-type propellers, paddles, and various forms of turbines—usually will perform the work of impellers of any other shape within reasonable limits. There are modifications of these principal types, but they are only for specific purposes. For example, a "weed-free" propeller has a blade design different from that of the ordinary marine-type propeller. The flat paddles may be curved rather than straight, and this will allow them to start with less power in highly viscous liquids. Except for such considerations, there is little need to consider the many thousands of impeller designs that have been suggested for mixing. Unless the particular flow characteristics required by an operation cannot be obtained from one of the ordinary-type propellers, or turbines, it is not necessary to resort to improvised impeller design; and all small-scale laboratory chemical research and pilot-plant work should be done with commercial forms of impellers. Chemical reactions which are functions of fluid motion (mixing) can only be reproduced on a larger scale when the same form of impeller, container, and fittings is used for each size.

## Mixing Requirements for Processing

The first consideration for mixing in a process is the choice of the flow pattern best suited to the operation. If solids are to be suspended, vertical flow currents must be developed to oppose the settling velocity of the particles, as in Figs. 4, 5, and 6. Turbines and paddles are effective at low rotational speeds and are preferred for large tanks, since they permit the use of long shafts without submerged bottom bearings. If liquids are to be blended, large flow volumes are required and radial-flow impellers (Figs. 2 and 5) or low speed, side-entering propeller mixers (Fig. 7) would be applied.

The power requirements for mixing depend upon the flow pattern desired, the velocities of flow which must be obtained at particular parts of the liquid, and the turbulent energy required. The velocity of flow is dependent upon the quantity of material in motion and the area through which it moves. Thus, a large quantity of flow produced by a small-diameter propeller will result in high velocities over small areas. Such flow will produce high intensity turbulence, but the scale of the turbulence may be low. On the other hand, low velocities of flow may be produced by a large-quantity flow produced by a large-diameter impeller. Some mixing operations may be performed best by this type of flow, whereas others might require the high velocity types of flow. In general, simple blending operations can be performed by large-volume flows produced over large areas, whereas the formation of an emulsion usually requires large-volume flows through small areas, thereby producing the more intense fluid shear and agitation. Power, then, is applied by means of the rotating impeller to move the fluid as desired. When the desired flow rates, velocities, and power input are known, an impeller size and speed can be selected to achieve the desired result. The determination of size and speed require data on the flow and power characteristics of impellers.

Finally, the only accurate way to determine the mixing requirements in terms of flow pattern, fluid-flow quantity and velocity, and power to be applied is to acquire data from past experience, similar operations, or from small-scale pilot-plant experimentation. Only by so doing can the specifications be written for a properly sized mixer.

## Flow from Impellers

Data are available for the flow produced in baffled tanks (Figs. 4 to 6) by square-pitch three-blade

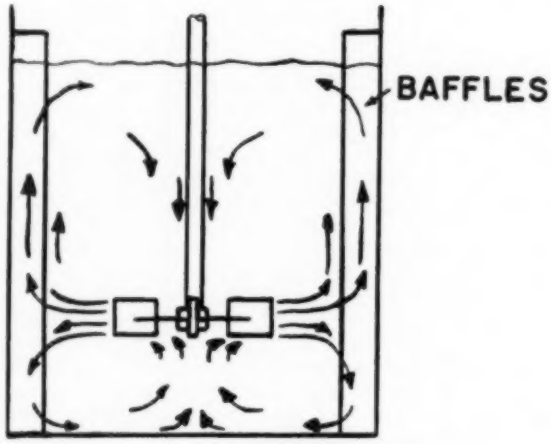


Side view.

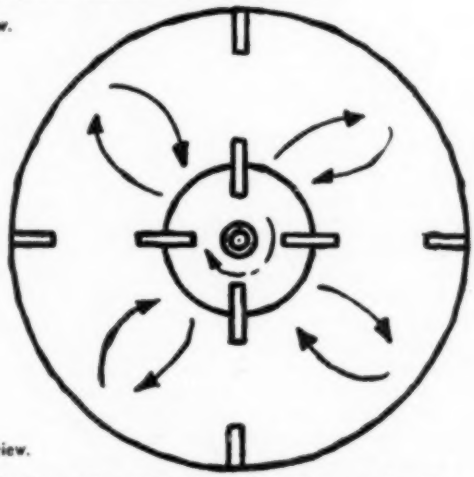

Bottom view.

Fig. 5—Flow pattern for turbine with baffles at tank wall.

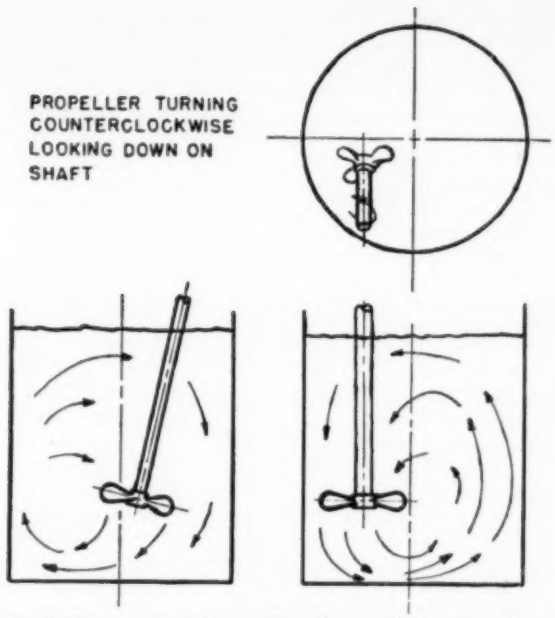


Fig. 6—Flow pattern with propeller off-centered in tank without baffles.

marine-type propellers manufactured by Mixing Equipment Co., Inc., and shown in Fig. 1.[3] Flow can be calculated for these propellers from

$$Q = K\,N\,D^3 \qquad [1]$$

where $Q$ is the flow in cu ft per sec, $N$ is rps, $D$ is the propeller diameter, ft, and the constant $K$ for water is 0.4. The equation shows that flow varies directly with impeller speed, and with the cube of the diameter. If propeller size is doubled and speed kept constant, the flow will be increased eight times.

Eq. 1 can be used for flow in baffled tanks from flat-blade turbines, and other-shape impellers by use of a proper value for the constant $K$. The value of $K$ for a turbine with six flat blades, like that shown in Fig. 2, is 0.5.

Eq. 1 is valid for different-sized impellers which are dimensionally similar. The value of $K$ is different for each type of impeller, and varies with the number of blades and position with respect to tank wall and bottom. For the propellers (Fig. 1) and turbines (Fig. 2), the values of $K$ are good over wide ranges of ratio of impeller to tank diameter ($D/T$) and can be used for ratios of $D/T$ up to 0.7.

### Power Required to Drive Impellers

The power required to drive a rotating impeller is a function of its shape, size ($D$), speed ($N$), and location, and of the fluid properties (density $\rho$ and viscosity $\mu$), and of the tank fittings and configuration.[4]

When the value of $(D^2N\rho/\mu)$, the Reynolds' number, is greater than 5000, and the liquid surface does not swirl in a vortex but has a flow as shown in Figs. 4 to 6, it can be safely assumed that the fluid motion is fully turbulent. For these conditions, power can be computed by

$$P = \frac{K}{g_c}\,\rho\,N^3\,D^5 \qquad [2]$$

where $P$ is power in ft-lb per sec, $g_c$ is the gravity constant, and $K$ is a constant (see Table I). The equation shows that for baffled conditions, if the speed of any impeller is doubled, the power required to turn it will be increased $(2)^3$, or eight times. Also, if a dimensionally similar impeller is twice the size of a smaller one, it will require $(2)^5$, or 32 times the power to rotate it at the same speed as the smaller one.

Values of $K$ for use in Eq. 2 are given in Table I for various impellers operating under standard baffled conditions; that is, four baffles, each extending into the tank 1/12 tank diameter at, or near, the wall or a properly off-centered propeller (Fig. 6) without baffles. Values of $K$ are lower for swirling conditions as shown in Fig. 3.[3]

Proximity of the impeller to tank bottom will change the value of $K$; in general, the closer the impeller is moved to the bottom, the lower will be the value of $K$, and of the power.

For viscous conditions, when the Reynolds number is less than 10,

$$P = \frac{K}{g_c}\,\mu\,N^2\,D^3 \qquad [3]$$

and the values of $K$ are given in Table I.

### Power, Flow, and Turbulence

Power information is not only essential for the proper sizing of large-scale equipment, but, for experimental and pilot-plant purposes, it is important for proper interpretation and evaluation of results. The performances of impellers to agitate and mix should be compared on the basis of equal power. For, if two impellers perform an operation equally well (rate, homogeneity, or other criteria are equivalent), then the impeller using the least amount of energy, or power, is to be preferred because it operates most efficiently. Thus, experimentation should be performed with standard shapes of impellers having well known characteristics as described above, so that the most effective size and speed may be used for a given agitation job.

To illustrate this point, consider an operation where it is desired to achieve the highest possible rate of reaction by using a rotating impeller. Fig. 8 illustrates three types of conditions which have been observed in application of mixing equipment. Reaction rate is plotted as a function of impeller size for dimensionally similar impellers in a given tank (ratio of $D/T$) for constant power demand of the impellers. Curve $A$ illustrates an action where the

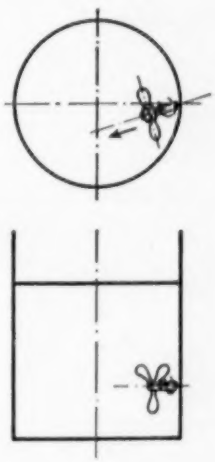

Fig. 7—Proper propeller position for propeller entering tank from side, turning clockwise.

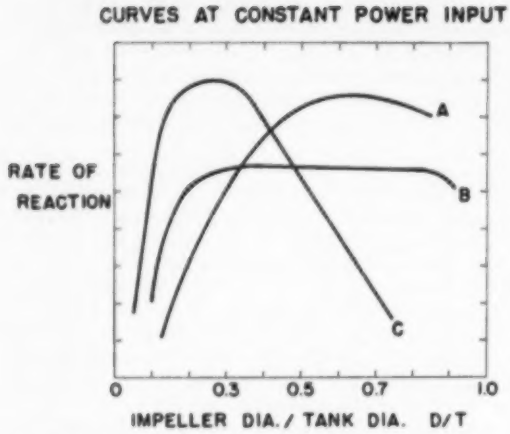


Fig. 8—Effect of impeller-tank diameter ratio at constant power input on three types of reactions.

rate of action increases up to a maximum as impeller size increases, after which the rate decreases with further increasing diameter. As diameter was increased, speed was decreased in order to maintain constant power (Eq. 2). Curve *B* shows another action where impeller size has little effect over a wide size range, and curve *C* shows the third type where a smaller impeller gives a larger rate than does the larger-size impeller at constant power.

It is clear that, if an operation is shown to be of type *A*, an impeller size of 60 pct of tank diameter will result in a much higher rate of action than a dimensionally similar impeller 25 pct of tank diameter, both operated at such speed as to impress the same power on the system. Many solid-suspension operations are of the type shown by curve *A*. On the other hand, some operations involving the dispersion of gas in a liquid behave like curve *C* where the impeller, sized 25 pct of tank diameter, is optimum and gives a much higher rate than the same shape impeller sized at 60 pct of tank diameter. Bench-scale and pilot-plant operations involving agitation and mixing should be designed to evaluate such trends.

The power imposed by an impeller results in flow against a total head

$$P = Q \rho H \qquad [4]$$

where $H$ is the total head in feet, and includes all static, pressure, velocity, and turbulent heads. Initial turbulence in a stream from an impeller is proportional to $H$; thus, the same amount of power can be applied to produce a large flow and small head (or turbulence), or a small flow with large head (or turbulence).[5] Curve *A* is typical of those operations most economically performed with large flow and relatively small turbulence. Curve *C* is typical of operations best performed by a large amount of turbulence and a relatively small quantity of flow.

Table II. Impeller Flow and Head Relations at Constant Power*

| Speed, Rpm | Diameter, $D$ | Volume, $Q$ | Head, $H$ | $Q/H$ |
|---|---|---|---|---|
| 1680 | 0.44 | 0.33 | 3.03 | 0.11 |
| 840 | 0.66 | 0.58 | 1.74 | 0.33 |
| 420 | 1.00 | 1.00 | 1.00 | 1.00 |
| 210 | 1.52 | 1.74 | 0.58 | 3.00 |
| 105 | 2.30 | 3.03 | 0.33 | 9.18 |

* Relative values based on a speed of 420 rpm.

Table II is illustrative of the relations between diameter, speed, flow, and head (or turbulence) for dimensionally similar impellers at constant power conditions with fully developed turbulence. For example, a propeller of some size operating at 420 rpm will produce one unit of flow at one unit of head. If a large impeller, 1.52 times the diameter of the first one, is operated, it must turn at 210 rpm to impress the same power. This will result in an increase in flow of 74 pct ($Q = 1.74$) and a decrease in head to 58 pct of that present with the smaller propeller. These relations can be derived from Eq. 2 resulting in

$$N_r = D_r^{-5/3} \qquad [5]$$

where the subscript $r$ indicates the ratio of large size to small size. These relations are the basis for the selection of proper mixing and agitation equipment and for scale up of experimental results to large-size equipment.[5] For, if it can be determined that an operation is best performed by large impellers rotating at low speed, then turbulence and agitation are less important than flow, and the proper size and speed impeller can be provided for whatever power input is desired. On the other hand, if a large amount of turbulence is shown to be necessary and relatively little flow is required, a smaller impeller running at high speed would be selected for the power desired.

To appreciate the magnitude of flow and power (Eqs. 1 and 2) for a marine-type propeller and for a flat-bladed turbine, the following figures are illustrative: a 6 in. propeller operated off-center (Fig. 6) or with standard baffles (Fig. 4) at a speed of 1120 rpm in water at 70°F will discharge 430 gal per min and will use 0.54 hp. If the speed is cut to half, then the flow will drop to 215 gal per min and the power to 0.07 hp. A 2 ft diam 6 flat-blade turbine running at 105 rpm in water will discharge 5150 gal per min and will require 3.82 hp. If a solid is suspended by this turbine so that the effective density is 95 lb per cu ft, then the power required by the impeller will be increased to 5.82 hp.

## Applications to Extractive Metallurgy

*Solids Handling:* It is common practice to convert solid materials into fluid masses by suspending the solids in water by means of mixers and then to pump the slurry at sufficient velocity to prevent settling of the solid particles. Slurries so formed can be used to advantage to control the feed of solids to continuous processes and to closed-pressure reactors.

Mixers may be used also to prepare a pulp of uniform concentration and particle-size distribution for feed to jigging tables or flotation cells where the capacity of the equipment may be increased by the improved uniformity.

The problems of impeller selection and location for the foregoing operations are of two types: those involving hindered settling and those involving free settling. The former are approached in terms of the size and type of mixer required to maintain a given slurry in a fluid condition and to keep the pulp in all parts of the tank in continuous motion, or, conversely, to determine the maximum concentration of solids that may be handled by an impeller which is known to be effective in this type of work. Operations with solid concentrations, such that free settling apply, are handled as "solid-suspension" problems, for which optimum $D/T$ ratios are known. The

preparation and maintenance of drilling mud for oil-well operations is a problem in this category, and within the past three years a large number of turbine-type and propeller mixers have been applied to this service.

*Mechanical and Physical Operations:* Blending of two or more ores is frequently necessary in order to obtain the desired composition for a refining or extraction process. While dry blending is possible, the handling of the material as a pulp often provides for better control of the system, assures a uniform blend, and eliminates troublesome dust problems. The addition of water in many cases is not a serious liability even though it is not required for subsequent processing steps. Wet grinding and feed of slurry to rotary kilns is common in the cement industry; it is done in a number of acidulating and roasting operations. Here again, the degree of uniformity of the feed provided by the mixer can improve the quality of the product and increase the through-put of the system.

*Flotation Applications:* Conditioning of the feed for flotation cells may be improved by the application of modern mixing equipment. The use of mixers of a type especially arranged to disperse the flotation agent most effectively and to contact the minerals to be wetted by the agent, materially reduce the power input required for a given result, or, by maintaining the same power input, increase the degree of contacting. A recent installation of turbine-type impellers in a relatively large conditioning cell proved operation to be as required at only one-half the power input used by the conventional impeller of a standard cell.

The problem in providing mixers for conditioning operations is twofold: the surface-active agents must be distributed quickly and uniformly, and there must be sufficient flow and turbulence to maintain solid suspension. Proper application of power by way of baffles, tank configuration, type of impeller to produce the optimum flow pattern, size, and position of the impeller, is necessary to obtain the necessary ratio of flow and turbulence. The previous discussion on effect of impeller size at constant power input (Fig. 8) is particularly applicable to wetting and flotation operations. It is becoming increasingly apparent that the effect of wetting and other surface-active agents is not alone one of specific activity, but the activity of many surface-active agents is a function of the uniformity of distribution on the finely divided solids and on the turbulence (or agitation) of the fluid surrounding the solids. When nonmiscible liquids are present in water, the turbulence will affect their drop size and distribution on solid surfaces. A study of the action of any wetting agent is incomplete if the effect of turbulence is not studied. Furthermore, as pointed out above, a mere increase in the size of a system will change the ratio of flow and turbulence for equal power input, hence unless this is taken into account, the activity of surface-active agents may well be markedly different for equal concentrations in a small test cell compared to a large commercial cell. This effect has been noted and evaluated to account for increased concentration of agents sometimes found necessary in larger systems. Work done to date indicates that further study of conditioning operations offers the possibility of appreciable improvement and cost reduction.

The flotation cell presents a similar problem. Here, however, the material to be dispersed is air, and contacting the wetted mineral values with it makes possible their flotation. Operation of a flotation cell is critical, however, because a layer of froth or foam is present. The mixing impeller must be so positioned that there is proper flow and turbulence necessary to disperse the gas, that the gas bubbles are contacted with the solid particles to form the foam and to allow the foam to separate from the more rapidly moving liquid beneath. The depth of the foam layer required for each operation will vary with the relative density, relative wettability, and particle size of the mineral, and upon the amount of classification desired in the foam layer. Studies of the effect of turbulence and flow and flow patterns by well known types of mixing impellers on flotation operations appear to offer attractive possibilities for substantial improvements. Enough bench-scale and plant tests have been made to give assurance of large potential improvements by the use of modern techniques of using mixing impellers.

*Crystallizing and Leaching:* In crystallizing operations throughout the chemical industry, mixers are employed to maintain uniformity of solution, maintain the solids in suspension in contact with the mother liquor, increase heat-transfer rates within the crystallizer, and to obtain a uniformity of crystal size in the product. These operations are primarily concerned with solid suspension, although the improvement of heat-transfer coefficient is not to be overlooked as a corollary advantage, since the improvement of heat-transfer rates will increase the equipment capacity by direct ratio. The potash industry depends largely on fractional solution and crystallization processes for the separation of sodium and potassium salts. Mixers are universally used to improve quality and increase through-put rates.

Leaching and dissolving are invariably done with mixing equipment designed to suspend or distribute the solids in the solvent and to increase mass transfer rates from solid to solution. Higher leaching rates and more complete removal of mineral values are obtained by applying the dynamic type of agitated system rather than with the type of leaching system in which only static contact is maintained between liquid and solid.

*Chemical Operations:* The chemical reactions of the metallurgical industry have been carried out for many years with equipment intended principally to "agitate" the solids or gases with the liquids. Only incidentally were flow patterns and turbulence produced which gave optimum use of energy. Rarely has an attempt been made to increase mass transfer rates, to dissolve, oxidize, or reduce the materials faster by applying known fluid-mechanics principles to reduce the resistance to mass transfer. Pachuca vats, air-lift agitators, and slow-moving rakes frequently can be replaced to advantage with mixers of known fluid-mechanics characteristics, resulting in increased process rates to the point where fewer reaction vessels may be required and large amounts of time and money can be saved. In general, the power input to a single reactor, using a mixer, will be considerably higher than that consumed by the equipment just mentioned, but the advantage and the opportunity lies in the increased production rate and quality control.

The efficiency of the extraction may be improved because of the more intense action, and more effective use may be made of the agents involved. Selective operations may be carried out wherein the major reaction may be controlled and completed,

and the less desirable or slower operation may be stopped before it has gone too far. Such a control is possible in the zinc, cadmium, arsenic, and antimony extraction system, to the extent that the zinc and cadmium may be extracted in appreciable quantities before the arsenic and antimony contents reach undesirable concentrations.

The dispersion of gases to bring about oxidations, reductions, ammoniations, or other reactions may be controlled by good mixer application. The dispersion of the gas and the increasing of the transfer rate from gaseous to liquid phase can be greatly improved by the proper use of mixers. This has the effect not only of raising the capacity of individual reactors, but also of increasing the degree of utilization of gas.

The foregoing discussion on chemical reaction and mass-transfer operations apply not only in general, but also in particular, to those recently developed processes in which high pressure operation is involved. When high pressures are required, the size of the reactor is limited by the tensile strength of the materials of construction. Therefore it is imperative that the individual reactor be as efficient as possible and the proper application of mixers can be used to advantage to accomplish this.

Mixers are also in regular use for the agitation of molten metals. Lead, zinc, magnesium, aluminum, and many eutectic alloys are mixed in their refining operations with the simple portable propeller mixers. Lead pots of as large as 50 ton capacity are mixed with heavier-duty equipment. The positive flow and agitation speeds the refining and alloying operations greatly and makes possible a quality control that has not been possible without their use. The resultant shorter operating time reduces the amount of oxidation and thus effects further savings.

*Mechanical Design:* A few notes about the mechanical design of modern mixing and agitating equipment are pertinent. Heavy-duty equipment is required in most metallurgical service because of the slurries of high solids concentration that must be handled, the dusty conditions, possible shock loads, and the necessity for continuous operation. The mixers must be capable of meeting momentary or short-time overloads due to higher-than-normal solids concentrations. Since the pulps are usually of abrasive character, the impellers, shafts, and baffles must be of resistant material and design, and easily and economically replaceable. It is most desirable that the units operate without the necessity of a steady bearing or other support bearings in the tank, thus requiring long overhung shafts on the mixer. Properly designed units can operate with such long shafts, and data are available on critical speeds of long overhung shafts carrying mixing impellers to enable accurate economical design.

Modern mixing equipment is designed to meet these conditions and to minimize maintenance costs.[1] Full advantage cannot be taken of the principles of fluid mechanics and mixing described earlier unless industrial mixing equipment is of sufficiently flexible design to allow for mixing changes as process requirements vary.

**References**


[1] R. D. Boutros: *Chemical Engineering Progress* (1952) **48**, p. 211.

[2] J. H. Rushton, E. W. Costich, and H. J. Everett: *Chemical Engineering Progress* (1950) **46**, Pt. I, p. 395, Pt. II, p. 467.

[3] J. H. Rushton and J. Y. Oldshue: *Chemical Engineering Progress* (1953) **49**, Pt. I, p. 161, Pt. II, p. 267.


---

**Technical Note**

# Effect of Subcritical Cooling Rate on the Brittle-Fracture Characteristics of Structural Steel


by L. Mair


A STUDY by J. R. Low, Jr.[1] on the effect of quench aging on the Charpy-impact specimens of semikilled 1020 steel disclosed that a decrease in cooling rate from 1275°F raised the transition temperature. This was demonstrated in his investigation by controlling the cooling rate of impact specimens to duplicate that of a heavier plate and comparing the properties with air-cooled specimens and quenched specimens. The transition temperature of the samples that had been cooled at a rate estimated to be similar to that of an air-cooled ¾ in. plate was approximately 45°F higher than the quenched samples. The transition temperature of the air-cooled series was between that of the slow-cooled and the quenched series.

On the basis of this work, it appeared that the cooling rate of plates after rolling in a hot mill would have a bearing on the brittle fracture of the


L. MAIR, Member AIME, is Research Metallurgist, Research & Development Dept., Inland Steel Co., East Chicago, Ind.



TN 224E. Manuscript, May 18, 1954.

## Table I. Tear-Test Results and Tensile Properties

| Check Analysis | | | | | Control-Cooling Temperature, °F | Tear-Test Transition Temperature, °F | Difference from Air-Cooled Sample, °F | Bhn | Yield No./In. | Tensile No./In. | Pct Elongation 8 In. | Pct Reduction of Area |
|---|---|---|---|---|---|---|---|---|---|---|---|---|
| Heat A | | | | | 1100 | + 95 | −20 | 140 | 33,150 | 65,400 | 27.0 | 55.4 |
| C | Mn | P | S | Si | 750 | +110 | − 5 | 140 | 33,700 | 64,600 | 29.8 | 50.7 |
| 0.29 | 0.49 | 0.008 | 0.039 | 0.02 | 400 | +110 | − 5 | 143 | — | — | — | — |
| | | | | | Air Cool | +115 | | 140 | 31,300 | 65,800 | 30.3 | 52.0 |
| Heat B | | | | | 1100 | + 90 | −10 | 131 | 35,250 | 63,800 | 28.3 | 57.0 |
| C | Mn | P | S | Si | 750 | + 85 | −15 | 134 | 34,550 | 63,200 | 31.3 | 56.3 |
| 0.28 | 0.45 | 0.010 | 0.038 | 0.02 | 400 | + 80 | −20 | 131 | 34,750 | 63,350 | 30.0 | 57.4 |
| | | | | | Air Cool | +100 | | 134 | 34,300 | 63,900 | 29.5 | 56.8 |
| Heat C | | | | | 900 | +105 | +10 | 128 | 32,350 | 61,600 | 30.0 | 56.7 |
| C | Mn | P | S | Si | 850 | +110 | +15 | 126 | 32,800 | 61,400 | 30.0 | 57.6 |
| 0.24 | 0.45 | 0.011 | 0.031 | 0.05 | 450 | +115 | +20 | 128 | 33,200 | 61,100 | 31.5 | 58.4 |
| | | | | | Air Cool | + 95 | | 128 | 32,850 | 62,000 | 28.0 | 57.3 |

steel. In general, the rate of drop from rolling temperatures is relatively fast because the plates are allowed to air cool to a low level. However, there are instances where plates are hot piled. Under this condition, cooling may be very slow. The mill layout is usually such that, in cases where pile cooling takes place, the temperature of the plates will be below 1200°F going into the lift, the range which may be critical as far as the brittle-fracture behavior is concerned.

Considering these various factors, it was deemed desirable to investigate the influence of cooling rate below 1200°F on the properties of structural steel. For this purpose an experiment was undertaken where samples of ¾ in. plate from three heats of structural steel were control cooled from the following temperatures: 1100°, 850°, and 450°F. This was accomplished by cutting three samples from the hot-rolled plate as it came off the mill and air cooling one sample to each of the three control-cooling temperatures. As the temperatures were reached, the samples were placed in individual boxes of Vermiculite and allowed to cool slowly for 24 hr. Cooling curves for the first four hours on samples placed in boxes at 850° and 450°F are shown in Fig. 1. After the 24 hr control-cooling period, the temperature of all of the samples had leveled off to approximately 125°F.

The evaluation of the brittle-fracture properties was based on the transition temperature of the Kahn tear test.[2] The testing was carried out in the prescribed manner with the sample being immersed in a controlled-temperature bath during testing. The testing temperature of the sample was assured by holding it at the testing level for 30 min prior to pulling. The transition temperatures were based on the point of 50 pct brittle fracture.

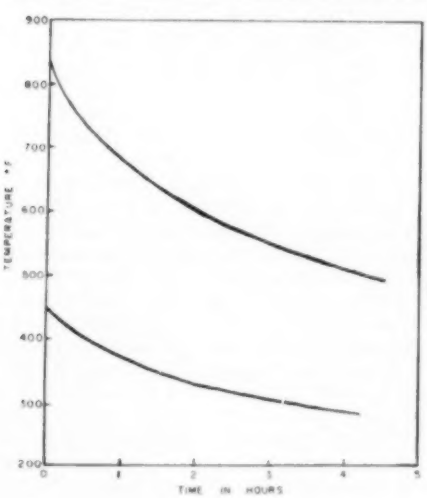


Fig. 1—Cooling curves for control-cooled plates, heat C.

The results of the tear tests and mechanical properties are shown in Table I. All of the tests were made in the longitudinal direction. A delay in cutting the samples from heat C resulted in the high temperature sample being placed in the box at 900°F rather than 1100°F as originally scheduled. The tear tests show a slight variation in transition temperature between the various controlled-cooling levels in the same heat. However, they are erratic and cannot be correlated with the treatment. No apparent change occurred in the mechanical properties as the result of the slow-cooling operation.

A microscopic examination was undertaken to determine if the cooling rates had an influence on the structure that may account for the variations in the transition temperatures. This revealed that all samples from the same heat, regardless of cooling rate, had a similar structure. Heat B, which ran 0.28 pct C, produced, on an overall average, the lowest transition temperature and had the finest grain. The remaining two heats exhibited a higher transition temperature and had a coarser grain with some indications of a Widmanstaetten structure. The difference in grain size between the heats probably resulted from finishing-temperature deviations.

The variations in cooling rate of structural steel plates between 1100° and 125°F as studied in this experiment did not affect the transition temperature of the Kahn tear test or the mechanical properties. Slow cooling from a temperature of 1100°F, the maximum used in the experiment, was an insufficient heat treatment to induce any changes in the steel that would affect the brittle-fracture behavior. This indicates that pile cooling of structural-steel plates below 1100°F is not detrimental to the brittle-fracture properties.

### Acknowledgments

The author wishes to express his appreciation to the Inland Steel Co. for permission to publish this data and to James W. Halley for his guidance.

[1] J. R. Low, Jr.: The Effect of Quench-Aging on the Notch Sensitivity of Steel. *Welding Research Supplement* (May 1952) V17, pp. 253S-256S.

[2] N. A. Kahn and E. A. Imbembo: A Method of Evaluating Transition from Shear to Cleavage Failure in Ship Plate and Its Correlation with Large-Scale Plate Tests. *Welding Journal* (April 1948) V27, pp. 169S-182S.

# Thoughts on Lead Blast-Furnace Smelting

## (With Discussion)

by L. B. Haney and R. J. Hopkins

**On the basis of limited experimental work conducted at the Port Pirie smelter, it would appear that, by increasing the specific surface of sinter, and possibly that of coke as well, a marked increase in the rate and degree of sinter reduction in the furnace shaft can be achieved. Fusion-point tests have shown that this increased reduction means a much higher sinter fusion point and narrower plastic zone, while the more efficient utilization of coke in the furnace is inherent in the intensification of reduction by the provision of a more reactive sinter surface. Investigations aimed at increasing the ability to operate the blast furnace with a higher lead tenor of sinter reducing fuel cost proportionately, and at eliminating the loss in reduction potential in coke entering the furnace, as shown by the presence of appreciable proportions of CO in the top gases, are reported. Several lines for future investigations that could result in improved smelting methods are proposed.**

A SOMEWHAT informal presentation of ideas on lead blast-furnace smelting will be given in this paper. These ideas have been developed during observations of furnace behavior at Port Pirie and earlier at Mt. Isa, and have been guided by the results of laboratory experiments at Port Pirie. The authors do not intend to propound any particularly new theories, but present their ideas as a basis for discussion which may help toward a better understanding and improved control of blast-furnace operation.

Performance variations of considerable magnitude occur from time to time at most lead blast-furnace plants. While Port Pirie is fortunate in having a very regular supply of high grade concentrates, it is no exception in this respect. Such irregularities are of considerable economic importance and they constitute a challenge to present-day metallurgists in their efforts to obtain an ever greater degree of control over furnace operation.

In operating as Port Pirie does with a relatively high lead charge, it has been recognized for a long time that shaft conditions are of the greatest importance. A practical, or engineering, attack on the problem of accretions consisted of changes in furnace design, e.g., by widening the shaft to 10 ft above the bottom row of tuyeres, and by the provision of curved ends and vertical walls.[1] That this attack has had a great measure of success is shown by the fact that barring down of these wide furnaces is rarely necessary, shaft conditions have greatly improved, and sensitivity to charge variations has been markedly reduced. These modifications, followed by some metallurgical changes (chiefly the incorporation of pig iron into the furnace charge in 1948), have brought furnace operation to a point where some variables which were previously masked can now be studied.

Accordingly, over different periods of time during the last five years, such variables as could be given numerical values have been recorded and subjected to statistical examination. The objectives of this work were: 1—to reveal the true importance of the different variables and 2—to show the proportion of total furnace variation which is unexplained and therefore referable to causes not measured at present, e.g., shaft accretions, sinter structure, coke structure, and others.

### Statistical Study of Variables

In this work factors relating to furnace speed and lead reduction have been examined: 1—slag com-

L. B. HANEY and R. J. HOPKINS, Member AIME, are Assistant Works Research Superintendent for Metallurgy and Works Research Superintendent, respectively, Broken Hill Associated Smelters Pty. Ltd., Port Pirie, South Australia.

Discussion on this paper, TP 3793D, may be sent, 2 copies, to AIME by Jan. 1, 1955. Manuscript, Jan. 14, 1954. New York Meeting, February 1954.

position ($SiO_2$, FeO + MnO, CaO, $Al_2O_3$, ZnO, and S),* 2—lead tenor of sinter, 3—percentage of coke on charge, 4—coke sizing (−5 +3 in., −3 +2 in., and −2 +¾ in.), 5—sinter-charge composition, and 6—lead fall during sintering.

* A typical Port Pirie slag composition is: 21.08 pct $SiO_2$, 26.72 pct FeO, 4.69 pct MnO, 14.52 pct CaO, 1.18 pct MgO, 6.55 pct $Al_2O_3$, 16.45 pct Zn, 1.8 pct S, and 1.32 pct Pb.

The first indications from the initial simple correlation survey were that coke sizing was of prime importance. Variations from an optimum of 45 pct of the total coke in the −5 +3 in. range adversely affected tuyere or shaft conditions. When this fraction was held at the optimum value, it was indicated also that as the −2 in. proportion increased, reduction improved.

In order to reveal something of the mutual influence of the different variables upon the effect of each other, multiple correlations were then made. Without going into the details of this work, beyond the scope of this paper, it can be stated that two factors were shown to have a strong influence on furnace performance: lime/silica ratio in the slag and lead fall during sintering.

At many plants the lime/silica ratio in slag has long been regarded as an important control factor. At Port Pirie, to some extent in the past, the desire to produce a high zinc slag has limited the range of permissible variation, and the effects of this factor have not been apparent.

The influence of lime in raising the softening point of sinter will be discussed later. Also, it can be mentioned that, from the current slag studies,[2] as the proportion of melilite components ($Ca_2$ *(R)* $Si_2O_7$ where *R* may be predominantly Zn and Fe) increases, the solvent power of the slag for ferrites increases, thus improving slag properties with regard to lead separation.[3]

In regard to the effect of lead fall during sintering on the subsequent behavior of the sinter in the blast furnace, it is considered that the improved furnace performance is not due solely to the fact that the sinter has a lower lead tenor. From the statistical studies there is evidence to support the view that the physical and chemical conditions which presumably favor roast reactions and bring about a high lead fall also yield a sinter which is more amenable to reduction in the blast furnace. Further laboratory examination of this feature is in progress.

As a whole, the statistical examination accounted for only about one-third of the total variation in furnace speed and reduction. It is unlikely that more than 50 pct of the variations could be accounted for by the application of statistical methods to normal plant records under even the most favorable conditions. Thus, at least half of the furnace variations are considered to be due to causes which escape evaluation at the present time.

In addition to the mathematical treatment of numerical data, operating observations have been recorded for the same time periods. Where only one furnace, of two or more operating, varied from normal, generally there was a practical reason that could be fairly readily assigned. However, when two furnaces similar in all respects produced slags assaying, for example, 0.9 to 1.1 pct lead steadily for a week, then together changed to 1.3 to 1.5 pct lead, and repeated this performance from time to time, it was necessary to examine the charge materials common to both furnaces to discover the reason for the shift.

At Port Pirie the furnace charge consists, for practical purposes, of sinter and coke. Therefore, attention has been concentrated on those properties of these materials which do not come within the scope of usual numerical evaluations.

## Coke Studies

From time to time a great deal of work has been carried out and reported on the properties of coke in relation to its performance in blast furnaces, mainly in the iron-smelting field. Recent observations at Port Pirie have been concerned principally with the lump-size factor, a regular supply of ore from one source ensuring a reasonable constancy of other properties.

It is generally recognized that coke must fulfill two distinct functions in the lead blast furnace. These functions are so radically different that the ability of one class of coke to satisfy both adequately may be questioned. 1—The liberation of heat energy should be concentrated at the tuyere zone. Therefore it is essential that the fuel to be burned there should persist to that zone in suitable size to ensure optimum permeability for deep and even blast penetration. It should burn predominantly to $CO_2$ to give maximum calorific intensity, resulting in hot slag of maximum fluidity. 2—The remaining portion of the coke must present a surface and reactivity that will result in the maintenance of suitable reducing conditions in the furnace shaft.

It is very important to absorb the heat energy leaving the tuyere zone in furnace gases as quickly as possible and to produce a high concentration of CO. The zone immediately above the tuyeres is the important region in this respect. The coke should be of such properties that the endothermic reduction of $CO_2$ to CO will proceed at maximum rate, rapidly bringing the temperature below the level at which the smelting column is plastic. Obviously, it is desirable that any plastic zone between solid and liquid charge should have the minimum vertical dimension and occur as near to the smelting zone as possible so that even permeability and maximum contact in the shaft between solid charge and rising gases is preserved. Failure to promote this endothermic reaction, with the consequent passage of high temperature gasses rich in $CO_2$ to the upper zones in the shaft, probably brings about more furnace instability than all other normal variables combined.*

* In reference to blast air volume, the Port Pirie furnaces are operated normally at constant pressure and variable volume. The normal volume of air used per large furnace, as recorded on the blast air meter, is 9,000 to 10,000 cu ft free air per min at about 32 oz pressure. The volume figure shown on the meter perhaps should be taken with a certain amount of latitude, since there are the usual variety of leaks at the tuyeres and other places before the air reaches the furnace. The Port Pirie operators have no means of accurately measuring the division of air between the upper and lower tuyeres. However, the air to the tuyeres is controlled so that the lower set are given all they will take, while the upper set are throttled back to a point that is sufficient to overcome back firing.

Results of the statistical work referred to earlier support the views expressed regarding the functions of coke. The minimum proportion of "tuyere coke" (+3 in. size) for satisfactory bottom conditions was clearly indicated; while, on the other hand, as the proportion of the −2 in. fraction increased over the range of 15 to 35 pct of the total weight of coke used, the available surface of coke for reaction in the shaft increased, top temperatures fell, and reduction improved.

As a result of these and earlier observations, an experimental coke-crushing and screening plant was installed, and coke was separated into two fractions:

Table I. Comparison of Analyses Before and After Crushing and Screening of Coke Became Standard Practice

| | 1948 | 1952 |
|---|---|---|
| Fixed carbon, pct of total charge weight | 8.0 | 7.4 |
| Pig iron, pct of total charge weight | 1.8 | 0.76 |
| $CO_2$, pct by volume in exit gases | 20.4 | 16.6 |
| CO, pct by volume in exit gases | 4.4 | 10.2 |
| Pct lead in slag | 1.52 | 1.2 |

−5 +3 in. and −3 +½ in. Each fraction was stored separately and charged to the furnaces in controlled proportions, a buffer stock of each size being maintained for normal adjustments.

This change (for some years now standard practice at Port Pirie) soon showed benefits in improved control of furnace conditions. Apart from the general improvement in furnace shaft conditions, one feature which characterized this period was the decrease in pig iron necessary to maintain a satisfactory lead tenor of slag. Also, the composition of furnace gases reflected the improved conditions. Typical figures obtained during a three-month period in 1948 and again for a similar period in 1952 (i.e., before and after crushing and screening of coke was standard practice) illustrate the change, Table I. Gas analyses quoted are of samples drawn from 3 ft below the charge surface.

As a further step in the control of coke sizing, the effect of increasing the proportion of −2 in. fraction while holding the +3 in. proportion constant has been examined during several test periods of about one-month duration each. The −2 in. proportion was increased by charging separately crushed and screened −2 in. +¾ in. coke to give a total −2 in. proportion of up to 45 pct of the fuel to the furnace. Although these tests were not carried to a conclusive stage, in each case improved reduction followed the increase in −2 in. fraction.

Structural limitations have delayed the incorporation of provisions for this adjustment in the coke-crushing and screening plant, but these will be provided as soon as possible.

## Sinter

The presence of 10.2 pct CO in furnace effleunt gas during the 1952 observations pointed strongly to the desirability of improving the opportunities for reaction between sinter and gases in the furnace shaft. Thus, the need for an investigation of sinter properties under shaft conditions was indicated.

*Fusibility Experiments:* As a first step, sinter fusibility was studied. A standard procedure was developed in which sinter samples were ground to −100 mesh (BSS), damped with water, and pressed into a tapered *V*-section groove filed in a block of steatite which had been dried at 100°C. After a few seconds, the steatite had absorbed the water and the triangular pyramid could then be pushed forward and out of the mold. After a further drying period, the pyramid could be handled into a muffle furnace for fusion-point determinations.

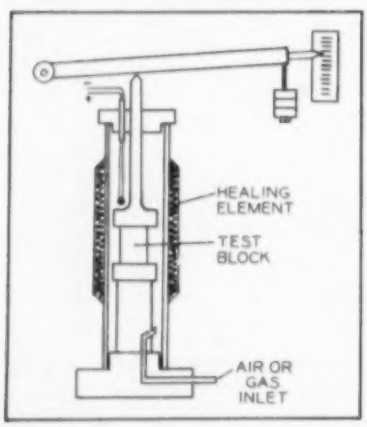


Fig. 1—Diagram of compression apparatus.

The pyramids were 3 in. long with base sides ⅝ in. high. They were set up on clay bases and treated like seger cones. It was found that, as long as care was taken to place the pyramids correctly in relation to the temperature zones in the muffle, reproducible softening and fusion-point results could be obtained. Temperature measurement was by chromel-alumel thermocouples brought in through the back of the muffle to a location in close proximity with the pyramids.

An initial contraction and deformation was recognized, usually in the temperature range 780° to 850°C, and was regarded as the softening point. This was followed, at temperatures of 150°C or higher, by the typical bending over of the pyramid as the fusion point was approached. The fusion point was taken as the temperature at which the upper part of the pyramid had reached a horizontal position.

In this work, the object was to compare the behavior of sinters of different types rather than to determine absolute fusion points. During the early stage of the work, several series of laboratory sinters were examined in which both lime/silica ratio and lead tenor had been varied. It was shown that, as the lime/silica ratio increased, the fusion point rose significantly, and also, as was expected, as the lead tenor rose, the fusion point fell.

These comparisons all were made under oxidizing conditions in the normal atmosphere. In order for the results to relate to behavior of the sinter when passing down the furnace shaft, it was necessary also for tests to be made under reducing conditions. The seger-cone method, carried out in a reducing atmosphere, indicated that fusion points were much higher than those measured in air, and some of the cones snapped before showing any sign of bending.

It appeared that a method of testing more nearly related to furnace shaft conditions would be that of measuring deformation under compression over a range of temperature in reducing conditions. Accordingly, the apparatus, a diagram of which is shown in Fig. 1, was set up and used for measuring the deformation of sinter cylinders 1 in. long and 0.8 in. diam. These cylinders were made by pressing dampened −100 mesh sinter at 3000 psi in a laboratory press.

The cylinders were held in an electric tube furnace, Fig. 1, between steel plates, and the desired load was applied to the top plate by a lever system. The movement of the lever, as the sinter specimen was compressed, was indicated by a pointer passing a scale. By raising the temperature of the tube furnace at a suitable rate, the softening point and the extent of the plastic range could be determined.

In Fig. 2, curve *A* shows the rate of deformation of a standard sinter cylinder in air, without prior reduction. Curve *B* relates to a sinter cylinder which previously had been reduced to 750°C in a 17 pct CO atmosphere until the rate of reaction fell to the point at which only 10 pct of the entering CO was being oxidized to $CO_2$. CO was then replaced by nitrogen,

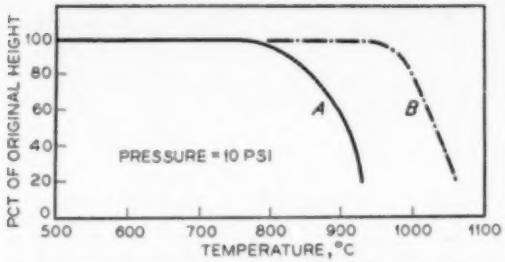


**Fig. 2—Sinter-compression tests, showing effect of gaseous reduction. *A* is unreduced sinter; *B*, reduced sinter.**

the furnace cooled to 300°C, a weight equivalent to a load of 10 psi was applied (as for curve *A*), and the deformation recorded. The rate of heating, as before, was held at a 5°C rise per min.

The progressive reduction of sinter passing downward in a blast-furnace shaft results in strengths intermediate between those depicted in Fig. 2, that is, unreduced and completely reduced sinter. In order to approach more closely actual blast-furnace-shaft conditions, changes in sinter strength with varying degrees of reduction were measured, with the results illustrated in Fig. 3.

Test specimens were heated to 850°C in air, 17 pct CO gas was passed for varying times indicated on the curves, nitrogen was then substituted for CO, and the weight applied.

The strengthening of sinter as reduction proceeds is clearly evident from the curves, and it may be inferred that the plastic condition within a furnace shaft can be related to the reduction characteristics of the sinter.

The progress of reduction will depend predominantly upon the available surface area of sinter. While control of coke size may improve CO concentration and temperature conditions, in the base of the furnace shaft it is necessary to provide suitable surface availability of the sinter in the upper part of the shaft to react with the CO and take full advantage of the benefits to be derived from the higher fusion point of sinter resulting from improved reduction.

It was clear from operating records that plant sinter was not always favorable for reaction with reducing gases and the considerations already given suggested a series of laboratory experiments aimed at studying the effect of various factors on the reaction between CO gas and sinter.

*Reduction Experiments:* Sinter samples were crushed and screened −3/16 +1/8 in. and contained in a silica tube so that passage of reducing gas (17 pct Co, 83 pct $N_2$) was uniform. The tube was heated to various temperatures and the degree of reduction taking place was recorded by $CO_2$ determinations on the tail gas.

Incoming gas from a reservoir, at a constant flow rate in all tests, was purified and tail gas passed through chromic-oxide solution for oxidation and absorption of $SO_2$ before $CO_2$ determination.

It was observed that at temperatures as low as 450°C some globules of lead appeared on the surfaces of the sinter granules and that from 650°C upward considerable activity was evident. When some sinter granules, after reduction for a period of time, were broken and examined, it was found that globules of reduced lead occupied the inner pores. When granules, after a reduction of 1 hr, were broken down in size and replaced in the reaction tube, there was renewed temporary activity, indicating the exposure of fresh surfaces previously unreduced, despite the deep penetration of reducing gas, as indicated by lead-prill formation.

Some differences in reduction rate were found to relate to changes in charge composition within the normal operating limits. These changes were small compared with the effects of some more radical changes, such as the inclusion of pyrite in the sinter charge. The use of pyrite has been suggested as a means of "puffing up" or extending the surface of sinter.

Reduction rates of normal sinter compared with those of sinter from charge containing 10 pct pyrite are shown in Fig. 4. In the latter the pyrite displaced hematite ore and part of the granulated slag while maintaining the lead level of both sinters at the same value.

The considerably higher reduction rates shown by the pyrite-bearing sinter are in line with the indications from practice at some overseas smelters where substantial furnace benefits are said to be derived from the use of pyrite in the sinter charge. Particularly noteworthy was the experience at Mt. Isa in the early years, where pyritic ore was specifically mined for its beneficial effect.[8]

The considerable improvement shown in these experiments, together with the increased activity shown by finely crushed and briquetted blocks used in sinter-compression tests, led to a study of the

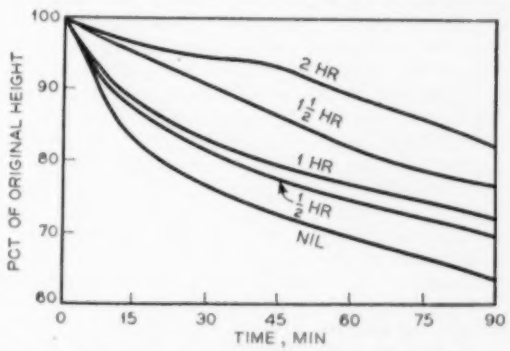


**Fig. 3—Sinter-compression tests after varying periods of reduction. Temperature is 850°C; pressure, 10 psi; and reducing gas, 17 pct Co, 83 pct $N_2$.**

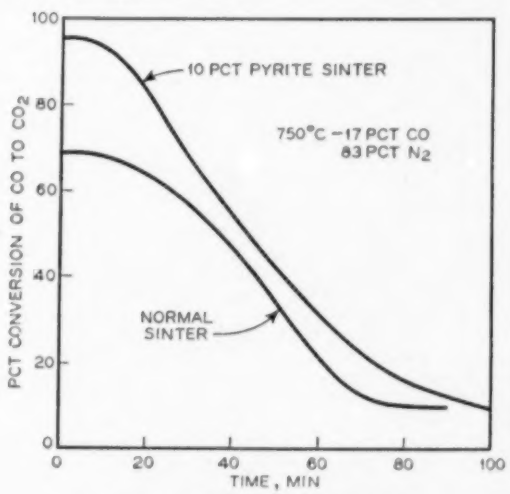


**Fig. 4—Effect of pyrite on sinter reduction.**

effect on reduction rates of increasing available sinter surface by fine crushing and briquetting.

*Effect of Sinter Surface:* The sinter samples remaining after separation of the −3/16 +1/8 in. portions (which comprised only a very small fraction of the total) were ground to −100 mesh, briquetted, and broken down to −3/16 +1/8 in. particles. These particles then were used for comparative reduction-rate tests with "solid" sinter particles.

The results obtained showed striking differences in reduction rates of briquetted and solid-sinter particles, as illustrated by the curves of Fig. 5. In this figure, curves *B* represent results from the briquetted particles and curves *A*, those from solid particles. It will be seen that an increase in the total sinter surface not only increased the rate of reaction with CO, but also markedly improved the overall degree of reduction under the fixed temperature conditions. It seems evident that, with solid sinter, a similar stage in the process of reduction can be reached only when the interiors of the sinter lumps are exposed by fusion.

Bearing in mind the results of sinter fusion-point tests referred to earlier in this paper, it appears that the solid, relatively unreduced sinter softens at a lower temperature and remains plastic over a wider temperature range than does the briquetted sinter with its extended surface and greater opportunity for reduction. This indicates that blast-furnace-shaft conditions can be influenced greatly by the surface exposure of sinter for gas-solid reactions.

Similar considerations presumably apply in the zinc-smelting industry where sinter is fritted rather than fused and where particle size and structure of the crushed sinter are important, particularly in briquetted charge for vertical retorts. Similarly, the iron smelters are evincing a growing interest in sintered charge with increased surface availability for blast furnaces. Perhaps the lead smelters, who, for a long time, have been accustomed to using a high proportion of sintered charge, should intensify their interest in sinter structure and particle size. Developments leading to a great increase in available specific surface area of sinter perhaps would bring about an important improvement in furnace capacity and efficiency.

In the experiments, results of which are given in Fig. 5, gas-solid contact times ranging from 0.5 sec

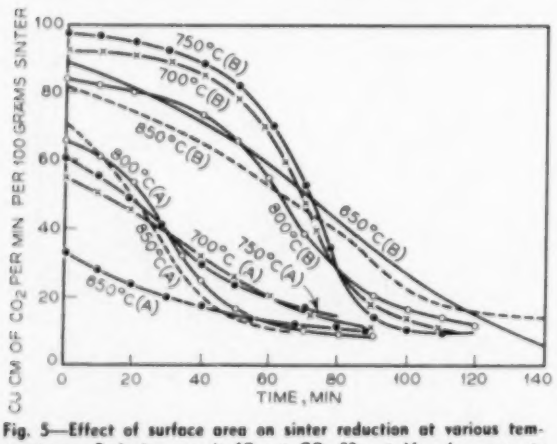


**Fig. 5—Effect of surface area on sinter reduction at various temperatures. Reducing gas is 17 pct CO, 83 pct $N_2$. *A* represents sinter granules −3/16+⅛ in. *B* represents sinter crushed −100 mesh, briquetted, then broken to granules −3/16+⅛ in.**

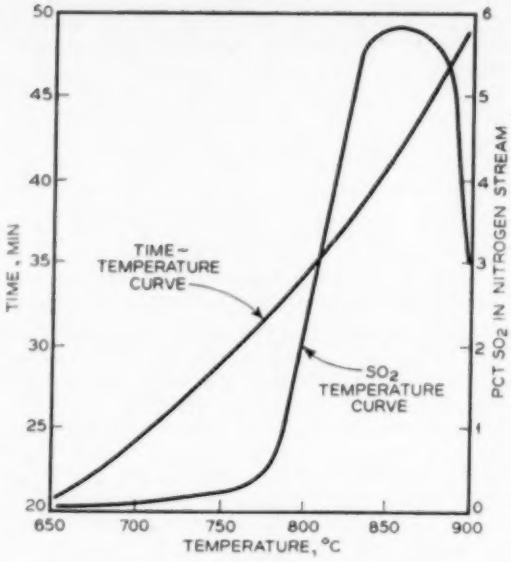


**Fig. 6—Variation in $SO_2$ evolution with temperature.**

at 850°C to 0.6 sec at 650°C were maintained, compared with an estimated time of 2 sec for gas passage through a Port Pirie blast furnace. Supplementary tests then were carried out in which sinter was moved progressively counter-current to the flow of reducing gas (17 pct CO, 83 pct $N_2$) which entered at 900°C and left the system at 600°C, with a gas-sinter contact time of 1.5 sec. Results showed that, when briquetted sinter was used, from 98 to 100 pct of the CO was oxidized to $CO_2$; while with solid-sinter granules only about 75 pct of the CO reacted.

Referring again to the curves in Fig. 5, it will be noticed that, at temperatures over 750°C, there is a decrease in reaction rates. This anomalous behavior was puzzling at first and led to further experimental work with the object of finding an explanation.

*Roast-Reaction Experiments:* In the earlier fusion-point tests, an initial deformation was observed at about 800°C and in some reduction tests, involving a progressive increase in temperature, similar decrease in activity occurred in the same temperature region. It was thought that roast reactions, resulting in the formation of metallic lead and $SO_2$ with possible "blanketing" of active surfaces, might proceed strongly at this temperature level. With this in mind, sinter samples were heated in a stream of nitrogen in a tube furnace as before, with a progressive increase in temperature, while $SO_2$ determinations were made on the effluent gas.

The results of these tests are plotted in Fig. 6 and show that a marked evolution of $SO_2$ begins at about 780°C, reaching a maximum in the region of 850°C, with a rapid decrease as temperature increased beyond that point. The sinter samples, when broken after the tests, showed much metallic lead.

These results clearly suggest that sinter activity is reduced by a decrease in available reactive surface area through incipient fusion and the presence of products of roast reactions. Therefore, it seems desirable to provide a maximum opportunity for contact between the sinter surface and reducing gas at temperatures approaching, but not exceeding, 800°C, and this calls for very steady blast-furnace-shaft conditions.

## Conclusion

Some lines of thought on factors affecting blast-furnace operation based on certain experimental results have been presented in this paper. The experimental work has been limited but, in as far as it has gone, it appears to show that, by increasing the specific surface of sinter, and possibly that of coke as well, a marked increase in the rate and degree of sinter reduction in the furnace shaft can be achieved.

Fusion tests have shown that this increased reduction means a much higher sinter fusion point and narrower plastic zone, while the more efficient utilization of coke in the furnace is inherent in the intensification of reduction by the provision of a more reactive sinter surface.

For a long time the lead-smelter metallurgist has been seriously reproached by the fact that high grade lead concentrates entering the smelter are invariably heavily diluted in producing sinter acceptable to the blast-furnace operator.

Everything possible should be done to control the sinter fusion point by taking advantage of reduction in the solid phase, since shaft conditions exercise a powerful influence on blast-furnace operation and economics, and since shaft conditions are, in themselves, closely related to charge fusibility. If this is done, possibly the most important benefit to be derived will be the ability to operate with a higher lead tenor of sinter and so reduce fuel cost proportionately.

Further, whenever appreciable proportions of CO are present in the gases leaving the top of the furnace, serious waste of coke occurs. Thus, in the instance mentioned earlier, when top gases contained 10 pct CO, about 25 pct of the reduction potential available in the coke entering the furnace was not used. If, by improved surface reactivity of charge, this loss can be avoided, not only will a fuel saving result, but the total gas volume would be reduced, giving generally cooler shaft conditions.

Finally, while great improvements may result from investigations into sintering methods in an attempt to give extended sinter surface without sacrificing other essential properties, would it not be worth while to study the possibilities of separate roasting of concentrates to give a strong gas and calcine which, mixed with necessary fluxes, would be briquetted to a size or sizes suitable for blast-furnace requirements?

Such a scheme would give complete control over the particle size of charge, other than coke, and would provide a maximum of reactive surface for reduction by CO gas. It is a direction in which there may be considerable opportunity for development of the lead-smelting practice of the future.


## Acknowledgment

The permission of the management of the Broken Hill Associated Smelters Pty. Ltd. to publish this paper is gratefully acknowledged.


## References


[1] L. A. White: The Development of the Lead Blast Furnace at Port Pirie, South Australia. *Trans.* AIME (1950) **188**, p. 1221; JOURNAL OF METALS (October 1950).

[2] A. B. Edwards: The Composition of Some Lead Blast Furnace Slags from Port Pirie. *Proc.* Australasian Institute of Mining and Metallurgy (1949) Nos. 154-155, pp. 41-68.

[3] F. A. Forward: Sintering and Smelting at Mt. Isa. *Proc.* Australasian Institute of Mining and Metallurgy (1933) No. 9, pp. 151-152.


*DISCUSSION, P. C. Fedderson and W. T. Isbell, Chairmen*

**G. L. Oldright** *(Salt Lake City, Utah)*—Doubtless for brevity, the authors have assumed that their readers would be intimately familiar with the Port Pirie plant and in particular with the development of the huge blast furnaces there. Some readers may find that it adds to both background and ease in following the paper to have before them earlier articles on the Port Pirie plant, especially the one by L. A. White.[1]

Of the combustion zones of the various types of lead blast furnaces examined by the Bureau of Mines, the Bunker Hill and Sullivan, with its rich lead charge containing a low percentage of coke so that considerable sulphur was removed as $SO_2$ from the charge, should resemble most closely the zones of the huge Port Pirie blast furnace.[4] However, in the absence of experimental data on the combustion conditions given by rows of tuyeres at two different elevations plus the use of coke that is either very coarse or quite fine, it is difficult to approximate the conditions of reduction at various horizontal planes across the shaft of the Port Pirie furnace. In smelting lead charges varying from the sulphides to an all-oxidized charge in the Scotch hearths with coal in sizes from dust to around ½ in. and using an excess of air blast,[5] there was still a distinct zonal arrangement of the combustion zones. The gases, however, in the interstices of the charge were largely $CO_2$, $SO_2$, O, and N, with only traces, if any, of CO. (The percentages of the lead volatilized and those finally liquated out as metal varied largely with the richness of the charge.)

The use of coarse and firm coke gives a zone of maximum temperature localized at the tuyere zone of the usual blast furnace, and thus this use aids uniformity of operation. Also, by furnishing a column of incandescent coke down through which fine streams of exceedingly fusible lead silicates can trickle, it is possible for the lead blast furnace to carry out its prime function of making clean slags to be discarded.

With the use of tuyeres at two elevations, the authors then raise the question of the optimum particle sizes (and presumably distribution) of reducer and of lead charge for the upper set of tuyeres; with the maximum temperature and accumulation of coke probably at the lower tuyeres, the lead charge there would be molten. The functions of each of the two sets of tuyeres would then seem to be different: at the upper tuyeres some residual sulphur is probably removed from the charge as $SO_2$, some iron-oxidized compounds are reduced, and the already sintered charge with its preformed slags starts to soften. At the lower tuyeres the more difficultly attacked lead compounds are reduced, the charge is completely fused, and the lead is largely liquated out.

That the sulphides are removed effectively would be judged from the negligible amount of time lost in barring the more deeply seated accretions, which are usually sulphides. Whether the lessened accretions at the top of the shaft are to be credited to the wider shaft or to other structural or operational changes is not obvious. By taking samples of the gases and, if possible, of the charge across the shaft of the operating furnace and by continuing experiments to determine the optimum nature of the charge and its relation to structural changes, it seems promising that still further improvements will be made to the notable ones already recorded. How rich a charge may be profitably smelted, however, may be governed by how concentratedly streams of molten lead may be run over coke at the bottom tuyeres without diminishing its reactive surface too greatly, as well as by the increase in plasticity and loss of permeability of richer charges at higher elevations in the shaft.

[4] *Reports of Investigations 3096.* United States Bureau of Mines.
[5] *Reports of Investigations 4591.* United States Bureau of Mines

# Applicability of Powder Metallurgy to Problems Of High Temperature Materials

## (With Discussion)

by G. M. Ault and G. C. Deutsch

**The paper reviews the efforts made to utilize powder metallurgy to solve problems encountered when using alloys at high temperatures. The following subjects are discussed: comparison of wrought and sintered super alloys, sintered aluminum powder, porous materials for transpiration cooling, molybdenum, and cermets.**

TODAY, powder-metallurgy techniques are becoming increasingly important, producing materials which at the present time cannot be made by any other method. Among these materials are high melting-point metals such as tantalum and tungsten, porous metals for filters and lubricant-containing bearings, electrical contacts and electrodes (i.e., tungsten-copper), cutting tools of the cemented carbides, and magnet alloys. In addition, the powder-metallurgy industry has grown because, through the application of its methods, shaped parts, such as gears, can be produced at tremendous rates with a low scrap loss in comparison with manufacture by casting or forging and machining.

In the past few years, by utilizing powder metallurgy, several approaches to the problem of high temperature materials have been investigated. In this paper the authors will review some of the studies on application of materials having properties above 1350°F. Since their experience lies in the aeronautical field, possible uses of powder-metallurgy techniques in the production of aircraft engines will be emphasized. A large portion of the work is classified, but such a restriction has not eliminated any field from discussion, although limiting the amount of detail it is possible to present.

The development of high temperature alloys from powders and porous metals for cooling will be discussed as well as research done on molybdenum and molybdenum alloys, cermets, and intermetallics. Some studies on the utilization of cermets will be considered along with special problems that have been revealed through these investigations. Special interest in certain factors of sintered aluminum powder (SAP) makes it desirable to discuss this material although its use temperature is below the 1350°F limitation set for this paper.

### High Temperature Alloys from Powders

In general, components made from powders for room-temperature application have been investigated with the primary purpose of taking advantage of the high production rates and economies made possible by powder metallurgy. From the standpoint of properties, the ojective of the powder metallurgist has been to obtain a product comparable to the cast or wrought product that is to be replaced.

Comparisons of the properties of alloys made by powder-metallurgy methods with those of similar compositions made by casting and forging are reported in the literature.[1-9] In many cases equivalent

G. M. AULT and G. C. DEUTSCH are associated with Lewis Flight Propulsion Laboratory, National Advisory Committee for Aeronautics, Cleveland.

Discussion on this paper, TP 3844E, may be sent, 2 copies, to AIME by Jan. 1, 1955. Manuscript, May 6, 1954. New York Meeting, February 1954.

strength properties have been achieved by powder metallurgy but usually with difficulty. For many applications, of course, strength equivalent to that of a wrought product is not required and the powder-metallurgy product is used because of manufacturing advantages. The point has been made[1] that, where equivalent properties have not been achieved by powder metallurgy, the weakness can be attributed mainly to the presence of pores. Experience has shown that pores can be eliminated best by forging after sintering or by hot pressing. In some cases it has been found to be beneficial to follow sintering or hot pressing by hot repressing. Forging of a powder-metallurgy product after sintering eliminates the manufacturing advantage of pressing to final shape to reduce machining costs. Thus, this is not too desirable if only equivalent properties are achieved.

Studies of the fabrication and properties of high temperature alloys produced by powder metallurgy have been reported.[2,3] In these studies, attempts have been made by the use of powder-metallurgy methods to obtain strengths equivalent to the normal cast strength of the cobalt-base alloy, X-40. Here it is essential to develop at least equivalent properties because for many high temperature applications the need is for better materials, not just equivalent ones. The data show that equivalent stress-rupture properties at 1500°F for rupture times out to at least 100 hr were obtained (Table I). This was accomplished through the development of a novel process called "hot coining" and through the use of fully alloyed powders.

Early in these studies it was found that satisfactory bodies could not be produced if elemental metal powders were used because the mechanism of solid diffusion of elements is so slow or so complicated as to preclude the preparation of successfully diffused alloys. With the development of alloy powders, the need for long sintering times at very high temperatures to cause homogenization of the alloy was eliminated and the powder-metallurgy problem resolved itself to that of making a dense body from homogeneous particles.

Table I. Comparison of Properties of X-40 Made by Hot Coining of Powders and by Casting

| | Hot Coined | Cast |
|---|---|---|
| **Room Temperature** | | |
| Tensile strength, psi | 162,500 | 101,000 |
| Elongation, pct | 23.5 | 11.0 |
| Reduction in area, pct | 18.6 | 14.0 |
| **1500°F** | | |
| Tensile strength, psi | 55,700 | 59,500 |
| Elongation, pct | 30.6 | 8.5 |
| Reduction in area, pct | 41.9 | 13.7 |
| Time for rupture at 28,000 psi, hr | 103 | 100 |
| Elongation, pct | 5 | 12 |

The steps in the hot-coining process are: 1—Cold pressing of the alloy powders to a density of about 70 pct to form a briquette; 2—Heating of the briquette in a protective atmosphere at a temperature somewhat above the normal forging temperature (this serves to provide some sinter bonds with, of course, some shrinkage and at the same time brings the alloy to the forging temperature); and 3—Forging or "coining." Here the porous briquette is forged to the final shape. This hot-forging operation serves to eliminate the voids.

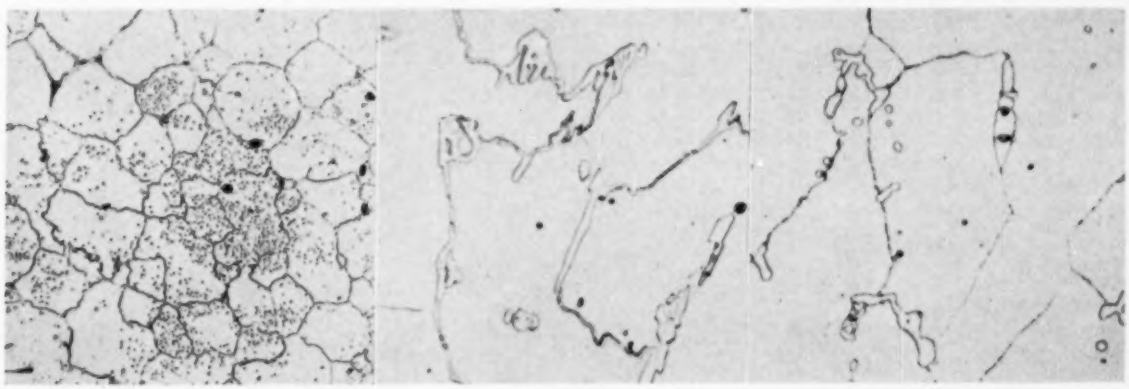

a—X-40, powder metallurgy (hot coined). b—X-40, cast. c—X-40, wrought.

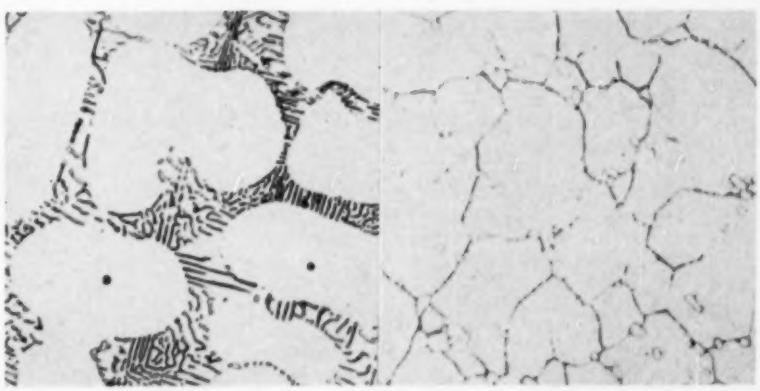

d—S-816, cast. e—S-816, wrought.

Fig. 1—Powder-metallurgy structure compared with microstructures of cast and wrought alloys. X500.

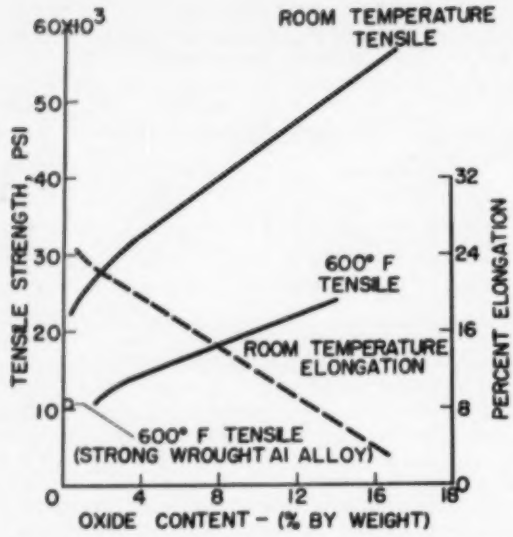


Fig. 2—Strength and ductility of sintered aluminum powder.

This process can result in densities fully equivalent to that of cast bodies of the same composition. When full densities are reached, good properties are obtained.

The fact that the 1500°F 100 hr stress-rupture strength is equivalent to that of the cast material might not have been expected in view of the pronounced differences in microstructure, Fig. 1. Here the microstructure in X-40 obtained by the powder-metallurgy process is compared with the microstructures of a typical cast and wrought X-40. (X-40 is not produced commercially in the wrought form and there is no typical structure.) Also shown is another cobalt-base alloy, S-816 (which is normally wrought), in both the cast and wrought forms. It is apparent that the structure of the X-40 alloy produced by the powder-metallurgy method is much more like a wrought structure (which it is) than a cast structure, since it has a much more finely dispersed carbide and much finer grain size than the cast product. However, it is known[4] that at room and elevated temperatures fatigue strengths of the wrought alloys as a group are superior to those of cast alloys. The fact that strengths in the best powder-metallurgy X-40 are equal to the cast suggests that this fatigue advantage might be gained while perhaps retaining much of the rupture strength of the cast. A comparison of the fatigue properties of the powder-metallurgy and cast materials would be of considerable interest.

In the wrought high temperature alloys of today, the amount of alloy additions that can be added for strength are limited by inability to break down the ingots because of segregations and other problems. The large segregations of the size that cause trouble in forging can be avoided through the use of prealloyed powders. These are obtained by freezing an atomized liquid stream, causing each powder particle to have the composition of the melt. Powder-metallurgy processes similar to the "hot coining" just described may permit alloys with greater strengthening additions to be forged into shapes such as turbine blades, giving the powder-metallurgy product a distinct strength advantage over the wrought.

### Sintered Aluminum Powder

Still another advantage which may be achieved through the use of powder alloys is illustrated by the example of "sintered aluminum powder" or SAP. The interest of powder metallurgists has been aroused by this development. The reason for the interest is that the sintered alloy promises to extend the maximum use temperature of aluminum by several hundred degrees.

The sintered aluminum alloy was made originally in Switzerland from extremely fine flake powder which was hot extruded. More recent work in this country[5] using atomized as well as flake particles has indicated that the remarkable strength of the alloy is primarily a function of the oxide content of the alloy. It has been hypothesized that during the hot working aluminum particles which have a thin oxide coating are plastically deformed, thus breaking their oxide films and permitting the aluminum particles to weld together. The strength properties are attributed to the entrapped and very finely dispersed oxide particles. Fig. 2 shows the strength and ductility of the wrought sintered aluminum powder plotted against oxide content at both room temperature and 600°F. For purposes of comparison, the strength of one of the best conventional wrought high temperature aluminum alloys has been included in Fig. 2. It is interesting to note that the strength increases almost linearly with increasing oxide content at both temperatures.

In the literature[6] it is noted that, as the oxide content increases, the distance between oxide particles tends to decrease, and this at least partly may account for the strengthening.

Increase in strength is accompanied by loss in ductility, and the choice of a composition would be a compromise of these properties. At 600°F, the wrought sintered alloys are much stronger than the cast and wrought alloys. This is particularly noteworthy, since the sintered product does not contain the conventional alloying elements.

Fig. 3[5] shows the stress-rupture properties at 900°F, a temperature generally considered to be above the useful temperatures for aluminum alloys. Again a strong wrought alloy has been included for purposes of comparison. The linearity of the curves for the wrought sintered aluminum indicates structural stability. The wrought sintered aluminum is superior at 900°F to the cast and wrought alloy at 600°F.

The method of accomplishing the improvement in high temperature strength of aluminum by dispersion of stable particles holds promise of similar accomplishment in other alloy systems. Similar improvements in platinum and particularly in tungsten have been noted. In tungsten this improvement has been achieved by the addition of thoria or by the additions of other materials containing aluminum or silicon.[7] It has been reported[7] that the General Electric Co. of England has achieved encouraging high temperature strength and creep properties in the cobalt-base alloy vitallium, by addition of thoria or other similar materials during fabrication by powder metallurgy. It would appear that powder metallurgists should exploit this phemonenon and apply it to other alloy systems.

### Porous Materials

Increase in gas temperatures for the turbojet engine will result in increased thrust.[8] There are several methods by which engine materials may be

made to sustain the increased temperature of operation. The most obvious, and also perhaps the most difficult to achieve, is through the use of more refractory or temperature-resistant materials throughout the engine. This approach will be discussed in greater detail in another section of this paper. Another way is through the use of cooled components. Because the most critical component in the engine is the turbine blade, most of the research effort for devising a cooling method has been concentrated here. Some of the designs that have been considered for cooled turbine blades are compared in Fig. 4.[9] The cooling methods fall into two categories: 1—Represented by the hollow and the finned blades, cooling is accomplished by conduction through the material; and 2—represented by porous or slotted material, cooling is accomplished primarily by providing an insulating or protective film of coolant. The use of porous blades is by far the most effective method of cooling to achieve a high temperature. For gas temperatures in the range of 2500° to 3000°F, this method has been estimated to require one-third to one-half the flow of the best of the more conventional cooling methods.

The use of a porous material for cooling is known as "transpiration" or sweat cooling. It should be emphasized that the cooling is achieved by the formation of a protective layer of coolant on the surface exposed to high temperature as well as through the cooling effect of the fluid on the porous metal. In transpiration cooling, there exists only a very slight drop in temperature across the porous plate, and the process is affected only very slightly by the thermal conductivity of the material.

In 1948[10] initial studies of materials for sweat-cooled components utilized liquids as the cooling media. This appeared very desirable because advantage could be taken of the cooling effects of vaporizing liquids (i.e., the heat of vaporization). The use of liquids is still desirable for stationary power plants and rocket motors where the fuel may be used as a coolant. Plugging of the pores by the coolant, however, is a serious problem. Primary sources of plugging are particles in the coolant, reactions with the coolant (particularly oxidation), and gases that are released with the coolant.

While some of these problems also exist when air is used as a coolant, they are minimized and can generally be handled either by material selection in the case of plugging by oxidation products, or by filtering in the case of plugging by particles in the gas stream. Another advantage of air cooling is that air is readily available at the pressures required. There is, however, a reduction in engine performance, since air that is normally burned to achieve

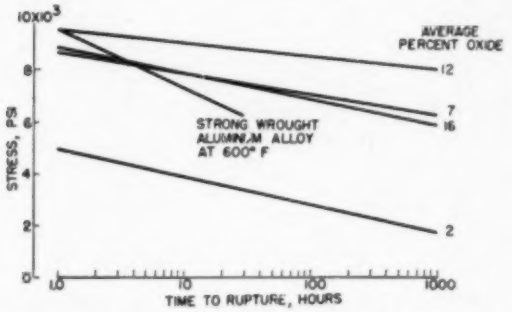


Fig. 3—Stress-rupture strength of sintered aluminum powder at 900°F, Gregory and Grant.[9]

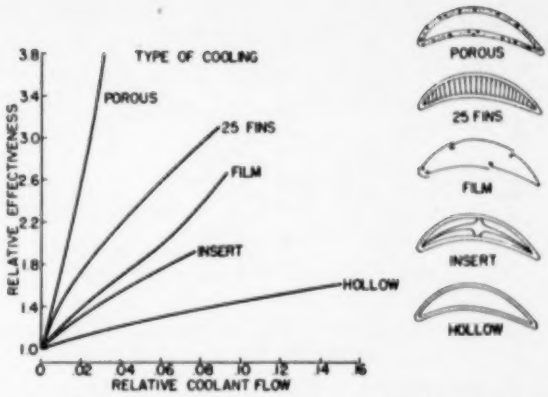


Fig. 4—Comparison of various types of air cooling for gas-turbine blades made of S-816.

thrust must be diverted to cool the blades. Although this disadvantage is avoided in the case of liquid cooling, the required weight of coolant that must be carried by the airplane may be prohibitive.[11]

The requirements for a porous component are: 1—chemical inertness, particularly with respect to the coolant, 2—adequate strength, and 3—the ability to permit passage of the required amount of coolant. The latter is defined as permeability, and materials are compared on the basis of a permeability coefficient. This permeability coefficient is a proportionality constant in Darcy's law[12] for laminar flow and requires special equipment for its determination. In the very early phases of the development of porous materials, it was customary to use the more readily determined density as a criterion for the ability of a porous material to pass coolant. For any one processing technique using a particular size and type of powder, a relation can be established between permeability and density. Subsequently the metallurgist can use changes in density as a measure of changes in permeability, and he can control permeability in much the same manner as density. If, however, the processing procedure is altered, for example, by a change in particle shape, then a new relation between density and permeability must be established.

It is difficult to discuss the strength requirements for materials for transpiration cooling because the critical values are interrelated with conditions of use. The strength must be such as to yield a reasonable life at temperatures of at least 900° to 1100°F when the thickness is reduced to yield the desired permeability. As a very rough approximation of the requirement, however, it appears that, at the proposed use temperature, the materials should have tensile strengths of from 20,000 to 25,000 psi and ductilities in excess of 2 pct. A typical variation in strength and ductility with density is given in ref. 13.

For actual turbine-blade use, of course, the stress-rupture strengths are of greater interest than the tensile strengths and values in the neighborhood of 500 hr of life at 900°F with a stress of 19,000 psi have been reported[14] for stainless steel with a permeability of interest.

It is a little unfair to discuss strengths at this point in the development of porous materials because thus far work has concentrated on the difficult production problem without too much consideration of the resultant strengths. It has been pretty generally felt that, if the production problems could be

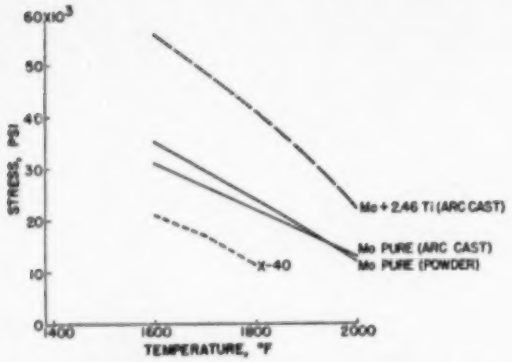


Fig. 5—Comparison of strengths of arc-cast and powder-metallurgy molybdenum. Stress for rupture in 100 hr.

resolved, then high strength heat-resistant materials could be produced by using heat-resistant alloys as starting materials. One such alloy that has been considered is X-40.[15]

The methods for the production of porous materials fall into four categories:[16] 1—sintering of loose powders, 2—sintering of loose powders having a wide range between the solidus and liquidus temperatures so that sintering is accomplished in the presence of a liquid phase, 3—sintering of compacted powders, and 4—sintering of compacted powders with a pore former.

The compacting operations may be conventional pressing or extrusion. After sintering, the product may be coined, rolled, and machined. In these finishing operations, the permeability can be reduced to desired values, although in some cases reduction of permeability has proved to be a problem. A surface etch to recover the permeability has been lost and in at least one case the closing of the pores during machining was avoided by impregnating the sintered compact with a soluble salt prior to machining.[17]

There are two principal problems in the fabrication of porous blades. One of these is that current procedures do not yield reproducible permeabilities from blade to blade. Secondly, if a blade is to be uniformly cooled, it should have a gradation in permeability which conforms to the changes in pressure in the blade external environment. Some progress has been made in eliminating (by design) the need for this gradation, but a blade having a controlled variation in porosity is much desired.

While porous materials appear to be promising from a standpoint of cooling effectiveness, it should be noted that they are in the early stages of development, and as yet there has been insufficient service-type experience to indicate all the problems which may be encountered. Also, recently, there have been developments with porous materials made from wire cloth or screen rather than by powder-metallurgical methods. These also are promising and at present appear to be competitive.

### Molybdenum and Molybdenum Alloys

Powder metallurgy has always found important application in making useful forms of metals, such as tungsten, tantalum, columbium, and molybdenum, that melt at extremely high temperatures. Of these, molybdenum is most promising for structural applications at high temperature because of its properties and availability. Early evaluations of molybdenum for elevated-temperature applications were based on the powder-metallurgy product, but, with the development of the arc-cast process for the melting of molybdenum and molybdenum alloys in vacuum or in atmosphere, an excellent competitive product has appeared. Fig. 5 shows a comparison of the wrought arc-cast and a good wrought powder-metallurgy product[18] on the basis of stress for rupture in 100 hr at 1600°, 1800°, and 2000°F.

It is difficult to make these comparisons because the strength of molybdenum is sensitive to amounts of stress relieving and recrystallization after working and it is not known if the metals are in comparable condition. It is apparent, however, that the powder-metallurgy product can be equivalent to the arc-cast material, at least on the basis of stress-rupture strength. Many alloys of molybdenum[19] that have been investigated using the arc-cast process are, however, far superior to the pure material on the basis of stress-rupture strength, as indicated by the data included on this figure for a molybdenum alloy containing 2.46 pct Ti. All of these molybdenum materials are far superior to the better cast

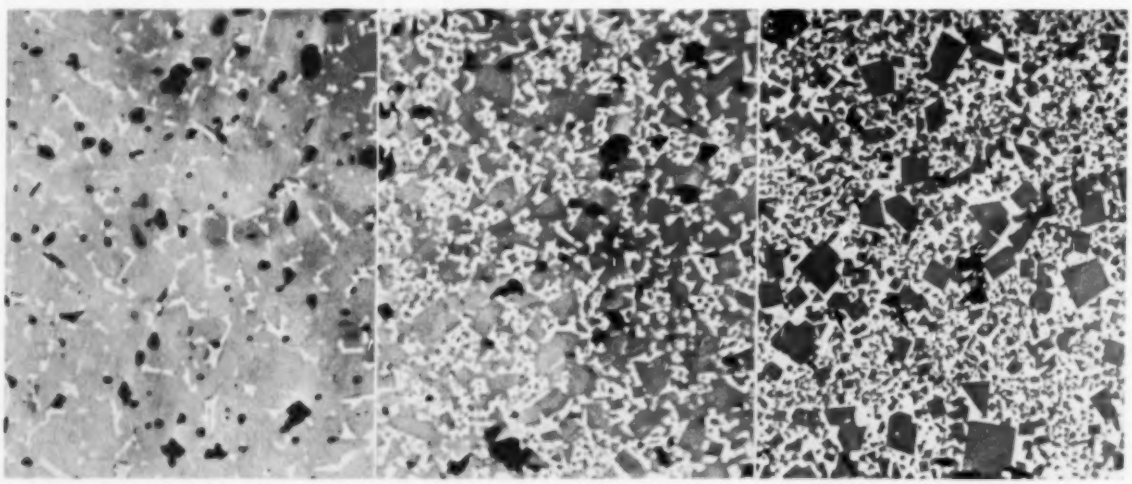

a—Percentage of metal by weight, 10; by volume (approximately), 5.8.

b—Percentage of metal by weight, 30; by volume (approximately), 19.2.

c—Percentage of metal by weight, 50; by volume (approximately), 35.6.

Fig. 6—Titanium carbide-base cermets with various metal contents. X1000. Area reduced approximately 60 pct for reproduction.

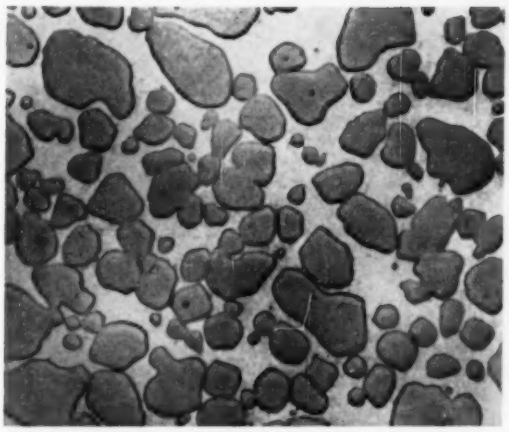

Fig. 7—Titanium carbide with nickel alloy. X1000. Area reduced approximately 55 pct for reproduction.

commercial super alloys represented by the data for X-40 also shown on the figure. Molybdenum and its alloys have not been widely used for structural components to date because they lack the resistance to oxidation required in most applications. Neither alloy additions nor coatings have been completely satisfactory for highly stressed structural parts, although coated pieces are being used for electric heating elements, nozzles and jets for burners, and thermocouple-protection tubes. An excellent summary of molybdenum data recently has been published.[25]

## Cermets

In the consideration of materials other than molybdenum alloys that might be superior to the "super alloys" of cobalt and nickel base for high temperature applications, it was natural to turn first to the ceramics, the oxides and silicates. In early studies, it was found that these materials generally were very strong and had low density, but were extremely brittle and generally had poor resistance to thermal shock.[25] It was proposed that what was required was a mixture of a ceramic and a metal to achieve a combination of the good properties of the two, thus giving a material having high strength at high temperature plus enough ductility or, in some cases thermal conductivity from the metal, to provide improved resistance to thermal shock. Much experience was available with such materials in the cemented-carbide tool industry where the high hardness and toughness of materials such as WC plus Co were well recognized. A producer of carbide tools was contacted by members of the research staff at the NACA and studies of the properties of a cemented carbide at elevated temperature were initiated. The first studies were on compositions of titanium carbide with cobalt. Titanium carbide was chosen in preference to tungsten carbide because of superior oxidation resistance and lower density. Cobalt was chosen because of the backlog of experience with additions of this element. Many other metal and alloy additions to titanium carbide have been investigated since, as well as metal additions to other carbides, oxides, nitrides, silicides, and borides. A listing of some of the typical compositions that have been studied are shown in Table II. It is apparent that these materials are receiving considerable attention.

Because these so-called ceramic-metal mixtures represented a new class of materials for structural

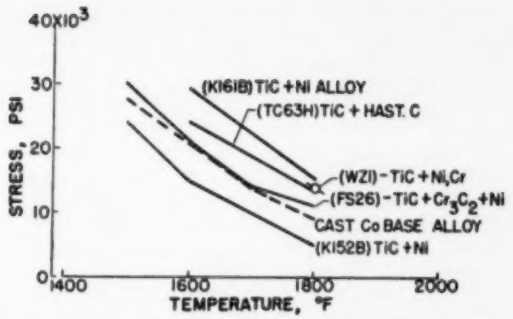


Fig. 8—Strength of titanium carbide cermets. Stress for rupture in 100 hr.

application at high temperature, many names were coined for them, i.e., "ceramals" and "cermets." It is felt that these names which combined parts of the words "metal" and "ceramic" were coined to represent a combination in properties; that is, to describe a body having a structure made up of a brittle phase and a more ductile metal phase, either continuous or discontinuous. In this light, many new materials that have been produced are not quite "cermets" even though the body has been produced by the sintering of a metal with a brittle phase. The resultant structure may be a combination of intermetallics instead of a structure with a metal or solid-solution alloy phase. An example is the addition of a metal to $MoSi_2$. Because of reactions during sintering, the final result is usually a mixture of complex silicides. In such cases major improvements in thermal shock or reduction in brittleness are not obtained, although unusual strength properties can result. Perhaps the materials that most nearly meet this definition of "cermet" are the previously mentioned titanium carbide with various metal and alloy additions. Typical structures are shown in Fig. 6. These are cold-pressed and sintered structures of titanium carbide with 10, 30, and 50 wt pct Ni. It is apparent that as the amount of metal increases, the metal phase becomes more continuous and thicker and it might be expected that more of the metallic properties would be obtained. A structure having even more isolated carbide particles in a metal-alloy matrix is shown in Fig. 7. Actually these combined structures are probably stronger at moderate temperatures than is either TiC or Ni alone.

J. T. Norton has defined[26] what he felt was the ideal structure of these cermets. He said that regular polyhedra surrounded by thin restrained films of metal were desirable. In this structure he felt that the metal would have an optimum thickness

Table II. Representative Cermets Under Investigation

| Class | Ceramic | Metal Addition |
|---|---|---|
| Oxides | $Al_2O_3$ | Al,Be,Co,Co-Cr,Fe, Stainless |
| | $Cr_2O_3$ | Cr |
| | MgO | Al,Be,Co,Fe,Mg |
| | $SiO_2$ | Cr,Si |
| | $ZrO_2$ | Zr |
| Carbides | SiC | Ag,Si,Co,Cr |
| | TiC | Mo,W,Fe,Ni,Co, S816 Inconel, Hastelloy, Stainless, Vitallium |
| | $Cr_3C_2$ | Ni,Si |
| Borides | $CrB_2$ | Ni |
| | $TiB_2$ | Fe,Ni,Co |
| | $ZrB_2$ | |
| Silicides | $MoSi_2$ | Ni,Co,Pt,Fe,Cr |
| Nitrides | TiN | Ni |

and behave in much the same way that thin films of copper behave in brazed joints. That is, since the copper is constrained by the surrounding metal, the braze copper is considerably stronger than copper in the massive form. To Norton's comments it might be added that the structure having improved ductility and impact strength may have thicker films than those for optimum strength, and a compromise to achieve the best combination of properties may have to be determined. Systematic studies of the relation of particle size and distribution to elevated-temperature creep and rupture strength, thermal shock, and impact strength would be helpful.

It is of interest to consider the elevated-temperature strength properties of these materials. Because of necessary limitations, the discussion of properties will be confined to those materials for which stress-rupture data are available. This immediately focuses attention on cermets of titanium carbide base. In Fig. 8 several outstanding TiC-base cermets are compared on the basis of stress for rupture in 100 hr at several temperature levels. Also shown on the curve is a good cast cobalt chrome-base super alloy. Many compositions having excellent strength compared with the super alloy have been developed. Since the cermets have about 0.7 the density of the super alloys, a comparison of strength on a relative-density basis would favor the cermets even more. For uses such as in the turbine bucket where stress is determined by centrifugal force, comparisons should be made on a strength-to-weight basis.

Primary composition differences in these materials exist although all contain titanium carbide and nickel. In some cases the nickel has been alloyed to provide increased strength as can be illustrated by comparison of the data for K152B containing nickel, and K161B containing a nickel alloy. Pure titanium carbide plus nickel does not have adequate oxidation resistance for long times at these temperatures and various additions have been developed to provide the necessary resistance. These additions are: 1—a solid-solution carbide of columbium, tantalum, and titanium,[25] 2—chromium carbide, $Cr_3C_2$,[26] and 3—chromium.[25] In addition, a ceramic coating that will provide resistance to oxidation has been developed by the National Bureau of Standards.[26] Development of the titanium carbide-base cermets produced by both cold pressing and sintering (Kennametal, American Electro Metals, Firth Sterling) and by infiltration (Sintercast, NACA) has resulted in a class of materials with outstanding strength at high temperatures and good resistance to oxidation and thermal shock.

Another material for which stress-rupture data are available is aluminum oxide plus 30 wt pct Cr.[27] This material is very strong at 2000°F and above (see Fig. 9). Since it consists principally of a saturated oxide, the oxidation resistance is excellent, but its applicability is limited to those environments where only moderate resistance to thermal shock is required.

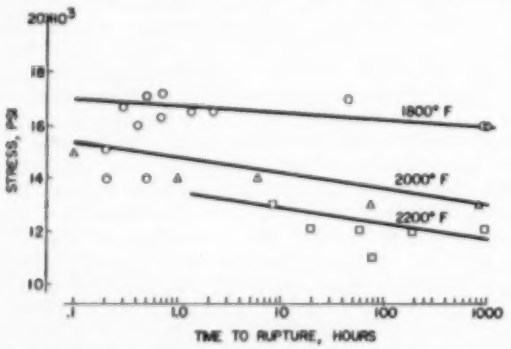


Fig. 9—Stress-rupture properties of alumina-30 pct chromium, Blackburn and Shevlin.[27]

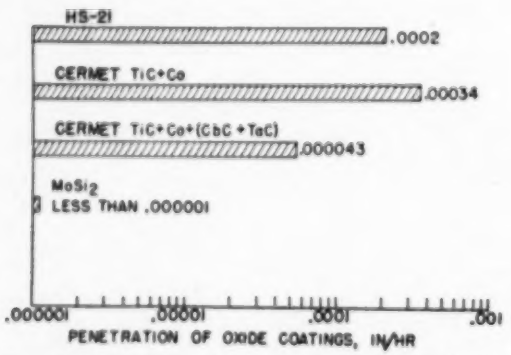


Fig. 10—Comparative oxidation resistance of molybdenum disilicide at 2000°F.

### Intermetallics and Hard Metals

In addition to the ceramics and cermets, materials called "hard metals" and "intermetallics" have been studied. These materials usually have been separately classified because they possess such metallic properties as metallic luster and good thermal and electrical conductivity, as contrasted to ceramics, and do not have a metal phase such as is commonly associated with cermets. This category includes carbides, nitrides, borides, and silicides of the transition metals. A large number of these have been investigated and an excellent summary of the research is given in Schwarzkopf and Kieffer's recent book.[28] A systematic study of many heretofore unexplored compositions, that may be of interest for high temperature applications, is now being made.[29]

Because of space limitations in the present discussion, the emphasis is placed again upon materials that have been developed to the point where at least some stress-rupture data are available.

A particularly interesting intermetallic that has been developed at the NACA is molybdenum disilicide, $MoSi_2$.[30-32] The electrical conductivity of this material is about that of stainless steel, and the thermal conductivity is about that of nickel at room temperature.

The most outstanding property of $MoSi_2$ is its resistance to oxidation. Some comparative data in terms of depth of oxide penetration is given in Fig. 10. Obviously $MoSi_2$ is far superior to a typical

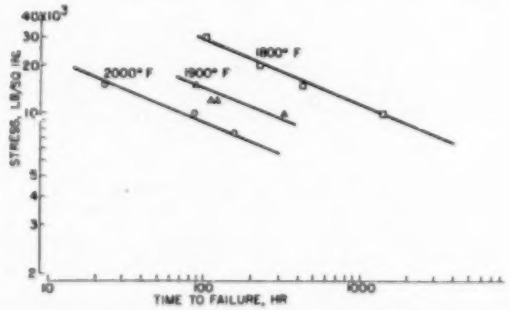


Fig. 11—Stress-rupture properties of $MoSi_2$.

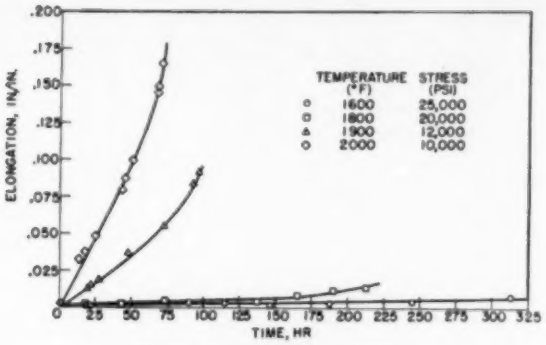


Fig. 12—Creep behavior of $MoSi_2$.

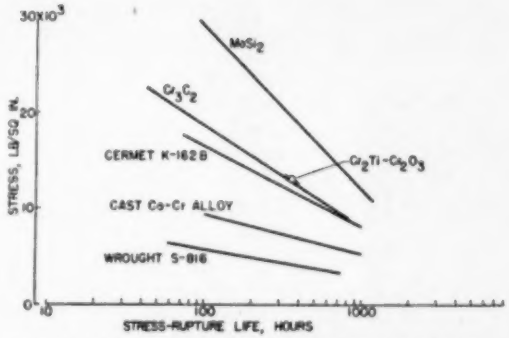


Fig. 13—Comparative stress-rupture strengths at 1800°F.

high temperature cobalt chrome-base alloy, Stellite 21, and to an outstanding cermet. The most dramatic demonstration is visual. A polished surface of $MoSi_2$ after 160 hr at 2000°F has darkened but still retains most of its original metallic luster. By X-ray diffraction it has been found that $MoSi_2$ obtains its oxidation resistance by a tightly adhering coating of $SiO_2$ that forms on the surface when $MoSi_2$ is exposed to oxidizing conditions.

In a study of fabrication variables, it was found that the short-time strength of the initially produced material could be approximately doubled by increasing the grain size and by the addition of carbon with a resulting decrease in oxygen content.

The stress-rupture strengths of the most promising material are shown in Fig. 11 at three temperatures, 1800°, 1900°, and 2000°F. The stress for 100 hr life at 1800°F is about 30,000 psi, about 15,000 psi at 1900°F, and at 2000°F about 9000 psi. These strengths are very high but, since the material flows plastically at these temperatures, it is of interest also to consider creep. Creep curves are shown in Fig. 12 for several stresses at 1600°, 1800°, 1900°, and 2000°F. The creep resistance of the material at 1600° and 1800°F is satisfactory. At 1900°F under a stress of 12,000 psi the elongation is of the order of 10 pct in 100 hr. This elongation would be beyond allowable limits for many structural uses; however, for lower stresses at 1900°F and at lower temperatures with higher stresses, $MoSi_2$ has satisfactory creep strength.

Other typical materials in this class, for which at least limited stress-rupture data are available, are chromium carbide, $Cr_3C_2$, and chromium titanide, $Cr_2Ti$. The kinetics of sintering during hot pressing with chromium carbide have been studied.[29-31] The material has demonstrated properties of interest at elevated temperatures. It has good oxidation resistance and is extremely metallic in appearance with a silvery color not unlike ordinary steels.

$Cr_2Ti$ is a new material[32] and only very limited data are available at this time. The resistance to oxidation at 1832°F is good and stress-rupture properties of a $Cr_2Ti$ plus 5 pct $Cr_2O_3$ body are being investigated at 1800°F. The data from the first preliminary test of this material and data for $Cr_3C_2$ are compared with several other materials, Fig. 13. These data show that the intermetallics have outstanding strength at 1800°F compared with the super alloys and also with the titanium-carbide cermets.

All these materials have excellent high temperature strength and good resistance to oxidation. Another very important property for many applications is resistance to thermal shock. A comparison of some of these materials is shown in Fig. 14. The data are from different pieces of test apparatus and represent differing severities of quench. In all cases the test specimen was a disk of 2 in. diam and ¼ in. thick. The specimens were quenched from a furnace at elevated temperature into different media at about room temperature. The temperature data plotted are essentially the temperature differences between the furnace and the quenching media.

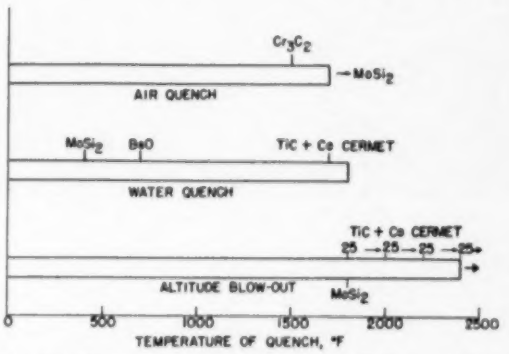


Fig. 14—Thermal-shock behavior of some brittle materials.

The first test, represented by the upper bar, consisted of a comparatively gentle quench in a low velocity air jet. Here $Cr_3C_2$ failed when quenched from 1500°F while $MoSi_2$ withstood a quench from the limiting temperature of the apparatus, 1700°F. The next test was more rigorous and consisted of a water quench in which only the outer periphery of the disk was quenched. Here $MoSi_2$ failed at a temperature differential of 400°F; whereas, for comparison, an outstanding ceramic BeO failed at 700°F. A titanium carbide-plus-cobalt cermet did not fail until quenched from 1700°F. The last test consisted of quenching a disk in a high velocity air stream where the velocities were similar in severity to those that might be encountered in a jet engine. Here $MoSi_2$ failed in the first one or two cycles at 1800°F, while the titanium carbide-plus-cobalt cermet withstood a total of 100 cycles — 25 cycles each at 1800°, 2000°, 2200°, and 2400°F. Cermets of titanium-carbide plus several other metal additions have consistently survived this test. Thus, although some of the intermetallics are strong at elevated temperatures, the resistance to thermal shock generally appears to be substantially less than that of the titanium carbide-plus-metal cermets. Because of their outstanding strength and good oxidation resistance, the intermetallics certainly will find appli-

Fig. 15—Cermet type-B turbine bucket after operation.

cation at elevated temperatures where only moderate resistance to thermal shock is required. This field is still relatively unexplored, and many new compositions of superior properties will undoubtedly be developed in the next few years.

### Application Studies of Cermets

*Turbine Buckets:* Because the cermet materials have demonstrated the best combination of strength, oxidation, and thermal-shock properties, application studies of refractory hard metals have emphasized cermets.

The application that is of greatest urgency is that of turbine buckets and some experiences in this field will be presented. The turbine buckets operate in a highly oxidizing atmosphere, under high stress at temperatures of 1500° to 1600°F and under conditions of thermal shock.

In the application of cermets to turbine buckets, the problem is one of the utilization of materials that are very strong at high temperatures but have no measured ductility at room temperature — and only traces of ductility of the type measured in a tensile test at high temperature. This combination of properties results in a material that is quite notch sensitive both at room and elevated temperatures.

The turbine-bucket designs must, therefore, embody two features. They must be of such geometry as to minimize notch effects. The design of the root must embody some method of uniformly redistributing the load concentrations imposed by the minor mismatching between bucket and wheel caused by dimensional variations.

The first turbine runs[20] were made using small buckets of a titanium-carbide cermet with the design shown in Fig. 15, which is a blade after operation. This blade is of simple design in that it has neither twist nor taper and is retained in the turbine wheel by a roll at the base of a rather thin neck. The operating conditions for this turbine were an estimated bucket temperature of about 1600°F and a centrifugal stress equal to that of one of the lower-stressed jet engines. From the first runs several things were learned:

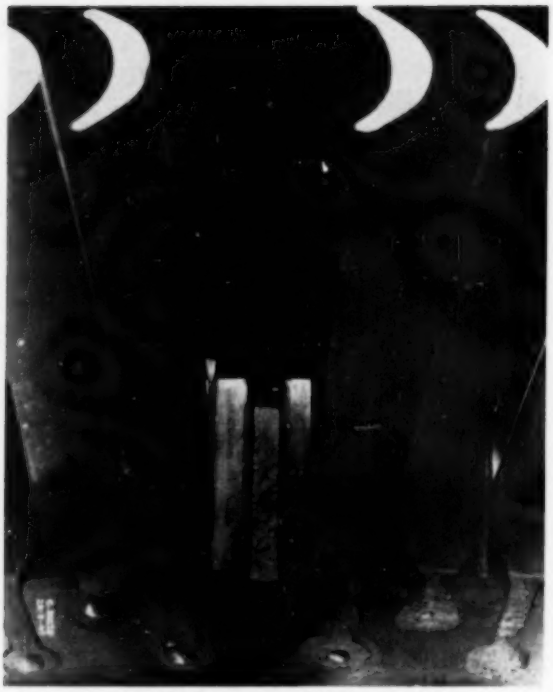

Fig. 16—Cermet type-B blade failure.

1—The critical or failure area of the bucket is in the root, particularly at the juncture of the neck with the roll. A typical failure of this type is shown in Fig. 16.

2—Since these materials have about twice the thermal conductivity of the currently used high temperature alloys, the wheel rim heats up more than it does with alloy buckets and is quite likely to fail locally.

3—Conventional methods of fastening the buckets in the wheel cannot be used.

In an effort to try to solve the problems associated with stress concentrations resulting from poor mating in the roots, a run was made using six cermet buckets in a wheel with a control sample of 136 alloy buckets.[20] Two of the cermet buckets were loosely mounted so that they could seat themselves as the turbine came up to speed, two had nickel-plated roots and two had copper-plated roots. The loosely mounted buckets failed rapidly, the better one failing after only about 5 hr of operation. The buckets having nickel-plated roots were only slightly better, the better one running for about 16 hr. The buckets with the copper-plated roots showed very marked superiority with one bucket lasting 111 hr, or longer than 95 pct of the alloy buckets. The failure in this cermet bucket, as in most of the previously run cermet buckets, was also in the root, whereas most of the alloy buckets failed in the airfoil.

*Design Studies:* These first runs pointed up the design aspects of bucket mounting. It was evident that new and drastically different types of roots would be required. A series of designs that were thought to be particularly adapted for use with brittle materials are shown in Fig. 17. For purposes of comparison, a standard serrated or fir-tree root that is widely used at the present time for alloy buckets has been included in the figure. It can be seen that all the roots have very generous radii. In

some, a ductile pin or shim retains the bucket in the wheel and imparts some of the ductility that is lacking in the cermet root. All root designs were evaluated in tension tests at 1200°F, both with and without an interposed layer of readily deformable nickel-plated copper screen. It was found that the fir-tree root could withstand about one-third more stress than is imposed on it in the engine, while one of the newer designs is capable of supporting in excess of twice the load imposed on it. The root designs not containing ductile retaining pins benefited considerably from the use of the screen. These tests indicate that the use of generous radii and ductile shims greatly improves the application potential of cermets. They also indicate the importance of proper design for brittle materials.

*Inspection:* Turbine operation of cermets has indicated that many buckets fail after only a very short time at the test conditions, while other buckets have very promising service lives. The problem of segregating these inferior buckets has been receiving increasing attention as the development of these materials progresses. In the inspection of cermets such conventional methods as density measurements, hardness tests, radiography, and various types of surface inspections utilizing penetrant dies have been used. While these techniques have eliminated buckets that had gross defects, the engine-operating experience indicates that they have not succeeded in eliminating all early bucket failures.

Proof testing in which components are subjected to simulated stress and temperature conditions for a prolonged time or a short time at over-stress conditions has also been used, and while this testing has succeeded in eliminating some buckets, early blade failures are still being encountered among those remaining. Other inspection techniques, such as supersonic methods, physical-proof tests on finished components, and magnetic measurements are being studied and have indicated some promise, but as yet have not solved the problem. Since magnetic measurements are the most unconventional, they will be discussed in greater detail.

Where nickel or high nickel alloys are used as the metal for the binder phase, measurements of the magnetic properties of the cermet material have been found to be useful for indicating composition changes in the metal phase. Fig. 18[27] shows the effect of various dissolved metals on the Curie temperature of nickel. The ferromagnetic elements iron and cobalt increase the Curie temperature linearly with quantity in solution and most of the nonmagnetic metals decrease Curie temperature linearly. Carbon is reported as not having an appreciable effect on the Curie temperature of nickel.[28] Titanium carbide is nonmagnetic, but cermets of titanium carbide and nickel are magnetic, of course. By measurements of the Curie temperature, an insight into the composition of the metal phase can be gained. A simple apparatus for the measurement of the Curie temperature of cermets is shown in Fig. 19a. Here the force required to remove a magnet from a cermet at various temperatures can be measured. The point where the magnet is no longer attracted by the cermet is the Curie temperature. If the data of magnetic pull against temperature are plotted (Fig. 19b), the curve can be extrapolated to zero magnetic pull, and the Curie point can be determined to an accuracy of about ±10°F. Plotting the data also has the advantage of pointing out breaks in the curve that might indicate the presence of magnetic phases of differing Curie points.

In the fabrication of cermets of titanium carbide-plus-nickel, any foreign atoms which may be present, including perhaps titanium, from the titanium carbide could be dissolved in the metal phase during sintering. In Fig. 18 the slope of the curve for iron indicates that a change in Curie temperature of 1°F is indicative of 0.04 pct change of iron in solution in nickel. Changes in Curie temperature thus appear to be a sensitive indication of the composition of the nickel phase.

The Curie point is being investigated at the NACA as a method of indicating differences in batch composition and particularly of changes in the metal phase resulting during a program of heat treatment of titanium carbide cermets. Typical changes in the Curie point of a specimen resulting from heat treatment are shown in Table III.

Measurements of only the force necessary to separate a standard magnet from a cermet at room tem-

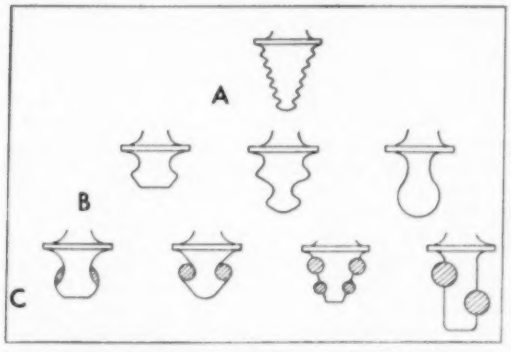


Fig. 17—Cermet blade-root design. a—Standard fir tree. b—Experimental cermet roots. c—Experimental cermet roots using ductile retaining pins.

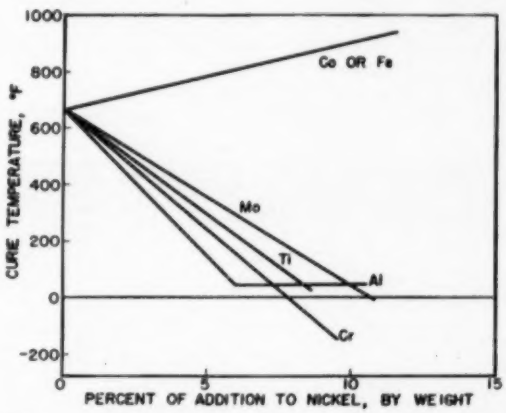


Fig. 18—Effect of alloying additions on the Curie point of nickel, Wise and Schaefer.[27]

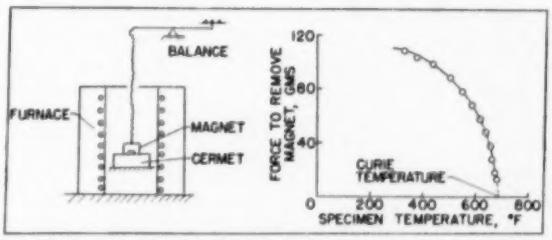


Fig. 19—Apparatus (*a*, right) and typical data curve for determination of Curie temperature (*b*, left).

Table III. Effect of Heat Treatment on Curie Temperature of a TiC + Ni Cermet

| Material Condition | Curie Temperature, °F |
|---|---|
| As sintered | 680 |
| Solution treated, 2375°F, 4 hr, air cooled | 600 |
| Above solution treatment plus age, 1550°F, 24 hr, air cooled | 685 |

perature is a quick method for indicating differences from lot to lot, and this avoids the heating cycle. Such measurements, however, do not give any indication of the cause for the differences, whereas measurements of Curie temperatures of cermets that give readings above the Curie temperature of pure nickel indicate the presence of magnetic materials such as iron or cobalt, and measurements below the Curie temperature of pure nickel indicate the presence of dissolved nonmagnetic materials. An important factor that must always be kept in mind is that a simultaneous solution of two elements, e.g., magnetic cobalt and nonmagnetic titanium, can cancel effects on Curie temperature. More information is needed about the magnetic properties of possible minor phases, such as intermetallics, before Curie temperatures can be used quantitatively with full confidence.

Another approach to the inspection problem is to assume that the failures are due to a random dispersion of minor surface flaws which are individually too small and not sufficiently concentrated to be detected by present surface-inspection techniques.

If this concept of a random dispersion of fine defects is accepted, it then becomes desirable to treat the surface in some manner which is designed to heal all the defects. Sometime ago Kennametal suggested that a film of nickel diffused into the surface of cermets may improve their properties. Tests at the NACA Lewis laboratory have indicated that a film of nickel can be readily diffused into the surface of both cold-pressed and sintered and infiltrated titanium carbide-base cermets.

Fig. 20 shows a titanium carbide-base cermet after a 0.004 in. thick film of nickel has been diffused into the surface. The surface appears to have been improved. Close examination of the structure reveals a higher metal content at the surface of the cermet. The nickel was applied by painting the surface with a nickel-powder slurry. The binder for the nickel powder was an ethyl methacrylate-touluene solution that has been developed for making brazing pastes. This solution volatilizes completely at about 750°F. This work on the surface treatment of cermets is still in a very preliminary stage, and there is evidence that cracks can be healed by this method. The effects on physical properties have not as yet been determined. If the properties are controlled by the surface conditions, large improvements may be encountered.

Fig. 20—Surface treatment of titanium carbide-base cermets. Unetched. X100. Area reduced approximately 55 pct for reproduction.

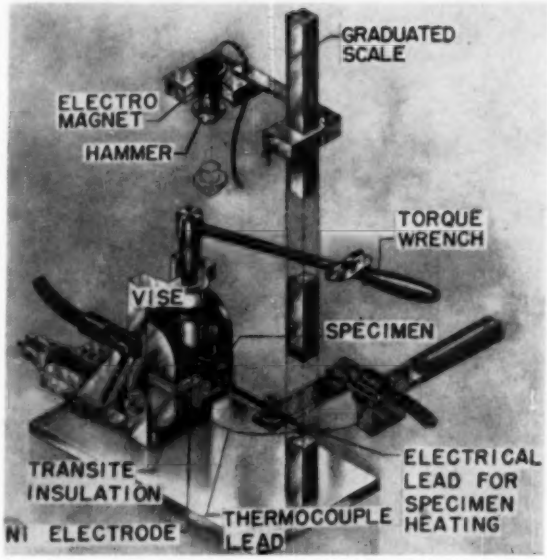


Fig. 21—Schematic diagram of NACA drop-impact test.

*Impact Strength:* Another property of cermets that is of considerable interest is the impact strength. In the case of the gas turbine, this property is required because of the danger that foreign objects, perhaps gravel picked up from runways, might pass through the engine or that fragments from a failed bucket might strike an adjacent bucket.

The measurement of the impact strengths of cermets has proved to be troublesome. One problem is that the values are below those usually encountered by the metallurgist and his equipment is not suitable. Values in the literature[39,40] obtained for cermets with conventional testing equipment lead to the conclusion that the results are reproducible and indicate that the impact resistance is inferior to conventional high temperature alloys.

In the plastics industry[41] where the impact-evaluation problem is analogous to that encountered with cermets, efforts have been made to eliminate any kinetic energy which may be imparted to the fragments of the test specimen by the impacting hammer from the recorded value of the impact strength. The elimination of this "toss energy" is felt to result in a more significant value of the impact strength. Equipment that has been proposed to accomplish this for cermets[42] is shown in Fig. 21. The apparatus consists essentially of a vise whose jaws are insulated with transite plates for gripping the specimen. To insure uniformity of gripping, the vise is closed at the test temperature using a torque wrench. The

## Table IV. Drop-Test Impact Data

| Material | Average Impact Strength, (In.-Lb) | | | | | | | | |
|---|---|---|---|---|---|---|---|---|---|
| | Room Temperature | | | 1200°F | | | 1500°F | | |
| | Notched | Unnotched | Ratio | Notched | Unnotched | Ratio | Notched | Unnotched | Ratio |
| **Cermets** | | | | | | | | | |
| K150B | 1.3 | — | — | 1.05 | — | — | — | — | — |
| K152B | 2.1 | 4.1 | 1.95 | 1.6 | 3.7 | 2.3 | 1.6 | — | — |
| K154B | 2.8 | 5.2 | 1.86 | 2.3 | 5.2 | 2.26 | 2.3 | 5.5 | 2.4 |
| K162B | 3.3 | 6.3 | 1.9 | 1.3 | 2.6 | 2.0 | — | — | — |
| FS-9 | 1.93 | — | — | 2.43 | — | — | 2.52 | — | — |
| FS-27 | 1.29 | — | — | 1.45 | — | — | 1.34 | — | — |
| **Alloys** | | | | | | | | | |
| X-40 | 48.05 | — | — | — | — | — | — | — | — |
| New-cast Co-base alloy | 2.2 | — | — | 2.1 | — | — | 2.1 | — | — |
| New-cast Ni-base alloy | — | 16.7 | — | — | — | — | — | — | — |

specimen is a ¼x¼x2 in. bar either with or without a notch at the center. The shape and the size of the specimen were chosen so that the specimen would be small and easy to fabricate and so that the thickness to be fractured would be of the same order of magnitude as the thickness of a turbine bucket.

In order to use this equipment for high temperature impact evaluation, the specimen is resistance heated by a low-voltage high-amperage current which is brought in through a movable electrode. The hammer strikes the cantilever-beam specimen near the free end and is dropped from successively increasing heights until the specimen is fractured.

In this test, the toss energy is eliminated by striking the specimen with just sufficient energy to create fracture. The energies necessary to cause fracture are shown in Table IV. Perhaps an even more significant value might be the maximum energy the specimen withstood without fracture. These values of impact strength are about 0.1 in.-lb less than the values shown in Table IV.

Initially there was concern that the blows which did not fracture the specimen might be damaging it and reducing the impact strength; however, the tests have indicated that with cermets this does not appear to be the case. Results have been consistent whether 2 or 16 blows were used.

Each value in Table IV is the average of values obtained with six specimens. These values are much lower than those in the literature because the specimen was smaller, the specimen was notched, and the toss energy was not included in the measured strength. The values of this investigation, however, are believed to be more significant for comparing cermets. For purposes of comparison, several alloys have been included in the table. All cermets shown are inferior to the conventional turbine-bucket alloy, X-40. The impact resistance of the cermets is, however, of the same order of magnitude as that of some

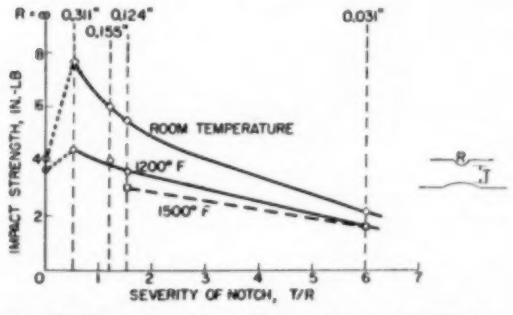


Fig. 22—Effect of notch severity on impact strength of a cermet.

of the newer and more refractory alloys that are currently being studied.

The first group of cermets, the K150B, K152B, and K154B have metal contents of 10, 30, and 50 wt pct, respectively, and as might be expected, the impact strength increases with increasing metal content. The effects of increasing temperature on impact strength were small and in some cases a decrease was noted.

In order to explore the effect of notches on impact strength, a series of tests was run in which the notch radius was varied but the notch depth was held constant, see Fig. 22. The values of impact strength have been plotted against the ratio of specimen thickness to notch radius. In this study, the specimen thickness $T$ was held constant. The purpose of the type of plot used was to enable the unnotched condition (infinitely large notch radius) to be included in the curve. This condition appears at zero notch severity. Perhaps of greatest interest in this figure is the shape of the curves. This shape is characteristic of ductile materials in tension where gentle notches produce a notch-strengthening effect over the unnotched condition, while severe notches produce a weakening effect.

### Summary

1—Powder-metallurgy techniques have proved of great value to the metallurgist interested in materials for high temperature applications by providing him with materials not otherwise available. This is true in the case of cermets, the intermetallics, and some refractory metals. Powder-metallurgy techniques provide him with materials in a form not otherwise available as in the case of porous materials.

2—With the possible exception of wrought molybdenum alloys, the techniques of powder metallurgy have produced materials — the cermets and intermetallics—that are superior to any other products on the basis of elevated-temperature strength. These materials have found some application, such as for heating elements, thermocouple-protection tubes, and high temperature abrasion-resistant parts. Before application to use in such critical components as turbine buckets can be made, solutions of several important problems must be found. These problems generally result from the lack of ductility and include methods of fastening, low impact resistance, and reliability. Progress is being made toward the accomplishment of these objectives.

3—The designer would prefer to have new materials available that will permit a higher use temperature without problems of low ductility, in other words, materials comparable to the present high temperature alloys but with an appreciably greater

strength. At least two approaches utilizing powder-metallurgy methods to achieve this are suggested: First, powder metallurgy holds some promise for the production of alloys having controlled microstructure and without the usual limitations in the quantities of alloying additions and permits the achievement of greater strengths. Second, the sintered aluminum powder has dramatized a mechanism for increasing limiting temperatures that may be applicable to other alloy systems.

## References


[1] P. Schwarzkopf: Engineering Properties of Sintered vs Cast Materials. *Product Engineering* (1946) **17**, No. 2, pp. 122-126.

[2] G. J. Comstock and J. D. Shaw: Alloy Powder Products from Fully Alloyed Powders. *The Physics of Powder Metallurgy* (1951) Edited by W. E. Kingston. P. 372. New York. McGraw-Hill Book Co.

[3] L. H. Mott: Progress Report on Hot Forging Prealloyed Metal Powders. *Precision Metal Molding* (1952) **10**, No. 10, p. 38.

[4] P. R. Toolin and N. L. Mochel: The High Temperature Fatigue Strengths of Several Gas Turbine Alloys. *Proceedings* ASTM (1947) **47**, pp. 677-691.

[5] J. P. Lyle, Jr.: Excellent Products of Aluminum Powder Metallurgy. *Metals Progress* (1952) **62**, No. 6, p. 109.

[6] E. Gregory and N. J. Grant: High Temperature Strength of Wrought Aluminum Powder Products. *Trans.* AIME (1954) **200**, pp. 247-252; JOURNAL OF METALS (February 1954).

[7] W. D. Jones: Progress in Powder Metallurgy. *Journal* Chemical, Metallurgical, & Mining Society, South Africa (1952) **52**, pp. 216-222.

[8] W. O. Schey: *The Advantages of High Inlet Temperature for Gas Turbines and Effectiveness of Various Methods of Cooling the Blades.* (1948) Paper presented at the Annual Meeting, ASME.

[9] H. H. Ellerbrook, Jr. and L. J. Schaefer, Jr.: Application of Blade Cooling to Gas Turbines. *NACA RM E50A04.*

[10] P. Duwez and H. L. Wheeler: Experimental Study of Cooling by Injection of a Fluid Through a Porous Material. Report, Jet Propulsion Laboratory. *Journal of Aero Science* (1948) **15**, pp. 509-521.

[11] G. J. Comstock, J. D. Shaw, C. L. Clark, W. V. Knopp, and G. M. Thomas: *Minutes* Meeting on Bureau of Aeronautics Sweat Cooling Project at Stevens Institute of Technology (February 24, 1949).

[12] R. L. Probst: Investigation of Sintered Loose Spherical Powders for Fabrication into Transpiration Cooled Turbine Blades. *Progress Reports Nos. 1, 2, and 3.* Research and Development Div., Federal Mogul Corp., Detroit, Mich.

[13] R. D. Grinthal, J. C. Bradbury, L. H. Mott, and G. J. Comstock: Investigation of Porous Material from Spherical Metal Powders. *Bi-monthly Progress Report No. 5* Navy Contract Noa(s)-51-185-c (1951) Stevens Institute of Technology.

[14] G. M. Thomas and G. J. Comstock: Process for Fabrication of Materials for Porous Turbine Blades. *Progress Reports Nos. 18 and 19. Summary of 19 Progress Reports* (June 1947 to April 1950), *Progress Report No. 20.* Powder Metallurgy Laboratory, Stevens Institute of Technology (1950).

[15] G. M. Thomas, C. L. Clark, W. V. Knopp, J. D. Shaw, and G. J. Comstock: Process for Fabrication of Materials for Porous Turbine Blades. *Progress Report No. 14* Powder Metallurgy Laboratory, Stevens Institute of Technology (Nov. 10, 1948).

[16] M. Hill, O. W. Reen, D. H. Vermelyea, and F. V. Lenel: Production of Porous Metal Compacts. *Bimonthly Progress Report No. 3* Navy Research Contract NOa(s) 11022 (October 1950) Rensselaer Polytechnic Institute.

[17] G. M. Thomas, C. L. Clark, W. V. Knopp, J. D. Shaw, G. J. Comstock, and K. B. Davis: Process for Fabrication of Materials for Porous Turbine Blades. *Progress Report No. 17* Powder Metallurgy Laboratory, Stevens Institute of Technology (June 30, 1949).

[18] E. G. Pekarek: Operation of Thompson Molybdenum Plant. *Final Report* to Headquarters of Air Material Command Contract W-33-038-ac-20672 (January 28, 1952).

[19] M. Semchyshen and H. E. Hastette: Arc-Cast Molybdenum Base Alloys. *Third Annual Report* (1952) Office of Naval Research Contract N8onr-78700, Task Order N8onr-78701, Project NR 034-401.

[20] J. J. Harwood: Molybdenum, Our Most Promising Refractory Metal. *Product Engineering* (1952) **23**, pp. 121-132.

[21] J. J. Gangler: Some Physical Properties of Eight Refractory Oxides and Carbides. *Journal* American Ceramic Society (1950) **33**, No. 12, pp. 367-374.

[22] J. T. Norton: Some Observations on the Role of the Binder in Cemented Refractory Alloys. *Powder Metallurgy Bulletin* (1951) No. 6, pp. 75-78.

[23] J. C. Redmond and E. N. Smith: Cemented Titanium Carbide. *Trans.* AIME (1949) **185**, p. 987; JOURNAL OF METALS (November 1949).

[24] E. M. Trent, A. Carter, and J. Bateman: High Temperature Alloys Based on Titanium Carbide. *Metallurgia* (1950) **42**, p. 111.

[25] P. Schwarzkopf and R. Kieffer: *Refractory Hard Metals.* (1953) pp. 396-397. New York. MacMillan Co.

[26] D. G. Moore, S. G. Benner, and W. N. Harrison: Studies of High Temperature Protection of a Titanium-Carbide Ceramel by Chromium-Type Ceramic-Metal Coatings. *NACA TN 2386* (1951).

[27] A. R. Blackburn and T. S. Shevlin: Fundamental Study and Equipment for Sintering and Testing of Cermet Bodies. V-Fabrication, Testing, and Properties of 30 Chromium-70 Alumina Cermets. *Journal* American Ceramic Society (1951) **34**, No. 11, pp. 327-331.

[28] P. Schwarzkopf and R. Kieffer: *Refractory Hard Metals.* (1953) New York. MacMillan Co.

[29] W. Arbiter: New High Temperature Intermetallic Materials. *WADC Technical Report 53-190* American Electro Metallurgical Corp., Yonkers, N. Y.

[30] W. A. Maxwell: Oxidation-Resistance Mechanism and Other Properties of Molybdenum Disilicide. *NACA RM E52A04* (1952).

[31] W. A. Maxwell: Properties of Certain Intermetallics as Related to Elevated-Temperature Applications. I-Molybdenum Disilicide. *NACA RM E9G01* (1949).

[32] W. A. Maxwell and R. W. Smith: Thermal Shock Resistance and High Temperature Strength of a Molybdenum Disilicide-Aluminum Oxide Ceramic. *NACA RM E53F26* (1953).

[33] W. G. Lidman and H. J. Hamjian: Kinetics of Sintering Chromium Carbide. *NACA TN 2491* (1951).

[34] H. J. Hamjian and W. G. Lidman: Influence of Structure on Properties of Sintered Chromium Carbide. *NACA TN 2731* (1952).

[35] C. A. Hoffman, G. M. Ault, and J. J. Gangler: Initial Investigation of Carbide-Type Ceramel of 80 Pct Titanium Carbide Plus 20 Pct Cobalt for Use as a Gas-Turbine-Blade Material. *NACA TN 1836* (1949).

[36] C. A. Hoffman and A. L. Cooper: Investigation of Titanium Carbide Base Ceramels Containing Either Nickel or Cobalt for Use as Gas-Turbine Blades. *NACA RM E52H05* (1952).

[37] E. M. Wise and R. H. Schaefer: The Properties of Pure Nickel-I. *Metals and Alloys* (1942) **16**, pp. 424-428.

[38] *Metals Handbook* (1948) p. 1183. Cleveland. ASM.

[39] W. L. Havekotte: Super Refractories for Use in Jet Engines. *Metals Progress* ASM (1953) **64**, No. 6, pp. 67-70.

[40] J. W. Graham: Sintered Titanium Carbides Open New Industrial Horizons. *Iron Age* (1953) **172**, pp. 148-152.

[41] B. Maxwell and L. F. Rahm: Impact Testing of Plastics: Elimination of the Toss Factor. *Bulletin* ASTM (October 1949).

[42] B. Pinkel, G. C. Deutsch, and N. Katz: The NACA Drop Test for the Evaluation of the Impact Strength of Cermets. *NACA RM E54D13* (1954).

*DISCUSSION, Claus Goetzel, Chairman*

**J. D. Roach** and **A. C. Haskell, Jr.** *(Titanium Alloy Mfg. Div., National Lead Co., Niagara Falls, N. Y.)*—Titanium carbide, while having been used for many years as a minor constituent in cemented carbides, recently has been receiving increasing attention as the basic material for a series of cemented products displaying interesting and unique properties. Characterized by excellent oxidation resistance, high strength, and low density, titanium carbide also displays the high hardness and modulus of elasticity, good wear resistance, and low thermal expansion typical of the refractory carbides generally.

In order to obtain a more complete knowledge of the characteristics of titanium carbide, available vacuum-fusion apparatus was applied to the gas analysis of this material, using equipment similar to that developed by Dr. G. Derge[44] of Carnegie Institute of Technology. Previous experience with this apparatus has shown that the apparent gas content of a given sample is greatly influenced by a number of factors encountered in the analytical procedure. Uniformity of this procedure is of great importance if accurate and consistent results are to be obtained. Fusion temperature, gas evolution and circulating time, the use of tin to prevent the gettering action of vaporized metal, and the ratio of the weight of the iron bath to that of the sample are important factors that have a definite effect on the analyses and therefore must be carefully controlled.

At first our vacuum-fusion work was concerned primarily with samples, which were compact or massive, in which the ratio of surface area to mass was relatively low. On dealing with a powdered material such as milled titanium carbide, however, this ratio is obviously increased many-fold. Hence, with powdered materials, the question of surface adsorption of gases, which may be neglected with a massive sample, becomes very important.

Rather than become involved in a detailed discussion of adsorption, it should suffice to say that adsorption, which is strictly a surface phenomenon as distinguished from absorption, generally occurs in two stages.[45, 46] The first is often referred to as Van der Waals adsorption, in which the forces involved are relatively weak so that the gases thus held can be easily and completely removed through decreased pressure and increased temperature. The second stage of adsorption, commonly called "chemisorption," is characterized by much greater bonding forces and hence is more difficult to overcome. Another peculiarity of adsorption is that it is quite often preferential, i.e., one gas from a mixture of gases can be adsorbed on a solid and essentially removed from the other gases in the mixture.

Methods were then considered for the removal of this adsorbed gas. The desorption technique chosen involved both heat and pressure. The sample was heated in an argon atmosphere for 1 hr at 750°C (1382°F). Actually, the argon was at atmospheric pressure, or slightly in excess thereof, but the effect is the same as employing low absolute pressure over the sample. The controlling factor causing the gas molecules to leave the surface is a low ratio of the partial pressure of that gas in the surrounding atmosphere to that of the same gas in the mixture adsorbed on the particle. Whether the time of 1 hr and the temperature of 750°C represent optimum conditions, we quite frankly do not know, but it is apparent nevertheless that these conditions are effective toward accomplishing at least considerable desorption.

Table V. Typical Analysis of High Purity Titanium Carbide

| | |
|---|---|
| Titanium | 79.1 pct |
| Total carbon | 19.46 pct |
| Free carbon | 0.29 pct |
| Combined carbon | 19.17 pct |
| Iron | 0.33 pct |

Table VI. Effect of Desorption of High Purity Titanium Carbide by Heating at 750°C in Argon for 1 Hr

| | Wt Pct | | |
|---|---|---|---|
| | Oxygen | Hydrogen | Nitrogen |
| Lot 4 as-produced | 0.630 | 0.014 | 0.088 |
| Lot 4 after desorption | 0.235 | 0.003 | 0.052 |

Thus, following some preliminary work with nickel and zirconium powders, an additional desorption step was added, for finely divided samples, to the standard vacuum-fusion procedure involving the following factors: 1—fusion temperature, 1950°C; 2—the addition of a small sample of tin for each sample analyzed; 3—dilution ratio, 500:1; and 4—uniform fusion and circulating time. The desorption step, which, of course, was applied first, consisted merely in heating 1 hr at 750°C in argon. Through standardization of the above factors, gas analyses obtained in this laboratory were duplicated, with very good agreement, by another laboratory.

It was realized that adsorption would play a major role in the gas content of titanium carbide due to the fineness of the material. This new grade of high purity, low free-carbon TAM titanium carbide has a maximum particle diameter of 44 microns (325 mesh) and down; approximately 38 wt pct is less than 10 microns. A typical chemical analysis of this titanium carbide is presented in Table V.

As has been noted, we are especially concerned here with the problem of determining the exact amount of contamination by the gases—oxygen, nitrogen, and hydrogen. It has not been known to what extent the gases are adsorbed or chemically combined. Incidentally, the importance of the contents of each of the common gases with respect to the ultimate processing, i.e., sintering, is also not known or fully appreciated. To secure some data on the first point, a sample of the finished carbide was split into two parts and subjected to gas analysis after one-half was desorbed, while the other half was analyzed as received. The results are presented in Table VI.

It is apparent, first of all, that the total gas content of the finished carbide is not excessive. But of more enlightening value is that large proportions of the gases, e.g., 57 pct of the oxygen, are adsorbed rather than chemically combined. The indications are that they are held in first-stage adsorption, since their removal was achieved quite readily. The remaining gas content, which was possibly chemically combined, was gratifyingly low.

Of interest next was the origin of these gases, and an investigation was begun to indicate how complete the reduction of the carbide was, and what effect the various steps of processing had on the gas contents. For this purpose, samples of the carbide were taken at various stages of manufacture. The sample designated "Prior to Milling" represents crushed carbide from the furnace, and its maximum particle size is approximately ⅛ in. A sample taken after milling was finer than 325 mesh. A third sample representing the

Table VII. Effect of Processing Steps on Gas Content of Titanium Carbide

| | Prior to Milling | | After Milling | | Finished Product | |
|---|---|---|---|---|---|---|
| Wt Pct | As-Received | After Desorption | As-Received | After Desorption | As-Received | After Desorption |
| Hydrogen | 0.007 | 0.0037 | 0.017 | 0.0002 | 0.014 | 0.005 |
| Oxygen | 0.134 | 0.059 | 0.548 | 0.246 | 0.630 | 0.235 |
| Nitrogen | 0.052 | 0.051 | 0.074 | 0.057 | 0.088 | 0.052 |

finished product indicates the effect of the beneficiation treatment. These samples were analyzed in the desorbed condition and by the standard method, as well as without desorption, in order that additional information could be obtained as to the nature and origin of contamination. These results are presented herewith in Table VII.

From these data a number of interesting conclusions can be drawn. First, in regard to the effects of processing, it is quite apparent that the reduction has been completed satisfactorily. The addition of gases by the milling operation is quite pronounced, whereas the pickup over the beneficiation phase was practically nil. The addition of gases by the milling operation is, of course, not unexpected, since it is this step which produces the tremendous surface area. The effect of this greatly increased surface area is very apparent from the tabulated data. Further comparison of the values cited for the milled product shows that some of the oxygen pickup is of a more permanent nature than that for hydrogen and nitrogen. This, too, is quite conceivable, as an appreciable amount of localized heat is liberated on milling. This led to the hypothesis that approximately 0.2 pct of the oxygen is held in second-stage adsorption. It is interesting to note that neither hydrogen nor nitrogen in the desorbed condition increased significantly during processing, thus providing an indication of preferential adsorption for oxygen. The hydrogen-nitrogen adsorption is quite plainly first-stage adsorption.

In addition to reporting progress towards an accurate method for the analysis of oxygen, nitrogen, and hydrogen in titanium carbide and presenting analyses thereof, these results seem mainly significant to us as an indication of the important role of adsorption. It was shown that a very appreciable percentage (more than 50 pct of the oxygen) of the gases was loosely held on the surfaces of the particles. The significance of this finding is that it suggests the possible utility of an analogous desorption technique during the fabrication or sintering of carbide particles. Admittedly, many sintering operations are conducted in vacuum at elevated temperatures, but the point is that allowance ought to be made for the greater densities and thicknesses of the shapes involved. In other words, the gases should be allowed to escape before they react with the carbide.

**F. W. Glaser** *(American Electro Metal Corp., Yonkers, N. Y.)*—Messrs. Ault and Deutsch, in surveying the field of high temperature materials as influenced by powder-metallurgy techniques, briefly made mention of some boron-containing cermets in their Table II.

Research in connection with transition metal borides for use as high temperature materials has been underway during the past several years and data as to the physical properties of interest to engine manufacturers have only recently become available for general publication. This is one of the reasons why the more often-publicized cermets of the titanium carbide-base type have become better known in comparison with the boride-base cermets, although the latter, in many instances, have shown stress-to-rupture strengths that were at least equivalent, if not superior, to those achieved by bonded TiC. To date, impact performance of the borides is still to be considered as relatively poor. However, results of research now in progress indicate that, at least at elevated temperatures, this lack of resistance to impact may be overcome in the very near future.

**Table VIII. "Borolite" Zirconium Boride 101, Physical Properties**

| | | |
|---|---|---|
| Chemical composition: | $ZrB_2$ + binder | |
| Apparent density: | 5.2 to 5.4 grams per cu cm | |
| Melting point: | 5400°F | |
| Hardness: | 88 to 91 $R_A$ | |
| Ultimate tensile strength: | 35,000 to 40,000 psi | |
| Transverse rupture strength (2 in. span): | 60°F | 66,000 psi |
| | 1800°F | 63,000 psi |
| | 2200°F | 55,000 psi |
| Stress to rupture strength (at 1800°F): | 5 hr | 30,000 psi |
| | 10 hr | 25,000 psi |
| | 100 hr | 18,500 psi |
| | 1000 hr | 14,000 psi |
| Modulus of elasticity: | 60°F | 31,600,000 psi |
| | 1800°F | 24,000,000 psi |
| Oxidation resistance: (Weight gain in still air at 2000°F) (Material not recommended beyond 200 hr at this temperature): | 50 hr: | 4 mg per sq cm |
| | 100 hr: | 6 mg per sq cm |
| | 200 hr: | 15 mg per sq cm |
| Corrosion resistance: | **Excellent** | **Good** |
| | Molten aluminum | Molten silicon |
| | Molten copper | Molten brass |
| | Molten tin | Hydrogen peroxide |
| | Molten magnesium | **Not Good** |
| | Molten fluorides | Molten iron |
| | Nitric acid | Inconel |
| | Hydrochloric acid | |
| Electrical resistivity: | 60°F | 17.3 microhm—sq cm per cm |
| | 1800°F | 240.0 microhm—sq cm per cm |
| | 3600°F | 280.0 microhm—sq cm per cm |
| Thermal shock resistance: | Good, passed NACA-type test | |
| Thermal conductivity: | 110°F, 15.0 Btu per ft per hr per sq ft per °F | |
| Expansion coefficient: | 75° to 1000°F, $2.7 \times 10^{-6}$ per °F | |
| | 75° to 2200°F, $3.2 \times 10^{-6}$ per °F | |
| Specific heat: | 60°F, 0.115 Btu per lb per °F | |
| | 1800°F, 0.250 Btu per lb per °F | |

The boride-base cermets exhibiting the best high temperature properties to date are not of the metal and ceramic-mixture type. In most instances, bonding was obtained by taking advantage of certain characteristics of the binary-phase diagrams, such as, for instance, a liquid phase produced at eutectic temperatures during sintering. The boron-bonded $ZrB_2$ sometimes referred to as Borolite I, is a typical example of this technique.

All borides of the transition metals of the 4th, 5th, and 6th groups are excellent metallic conductors and therefore exhibit generally satisfactory heat shock resistance. Physical properties of some of the more prominent boride grades are shown in Tables VIII and IX.

**John C. Redmond** *(Kennametal Inc., Latrobe, Pa.)*—It is desirable to clarify the impact values for cermets reported by Messrs. Ault and Deutsch, since they can be interpreted in a misleading fashion. To those accus-

**Table IX. "Borolite" Chromium Boride 400 Series, Physical Properties**

| Grade | 401 | 402 | 403 | 404 |
|---|---|---|---|---|
| Density, grams per cu cm | 7.31 | 7.13 | 6.87 | 6.77 |
| Hardness, $R_A$ | 77.6 | 81.5 | 85.5 | 88.2 |
| Electrical resistivity | 26.8 microhm-cm | 34.2 microhm cm | 52.8 microhm-cm | 54.0 microhm-cm |
| Transverse rupture strength, 1800°F | 139,000 psi | 150,000 psi | 90,000 psi | 120,000 psi |
| Stress-to-rupture life, 1800°F and 14,000 psi | 2000 hr | 3000 hr | In test | In test |
| Oxidation resistance (weight gain—100 hr in air at 2000°F) | 0 | 10.6 mg per sq cm | 13.1 mg per sq cm | Not recommended |
| Heat shock—NACA terminal temperature 2400°F | 200 cycles | 200 cycles | 200 cycles | Not tested |

tomed to thinking in terms of ft-lb values for alloys, it may appear that the in.-lb values are much lower than they are. The in.-lb values were obtained on a small bar with a ¼x3/16 in. cross-section. If impact values are obtained in ft-lb on a standard unnotched 0.394 in. Charpy bar, values of the order of 7 ft-lb may be shown for cermets having an in.-lb value around 3, and we have produced compositions having impact strength of the order of 10 to 12 ft-lb.

Our experience with the running of cermets in turbines also bears out the importance of design. To obtain information as to the capabilities of cermets at higher temperatures, our company has built and has been operating a small radial inward-flow turbine. No satisfactory results were obtained as long as conventional impeller design suitable for alloys was followed. A successful design has now been evolved which is operating satisfactorily at 1800° to 1900°F inlet temperature.

**J. R. Tinklepaugh** *(Alfred University, Alfred, N. Y.)*—The authors have presented an exceptionally complete picture of the status of high temperature-stress material development. It is evident that the titanium carbide-base cermets have been improved significantly during the last two years and that such improvement will continue, particularly in the property of impact resistance.

It should be noted that the development of other types of cermets has not been neglected in spite of the obvious current promise of the titanium carbide-base cermets. Research is continuing at Alfred University on metal-bonded silicon carbide and in many other laboratories on the oxide-base cermets and intermetallics.

The use of Curie temperature by the authors in the study of the solution treatment of cermets is commendable and of real interest, although the apparatus described for these measurements seems almost too simple to obtain the results desired.

The apparatus and techniques used by the various laboratories engaged in the impact testing of cermets has varied widely. On Feb. 2, 1954 representatives of these laboratories met at Alfred University and reviewed the testing methods used and proposed. The techniques and equipment for the Charpy test varied considerably and a large number of those present agreed to set up a "drop test," based on the test described by the authors of this paper, as an approach to standardization of cermet impact testing.

**W. F. Zimmerman** *(General Electric Co., Cincinnati)*—The importance of work related to the improvement of the impact resistance of cermets cannot be overemphasized. Whether this improvement will be accomplished by compositional variations, novel microstructures, heat treatment, or surface conditioning of some type is still uncertain. The fact remains that, as a result of the present low impact strength of cermets, engine-test results to date illustrate the possible catastrophic effects of the first failure of a cermet component from whatever cause, i.e., fatigue, thermal shock, etc.

Modifications in part design and engine-operating conditions are additional factors which are receiving much attention at present. If successful, these factors may serve to control the type of failure to minimize resulting catastrophic effects.

**Dr. Amos J. Shaler** *(The Pennsylvania State University, State College, Pa.)*—How much impact, in a definite numerical figure in in.-lb, is needed?

**J. Bateman** *(formerly with Firth-Sterling, Inc., Pittsburgh)*—I should like to congratulate the authors on their very fine survey of the subject. It is very interesting to note how they stress the design problems involved in the application of these brittle materials.

My work on the subject has been confined to the development of cermets based on titanium carbide in England and lately in the United States. At Hard Metal Tools Ltd., England, we manufactured cermet blades to close dimensional tolerances using similar techniques to those used in the tungsten carbide industry. For engine testing, due to the lack of suitable facilities, we had to test the blades in a production engine which necessitated the use of the conventional fir-tree root fixing.[48] Our method was to replace some of the Nimonic blades with a few cermet ones and to run the engine on a normal test-bed schedule. In all cases, cracking occurred in the root fixing at the reduced cross-section of the serration, which emphasized the notch sensitivity of this type of cermet. Nevertheless, with the first engine test on blades of composition 50 pct Ni-50 pct Ti-Cr carbide, a running time in excess of 100 hr was attained.

Table X. Results for the Two Tests

| Firth-Sterling Inc. | Pratt & Whitney Aircraft Corp. |
|---|---|
| Average, 4.7 ft-lb<br>Range, 4.2 to 5.0 ft-lb | Average, 3.2 in.-lb<br>Range, 2.5 to 3.6 in.-lb |

The majority of the recent work at Firth-Sterling Inc., has been directed towards increasing the impact strength of cermets. One disconcerting feature of this work is the lack of standardization among the industry as to a method of impact testing, a subject which is now receiving some consideration. To establish some relationship between two such tests, bars of FS27 cermet were prepared of sufficient length so that two different unnotched impact specimens could be obtained from them. One set of specimens was tested on a 20 ft-lb capacity Charpy machine and the other set tested on the machine used by Pratt & Whitney Aircraft Corp. The results given in Table X were obtained on specimens of dimensions 0.394x0.394x2.165 in. and 0.187x0.187x2 in., respectively.

These results show that this problem of standardization is a very urgent one and the machine described by the authors is a step in the right direction, for it similates service conditions more than the conventional impact test.

Titanium carbide-base cermets have been found to possess a much higher resistance to deformation when tested in compression-creep tests than when tested in tensile-creep tests. This is due to the hard particles being forced together instead of pulled apart, as is the case when tensile tested. This property should make these cermets a potentially useful material for other applications.

**Julius J. Harwood** *(Office of Naval Research, Washington)*—Resistance to impact may not be as fair a test of the suitability of a material for engine components as resistance to fragmentation. The impact test that is in fairly wide usage is not the same type of impact as engine components receive. Aircraft blading receives high velocity small-mass impacts which tend toward chipping or possible cracking. The correlation between any laboratory test and service experience should be looked into very closely and all possible effort should be made toward designing a laboratory test which adequately represents the conditions in actual turbine operation. What is desired is a test which will provide information about those ductile and toughness properties of materials which are meaningful in terms of the service-performance characteristics which they have to meet.

**G. M. Ault** and **G. C. Deutsch** (authors' reply)—In regard to the comments pertaining to impact, the authors wish to caution against comparison of impact data from different types of test. This was pointed out by Messrs. Redmond and Bateman who gave examples of the variation in magnitude of impact values that can be obtained when different methods of test

are used. These data also emphasize the need for standardization of test mentioned by Messrs. Bateman and Tinklepaugh.

In response to the question by Dr. Shaler, it is impossible at this time to assign a value to the minimum impact strength required for jet-engine turbine blades. The alloy X-40, shown in Table IV to have an impact strength of 48 in.-lb, has been used widely for jet-engine blades and, therefore, can be presumed to have adequate impact strength. Experimental alloys having impact strengths in the neighborhood of 20 in.-lb have been operated successfully as blades in a laboratory-test jet engine at the NACA.

As pointed out by Mr. Harwood, impact failures occurring in engines usually are the result of collision at high velocities and are localized at the point of impact. The present test has been proposed to enable the quick comparison of materials and to aid in development work. A high velocity test simulating the conditions encountered in engines also warrants study.

The authors would like to thank Mr. Bateman for referring to the British experience with cermet turbine blades. This reference is a valuable addition.

Mr. Zimmerman suggests that additional operational gains can be achieved through modifications in part design and engine-operating conditions. Prior design studies have been attempts to improve the blade attachment and have not considered modifications in airfoil designs. The reason for this is twofold: First, a major modification would require the construction of expensive testing facilities for evaluation if necessary; secondly, it has been the desire of the various laboratories to make cermets work in conventional engines without compromise in either blade shape or tolerance. It is known, however, that some changes can be made without affecting the aerodynamic performance of the engine. It appears likely that designs favoring the material properties can be developed and this is believed to offer a fruitful avenue for further research.

**George Stern** *(American Electro Metal Corp., Yonkers, N. Y.)*—American Electro Metal Corp. has been working for some time on porous stainless-steel materials. We have done considerable work with type 316 stainless-steel powder, sintering both in dry hydrogen and in vacuum in order to obtain maximum physical properties. Test shapes have recently been made for evaluation in transpiration cooling and, in these bodies, a combination of sintering and infiltration techniques have been used to achieve maximum strength in critical areas.

**Leonard P. Skolnick** *(Sintercast Corp. of America, Yonkers, N. Y.)*—The authors have mentioned the use of magnetic testing of cermets only on titanium carbide-nickel compositions. I wonder whether this method has been applied to those compositions which contain an alloy matrix.

I should also like to inquire whether heat treatment of the cermet results in a change in the Curie point and whether a relationship exists between the Curie point and the physical properties of the heat-treated titanium carbide cermet.

**Messrs. Ault** and **Deutsch**—In regard to Mr. Tinklepaugh's comment pertaining to the simplicity of the Curie-point apparatus, the authors wish to state that the apparatus is actually very simple and involves only measuring (with a simple beam balance) the force necessary to pull a small permanent magnet away from a flat surface of the cermet specimen in question. The measurements are plotted as a function of specimen temperature and extrapolated to zero force. Repeated calibrations against a pure nickel standard has proven that the method gives an accurate reproducible value for Curie point.

In reply to Mr. Skolnick's question, most of the measurements to date have been made on cermets containing only nickel as the metal addition. Although studies are now underway, no data are available on the relation of Curie point to material properties.

**Dr. Shaler**—The fact that fractures begin at the surface of the cermet should be emphasized. Would surface treatments promise any property improvements?

**Messrs. Ault** and **Deutsch**—Dr. Shaler emphasizes the possible role of the surface in the fracture of brittle materials. In the text, it has been shown that the surface can be improved by diffusion treatments. Preliminary data indicate that this treatment results in an improvement of between 20 and 25 pct in tensile strength; however, some of this increase may be due to the heat treatment which is required to diffuse the surface coating.

**John Preston** *(Curtiss-Wright Corp., Wood-Ridge, N. J.)*—The comprehensive data in the paper by Messrs. Ault and Deutsch is a valuable contribution to the field of powder metallurgy. Materials for high temperature service, especially the refractory alloys produced by powder-metallurgy techniques, are especially interesting to those engaged in the manufacture of aircraft gas-turbine engines.

It is apparent that considerable effort is being expended in impact testing cermets at room and elevated temperatures. There are some who believe that impact strength is the major property for determining the suitability of cermet materials for gas turbines. However, it is recognized that cermets are being developed to function at higher temperatures than are now possible for most cast alloys. Insufficient data have been presented to indicate the thermal-fatigue resistance of cermets at these elevated temperatures. Others believe that thermal-fatigue properties are more important than impact strength. It is suggested that consideration be given to placing more emphasis on resistance to thermal fatigue in evaluating cermets for gas-turbine applications.

I would like to know, from a representative of a carbide producer, what tolerances could be expected on cermet blades in production quantities? Another important consideration to the engine manufacturer is the machining characteristics of cermets. For instance, it would be helpful to us to have a comparison of the machinability of cermets to the cast cobalt-base alloys.

**Mr. Redmond**—I can assure Mr. Preston that tolerances can be met. We have produced several hundred buckets and are now able to meet metal-blade tolerances. The airfoils are now being produced by methods suitable for large-quantity production. The root-grinding methods now in use are not suitable for production, but several methods are being investigated, and a production-grinding process will be available.

I believe Messrs. Ault and Deutsch will agree that there is no problem with surface defects. Inspection methods for internal defects leave something to be desired, but work is under way to investigate such methods as supersonic testing.

**Messrs. Ault** and **Deutsch**—It is understood that by thermal fatigue Mr. Preston means resistance to repeated thermal stress or thermal cycles. Many of the cermet materials have been evaluated in this property and some of the early data are given in refs. 35, 36, and 47. These references indicate that most titanium carbide-base cermets are very resistant to repeated thermal stressing. It should be pointed out that they are not equivalent to the alloys currently being used; however, in a large number of engine runs, the rotating blades have never failed by thermal shock. In the case of the nozzle vanes, the problem may be more critical.

[43] G. Derge: Vacuum Fusion Analysis of Steel for Hydrogen. *Trans.* AIME (1945) **162**, p. 361.
[44] S. Glasstone: *Textbook of Physical Chemistry.* (1951) 2nd Ed., Chap. XIV, pp. 1194-1210. New York. D. Van Nostrand Co.
[45] S. Dushman: *Vacuum Technique* (1949) Chap. 7, pp. 387-390. New York. John Wiley & Sons.
[46] S. T. Harrison: *Special Report No. 43* Iron & Steel Institute, p. 347.
[47] A. L. Cooper and L. E. Colteryahn: The Elevated Temperature Properties of Titanium-Carbide Base Ceramals Containing Nickel or Iron. *RM E51I10* NACA.

**AIME OFFICERS:**
**President**—Leo F. Reinartz
**Vice-Presidents**—T. B. Counselman, L. E. Elkins, Harold Decker, O. B. J. Fraser, A. B. Kinzel, J. B. Morrow
**President-Elect**—H. DeWitt Smith
**Treasurer**—G. F. Moulton
**AIME STAFF:**
**Secretary**—E. H. Robie
**Administrative Ass't. Sec'y.**—Ernest Kirkendall
**Ass't. Secretaries**—J. B. Alford, H. N. Appleton, E. J. Kennedy, Jr., R. E. O'Brien
**Ass't. Treasurer**—P. J. Apol

aime NEWS

# Plant Trips Lead Off Twelfth Electric Furnace Steel Conference

THE Electric Furnace Steel Committee of the AIME will hold its Twelfth Annual Conference at the William Penn Hotel, Pittsburgh, Pa., Dec. 1 to 3, 1954.

Plant trips to McConway & Torley Corp. and U. S. Steel Corp. Duquesne Works have been scheduled for the afternoon of the day preceding the technical sessions. These plant trips will replace the Saturday morning Educational Session and still limit the meeting to three days.

All operating men, repair and maintenance men, metallurgists, ceramic and refractory engineers, observers, and any others interested in the production of more steel, better steel, and cheaper steel are invited to attend. The complete program will be mailed in November, but make plans now to attend this important Conference.

Hotel reservations should be made directly with the headquarters hotel or other Pittsburgh hotels.

The $7.00 registration fee includes a copy of the bound Proceedings when published. There is no registration fee for students at any of the sessions unless they desire a copy of the Proceedings. AIME Members are entitled to a $2.00 reduction in the registration fee.

Bound copies of the 1953 Conference Proceedings are now available at Institute headquarters. Price is $10.00 to the public, ($10.50 foreign) less 30 pct to AIME Members and past registrants.

## *Preliminary Program For Electric Furnace Steel Conference*

**WEDNESDAY, DECEMBER 1**

9:00 am to 9:00 pm
**Registration**

1:00 pm
**Plant Trips**

Leave and return by chartered buses from the William Penn Hotel for two simultaneous plant trips: the McConway & Torley Corp. plant to see a castings shop; the Duquesne Works of the U. S. Steel Corp. to see an ingot shop.

**THURSDAY, DECEMBER 2**

8:30 am
**Registration**

9:30 am
**Opening Session**

Welcoming remarks; announcements and reports.

9:45 am
**Joint Session on Vacuum Melting**

General problems and results of refining techniques; reasons for vacuum melting; experience on pilot scale; improved properties; experience in mechanical working; consumers interest in vacuum melted alloys; European history and practice.

2:00 pm
**Refractories and Masonry**

Evaluation of refractories; bottom materials maintenance; side walls and their maintenance; roof construction and maintenance; effect of intermittent operations on refractories.

2:00 pm
**Castings Metallurgical Session on Melting**

Basic melting practice for quality steel; acid melting practice; high alloy steel melting in basic furnace; melting practice comparison for high alloys.

6:30 pm
**Reception and Cocktail Party**

7:00 pm
**Annual Fellowship Dinner**

**FRIDAY, DECEMBER 3**

8:30 am
**Registration**

9:30 am
**Ingot Session on Quality**

Fluorescent X-ray spectrometer for rapid analysis; low volume hot top for yield; exo-

thermic hot topping; addition of special minor elements to heats.

9:30 am

**Operations in Foundry Melting Session**

Use of high alumina brick in a single slag basic practice; operational experience with a new type control; foundry ladle practice for acid steel; foundry ladle practice for basic steel.

2:00 pm

**Ingot Bull Session**

2:00 pm

**Castings Bull Session**

## Ernest O. Kirkendall Named Administrative Assistant Secretary

E. O. KIRKENDALL

Having in mind the approaching retirement of Edward H. Robie as Secretary of the Institute, the Board of Directors, at their meeting on September 21, named E. O. Kirkendall as Administrative Assistant Secretary effective October 1. Dr. Kirkendall, since January 1946, has been Assistant Secretary of the AIME, also serving as Secretary of the Metals Branch and its constituent Divisions. He is 40 years old and a Michigander by birth. His bachelor degree was earned at Wayne University where he taught metallurgical and chemical engineering for ten years, and his master's and doctor's at the University of Michigan. While in Detroit he was employed on several consulting jobs.

The Board has recommended to the *new* Board taking office in February that Dr. Kirkendall at that time be made Secretary of the Institute, and that Mr. Robie be made Secretary Emeritus for the ensuing year, with duties to be assigned.

## Divisions May Name Nuclear Committees

With a constantly growing number of AIME Members interested in one or another of the phases of the generation and use of nuclear energy, much interest has been expressed in the proposed all-Institute committee on this subject. It is now felt that the most practical method of recognizing Members' interest in the subject is through the appointment of divisional committees, each of which would develop papers and arrange for sessions in the specific field of the division. Such committees would in all likelihood work jointly to a considerable extent, with each other and with similar committees of other societies. Sessions involving various aspects of the finding and utilization of uranium and the other metals of possible similar use may be arranged for the Annual Meeting of the Institute, and for a potential meeting with other societies currently being arranged by Engineers Joint Council the date of which is tentatively set for July 11 to 16, 1955.

The chairmen of the various divisional AIME committees on nuclear energy might compose an all-Institute committee to arrange for joint meetings and publication. To date, only the Institute of Metals Div. has a committee on this subject—its Nuclear Metallurgy Committee.

## Bureau of Mines Station Dedicated

At Reno, Nevada, on September 25, some 200 guests gathered to dedicate the impressive new Rare and Precious Metals Experiment Station of the U. S. Bureau of Mines. Seated in the bright Nevada sunshine on the lawn in front of the building (referred to by one of the speakers as perhaps the largest patch of grass in the state!), the guests enjoyed a short program which included talks by Dr. Minard W. Stout, president of the University of Nevada; J. J. Forbes, director of the Bureau of Mines; Pat McCarran, U. S. Senator from Nevada, (the sudden death of Senator McCarran, a few days later, was a grievous shock to all who knew him); and Felix E. Wormser, assistant secretary of the Interior. Other distinguished guests introduced included: Clifton Young and Walter S. Baring, representatives in Congress from Nevada; Vernon E. Scheid, director of the Mackay School of Mines and the Nevada State Mining Bureau; Jesse Johnson, director of raw materials for the Atomic Energy Commission; T. B. Counselman, vice president of the AIME; Charles W. Mapes, Jr.; Frederick J. DeLongchamps, designer of the building; Steve O'Connor, builder of the structure; Harold C. Miller, regional director of the Bureau of Mines; and Thomas H. Miller, assistant director of the U. S. Geological Survey.

An inspection of the building followed, and then a luncheon at the Riverside Hotel, sponsored by the Nevada Mining Assn. and the Reno Chamber of Commerce. Shortly afterward, Mrs. Felix E. Wormser, president of the Woman's Auxiliary to the AIME, spoke informally before some of the ladies.

## Connecticut Section Opens 1954-55 Season

The first technical session of the Connecticut Section AIME for the 1954-1955 season was held on Wednesday evening, September 22, at the Connecticut Light & Power Co. Auditorium, Waterbury, Conn. Thirty persons attended the session, including 25 members and 5 guests.

Following introductory remarks by Richard J. Christine, Chairman of the Connecticut Section, William E. Milligan of Yale University was presented with a gift in appreciation of his long services as Secretary-Treasurer of the Connecticut Section.

The guest speaker for the evening was W. R. Hibbard, Jr. former associate professor of Metallurgy at Yale University and presently engaged in research for General Electric Co. The subject of his illustrated talk was *Progress In The Understanding of The Properties of Alloys.* By the use of equilibrium diagrams and especially the solid solution systems, Dr. Hibbard discussed the electrical and magnetic properties of alloys. He also included in this interesting talk the high temperature properties and the effect of other alloying elements from the periodic table. The door prize consisting of a book was won by James Kemp at the conclusion of the meeting.

The next meeting will be held November 10 at the Hammond Metallurgical Laboratory, Yale University, New Haven, Conn. Sidney Siegal of the general plate div., Metals & Controls Corp. will speak on, *The Production and Application of Composite Metals.*

## Metals Divisions Plan Annual Meeting Papers

Men at work signs are up all over the country as AIME Members sit down to write the papers, schedule the sessions, and work out the mechanics of the 1955 Annual Meeting slated for the Conrad Hilton Hotel, Chicago, February 14 to 17.

Right now the Chicago Section is making the physical arrangements for the meeting. Other groups, such as the award committees, have been working since the end of the last annual meeting. Two of the high spots of every Annual Meeting have already been filled. Clarence Zener will deliver the IMD Lecture, *Metallurgy of the d-Electrons*, while John Marsh will be the Howe Memorial Lecturer. Mr. Marsh is the 1954 Iron and Steel Div. Chairman.

The Extractive Metallurgy Div. has already formulated a tentative schedule of sessions. Two papers expected to be on the aluminum agenda are: Gas Content of Solid Aluminum by Solid Extraction and Vacuum Fusion, by J. L. Brandt and N. Cockran; and Production of Alumina from Anorthosite, by H. W. St. Clair.

Zinc and lead papers scheduled are Slag Fuming at Flin Flon, by R. E. Mast and G. H. Kent; Processing of Zinc Oxide Fume at Flin Flon, by R. Ellerman; and Separation of Germanium and Cadmium from Zinc Concentrate by Fuming, by H. Kenworthy, A. G. Starleper, and A. Ollar.

Other sessions will include hydrometallurgy, physical chemistry of extractive metallurgy, and titanium. A joint session will cover physical chemistry of extractive metallurgy and physical chemistry of steelmaking. There will be a symposium on refractories for liquid metals and slags.

Outline for the Iron and Steel Div. program is beginning to take shape. Slated for presentation are Solid State Diffusion in the Reduction of Magnetite, by J. O. Edstrom and Gust Bitsianes; Rate of Reduction of FeO From a Lime-Silica-Alumina Slag Over Carbon Saturated Iron, by W. O. Philbrook; and Surface Tension of Slags, by G. Derge.

Another session will feature High Temperature Metallurgy; Rates of Desulphurization at Various Pressures of Carbon Monoxide, by N. J. Grant; Equilibria in Systems Containing Oxygen and Sulphur, by Chipman and Grant; and Desulphurization of Carbon Saturated Iron, by G. Derge and W. O. Philbrook. All told, eight sessions have been scheduled by the division, with one of them reserved for the Chicago Section.

The Institute of Metals Div. has scheduled sessions on powder metallurgy as well as one on titanium. An entirely new session makes its bow at the February meeting with the first Nuclear Metallurgy program.

## Half of Metals Branch Research Fund Received

Approximately half of the $50,000 goal for the Metals Research Publication Fund had been received by the end of September. At its September meeting, the Board of Directors authorized a levy on this fund sufficient to publish approximately 868 pages of Metals Transactions material this year, as had originally been planned, without increasing the Metals Branch deficit beyond the $29,000 figure set in the revised budget. Otherwise a sharp reduction in the amount of metals research papers would have been necessary. Some $7600 will be used from the new Fund for this purpose. The Board also authorized publication of an extra 144-page Transactions supplement in January 1955, the cost of which would be borne by the Fund.

## Change To Be Made In Presidential Rotation

Normally, with the usual rotation, a mining man would be destined to be President of the AIME in 1959. However, that will be the year of the 100th anniversary of petroleum industry in this country and therefore it would be appropriate for the president of the Institute to be representative of that industry. The Mining Branch Council has given its assent, provided a Mining man would be selected for the presidency in 1960 and 1961. The rotation will therefore be: 1955, Mining; 1956, Petroleum; 1957, Mining; 1958, Metals; 1959, Petroleum; 1960 and 1961, Mining; 1962, Metals. The president of course serves as president-elect in the preceding year.

## Name Committee For Fairless Award

A year ago L. F. Reinartz announced to the AIME Board that a new award was being established to be presented annually to an outstanding man in the ferrous field. Last spring the U. S. Steel Corp. provided $13,000 as the principal of a fund to make the award possible, and it was decided that it would be known as the, "Benjamin F. Fairless Award in Iron and Steel Production and Ferrous Metallurgy."

Rules of the award have now been approved by the Board. Briefly they are as follows: The award shall be a bronze plaque. There are no limitations regarding nationality or membership in the Institute. The candidate must be a living person, willing to be present in person to receive the award. A person who has been awarded one of the other major awards of the Institute is ineligible. Nine members of the AIME constitute the award committee. The procedure of selection is essentially the same as for the other major awards of the Institute (details on request from the Secretary's office); nominations must be made by the committee but anyone can suggest suitable names to the committee.

The names of the committee which will select a candidate for the award for the presentation at the Annual Meeting of the Institute in February 1955 are as follows, for terms expiring as indicated: L. E. Berner, Chairman, 1955; E. C. Smith, 1955; K. C. McCutcheon, 1956; J. N. Marshall, 1956; J. S. Marsh, 1957; H. W. Graham, 1957; John Chipman, 1958; G. B. McMeans, 1958; L. F. Reinartz, President AIME, ex officio, 1955.


**PROFESSIONAL SERVICES**

Limited to AIME members, or to companies that have at least one AIME member on their staffs. Rates $40 per year per inch.

ST & CO INC

SCIENTISTS
CONSULTANTS
METALLURGISTS

Small Jobs Welcomed

**SAM TOUR & CO., INC.**

Laboratories and offices
44 Trinity Place, New York 6, N. Y.

Testing—Certifying
American Standards
Testing Bureau, Inc.

ASTB

**OXYGEN IN METALS**
By Wet Procedure
LEDOUX & COMPANY
*Metallurgical Chemists—Spectroscopists*
359 Alfred Ave., Teaneck, New Jersey

**HANS NEUBERT**
PRECISE PROMPT
TECHNICAL TRANSLATIONS FROM GERMAN, SPANISH, FRENCH INTO ENGLISH. $1.00 per 100 WORDS OF THE ENGLISH TRANSLATION.
31 Hilltop Ave. Clark-Rahway, N.J.

**MAX STERN**
Consulting Engineer
Expert for Scrap Recovery and Shipwrecking — Modernization of Plants and Yards for Ferrous and Nonferrous Metal Scrap
149 Broadway New York 6, N. Y.

**H. L. TALBOT**
Consulting Metallurgical Engineer
Extraction and Refining of Base Metals
Specializing in Cobalt and Copper
Room 331, 84 State St., Boston 9, Mass.

# National Open Hearth Committee Local Section Meetings

## EASTERN SECTION

Left: H. W. Potter, C. D. Moore, and C. B. Jenni chat during the afternoon technical session. Above: Panel of experts consisted of D. R. Mathews, Harry Davis, Walter Griffith, E. J. Dattisman, C. F. Chandler, and W. S. Webb.

THE Eastern Section of the AIME National Open Hearth Committee held its annual meeting at the Warwick Hotel, Philadelphia, on Oct. 8, 1954, with 244 registrants. The morning session featured a panel discussion, with audience participation, that could well develop into an all-day session at future meetings. Registrants posed operating problems to the panel of experts: D. R. Mathews, Alan Wood Steel Co., Chairman; Harry Davis, Bethlehem Steel Co.; Walter Griffith, Colorado Fuel & Iron Corp.; E. J. Dattisman, U. S. Steel Corp.; C. F. Chandler, Bethlehem Steel Co.; and W. S. Webb, Barium Steel Co. The experts attempted to answer the questions by drawing on their experience and that of their respective companies. Additional discussion and answers were drawn from the floor. The topics covered all phases of open hearth procedure, with time as the only limiting factor. The full cooperation of the audience kept the session lively.

The afternoon sessions had as Co-chairmen H. W. Potter of Lukens Steel Co., and C. B. Jenni, General Steel Castings Corp. In the session on Furnace Control Equipment, L. W. Eisenhart, U. S. Steel Corp.; F. Klosowski, Colorado Fuel & Iron Corp.; Harry Spiess, Alan Wood Steel Co.; and William Enders, Bethlehem Steel Co. reported on the instrumentation in their particular plants. R. P. Smith, Bethlehem Steel Co. led off the session on Pouring Pit Practice. G. H. Enzian, Jones & Laughlin Steel Corp. showed a high speed movie on pouring taken in the laboratory. A regular film showing bottom pouring practice was narrated by H. A. Grubb and H. W. Potter of Lukens Steel Co. S. A. Ott, Midvale Steel Co. discussed the pouring of large ingots, and W. S. Webb, Barium Steel Co. spoke on basket pouring.

The Eastern Section's annual dinner followed a cocktail party provided by the suppliers committee. C. D. Moore, Vice-chairman of the section welcomed all those in attendance, and introduced the head table guests. Lee Lambing, Chairman of the National Open Hearth Committee spoke about the 1955 National Open Hearth Conference which will be held in Philadelphia. R. L. Batteiger, Chairman of the Suppliers Committee was introduced, and he in turn brought out the Mummers Band that provided the entertainment for the evening. Eastern Section Chairman P. R. Sultzbach was unable to attend the meeting because of illness.

## SOUTHWESTERN SECTION

THE Southwestern Section of the National Open Hearth Committee known as the "Globe trotters" again traveled a considerable distance to hold their fall meeting in Atlanta, Ga. Some 60 left St. Louis and Chicago in two special cars on the afternoon before the meeting arriving in Atlanta on the morning of October 7. Approximately 125 took the plant trip through the Atlantic Steel Co. that afterncon and attended the technical sessions the following day. A souvenir bound volume of the history of the company was presented to those who made the plant trip. The company, one of the small semi-integrated steel plants that are aiding the growth of the Industrial South, specializes in small bars, narrow strip, and wire products for a predominantly agricultural trade. Atlantic Steel also provided a helpful conference program booklet and notebook combination. A special short trip was arranged through the electric furnace dept. for the two dozen ladies who attended. Dinner that evening consisted of a southern barbecue supper at Atlantic Steel Co.'s Glenn Field.

Technical sessions were held both morning and afternoon of the second day. The first paper *Steel Manufacturing Practice at Monterrey, Mexico* by N. Morales of the Cia. Fundidora de Fierro Y Acero de Monterrey was presented by Mr. Gonsales. It was pointed out that the scarcity of scrap in Mexico required a high percentage of hot metal charge. Both the acid bessemer and basic open hearth were therefore used in their practice. The pig iron tends to be high in phosphorus requiring larger than normal amounts of limestone. The second paper, *Recent Developments in Continuous Casting* by John F. Black of Koppers Co., Inc., was effectively presented by using both slides and movies. As was the case with the preceding paper, good discussion followed its presentation.

*Some Observations on the Metallurgical Aspects of Billet-Size Ingot Practice* by R. W. Sandelin of H. K. Porter Co., Inc., reviewed the practice developed over a period of 15 years of producing small size ingots. Demand was sufficient to keep the plant operating at full production. Plain carbon steels with carbon contents running from 10 to 80 points were being produced. Segregation in the smaller ingots, of course, was low. This advantage was counterbalanced by the disadvantage of time required to pour almost 200 ingots per heat. The morning session

closed with a paper entitled *Use of Basic Checkers at Algoma* by C. C. Benton of Algoma Steel Corp. The author pointed out that the maximum advantage of the all basic furnace could only be realized by using checkers at least in the top part of the regenerators. The higher temperatures from the increased firing rates resulted in the use of less fuel per ton. Discussion included some results on the successful use of a suspended flat basic roof.

The afternoon sessions started with the paper *Observations on European Steel Making Operations* by T. T. Watson of Lukens Steel Co. Mr. Watson emphasized that the furnaces used in Europe were small compared to those normally used in the United States and that the raw materials used to make a particular heat of steel frequently varied with the materials available. Thus uniform heat to heat practice similar to that used in this country was not possible. Scrap was scarce, pig was high in phosphorus and metallurgical coke was not available. The low shaft blast furnace lent itself to such conditions. He did point out, however, that at least two steel plants in Europe were both modern and large and were patterned after some of the best steel plants in this country. The ratio of the cost of basic to acid brick is not as great in Europe as it is in this country. Basic bessemer process is extensively used as is oxygen. The bad effects of nitrogen in bessemer steel are counteracted by the use of oxygen and by avoiding a bottom flow as in the Linz-Donawitz process. As much as 40 tons per hr can be produced from this process. K. P. Campbell, metallurgist at the Sheffield Steel Co., presented the paper *Installation and Application of an Electronic Recording Analyzer in a Steel Plant.* While the complete cost of such an installation was approximately $100,000, it was expected that this cost would be repaid through savings in chemicals and the number of technicians required to carry out this very fast process. Samples are sent to the laboratory by means of the pneumatic tube, a flat surface ground, the tests run and the results reported by telegraph within five min. The accuracy is almost as good as the best wet analysis provided the laboratory is located in a constant temperature, constant humidity building.

J. E. Wilbanks, superintendent of melting, Atlantic Steel Co., presented the paper *An Up-to-Date Comparison of Open Hearth and Electric Furnace Operating Costs in a Cold Metal Plant.* Mr. Wilbanks gave actual costs for the year 1953 when both open hearth and electric furnaces were being used at their plant. The figures indicated a very definite advantage for the electric furnaces. The last paper in the afternoon was by Lee Jennings, open hearth superintendent, General Steel Castings Co. in St. Louis, on the subject *Pouring Small Molds with Large Ladle.* The problem faced was that of pouring large and small castings from the same ladle. He described the successful use of a reducer made of bonded graphite cemented inside the nozzle after the large castings were poured. This permitted the pouring of small castings subsequently without the necessity of such sensitive control of the stopper rod.

Friday evening the suppliers provided a cocktail party and the dinner followed in the Dixie Ballroom of the Henry Grady Hotel, the headquarters hotel for this meeting. A watch was presented to Hugh Clark of the American Steel Foundries, the retiring Chairman of the Section who had spent over 40 years in the steel foundry business. The new Chairman of the Section will be J. M. Brashear of the Lone Star Steel Co.

The speaker of the evening was Harry Mehre, Atlanta Journal sports columnist and former football star at the University of Notre Dame, who gave an interesting talk on his experience as football coach. He indicated that those in attendance might feel that they had a hot and difficult job in working around furnaces but his position and the alumni kept him in the furnace. His talk was followed by some excellent movies of Georgia Tech games.

## BUFFALO SECTION

The Buffalo Section of the NOHC opened its meeting on Tuesday, October 5 with a plant tour of the Republic Steel Corp. plant. The technical session convened in the New York Room of the Hotel Statler in the afternoon.

Featured in the technical session was a discussion of refractories for the open hearth which was introduced by M. A. Fay. Other papers given during the afternoon were: *The Flat, Suspended Open Hearth Roof* by R. E. Over, *You Bet Your Life* by Thomas W. Wilson, and *The Oxygen Steelmaking Process* by E. J. McMulkin.

Following the cocktail hour the meeting closed with the annual banquet. Robert P. Gibson, Field Engineer, Republic Steel Corp., spoke on Operation Red Gold. The meeting and banquet was attended by 180 guests and members.

H. H. Northrup, Section Chairman, Joseph L. Walton, Technical Program Chairman, and Harry A. Morlock, Section Secretary, were in charge of the meeting.

In charge of the Buffalo Section meeting were: Joseph L. Walton, Superintendent of Open Hearths, Bethlehem Steel Corp., Lackawanna, N. Y.; Harry A. Morlock, General Refractories Co., Buffalo; and H. H. Northrup, Open Hearth Superintendent, Republic Steel Corp., Buffalo.

Authors presenting papers during the technical session were: R. E. Over, Manager, Open Hearth Department, M. E. Detrick Co.; Thomas W. Wilson, Safety Supervisor, Republic Steel Corp.; and E. J. McMulkin, Research and Development Engineer, Dominion Foundries & Steel Ltd.

# Personals

**J. H. Brannan** has been transferred from the Chicago office of the National Carbon Co., to Cleveland.

J. W. BOLTON

**Marvin L. Steinbuch** has been appointed chief metallurgist and research director of the Lunkenheimer Co., Cincinnati. He succeeds **John W. Bolton** who is retiring. Mr. Bolton had directed the firm's metallurgical research and testing div. for 27 years. Mr. Steinbuch joined Lunkenheimer in 1947.

**Sam Tour,** president of Sam Tour & Co., was recently given an award of merit by the ASTM for service to the Society.

**C. S. Barker** has joined the wheel and brake div. of the Goodyear Aircraft Corp., Akron, Ohio. He had been associated with the metallurgical dept., Westinghouse Research Laboratory, East Pittsburgh, Pa.

**Edwin S. Tankins** has joined the Westinghouse Educational Center, Pittsburgh, Pa.

**Pol Duwez,** professor of mechanical engineering, California Institute of Technology, has terminated his association with the jet propulsion laboratory and will devote all his time to teaching and carrying out research at the Institute.

**Wade W. Winner, Jr.,** U. S. Steel Corp., Pittsburgh, has been transferred to the research laboratory, Kearny, N. J., as turn supervisor, process control.

**Julian Glasser** is technical director for Cramet, Inc., Chattanooga, Tenn. He had been associated with the Armour Research Foundation, Chicago, Ill.

**David S. McLellan,** Reynolds Metals Co., has been transferred from Brookfield, Ill., to Phoenix, Ariz.

**G. Hastings** is with Chromium Mining & Smelting Corp., Ltd., Sault-Ste-Marie, Ont., Canada. He had been located at Beauharnois, Quebec, with Electro-Reagents (Quebec) Ltd.

**William C. Hagel** has accepted a position with the materials and processes laboratory, large steam turbine generator dept., General Electric Co., Schenectady, N. Y.

**L. D. Jaffe** has resigned as chief of the metals research branch of the Watertown Arsenal Laboratory, Watertown, Mass. He has become chief of the materials section of the jet propulsion laboratory of the California Institute of Technology, Pasadena, Calif.

**G. E. Willey** formerly with Algoma Steel Corp., Ltd., Sault Ste Marie, Ontario, has joined the Electro Metallurgical Co., Welland, Ontario.

**John Wallace Barnes** has joined the staff of the processing div., Grand Junctions operations, Atomic Energy Commission. Mr. Barnes has had more than 17 years experience in private industry. He has assisted in building plants and facilities for the Southwest Potash Co., Stanolind Oil & Gas Co., Duval Sulfur & Potash Co., International Minerals & Chemical Corp., and others.

C. E. PETERSON

**Charles E. Peterson** is now chief metallurgist of Mackintosh-Hemphill Co., Pittsburgh, Pa. Mr. Peterson joined Mackintosh-Hemphill in 1949 as a metallurgical assistant. He left the company in 1953 and until recently was a sales and research metallurgist for the rolls div., Blaw-Knox Co.

**William E. Tragert** has been named to the staff of the General Electric Co., research laboratory, Schenectady, N. Y.

**C. W. Jordon, Jr.,** recently accepted a position with International Business Machines Corp., Endicott, N. Y.

F. B. SPEAKER

**Francis B. Speaker** has been named manager of nonferrous metal mining industry sales development by Hewitt-Robins, Inc., Stamford, Conn. He has been with the company since 1945.

**Richard H. Thompson** is now associated with ACF Industries, Inc., New York. Mr. Thompson had been with the American Car & Foundry Co., Berwick, Pa.

**Bernard A. Gruber** has joined the Ethyl Corp., research and engineering dept., Baton Rouge, La. Mr. Gruber had been associated with Metal Hydrides, Inc., Beverly, Mass.

**Robert E. Minto** has been appointed chief metallurgist for Jones & Laughlin Steel Corp., Cleveland Works. Mr. Minto has been associated with Jones & Laughlin since 1923 and has been assistant chief metallurgist since 1950.

**Heath Steele,** vice president and director of the American Metal Co., Ltd., is planning to retire from active service at the end of 1954. He is also retiring as president and director of several subsidiary companies of the firm.

**F. E. Walling** has resigned as general manager of Quebec Iron & Titanium Corp., Quebec. **Roy B. Young** has been appointed to succeed him. Mr. Walling is now associated with Emhart Mfg. Co., Hartford, Conn.

**F. C. Krebs, Jr.,** has accepted a position with the metals div., Utica Drop Forge & Tool Corp., Utica, N. Y., as metallurgical engineer in charge of research and development of powder metallurgy.

**Wayne C. Hazen** has accepted a position with the Kerr-McGee Oil Industries, Inc., Boulder, Colo. He was an alternate group leader for the Los Alamos Scientific Laboratory, Los Alamos, N. M.

**E. C. Van Blarcom** has accepted an appointment to the raw materials div., of the Atomic Energy Commission, Washington, D. C. For the last four years Mr. Van Blarcom has been a consulting metallurgist with Singmaster & Breyer, New York, N. Y.

**L. F. Rains** has retired as president of A. M. Byers Co., Pittsburgh. Mr. Rains had served for 23 years as president and a director. **A. B. Drastrup** succeeds him as president. Mr. Drastrup has been executive vice president since February 1954.

**B. A. Axelrad,** Freeport Sulphur Co., has been transferred from Freeport, Texas to Port Sulphur, La.

**Robert G. Swift** is a metallurgical assistant in the smelter, Phelps Dodge Corp., Morenci, Ariz. Mr. Swift had been superintendent of roasting and leaching with the Tin Processing Corp., Texas City.

**Rudolph E. Peterson** is a metallurgist for the Stanford Research Institute, Menlo Park, Calif. He had been a research metallurgist with Kaiser Aluminum & Chemical Corp., Spokane, Wash.

**Robert W. Balluffi** has been named an assistant professor at the University of Illinois, Urbana, Ill., in the dept. of mining and metallurgy. He had been associated with the Sylvania Electric Products Inc., Bayside, N. Y.

**William J. Kroll,** Corvallis, Ore., has been awarded a Francis J. Clamer Medal by the Franklin Institute, Philadelphia.

**Robert L. Womer** has been appointed vice president in charge of research and development for Speer Carbon Co., St. Marys, Pa. Dr. Womer was formerly assistant for divisional research, Olin Mathieson Chemical Corp.

**Bruce Cramer** has been appointed refractories engineer by the Norton Co., Worcester, Mass., for a new territory consisting of the principal parts of Texas, Oklahoma, Arkansas, and a small part of Louisiana.

**Clyde C. Williams** has been elected vice president of sales, marine and industrial engine div., Chrysler Corp., Detroit.

**Ward W. Minkler,** formerly Pacific coast manager of sales and technical service, has been named assistant manager of market development of the Titanium Metals Corp. of America, New York.

**Marvin C. Y. Lee** is now with the dept. of metallurgy, Lehigh University, Bethlehem, Pa. Mr. Lee had been at the Hammond metallurgical laboratory, dept. of metallurgy, Yale University, New Haven, Conn.

**George J. Zimmerman,** formerly chief of the technical liaison div., office of chief of engineers, Corps of Engineers, U. S. Army, has been appointed staff assistant for management controls of the Carborundum Co., Niagara Falls, N. Y.

**Ronald D. Gumbert** has been appointed a vice president of the Mercast Corp., New York. Mr. Gumbert will continue as executive vice president of Alloy Precision Castings Co., Cleveland, a Mercast licensee.

**George W. Belcher** has been appointed central district manager of sales and technical service, Titanium Metals Corp. of America, Chicago.

**Lawrence E. O'Donnell, Raymond R. Hindersinn,** and **William J. Strachan,** have joined the staff of the research and development dept., Hooker Electrochemical Co., Niagara Falls, N. Y.

**Herbert Hoover,** former president of the United States and a former president of AIME, was awarded the status of Fellow in the Standards Engineers Society, Camden, N. J. This is the highest award of the Society.

**John R. Parks** has been named flotation sales engineer for the chemical div. of Armour & Co., Chicago.

**Kenneth C. Vincent,** ceramics and minerals research dept., Armour Research Foundation, Illinois Institute of Technology, Chicago, now heads the ore dressing section. This newly organized section is concerned with the beneficiation of both nonmetallic and metallic ores. Mr. Vincent was formerly chief metallurgist, Baroid Sales Div., National Lead Co., Malvern, Ark.

**George E. Keller** is manager, coal evaluation, U. S. Steel Corp., Pittsburgh. He was chemical director, manager, Commercial Testing & Equipment Co., Charleston, W. Va.

**Fred J. Hoff** is with Climax Molybdenum Co., Climax, Colo.

**Carlos E. Roggero** is shift foreman, Electrothermic Zinc Plant Co., Cerro de Pasco Corp., La Oroya, Peru.

# Proposed for Membership
## — Metals Branch AIME —

*Total AIME membership on Sept. 30, 1954 was 21,466; in addition 1738 Student Associates were enrolled.*

*ADMISSIONS COMMITTEE*

*O. B. J. Fraser, Chairman; R. B. Caples, Vice-Chairman; F. A. Ayer, A. C. Brinker, R. H. Dickson, Max Gensamer, Ivan A. Given, Fred W. Hanson, T. D. Jones, Sidney Rolle, J. H. Scaff, John T. Sherman, F. T. Sisco, Frank T. Weems, R. L. Ziegfeld.*

*The Institute desires to extend its privileges to every person to whom it can be of service, but does not desire as members persons who are unqualified. Institute members are urged to review this list as soon as possible and immediately to inform the Secretary's office if names of people are found who are known to be unqualified for AIME membership.*

*In the following list C/S means change of status; R, reinstatement; M, Member; J, Junior Member; A, Associate Member; S, Student Associate.*

**Arizona**
*Douglas*—Lindsey, Harry F. (M)

**California**
*Berkeley*—Washburn, Jack (M)

**Connecticut**
*New Canaan*—Bittenbender, William P. (A)

**Illinois**
*Chicago*—Anthonisen, Robert P. (M) (C/S—A-M)
*Chicago*—Hall, Camden E. (A)
*Chicago*—Lloyd, Donald W. (M)
*Chicago*—Tarr, Clarence M. (J)
*East Alton*—Seastone, John B. (M)
*Elmhurst*—Mueller, Melvin H. (M)

**Indiana**
*East Chicago*—Dotlich, Mike (M)
*East Chicago*—Weydert, Vernon C. (A)
*Gary*—Hubbard, Frank B. (M)
*Hammond*—White, Robert D. (M)
*Munster*—Dann, Theodore E. (M) (R. M)

**Michigan**
*Allen Park*—Hart, Warren E. (A)

**New Jersey**
*Fairlawn*—Connelly, Joseph J. (M)
*Hackensack*—Mazza, Edmund N. (M)
*Pennsauken*—Pease, Charles C. (J)

**New York**
*Hamburg*—Walton, Joseph L. (M) (C/S—A-M)

**Ohio**
*Akron*—Wittenberg, Robert B. (A)
*Alliance*—Schwartz, George J. (A)
*Canton*—Fogarty, John E. (J)
*Cleveland*—Hodge, James C. (A)
*Columbus*—Wahli, Marshall J. (M)
*Steubenville*—Wallace, Samuel I. (M) (C/S—A-M)
*Terrace Park*—Collier, Russell L. (A)

**Pennsylvania**
*Clairton*—Halpin, John A. (A) (R. C/S—S-A)
*Johnstown*—Pullen, Frederick R. (A)
*Palmerton*—Brock, Geoffrey E. (J)
*Pittsburgh*—Conway, Leon F. (A)
*Pittsburgh*—Egger, Eduard J. W. (A)
*Pittsburgh*—Foster, Floyd W. (A)
*Pittsburgh*—Hartman, Earl R. (A)

**South Dakota**
*Rapid City*—Anderson, Paul H. (M) (R. C/S—A-M)

**Texas**
*Lone Star*—Anderson, S. Glenn (M)

**West Virginia**
*Charleston*—Fetzer, William W. (J)

**Ceylon**
*Kottiyakumbura*—Perera, Weerakondabaduge, A. (A)

**England**
*Warwickshire*—Allender, Peter J. (M)

**Germany**
*Bremen-St. Magnus*—Schaaber, Otto (M)

**India**
*Calcutta*—Jain, Sumeru C. (M)

**Sweden**
*Stockholm*—Willners, Sven H. (A)

# Obituaries

An Appreciation of

**Charles Augustus Carlow**

By Eugene McAuliffe

There passed away at his home, Kincaple, St. Andrews, Scotland, on the morning of Friday, 13th August, one of the great leaders of the British coal mining industry, Mr. Charles Augustus Carlow, the former chairman and managing director of the Fife Coal Co., Ltd., the company's mines located in Fifeshire, Scotland.

Mr. Carlow came of a family connected with the Scottish coal industry for more than a century. His first position was that of a mining engineer student in the Leven office. Quickly adapting himself to the work, he was made medalist Cowdenbeath Mining School during the years 1897 to 1898 and again in 1898 to 1899. He was also medalist in Cowdenbeath Mining School in 1899. On the fiftieth anniversary of the company, he gave his home, Linwood Hall, Leven, as a convalescent home for miners' wives and the company's women workers. Throughout his entire career, he gave much of his time and means to the welfare of his employees, their families and the public. Dr. Carlow never married.

Many honors came to Dr. Carlow, including the presidency of the Mining Institute of Scotland, 1932-36; president of the Institution of Mining Engineers, 1936-38; and in 1946 he was made an Honorary Member of the AIME and a similar honor was conferred on him by the British Institution of Mining Engineers in 1952. The last major honor received by him in 1952, was that of an Honorary L.L.D. by St. Andrews University, the oldest university in Scotland, which dates back to the year 1411.

Mr. Carlow wrote many technical papers relating to coal mining and management, perhaps his *magnum opus* was his paper "World Coal Resources," read at the Seventy-fifth Anniversary meeting of the AIME in March 1947, this paper covering fifty pages in the Anniversary Volume. At this meeting, held in New York City, Dr. Carlow, a man of commanding presence, of affable and courteous demeanor, made many, many friends within the ranks of the Institute.

With thousands here and abroad, it was a great privilege to call Dr. Carlow "my friend."

An Appreciation of

**Albert A. Hoffman**

By William Wallace Mein

It is with a sense of deep personal loss that I must record the passing in Oakland, Calif., on May 4, 1954 of Albert A. Hoffman, vice president, consulting engineer and director of Calaveras Cement Co. for 10 years.

Bert Hoffman was a distinguished engineer and mine manager of wide experience. He came to Calaveras Cement Co. in 1944 to supervise the erection of a new kiln, and remained to steer us through two major plant expansions that trebled our capacity. His foresight and guidance were an inspiration to all who worked with him.

Hoffman was born in Parsons, Kan., July 28, 1880, and was graduated from the University of Kansas with a B.S. in mining engineering. His great mechanical aptitude showed itself early, and after two years' experience as repair foreman for the Green Cananea Copper Co., he became mechanical superintendent for Braden Copper Co. where he remained until 1912. He then moved to Chile Copper Co. where he was construction superintendent from 1912 to 1916, until World War I called him as a Captain of Ordnance, U. S. Army.

At the end of the war he returned to South America where he was successively assistant general manager of Andes Copper Co. from 1919 to 1929, and manager of Anglo Chilean Nitrate Co. from 1929 to 1932.

In 1932 he returned to the United States where he was an independent consultant until 1936. In 1936 industry called him again. From 1936 to 1942 he was California manager of the American Potash & Chemical Corp. and president of Trona Ry. Co.; from 1942 to 1943 manager of the Nicaro Nickel Co., New York and Cuba; and from 1943 to 1944 manager of the Manganese Ore Co., Henderson, Nev. It was when this plant closed down that he joined the staff of Calaveras Cement Co.

Hoffman was a member of the AIME, ASME, MMSA, AOA, AF & AM, and the Engineers Club of San Francisco.

Hoffman was married in Chile in 1915 to Edith Morgan of Nevada City, Calif., who survives him. He is also survived by a son, John Morgan Hoffman of Porterillos, Chile; two daughters, Mrs. Rachel Woolett of Whittier, Calif., and Mrs. Fergus Joy of Los Altos, Calif., and six grandchildren.

## Necrology

| Date Elected | Name | Date of Death |
|---|---|---|
| 1934 | C. Augustus Carlow | Aug. 13, 1954 |
| 1949 | E. Y. Ellis | Aug. 24, 1954 |
| 1926 | Thomas W. Guy | Sept. 9, 1954 |
| 1937 | C. H. Heist | Unknown |
| 1928 | Walter L. Kohlberg | July 22, 1949 |
| 1907 | John H. Leavell | Sept. 15, 1954 |
| 1890 | Spencer Miller | June 1953 |
| 1919 | John Hunter Nead | Sept. 13, 1954 |
| 1954 | Charles M. Paul | Sept. 1, 1954 |
| 1937 | Roger H. Sherman | Sept. 5, 1954 |
| 1944 | Rush T. Sill | Aug. 19, 1954 |
| 1951 | Charles E. Sumpter | Sept. 13, 1954 |
| 1916 | Arthur D. Terrell | February 1954 |
| 1948 | Stanley M. Walker | June 17, 1954 |
| 1923 | Nicholas A. Ziegler | Aug. 20, 1954 |

# Advertisers' Index


| | |
|---|---|
| Air Reduction Co., Inc.<br>*G. M. Basford* | * |
| Ajax Engineering Corp.<br>*Eldridge, Inc.* | 1175 |
| Aluminum Co. of America<br>*Fuller & Smith & Ross Inc.* | 1188 |
| American Bridge Div., U. S. Steel Corp.<br>*Batten, Barton, Durstine & Osborn, Inc.* | 1173 |
| Bailey Co., Wm. M.<br>*Walker & Downing* | Third Cover |
| Bell Telephone Labs.<br>*N. W. Ayer & Son, Inc.* | * |
| Buehler Ltd.<br>*Kreicker & Meloan, Inc.* | * |
| Carondelet Foundry Co.<br>*Whitehead & Sprague, Inc.* | Second Cover |
| Chemical Construction Co.<br>*Michel-Cather, Inc.* | * |
| Electro Met. Div., Union Carbide & Carbon Corp.<br>*J. M. Mathes, Inc.* | 1177 |
| General Electric Co., X-Ray Dept.<br>*Klau, Van Pietersom-Dunlap Assoc.* | * |
| Great Lakes Carbon Corp.<br>*Davis, Parsons & Strohmeier, Inc.* | 1181 |
| Harbison-Walker Refractories Co.<br>*Walker & Downing* | * |
| Hevi Duty Electric Co.<br>*Camm & Costigan Inc.* | * |
| International Nickel Co.<br>*Marschalk & Pratt Co.* | 1186 |
| Minneapolis-Honeywell Regulator Co.<br>*Aitkin-Kynett Co., The* | * |
| Molybdenum Corp. of America<br>*Smith, Taylor & Jenkins, Inc.* | * |
| Morgan Construction Co.<br>*Davis Press, Inc., The* | 1185 |
| National Carbon Div., Union Carbide & Carbon Corp.<br>*William Esty Co., Inc.* | Fourth Cover |
| Pittsburgh Lectromelt Furnace Corp.<br>*Fuller & Smith & Ross Inc.* | * |
| Ramtite Co., The<br>*Marsteller, Gebhardt and Reed Inc.* | * |
| Smeeth-Harwood Co.<br>*Allbright Associates Adv.* | * |
| Stokes Machine Co., F. J.<br>*John Mather Lupton Co., Inc.* | * |
| Titanium Alloy Mfg. Div., National Lead Co.<br>*Comstock & Co.* | 1178 |
| U. S. Steel Corp.<br>Columbia-Geneva Steel Div.<br>Tennessee Coal & Iron Div.<br>U. S. Steel Supply Div.<br>U. S. Steel Export Co.<br>*Batten, Barton, Durstine & Osborn, Inc.* | * |
| Vacuum Metals, Inc.<br>*Sutherland-Abbott* | * |
| Wyman-Gordon Co.<br>*John W. Odlin Co., Inc.* | 1172 |


* Previous issue.

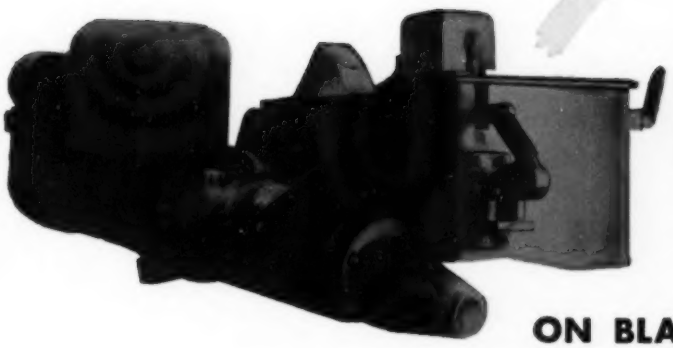

# Controlled POWER

FOR PLUGGING
TAPPING HOLES

**ON BLAST FURNACES**
**ON LARGE ELECTRIC FURNACES**

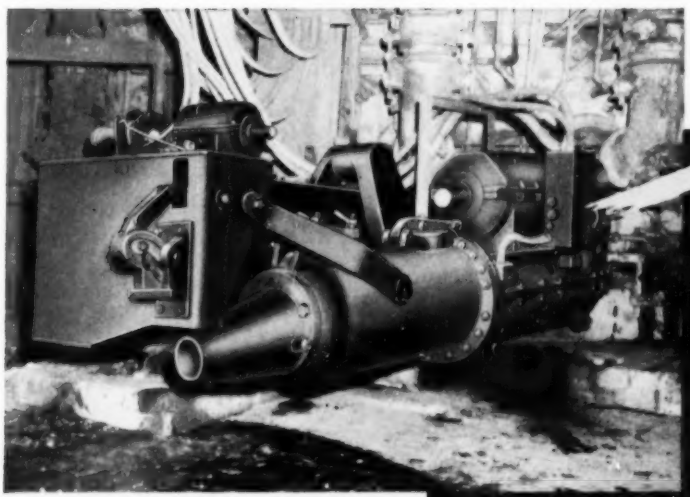

## Bailey CLAY GUNS

Long a standard of precision and safety on blast furnaces, Bailey Clay Guns now are used on large electric furnaces as well.

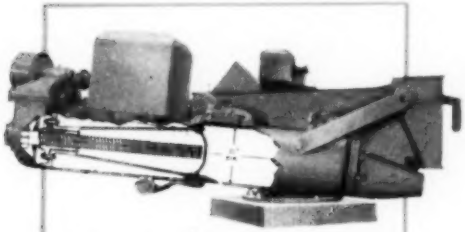

The plunger is driven by a highly efficient power screw and double reduction gear drive. Design is such that Bailey Clay Guns are operated by three separate motor drives.

These guns supply clay under high pressure exactly where it is needed to give best results and safety in quickly plugging tapping holes. Fast, accurate and solid positioning is assured by an exclusive pedestal support and lever mechanism. Since the electrically-driven piston develops a clay pressure of 600 psi, there is ample power to maintain long tapping holes.

WILLIAM M. Bailey COMPANY
ENGINEERS
LEADERSHIP THROUGH QUALITY

1221 BANKSVILLE ROAD — PITTSBURGH 16, PA

# Want greater Electrode Savings?

*Take these tips from*

## NATIONAL CARBON

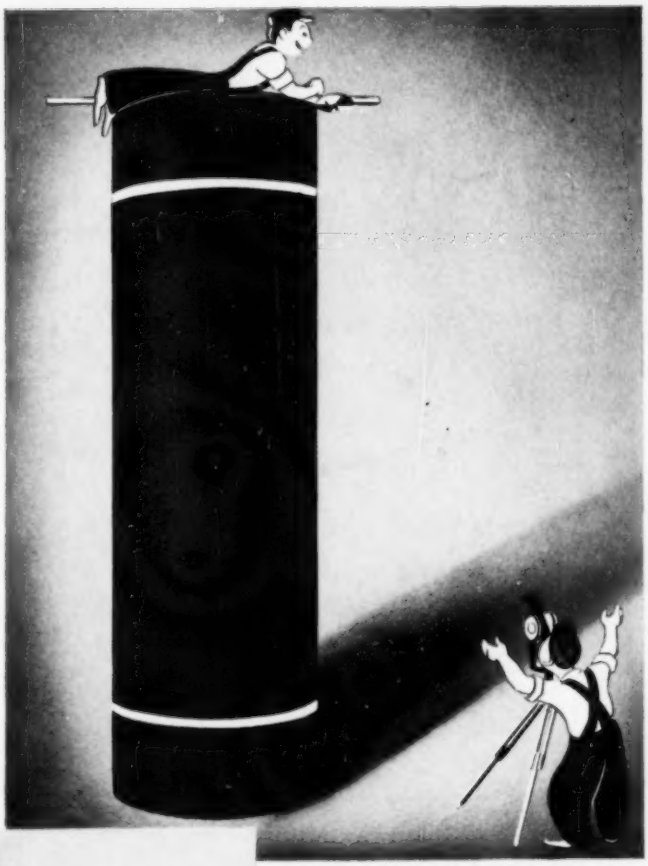

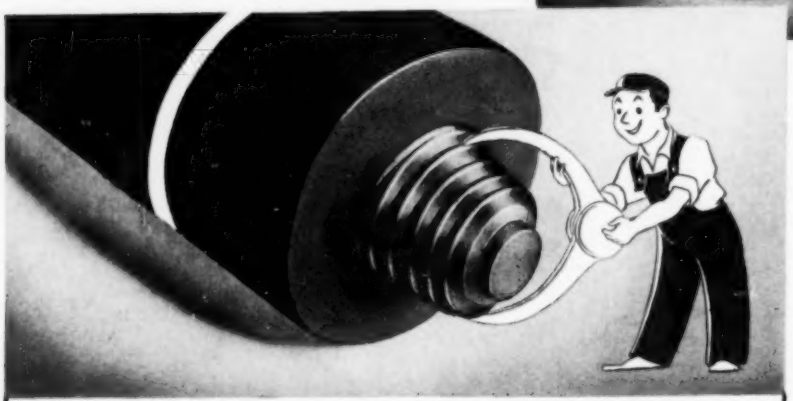

**LOOK AT NIPPLE SIZE.** Electrode nipples are another potential source of economy and improved performance. For example, if you use electrodes of 16" diameter or larger, and you are not already using the smaller nipples *pioneered by* NATIONAL CARBON COMPANY, you may be able to make this switch and save money while getting even stronger joints due to the thicker socket-walls provided by the smaller nipple sizes.

**LOOK AT ELECTRODE LENGTH.** Frequently we are able to direct customers to valuable economies in cost-per-pound of electrode, as well as to other cost-saving advantages, simply by recommending a longer length than they are already using. For instance, when you switch from a 60" electrode to one of 72", you reduce the number of electrodes, handled and used, by *one in six,* and, even more important, you cut down the number of joints made by the same high percentage. Obviously, this increases furnace-availability and boosts production.

• These are only two of many ways that NATIONAL CARBON'S electrode technical-service facilities have helped users get the most for their electrode dollar. Let your NATIONAL CARBON representative survey your electrode and nipple requirements. He may help you get substantial savings and improved electrode performance.

**FOR ELECTRODES AND ELECTRODE SERVICE...rely on NATIONAL CARBON COMPANY!**

*The term "National" is a registered trade-mark of Union Carbide and Carbon Corporation*

**NATIONAL CARBON COMPANY**

**A Division of Union Carbide and Carbon Corporation • 30 East 42nd Street, New York 17, N. Y.**

*Sales Offices:* Atlanta, Chicago, Dallas, Kansas City, New York, Pittsburgh, San Francisco

IN CANADA: Union Carbide Canada Limited, Toronto

# Journal of METALS

TRANSACTIONS SECTION

# Strain Hardening of Latent Slip Systems in Zinc Crystals

by E. H. Edwards and Jack Washburn

**Zinc crystals were deformed in simple shear and it was found that anisotropic strain hardening occurred in which the inactive slip systems were hardened more than the active system. The formation of dislocation barriers by dislocation interaction was discussed as a possible explanation of the hardening of the latent systems.**

STRAIN hardening which accompanies slip in a metal crystal is not limited to the slip systems actively contributing to the plastic strain. There is also a strengthening of the latent slip systems which are crystallographically equivalent to the active system. In the case of aluminum deformed in tension, Taylor and Elam[1] found that plastic flow on one set of octahedral planes caused either the same or a slightly greater hardening on an inactive set. Similar results have been obtained for crystals of $\alpha$ brass[2] and of Cu-Al solid solutions.[3] Experiments by Röhm and Kochendörfer[4] indicated that the hardening of the active system exceeded the hardening of any latent system for aluminum crystals deformed in shear. On the other hand, strain hardening in zinc and cadmium crystals tested in simple shear at −196°C was recently found to be greater in the latent than in the active slip direction.[5] When the strain direction was shifted during testing to a direction 60° from the original, a higher stress was required for glide to continue than would have been needed for flow to proceed in the original direction.

The relation between the hardening of active and latent systems must be complex, depending upon the relative orientations of the systems and upon the experimental techniques used to deform the crystal. A detailed knowledge of the hardening produced in latent systems would be valuable in choosing between possible dislocation models of the strain-hardening process. The experimental data now available are incomplete and even contradictory. The present study was undertaken to provide quantitative information regarding the relative amount of hardening of active and latent systems for a particularly simple case. Zinc crystals were deformed in simple shear along one of the three crystallographically equivalent directions $[2\bar{1}\bar{1}0]$, $[\bar{1}2\bar{1}0]$, and $[\bar{1}\bar{1}20]$ in the slip plane, and the relative hardening produced in each of these directions was compared.

## Experimental Procedure and Results

The single crystals of 99.99 pct purity zinc used in this investigation were grown from the melt in the form of 1 in. diam spheres. Shear specimens were acid-machined from the crystals by a method which has been described previously.[6] The gage section of the test specimen was a cylinder having a height of 1/8 in. and a cross-sectional area of approximately 1/3 sq in. All specimens were machined with the axis of this cylindrical gage section aligned with the [0001] axis of the crystal.

An innovation in the design of the shearing apparatus for these tests was the provision for a rapid shift in the direction of the applied stress from one slip direction to any other slip direction lying in the same slip plane. Fig. 1 shows a section through the specimen and shearing apparatus, and Fig. 2 is a

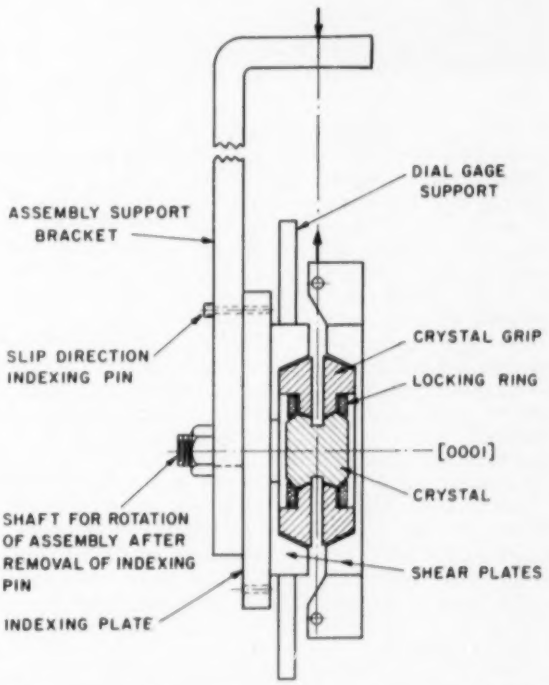


Fig. 1—Schematic diagram of apparatus used for testing crystals in simple shear at −196°C. Direction of straining could be shifted during testing from a given slip direction to any other slip direction lying in the same slip plane. Assembly was submerged during testing in liquid nitrogen contained in a Dewar flask.

E. H. EDWARDS is Materials Engineer, Standard Oil Co. of California, San Francisco, and J. WASHBURN is Assistant Professor of Metallurgy, University of California, Berkeley, Calif.

Discussion on this paper, TP 3826E, may be sent, 2 copies, to AIME by Jan. 1, 1955. Manuscript, Apr. 15, 1954. Chicago Meeting, November 1954.



*The Transactions papers appearing in the Journal of Metals during 1954 will subsequently appear in AIME Transactions Volume 200, and may be permanently referenced to that volume.*

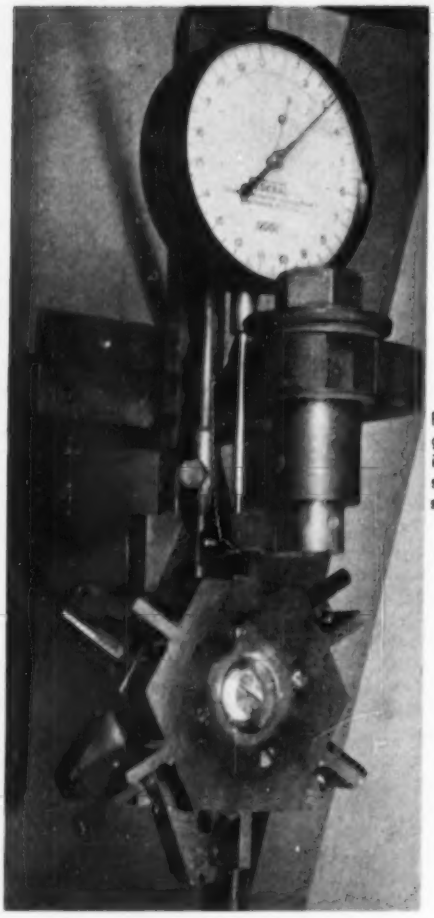

Fig. 2—Photograph showing details of shearing assembly.

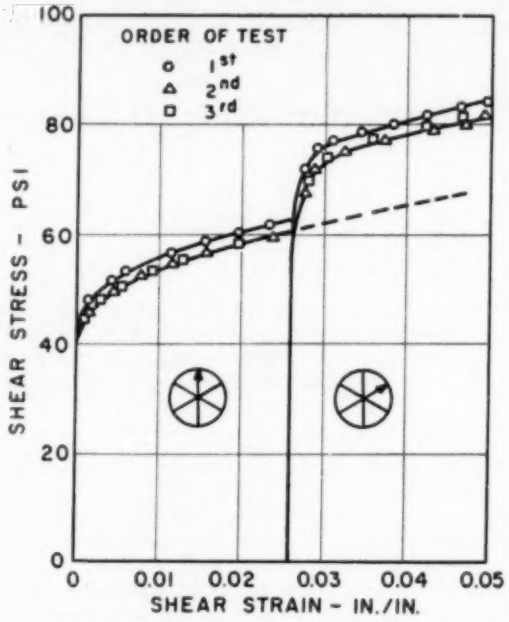


Fig. 3—Three successive stress-strain curves from a zinc crystal showing the effect of shifting the strain direction during testing to a new direction 60° from the original direction of slip. Complete recovery of mechanical properties was achieved by an anneal of 1 hr at 400°C before each test.

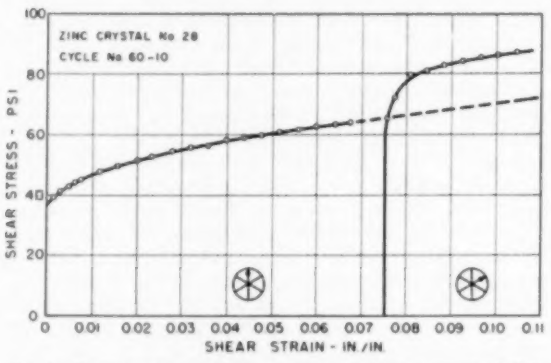


Fig. 4—Stress-strain curve for a zinc crystal showing effect of shifting the strain direction during testing at —196°C to a new direction 60° from the original direction of slip after a strain of 0.076 in the original direction.

photograph of the complete assembly with extensometer in position. During a test the specimen and shearing apparatus were submerged in liquid nitrogen. A shift from one slip direction to another could be accomplished without removal of the assembly from the nitrogen, thus avoiding the possibility of recovery occurring during the interval in which the direction change was being made. The crystals were sheared at a constant strain rate of 3 pct per min.

The observation that hardening of a latent slip system may exceed that of the active system appears to be generally valid for zinc. A considerable number of crystals with somewhat different previous histories with regard to orientation during growth, heat treatment, and macrosubstructure were strained approximately 4 pct in a given slip direction at —196°C, unloaded, and immediately strained in a second slip direction 60° from the original direction. In every instance, after exceeding a small value of strain in the second direction, the shear stress corresponding to a given total strain was higher than would have been observed had slip continued in the original direction.

The strain hardening, including the increment due to this change in slip directions, could be completely eliminated by annealing. Fig. 3 shows three successive stress-strain curves obtained from the same crystal for which the direction of straining was shifted during each test to a new slip direction 60° from the first after a strain of 2.6 pct in the original direction. The crystal was annealed for 1 hr at 400°C before each test. Selection of any one of the three slip directions as the first active direction after annealing produced the same set of curves. As a consequence of this complete recovery, it was practicable to study, in the same crystal, the magnitude of the hardening of each latent system in relation to the amount of previous strain in the active system. Errors which might have been introduced by comparing data obtained from crystals of different degrees of internal perfection were thus avoided.

A series of tests was performed on a crystal in which the strain in the original direction was varied from 0.3 to 10 pct before shifting to a second strain direction. Representative examples of the individual tests are reproduced in Figs. 4 and 5, showing the effect of shifting to a new slip direction 60° and 120°, respectively, from the original direction. The shear-stress increase accompanying such a shift in strain directions (measured after a strain of 3.0 pct in the

second direction) was found to increase as a function of strain in the original direction (Fig. 6). The magnitude of this shear-stress increase rises sharply for small strains in the original direction, but at larger strains, the rate of increase diminishes and becomes linear with strain in the first direction. All the data recorded in Fig. 6 were obtained from a single specimen. The only significant difference between the results obtained from 120° shifts of direction as compared to those from 60° shifts was the occurrence of a small amount of strain at low stress levels when the strain direction was shifted 120°.

Another series of tests were performed in which the strain direction was changed by 180°, using the same crystal from which the data in 60° and 120° shifts in strain direction were obtained. A representative example of one of these tests is shown in Fig. 7. A measurable amount of strain in the reverse direction was always observed at a very low applied stress, and a considerable reverse strain occurred before a stress equal to the maximum achieved in the forward direction was reached. Even at very large strains in the reverse direction, the stress was less than the value it would have reached at the same total strain had the reversal not taken place. A portion of the strain hardening thus was permanently lost as a result of the reversal. Fig. 8 shows that the stress-strain curve after reversal of the strain direction fell below the extrapolated original curve by an amount that increased in an approximately linear manner with strain in the original direction. The decrease in the flow stress plotted in Fig. 8 was measured after a strain of 3 pct in the reverse direction.

## Discussion and Conclusions

No adequate theory for strain hardening accompanying the plastic deformation of metal crystals by simple slip (easy glide, lamellar slip) has yet been proposed. Kochendorfer[4] has suggested that this hardening, which is approximately linear with strain, is due to the action of back stresses created by dislocations piled up at regions of crystal imperfection. The local stress at dislocation sources was assumed thereby to be decreased and continued slip would then require an increase in applied stress. Mott[7] has suggested that the primary barrier to the motion of dislocations is probably other dislocations which cut across the active slip plane and have a Burgers-vector component normal to the slip plane. In cubic structures, these dislocations could lie on other equivalent slip planes; in hexagonal crystals, they would be dislocations with a Burgers vector in the c direction. The motion of the screw segments of the dislocation loops expanding from a source in the slip plane would be retarded by these intersecting dislocations. Read[8] has pointed out that the crossing of two screw dislocations at right angles produces a step in each of the dislocations. Any motion of the stepped screw dislocation is accompanied by the formation of a row of lattice vacancies or interstitial atoms which are left behind the moving step.

The experimental results obtained from the 180° reversal of applied stress are not inconsistent with

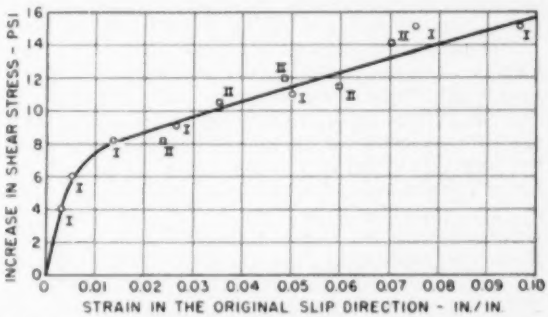


Fig. 6—Increase in shear stress as a result of shifting the strain direction to a new direction during testing at —196°C as a function of strain in the original slip direction. I—New slip direction 60° from the original direction. II—New slip direction 120° from the original direction. Stress increase measured after a strain of 0.03 in the new direction.

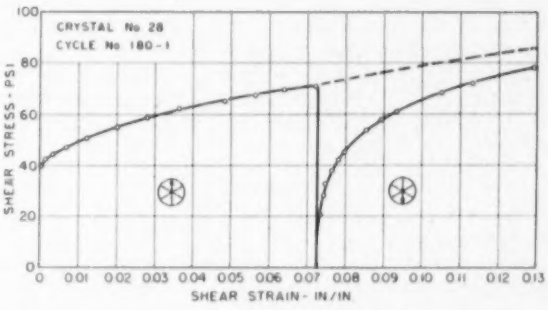


Fig. 7—Stress-strain curve for a zinc crystal showing the effect of reversing the direction of straining after a strain of 0.073 in the original direction during testing in simple shear at —196°C.

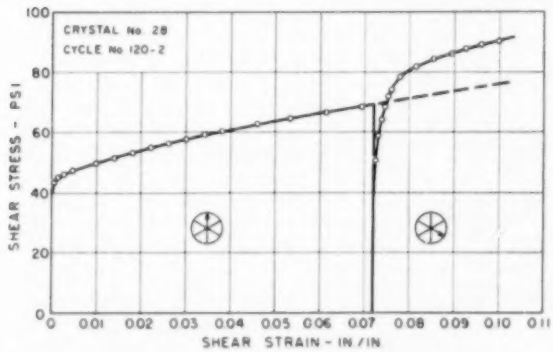


Fig. 5—Stress-strain curve for a zinc crystal showing the effect of shifting the strain direction during testing at —196°C to a new direction 120° from the original direction of slip after a strain of 0.072 in the original direction.

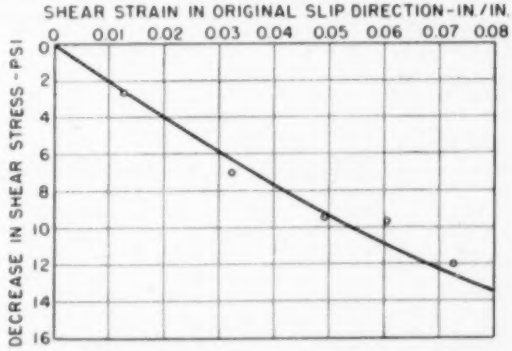


Fig. 8—Curve showing decrease in the shear stress accompanying reversal of direction of straining during testing in simple shear at —196°C as a function of the strain in the original direction. Decrease in stress was measured after a strain of 0.03 in the reverse direction.

the thought that a strained crystal may contain dislocation loops which have encountered obstacles and therefore have not been able to spread completely across the slip plane. The low stress required to initiate strain in the reverse direction appears to confirm the idea of a back stress due to such partially expanded loops. The permanent loss of strain hardening accompanying continued strain in the back direction might be due to dislocations of opposite sign issuing from the same sources which were responsible for the strain in the first direction. These could have the effect of partially eliminating the barriers by combination of dislocations of opposite sign. Only a shift of 180° in the direction of straining would be expected to be accompanied by a permanent loss of a portion of the strain hardening.

The results of the 60° and 120° shifts of strain direction are not easily understood on the basis of a simple picture of back stresses. The component of the back stress acting in any direction in the same slip plane should vary with the cosine of the angle between this direction and the initial direction,[4] and hence the strain hardening should be greatest in the original direction. Contrary to this conclusion, it was found that the hardening in 60° and 120° directions was greater than the hardening in the original direction. It would appear, therefore, that the action of back stresses on the sources of dislocations is not the controlling factor. An alternative approach is to assume that additional barriers are formed in the early stages of strain in the new direction, perhaps as a result of dislocation reactions of the type $a/3[2\bar{1}\bar{1}0] + a/3[\bar{1}\bar{1}20] \rightarrow a/3[1\bar{2}10]$ between the dislocations being generated by the applied stress in the new direction and those already present due to strain in the first direction. The magnitude of the hardening effect due to the barriers of this type might be expected to be proportional to the number of them formed, which in turn might be proportional to the density of dislocations left in the crystal after straining in the first direction.


### Summary

When a zinc crystal is deformed in simple shear, anisotropic strain hardening occurs in which the inactive slip systems are hardened more than the active one. The hardening effect is substantially the same for latent systems whose directions lie at 60° and 120° to the slip direction of the active system. The hardening of the latent systems is apparently due to dislocation barriers formed in the crystal during the initial stages of plastic flow in the latent directions. These barriers to dislocation movement in latent directions are of a type which can be removed by annealing.

When the direction of straining is reversed, plastic flow begins at a stress much lower than that required for the onset of slip in the original direction. This effect is attributed to movement of dislocations which are trapped at internal barriers during deformation in the forward direction but which can move freely in the reverse direction. The permanent loss of a portion of the strain hardening when the direction of straining is reversed may be due to annihilation of some of the dislocations trapped in the crystal during straining in the first direction.



### Acknowledgment

The authors are grateful for the support of the Office of Naval Research which made a portion of this work possible. The authors are especially indebted to Professor Earl R. Parker for his valuable advice and his constructive suggestions. Thanks are also due to Dr. Betsy Ancker and C. H. Li for their helpful discussions and to Leslie Seaborn and Robert Arneson for their assistance in the construction of apparatus.


### References


[1] G. I. Taylor and C. F. Elam: *Proceedings* Royal Society (1925) **A108**, p. 28.

[2] v. Golar and G. Sacks: *Ztsch. Physik* (1929) **55**, p. 581.

[3] C. F. Elam: *Proceedings* Royal Society (1927) **A115**, p. 133.

[4] F. Rohm and A. Kochendorfer: *Ztsch. Metallkunde* (1950) **41**, p. 265.

[5] E. H. Edwards, J. Washburn, and E. R. Parker: *Trans.* AIME (1953) **197**, p. 1525; JOURNAL OF METALS (November 1953).

[6] E. R. Parker and J. Washburn: Deformation of Single Crystals. *Modern Research Techniques* ASM Seminar (1952).

[7] N. F. Mott: *Philosophical Magazine* (1952) **43**, p. 1151.

[8] W. T. Read: *Dislocations in Crystals* (1953) New York. McGraw-Hill Book Co.


---

**Technical Note**

## Effect of Carbon Content on the 500°F Embrittlement of Tempered Martensite


by P. Payson


EMBRITTLEMENT of hard-tempered martensite (500°F embrittlement) appears to be coincident with the beginning of the third stage of tempering. During the first stage, primary martensite of steels containing over 0.25 pct C decomposes to a mixture of $\epsilon$ carbide and martensite of appreciably constant carbon content close to 0.25 pct.[1] During the third stage of tempering, cementite forms. In steels with

a carbon content over 0.25 pct, the formation of cementite probably involves the simultaneous solution of $\epsilon$ carbide in the matrix. In steels with less than about 0.25 pct C, cementite apparently forms directly from the primary martensite.

It seemed reasonable to inquire whether the very low carbon martensite, which decomposes to cementite in a manner different from that of higher carbon martensite, would show the embrittlement commonly found in the higher carbon steels when tempered at about 500°F. Although this embrittlement has been discussed at considerable length in recent years,[2-5] very few data have been presented on steel with carbon under about 0.20 pct. Therefore, three steels were made up in 30 lb heats, two with carbon under 0.15 pct and the third with carbon at 0.25 pct. To assure sufficient hardenability so that only martensite would form in the heat treatment of blanks for standard Charpy-test pieces, the steels were made with about 0.5 pct Mn, 0.5 pct Cr, 0.3 pct Mo, and in addition varying amounts of Ni, from 5.0 pct in the lowest carbon steel to 2.5 pct in the 0.25 pct C steel. The nickel was decreased with increase in carbon to minimize retained austenite.

The ⅝ in. square bars rolled from 30 lb ingots were annealed by an air cool from 1600°F followed by a temper at 1100°F for 16 hr. Blanks for Charpy-test pieces were then machined to 0.470 x 0.470 x 2 1/16 in. These were austenitized at 1700°F for 30 min, quenched in water, and immediately refrigerated in liquid nitrogen at about −320°F. A check on the microstructures showed that all steels were martensitic as-quenched and refrigerated, but no steps were taken to determine how much, if any, retained austenite was present.

One pair of blanks from each heat was left as-hardened, and others were tempered over the range from 200° to 1000°F in 100° intervals. All were then finished to standard-sized Charpy pieces with 0.010 in. radius *V*-notch.

A complete set of Charpy pieces of each steel was tested for hardness and broken at room temperature. Additional Charpy pieces were broken at other temperatures, some at −100°F, some at 300°F. The purpose of the tests at temperatures other than room temperature was to get an indication of the transition temperatures of the steels for several tempered conditions. Complete transitions curves for the steels in these different conditions were not obtained because of the large amount of work necessary to get this information and because it was felt that quantitative data on transition temperatures were not any more valuable for an understanding of the phenomena involved than qualitative data.

The results plotted in the accompanying curve sheet, Fig. 1, show clearly that carbon content of the martensite does not change the fundamental condition responsible for the embrittlement produced by tempering in the range between 500° and 700°F, but merely affects the transition temperature of the products resulting from such tempering. Apparently, the lower the carbon content of the martensite is, the lower the transition temperature. In the 0.06 pct C steel, the transition temperature of the 600°F tempered product is below room temperature, whereas in the 0.25 pct C steel the transition temperature is well above room temperature.

P. PAYSON is Assistant Director of Research, Research Laboratory, Crucible Steel Co. of America, Harrison, N. J.

TN 234E. Manuscript, June 17, 1954.

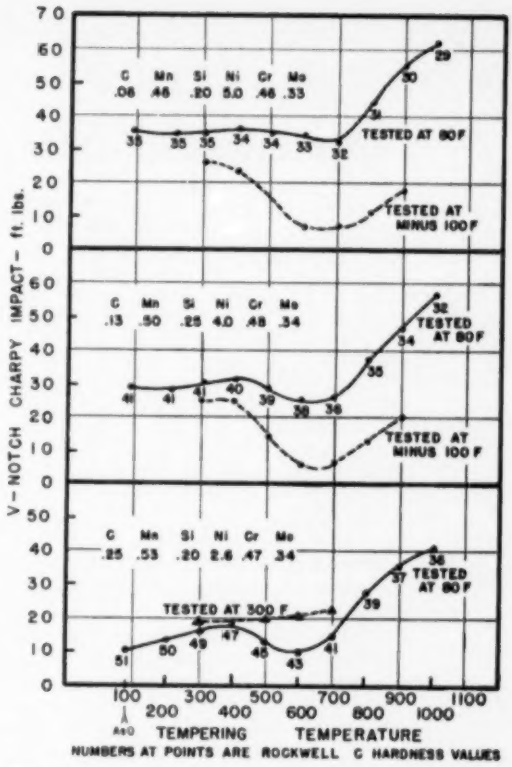
V-NOTCH CHARPY IMPACT – ft. lbs.
C Mn Si Ni Cr Mo
.06 .46 .20 5.0 .46 .33
TESTED AT 80 F
TESTED AT MINUS 100 F
C Mn Si Ni Cr Mo
.13 .50 .25 4.0 .48 .34
TESTED AT 80 F
TESTED AT MINUS 100 F
C Mn Si Ni Cr Mo
.25 .53 .20 2.6 .47 .34
TESTED AT 300 F
TESTED AT 80 F
TEMPERING TEMPERATURE
NUMBERS AT POINTS ARE ROCKWELL C HARDNESS VALUES

Fig. 1—Effects of composition of steel and testing temperature on minimum in notch impact vs tempering-temperature curve.

It may be concluded, therefore, that regardless of composition, tempered martensite is embrittled when cementite first forms during the third stage of tempering. The only effect to be expected by variation of composition is a change in transition temperature of the tempered product. The data on the series of steels studied show that the lower the carbon of the tempered martensite, the lower is the transition temperature. However, they also show that the higher the nickel content, the lower the transition temperature. Additional steels would have to be studied to establish the effects of carbon and nickel separately.

It appears further from these data that the embrittlement seems independent of the quantity of the freshly formed cementite, since it is obvious that in the very low carbon steels the quantity of cementite is much less than that in the 0.25 pct C steel.

## References

[1] C. S. Roberts, B. L. Averbach, and M. Cohen: The Mechanism and Kinetics of the First Stage of Tempering. *Trans.* ASM (1953) **45**, p. 576.

[2] M. Baeyertz, W. F. Craig, Jr., and J. P. Sheehan: Effect of Alloying Elements on Impact Properties of Quenched and Tempered Steels. *Project NR031-115*. Office of Naval Research (1949).

[3] P. Payson: Embrittlement of Tempered Martensite Better Defined. *The Iron Age*. (1951) **168**.

[4] R. L. Rickett and J. M. Hodge: Notch Toughness of Fully Hardened and Tempered Low Alloy Steels. *Proceedings* ASTM (1951) **51**.

[5] L. J. Klingler, W. J. Barnett, R. P. Frohmberg, and A. R. Troiano: The Embrittlement of Alloy Steels at High Strength Levels. *Trans.* ASM (1954) **46**, p. 1557.

# An Examination of the Decrease of Surface-Activity Method Of Measuring Self-Diffusion Coefficients in Wustite And Cobaltous Oxide

by R. E. Carter and F. D. Richardson

**Self-diffusion coefficients have been measured for iron in wustite (700° to 1000°C) and for cobalt in cobaltous oxide (800° to 1350°C) by means of radio-isotopes. Both sectioning and decrease of surface-activity methods have been used and a particular shortcoming of the latter method has been disclosed for wustite.**

**The effects of oxygen pressure on the composition of cobaltous oxide and on the diffusion coefficient of cobalt in the oxide have been established. The effect of the preparation conditions of the cobalt-oxide specimens on the diffusion measurements has been determined. It has been concluded that diffusion of cobalt occurs via vacant cation sites and that a cobaltous-oxide disk reaches equilibrium with its environment in a time which is very short compared with that needed for diffusion of the radio-isotope.**

THE availability of radioactive isotopes in recent years has permitted the measurement of many self-diffusion coefficients which were hitherto impossible to determine. With the advent of radioactivity, the method of measuring diffusion coefficients has also changed. The earlier sectioning method by which the concentration profile of the diffusing species was determined in the diffusion specimen has often been rejected in favor of the decrease of surface-activity method first developed by Von Hevesy,[1] and extended by Steigman, Shockley, and Nix,[2] and Raynor, Thomassen, and Rouse.[3]

With the experimental arrangement where an infinitely thin deposit of tracer is diffused into a semi-infinite cylinder, the decrease in activity of the active face due to diffusion of the tracer into the specimen is measured by counting the active face before and after diffusion. Under these conditions, the appropriate solution of the diffusion equation is

$$R = e^{z}(1 - \phi\sqrt{Z}) \qquad [1]$$

where $R$ is the ratio of the counting rates after-to-before diffusion, $\phi\sqrt{Z}$ is the Gaussian error integral of $\sqrt{Z}$, and $Z$ is defined as $Z = \mu^2 Dt$, $\mu$ being the linear-absorption coefficient of the detected radiation in the diffusion specimen, $D$ the self-diffusion coefficient, and $t$ the diffusion time.

In the older sectioning method the concentration distribution of the tracer is found after diffusion by analysing thin parallel sections cut from the active face of the diffusion specimen. As seen from the solution of Fick's second law for the distribution of an infinitely thin source after diffusion into a semi-infinite cylinder

$$c = \frac{Q}{\sqrt{\pi Dt}}\, e^{-x^2/4Dt} \qquad [2]$$

the log of the concentration plotted against $x^2$ will be a straight line of slope log $e/4\ Dt$. The diffusion coefficient thus can be calculated directly. The units of the tracer concentration are completely arbitrary, since any change in units does not change the slope of the log $c$ vs $x^2$ plot.

Although both of the above methods have been widely used, a thorough experimental comparison does not appear to have been made. Birchenall and Mehl,[4] during an investigation of the self-diffusion rate of $\alpha$ and $\gamma$ iron by the surface method using $Fe^{59}$ tracer, diffused and sectioned one welded couple. The diffusion coefficient from this run agreed with those by the surface method. Buffington, Bakalar, and Cohen,[5] during an investigation on $\alpha$ and $\gamma$ iron

R. E. CARTER, Junior Member AIME, is associated with the Mines Branch, Dept. of Mines and Technical Surveys, Ottawa, Ont., Canada, and F. D. RICHARDSON, Member AIME, is Director, Nuffield Research Group in Extraction Metallurgy, Royal School of Mines, London, England.

Discussion on this paper, TP 3839E, may be sent, 2 copies, to AIME by Jan. 1, 1955. Manuscript, Apr. 14, 1954. Chicago Meeting, November 1954.

by the surface method, also sectioned one specimen. The resulting diffusion coefficient was 61 pct of that by the surface method. The experimental scatter in this investigation was about ±25 pct. Hedvall, Brise, and Lindner,[6] measuring the diffusion rate of $Ca^{45}$ in $CaO \cdot Fe_2O_3$ by both methods, found lower results by the sectioning method than by the surface method. Their log concentration vs $x^2$ curve, however, was not straight but curved upwards near the specimen surface. They attributed this curvature to two diffusion mechanisms, and claimed that the surface method was measuring the diffusion rate deep within the specimen, as the 0.25 mev $\beta$ particles were too penetrating to measure the surface effect. In the opinion of the authors, this explanation now appears doubtful.

The comparison of the two methods outlined above was carried out on wüstite of composition '$FeO_{1.087}$' with $Fe^{55}$, and on 'CoO' over a range of compositions with $Co^{60}$. The comparison using $Fe^{55}$ was made to test the surface method under the most favorable conditions, i.e., where the emission obeys Beer's law exactly. The $Fe^{55}$, which has a manganese nucleus, decays by K-electron capture with the emission of Mn kX. The comparison with $Co^{60}$, which decays by the emission of a 0.3 mev $\beta$ particle and 1.1 and 1.3 mev $\gamma$ rays, was made to test the surface method with a $\beta$ plus $\gamma$ emitting isotope.

Because the range of nonstoichiometry of CoO had not been measured previously, experiments were made to determine this. The method used was to measure the weight of oxygen taken up during complete oxidation of cobalt sheet to CoO in equilibrium with controlled pressures of oxygen. Measurements were also made of weight losses which occurred when these fully oxidized specimens were reduced back to metal in hydrogen.

According to Bardeen and Herring,[7] the diffusion coefficient of a tracer atom in a face-centered-cubic structure (which the cations in FeO and CoO may be considered to occupy in a rigid oxygen framework) is 10 pct lower than the true self-diffusion coefficient of the cations. Since this difference is smaller than the accuracy limits for the diffusion coefficients measured in this investigation, it has not been taken into account.

## Experimental Diffusion

The wüstite and cobaltous-oxide disks used in this work were all made by complete oxidation of high purity metal. The metal starting disks were 0.55 in. in diameter and 0.040 in. thick. They were polished to 3/0, cleaned in acetone, and completely oxidized to FeO or CoO under known partial pressures of oxygen.

The iron was supplied as rolled rod by the British Iron and Steel Research Assoc. The impurities were 0.002 pct C, 0.002 pct Si, <0.005 pct Mn, 0.003 pct S, <0.001 pct P, 0.0027 pct $O_2$, and 0.0014 pct $N_2$. No attempt was made to refine this iron further. The high purity cobalt, supplied by Johnson Matthey and Co. Ltd., was 99.99 pct pure, and had been rolled from hydrogen-reduced sponge. A microscopic examination showed long thin inclusions which could act as barriers to diffusion if they were maintained in the oxide specimens. The cobalt was melted therefore into ingots in alumina crucibles in vacuo in an induction furnace.

The $Fe^{55}$, half-life 5.0 years, was obtained as "carrier-free" ferric-sulphate solution. The iron content was 50 micrograms per ml and the specific activity 10 microcuries per ml. The analysis was as given in Table I.

Table I. Analysis of $Fe_2^{55}(SO_4)_3$ Solution: Activity 10 Microcuries per Ml

| Element | Micrograms per Ml | Element | Micrograms per Ml |
|---|---|---|---|
| Cd | <0.05 | Pb | 2 |
| As | 5 | Cr | <0.5 |
| Be | 0.1 | Ni | <0.5 |
| B | <0.5 | Al | 50 |
| Fe | 50 | Ca | 20 |
| Mn | <0.1 | Cu | 20 |
| Mg | 5 | Na | 50 |

The $Co^{60}$, half-life 5.3 years, was obtained as irradiated filaments of No. 26 standard wire gage, 99.99 pct pure cobalt wire, specific activity 2.1 millicuries per gram.

*Gas Mixtures:* The gas trains were of conventional pattern. They were made entirely of pyrex except for short lengths of poly-vinyl-chloride tubing between the gas cylinders and the blowoffs and from the hydrogen flowmeter to the saturator in the $H_2/H_2O$ train.

In the $H_2/H_2O$ system used for the FeO work, commercial hydrogen was maintained at constant pressure by an *n*-dibutyl phthalate blowoff, and dried by passing through calcium chloride. After removal of the oxygen by conversion to water over palladized asbestos at 300°C, the gas was dried and then metered. The purified hydrogen was passed either through magnesium perchlorate and then to the furnace or to a water saturator for preparation of $H_2/H_2O$ mixtures.

The saturator, a one-liter flask, heated by an electric mantle, was maintained about 10°C above that required to give the desired water pressure. Hydrogen was admitted to the saturator in small bubbles by means of a fritted glass disk. Past the saturator, the gas line was wound with heating tape to prevent condensation of water. The excess water was condensed from the gas stream by passing the gas line through a large well stirred constant-temperature bath, the condensed water draining into a sump. The $H_2/H_2O$ stream then passed to the furnace. The bath temperature was controlled to ±0.1°C by a bimetal spiral regulator, and was read on a calibrated mercury-in-glass thermometer alongside the gas exit line.

The nitrogen used for flushing was prepared from "oxygen-free" nitrogen. This was passed over calcium chloride and soda lime, over copper at 600°C, metered, and finally dried over magnesium perchlorate and passed to the furnace.

In the preparation of the nitrogen/oxygen mixtures required for the CoO work, commercial oxygen-free nitrogen, air, and oxygen were passed over calcium chloride, soda lime, and magnesium perchlorate, metered, and passed to the furnace.

No special efforts were made to mix the oxygen and nitrogen but, as the mixed gasses passed through 6 ft of 6 mm tubing with many sharp bends, it was assumed that the gas composition would be uniform over the diffusion specimens.

The flowmeters were all calibrated at frequent intervals by the soap-bubble flowmeter method in which the time required for a stream of gas saturated with water vapor to sweep a soap film through a known volume is measured. The reproducibility of these calibrations was ±0.5 pct, but the absolute accuracy is probably not more than 1 pct.

*Apparatus for Diffusion Anneal:* A platinum-

wound furnace was used for all work on FeO and for all work above 1150°C on CoO. This furnace had a constant temperature zone of ±2°C over a length of 2 in. at 1200°C. A differentially wound kanthal furnace was used for the work on CoO at 1150°C, and below. The outside of this furnace was differentially lagged to give a zone constant to within ±2°C over a length of 4 in. A schematic section of the furnace assembly is shown in Fig. 1.

For work at 1150°C and below, quartz reaction tubes with B-29 cone ends were used. At higher temperatures, alumina or mullite tubes were used with pyrex cones cemented with "araldite," a thermosetting cement made by Aero Manufacturing Co.

For experiments requiring a $H_2/H_2O$ atmosphere, the cold parts of the assembly were wound with heating tape to prevent condensation of water. Both furnaces were controlled to within ±2°C by Kent potentiometer-type controllers. The whole apparatus was tested for leaks at frequent intervals.

*Preparation and Treatment of Diffusion Specimens:* The polished and degreased iron and cobalt disks were supported by pure iron or cobalt holders inside alumina boats and oxidized to completion. The holders were so arranged that the specimens were never in contact with the boat during oxidation.

The iron was oxidized at 1000°C in a $H_2/H_2O$ atmosphere fixed to give an O/Fe ratio of 1.087 as calculated from the data of Darken and Gurry.[8] The cobalt was oxidized at 1250°C in air. Both the iron and cobalt were completely oxidized in 24 hr, but a further 24 hr were allowed to remove the oxygen gradient across the disk, although subsequent work showed that this was not necessary. In all oxidation and diffusion runs, the total gas flow was about 250 ml per min at stp (3 to 5 cm per sec linear flow over the specimens). The measurements therefore could not be influenced by thermal segregation in the gas mixtures.

After the anneal period, the FeO disks were quenched by quickly drawing the oxidation boat into the cold end of the quartz furnace tube and pouring water over the tube. At the same time the $H_2/H_2O$ stream was shut off and the furnace flushed with purified nitrogen. As the CoO disks were made in air, they were quickly drawn out of the furnace and cooled by placing the boat on a sheet of asbestos board. The quenching cracked many of the FeO disks but the CoO showed no sign of damage.

Both sides of the disks were then ground flat with No. 1 emery paper and one face polished to 3/0 emery paper. This face, which was to be used for the diffusion measurement, was not polished further, as grain growth during diffusion resulted in surface irregularities much larger than the polishing scratches. After polishing, the surface was completely covered by fine parallel scratches and no grain boundaries could be seen.

The ground disks were then normally annealed in a small platinum boat fastened to the thermocouple sheath at the oxygen pressure and temperature, but for twice the time of the subsequent diffusion anneal. This annealing removed most of the polishing scratches and developed the grain boundaries and grain orientation as seen in Fig. 2a and b. To save time, most of the FeO disks which were diffused at 800°C and below, were annealed at 925°C for 2 hr in a $H_2/H_2O$ atmosphere which would maintain the O/Fe ratio of 1.087. This procedure was equivalent to an anneal twice as long as the subsequent diffusion anneal. After this prediffusion anneal, the surfaces of the disks were examined at a magnification of X540 to see that they were free of obvious foreign material that could interfere with diffusion.

A thin layer of $Fe^{59}$ or $Co^{60}$ was placed on each annealed diffusion specimen, the surface re-examined, and the deposit counted. To determine whether the method of placing the tracer on the specimen influenced the diffusion coefficient, three methods were used during the FeO work:

1—A drop of the active ferric-sulphate solution was dried on the surface of the disk. Because the edges of the disks were porous, the activity was confined in a 1 cm diam area in the center of the 1.4 cm diam disks. The analysis of the $Fe^{59}$ solution (Table I) shows that this deposit could only have been a few atom layers thick.

2—A layer of $Fe^{59}$ was evaporated from a tungsten filament on which a few drops of the ferric sulphate had previously been dried, ignited, and reduced in $H_2$. During this evaporation, the disk was held in a recessed ring so that the tracer was again confined in a 1 cm diam area in the center of the diffusion specimen.

3—A deposit of $Fe^{59}$ was electroplated on the oxide by placing a drop of the active ferric sulphate on the center of the disk and placing a pure iron anode above and parallel to it and in contact with the active solution. A current of 3 microamp per sq cm for 5 to 10 min was required to deposit the required activity. Even at a 100 pct current efficiency, the thickness of this deposit could not have exceeded $3.5 \times 10^{-4}$ cm.

For the CoO investigation, the $Co^{60}$ was evaporated from irradiated cobalt filaments on to the center of the diffusion specimens by a conventional hot-wire technique. From the specific activity of the filament and the counting geometry used, the thickness of this deposit could not have exceeded $2 \times 10^{-4}$ cm.

After the thin active layers had been counted, the disks were heated in pairs with their active faces toward each other to decrease any loss of tracer by evaporation. To allow free access of oxygen, the active faces were kept 0.01 in. apart by spacers of platinum wire at the edges. These diffusion anneals were made in the same platinum boat used for the

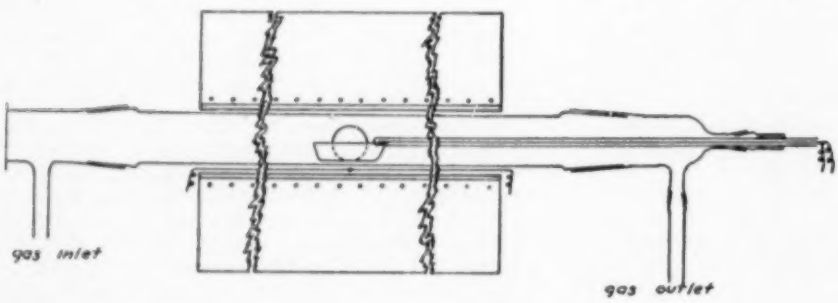


Fig. 1—Schematic representation of furnace assembly.

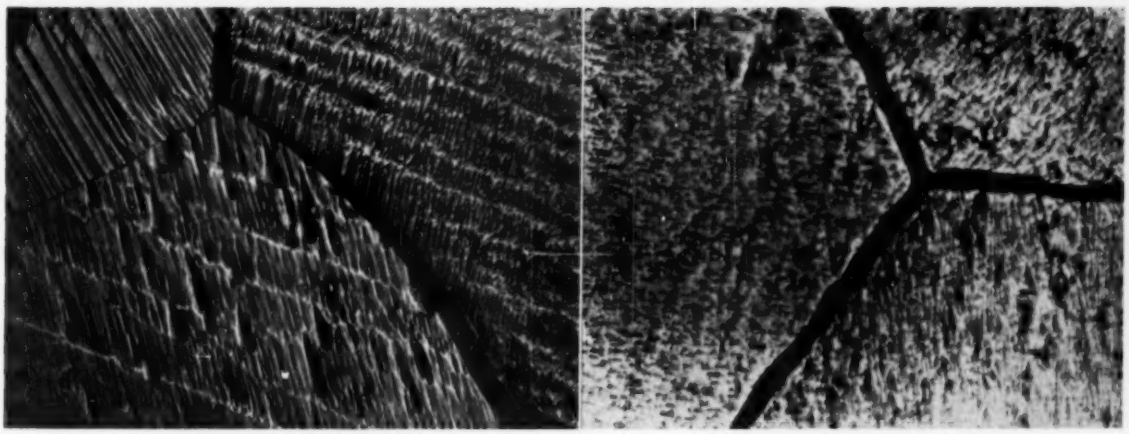

a—Wustite after 2 hr at 925°C. b—Cobaltous oxide after 2 hr at 1003°C.

Fig. 2—Surfaces of oxide specimens after annealing before diffusion. X275. Area reduced approximately 25 pct for reproduction.

prediffusion anneals. This boat was constructed of 0.005 in. platinum sheet just large enough to hold the two oxide disks; this reduced the heat capacity of the assembly and so decreased the heating and cooling times.

In both the prediffusion and diffusion anneals, the specimens were loaded into the cold end of the furnace tube, which was then closed and flushed for 1 hr with the gas mixture of the subsequent anneal. The specimens were then pushed quickly into the center of the furnace. After the anneal, the specimens were quenched by drawing them quickly to the cold end of the furnace tube. After about 15 min the furnace tube was opened and the specimens were removed. This quenching procedure was possible with alumina and mullite as well as quartz tubes because of the small heat capacity of the platinum trays and oxide specimens.

After diffusion, the disks were recounted so that the diffusion coefficient could be calculated by the decrease of surface-activity method. The active surfaces of the disks were then re-examined under the microscope.

*Decrease of Surface-Activity Technique:* The calculation of the absorption coefficient required for the decrease of surface-activity method needs careful consideration. The absorption of the radiation from the $Fe^{55}$ (Mn kX) was determined with aluminum, iron, and FeO absorbers in contact with the source. The measured absorption coefficients with all three obeyed Beer's law and agreed closely with the known absorption coefficients of these substances for Mn kX. For the wüstite used in this investigation, O/Fe ratio 1.087, the linear absorption coefficient was 432 $cm^{-1}$.

Because of the complicated absorption and scattering of $\beta$ particles, a linear absorption coefficient cannot hold for the radiation from $Co^{60}$. A purely graphical method of determining the diffusion coefficient by the decrease of surface-activity method, developed by Ruder and Birchenall,[9] was therefore used, instead of the analytical solution (Eq. 1). The method was based on an absorption curve determined for the total $\beta + \gamma$ radiation under the same geometrical conditions as obtained in the counting of the diffusion disks.* The product of the concentration-distance curve for a typical $Dt$ product (Eq. 2) and the transmission-distance curve was integrated graphically from the surface to an infinite depth into the oxide disk. This integral divided by the corresponding integral of the concentration-distance curve then gave the ratio of the surface counts after a diffusion anneal to the counts before an anneal for the $Dt$ product used in setting up the initial concentration-distance curve. This procedure was repeated for a series of $Dt$ products. The resulting curve of activity ratio vs $Dt$ was then used to calculate the self-diffusion coefficient of CoO. It must be emphasized that this curve is appropriate only to the tracer counting arrangement used in determining the absorption curve and must be redetermined every time the experimental conditions are changed.

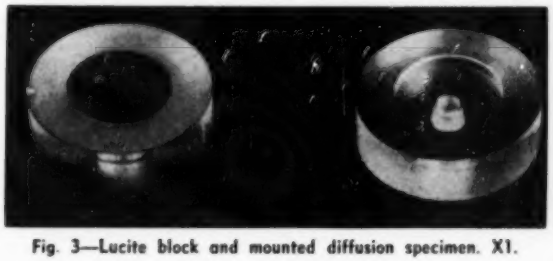

Fig. 3—Lucite block and mounted diffusion specimen. X1.

As this graphical method involves no assumptions about the absorption of the tracer radiation, it is suitable for any tracer whose radiation is attenuated sufficiently to make the surface method possible.

*Sectioning Technique:* Those specimens from which the diffusion coefficient was to be determined by the sectioning method were cemented with a thin gel of methyl methacrylate into "lucite" blocks. A photograph of a lucite block and a mounted disk is shown in Fig. 3.

Any cement which had crept over the edges of the disk was carefully removed with 2/0 emery paper, and the back face of the mount was ground parallel to the active face within 0.0003 cm as measured by a micrometer at four points. Thin slices were then ground from the active face with 3F carborundum powder on a glass plate. By this method, sections of any thickness could be easily removed with little

* Cobalt and aluminium foils of various thicknesses were interposed between a cobalt disk coated with $Co^{60}$ and the counter, the absorber and disk being held in contact. The mass absorption coefficients of these materials are nearly the same, the aluminium giving $I/I_0$ values which were about 7 pct greater than those of cobalt at low thicknesses and 15 pct greater at high thicknesses. Since it is the low thicknesses which are important in this work, and light oxygen atoms as well as cobalt atoms are present in the cobalt oxide which is the absorbing medium in the diffused disk, the mean curve was used. The resulting error is relatively small, i.e., less than 5 pct. Three check points determined with CoO foils agreed closely with this mean curve.

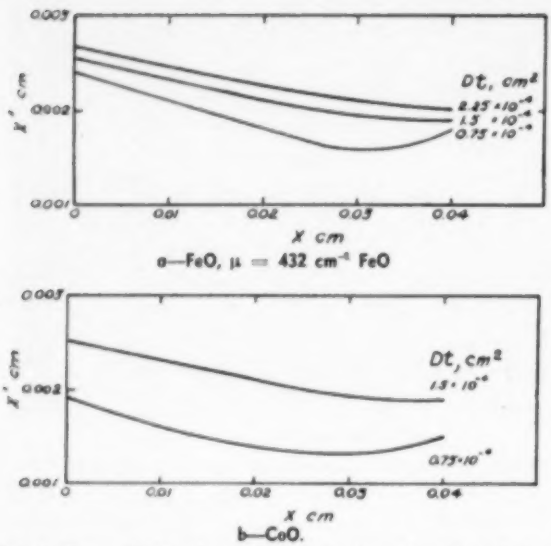


a—FeO, $\mu$ = 432 cm$^{-1}$ FeO




b—CoO.

Fig. 4—Curves showing $x'$ as a function of $x$ for various $Dt$ products.

tendency for the disk to grind unevenly. After each grinding, the thickness of the slice removed was measured by the decrease in mount thickness at four points around the disk face. The thickness recorded was always the average of at least two sets of measurements. In no case did two sets of measurements differ by more than 0.0002 cm and the active and back faces of the disks were always parallel within 0.0003 cm. With this procedure, no disks were lost because of breaking or cracking of the oxide. The ground surfaces were smooth up to the last one or two slices, where a few very small pits developed. These pits, which were never large enough to influence the concentration-distance curve, were probably caused by the beginning of porosity in the oxide disk, see Figs. 5a and b.

The concentration profile was originally determined by counting each of the thin sections removed. Each section was dissolved in hydrochloric acid and filtered to remove the insoluble carborundum powder. It was then evaporated to 20 ml and analyzed in a thin-walled liquid counter. In all cases the carborundum removed was free from activity. Because the soft Mn kX and 0.3 mev $\beta$ particles were greatly attenuated by the solution and counter walls, the counting rate was low, 60 to 150 counts per min. The method therefore was modified so that the residual activity in the disk was counted after each thin section had been removed. The counting rate, $A$, from the disk was taken as proportional to the tracer concentration at the distance of the fresh surface below the original surface, distance $x$, plus a small correction, $x'$, to allow for the detected radiation being distributed below the exposed surface. The slope of the log $A$ vs $(x + x')^2$ plot, a straight line, then gave the diffusion coefficient directly from Eq. 2. $x'$ was determined as follows:

A c vs $x$ curve was drawn from Eq. 2 for a fixed value of $Dt$, approximately equal to that obtaining in the diffusion experiments. From this curve, an $A$ vs $x$ curve was derived in the case of FeO by applying Beer's Law:

$$A = c\, e^{-\mu x}$$

where $A$ is the effect at the surface of the tracer at $x$, c is the concentration of tracer given by the c vs $x$ curve, $x$ is the distance below the surface exposed for counting, and $\mu$ is the linear absorption coefficient in cm$^{-1}$. This procedure was repeated after each of a series of thin sections had been removed from the head of the c vs $x$ curve normal to the distance axis. The center of gravity of each of these curves was then determined experimentally, the distance of this point from the exposed surface being taken as $x'$. Families of curves showing $x'$ as a function for $x$ of various $Dt$ products for both FeO and CoO are shown in Figs. 4a and b. For a typical diffusion experiment in which the rms penetration was about 0.02 cm, the correction factor $x'$ changed $D$ by about 10 pct.

This method was tested graphically by plotting the log of the area of each $A$ vs $x$ curve against $(x + x')^2$ and showing that the resultant value of $Dt$ was equal (within $\pm$1 pct) to that used for setting up the original c vs $x$ curve. The diffusion coefficients obtained by this method agreed within $\pm$10 pct (see Tables II and IV) with those derived from the solution counting technique. In addition, Gruzin's[10] analytical expression relating the diffusion coefficient to the counts from a diffusion specimen after each thin section was removed gave results which agreed with those calculated graphically within the limits of the experimental error.

A similar procedure was adopted for CoO but, because of the complicated scattering of the radiation from $Co^{60}$, the experimentally determined transmission curve was used in calculating $x'$ and the counting technique had to be modified. As the very penetrating $\gamma$ rays would have made the correction $x'$ large, only the $\beta$ count could be used. This was obtained by subtracting the $\gamma$ count from the total $\beta+\gamma$ count. The $\gamma$ count was determined with a

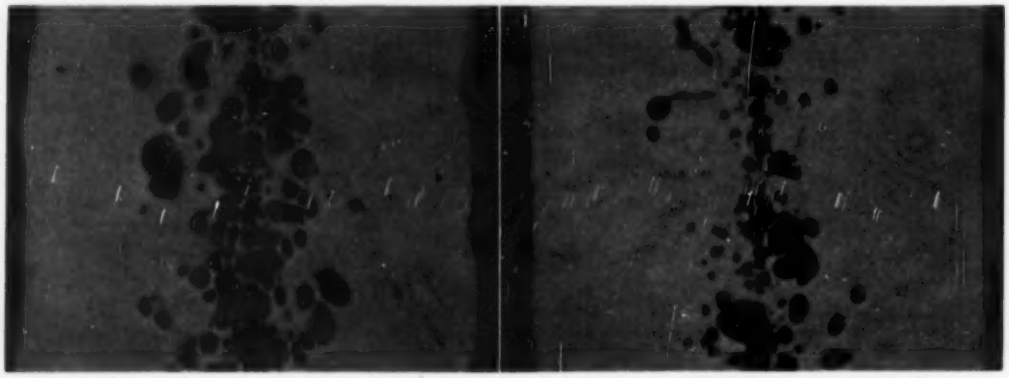

a b

Fig. 5—Cross sections of disks. X50. a—FeO, and b—CoO. Area reduced approximately 25 pct for reproduction.

0.024 in. Fe $\beta$ absorber in contact with the counter window. The $\gamma$ count as measured with this absorber was high due to the emission of secondary electrons from the absorber. The true $\gamma$ count must lie somewhere between 100 and 50 pct of the measured count because some, but not all, of these secondary electrons are detected by the counter. The true $\gamma$ count was therefore taken as 75 pct of the observed count, the maximum uncertainty being ±33 pct. A simple calculation shows that the effect of this uncertainty in the $\gamma$, and hence the $\beta$ count, since the $\beta$ activity is many times the $\gamma$ activity, can only influence the diffusion coefficient by about 3 pct (see Table V).

*Counting:* Counting was done with a standard decade scaler using a mica end-window X-ray-sensitive Geiger-Müller tube, a mica end-window $\beta$-sensitive tube, and a thin-walled $\beta$-sensitive liquid tube. Each specimen was counted twice to a minimum of 10,000 counts. All counts were compared with iron and cobalt standards to eliminate day-to-day variations in the counting efficiency and the usual corrections were made for the background and tube dead time. All specimens were held in closely fitting recesses in dural specimen holders. This permitted the sources to be replaced for counting with an error in geometry that was less than the counting error.

## Experimental Composition of CoO

About 2 grams of 0.005 in. Co sheet was cleaned with 1/0 emery paper and reduced in hydrogen at 1000°C for 1 hr. The clean metal was next placed in a fired and weighed alumina boat and the assembly reweighed. The cobalt was then completely oxidized in the closed furnace assembly (Fig. 1). The oxidation was carried out for a period equal to three times that required for complete oxidation.

After oxidation in the low oxygen atmosphere, i.e., 0.5 pct $O_2$, at 1000° and 1150°C, the boat was quickly drawn into the cold end of the quartz reaction tube and cold water poured over the tube. At 1350°C the boats were quickly drawn through the mullite reaction tube into a quartz cooling tube fitted to the B-29 cone. This quenching procedure cooled the oxide specimens to below red heat in 15 sec and cooled the boat to below red heat in 35 sec. Even if all the oxygen passing over the specimens *during the cooling period* was absorbed by the oxide to form $Co_2O_3$, the O:Co ratio would be raised by only 0.001.

After oxidation in pure oxygen, the specimens were quickly drawn out of the furnace and cooled in still air. This air quench cooled the specimens below red heat in 20 sec. To determine if oxygen was lost or gained during the cooling period, three specimens were quenched in cold water as soon as they were drawn from the furnace. The analysis of these specimens by reduction in $H_2$ was identical with those cooled in air. After cooling the oxide and boat were reweighed and the O:Co ratio calculated.

The oxide was then ground to −60 mesh and about 1.5 grams placed in a weighed alumina boat which had been previously fired in hydrogen to constant weight. After reweighing, the oxide was reduced in hydrogen at 900°C for 24 hr, the assembly reweighed and the oxygen:metal ratio calculated. All weighings, which were by the method of swings, were reproducible to ±0.00003 grams.

## Results

The oxide-diffusion disks used in this investigation were free from cracks and voids to a depth of approximately 0.05 cm, which is about a quarter of the total disk thickness. Cross sections of typical FeO and CoO disks are shown in Figs. 5a and b. Both the FeO and CoO were coarsely polycrystalline with a well developed columnar grain structure. The average grain diameter was between 1 and 2 mm for the wüstite and between 0.5 and 1 mm for the CoO as measured on the polished and annealed diffusion surface. The average grain length was about 0.8 mm. In all experiments the rms penetration of the tracer was less than half the thickness of the dense outer layer of the diffusion disk.

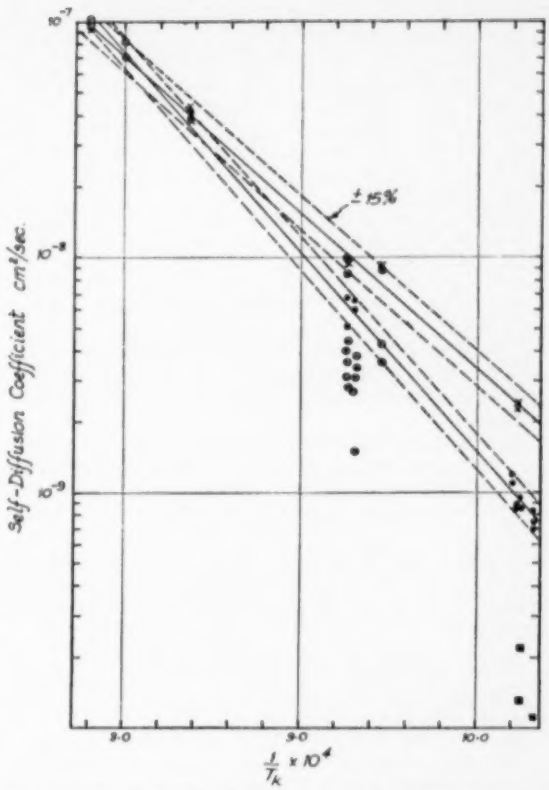


Fig. 6—Self-diffusion coefficient of iron in wustite (Fe:O = 1:1.087) as a function of temperature. Circled X represents sectioning method; X, modified sectioning method; filled circle, tracer-plated surface methods; filled square, tracer-evaporated surface methods; and circled dot, tracer-dried surface methods.

The rapid quench after the oxidation and after the annealings appeared to prevent the decomposition of the FeO used in this investigation, O/Fe = 1.087. Even at X1500, the oxide always appeared as a single phase. This is in agreement with the findings of Himmel, Mehl, and Birchenall[11] who reported that the decomposition could be prevented in wüstites containing more than 76.3 pct Fe, O/Fe = 1.084.

An examination of the CoO at X1000, however, always revealed a second phase in the centers of the grains and along the grain boundaries. During the subsequent diffusion anneals, it was assumed that this phase dissolved to form single phase CoO.

*Self-Diffusion in Wüstite:* A summary of the conditions of the preparation, prediffusion anneal, and diffusion anneal of the wüstite experiments is given in Table II. A summary of the self-diffusion coefficients by the surface method and the two sectioning methods is given in Table II and in Fig. 6, where the

best straight lines have been calculated by the method of least squares.

As can be seen from Table II, all the wüstites used in this investigation had an O:Fe ratio within 0.003 of 1.087 (76.2 pct Fe). All the diffusion coefficients listed are therefore taken to be for wüstite of this composition. The resulting error in the diffusion coefficient of 3 pct is small compared to the total error in this work.

For a wüstite of this composition, the self-diffusion coefficient determined by the sectioning methods is well represented by

$$D = 0.014\ e^{-50,200/RT}\ \text{sq cm per sec.} \qquad [3]$$

The statistical probable error in the energy is 1.8 pct and in the frequency factor, 25 pct.

*Composition of CoO:* The results are summarized in Table III.

Each analysis is the average of at least two oxidation and four reduction experiments. The oxygen: metal ratios determined by either oxidation or reduction were consistent to ±0.0005 but the ratios by the oxidation method were always about 0.002 lower than those by reduction.* As the cause of this difference was not determined, the average was taken with a resulting uncertainty of ±0.0015 in the O:Co ratio.

* Such a difference might conceivably have been caused by the presence of some impurity such as silica present at a concentration of about 1.0 pct in the original cobalt sheet. This might have escaped reduction in the initial 1 hr $H_2$ treatment of the cobalt sheet. The quantity of silica required, however, is greater than that likely to be present in the 99.99 pct metal.

*Self-Diffusion in Cobaltous Oxide:* Since the O:Co ratio of CoO as a function of oxygen pressure could only be determined approximately, the self-diffusion rate in the oxide was measured as a function of the oxygen pressure over a range of temperatures. These results are summarized in Table IV and in Figs. 7 and 8, where the best straight lines have been calculated by the method of least squares.

The diffusion coefficient at constant temperature was proportional to a power of the oxygen pressure, which decreased with rising temperature, as represented by the following equations:

$$\text{At } 1000°\text{C}, D = 2.6\text{x}10^{-5}\ (P_{O_2})^{0.35}\ \text{sq cm per sec.} \qquad [4]$$

$$\text{At } 1150°\text{C}, D = 9.0\text{x}10^{-6}\ (P_{O_2})^{0.30}\ \text{sq cm per sec.} \qquad [5]$$

$$\text{At } 1350°\text{C}, D = 5.1\text{x}10^{-5}\ (P_{O_2})^{0.28}\ \text{sq cm per sec.} \qquad [6]$$

The statistical probable error in the power is approximately 2 pct.

At an oxygen pressure of 1 atm (oxide composition changing) the self-diffusion coefficient of cobalt in CoO is well represented by

$$D = 2.15\text{x}10^{-6}\ e^{-34,500/RT}\ \text{sq cm per sec.} \qquad [7]$$

The statistical probable error in the energy term is 1.2 pct and in the frequency factor, 16 pct.

Throughout this investigation, activity could never be detected in the exit gases, and the furnace tube remained inactive after more than 50 diffusion runs had been made in the system. Volatilization losses therefore could not have been a significant source of error. Autoradiographs taken before and after diffusion showed that surface diffusion could not have been significantly, if at all, greater than the bulk diffusion, indicating that there could have been no error arising from changes in counting geometry.

**Table II. Details of Preparation, Prediffusion Anneal, and Diffusion Anneal of Wustite Specimens**

| Specimen No. | Oxidation | | | | Prediffusion Anneal | | | | Diffusion Anneal | | | |
|---|---|---|---|---|---|---|---|---|---|---|---|---|
| | Temperature, °C | Time, Hr | Atm, $H_2O/H_2$ | Composition, O/Fe | Temperature, °C | Time, Hr | Atm, $H_2O/H_2$ | Composition, O/Fe | Temperature, °C | Time, Min | Atm, $H_2O/H_2$ | Composition, O/Fe |
| F-51-A | 1000 | 48 | 1.70 | 1.086 | — | — | — | — | 1010 | 53 | 1.72 | 1.086 |
| F-52-A | 1000 | 48 | 1.70 | 1.086 | — | — | — | — | 1010 | 40 | 1.72 | 1.086 |
| F-53-A | 1000 | 48 | 1.70 | 1.086 | — | — | — | — | 784 | 449 | 1.25 | 1.090 |
| F-53-B | 1000 | 48 | 1.70 | 1.086 | — | — | — | — | 784 | 449 | 1.25 | 1.090 |
| F-54-A | 1000 | 48 | 1.70 | 1.086 | — | — | — | — | 802 | 472 | 1.30 | 1.090 |
| F-57-A | 1000 | 48 | 1.70 | 1.086 | — | — | — | — | 800 | 412 | 1.30 | 1.090 |
| F-57-B | 1000 | 48 | 1.70 | 1.086 | — | — | — | — | 800 | 412 | 1.30 | 1.090 |
| F-57-C | 1000 | 48 | 1.70 | 1.086 | — | — | — | — | 801 | 412 | 1.30 | 1.090 |
| F-57-D | 1000 | 48 | 1.70 | 1.086 | — | — | — | — | 801 | 412 | 1.30 | 1.090 |
| F-58-A | 1000 | 48 | 1.70 | 1.086 | 1000 | 2 | 1.70 | 1.086 | 811 | 306 | 1.33 | 1.090 |
| F-58-B | 1000 | 48 | 1.70 | 1.086 | — | — | — | — | 811 | 306 | 1.33 | 1.090 |
| F-58-C | 1000 | 48 | 1.70 | 1.086 | — | — | — | — | 811 | 306 | 1.33 | 1.090 |
| F-59-A | 1000 | 48 | 1.70 | 1.086 | 1000 | 1 | 1.70 | 1.086 | 802 | 348 | 1.27 | 1.089 |
| F-59-B | 1000 | 48 | 1.70 | 1.086 | 1000 | 1 | 1.70 | 1.086 | 802 | 348 | 1.27 | 1.089 |
| F-59-C | 1000 | 48 | 1.70 | 1.086 | 1000 | 1 | 1.70 | 1.086 | 807 | 253 | 1.25 | 1.088 |
| F-61-A | 1000 | 48 | 1.70 | 1.086 | 1000 | 1 | 1.70 | 1.086 | 807 | 249 | 1.25 | 1.088 |
| F-61-B | 1000 | 48 | 1.70 | 1.086 | 1000 | 1 | 1.70 | 1.086 | 807 | 249 | 1.25 | 1.088 |
| F-61-C | 1000 | 48 | 1.70 | 1.086 | 1000 | 1 | 1.70 | 1.086 | 807 | 253 | 1.25 | 1.088 |
| F-62-A | 1000 | 48 | 1.70 | 1.086 | 925 | 2 | 1.49 | 1.087 | 705 | 1453 | 1.00 | 1.089 |
| F-62-B | 1000 | 48 | 1.70 | 1.086 | 925 | 2 | 1.49 | 1.087 | 705 | 1453 | 1.00 | 1.089 |
| F-62-C | 1000 | 48 | 1.70 | 1.086 | 700 | 51 | 1.00 | 1.089 | 696 | 1547 | 1.00 | 1.089 |
| F-64-B | 1000 | 48 | 1.70 | 1.086 | 700 | 51 | 1.00 | 1.089 | 696 | 1547 | 1.00 | 1.089 |
| F-65-A | 923 | 180 | 1.48 | 1.087 | 925 | 2 | 1.49 | 1.087 | 923 | 30 | 1.48 | 1.087 |
| F-65-B | 923 | 180 | 1.48 | 1.087 | 925 | 2 | 1.49 | 1.087 | 923 | 30 | 1.48 | 1.087 |
| F-65-C | 923 | 180 | 1.48 | 1.087 | 925 | 2.6 | 1.48 | 1.086 | 707 | 1464 | 0.95 | 1.086 |
| F-68-A | 1000 | 48 | 1.70 | 1.086 | 925 | 2.5 | 1.48 | 1.086 | 703 | 1441 | 0.94 | 1.086 |
| F-68-B | 1000 | 48 | 1.70 | 1.086 | 925 | 2.5 | 1.48 | 1.086 | 703 | 1441 | 0.94 | 1.086 |
| F-68-C | 1000 | 48 | 1.70 | 1.086 | 925 | 2.6 | 1.48 | 1.086 | 707 | 1464 | 0.95 | 1.086 |
| F-68-C-B | 1000 | 48 | 1.70 | 1.086 | 925 | 2.6 | 1.48 | 1.086 | 696 | 1487 | 0.93 | 1.086 |
| F-69-A | 1000 | 48 | 1.70 | 1.086 | 925 | 2 | 1.48 | 1.086 | 703 | 1397 | 0.94 | 1.086 |
| F-69-C | 1000 | 48 | 1.70 | 1.086 | 925 | 2 | 1.48 | 1.086 | 703 | 1397 | 0.94 | 1.086 |
| F-69-C-B | 1000 | 48 | 1.70 | 1.086 | 925 | 2.6 | 1.48 | 1.086 | 696 | 1487 | 0.93 | 1.086 |

* Concentration profile determined by counting residual activity after each thin section was removed.

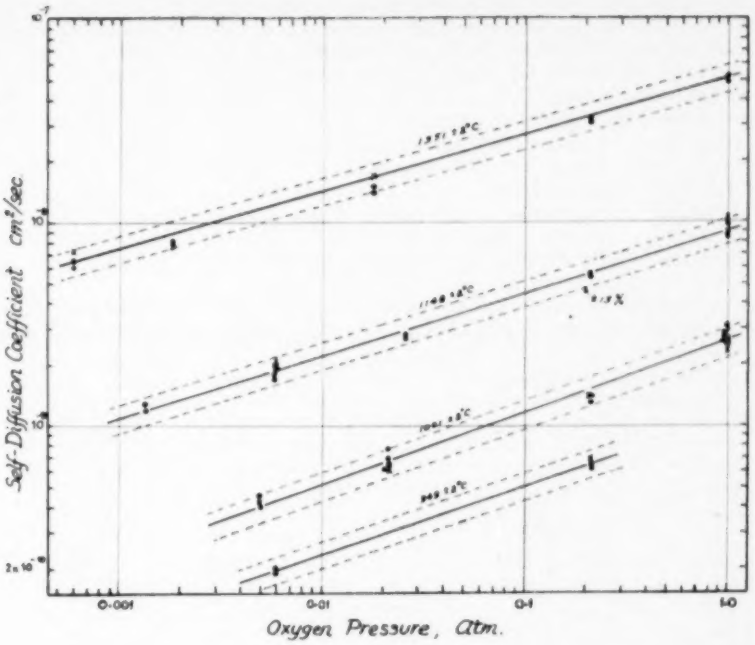


Fig. 7—Self-diffusion coefficient of cobalt in cobaltous oxide as a function of oxygen pressure at various temperatures. X represents sectioning method; filled circle, surface method.

To determine whether the oxide was always in equilibrium with its environment during the diffusion anneal, diffusion runs were made on CoO disks which had been prepared at high and low oxygen pressures both with and without prediffusion anneal.

**Table II. Continued**

| Tracer Application | Surface Activity Ratio, After: Before | Self-Diffusion Coefficient, Sq Cm per Sec: Surface Method | Self-Diffusion Coefficient, Sq Cm per Sec: Sectioning Method |
|---|---|---|---|
| Plating | 0.069 | $1.1\times10^{-7}$ | — |
| Drying | 0.083 | $1.0\times10^{-7}$ | $9.3\times10^{-8}$* |
| | | | $9.7\times10^{-8}$† |
| Drying | 0.119 | $4.3\times10^{-8}$ | $9.1\times10^{-8}$* |
| | | | $8.8\times10^{-8}$† |
| Drying | 0.129 | $3.6\times10^{-8}$ | — |
| Drying | 0.148 | $2.7\times10^{-8}$ | — |
| Drying | 0.132 | $3.8\times10^{-8}$ | — |
| Drying | 0.142 | $3.4\times10^{-8}$ | — |
| Drying | 0.147 | $3.1\times10^{-8}$ | — |
| Drying, surface very dirty | 0.205 | $1.5\times10^{-8}$ | — |
| Drying | 0.154 | $3.6\times10^{-8}$ | — |
| Drying | 0.144 | $4.2\times10^{-8}$ | — |
| Drying, surface very dirty | 0.170 | $2.8\times10^{-8}$ | — |
| Evaporation | 0.115 | $6.0\times10^{-8}$ | — |
| Plating | 0.108 | $6.6\times10^{-8}$ | — |
| Drying | 0.180 | $3.1\times10^{-8}$ | — |
| Evaporation | 0.147 | $5.1\times10^{-8}$ | — |
| Plating | 0.127 | $6.8\times10^{-8}$ | $9.6\times10^{-8}$* |
| | | | $1.0\times10^{-8}$† |
| Drying | 0.163 | $4.0\times10^{-8}$ | $9.6\times10^{-8}$* |
| | | | $8.5\times10^{-8}$† |
| Plating | 0.144 | $8.9\times10^{-10}$ | $2.3\times10^{-9}$* |
| Plating | 0.147 | $8.5\times10^{-10}$ | $2.3\times10^{-9}$* |
| Plating | 0.153 | $7.5\times10^{-10}$ | — |
| Plating | 0.157 | $7.0\times10^{-10}$ | — |
| Plating | 0.151 | $3.9\times10^{-8}$ | $4.3\times10^{-8}$* |
| Plating | 0.152 | $3.9\times10^{-8}$ | $3.9\times10^{-8}$* |
| Plating | 0.123 | $1.2\times10^{-9}$ | — |
| Plating | 0.139 | $9.6\times10^{-10}$ | — |
| Plating | 0.148 | $8.5\times10^{-10}$ | — |
| Plating | 0.132 | $1.1\times10^{-9}$ | — |
| Evaporation | 0.350 | $1.1\times10^{-10}$ | — |
| Evaporation | 0.340 | $1.3\times10^{-10}$ | — |
| Evaporation | 0.274 | $2.2\times10^{-10}$ | — |
| Plating | 0.147 | $8.4\times10^{-10}$ | — |

† Concentration profile determined by counting the activity in each of the thin sections removed.

**Table III. Oxygen:Metal Ratio in Cobaltous Oxide**

| Temperature, °C | O/Co Ratio: $P_{O_2}$ = 1.0 Atm | O/Co Ratio: $P_{O_2}$ = 0.005 Atm | Mol Pct Excess Oxygen: $P_{O_2}$ = 1.0 Atm | Mol Pct Excess Oxygen: $P_{O_2}$ = 0.005 Atm |
|---|---|---|---|---|
| 1000 | 1.0063±0.0015 | 1.0017±0.0015 | 0.63±0.15 | 0.17±0.15 |
| 1150 | 1.0080±0.0015 | 1.0018±0.0015 | 0.80±0.15 | 0.18±0.15 |
| 1359 | 1.0098±0.0015 | 1.0024±0.0015 | 0.98±0.15 | 0.24±0.15 |

As the first 20 specimens in Table IV show, the diffusion coefficient in all cases was independent of the conditions of the oxide preparation.

*Errors:* A summary of the possible errors is given in Table V.

## Discussion

There can be no doubt that the diffusion coefficients measured here are those for lattice diffusion in both wüstite and cobaltous oxide. The tracer distribution in all specimens (other than those of wüstite below 850°C), can be represented as a good straight line on a log concentration vs $x^2$ plot (e.g., Fig. 9a). If grain-boundary diffusion had been of major importance, a straight line would have been obtained only on a log concentration vs $x$ plot.[12] This conclusion is corroborated by the fact that autoradiographs taken at the surface of specimens, at a depth equal to the rms tracer penetration below the surface and at approximately twice the rms penetration, never showed concentration of the activity at the grain boundaries. Since the resolution of the autoradiographs, better than 0.2 mm, was smaller than the oxide grain diameters, approximately 1 mm in the wüstite and 0.5 mm in the cobaltous oxide, and smaller than the rms penetration of the tracer into the specimens, any preferential concentration of the tracer along the grain boundaries would have been detected easily.

*Diffusion in Wüstite:* The reproducibility achieved in these measurements is good, and the scatter of ±15 pct exhibited by the results shown in Fig. 6 is

fully consistent with the possible errors listed in Table V. There is close agreement between the results obtained by the surface and sectioning techniques above 850°C, but below this temperature the results obtained by the former method are much lower than those from the latter.

The self-diffusion coefficients determined in this investigation for wüstite of composition O:Fe = 1.087:1, by the sectioning method and also by the surface-activity method *above 850°C*, agree within 10 pct with those obtained by Himmel, Mehl, and Birchenall (their Fig. 6)[11] between 700° and 1000°C.

The difference in the results obtained by the sectioning and decrease of surface-activity methods is thought to be due to a small amount, 5 to 10 pct, of the initial activity being "bound" to the surface of the diffusion specimen. At 923°C, where the sectioning and surface methods agree closely, the concentration vs distance curve agrees with Eq. 2 and the log concentration vs $x^2$ plot (Fig. 9a) is a good straight line. This indicates that there was good bonding between the tracer and bulk oxide and that the diffusion coefficient was constant with depth, i.e., all of the oxide was in equilibrium with its en-

**Table IV. Details of Preparation, Prediffusion Anneal, and Diffusion Anneal of Cobaltous Oxide Specimens**

| Specimen No. | Oxidation | | | Prediffusion Anneal | | | Diffusion Anneal | | |
|---|---|---|---|---|---|---|---|---|---|
| | Temperature, °C | Time, Hr | Oxygen Pressure, Atm | Temperature, °C | Time, Hr | Oxygen Pressure, Atm | Temperature, °C | Time, Min | Oxygen Pressure, Atm |
| C-4-A | 1148 | 167 | 0.0055 | 999 | 14.1 | 1.0 | 1000 | 417 | 1.0 |
| C-4-B | 1148 | 167 | 0.0055 | 1001 | 14.4 | 1.0 | 1000 | 417 | 1.0 |
| C-5-A | 1149 | 85 | 1.0 | 999 | 14.1 | 1.0 | 1000 | 417 | 1.0 |
| C-5-B | 1149 | 85 | 1.0 | 1001 | 14.4 | 1.0 | 1000 | 417 | 1.0 |
| C-4-C | 1148 | 167 | 0.0055 | 1000 | 73.5 | 0.0212 | 1001 | 1,167 | 0.0212 |
| C-5-C | 1149 | 85 | 1.0 | 1000 | 73.5 | 0.0212 | 1002 | 1,166 | 0.0212 |
| C-5-D | 1149 | 85 | 1.0 | 1000 | 73.5 | 0.0212 | 1002 | 1,166 | 0.0212 |
| C-6-A | 1146 | 144 | 0.15 | 1000 | 73.5 | 0.0212 | 1001 | 1,167 | 0.0212 |
| C-7-C | 1250 | 48 | 0.21 | 1150 | 15 | 1.0 | 1150 | 285 | 1.0 |
| C-9-C | 1250 | 49 | 0.21 | 1150 | 15 | 1.0 | 1150 | 285 | 1.0 |
| C-14-A | 1250 | 48 | 0.21 | — | — | — | 1147 | 225 | 1.0 |
| C-14-B | 1250 | 48 | 0.21 | — | — | — | 1147 | 225 | 1.0 |
| C-7-D | 1250 | 48 | 0.21 | 1150 | 46 | 0.0061 | 1146 | 1,377 | 0.0058 |
| C-10-A | 1250 | 48 | 0.21 | 1150 | 46 | 0.0061 | 1146 | 1,377 | 0.0058 |
| C-14-C | 1250 | 48 | 0.21 | — | — | — | 1148 | 1,104 | 0.00593 |
| C-14-D | 1250 | 48 | 0.21 | — | — | — | 1148 | 1,104 | 0.00593 |
| C-16-A | 1250 | 48 | 0.21 | 800 | 96 | 0.0035 | 800 | 11,780 | 0.0031 |
| | | | | | | | 800 | 21,320 | 0.0031 |
| C-16-D | 1250 | 48 | 0.21 | 800 | 96 | 0.0035 | 800 | 11,780 | 0.0031 |
| | | | | | | | 800 | 21,320 | 0.0031 |
| C-19-A | 1250 | 48 | 0.21 | — | — | — | 800 | 11,780 | 0.0031 |
| | | | | | | | 800 | 21,320 | 0.0031 |
| C-19-B | 1250 | 48 | 0.21 | — | — | — | 800 | 11,780 | 0.0031 |
| | | | | | | | 800 | 21,320 | 0.0031 |
| C-3-A+B | 996 | 134 | 1.0 | 1000 | 4.5 | 1.0 | 1000 | 77 | 1.0 |
| | | | | | | | 1000 | 426 | 1.0 |
| C-6-B | 1146 | 144 | 0.15 | 1003 | 63.6 | 0.00498 | 1003 | 1,932 | 0.00498 |
| C-6-C | 1146 | 144 | 0.15 | 1003 | 63.6 | 0.00498 | 1003 | 1,932 | 0.00498 |
| C-6-D | 1146 | 144 | 0.15 | 1150 | 28 | 0.21 | 1146 | 401 | 0.21 |
| C-7-A | 1250 | 48 | 0.21 | 1003 | 39.2 | 0.21 | 1003 | 608 | 0.21 |
| C-7-B | 1250 | 48 | 0.21 | 1003 | 39.2 | 0.21 | 1003 | 608 | 0.21 |
| C-8-A | 1250 | 48 | 0.21 | 1003 | 17.6 | 1.0 | 1003 | 412 | 1.0 |
| C-8-B | 1250 | 48 | 0.21 | 1003 | 17.6 | 1.0 | 1003 | 412 | 1.0 |
| C-8-C | 1250 | 48 | 0.21 | 1150 | 38.3 | 0.0269 | 1146 | 717 | 0.0258 |
| C-9-A | 1250 | 49 | 0.21 | 1003 | 27 | 1.0 | 1003 | 704 | 1.0 |
| C-9-B | 1250 | 49 | 0.21 | 1003 | 27 | 1.0 | 1003 | 704 | 1.0 |
| C-9-D | 1250 | 49 | 0.21 | 1150 | 28 | 0.21 | 1146 | 401 | 0.21 |
| C-10-B | 1250 | 48 | 0.21 | 1150 | 38.3 | 0.0263 | 1146 | 717 | 0.0258 |
| C-10-C | 1250 | 48 | 0.21 | 1146 | 48.5 | 0.00136 | 1147 | 1,624 | 0.00134 |
| C-10-D | 1250 | 48 | 0.21 | 1146 | 48.5 | 0.00136 | 1147 | 1,624 | 0.00134 |
| C-11-A | 1250 | 46 | 0.21 | 1349 | 1.66 | 1.0 | 1349 | 37 | 1.0 |
| C-11-B | 1250 | 46 | 0.21 | 1349 | 4.83 | 0.0175 | 1349 | 154 | 0.0179 |
| C-11-C | 1250 | 46 | 0.21 | 1348 | 2.33 | 0.21 | 1353 | 60 | 0.21 |
| C-11-D | 1250 | 46 | 0.21 | 1351 | 22 | 0.00059 | 1353 | 350 | 0.00059 |
| C-12-A | 1250 | 48 | 0.21 | 1349 | 1.66 | 1.0 | 1349 | 37 | 1.0 |
| C-12-B | 1250 | 48 | 0.21 | 1349 | 4.83 | 0.0175 | 1349 | 154 | 0.0179 |
| C-12-C | 1250 | 48 | 0.21 | 1348 | 2.33 | 0.21 | 1353 | 60 | 0.21 |
| C-12-D | 1250 | 48 | 0.21 | 1351 | 22 | 0.00059 | 1353 | 350 | 0.00059 |
| C-13-A | 1250 | 48 | 0.21 | 1101 | 10.5 | 1.0 | 1101 | 327 | 1.0 |
| C-13-B | 1250 | 48 | 0.21 | 1101 | 10.5 | 1.0 | 1101 | 327 | 1.0 |
| C-13-C | 1250 | 48 | 0.21 | 1049 | 17.3 | 1.0 | 1050 | 474 | 1.0 |
| C-13-D | 1250 | 48 | 0.21 | 1049 | 17.3 | 1.0 | 1050 | 474 | 1.0 |
| C-15-A | 1250 | 48 | 0.21 | 950 | 24 | 0.21 | 950 | 1,684 | 0.21 |
| C-15-B | 1250 | 48 | 0.21 | 950 | 24 | 0.21 | 950 | 1,684 | 0.21 |
| C-15-C | 1250 | 48 | 0.21 | 950 | 35 | 0.0060 | 948 | 6,632 | 0.0059 |
| C-15-D | 1250 | 48 | 0.21 | 950 | 35 | 0.0060 | 948 | 6,632 | 0.0059 |
| C-16-B | 1250 | 48 | 0.21 | 800 | 96 | 0.0035 | 800 | 21,150 | 0.0026 |
| | | | | | | | 800 | 55,872 | 0.0026 |
| C-17-A | 1250 | 48 | 0.21 | 1299 | 2.1 | 1.0 | 1300 | 84 | 1.0 |
| C-17-B | 1250 | 48 | 0.21 | 1299 | 2.1 | 1.0 | 1300 | 84 | 1.0 |
| C-17-C | 1250 | 48 | 0.21 | 1198 | 4.3 | 1.0 | 1201 | 125 | 1.0 |
| C-17-D | 1250 | 48 | 0.21 | 1198 | 4.3 | 1.0 | 1201 | 125 | 1.0 |
| C-20-A | 1250 | 62 | 0.21 | 1249 | 3 | 1.0 | 1248 | 82 | 1.0 |
| C-20-B | 1250 | 62 | 0.21 | 1249 | 3 | 1.0 | 1248 | 82 | 1.0 |
| C-20-C | 1250 | 62 | 0.21 | 1352 | 10 | 0.00179 | 1352 | 254 | 0.00181 |
| C-20-D | 1250 | 62 | 0.21 | 1352 | 10 | 0.00179 | 1352 | 254 | 0.00181 |
| C-21-A | — | — | — | — | — | — | 1147 | 237 | 1.0 |
| C-21-B | — | — | — | — | — | — | 1147 | 237 | 1.0 |
| C-22-A | 1250 | 54 | 0.21 | 800 | 213 | 0.0027 | 800 | 21,150 | 0.0026 |
| C-22-B | 1250 | 54 | 0.21 | 800 | 213 | 0.0027 | 800 | 21,150 | 0.0026 |
| | | | | | | | 800 | 55,872 | 0.0026 |
| C-22-C | 1250 | 54 | 0.21 | 800 | 213 | 0.0027 | 800 | 21,150 | 0.0026 |
| | | | | | | | 800 | 55,872 | 0.0026 |
| C-24-A | — | — | — | — | — | — | 1155 | 932 | 1.0 |
| C-24-B | — | — | — | — | — | — | 1155 | 932 | 1.0 |

* Concentration profile determined by counting residual activity after each thin section was removed.

vironment. At 705°C, however, the concentration vs distance curve shows an increasing rather than decreasing slope near the surface of the disk, and on the log concentration vs $x^2$ plot (Fig. 9b) points near the surface lie far above the straight line joining the points obtained deep in the oxide disk. As the diffusion temperature was raised from 705° to 900°C, the curves gradually changed from the form shown in Fig. 9b to that in Fig. 9a, and above 800°C often only a single initial high point was found. The curvature in Fig. 9b could not have been caused by reflection from an internal barrier, as the semi-logarithmic plots deep within the disks were always linear. Nor could the diffusion coefficient have changed with depth. Not only were most of the disks given a prediffusion anneal, but also both theory and experiment indicate that, when diffusion occurs via lattice vacancies, the diffusion specimen will come to equilibrium with its environment very early in the diffusion anneal.

When the surfaces of the oxide disks were examined under X540 at various stages in the diffusion procedure, it was found that a number of changes took place during the annealing periods. After polishing with 3/0 paper, the surface was covered by fine parallel scratches and grain boundaries were invisible. After a prediffusion anneal at 900°C and above, the surface became almost free of polishing scratches, the orientation of the different grains could be clearly seen, and the grain boundaries were obvious (Fig. 2a). After applying the $Fe^{59}$ by evaporation from a hot filament, the appearance of the surface was unchanged; after plating on the tracer, the original surface was still visible although not as clearly as before. After a diffusion anneal at 900°C and above, the surface was unchanged from that shown in Fig. 2a. After a diffusion anneal below 900°C, however, the surface was covered by a mass of very fine crystals, which hid the grain orientation and most of the grain boundaries. Fig. 10a shows the surface of an electroplated specimen near the edge of the active deposit showing the surface of the underyling oxide. When the activity was evaporated on, the deposit was much thinner and the needles correspondingly finer (Fig. 10b). The thickness of deposited layer therefore seems to control

**Table IV. Continued**

| Surface Activity Ratio, After: Before | Self-Diffusion Coefficient Sq Cm per Sec | |
|---|---|---|
| | Surface Method | Sectioning Method |
| 0.217 | 2.6x10⁻⁹ | — |
| 0.225 | 2.4x10⁻⁹ | — |
| 0.200 | 3.0x10⁻⁹ | 2.6x10⁻⁹* |
| 0.207 | 3.1x10⁻⁹ | — |
| 0.239 | 7.0x10⁻¹⁰ | — |
| 0.245 | 6.5x10⁻¹⁰ | 6.2x10⁻¹⁰* |
| 0.230 | 7.8x10⁻¹⁰ | — |
| 0.247 | 6.2x10⁻¹⁰ | — |
| 0.172 | 8.7x10⁻⁹ | — |
| 0.172 | 8.7x10⁻⁹ | 8.9x10⁻⁹* |
| 0.178 | 9.8x10⁻⁹ | — |
| 0.182 | 9.0x10⁻⁹ | 1.05x10⁻⁸* |
| 0.175 | 1.7x10⁻⁹ | — |
| 0.171 | 1.8x10⁻⁹ | 2.0x10⁻⁹* |
| 0.181 | 1.9x10⁻⁹ | 2.1x10⁻⁹* |
| | | 2.0x10⁻⁹† |
| 0.179 | 2.0x10⁻⁹ | — |
| 0.342 | 2.4x10⁻¹¹ | — |
| 0.274 | 2.4x10⁻¹¹ | — |
| 0.345 | 2.4x10⁻¹¹ | — |
| 0.270 | 2.5x10⁻¹¹ | — |
| 0.332 | 2.7x10⁻¹¹ | — |
| 0.274 | 2.4x10⁻¹¹ | — |
| 0.338 | 2.5x10⁻¹¹ | — |
| 0.276 | 2.4x10⁻¹¹ | — |
| 0.386 | 2.9x10⁻⁹ | — |
| 0.215 | 2.7x10⁻⁹ | 2.3x10⁻⁹* |
| | | 2.6x10⁻⁹† |
| 0.243 | 4.0x10⁻¹⁰ | 4.2x10⁻¹⁰* |
| 0.234 | 4.5x10⁻¹⁰ | — |
| 0.178 | 5.4x10⁻⁹ | — |
| 0.237 | 1.4x10⁻⁹ | — |
| 0.240 | 1.3x10⁻⁹ | 1.4x10⁻⁹* |
| 0.211 | 2.9x10⁻⁹ | — |
| 0.215 | 2.7x10⁻⁹ | — |
| 0.184 | 2.7x10⁻⁹ | — |
| 0.189 | 2.5x10⁻⁹ | 2.5x10⁻⁹* |
| 0.187 | 2.6x10⁻⁹ | — |
| 0.179 | 5.4x10⁻⁹ | — |
| 0.182 | 2.8x10⁻⁹ | — |
| 0.187 | 1.2x10⁻⁹ | — |
| 0.179 | 1.3x10⁻⁹ | — |
| 0.186 | 5.1x10⁻⁹ | 5.0x10⁻⁹* |
| 0.177 | 1.5x10⁻⁹ | — |
| 0.187 | 3.1x10⁻⁹ | — |
| 0.177 | 6.5x10⁻⁹ | 7.3x10⁻⁹* |
| 0.189 | 4.9x10⁻⁹ | — |
| 0.178 | 1.4x10⁻⁹ | 1.7x10⁻⁹* |
| 0.187 | 3.1x10⁻⁹ | — |
| 0.181 | 6.0x10⁻⁹ | — |
| 0.182 | 6.2x10⁻⁹ | — |
| 0.178 | 6.7x10⁻⁹ | — |
| 0.191 | 3.7x10⁻⁹ | — |
| 0.189 | 3.8x10⁻⁹ | — |
| 0.221 | 6.1x10⁻¹⁰ | — |
| 0.219 | 6.3x10⁻¹⁰ | 6.9x10⁻¹⁰* |
| 0.206 | 2.0x10⁻⁹ | — |
| 0.207 | 1.9x10⁻¹⁰ | — |
| 0.299 | 1.9x10⁻¹¹ | — |
| 0.215 | 2.0x10⁻¹¹ | 1.9x10⁻¹¹* |
| 0.162 | 3.6x10⁻⁹ | — |
| 0.164 | 3.5x10⁻⁹ | — |
| 0.179 | 1.7x10⁻⁹ | — |
| 0.180 | 1.7x10⁻⁹ | — |
| 0.185 | 2.4x10⁻⁹ | — |
| 0.185 | 2.4x10⁻⁹ | 2.7x10⁻⁹* |
| 0.181 | 8.1x10⁻⁹ | — |
| 0.184 | 7.7x10⁻⁹ | — |
| 0.220 | 4.4x10⁻⁹ | — |
| 0.216 | 4.7x10⁻⁹ | — |
| 0.291 | 2.0x10⁻¹¹ | — |
| 0.306 | 1.7x10⁻¹¹ | — |
| 0.221 | 1.9x10⁻¹¹ | 2.0x10⁻¹¹* |
| 0.294 | 1.9x10⁻¹¹ | — |
| 0.216 | 2.0x10⁻¹¹ | — |
| 0.142 | 4.5x10⁻⁹ | — |
| 0.141 | 4.5x10⁻⁹ | — |

† Concentration profile determined by counting the activity in each of the thin sections removed.

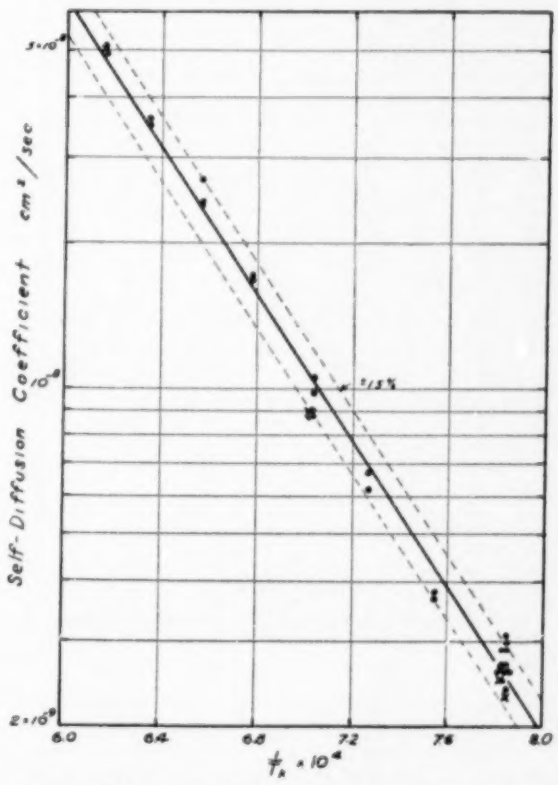


Fig. 8—Self-diffusion coefficient of cobalt in cobaltous oxide at an oxygen pressure of 1 atm as a function of temperature. X represents sectioning method; filled circle, surface method.

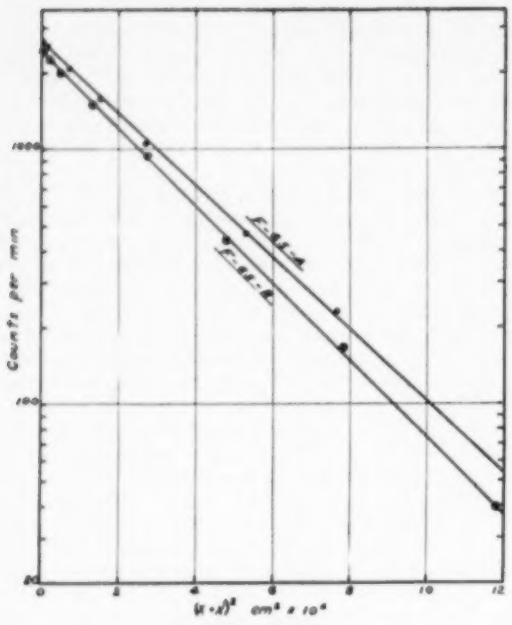


a—FeO at 923°C.

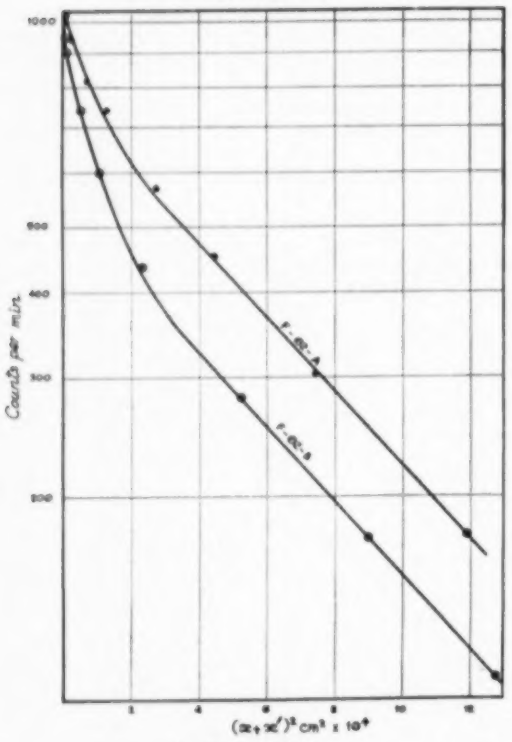


b—FeO at 705°C.

Fig. 9—Graph showing the log of the concentration of tracer (counts per min) as a function of the square of the distance in FeO.

the size of the crystals formed. To determine if a disturbed oxide layer would develop a covering of fine crystals when annealed below 900°C, a disk polished to 3/0 was annealed at 700°C for 48 hr. Again, the surface became covered exactly as shown in Fig. 10a. When a disk covered by a mass of fine crystals was re-annealed at 1000°C for 1 hr, the original surface and grain boundaries became visible over most of the disk and the remaining needles were much larger.

Below 900°C, therefore, strained layers of iron or wüstite apparently form needlelike crystals of FeO in $H_2/H_2O$ atmospheres. When this occurs with a deposit of $Fe^{55}$ on an FeO disk during a diffusion anneal because of the almost point contacts between the crystals and the underlying oxide, the tracer is able to diffuse only very slowly out of the needles and into the bulk phase. Thus, the tracer may be said to be "bound" to the surface of the diffusion specimens.

The formation of such fine crystals and of long thin needles has also been found in this laboratory during the oxidation of strained iron to wüstite in $H_2/H_2O$ atmospheres.

If some of the tracer is bound to the surface of the oxide disk, the apparent diffusion coefficient by the surface method will decrease with increasing diffusion times. The diffusion anneals at 700°C of several disks therefore were interrupted several times, the specimens counted, and the apparent diffusion coefficient calculated. The results were exactly as anticipated: the apparent diffusion coefficient after an anneal of 24 hr being only 60 pct of what it was after an anneal of 1 hr.

A diffusion coefficient which appears to decrease with increasing diffusion times was also found by Ruder and Birchenall[9] during a self-diffusion study of cobalt metal by the surface method. They explained the effect as being due to a change in the scattering of $\beta$ particles by the specimen surface as the $Co^{60}$ diffused inward. This explanation is not justified here, however, because of the photoelectric absorption of the X-rays with no resulting scatter.

The phenomenon of bound tracer was not found by Himmel, Mehl, and Birchenall[11] during their FeO self-diffusion studies. As mentioned, their results agree closely with the sectioning results reported here. In addition, they found no change in the apparent diffusion coefficient with diffusion time at 700°C. The only significant difference between the procedure adopted by Himmel et al. and that used in this investigation was that immediately after plating they swabbed their $Fe^{59}$ deposits under alcohol. It appears that this swabbing may have removed some loosely adherent tracer, which could have been responsible for the bound activity found here. This mechanism does not, of course, explain the low results obtained when the tracer was evaporated onto the oxide. This deposit may also have been loose and porous, but thin evaporated layers are usually assumed to be dense and adherent to the underlying material.

High points on log concentration vs $x^2$ plots similar to those shown in Fig. 9b have been found during diffusion studies on both metals and nonmetals.[15-17] This strongly suggests that the phenomenon of bound tracer on the surface of diffusion specimens may be common. If so, this would explain much of the scatter between the results obtained by the surface method by different investigators. A remarkable feature of the phenomenon is the consistency of the apparent diffusion coefficient obtained with a fixed experimental procedure and the way the logarithm of the diffusion coefficient gives a straight line against $1/T$. An investigator using the surface method, who does not check his results by the sectioning method, therefore may be given a false sense of accuracy.

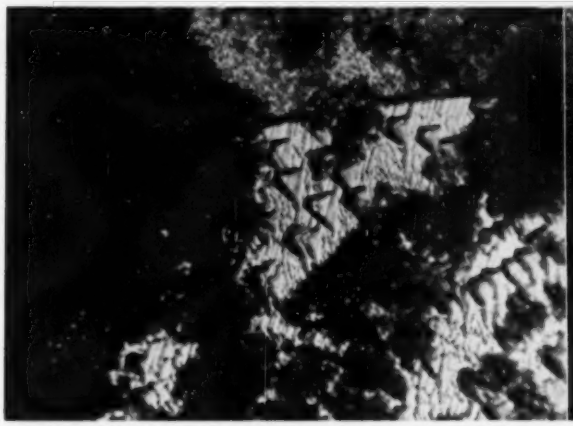

Fig. 10a—Surface of a prediffused wustite specimen after the active deposit had been plated on and the specimen annealed for 24 hr at 703°C. X275. Area reduced approximately 25 pct for reproduction.

Fig. 10b—Surface of a disk after the active deposit had been evaporated on and diffused for 24 hr at 696°C. X350. Area reduced approximately 25 pct for reproduction.

*Diffusion in Cobaltous Oxide:* The reproducibility obtained in these measurements (the scatter in Fig. 7 is less than ±15 pct) was most satisfactory. At all temperatures (950° to 1350°C) the tracer distribution was exactly as given by Eq. 2 and the log concentration vs $x^2$ plots were good straight lines. This indicates that: 1—The tracer was never bound to the oxide surface at any of the temperatures used in the investigation. 2—The oxide was always in equilibrium with its gaseous environment to a depth greater than the penetration of the tracer atoms. 3—There was no reflection of tracer from an internal barrier.

The good agreement between the surface and sectioning methods indicates that the surface method can give accurate results with a $\beta+\gamma$ emitting tracer if a graphical solution of the experimental data is used. In view of the roughness of the oxide surface because of grain growth during the prediffusion and diffusion anneals, the excellent agreement between the surface and grinding methods casts doubt on the "roughness" hypothesis of Ruder and Birchenall.[8]

In view of the trouble experienced with bound activity in the wüstite work, the excellent contact obtained in this work was rather surprising. Further evidence of the absence of this effect was given by a microscopic examination of the oxide surfaces both before and after the diffusion anneals. In every case the surface remained clean and bright. As a further check, the diffusion anneal of several disks was interrupted as described for the wüstite work. In every case, however, the apparent diffusion coefficient was independent of the diffusion time.

As all the work on CoO was above the temperature where difficulty was encountered with the wüstite, four CoO disks were annealed for 96 hr and diffused for 196 and 355 hr at 800°C in an oxygen pressure of 0.0031 atm, and another four specimens were annealed for 213 hr and diffused for 352 and 931 hr at an oxygen pressure of 0.0027 atm. Several of the disks were then mounted and sectioned. At both oxygen pressures, the apparent diffusion coefficient was independent of the diffusion time, and good checks were obtained both between different disks and by the surface and sectioning methods on the same disk, see specimens C-16, C-19, and C-22 in Table IV. Although the surface of some of the disks developed a brownish coating during the prediffusion anneal and at X540 the grain boundaries of all the disks were covered by a layer of very small crystals, none of the $Co^{60}$ tracer appeared to be bound to the surface. Because of this conflicting

## Table V. Summary of Possible Errors

| Source | Possible Error | Effect on $D$ | |
|---|---|---|---|
| | | Surface Method | Sectioning Method |
| **Errors in the Measurements with Wüstite** | | | |
| $p$, $H_2/H_2O$ | ±4 pct | ±3 pct | ±3 pct |
| Temperature measurement | ±2°C | ±3 pct | ±3 pct |
| Temperature fluctuations | ±2°C | ±3 pct | ±3 pct |
| Statistical counting errors | ±1 pct | ±2 pct | — |
| Diffusion time | ±3 min | ±10 pct at 1000°C, nil below 900°C | ±10 pct at 1000°C, nil below 900°C |
| Measurement of penetration | ±2x10⁻⁴ cm | — | ±1 pct |
| Absorption coefficient | ±5 pct | ±10 pct | Nil |
| **Errors in the Measurements with Cobaltous Oxide** | | | |
| $P_{O_2}$ | ±2 pct | ±1 pct | ±1 pct |
| Temperature measurement | ±2°C | ±3 pct | ±3 pct |
| Temperature fluctuations | ±2°C | ±3 pct | ±3 pct |
| Statistical counting errors | ±1 pct | ±2 pct | — |
| Diffusion time | ±3 min | ±8 pct at $P_{O_2}$ = 1.0, $T$ = 1350°C, nil below 1150°C | ±8 pct at $P_{O_2}$ = 1.0, $T$ = 1350°C, nil below 1150°C |
| Measurement of penetration | ±2x10⁻⁴ cm | — | ±1 pct |
| Absorption coefficient for sectioning method | ±25 pct | — | ±2 pct |
| Error in $\gamma$ count for sectioning method | ±33 pct | — | ±3 pct |
| $\beta+\gamma$ absorption curve for surface method | ±5 pct | ±5 pct | — |

evidence for and against bound tracer, it is impossible to say whether or not binding of the tracer would occur on CoO disks at lower temperatures. It is obvious, however, that no significant binding occurs down to 800°C.

*Composition of Cobaltous Oxide and the Diffusion Mechanism:* The concentration of excess oxygen found in cobaltous oxide in this study (Table III) was proportional to the 0.26 ±0.1 power of the oxygen pressure between 1000° and 1350°C. This fact, taken in conjunction with the finding that the diffusion coefficient of cobalt in the oxide is also proportional to a similar power of the oxygen pressure, shows that the nonstoichiometry is caused by vacant cation sites and that cation diffusion occurs via these sites as in the case of iron in wüstite.[11]

The O:Co ratios found here are much lower than the value of 1.04:1 found by Preece and Lucas[16] at 1000°C. These investigators do not describe their procedure beyond saying that they heated $Co_3O_4$ which "reverted" to CoO, which they then heated at 1000°C and weighed. Unless they cooled their specimens quickly before weighing, much of their excess oxygen can be attributed to the formation of $Co_3O_4$ during cooling.

Himmel, Mehl, and Birchenall[11] showed that, within the relatively large limits of error of their measurements, the self-diffusion coefficient of iron in wüstite is approximately proportional to the concentration of vacant iron lattice sites at 897°C (see their Fig. 6). At 800°C, however, the diffusion coefficient is almost independent of the vacancy concentration, but at 983°C it is proportional to the 1.25 power of the vacancy concentration. The fact that the number of vacant cation sites in wüstite is proportional to powers of the oxygen pressure much greater than 0.167 suggests, as Richardson[10] and Hoar[20] have already indicated, that there may be a considerable degree of association between the vacancies and the ferric iron atoms,* as well as possible variations of the activity coefficients with concentration.

* The equilibria may be represented as follows:
$2\,Fe\cdots + \tfrac{1}{2}O_2 = 2\,Fe\cdots + \square + O^{-}$; $\square \propto (P_{O_2})^{1/6}$
$2\,Fe\cdots + \tfrac{1}{2}O_2 = Fe\cdots + (Fe\cdots\square) + O^{-}$; $\square \propto (P_{O_2})^{1/4}$
$2\,Fe\cdots + \tfrac{1}{2}O_2 = (Fe\cdots\square\,Fe\cdots) + O^{-}$; $\square \propto (P_{O_2})^{1/2}$.

It would be expected that the completely associated sites in wüstite would be less useful for diffusion than those partially associated and these again less useful than the fully dissociated sites. The diffusion of a ferrous ion into an associated vacancy commonly must involve the simultaneous partial or complete dissociation of the vacancy, although there are a restricted number of ways in which a ferrous ion could diffuse into an associated vacancy without dissociating it further. The accuracy of the data on self-diffusion in wüstite does not permit a decision to be made, although the fact that at the lowest temperatures the self-diffusion coefficient is almost independent of the total number of vacant sites suggests that it is the fully dissociated sites which are most important. It can be calculated, for example, from the three simplest equilibria* that, under conditions where the proportion of fully dissociated vacancies is very small, the molar concentration of fully dissociated vacancies is independent of the oxygen pressure and of the total vacancy concentration.

* See footnote above.

Unfortunately the accuracy of the authors' relation between composition and oxygen pressure for cobaltous oxide is insufficient to show how the cation diffusion coefficient varies with the total concentration of vacant cobalt-lattice sites. Since $D$ is proportional to powers of the oxygen pressure much greater than 0.167, however, there may be considerable association of the vacancies. These powers are approximately the same as those which can be calculated from the measurements of Darken and Gurry[9] for the total concentration of vacancies in wüstite nearly saturated with iron, i.e., 0.33 at 1100°C and 0.27 at 1400°C.

If the activity coefficients of the cobaltic ions and the vacancies were independent of concentration and diffusion were to occur via all three types of vacancy, it would be expected that the slopes of the lines in Fig. 7 would increase with increasing oxygen pressure and, hence, increasing total concentration of the vacancies. If diffusion occurred primarily via fully dissociated vacancies, the slopes would be expected to decrease with increasing oxygen pressure. The actual points suggest that, if there is a change in slope, it is a slight increase with increasing oxygen pressure, although the precision of the results is insufficient to confirm this.

Wagner and Koch[21] found that the conductivity of CoO at 1000°C varied as the 0.23 power of the oxygen pressure, again indicating considerable association between cobaltic ions and vacancies. The difference between 0.23 and 0.351 for the oxygen dependence of the conductivity and self-diffusion in CoO appears to be outside the experimental errors. Possibly it may be attributed to impurities such as iron in the cobalt used by Wagner and Koch. Under the range of conditions of their experiments, all such iron would be in the ferric state and the dependence of the conductivity on oxygen pressure thereby decreased.

*Rate of Equilibration of Cobaltous Oxide:* Since cation diffusion in cobaltous oxide occurs via cation vacancies, it follows (if the isotope effect of Bardeen and Herring[7] is neglected) that

$$D_t = D_c = D_v \frac{n}{N} \qquad [8]$$

where $D_t$ is the diffusion coefficient of the tracer, $D_c$ is the diffusion coefficient of the cations, $D_v$ is the diffusion coefficient of the vacancies, and, $\frac{n}{N}$ is the lattice-defect concentration.

From Eq. 8 the diffusion coefficient of the vacancies is many times that of the cations. From this, Seitz[22] concluded that the lattice-vacancy concentration should approach the equilibrium value for the environment in a time short compared with that required for a substantial movement of cations (e.g., of tracer in a diffusion anneal). It would seem therefore that, if at the commencement of a diffusion experiment there is a vacancy gradient across a single phase specimen (as could, for example, be set up in an oxide by making the oxide at an oxygen pressure different from that obtaining in the diffusion anneal), this gradient should almost disappear in a time which is short compared to that of the diffusion anneal. It should not, therefore, have any significant influence on the movement of the tracer and, hence, on the measured diffusion coefficients. That this hypothesis has been proven for cobaltous oxide can be seen from the results given in Table IV, where the measured diffusion coefficient is shown to be independent of the preparation of the diffusion specimens. Although the lattice defects in metal-

deficient compounds are not stabilized by thermal effects as they are in pure metals, this rapid equilibration must cast doubt on the conclusions of many who have attributed anomalous diffusion results to the "freezing in" of lattice defects. This doubt must remain until it has been proven that these anomalous results do result from the freezing in of defects.


## Summary

Measurements have been made of the self-diffusion coefficients of iron in wüstite at one composition and of cobalt in cobaltous oxide over a range of compositions. Both sectioning and decrease of surface-activity methods have been used and the results compared. It has been found that with wüstite below 850°C, the results obtained by the decrease of surface-activity method can be incorrect due to the deposited tracer forming tiny crystals during the diffusion anneal and thus not bonding properly to the basic oxide. With cobaltous oxide, this phenomenon was not observed down to 800°C.

The decrease of surface-activity method therefore is not as reliable as a sectioning technique, and whenever used it should be checked by a few sectioning experiments over the range of conditions studied.

The diffusion coefficients measured for cobaltous oxide were

At 1000°C, $D = 2.6\text{x}10^{-9}\ (P_{O_2})^{0.86}$ sq cm per sec$^{-1}$.
At 1150°C, $D = 9.0\text{x}10^{-8}\ (P_{O_2})^{0.89}$ sq cm per sec$^{-1}$.
At 1350°C, $D = 5.1\text{x}10^{-6}\ (P_{O_2})^{0.88}$ sq cm per sec$^{-1}$.

The statistical probable errors are approximately 5 pct in $D$ and 2 pct in the power of the oxygen pressure.

The composition of CoO in equilibrium with 1 atm of oxygen was found by analysis to range from $CoO_{1.005}$ at 1000°C to $CoO_{1.010}$ at 1350°C; the concentration of excess oxygen was found to be proportional to the 0.26±0.1 power of the oxygen pressure between these temperatures.

It has been concluded that in CoO diffusion of cobalt occurs via vacant cation sites. It is not clear, however, whether all the vacant sites or only those fully dissociated from the cobaltic ions are involved in the process. A cobaltous oxide disk reaches equilibrium with its environment in a time which is very short compared to the time for diffusion of a tracer into the disk.



## Acknowledgments

The authors wish to thank Mr. C. B. Alcock for his helpful advice and interest. They are indebted to the National Research Council of Canada for an overseas scholarship granted one of the authors.


## References


[1] G. von Hevesey and W. Seith: *Ztsch. Physik. Chemie* (1929) **56**, p. 790.
[2] J. Steigman, N. Shockley, and F. Nix: *Physical Review* (1939) **56**, p. 13.
[3] C. Raynor, L. Thomassen, and L. Rouse: *Trans.* ASM (1942) **30**, p. 313.
[4] C. Birchenall and R. Mehl: *Trans.* AIME (1950) **188**, p. 144; JOURNAL OF METALS (January 1950).
[5] F. Buffington, I. Bakalar, and M. Cohen: *Physics of Powder Metallurgy.* (1951) Edited by W. Kingston, p. 92. New York. McGraw-Hill Book Co.
[6] A. Hedvall, C. Brisi, and R. Lindner: *Archiv. for Kemi* (1952) **4**, p. 377.
[7] J. Bardeen and C. Herring: *Atom Movements.* (1951) p. 87. Cleveland. ASM.
[8] L. S. Darken and R. W. Gurry: *Journal* American Chemical Soc. (1945) **67**, p. 1398.
[9] R. Ruder and C. Birchenall: *Trans.* AIME (1951) **191**, p. 142; JOURNAL OF METALS (February 1951).
[10] P. Gruzin: *Doklady Akademii Nauk* SSSR (1952) **86**, No. 2, p. 289.
[11] L. Himmel, R. Mehl, and C. Birchenall: *Trans.* AIME (1953) **197**, p. 827; JOURNAL OF METALS (June 1953).
[12] J. Fisher: *Journal of Applied Physics* (1951) **22**, p. 74.
[13] R. Eckert and H. Drickamer: *Journal of Chemical Physics* (1952) **20**, p. 13.
[14] P. Miller and F. Banks: *Physical Review* (1942) **61**, p. 648.
[15] F. Banks: *Physical Review* (1941) **59**, p. 376.
[16] D. Mapother and R. Maurer: *Physical Review* (1948) **73**, p. 1260; *Journal of Chemical Physics* (1950) **18**, p. 1231.
[17] M. Feldman, W. Goeddel, and G. Dienes: *Journal of Applied Physics* (1952) **23**, p. 1200.
[18] A. Preece and G. Lucas: *Journal* Institute of Metals, London (1952) **81**, p. 219.
[19] F. D. Richardson: *Discussions* Faraday Society (1948) **4**, p. 286.
[20] T. P. Hoar: *Discussions* Faraday Society (1948) **4**, p. 320.
[21] C. Wagner and E. Koch: *Ztsch. Physik. Chemie* (1936) **B32**, p. 439.
[22] F. Seitz: *Phase Transformations in Solids.* (1951) p. 77. New York. John Wiley and Sons.


---

**Technical Note**

# A Calorimetric Investigation of Heats of Formation and Precipitation In Some Cu-Sn Alloys


by J. B. Cohen, J. S. Ll. Leach, and M. B. Bever


IN the work reported here, the heats of formation of a copper-rich Cu-Sn ($\alpha$) solid solution and of the $Cu_3Sn$ ($\epsilon$) phase were measured by tin solution calorimetry. An approximate determination of the heat effect attending the precipitation of $\epsilon$ from a supersaturated $\alpha$ solid solution was also made.

Alloys and mechanical mixtures were prepared from OFHC copper, reported to be 99.975 pct pure, and tin containing less than 0.03 pct analyzed impurities. The alloys were melted by induction in a graphite crucible, chill cast, and annealed in vacuo to obtain homogeneous single-phase structures. The alloys were analyzed for copper, and tin was assumed to be the only other constituent; contamination was unlikely, and, in particular, the solubility of carbon in Cu-Sn alloys is negligibly small.[1] On this basis, the alloys contained 8.10 and 37.95 wt pct Sn. The 8.10 pct alloy, after quenching from the annealing temperature, was supersaturated metastable $\alpha$ and the 37.95 pct alloy fell within the narrow composition range of the $\epsilon$ phase;[2] metallographic inspection showed that only these single-phase structures were present.

Samples of $\alpha$ and copper were rolled into thin strips to provide maximum surface for dissolution, while those of $\epsilon$ and tin were prepared as small lumps. All samples were cleaned thoroughly.

The calorimetric method has been described previously.[3] Samples at 0°C were added to a bath of liquid tin at 350°C. The observed heat effect was composed of the heat required for raising a sample from 0°C to 350°C and the heat of dissolution. The difference between the heat effects associated with the addition of an alloy and the addition of a mechanical mixture of the same composition represents the difference in their energy contents in the initial states, that is, the heat of formation of the alloy at 0°C.

In each calorimetric run, two samples of alloy and two samples of mechanical mixture were added. The heat effect, referred to infinite dilution, for each mixture addition was subtracted from that for each alloy addition. Four values of the heat of formation thus were obtained in a run.

*$\epsilon$ Phase:* Twelve values of the heat of the formation of $\epsilon$ at 0°C were obtained. Their mean and the rms error were $-1870 \pm 157$ cal per gram-atom of $\epsilon$. (One gram-atom of $\epsilon$ is equal to 77.12 grams.) The heat of formation of $\epsilon$ has been determined by other investigators. They used dissolution in aqueous bromine-potassium bromide solutions at 20°C[4, 5] or determined the difference in the heat effects associated with cooling alloys and the constituent elements from the liquid state to room temperature, which yielded the heat of formation of the alloy at 20°C.[6] With these methods, the quantity sought is a small difference of large values, while in the work reported here the heat of formation of $\epsilon$ was of the same order of magnitude as the observed heat effects. The published values of the heat of formation of $\epsilon$ are $-1.5$,[4] $-1.8$,[5] $-1.9$,[6] and $-2.0$[6] cal per gram-atom of alloy.

*$\alpha$ Solid Solution:* The heat of formation of supersaturated $\alpha$ containing 8.10 pct Sn was determined as approximately $-175$ cal per gram-atom (equal to 66.01 grams) of alloy. This figure is based on the best five of 12 values; the others were discarded because of known experimental difficulties or excessive deviations from the mean.

*Precipitation from $\alpha$ Solid Solution:* Samples of the supersaturated $\alpha$ solid solution were annealed at 254°C for 219 hr. Metallographic inspection indicated the presence of two phases, but these may not have been equilibrium $\alpha$ and $\epsilon$.[7]

The energy effect associated with the precipitation is the difference between the heats of formation of the supersaturated solid solution and the alloy in which precipitation has occurred. The heat of formation of the latter was determined as approximately $-256$ cal per gram-atom. This figure is based on only three of four values and additional work would be necessary to establish it firmly. The energy change associated with precipitation was, therefore, approximately $-81$ cal per gram-atom or $-1.2$ cal per gram of alloy, referred to 0°C.

Energy effects associated with precipitation from solid solutions in various systems have been determined by several investigators,[8-13] who measured the evolution of heat during the process of precipitation. Their results demonstrate that the heat effect of precipitation depends on the amount of precipitate and, hence, on the temperature of precipitation and the overall composition of the alloy. No data are available for the Cu-Sn system.


## Acknowledgment

The authors thank Professor C. Wagner for helpful discussions and Mr. L. R. Rubin for advice and assistance. This work was supported in part by the United States Atomic Energy Commission under Contract AT(30-1)-1002.


## References


[1] M. B. Bever and C. F. Floe: *Trans.* AIME (1946) **166**, p. 128.

[2] G. V. Raynor: *Annotated Equilibrium Diagram Series.* Institute of Metals, London (1944) No. 2.

[3] L. B. Ticknor and M. B. Bever: *Trans.* AIME (1952) **194**, p. 941; JOURNAL OF METALS (September 1952).

[4] M. Herschkowitsch: *Ztsch. Physik. Chemie* (1898) **27**, p. 123.

[5] W. Biltz, W. Wagner, H. Pieper, and W. Holverscheit: *Ztsch. Anorg. Allgem. Chemie* (1924) **134**, p. 25.

[6] F. Körber and W. Oelsen: *Mitteilungen* Kaiser-Wilhelm Institut für Eisenforschung, Düsseldorf (1937) **19**, p. 209.

[7] C. Haase and F. Pawlek: *Ztsch. Metallkunde* (1936) **28**, p. 73.

[8] W. Swietoslawski, J. Czochralski, et al.: *Wiadomosci Instytutu Metalurgji* (1936) **3**, p. 59; (1937) **4**, p. 45 (after *Metall Abstracts* (Series 2) **3**, p. 296; **4**, p. 505.

[9] H. Calus and R. Smoluchowski: *Physical Review* (1940) **58**, p. 205.

[10] J. Nyström: *Arkiv för Fysik* (1949) **1**, p. 359.

[11] G. Borelius, J. Andersson, and K. Gullberg: *Ingeniörsvetenskapsakademien Handlingr Nr 169* (1943).

[12] G. Borelius, S. Berglund, and O. Avsan: *Arkiv för Fysik* (1951) **2**, p. 551.

[13] G. Borelius and S. Berglund: *Arkiv för Fysik* (1951) **4**, p. 173.



J. B. COHEN, Student Associate AIME, J. S. LL. LEACH, and M. B. BEVER, Member AIME, are Research Assistant, Dept. of Metallurgy, Staff Member, Div. of Industrial Cooperation, and Associate Professor, Dept. of Metallurgy, respectively, Massachusetts Institute of Technology, Cambridge, Mass.



TN 233E. Manuscript, June 30, 1954.

This note is based on a thesis by J. B. Cohen submitted, in partial fulfillment of the requirements for the degree of Bachelor of Science, to the Massachusetts Institute of Technology.

# Effect of Nitrogen on Sigma Formation in Cr-Ni Steels At 1200°F (650°C)

by G. F. Tisinai, J. K. Stanley, and C. H. Samans

**The addition of nitrogen (0.10 to 0.20 pct) to Fe-Cr-Ni alloys of simulated commercial purity results in a real displacement of the $\sigma$ phase boundaries to higher chromium contents. The effect is small for the $(\gamma + \sigma)/\gamma$ boundary, but is pronounced for the $(\gamma + \alpha + \sigma)/(\gamma + \alpha)$ boundary. Although there is an indication of an exceptionally large shift of the $\sigma$ boundaries to higher chromium contents, especially in steels with nitrogen over 0.2 pct, the major portion of this apparent shift results from the fact that carbide and nitride precipitation cause "chromium impoverishment" of the matrices. The effect of combined additions of nitrogen and silicon to the Fe-Cr-Ni phase diagram is demonstrated also. Nitrogen can nullify the effect of about 1 pct Si in shifting the $(\gamma + \sigma)/\gamma$ phase boundary to lower values of chromium at all nickel levels from 8 to 20 pct. Nitrogen can nullify this $\sigma$-forming effect of about 2 pct Si at the 8 pct Ni level, but not at the 20 pct Ni level. The alloys studied were in both the cast and the wrought conditions. There are indications that the $\sigma$ phase forms more slowly in the cast alloys than in the wrought alloys if both are in the completely austenitic state. The presence of $\delta$ ferrite in the cast alloys accelerates the formation of $\sigma$. Cold working increases the rate of $\sigma$ formation in both cast and wrought alloys.**

THE major improvement in Fe-Cr-Ni austenitic alloys in recent years has been in the addition or removal of minor alloying elements to facilitate better control of corrosion resistance, sensitization, and heat resistance. One shortcoming of the austenitic Fe-Cr-Ni alloys, which never has been completely circumvented, is their propensity toward $\sigma$ formation. In the AISI-type 310 (25 pct Cr-20 pct Ni) and type 309 (25 pct Cr-12 pct Ni) steels, sufficient amounts of $\sigma$ phase can form, if service or treatment is in a suitable temperature range, to cause severe embrittlement. Also, there is a growing conviction that this phase may be contributory to some unexpected decreases in the corrosion resistance of certain of the 18 pct Cr-8 pct Ni-type steels.

The present paper discusses the effect of nitrogen additions on the location of the $(\gamma+\sigma)/\gamma$ and the $(\gamma+\alpha+\sigma)/(\gamma+\alpha)$ phase boundaries in the ternary Fe-Cr-Ni system, for cast and wrought alloys of simulated commercial purity, and in similar alloys containing up to about 2.5 pct Si. The objective is to define compositional limits for alloys which will not be susceptible to $\sigma$ formation when used near 1200°F (650°C).

An excellent review of the early studies of the $\sigma$ phase in the Fe-Cr-Ni system has been compiled by Foley.[1] Rees, Burns, and Cook[2] have determined a high purity phase diagram for the ternary system, whereas Nicholson, Samans, and Shortsleeve[3] restricted themselves to a portion of the simulated commercial-purity phase diagram. Both groups of investigators show almost an identical position for the commercially significant $(\gamma+\sigma)/\gamma$ phase boundary. Further comparison of the work of the two groups indicates that, below the 8 pct Ni level, the commercial alloys have a decidedly greater propensity toward $\sigma$ formation than the high purity alloys. The two groups of workers agreed that both the AISI-type 310 (25 pct Cr-20 pct Ni) and the type 309 (25 pct Cr-12 pct Ni) steels are well within the $(\gamma+\sigma)$ region and that the 18 pct Cr-8 pct Ni-type alloys straddle the $\sigma$-forming phase boundaries. Nicholson et al.[3] showed, in addition, that these boundaries shift toward lower chromium contents if greater than nominal amounts of silicon or molybdenum are added.

The effect of nitrogen on the location of the $\sigma$ phase boundaries in the Fe-Cr-Ni system has not been known with any certainty. In 1942, an approach to this problem was made by Krainer and Leoville-Nowak,[4] but at that time they apparently were unaware of the slow rate of $\sigma$ formation in strain-free samples and aged their samples for insufficient times, e.g., 100 hr at 650°C (1200°F) and 800°C (1470°F). For this reason, it would be expected that their $(\gamma+\sigma)/\gamma$ boundary would be shifted toward lower chromium contents (restricted $\gamma$-field) when equilibrium conditions were approximated more closely.

### Procedure for Studying the Alloys

The alloys used were prepared in the following way: Heats of 200 lb each were melted in an induction furnace. A 5 lb portion of each heat was poured into a ladle containing an aluminum slug for de-

G. F. TISINAI, J. K. STANLEY, and C. H. SAMANS, Members AIME, are Research Engineer, Section Head, and Associate Director, respectively, Materials Div., Engineering Research Dept., Standard Oil Co. (Indiana), Whiting, Ind.

Discussion on this paper, TP 3836E, may be sent, 2 copies, to AIME by Jan. 1, 1955. Manuscript, Apr. 15, 1954. Chicago Meeting, November 1954.

## Table I. Compositions of Alloys Investigated, Wt Pct

| Alloy | | Cr | Ni | Si | Mn | C | Mo | S | P | N | Matrix Composition* Cr | Matrix Composition* Ni |
|---|---|---|---|---|---|---|---|---|---|---|---|---|
| 1 | a** | 14.90 | 4.63 | 0.40 | 0.34 | 0.03 | 0.01 | — | — | 0.10 | 12.78 | 5.08 |
| | b | 15.45 | 5.37 | 0.37 | 0.39 | 0.06 | 0.01 | 0.020 | 0.004 | 0.10 | | |
| 2 | a | 14.82 | 7.60 | 0.47 | 0.40 | 0.02 | 0.01 | — | — | 0.10 | 13.03 | 8.19 |
| | b | 14.15 | 8.52 | 0.40 | 0.42 | 0.07 | 0.02 | 0.018 | 0.010 | 0.12 | | |
| 3 | a | 14.59 | 12.40 | 0.52 | 0.52 | 0.03 | 0.01 | — | — | 0.10 | 13.27 | 12.66 |
| | b | 14.68 | 12.49 | 0.42 | 0.44 | 0.06 | 0.02 | 0.016 | 0.010 | 0.11 | | |
| 4 | a | —† | — | — | — | — | — | — | — | — | 12.86 | 19.62 |
| | b | 14.40 | 19.26 | 0.35 | 0.53 | 0.06 | 0.02 | 0.021 | 0.004 | 0.10 | | |
| 5 | a | 18.27 | 2.79 | 0.59 | 0.57 | 0.03 | 0.01 | — | — | 0.10 | 16.63 | 3.87 |
| | b | 17.68 | 4.82 | 0.47 | 0.58 | 0.07 | 0.02 | 0.014 | 0.004 | 0.10 | | |
| 6 | a | — | — | — | — | — | — | — | — | 0.23 | 16.13 | 8.81 |
| | b | 18.35 | 8.58 | 0.42 | 0.40 | 0.07 | 0.02 | 0.015 | 0.010 | 0.20 | | |
| 7 | a | 16.83 | 10.21 | 0.59 | 0.52 | 0.03 | 0.01 | 0.017 | 0.010 | 0.19 | 15.21 | 10.40 |
| 8 | a | 18.11 | 12.68 | 0.51 | 0.52 | 0.04 | 0.01 | — | — | 0.15 | 16.21 | 13.21 |
| | b | 17.96 | 13.17 | 0.47 | 0.62 | 0.07 | 0.02 | 0.017 | 0.010 | 0.19 | | |
| 9 | a | — | — | — | — | — | — | — | — | — | 15.69 | 18.73 |
| | b | 17.16 | 18.41 | 0.42 | 0.39 | 0.06 | 0.01 | 0.021 | 0.004 | 0.10 | | |
| 10 | a | — | — | — | — | — | — | — | — | — | 19.20 | 2.37 |
| | b | 20.80 | 2.32 | 0.40 | 0.50 | 0.07 | 0.02 | 0.022 | 0.006 | 0.12 | | |
| 11 | a | 21.40 | 3.23 | 0.49 | 0.51 | 0.04 | 0.01 | — | — | 0.15 | 19.98 | 3.29 |
| 12 | a | 21.94 | 4.13 | 0.47 | 0.53 | 0.04 | 0.01 | 0.010 | 0.012 | 0.10 | 20.82 | 4.19 |
| 13 | a | 20.00 | 8.28 | 0.49 | 0.34 | 0.03 | 0.01 | — | — | 0.11 | 18.60 | 8.90 |
| | b | 19.89 | 9.23 | 0.42 | 0.44 | 0.06 | 0.02 | 0.015 | 0.004 | 0.09 | | |
| 14 | a | 20.54 | 13.04 | 0.42 | 0.38 | 0.03 | 0.01 | — | — | 0.10 | 19.28 | 13.50 |
| | b | 20.62 | 13.53 | 0.35 | 0.50 | 0.06 | 0.01 | 0.014 | 0.006 | 0.13 | | |
| 15 | a | — | — | — | — | — | — | — | — | — | 18.57 | 20.88 |
| | b | 19.99 | 20.52 | 0.42 | 0.50 | 0.06 | 0.01 | 0.014 | 0.004 | 0.10 | | |
| 16 | a | — | — | — | — | — | — | — | — | — | 22.45 | 2.43 |
| | b | 23.80 | 2.39 | 0.47 | 0.50 | 0.06 | 0.02 | 0.021 | 0.006 | 0.10 | | |
| 17 | a | 23.76 | 2.93 | 0.41 | 0.36 | 0.03 | 0.01 | — | — | 0.11 | 22.74 | 2.97 |
| 18 | a | 23.69 | 3.93 | 0.61 | 0.54 | 0.07 | 0.01 | 0.008 | 0.009 | 0.14 | 21.97 | 4.02 |
| 19 | a | 24.09 | 6.28 | 0.49 | 0.50 | 0.04 | 0.05 | 0.007 | 0.010 | 0.16 | 22.56 | 6.40 |
| 20 | a | 23.76 | 7.12 | 0.52 | 0.41 | 0.04 | 0.01 | — | — | 0.11 | 22.62 | 7.23 |
| 21 | a | 23.68 | 12.84 | 0.54 | 0.45 | 0.05 | 0.01 | — | — | 0.10 | 21.90 | 13.42 |
| | b | 23.35 | 13.44 | 0.47 | 0.36 | 0.07 | 0.01 | 0.016 | 0.004 | 0.14 | | |
| 22 | a | — | — | — | — | — | — | — | — | — | 22.37 | 19.77 |
| | b | 23.77 | 19.42 | 0.66 | 0.47 | 0.05 | 0.01 | 0.018 | 0.006 | 0.13 | | |
| 23 | b | 27.63 | 0.20 | 0.47 | 0.62 | 0.03 | 0.01 | 0.007 | 0.009 | 0.10 | 26.70 | 0.20 |
| 24 | b | 30.40 | 0.20 | 0.51 | 0.52 | 0.05 | 0.01 | 0.009 | 0.012 | 0.12 | 29.18 | 0.20 |

* Based on complete insolubility of C and N at 1200°F and formation of pure $Cr_7C$ and $Cr_2N$. Where both cast and wrought compositions are given, the average value was used in calculating the modified matrix compositions.
** Series *a* alloys are castings made from slugs of the respective heat which were deoxidized with aluminum.
Series *b* alloys are wrought, made from the remainder of the respective heats after deoxidizing with magnesium.
† Analyses are not available.

oxidation and then was cast into a block approximately 3x3x2 in. The remainder of the heat was deoxidized with a Ni-Mg alloy and was poured into a cast-iron mold. The resulting ingot was hot rolled to ⅞ in. diam.

The 24 Fe-Cr-Ni base compositions investigated are given in Table I and the 44 Fe-Cr-Ni-Si base alloys are given in Tables II through IV.

Filings of −120 mesh size were prepared from both wrought and cast forms of the alloys and were sealed in individual Vycor tubes under partial vacuum. Except for the alloys containing silicon (which were held only 500 hr, since longer times were not necessary), the tubes with their contents were held at 1200°±10°F (650°C) for 2000 hr and water quenched. The X-ray diffraction powder method, using Cr K$\alpha$, was used to examine the filings. Phases were identified by direct comparison with previously prepared standard patterns of austenite, ferrite, $\sigma$, carbides, nitrides, and oxides. In many instances, the filings also were examined metallographically to see if the $\sigma$ phase was present.

For metallographic examination, bulk samples, approximately ⅜ in. cubes, were cut from the cast and the wrought alloys (except alloys 23 and 24). Unstrained samples from the cast alloys (except alloys 12, 18, and 19) were aged at 1200°F for 96, 500, 2000, and 5000 hr, and unstrained samples from the wrought alloys were aged at 1200°F for 170, 620, and 2000 hr. Other samples from both the cast and wrought alloys then were strained (cold hammered to a 50 pct reduction in height). Alloys 12, 18, and 19 were aged at 1200°F for 500 hr and all the others were aged for 910 hr. All the silicon-containing alloys were cold worked 50 pct by hammering. The cast alloys were aged 500 hr, the wrought alloys, 1000 hr. The samples were examined metallographically, after etching with glyceregia (3 parts glyc-

## Table II. Compositions and Equilibrium Phases of Fe-Cr-Ni—2.5 Pct Si Alloys Before and After Nitrogenization

| | Before Nitrogenization | | | | | | | | | After Nitrogenization | | | |
|---|---|---|---|---|---|---|---|---|---|---|---|---|---|
| | | | | | | | Matrix Compositions | | Equilibrium Phases, 1200°F | Matrix Compositions | | | Equilibrium Phases, 1200°F |
| Alloy | Cr | Ni | Mo | Si | Mn | C | Cr | Ni | | N | Cr | Ni | |
| 6174 | 14.93 | 19.90 | 0.01 | 1.87 | 0.66 | 0.05 | 13.88 | 20.15 | $\gamma + CC$ | — | | | |
| 6175 | 17.61 | 20.20 | 0.01 | 1.94 | 0.72 | 0.04 | 16.73 | 20.45 | $\gamma + CC + \sigma$ | — | | | |
| 6134 | 18.11 | 19.64 | — | 2.11 | 0.68 | 0.04 | 17.25 | 19.85 | $\gamma + \sigma$ | — | | | |
| 6133 | 17.74 | 18.33 | — | 2.27 | 1.82 | 0.04 | 16.97 | 18.53 | $\gamma + \sigma$ | — | | | |
| 6416 | 17.41 | 14.27 | 0.02 | 1.73 | 0.57 | 0.05 | 16.38 | 14.46 | $\gamma + \sigma$ | — | | | |
| 6243 | 14.65 | 13.75 | 0.01 | 2.34 | 0.51 | 0.04 | 13.73 | 13.90 | $\gamma$ | — | | | |
| 6244* | 17.24 | 13.88 | 0.01 | 2.53 | 0.51 | 0.04 | 16.52 | 14.00 | $\gamma + \sigma$ | 0.24 | 15.13 | 14.23 | $\gamma + \sigma + CC$ |
| 6260* | 18.93 | 15.15 | 0.01 | 2.62 | 0.40 | 0.03 | 16.31 | 15.26 | $\gamma + \sigma$ | 0.20 | 15.24 | 15.47 | $\alpha' + \gamma + CC + Cr_2N$ |

* Before nitrogenizing both 6244 and 6260 contained 0.03 pct N. The value of 0.05 pct was chosen arbitrarily for the other samples.

## Table III. Compositions and Equilibrium Phases of Fe-Cr-Ni-Si-N Alloys Before and After Nitrogenization

| | Before Nitrogenization | | | | | | | Matrix Compositions** | | Equilibrium† Phases, 1200°F | After Nitrogenization | | | |
|---|---|---|---|---|---|---|---|---|---|---|---|---|---|---|
| | | | | | | | | | | | Matrix Compositions** | | | Equilibrium Phases, 1200°F |
| | Cr* | Ni | Mo | Si | Mn | C | N | Cr | Ni | | N | Cr | Ni | |
| 6458 | 15.66 | 8.21 | 0.09 | 2.18 | 1.12 | 0.03 | 0.098 | 14.65 | 8.30 | $\alpha+\gamma+\sigma+CC$ | 0.271 | 13.50 | 8.43 | $\alpha'+\gamma+CC$ |
| 6454 | 15.87 | 13.73 | 0.10 | 2.09 | 0.93 | 0.02 | 0.115 | 14.84 | 13.90 | $\gamma+CC$ | 0.333 | 13.43 | 14.15 | $\gamma+CC$ |
| 6455 | 15.75 | 19.81 | 0.12 | 2.10 | 0.91 | 0.02 | 0.119 | 14.71 | 20.10 | $\gamma+CC$ | 0.271 | 13.73 | 20.30 | $\gamma+CC$ |
| 6462 | 18.25 | 7.92 | 0.06 | 2.34 | 0.88 | 0.03 | 0.104 | 17.18 | 8.02 | $\gamma+\sigma$ | 0.274 | 16.12 | 8.06 | $\alpha'+\gamma+X$ |
| 6463 | 18.28 | 13.58 | 0.04 | 2.41 | 0.88 | 0.04 | 0.118 | 17.00 | 13.80 | $\gamma+\sigma$ | 0.303 | 15.81 | 14.00 | $\gamma+X$ |
| 6464 | 18.30 | 19.44 | 0.03 | 2.44 | 0.96 | 0.03 | 0.123 | 17.09 | 19.75 | $\gamma+\sigma$ | 0.363 | 15.62 | 20.10 | $\gamma+\sigma+X$ |
| 6465 | 21.32 | 8.09 | 0.08 | 2.54 | 1.04 | 0.03 | 0.118 | 20.20 | 8.21 | $\gamma+\sigma$ | 0.370 | 18.80 | 8.37 | $\alpha'+\gamma+\sigma$ |
| 6466 | 21.21 | 13.56 | 0.03 | 2.55 | 0.96 | 0.03 | 0.135 | 20.00 | 13.78 | $\gamma+\sigma$ | 0.455 | 18.13 | 14.10 | $\gamma+\sigma+X$ |
| 6484 | 22.50 | 19.58 | 0.03 | 2.06 | 0.83 | 0.07 | 0.190 | 20.40 | 20.10 | $\gamma+\sigma$ | 0.665 | 17.45 | 20.90 | $\gamma+\sigma+CC+X$ |
| 6498 | 24.87 | 7.99 | 0.03 | 2.11 | 0.90 | 0.04 | 0.119 | 23.70 | 8.13 | $\gamma+\sigma$ | — | — | — | — |
| 6495 | 23.74 | 13.42 | 0.01 | 1.87 | 0.97 | 0.04 | 0.113 | 22.59 | 13.63 | $\gamma+\sigma$ | 0.998 | 17.05 | 14.59 | $\gamma+\sigma+X$ |
| 6494 | 24.84 | 19.70 | 0.01 | 1.95 | 0.93 | 0.05 | 0.125 | 23.50 | 20.10 | $\gamma+\sigma$ | 0.603 | 20.82 | 20.77 | $\gamma+\sigma+X$ |
| 6457†† | 15.19 | 4.24 | 0.01 | 1.67 | 0.75 | 0.04 | 0.102 | 13.97 | 4.31 | $\alpha+\alpha'+\gamma+Cr_2N$ | | | | |
| 6493‡ | 17.75 | 3.85 | 0.01 | 2.15 | 0.82 | 0.04 | 0.036 | 16.95 | 3.89 | $\alpha+\alpha'+\gamma+\sigma$ | | | | |
| 6500 | 22.18 | 3.85 | 0.01 | 2.20 | 0.61 | 0.05 | 0.086 | 20.99 | 3.91 | $\alpha+\gamma+\sigma$ | | | | |

* Analyses for Cr and Ni were made from both cast and wrought forms; these values are the average of the two. All other analyses were made from the castings. Sulphur ranged from 0.009 to 0.030 pct, phosphorus from 0.009 to 0.022 pct.
** Matrix compositions are based on the assumption of complete precipitation of carbon and nitrogen as $Cr_4C$ and $Cr_2N$, respectively, at 1200°F.
† Equilibrium phases were determined in the wrought forms of the alloys.
†† These three alloys were received in the form of very gassy ingots.
‡ This alloy was not plotted on Fig. 1 because of its very low nitrogen content.

erin, 2 parts concentrated HCl, and 1 part concentrated $HNO_3$). This etchant attacks the $\sigma$ phase very heavily without overetching the other phases.

Samples of cast and wrought alloys which were shown to be susceptible to $\sigma$ formation were nitrided and homogenized to increase their nitrogen contents. Filings were prepared from these samples, and the samples then were aged in Vycor for 500 hr at 1200°F. The phases in the filings were identified by X-ray diffraction and metallography. Some bulk samples, which had been protected by Vycor during aging, also were examined metallographically. Later these samples were dissolved in an electrolytic $FeCl_3$ solution and the residues were examined by X-ray diffraction.

### Results and Discussion

*Fe-Cr-Ni Alloys with High Nitrogen:* In drawing the ternary diagrams of the various Fe-Cr-Ni systems, e.g., high purity, commercial purity, high nitrogen, high silicon, etc., it is somewhat misleading to plot the compositions of the alloys in accordance with the analytically determined elemental components. Because of the presence of carbides, nitrides, and inclusions, the matrix composition, which is an important factor in determining susceptibility to $\sigma$ formation, actually is not determined by a simple chemical analysis for chromium, nickel, or iron.

The presence of carbides and nitrides (the oxides are excluded purposely) reduces the relative amount of chromium and increases the relative amounts of iron and nickel in actual solid solution. Also, the amount of carbon and nitrogen in solid solution in the alloys is reduced to smaller, although indeterminate, values at 1200°F by the precipitation of carbides and nitrides in the form of $Cr_4C$ and $Cr_2N$. These compounds were analysed by X-ray fluorescence analysis and were found to be predominantly chromium but also to contain some iron; no nickel was found in the compounds. For example, the Cr:Fe ratio of nitrides, precipitated at 1200°F and extracted by an electrolytic $FeCl_3$ etch, was found to be 15.7:1 for a high nitrogen 24 pct Cr-2 pct Ni alloy, and 8:1 for a high nitrogen 30 pct Cr alloy.

## Table IV. Compositions and Equilibrium Phases of Fe-Cr-Ni—1 Pct Si Alloys Before and After Nitrogenization

| | Before Nitrogenization | | | | | | Matrix Compositions | | Equilibrium Phases, 1200°F | After Nitrogenization | | | |
|---|---|---|---|---|---|---|---|---|---|---|---|---|---|
| | | | | | | | | | | Matrix Compositions | | | Equilibrium Phases, 1200°F |
| Alloy | Cr | Ni | Mo | Si | Mn | C | Cr | Ni | | N | Cr | Ni | |
| 6122 | 12.36 | 8.51 | 0.01 | 0.94 | 0.63 | 0.03 | 11.58 | 8.58 | $\alpha'+\gamma$ | — | — | — | — |
| 6123 | 15.23 | 8.51 | 0.01 | 0.98 | 0.61 | 0.04 | 14.31 | 8.61 | $\alpha'+\gamma+\sigma$ | 0.20 | 13.35 | 8.71 | $\alpha'+\gamma$ |
| 6125 | 17.87 | 8.38 | 0.02 | 1.01 | 0.55 | 0.03 | 17.13 | 8.47 | $\alpha'+\gamma+\alpha+\sigma$ | 0.24 | 15.95 | 8.58 | $\gamma+\alpha'+Cr_2N+CC$ |
| 6126 | 21.00 | 8.35 | 0.01 | 0.96 | 0.66 | 0.03 | 20.30 | 8.43 | $\gamma+\sigma$ | 0.39 | 18.22 | 8.65 | $\gamma+\sigma$ |
| 6134 | 24.13 | 8.50 | 0.01 | 0.87 | 0.50 | 0.06 | 23.08 | 8.63 | $\gamma+\sigma$ | 0.61 | 19.66 | 8.92 | $\gamma+\sigma+X$ |
| 6136 | 12.70 | 14.54 | — | 1.01 | 0.49 | 0.05 | 11.59 | 14.72 | $\gamma+CC$ | — | — | — | — |
| 6140 | 15.00 | 13.62 | 0.01 | 0.96 | 0.66 | 0.05 | 13.94 | 13.79 | $\gamma$ | 0.32 | 12.16 | 14.08 | $\gamma+CC$ |
| 6144* | 17.83 | 14.27 | 0.01 | 1.03 | 0.55 | 0.05 | 16.85 | 14.42 | $\gamma+\sigma$ | 0.23 | 15.58 | 14.65 | $\gamma+X$ |
| 6145* | 21.07 | 14.93 | 0.01 | 1.05 | 0.58 | 0.05 | 20.14 | 15.11 | $\gamma+\sigma$ | 0.36 | 18.19 | 15.48 | $\gamma+CC+X$ |
| 6149* | 23.80 | 14.14 | 0.02 | 1.22 | 0.54 | 0.05 | 22.81 | 14.31 | $\gamma+\sigma$ | — | — | — | — |
| 6150 | 11.56 | 19.38 | 0.01 | 1.13 | 0.77 | 0.04 | 10.60 | 19.60 | $\gamma+CC$ | — | — | — | — |
| 6160 | 15.30 | 20.30 | — | 1.10 | 0.89 | 0.05 | 14.25 | 20.55 | $\gamma+CC$ | — | — | — | — |
| 6161 | 18.90 | 20.09 | — | 1.19 | 0.82 | 0.05 | 17.90 | 20.96 | $\gamma+CC+\sigma$ | 0.28 | 16.45 | 21.34 | $\gamma+CC$ |
| 6164 | 20.58 | 19.77 | — | 1.19 | 0.65 | 0.06 | 19.48 | 20.09 | $\gamma+\sigma+CC$ | 0.31 | 17.83 | 20.41 | $\gamma+CC$ |
| 6165 | 24.00 | 19.51 | 0.02 | 1.24 | 0.60 | 0.06 | 22.92 | 19.82 | $\gamma+\sigma$ | 0.50 | 20.22 | 20.48 | $\gamma+\sigma+CC$ |
| 6408 | 25.01 | 12.57 | 0.12 | 1.08 | 0.62 | 0.06 | 23.98 | 12.76 | $\gamma+\sigma$ | 0.52 | 20.99 | 13.25 | $\gamma+\sigma$ |
| 6403 | 17.51 | 13.75 | 0.12 | 0.93 | 0.52 | 0.04 | 16.65 | 13.89 | $\gamma+CC$ | — | — | — | — |
| 6414 | 17.17 | 19.64 | 0.10 | 0.96 | 0.68 | 0.06 | 15.99 | 19.97 | $\gamma+CC$ | — | — | — | — |
| 6417 | 25.35 | 20.95 | 0.10 | 1.14 | 0.69 | 0.07 | 24.15 | 21.30 | $\gamma+\sigma$ | 0.41 | 22.06 | 21.87 | $\gamma+\sigma+X$ |
| 613-1 | 18.58 | 18.86 | — | 0.84 | 0.85 | 0.04 | 17.72 | 19.05 | $\gamma+CC+\sigma$ | — | — | — | — |
| 613-2 | 18.88 | 18.99 | — | 1.01 | 1.75 | 0.04 | 18.02 | 19.19 | $\gamma+CC+\sigma$ | — | — | — | — |

* Nitrogen analyses show 0.04 pct for both 6144 and 6145, and 0.05 pct for 6149. The value of 0.05 pct was chosen arbitrarily for the remaining samples. In no instance did sulphur exceed 0.020 pct and the phosphorus 0.024 pct.

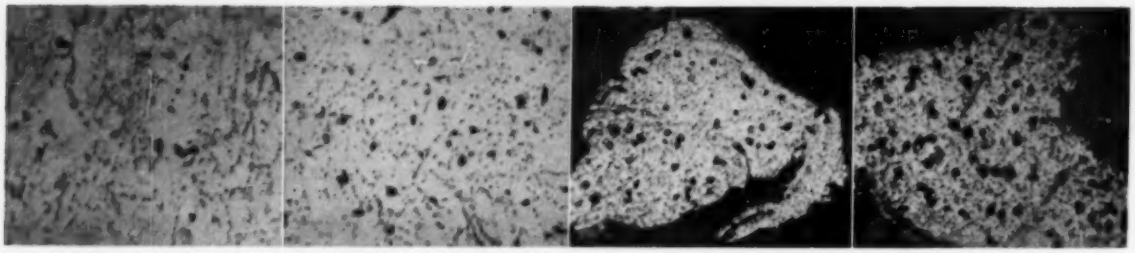

a—Alloy No. 6 (18.35 pct Cr-8.58 pct Ni) bulk specimen compressed cold about 50 pct. X750. Area reduced approximately 45 pct for reproduction.

b—Alloy No. 15 (19.99 pct Cr-20.52 pct Ni) bulk specimen compressed cold about 50 pct. X750. Area reduced approximately 45 pct for reproduction.

c—Alloy 8N-18 (17.80 pct Cr-8.18 pct Ni) filings. X1000. Area reduced approximately 45 pct for reproduction.

d—Alloy 20N-18 (18.53 pct Cr-19.25 pct Ni) filings. X1000. Area reduced approximately 45 pct for reproduction.

Fig. 1—Metallographic evidence of $\sigma$ formation (large dark-etching regions) in cold-worked low and high nitrogen alloys in which X-ray diffraction (powder method) did not reveal $\sigma$ phase. Glyceregia etch. Alloys *c* and *d* were two of those used by Nicholson et al.[5]

For this reason, in plotting the compositions of the alloys the existence of chromium-impoverished matrices should be recognized.

Because of the lack of information on the solubility of nitrogen and carbon in these steels as well as on the exact Cr:Fe:Ni ratio of the various nitrides and carbides, the most conservative assumption was made that only pure $Cr_4C$ and $Cr_2N$ are precipitated at 1200°F. It then becomes apparent that, as the carbon or nitrogen content of an alloy is increased, the accuracy possible in estimating the degree of chromium impoverishment will decrease, simply because the carbides and nitrides remove small but indeterminate amounts of iron and nickel as well as relatively large amounts of chromium from the solid solution.

Correction for chromium impoverishment was not considered by Nicholson et al.,[5] who plotted their data in the more conventional manner, in determining the $(\gamma+\sigma)/\gamma$ boundary for the commercially pure Fe-Cr-Ni system. Also, it was found in the present study that, when the amount of $\sigma$ formation is small, i.e., less than about 5 vol pct, $\sigma$ cannot be detected by X-ray diffraction but it can be detected by metallographic examination. Filings of some of the samples used by Nicholson et al.,[5] which did not show the $\sigma$ phase by X-rays, were available to the authors. When checked metallographically, many of these were found to contain $\sigma$ (see Table V). Fig. 1 illustrates the general appearance of $\sigma$ in filings.

A portion of the modified commercial-purity ternary Fe-Cr-Ni diagram, plotted on the basis of this new viewpoint as well as on that of chromium impoverishment, is given in Fig. 2. For the remainder of this report, the term "commercial-purity boundaries" will refer to these redetermined boundaries separating the $\sigma$-free and $\sigma$-containing alloys.

The comparison between the boundaries of the commercially pure system and those of the high nitrogen Fe-Cr-Ni system shows that nitrogen causes a shift of the $\sigma$ phase boundaries to higher chromium contents (larger $\gamma$ and $(\gamma+\alpha)$ fields) (see Fig. 3 and Tables VI through VIII). The shifts shown here must represent the minimum effects of nitrogen addition, since any consideration of the small amounts of iron (and nickel) in $Cr_4C$ and $Cr_2N$ would result in a greater shift towards higher chromium contents for the high nitrogen system than for the commercial-purity system. As shown here, the $(\gamma+\sigma)/\gamma$ boundary is shifted approximately 1 pct by nitrogen to a higher chromium content except at the $\gamma$ triple point where it is substantially the same as for the

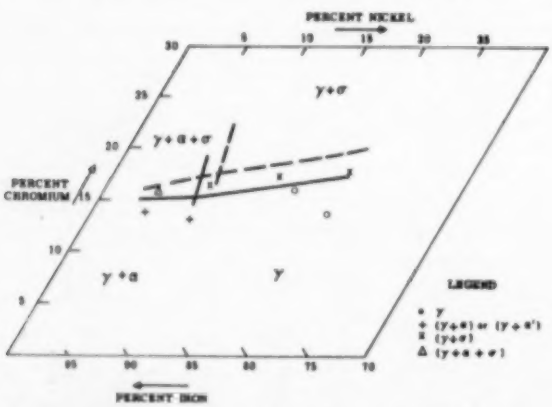


Fig. 2—Phase boundaries at which $\sigma$ forms at 1200°F in commercially pure Fe-Cr-Ni steels. Dashed lines are as reported by Nicholson et al.[5] from X-ray diffraction results; solid lines are as arrived at after metallographic examination of the same specimens (heat-treated filings) and correction for chromium-impoverishment effects.

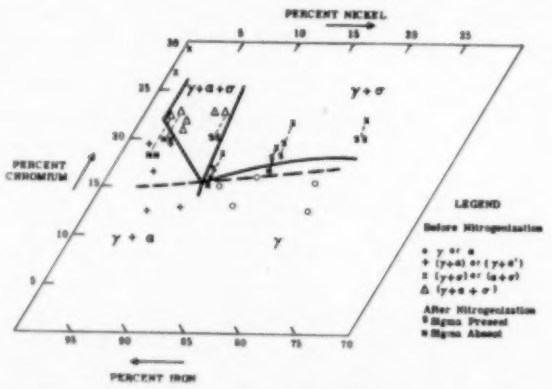


Fig. 3—Effect of nitrogen on phase boundaries at which $\sigma$ forms at 1200°F in commercially pure Fe-Cr-Ni steels. Dashed lines are modified boundaries given in Fig. 2; solid lines are boundaries as affected by increasing nitrogen content. All matrix compositions have been corrected for chromium impoverishment. The short dash lines of nearly constant nickel content show the effect of increasing the nitrogen content of specific compositions (by nitriding and homogenizing). In each instance the original (matrix) composition is indicated by an X or triangle and the (matrix) compositions after nitriding are indicated by an *S* or *N*, depending on whether or not $\sigma$ phase was present.

## Table V. Alloys of Nicholson et al.[3] Re-examined Metallographically

| Alloy | Cr | Ni | Mo | Si | Mn | C | Matrix Composition* Cr | Matrix Composition* Ni | Equilibrium Phases, 1200°F |
|---|---|---|---|---|---|---|---|---|---|
| 4N-15 | 15.30 | 4.33 | 0.02 | 0.54 | 0.48 | 0.07 | 13.98 | 4.40 | $\alpha+\gamma$ |
| 4N-18 | 17.17 | 4.49 | 0.01 | 0.63 | 0.57 | 0.07 | 15.88 | 4.56 | $\alpha+\gamma+\sigma$ |
| 8N-15 | 14.42 | 8.25 | 0.03 | 0.70 | 0.78 | 0.06 | 13.23 | 8.36 | $\alpha+\gamma$ |
| 8N-18 | 17.80 | 8.18 | — | 0.42 | 0.39 | 0.07 | 16.52 | 8.31 | $\gamma+\sigma$ |
| 14N-15 | 17.13 | 15.51 | 0.01 | 0.26 | 0.33 | 0.04 | 16.27 | 15.67 | $\gamma$ |
| 14N-18 | 17.98 | 13.88 | 0.01 | 0.33 | 0.36 | 0.02 | 17.48 | 13.96 | $\gamma+\sigma$ |
| 20N-15 | 14.87 | 19.69 | 0.03 | 0.40 | 0.49 | 0.06 | 13.69 | 19.96 | $\gamma$ |
| 20N-18 | 18.53 | 19.25 | 0.01 | 0.51 | 0.59 | 0.03 | 17.82 | 19.32 | $\gamma+\sigma$ |

* A value of 0.05 pct N was selected in making the calculations for matrix compositions

## Table VI. Phase Relationships in Wrought Alloys (0.10 to 0.20 Pct N) at 1200°F

| Alloy No. | Nominal Composition Cr | Nominal Composition Ni | Cold-Worked Filings,* 2000 Hr | As-rolled Bulk Specimens* 170 Hr | As-rolled Bulk Specimens* 620 Hr | As-rolled Bulk Specimens* 2000 Hr | Cold-Worked Bulk Specimens,* 910 Hr |
|---|---|---|---|---|---|---|---|
| 1 | 15 | 4 | *A,M* | *M* | *M* | *M,P* | *M,P* |
| 2 | 15 | 8 | *A,M,N* | *A,M* | *A,M,P* | *M,P* | *M,P* |
| 3 | 15 | 14 | *A* | *A,X* | *A,X* | *A,X* | *A,P* |
| 4 | 15 | 20 | *A,C,N* | *A,X* | *A,X* | *A,X* | *A,P* |
| 5 | 18 | 4 | *A,M,N* | *F,M* | *F,M* | *F,M,P* | *F,M,P* |
| 6 | 18 | 8 | *A,C,N* | *A,X* | *A,P* | *A,P* | *A,S,P* |
| 8 | 18 | 14 | *A,N* | *A,X* | *A,X* | *A,X* | *A,P* |
| 9 | 18 | 20 | *A,C,N* | *A,X* | *A,X* | *A,X* | *A,P* |
| 10 | 21 | 2 | *F,A,N* | *F,M* | *F,M,P* | *F,M,P* | *F,M,P* |
| 13 | 21 | 8 | *A,M,S,C* | *A,X* | *A,X* | *A,S,X* | *A,S,P* |
| 14 | 21 | 14 | *A,C,N* | *A,X* | *A,X* | *A,S,X* | *A,S,P* |
| 15 | 21 | 20 | *A,C,N* | *A,X* | *A,X* | *A,X* | *A,S,P* |
| 16 | 24 | 2 | *F,A,S,N* | *F,M* | *F,M,S* | *F,M,S,P* | *F,M,S,P* |
| 21 | 24 | 14 | *A,S* | *A,X* | *A,S,X* | *A,S,X* | *A,S,P* |
| 22 | 24 | 20 | *A,S* | *A,X* | *A,S,X* | *A,S,X* | *A,S,P* |
| 23 | 27 | 0 | *F,S,N* | — | — | — | — |
| 24 | 30 | 0 | *F,S,N* | — | — | — | — |

* Letters stand for: *F* is chromium ferrite, *M* is martensite, *A* is austenite, *C* is cubic carbide, $Cr_4C$, *N* is nitride, $Cr_2N$, *S* is $\sigma$, *P* is random, resolvable particles, a mixture of $Cr_2N$ and $Cr_4C$, *X* is grain-boundary precipitate, probably $Cr_4C$.

commercially pure system. Depending upon composition, the $(\gamma+\alpha+\sigma)/(\gamma+\alpha)$ boundary also is shifted to higher chromium contents, varying linearly from substantially no change at the $\gamma$ triple point to a change of approximately 7 pct (i.e., from 15 to 22 pct Cr) at the $\alpha$ triple point.

The nitriding and homogenizing treatments given to $\sigma$ susceptible alloys 13, 14, 16, 17, 20, 21, and 22 caused definite changes in their propensity towards $\sigma$ formation at 1200°F (Table VIII). Alloy 13 still formed $\sigma$ when its nitrogen content was raised to 0.35 pct but not when it was raised to 0.70 pct. Alloy 14 still formed $\sigma$ when its nitrogen content was raised to 0.30 pct but not when it was raised to 0.41 pct. Alloy 16 was immune to $\sigma$ formation when its nitrogen content was raised to either 0.74 or 0.79 pct. Alloy 17 was immune to $\sigma$ formation at nitrogen contents of 0.55 and 0.65 pct. Alloys 20, 21, and 22 formed $\sigma$ at all nitrogen contents reached.

X-ray diffraction studies of the residues, from the set of high nitrogen samples which had been successively cold hammered, aged at 1200°F, and dissolved in the electrolytic $FeCl_3$ etch, all showed the pattern of the compound $Cr_2N$ as the strongest one present. Studies of alloys 13 and 21 showed the $\sigma$ phase. Those of 14, 17, 20, 21, and 22 all had some unknown lines which, however, were not necessarily common to all the films. A metallographic examination of both sets of samples, i.e., both those aged as filings and those aged as bulk samples, showed that all filings contained a considerable amount of small light-colored particles which probably are nitrides and that the bulk samples contained a lamellar structure which probably contains nitrides (Fig. 4). Calculations of the matrix compositions show that, for the most part, the immunity toward $\sigma$ formation after nitriding and homogenizing most probably is due to chromium impoverishment caused by nitride and carbide precipitation.

*Fe-Cr-Ni-Alloys Containing Silicon and Nitrogen:* The addition of nitrogen to the Fe-Cr-Ni system causes both a small but true shift of the $(\gamma+\sigma)/\gamma$ phase boundary at 1200°F to higher chromium values, and a large but illusory shift to higher chro-

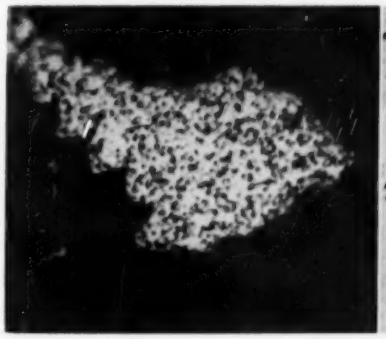

Fig. 4a—Microstructure of a filing (—120 mesh) of alloy No. 17 (24 pct Cr-4 pct Ni) containing 0.65 pct N, after holding 148 hr at 1200°F. The particles are nitrides. Glyceregia etch. X1000.

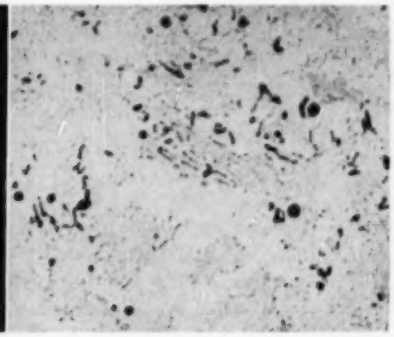

Fig. 4b—Microstructure of a cold-worked bulk sample of alloy No. 22 (24 pct Cr-20 pct Ni) containing 0.50 pct N, after holding 500 hr at 1200°F. The dark-etching particles are $\sigma$, and the lamellar structure contains nitrides. Glyceregia etch. X500.

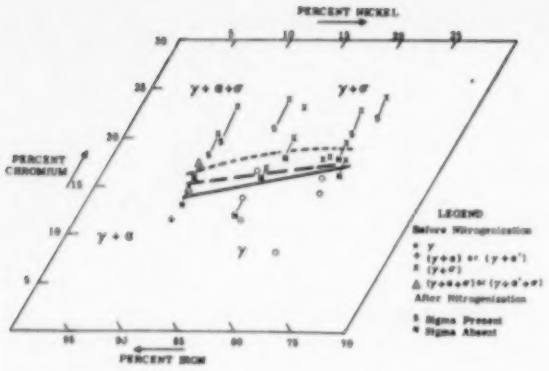


Fig. 5—Effect of nitrogen and of about 1 pct Si on phase boundaries at which $\sigma$ forms from austenite ($\gamma$) in commercially pure Fe-Cr-Ni steels at 1200°F. Long dash line is modified boundary given in Fig. 2; solid line is boundary for alloys containing about 1 pct Si; short dash line is boundary for 1 pct Si alloys with increased nitrogen contents. The short solid lines of nearly constant nickel content show the effect of increasing the nitrogen content of specific compositions (by nitriding and homogenizing). In each instance the original (matrix) composition is indicated by an X or triangle and the (matrix) composition after nitriding is indicated by an S or N, depending upon whether or not $\sigma$ phase was formed.

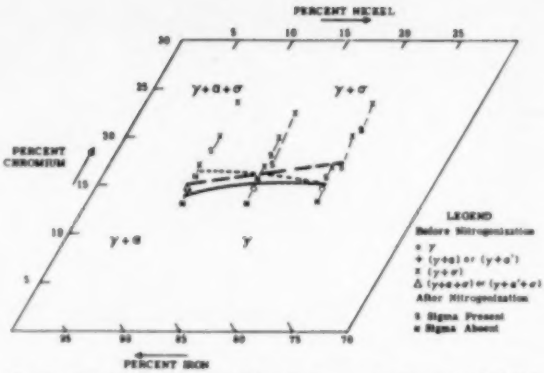


Fig. 6—Effect of about 2 pct Si and nitrogen in the range 0.088 to 0.190 pct on the phase boundary at which $\sigma$ forms from austenite ($\gamma$) in commercially pure Fe-Cr-Ni steels at 1200°F. Long dash line is modified boundary given in Fig. 2; solid line is boundary as affected by about 2 pct Si and nitrogen in the range 0.088 to 0.190 pct; short dash line is boundary for 2 pct Si, 0.088 to 0.190 pct N alloys after a further increase in nitrogen content. The short dash lines of nearly constant nickel content show the effect of increasing the nitrogen content of specific compositions (by nitriding and homogenizing). In each instance the original (matrix) composition is indicated by an X, triangle, or circle, and the (matrix) composition after nitriding is indicated by an S or N, depending upon whether or not $\sigma$ phase was formed.

## Table VII. Phase Relationships in Cast Alloys (0.10 to 0.20 Pct N) at 1200°F

| Alloy No. | Nominal Composition, Cr | Nominal Composition, Ni | Cold-Worked Filings,* 2000 Hr | As-Cast Bulk Specimens* 0 Hr | 96 Hr | 500 Hr | 2000 Hr | 5000 Hr | Cold-Worked Bulk Specimens,* 910 Hr |
|---|---|---|---|---|---|---|---|---|---|
| 1 | 15 | 4 | *M,A,C,N* | *M* | *M* | *M* | *M,P* | *M,P* | *M,P* |
| 2 | 15 | 8 | *M,A,N* | *M* | *M* | *M* | *M,P* | *M,P* | *M,P* |
| 3 | 15 | 14 | *A,N* | *A* | *A,X* | *A,X* | *A,X,Z* | *A,X,Z* | *A,P* |
| 4 | 15 | 20 | *A,C,N* | *A* | *A,X* | *A,X* | *A,X,Z* | *A,X,Z* | *A,P* |
| 5 | 18 | 4 | *M,C,N* | *F,M* | *F,M,X* | *F,M,X* | *F,M,X* | *F,M,X* | *F,M,P* |
| 6 | 18 | 8 | *A,C,N* | *A* | *A,X* | *A,X* | *A,X,Z* | *A,X,Z* | *A,S,P* |
| 7 | 18 | 8 | *A,N* | *A* | *A,X* | *A,X* | *A,X,Z* | *A,X,Z* | *A,P* |
| 8 | 18 | 14 | *A,C,N* | *A* | *A,X* | *A,X* | *A,X* | *A,X,Z* | *A,P* |
| 9 | 18 | 20 | *A,C,N* | *A* | *A,X* | *A,X* | *A,X* | *A,X* | *A,P* |
| 10 | 21 | 2 | *F,A,C,N* | *F,A,M* | *F,A* | *F,A* | *F,A,P* | *F,A,P* | *F, A, P* |
| 11 | 21 | 4 | *F,A,C,N* | *F,A* | *F,A,M,X* | *F,A,M,X* | *F,A,M,X* | *F,A,X* | *F, A, P* |
| 12 | 21 | 4 | *F,A,S* | — | — | — | — | — | *F,A,S* (500 hr) |
| 13 | 21 | 8 | *A,S* | *F,A* | *F,A,S* | *F,A,S* | *F,A,S* | *F,A,S,P* | *F,A,S,P* |
| 14 | 21 | 14 | *A,S* | *A* | *A,S,P* | *A,S,P* | *A,S,P* | *A,S,P* | *A,S,P* |
| 15 | 21 | 20 | *A,C* | *A* | *A,X* | *A,X* | *A,X,Z* | *A,X,Z* | *A,S,P* |
| 16 | 24 | 2 | *F,S* | *F,A* | *F,A* | *F,A* | *F,A* | *F,A* | *F,S,P* |
| 17 | 24 | 4 | *F,A,S* | *F,A* | *F,A* | *F,A,S,P* | *F,A,S,P* | *F,A,S,P* | *F,A,S,P* |
| 18 | 24 | 4 | *F,A,S* | — | — | — | — | — | *F,A,S* (500 hr) |
| 19 | 24 | 6 | *F,A,S* | — | — | — | — | — | *F,A,S* (500 hr) |
| 20 | 24 | 8 | *A,S,N* | *F,A* | *F,A,S* | *F,A,S* | *F,A,S* | *F,A,S,P* | *F,A,S,P* |
| 21 | 24 | 14 | *A,S* | *F,A* | *F,A,S* | *A,S* | *A,S* | *A,S* | *A,S,P* |
| 22 | 24 | 20 | *A,S* | *A* | *A,X* | *A,X* | *A,X,Z* | *A,X,Z* | *A,S,P* |

* Letters stand for: *F* is chromium ferrite, *M* is martensite, *A* is austenite, *C* is cubic carbide, $Cr_4C$, *N* is nitride, $Cr_2N$, *S* is $\sigma$, *P* is random resolvable particles, a mixture of $Cr_2N$ and $Cr_4C$, *X* is grain boundary precipitate, probably $Cr_4C$, and *Z* is dispersed, unresolved precipitate, probably $Cr_2N$.

## Table VIII. Effect of Nitriding and Homogenizing on Phase Relationships in Cast Alloys

| Alloy No. | Treatment No. 1: Matrix Compositions, N | Cr | Ni | Equilibrium Phases, 1200°F in Filings: X-ray* | Metallographic* | Treatment No. 2: Matrix Compositions, N | Cr | Ni | Equilibrium Phases, 1200°F Cold-Worked Bulk Samples: Metallographic† | X-ray $FeCl_3$ Residues* |
|---|---|---|---|---|---|---|---|---|---|---|
| 13 | 0.70 | 15.18 | 9.27 | *A,N* | Matrix, *P* | 0.35 | 17.08 | 9.07 | Matrix, *L,S* | *N,S* |
| 14 | 0.41 | 17.38 | 13.82 | *A,N* | Matrix, *P* | 0.30 | 18.05 | 13.71 | Matrix, *L,P,S* | *N*† |
| 16 | 0.79 | 18.13 | 2.57 | *F,N* | Matrix, *P* | 0.74 | 18.49 | 2.56 | Matrix, *P* | *N* |
| 17 | 0.65 | 19.48 | 3.09 | *F,A,N* | Matrix, *P* | 0.55 | 20.10 | 3.07 | Matrix, *L* | *N*† |
| 20 | 0.56 | 19.91 | 7.47 | *A,S,N* | Matrix, *P,S* | 0.50 | 20.25 | 7.44 | Matrix, *L,S* | *N*† |
| 21 | 0.69 | 18.80 | 13.98 | *A,S,N*† | — | 0.50 | 19.91 | 13.81 | Matrix, *L,S* | *N,S* |
| 22 | 0.49 | 20.21 | 20.32 | *F,A*† | Matrix, *P,S* | 0.45 | 20.32 | 20.25 | Matrix, *L,S* | *N*† |

* Letters stand for: *F* is chromium ferrite, *A* is austenite, *N* is Nitride, $Cr_2N$, *S* is $\sigma$, *P* is random, resolvable particles, a mixture of $Cr_2N$ and $Cr_4C$, and *L* is a lamellar structure which probably is $Cr_2N$.
† Also unidentified lines which, however, are not necessarily common to each other among the various patterns.

mium values because of chromium impoverishment of the matrices of the alloys resulting from nitride and carbide precipitation. On the other hand, silicon additions have been reported as causing an opposite, small but true, shift of this boundary to lower chromium values.[8]

The phase relationships for alloys containing approximately 1 pct Si, in both the low nitrogen and high nitrogen (nitrided and homogenized) states, are illustrated in Fig. 5. The presence of $\sigma$ was checked by metallographic examination and the compositions of the matrices are those calculated on the basis of chromium impoverishment. The boundary shown for the high $N_2$-1 pct Si alloys can be drawn much like that of the high nitrogen alloys in Fig. 3. Not only has the shift of the $(\gamma+\sigma)/\gamma$ boundary caused by silicon been nullified by nitrogen, but also the added influence of nitrogen in shifting this boundary to higher chromium contents, as shown in Fig. 3, still is present.

With the addition of more than about 1 pct Si, the effect of nitrogen definitely is decreased. Although nitrogen still is effective at the 8 pct Ni level, it becomes progressively less effective as the nickel is increased further, until at the 20 pct Ni level, nitrogen has virtually no effect. The addition of 0.088 to 0.190 pct N to the 2 pct Si alloys, by use of suitable melting practice, has prevented a shift in the $(\gamma+\sigma)/\gamma$ boundary at the 8 pct Ni level to values of chromium lower than those shown for the 1 pct Si alloys in Fig. 5 (see Fig. 6). However, at the 20 pct Ni level, the nitrogen appears to be ineffective in preventing the shift caused by silicon, since the boundary composition here is the same as that found for 2 pct Si alloys containing low amounts of nitrogen (see Fig. 7).

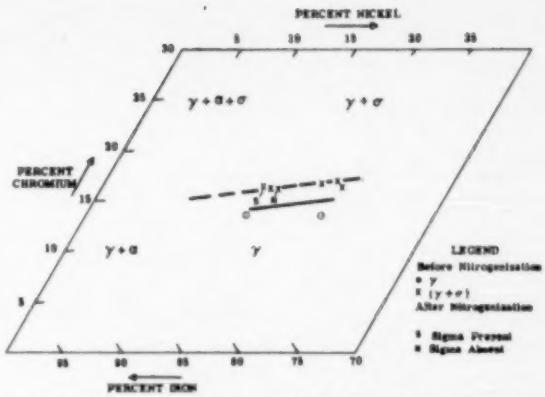


Fig. 7—Effect of about 2 pct Si (about 0.05 pct N) on the phase boundary at which $\sigma$ forms from austenite ($\gamma$) in commercially pure Fe-Cr-Ni steels at 1200°F. Long dash line is modified boundary given in Fig. 2; solid line is boundary as affected by about 2 pct Si. For two of the alloys the nitrogen contents were increased further (by nitriding and homogenizing). The initial (matrix) composition is indicated by an X and the (matrix) composition after nitriding is indicated by an S or N, depending on whether or not $\sigma$ phase formed.

Introduction of greater amounts of nitrogen (by nitriding and homogenizing) into two $\sigma$ susceptible 15 pct Ni-2 pct Si alloys of low nitrogen content caused no change in their phase relationships at 1200°F that cannot be accounted for by chromium impoverishment alone (see Fig. 7).

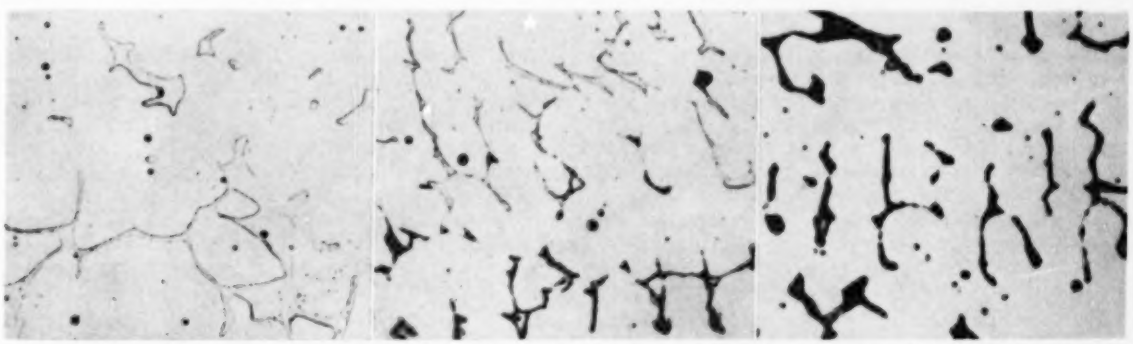

a—As-cast showing δ ferrite in austenite matrix. X500.

b—Casting after holding 96 hr at 1200°F. X500.

c—Casting after holding 500 hr at 1200°F. X500.

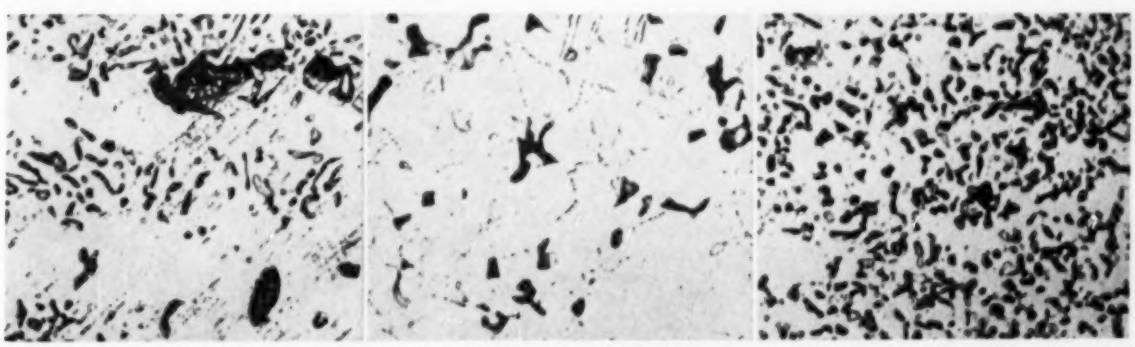

d—Casting after cold working and holding 910 hr at 1200°F. X750.

e—Wrought alloy after holding 2000 hr at 1200°F. X750.

f—Wrought alloy after cold working and holding 910 hr at 1200°F. X750

Fig. 8—Mode of sigma formation at 1200°F in the cast and wrought forms of alloy No. 21 (24 pct Cr-14 pct Ni). Dark-etching regions are $\sigma$ phase. Glyceregia etch.

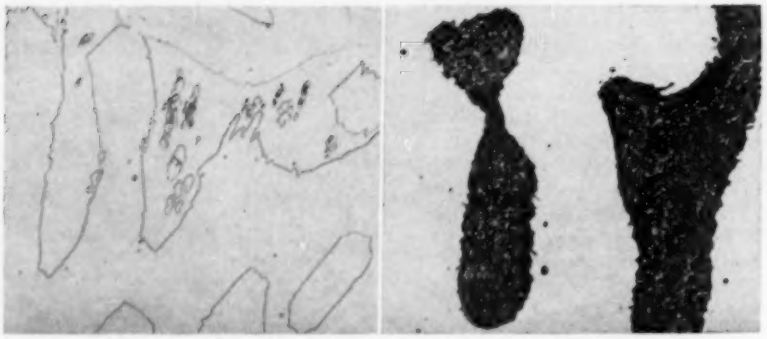

a—After holding for 24 hr at 2250°F in argon and water quenching. δ ferrite in an austenite matrix.

b—After giving sample *a* a further heat treatment of 24 hr at 1200°F. δ ferrite transformed almost completely to σ phase.

Fig. 9—Metallographic evidence of σ formation in δ ferrite of cast alloy No. 21 (24 pct Cr-14 pct Ni). Glyceregia etch. X250.

*Metallographic Observations on Cast and Wrought Alloys:* Insofar as susceptibility to σ phase formation is concerned, no differences were noted between the nitrogen-containing cast and wrought alloys. However, differences in the rate of formation of σ were noted between these forms. The σ phase is reported to form more readily in the wrought alloys than in the cast forms.[5-7] The present work indicates this to be true only of single-phase alloys. For example, in the fully austenitic alloy 22 (24 pct Cr-20 pct Ni) σ formed more rapidly in the wrought than in the cast form. However, the effect was reversed for alloys 13 (21 pct Cr-8 pct Ni) and 21 (24 pct Cr-14 pct Ni) in which σ formed more rapidly in the cast forms which contained δ ferrite, than in the wrought forms. It is well known that the σ phase will form very readily in δ ferrite.

The mode of σ precipitation in alloy 21 (24 pct Cr-14 pct Ni) is shown in Fig. 8. In the unstrained cast form, σ formation occurs readily in the δ ferrite but not in the austenite matrix. However, when the cast form is strained, the σ phase forms both in the δ ferrite and in the austenite matrix. In the unstrained wrought form, the σ phase forms at the grain boundaries. In the strained wrought form, it occurs both at the grain boundaries and within the grains. Note also the greater amount of σ that has formed in the strained alloys, illustrating the accelerating effects of straining on σ formation.

The greater tendency for σ phase formation in δ ferrite is illustrated also in Fig. 9. The cast form of alloy 21 was held at 2250°F for 24 hr in argon to increase the amount of δ ferrite, and then was aged at 1200°F. Within 24 hr at 1200°F, δ ferrite was converted almost completely to σ.

Fig. 10 shows a dark-etching constituent which formed within 96 hr at 1200°F in the grain boundaries of alloy 14 (21 pct Cr-14 pct Ni) which is completely austenitic in the cast form. The nature of the precipitate is not known. Although it etches somewhat like σ, it does not look like it under the microscope. Moreover, an X-ray diffraction examination of the residue of an electrolytic $FeCl_3$ extraction did not show any evidence of σ phase.

## Conclusions

1—The addition of nitrogen above amounts ordinarily found in steels of the Fe-Cr-Ni system has two effects: A—By precipitation of nitrides (as well as carbides), a chromium impoverishment of the matrix occurs which gives an apparent though erroneous impression of large shifts of the σ boundaries to higher chromium contents. B—Over and above the chromium-impoverishment effect, the residual nitrogen significantly displaces the $(\gamma+\sigma)/\gamma$ phase boundary at least 1 pct to higher chromium contents for alloys containing more than about 8 pct Ni; and, for alloys containing less than about 8 pct Ni, the nitrogen displaces the $(\gamma+\alpha+\sigma)/(\gamma+\alpha)$ phase boundary to higher chromium contents by an amount varying linearly from about 0 pct at the γ triple point to about 7 pct at the α triple point. These displacements are considered as the minimum displacements possible. Consideration of the small amount of iron and nickel in the nitrides as well as the small amount of nitrogen in solution would cause somewhat greater displacement of the σ-forming boundaries toward higher chromium contents.

2—Even in the presence of silicon (up to about 1 pct), nitrogen has the ability to shift the $(\gamma+\sigma)/\gamma$ phase boundary of the Fe-Cr-Ni system to higher values of chromium. This is evident at all nickel levels, in alloys containing about 1 pct Si. However, in alloys containing about 2 pct Si, this ability to

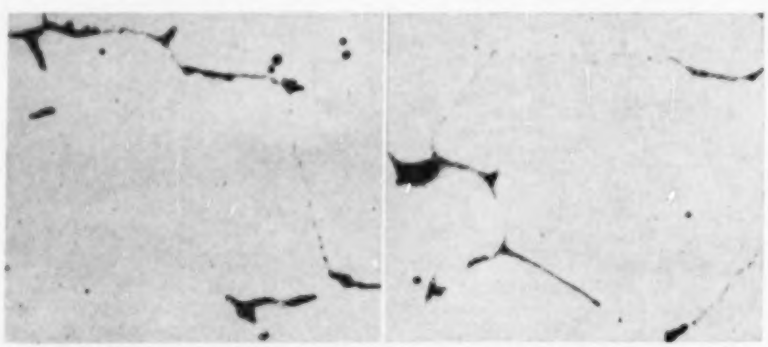

a—After holding 96 hr at 1200°F.

b—After holding 2000 hr at 1200°F.

Fig. 10—Unidentified precipitate (not σ) in the as-cast austenitic alloy No. 14 (21 pct Cr-14 pct Ni). Glyceregia etch. X500.

shift the $(\gamma+\sigma)/\gamma$ boundary exists at the 8 pct Ni level but has virtually disappeared at the 20 pct Ni level.

3—Except in the presence of $\delta$ ferrite, $\sigma$ forms at a slower rate (at 1200°F) in the as-cast alloys than in the wrought alloys. The accelerating effect of cold work on $\sigma$ formation in both cast and wrought alloys is demonstrated clearly.


### Acknowledgments

The authors are indebted to F. L. Eberle, A. L. Malacky, and H. R. Seagren for the assistance provided in this work. Many of the data were secured as parts of a cooperative program on stainless steels between Standard Oil Co. (Indiana) and Crane Co.; permission of both companies to publish this work is gratefully acknowledged.


### References


[1] F. B. Foley: The Sigma Phase in Certain High-Chromium Steels. *Metallurgia* (1946) **34**, p. 139.

[2] W. P. Rees, B. D. Burns, and A. J. Cook: Constitution of Iron-Nickel-Chromium Alloys at 650° to 800°C. *Journal* Iron and Steel Institute (1949) **162**, p. 325.

[3] M. E. Nicholson, C. H. Samans, and F. J. Shortsleeve: Composition Limits of Sigma Formation in Nickel-Chromium Steels at 1200°F (650°C). *Trans.* ASM (1952) **44**, p. 601.

[4] H. Krainer and M. Leoville-Nowak: The Constitution Diagram of Nitrogen-Containing Chromium-Nickel Steels. *Archiv. Eisenhuttenwesen* (1942) **15**, p. 507.

[5] A. M. Talbot and D. E. Furman: Sigma Formation and its Effect on the Impact Properties of Iron-Nickel-Chromium Alloys. *Trans.* ASM (1953) **45**, p. 429.

[6] G. N. Emmanuel: Sigma Phase and Other Effects of Prolonged Heating at Elevated Temperatures on 25 pct Cr-20 pct Ni Steel. Symposium on Nature, Occurrence, and Effects of Sigma Phase. *ASTM Bulletin 110* (1950) pp. 82-99.

[7] W. O. Binder: Some Notes on the Structure and Impact Resistance of Columbium-Bearing 18-8 Steels After Exposure to Elevated Temperatures. Symposium on Nature, Occurrence, and Effects of Sigma Phase. *ASTM Bulletin 110* (1950) pp. 146-164.


---

Technical Note

# Titanium-Manganese Phases


by Harold Margolin and Elmars Ence


TWO versions of the Ti-Mn binary diagram have been published recently.[1, 2] Both diagrams show two compounds in the region between 40 and 70 wt pct Mn, but disagree as to the reaction in which these compounds are involved. The investigation of the manganese-rich portion of the Ti-Mn binary diagram was undertaken at New York University as part of an investigation of ternary systems with titanium and manganese in order to determine which of the proposed diagrams is correct.

A number of alloys between 31 and 70 pct Mn were prepared in a manner similar to that described by Cadoff and Nielsen,[3] except that low currents (110 amp in argon atmosphere) and long melting times (up to 20 min) were used to prepare the alloys. Compositions were determined from weight-loss data, assuming all loss as due to manganese. Heat treatments were carried out with relatively large pieces, since there was a tendency for manganese to be lost during heat treatment. When X-ray diffraction data was to be obtained, the central parts of heat-treated specimens were used to make filings or powders which were not heat treated.

Specimens were heat treated from the as-cast state. Heat-treatment times were as follows: 1150°C, 1 day; 1100°C, 2 days; 1000°C, 5 days; and 900°C, 15 days. It should be noted that equilibrium was not attained at 900°, 1000°, and in one case, at 1150°C. Metallographic specimens were electrolytically polished and strain etched by a technique described elsewhere.[4]


H. MARGOLIN, Junior Member AIME, and E. ENCE, Member AIME, are Research Associates, Engineering Research Div., New York University, New York.



TN 230E. Manuscript, Apr. 19, 1954.


At least four, and possibly six, phases were found in the region investigated. On the basis of information available at this time, a completely self-consistent diagram cannot be constructed, and therefore data are presented only for those phases which have been identified by both X-ray and microstructure.

Of the compounds detected, the one highest in manganese is the Laves phase, $TiMn_2$, which is hexagonal with a $MgZn_2$ type of structure.[5] The diffraction data for $TiMn_2$ from a 70 pct Mn alloy annealed at 1150°C are shown in Table I. The $c/a$ ratio and parameters of $TiMn_2$ agree well with those of Wallbaum[6] and Rostoker et al.[5] The values obtained here are $c/a = 1.641$, $a = 4.825$Å. Another compound is the $\gamma$-phase which is estimated to contain about 60 pct Mn. The $\gamma$-phase has a structure which is identical to that of $TiMn_2$ with $c/a = 1.639$, $a = 4.906$Å. The fact that $\gamma$ has a Laves-type lattice would suggest that $TiMn_2$ has a range of solubility which extends from the composition of $TiMn_2$ (69.6 Mn) to that of $\gamma$ (60 pct Mn). However, this could not account for microstructures which, in the 60 to 70 pct Mn region, show several phases in both the as-cast state and after annealing at 1150°C.

Fig. 1 shows a two-phase structure of a 60 pct Mn alloy annealed at 1150°C. The phases present are $\gamma$ (white) and $\epsilon$ (dark). If $\gamma$ were $TiMn_2$ then, according to Rostoker et al.,[5] the second phase of Fig. 1 should be $\beta$-Ti. The diffraction data for the 60 pct Mn alloy of Fig. 1 are shown in Table I. The starred $d$-values are from the $\epsilon$-phase and these lines do not correspond to those of $\beta$-Ti. Comparison of as-cast and 1150°C microstructures of the 60 pct Mn alloy indicates that $\epsilon$ precipitated from $\gamma$. Since $\gamma$ has a

## Table I. Diffraction Data of Ti-Mn Phases

| $TiMn_2$: $c/a = 1.641$ $a = 4.825$Å, $c = 7.917$Å | | | | $\gamma$ Phase: $c/a = 1.639$ $a = 4.906$Å, $c = 8.040$Å | | | | Ti—60 Pct Mn | | $\delta$-Phase: Ti—50.5 Pct Mn | |
|---|---|---|---|---|---|---|---|---|---|---|---|
| Ti—70 Pct Mn Annealed At 1150°C | | Calculated | | Ti—50.5 Pct Mn As Cast | | Calculated | | Annealed 24 Hr at 1150°C | | Annealed 24 Hr at 1150°C | |
| d, A | Relative Intensity | d, A | Indices | d, A | Relative Intensity | d, A | Indices | d, A | Relative Intensity | d, A | Relative Intensity |
| 4.168 | 0.1 | 4.162 | 100 | 4.255 | 0.15 | 4.249 | 100 | 4.445 | 0.05 | | |
| 3.948 | 0.1 | 3.958 | 002 | 4.019 | 0.08 | 4.020 | 002 | 4.219 | 0.1 | | |
| 3.696 | 0.07 | 3.700 | 101 | 3.763 | 0.15 | 3.757 | 101 | 3.963 | 0.08 | | |
| | | 2.874 | 102 | | | 2.920 | 102 | 3.745 | 0.1 | | |
| 2.412 | 0.5 | 2.412 | 110 | 2.451 | 0.5 | 2.453 | 110 | 2.487* | 0.05 | 2.425 | 0.1 |
| 2.232 | 1 | 2.231 | 103 | 2.267 | 0.8 | 2.267 | 103 | 2.453 | 0.5 | 2.292 | 0.3 |
| 2.062 | 1 | 2.059 | 112 | 2.090 | 1 | 2.094 | 112 | 2.385* | 0.01 | 2.189 | 1 |
| 2.026 | 0.8 | 2.020 | 201 | 2.054 | 1 | 2.054 | 201 | 2.331* | 0.01 | 2.091 | 1 |
| 1.981 | 0.3 | 1.979 | 004 | 2.010 | 0.05 | 2.010 | 004 | 2.300* | 0.01 | 2.056 | 0.6 |
| 1.848 | 0.4 | 1.848 | 202 | 1.876 | 0.4 | 1.878 | 202 | 2.262 | 1 | 2.033 | 0.2 |
| 1.789 | 0.4 | 1.789 | 104 | 1.816 | 0.2 | 1.817 | 104 | 2.202* | 0.2 | 1.925 | 0.15 |
| 1.640 | 0.1 | 1.638 | 203 | 1.666 | 0.15 | 1.665 | 203 | 2.177* | 0.08 | 1.860 | 0.08 |
| 1.394 | 0.08 | 1.393 | 300 | 1.416 | 0.08 | 1.416 | 300 | 2.165* | 0.08 | 1.820 | 0.03 |
| 1.357 | 0.4 | 1.356 | 213 | 1.379 | 0.4 | 1.378 | 213 | 2.123* | 0.5 | 1.741 | 0.05 |
| 1.315 | 0.4 | 1.314 | 302 | 1.336 | 0.3 | 1.336 | 302 | 2.093 | 1 | 1.380 | 0.2 |
| 1.262 | 0.4 | 1.262 | 205 | 1.279 | 0.5 | 1.278 | 205 | 2.050 | 1 | 1.360 | 0.2 |
| 1.236 | 0.2 | 1.234 | 214 | 1.255 | 0.1 | 1.256 | 214 | 2.010 | 0.5 | 1.334 | 0.2 |
| 1.207 | 0.3 | 1.205 | 220 | 1.228 | 0.2 | 1.227 | 220 | 1.886 | 0.1 | 1.316 | 0.2 |
| 1.117 | 0.3 | 1.115 | 206 | | | | | 1.878 | 0.5 | 1.294 | 0.2 |
| 1.094 | 0.07 | 1.092 | 107 | | | | | 1.814 | 0.4 | 1.219 | 0.2 |
| 1.063 | 0.3 | 1.061 | 313 | | | | | 1.662 | 0.1 | | |
| | | | | | | | | 1.610* | 0.08 | | |
| | | | | | | | | 1.411 | 0.04 | | |
| | | | | | | | | 1.377 | 0.4 | | |
| | | | | | | | | 1.335 | 0.4 | | |
| | | | | | | | | 1.315* | 0.1 | | |
| | | | | | | | | 1.290* | 0.02 | | |
| | | | | | | | | 1.279 | 0.4 | | |
| | | | | | | | | 1.251 | 0.06 | | |
| | | | | | | | | 1.226 | 0.4 | | |

* In this column starred $d$-values belong to $\epsilon$, others are from $\gamma$.

range of compositions which extends from 60 to possibly 58 pct Mn with decreasing temperature,[7] this suggests that $\epsilon$ lies between $\gamma$ and $TiMn_2$.

$\gamma$ has been found in the diffraction patterns of as-cast alloys containing from 45 to 60 pct Mn and for a 1150°C anneal only in the 60 pct Mn alloy of Fig. 1. Diffraction data of $\gamma$ for both the as-cast and annealed conditions are shown in Table I together with calculated $d$-values. It can be seen from Table I that there is close agreement between the $d$-values of $\gamma$ obtained from as-cast and annealed alloys. In both cases the $d$-values are not the same as those of $TiMn_2$.

It has been pointed out that the diffraction pattern of $\gamma$ appears only in the 60 pct Mn alloy after annealing at 1150°C. In alloys containing less than 60 pct Mn, a new diffraction pattern appears after an anneal at this temperature. This new phase is indistinguishable microstructurally from $\gamma$. Evidence is available[7] which suggests that this compound, $\delta$, is close to the composition of $\gamma$ and either may form by peritectoid reaction between $\beta$-Ti and $\gamma$ or may be an allotropic modification of $\gamma$. The diffraction data for $\delta$ were obtained from three alloys containing approximately 45, 48, and 50.5 pct Mn and the $d$-values from the 50.5 pct Mn alloy are shown in Table I.

The stain-etched colors of the phases discussed above, as etched with HG-electrolyte,[4] are as follows: $TiMn_2$, pink; $\epsilon$, similar to $TiMn_2$ but lighter; $\gamma$, bluish-green; and $\delta$, similar to $\gamma$.

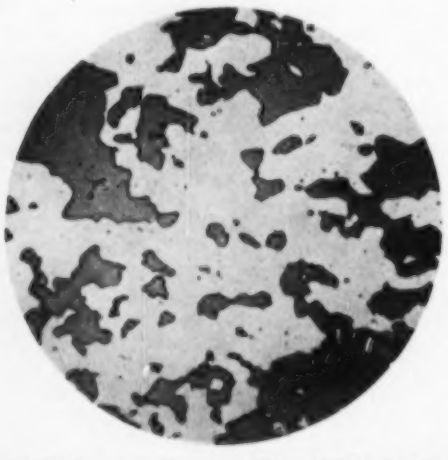

Fig. 1—Ti-60 pct Mn alloy, annealed at 1150°C for 24 hr, water quenched. Electrolytically stained, "HG" electrolyte. $\gamma$ is white (actually bluish-green) and $\epsilon$ is gray (actually violet). X350.


### Acknowledgment

The authors wish to thank the United States Army Ordnance Corps, Watertown Arsenal, for permission to publish this work. The investigation was carried out under Watertown Arsenal Contract No. DA-30-069-ORD-208.


### References


[1] D. J. Maykuth, H. R. Ogden, and R. I. Jaffee: Titanium-Manganese System. *Trans.* AIME (1953) **197**, p. 225; JOURNAL OF METALS (February 1953).

[2] W. Rostoker, R. P. Elliot, and D. J. McPherson: Discussion of Titanium-Manganese System. *Trans.* AIME (1953) **197**, p. 248; JOURNAL OF METALS (February 1953).

[3] I. Cadoff and J. P. Nielsen: Titanium-Carbon Phase Diagram. *Trans.* AIME (1953) **197**, p. 248; JOURNAL OF METALS (February 1953).

[4] E. Ence and H. Margolin: Titanium Phases Identified by Cumulative Etching. *Trans.* AIME (1954) **200**, p. 346; JOURNAL OF METALS (February 1954).

[5] H. J. Walbaum: *Ztsch. Kristallographie* (1941) **103**, p. 391.

[6] B. W. Levinger et al.: Armour Research Foundation. *Final Report on Contract No. DA-11-022-ORD-272* to Watertown Arsenal (February 1953).

[7] New York University: *Final Report on Contract No. DA-30-069-ORD-208* to Watertown Arsenal (April 1954).

# Temper Embrittlement of 5140 Steel

by S. H. Bush and C. A. Siebert

**Isothermal temper-embrittlement studies were conducted on a 5140 steel at various temperatures for times as long as 3000 hr. Specimens from the embrittled steel were subjected to impact tests, metallographic examination, microhardness, and lattice-parameter measurements.**

SEVERAL of the steels in the low alloy group are subject to a pronounced decrease in impact energy if held within, or cooled slowly through, a range of temperatures below the lower critical. This phenomenon, known as temper embrittlement, is quite pronounced in the chromium steels of which AISI 5140 is typical.

This study considered the response of one heat of 5140 steel when embrittled isothermally at various temperatures for times as long as 3000 hr.

Excellent reviews of the work done in the field of temper embrittlement have been written by Hollomon[1] and Woodfine.[2] Both authors list the various theories which have been advanced to explain temper embrittlement. Some of the mechanisms considered were: 1—a transformation below 700°C; 2—an allotropic modification of iron; 3—precipitation from the ferrite of such compounds as carbides, nitrides, phosphides, or chromium oxides; 4—decomposition of retained austenite; 5—modification of special carbides; 6—grain-boundary segregation; and 7—selective distribution of carbides.

The present study investigated the changes in hardness, Meyer's number, impact properties, microstructure, and lattice parameter which occurred on embrittlement. Previous studies considered the influence of microstructure and of prior austenitic grain size[3] on the response of 5140 steel to temper embrittlement.

S. H. BUSH and C. A. SIEBERT, Members AIME, are Instructor in Dental Materials and Professor of Metallurgical Engineering, respectively, University of Michigan, Ann Arbor, Mich.

Discussion on this paper, TP 3849E, may be sent, 2 copies, to AIME by Jan. 1, 1955. Manuscript, Aug. 27, 1953. Chicago Meeting, November 1954.

## Equipment and Procedure

All samples were taken from one heat of 5140 steel; the chemical composition of this steel was: 0.43 pct C, 0.86 pct Mn, 0.020 pct P, 0.019 pct S, 0.27 pct Si, 0.84 pct Cr, 0.10 pct Ni, 0.06 pct Mo, 0.10 pct Cu, and the remainder Fe. The material was received as ¾ in. rounds. This stock was cut down to blanks measuring approximately 0.425x0.425x2.196 in.

*Heat Treatment:* The rough blanks were normalized at 1600°F (870°C) for 1 hr, then austenitized at 1600°F (870°C) for 1½ hr, and quenched into an agitated oil bath. The specimens were tempered at 1275°F (690°C) for 5 hr and water quenched. These tempered specimens were designated as the toughened state.

*Embrittling Treatments:* The tempered bars were divided into sets and subjected to the various embrittling treatments listed in Table I. Temperatures from 750° to 1050°F were investigated for times of 1 to 3000 hr. Special tests to determine the effect of heating a short time at a higher temperature after long-time embrittlement at some lower temperature were also conducted. All specimens were water quenched at the end of the embrittling cycle, then ground and notched to obtain standard Charpy *V*-notch specimens.

*Impact Tests:* The bars were fractured in a 260 ft-lb Charpy impact unit; specimens were fractured at temperatures ranging from −315°F to room temperature. Fixed temperatures used consisted of −315°F with liquid nitrogen, −115°F with dry ice and acetone, and 32°F with ice and water. Intermediate temperatures were obtained by suspending the bars in a jig over the liquid nitrogen, dry ice and acetone, or ice and water.

After determining the impact energies, the specimens were immersed in acetone to protect the fractures until the bars reached room temperature. The specimens were removed, dried, and the percentage of brittle fracture determined by comparing with a series of calibration fractures. These values were plotted as impact energy vs testing temperature, or the percentage of brittle fracture vs testing temperature.

*Metallographic Examination:* Sections were taken from the bars fractured at room temperature for each heat treatment or embrittling cycle. These specimens were polished electrolytically and etched with ethereal picric acid following the method suggested by Jacquet.[4, 5] These samples were examined at X2000 for selective attack of the embrittled specimens. A typical series covering embrittlement at 950°F for 100 hr, reversals at 1250°F, and re-embrittlement at 950°F is included, together with a micrograph of the steel in the toughened state.

*Microhardness:* Some of the electrolytically polished specimens were tested to determine the Meyer's numbers in the various states. A series of microhardness measurements were made at loads of 100 and 1000 grams using a Tukon unit with the 136° diamond pyramid point. Values were averaged for each specimen and load, and *n*, the Meyer's number, determined analytically as suggested by Bückle.[6]

*Lattice-Parameter Measurements:* The electrolytically polished specimens used for the metallographic survey were examined with X-rays, using a back-reflection technique, to determine if any change occurred due to embrittlement. Unfiltered cobalt radiation was used with a small symmetric-back-reflection camera. The lattice parameters were determined using the graphical method suggested by Cohen.[7]

**Table I. Transition Temperatures, Lattice Parameters, and Meyer's Numbers for Various Times and Embrittling Temperatures**

| Heat Treatment | Transition Temperature | | | |
|---|---|---|---|---|
| | 50 Ft-Lb Impact Energy, °F | 50 Pct Brittle Fracture, °F | Extrapolated Lattice Parameters | Meyer's Number |
| 1600°F, 1275°F, 5 hr* | −103 | −103 | 2.8620 | 1.89 |
| 750°F, 100 hr; 1250°F, 1 hr | −103 | −98 | 2.8616 | 1.96 |
| 950°F, 100 hr; 1250°F, 1 hr | −80 | −85 | 2.8620 | — |
| 950°F, 100 hr; 1250°F, 1 hr; 950°F, 100 hr | −18 | −26 | 2.8614 | — |
| 750°F, 1 hr | −92 | −90 | — | — |
| 750°F, 10 hr | −90 | −88 | — | — |
| 750°F, 24 hr | −80 | −83 | — | — |
| 750°F, 100 hr | −78 | −88 | 2.8616 | — |
| 750°F, 1000 hr | −80 | −96 | — | — |
| 750°F, 3000 hr | −87 | −87 | 2.8615 | — |
| 850°F, 1 hr | −87 | −90 | — | — |
| 850°F, 10 hr | −80 | −81 | — | — |
| 850°F, 24 hr | −69 | −54 | — | — |
| 850°F, 100 hr | −45 | −51 | 2.8610 | — |
| 850°F, 1000 hr | 1 | 1 | — | — |
| 850°F, 3000 hr | 27 | 34 | 2.8608 | — |
| 950°F, 1 hr | −85 | −83 | 2.8619 | 1.97 |
| 950°F, 10 hr | −40 | −47 | 2.8616 | 1.92 |
| 950°F, 24 hr | −24 | −33 | 2.8613 | 1.95 |
| 950°F, 100 hr | −4 | −9 | 2.8612 | 1.94 |
| 950°F, 1000 hr | −6 | −6 | 2.8610 | — |
| 950°F, 3000 hr | −15 | −15 | 2.8610 | — |
| 1000°F, 1 hr | −74 | −74 | — | — |
| 1000°F, 10 hr | −42 | −53 | — | — |
| 1000°F, 24 hr | −34 | −42 | — | — |
| 1000°F, 100 hr | −34 | −42 | 2.8613 | — |
| 1080°F, 1 hr | −31 | −81 | 2.8614 | 1.97 |
| 1050°F, 10 hr | −51 | −53 | 2.8614 | 1.90 |
| 1080°F, 24 hr | −63 | −49 | 2.8610 | 1.95 |
| 1050°F, 100 hr | −74 | −67 | 2.8614 | 1.98 |
| 1050°F, 1000 hr | −56 | −56 | 2.8611 | — |
| 1080°F, 3000 hr | −67 | −58 | 2.8614 | — |
| 1100°F, 10 hr | −58 | −71 | — | — |
| 1100°F, 24 hr | −60 | −69 | — | — |
| 1100°F, 100 hr | −49 | −49 | 2.8614 | — |
| Pure iron | — | — | 2.8606 | — |
| As-quenched (5140 steel) | — | — | — | 1.93 |

* Toughened condition used as a base for determining transition-temperature shift.

## Discussion

The RB hardnesses of all specimens were determined before the impact test. It is interesting to note that the maximum shift in average RB hardness from the toughened state to the softest condition encountered in the embrittling cycle was less than six points, and the range of values from the highest to the lowest was less than nine points. Therefore, it is believed that any change in hardness is too small to affect the impact values noticeably.

An examination of Table I will prove the reversibility of the temper-embrittlement reaction. The 950°F, 100 hr cycle shifts the transition temperature approximately 100°F from the base or toughened state. One hour at 1250°F after 100 hr at 950°F is sufficient to decrease this shift to less than 25°F. An additional 100 hr at 950°F increases the shift to about 80°F.

Temperatures as low as 750°F do not appear to promote temper embrittlement. The maximum shift observed is only 25°F. It is interesting to note that a slight reversal apparently occurs at 3000 hr. However, the decrease is so limited that it may be meaningless.

The optimum long-time embrittling temperature of those investigated was found to be 850°F. Embrittlement was not pronounced in the short-time cycles, but a shift of about 130°F occurred in 3000 hr, the greatest shift observed.

Pronounced embrittlement occurred in relatively short times at 950°F. A shift of approximately 100°F was observed within 100 hr. After 100 hr the embrittlement decreased gradually.

In the case of the embrittling tests at 1050°F, two maxima were observed in the transition-temperature shift. The first occurred in 10 hr after which a decrease was noted until 100 hr when an increase occurred to a maximum at 1000 hr followed by another decrease. These general trends were confirmed by tests at 1000° and 1100°F.

The lattice parameters appearing in Table I confirm the shifts noted in the transition temperature. As the transition-temperature shift increases, the lattice parameter decreases. A reversal in the one is accompanied by a reversal in the other. This indicates a decrease in lattice size due to a removal of an interstitial component such as carbon or the rearrangement of the substitutional constituents. The changes in parameter are not pronounced, but the fact that there is such a definite correlation between the transition-temperature shift and the parameter tends to confirm the reversals observed in some of the cycles.

The Meyer's numbers given in Table I qualitatively confirm the embrittlement of the steel, but there does not appear to be a quantitative relationship. An increase in the Meyer's number is observed with embrittlement, indicating an increase in strain in the structure. Unfortunately, the Meyer's numbers increase and decrease while a continuous increase in transition-temperature shift occurs. This is particularly noticeable at 950°F. As a result, this test is not believed to be satisfactory for following the temper embrittlement of a 5140 steel.

The reversal occurring after embrittling, then reheating to some temperature close to the lower critical, is very apparent in Fig. 1. After 100 hr at 950°F,

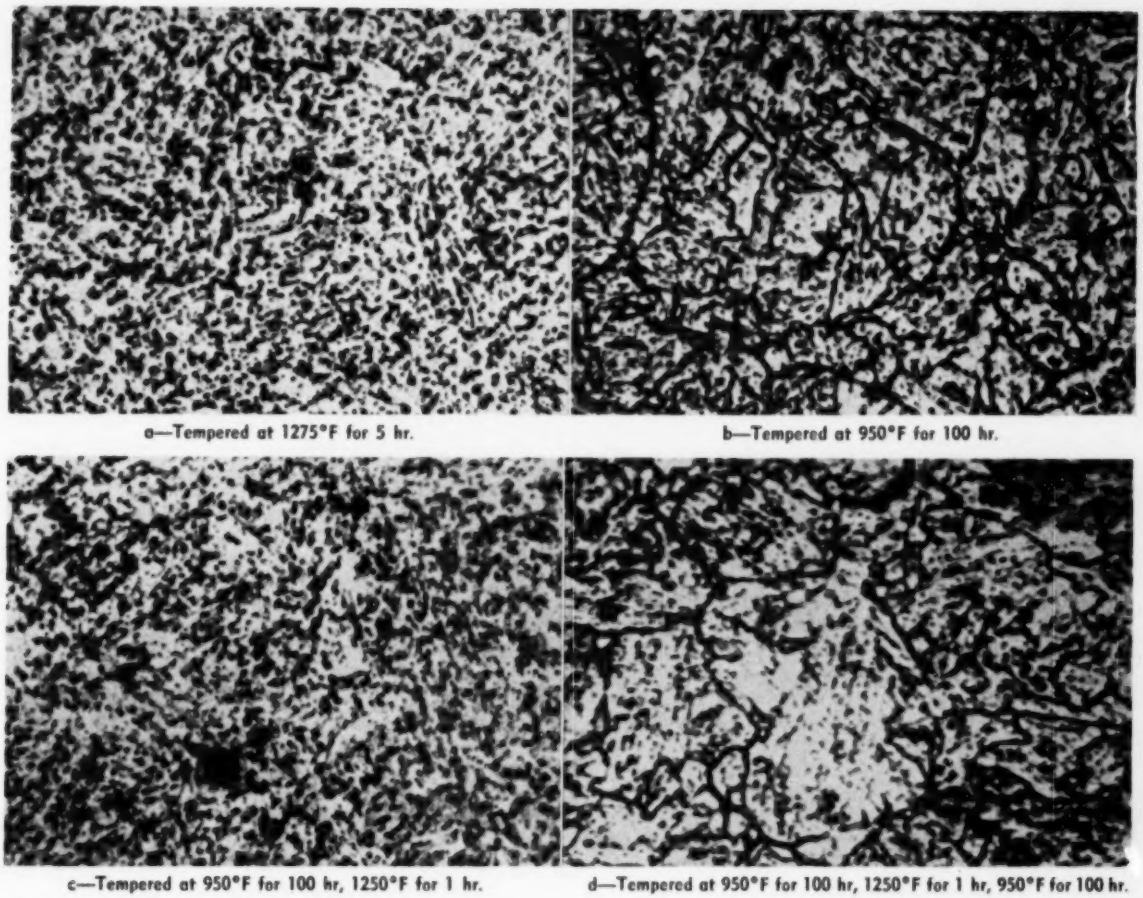

a—Tempered at 1275°F for 5 hr. b—Tempered at 950°F for 100 hr.

c—Tempered at 950°F for 100 hr, 1250°F for 1 hr. d—Tempered at 950°F for 100 hr, 1250°F for 1 hr, 950°F for 100 hr.

**Fig. 1—Reversal of embrittlement by heating to a higher temperature. Ethereal picric immersion etch, 2.5 min. X2000. Area reduced approximately 35 pct for reproduction.**

the steel displays a continuous grain-boundary etch pattern. One hour at 1250°F removes this attack completely and the structure is the same as the toughened state. An additional embrittling cycle of 100 hr at 950°F is sufficient to cause essentially the same degree of attack as that observed after the first 100 hr. In this case there is complete correlation among transition-temperature shift, lattice parameter, and microstructure. In no case was a precipitate observed at the grain boundaries when examined with optical or electron microscopes.

## Conclusions

1—A reversal in the temper embrittlement of a steel may occur if held at some temperature sufficiently long. This reversal may be followed by an increased embrittlement when held for a longer time; this in turn may decrease on further holding.

2—A short time at a temperature near the lower critical is sufficient to remove extensive embrittlement developed by holding a long time at some lower temperature.

3—In a quenched and drawn structure, the degree of attack of the austenitic grain boundaries conforms to the shifts in transition temperature caused by embrittlement.

4—The Meyer's number qualitatively differentiates between a tough and temper-embrittled steel, but does not accurately portray an increase or decrease in embrittlement.

5—An increase in embrittlement is accompanied by a decrease in the lattice parameter; similarly, a decrease in embrittlement is accompanied by an increase in lattice parameter. The shift in lattice parameter is an indication of the degree of embrittlement as noted by a transition-temperature shift.


## Acknowledgment

The authors wish to thank the Timken Roller Bearing Co. for the steel used in this investigation.


## References


[1] J. H. Hollomon: Temper Brittleness. *Trans.* ASM (1946) **36**, pp. 473-542.

[2] B. C. Woodfine: Temper Brittleness: A Critical Review of the Literature. *Journal* Iron and Steel Institute (1953) **173**, No. 3, pp. 229-240.

[3] S. H. Bush and C. A. Siebert: *The Effect of Microstructure and Austenitic Grain Size on the Temper Embrittlement of a 5140 Steel.* Unpublished.

[4] P. A. Jacquet: Etude Micrographie de la Fragilite de Revenu des Aciers au Carbone Faiblement Allies. *Revue de Metallurgie* (1951) **48**, pp. 825-852.

[5] P. A. Jacquet: Etude Micrographie des Etats Fragile et Tenace des Aciers au Carbone Faiblement Allies. *Revue de Metallurgie* (1952) **49**, pp. 195-207.

[6] H. Bückle: L'Application de L'Analyse. Meyer. Microsclero-metrique a la Fragilite de Revenu. *Revue de Metallurgie* (1951) **48**, pp. 858-863.

[7] M. V. Cohen: Precision Lattice Constants from X-ray Powder Photographs. *Review of Scientific Instruments* (1935) **6**, pp. 68-74.

# Stabilization of the Bainite Reaction

by R. F. Hehemann and A. R. Troiano

**The influence of partial decomposition to high temperature bainite on reaction kinetics at a lower temperature has been studied in two alloy steels. Reaction at the lower temperature is retarded by the prior treatment, and the extent of decomposition may be reduced. Interpretation of these results is based on a mechanism involving a limitation in the nucleation and growth of bainite plates.**

OF the major transformations in steel, the characteristics and general behavior of the bainite reaction are probably the least understood and appreciated. Limitations of space preclude a critical evaluation of the present status of the bainite transformation in this presentation; however, such a treatment will shortly appear elsewhere.

Only the salient features pertinent to the present investigation will be introduced briefly here. Although the reaction curve for the formation of bainite is similar to that for a nucleation and growth process, other kinetic features are more in keeping with the martensitic mode of transformation. A definite temperature exists above which austenite will not transform to bainite.[1-4] This temperature, which has been designated $B_s$, is determined by the composition of the austenite. Unlike other nucleation and growth processes, the amount of austenite transformed to bainite is a function of reaction temperature. The extent of decomposition increases from 0 at $B_s$ to 100 pct at some lower temperature.[1, 2] This lower temperature will be designated $B_f$ and appears to be relatively insensitive to austenite composition.[5, 7] The similarity in the effect of reaction temperature on the bainite and martensite transformations serves to emphasize the close connection between these two decomposition processes.

Austenite decomposition in the bainite range proceeds without partition of the alloying elements.[8-11] Partition of carbon has been proposed[12] primarily on the basis that partial transformation to bainite lowers $M_s$ and increases the amount of austenite retained at room temperature. Carbon enrichment resulting from such partition has been employed to explain the influence of reaction temperature on the extent of decomposition.[13] It should be noted, however, that no enrichment has been detected experimentally in high carbon steels.[3, 14, 15] Lattice-parameter measurements of retained austenite in steels containing 0.3 to 0.4 pct C have indicated carbon enrichment,[5, 16-19] although the split indicative of a high carbon martensite has not been reported. Carbon enrichment, if it does occur, must be highly localized around the bainite plates. Therefore, carbon enrichment does not account for the influence of temperature on the progress of the bainite reaction.[20]

Thermal history is known to influence the martensite transformation through stabilization.[20, 21] No similar phenomenon in the bainite transformation has been reported.

## Materials and Procedure

Two triple-alloy steels were chosen for this investigation. Their compositions were as given in Table I. These steels were chosen because the pearlite reaction did not interfere with the bainite reaction.

Steel K was received in the cast condition and forged from 2 in. square bars to ½x1¾ in. plates. The 4340 was received as 1¼ in. hot-rolled rounds. Both steels were homogenized in vacuum for one week at 2300°F in order to minimize segregation.

A quenching dilatometer similar to that described by Flinn, Cook, and Fellows[9] was employed for the kinetic measurements. Dimensional changes were detected by a differential transformer coupled with a high speed recorder. The dilatometer was mounted so that it could be transferred to any one of three furnaces: a nitrogen-atmosphere austenitizing furnace and two salt-bath furnaces for isothermal transformation. Dilatometer specimens were 1/32x¼x½ in. with a gage length of 1.4 in. All specimens were nickel plated in order to minimize decarburization during austenitizing. The austenitizing conditions consisted of 10 min at the temperatures given above. Austenitizing temperatures were controlled to ±10°F and transformation temperatures to ±3°F. The precision of the dimensional measurements was estimated to be $\pm 5 \times 10^{-4}$ in. per in.

## Results and Discussion

*Isothermal Transformation:* The characteristics of the isothermal bainite reaction will be described

R. F. HEHEMANN, Junior Member AIME, and A. R. TROIANO, Member AIME, are Assistant Professor and Professor and Head, respectively, Dept. of Metallurgical Engineering, Case Institute of Technology, Cleveland.

Discussion on this paper, TP 3896E, may be sent, 2 copies, to AIME by Jan. 1, 1955. Manuscript, Apr. 13, 1954. Chicago Meetings, November 1954.

This paper is based on a thesis by R. F. Hehemann submitted, in partial fulfillment of the requirements for the degree of Doctor of Philosophy, to the Dept. of Metallurgical Engineering, Case Institute of Technology.

Table I. Composition of Two Triple-Alloy Steels

| Designation | Composition, Wt Pct | | | | | | Austenite Temperature, °F |
|---|---|---|---|---|---|---|---|
| | C | Si | Mn | Ni | Cr | Mo | |
| 4340 | 0.38 | 0.28 | 0.74 | 1.79 | 0.81 | 0.26 | 1550 |
| K | 0.31 | 0.30 | 0.76 | 3.07 | 1.22 | 0.49 | 1650 |

in order to provide a reference framework for evaluation of the influence of partial reaction at one temperature on the kinetics of reaction at a lower temperature. Isothermal-expansion curves for the bainite reaction in 4340 are illustrated in Fig. 1. These curves are typical of the behavior of both 4340 and the K steels.

The general shape of the reaction curve remains unchanged throughout the temperature interval above $M_s$. The isothermal reaction is characterized by a short induction period during which expansion is negligible, followed by a time period during which transformation proceeds rapidly. Reaction soon stops, but all of the austenite does not transform. This characteristic of the bainite reaction is most evident in the reduced overall expansion resulting from reaction at the higher temperatures.

A semiquantitative picture of the way in which the extent of decomposition depends on transformation temperature ($B$-$T$ curve) can be obtained from the total isothermal expansion.[1, 2] This is presented as a function of reaction temperature in Fig. 2 for 4340 and Fig. 3 for the K steel. The $B_s$ temperature is determined by extrapolation of this curve to 0 pct expansion. Thus, it becomes apparent that bainite forms only below this characteristic temperature and the amount of bainite becomes greater as the temperature is lowered. Metallographic examination indicated that $B_f$ was 730°F for 4340 and 610°F for the K steel. The total dilation continued to increase as the reaction temperature was lowered below $B_f$. Some increase in total dilation must be anticipated here because of the difference in the coefficients of thermal expansion of the austenitic and ferritic phases; however, the slope of the curve below $B_f$ is too great to be accounted for by this means. The reason for this anomalous behavior is not clear.

The shape of the reaction curve at temperatures below $M_s$ (curve for 575°F in Fig. 1) is different from that observed above $M_s$. This does not reflect a fundamental change in the characteristics of the bainite reaction but rather results from the integrated contributions of the martensite and bainite transformations. The initial expansion starting at 4 to 5 sec results from the athermal martensite transformation; whereas the isothermal martensite reaction[3] permits transformation to continue even after the specimen has attained the bath temperature (10 sec). The inflection point at approximately

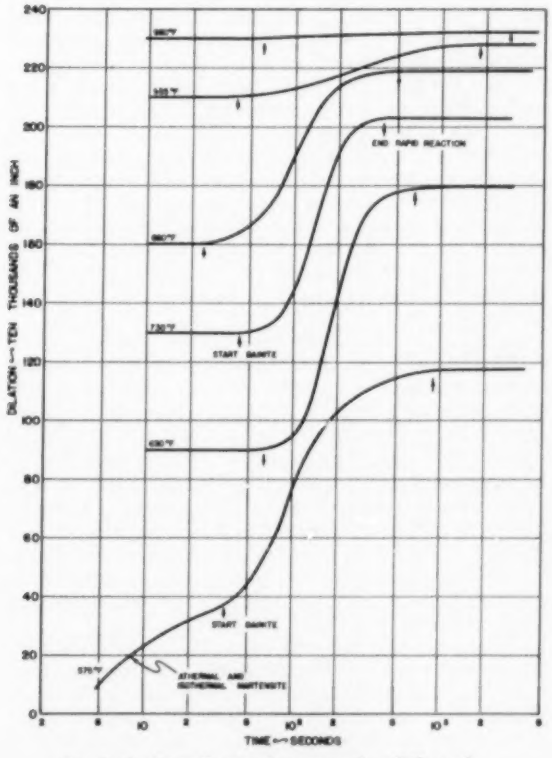


Fig. 1—Isothermal-expansion curves for 4340 steel.

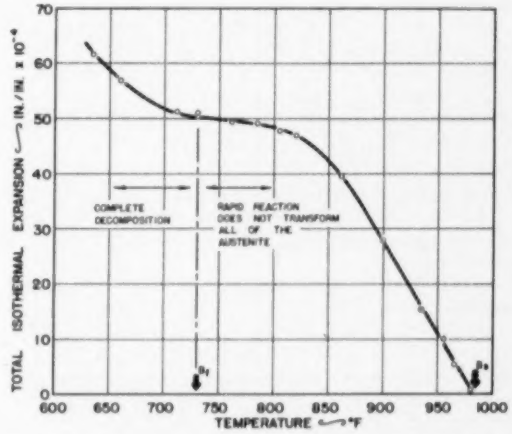


Fig. 2—Total expansion vs transformation temperature for 4340 steel.

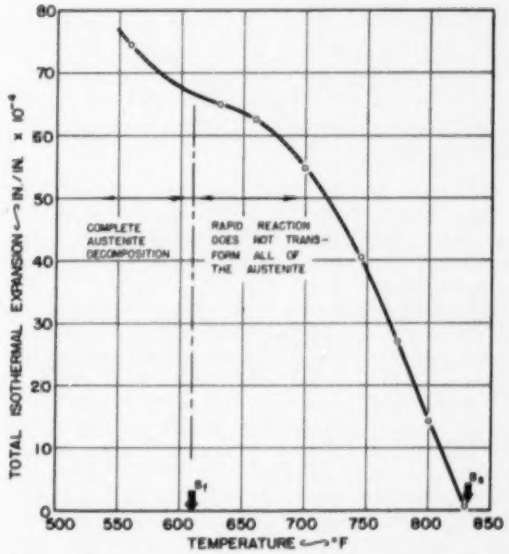
TOTAL ISOTHERMAL EXPANSION — IN./IN. x 10⁻⁴
TEMPERATURE — °F
COMPLETE AUSTENITE DECOMPOSITION
RAPID REACTION DOES NOT TRANSFORM ALL OF THE AUSTENITE
$B_f$
$B_s$

Fig. 3—Total expansion vs transformation temperature for K steel.

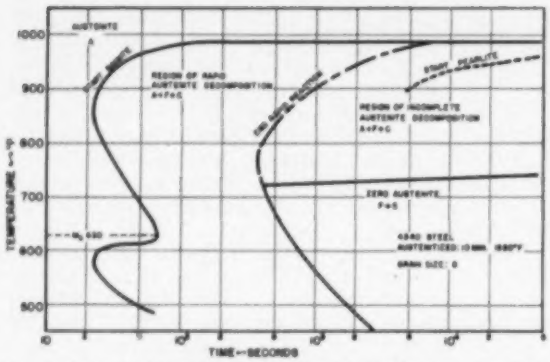


Fig. 4—Isothermal-transformation diagram for bainite range of 4340 steel.

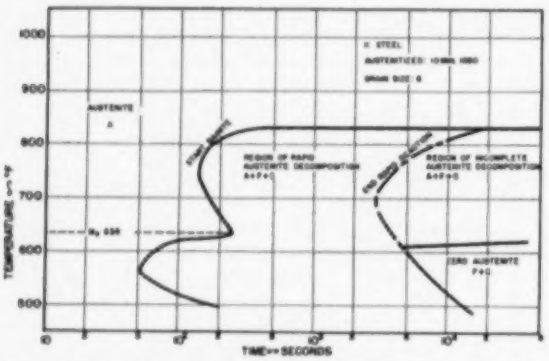


Fig. 5—Isothermal-transformation diagram for bainite range of K steel.

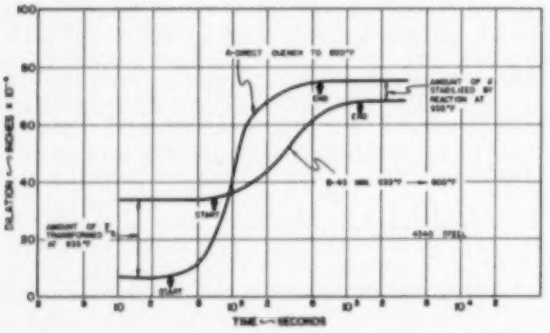


Fig. 6—Effect of partial reaction at 935°F on progress of transformation at 800°F.

35 sec thus signifies the start of the normal bainite reaction. Aside from the marked acceleration in reaction rate, the prior formation of martensite has not altered the basic kinetic features of the bainite transformation.

Time-temperature-transformation diagrams for the bainite range of the 4340 and K steels were constructed from the dilatometric data and are presented in Figs. 4 and 5. The time for the start and end of the rapid reaction was arbitrarily chosen as that at which the expansion attained 1 and 99 pct, respectively, of the total isothermal expansion.

At temperatures near the top of the bainite range in 4340, the pearlite reaction is initiated if the isothermal treatment is continued well beyond the end of the bainite reaction. As illustrated in Fig. 4, the pearlite reaction is accelerated by the prior formation of bainite in the same fashion as the bainite

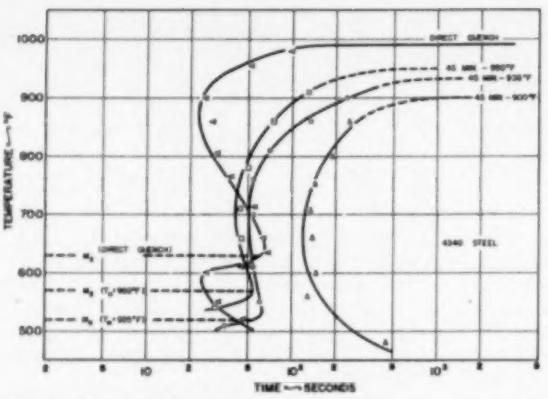


Fig. 7—Effect of 45 min at several temperatures on induction period at lower temperatures.

reaction is accelerated by the prior formation of martensite at reaction temperatures below $M_s$. The pearlite reaction in the K steel was not initiated within five days at any temperature in the bainite range.

*Stepped Reactions:* Conventional nucleation and growth concepts suggest that a reaction initiated at one temperature in a metastable region should continue upon quenching to a different temperature. A new induction period should not be required at the second temperature. In view of the significance of such thermal-history effects in the formulation of an adequate hypothesis for the reaction mechanism, a detailed knowledge of these kinetic features becomes virtually mandatory. Therefore, specimens were reacted at a high temperature in the bainite range*

* In the following, the first reaction temperature will be designated $T_h$ and the second $T_r$.

for a predetermined period of time and then quenched to a lower temperature. Fig. 6 compares two curves for reaction at 800°F. Curve *A* illustrates the progress of the normal reaction (direct quench) at this temperature. In curve *B*, transformation at 800°F was preceded by reaction for 45 min at 935°F. The 935°F treatment resulted in 24 pct bainite, the maximum amount attainable at this temperature. Reaction at $T_h$ has increased the induction period from 28 to 64 sec and has appreciably reduced the rate of transformation. Although the reaction rate at $T_r$ has been lowered, the fundamental kinetic feature of a rapid, incomplete reaction has been preserved.

In addition to the retardation of reaction, prior transformation has stabilized part of the austenite against decomposition at $T_r$. This is revealed clearly in the influence of prior transformation on the total dilation at $T_r$. Obviously, transformation at $T_h$ must reduce the total expansion at $T_r$; however, even after correction for the decomposition at $T_h$, the total dilation is less than that obtained by direct reaction. This difference in total expansion (see Fig. 6) is a measure of the amount of austenite stabilized by the prior treatment. The semiquantitative observations of stabilization obtained with the dilatometer have been confirmed by lineal analysis.

The principal factors controlling the retardation process are the holding time, the holding temperature ($T_h$), the amount of transformation, and the reaction temperature $T_r$. All these are not independent variables and insufficient data are available to permit a complete separation of their individual

contributions. It is possible, nevertheless, to define the general features of the retardation phenomenon and to indicate some of the interrelationships between contributing factors. For this purpose, the induction period at $T_r$ will be employed as a criterion of the amount of retardation.

*Effect of Reaction Temperature ($T_r$):* The dependence of the induction period of 4340 on reaction temperature ($T_r$) is illustrated in Fig. 7. Here, the induction period observed after treatment for 45 min at $T_h$ levels of 950°, 935°, and 900°F is compared with that resulting from direct reaction. At reaction temperatures near the holding temperature, the induction period at $T_r$ has been lengthened appreciably by the prior transformation at $T_h$. The amount of retardation becomes less as the difference between $T_h$ and $T_r$ is increased. In fact, there is an apparent reversal of the retardation effect at reaction temperatures below approximately 700°F.

The K steel responded to prior treatment at $T_h$ = 800°F in a manner analogous to that of 4340, see Fig. 8. Holding for 2 hr at 800°F has retarded transformation at all lower temperatures. Again, the amount of retardation decreased as the reaction temperature was lowered.

In each of the cases examined, an induction period has been required at the second reaction temperature ($T_r$) which suggests that transformation initiated at $T_h$ has not continued at $T_r$. This concept receives added weight from an examination of the microstructures produced at $T_r$. If the transformation product formed at $T_h$ had continued its growth at $T_r$, then the microstructure should consist of platelets of the high temperature product more or less completely surrounded by low temperature bainite. The structure of 4340 obtained by treating 1 hr at 930°F followed by 3 min at 700°F is reproduced in Fig. 9. Although the low temperature product (dark platelets) does appear to nucleate in the vicinity of the high temperature bainite (light platelets), its principal direction of growth does not, in general, coincide with that of the high temperature plate. None of the low temperature product is visible around a majority of the high temperature plates. It appears that growth of the high temperature product does not take place at the lower temperature. New plates of low temperature bainite are formed both within the austenite and at the austenite/prior-bainite interface.

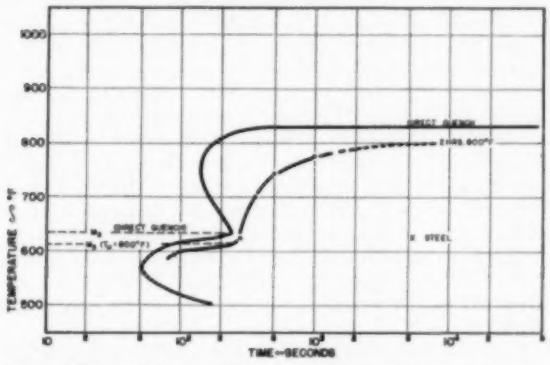


Fig. 8—Effect of 2 hr at 800°F on induction period at lower temperatures.

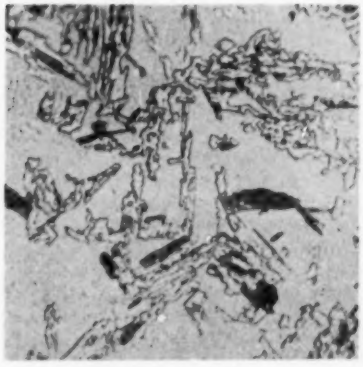

Fig. 9—Structure of 4340 steel produced by reaction for 1 hr at 930°F followed by 3 min at 700°F. Nital etch. X1200. Area reduced approximately 40 pct for reproduction.

*Effect of Time at the Holding Temperature ($T_h$):* In the above experiments, the time at $T_h$ (45 min) has been equal to or greater than that required for expiration of transformation. The results therefore are clouded by the fact that the amount of bainite formed at $T_h$ becomes greater as this temperature is lowered. In an attempt to separate the effects of holding time, holding temperature, and amount of bainite, specimens of 4340 were reacted for various times at $T_h$ levels of 965°, 935°, and 900°F and then quenched to 800°F. The induction period at $T_r$ = 800°F is presented as a function of holding time at $T_h$ in Fig. 10. Analogous results have been obtained for other combinations of $T_h$ and $T_r$.

The holding time at $T_h$ exerts a potent influence on the behavior at $T_r$. Short holding times may reduce slightly the induction period at $T_r$; however, in no case has it been eliminated. Therefore, the reaction initiated at $T_h$ does not continue at $T_r$ even when transformation is still in progress at the instant of quenching. This is substantiated by the structure produced in 4340 by reaction for 2 min at 940°F followed by 50 sec at 660°F. This structure is illustrated in Fig. 11.

Since holding for a short time at $T_h$ reduces the induction period at $T_r$ to something less than its normal value, it would appear that the reaction at $T_r$ has been accelerated by the prior treatment. This, however, is more apparent than real. On the basis of total reaction time, the mere fact that a new induction period is required indicates that the reaction, in reality, has been retarded by the prior treatment. This retardation of reaction at $T_r$ becomes more pronounced as the holding time at $T_h$ is prolonged. The induction period at the second temperature ($T_r$) exceeds its normal value when reaction at the holding temperature ($T_h$) has proceeded to an appreciable extent. The arrows in Fig. 10 designate the time at which the rapid reaction at

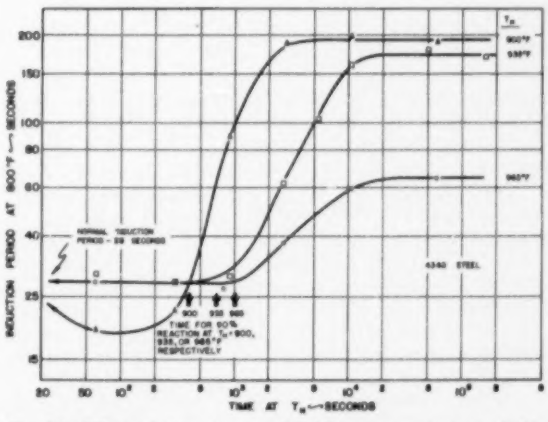


Fig. 10—Effect of time at several holding temperatures on induction period at 800°F.

Fig. 11—Structure of 4340 steel produced by reaction for 2 min at 940°F followed by 50 sec at 660°F. Nital etch. X800. Area reduced approximately 30 pct for reproduction.

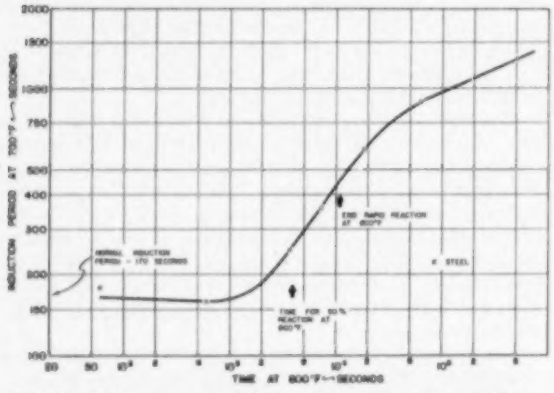

Fig. 12—Effect of time at 800°F on induction period at 700°F.

$T_h$ attains 90 pct of its total. It may be noted that only the last 10 pct* of the reaction at $T_h$ results in significant retardation at lower temperatures. Indeed, the phenomenon producing retardation continues even in the absence of detectable transformation. Fig. 12 demonstrates that the K steel responds to variation of the holding time in much the same manner as 4340. The major retardation again is associated with holding periods near the end of reaction at $T_h$.

* 10 pct of the transformable amount and not 10 pct reaction product.

By analogy with the stabilization process associated with the martensite transformation,[11] it might be anticipated that the amount of retardation would approach a limiting value as the holding time at $T_h$ is extended. The maximum amount of retardation should increase as $T_h$ is lowered. Fig. 10 indicates that this is true for 4340 although the limiting value of the induction period is not much greater after treatment at $T_h = 900°F$ than it is at $T_h = 935°F$. In the K steel, the induction period at 700°F continues to increase after prior treatment for five days at 800°F. Evidently, a time longer than five days is required to achieve the limiting state in this steel.

*Relative Influence of $T_h$ and Percentage of Bainite:* Fig. 10 demonstrates that the maximum amount of retardation at a given reaction temperature ($T_r$) increases as the holding temperature ($T_h$) is lowered. Since the amount of bainite at the end of transformation also increases as $T_h$ is lowered, the relative effect of holding temperature and percentage of bainite on retardation is not apparent. On the other hand, it is evident that the retardation process cannot be attributed solely to the amount of transformation at $T_h$. Thus, 18 pct bainite formed by holding for 45 min at 950°F lengthens the induction period at 800°F from 28 to 50 sec. The same amount of bainite formed by holding for 2 min at 900°F shortens the induction period at 800°F from 28 to 18 sec. Since major retardations are associated only with the last few percent of transformation at $T_h$, regardless of the actual level of transformation, the retardation phenomenon may result from the same process which produces the incomplete nature of the bainite reaction.

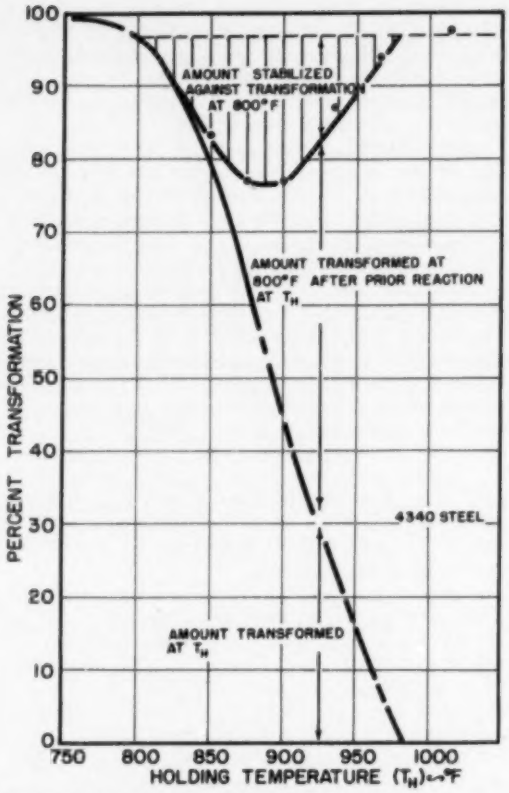
AMOUNT STABILIZED AGAINST TRANSFORMATION AT 800°F
AMOUNT TRANSFORMED AT 800°F AFTER PRIOR REACTION AT $T_H$
4340 STEEL
AMOUNT TRANSFORMED AT $T_H$
PERCENT TRANSFORMATION
HOLDING TEMPERATURE ($T_H$)—°F

Fig. 13—Stabilization of austenite at 800°F produced by reaction for 45 min at various $T_h$ levels.

In addition to a general retardation of reaction rate, Figs. 7 and 8 reveal that prior transformation at $T_h$ also causes a lowering of $M_s$. The similarity between the effects of holding in the bainite and in the martensite[11] ranges on $M_s$ is striking, and as in the latter case, depression of $M_s$ by prior transformation signifies the operation of a stabilization process.

*Stabilization of the Austenite-Bainite Reaction:* It has been indicated that partial reaction at $T_h$ does not eliminate the incomplete nature of the bainite reaction but actually decreases the amount of bainite attainable under certain circumstances. This stabilization of the bainite transformation has been studied by the lineal-analysis technique.[10] The effect of 45 min at several holding temperatures on the total extent of reaction after subsequent treatment at 800°F is illustrated in Fig. 13. A decomposition of 97 pct is obtained by direct reaction at this temperature. As an illustration of the interpretation of

this figure, consider reaction at $T_a$ = 925°F. It is observed that 31 pct austenite is transformed to bainite at $T_a$ and that an additional 52 pct transforms during subsequent reaction at 800°F. Prior transformation at 925°F thus has reduced the total transformation from 97 to 83 pct. The cross-hatched region in Fig. 13 thus represents the amount of austenite stabilized against reaction at 800°F.

The amount of stabilized austenite increases as $T_a$ is lowered below 985°F, passes through a maximum, and decreases again as the holding temperature approaches the reaction temperature. This characteristic of stabilization of the bainite reaction is, therefore, very similar to the corresponding characteristic of the martensite transformation.[21] In the latter case, the maximum amount of stabilization occurs at that temperature at which all of the austenite not transformed at $T_a$ is stabilized against reaction at $T_r$. This is not the situation in the stabilization process associated with the transformation of austenite to bainite.

Transformation at one temperature will affect the course of the *B-T* curve at lower temperatures. The effect of transformation for 45 min at 935°F on the shape of the *B-T* curve is depicted in Fig. 14. The stabilization treatment has reduced the total amount of decomposition for all reaction temperatures between 935° and 750°F; however, the $B_f$ temperature was unaffected by the stabilization treatment. Stabilization at holding temperatures of 900° and 965°F was also without effect upon the $B_f$ temperature. In fact, no thermal treatment capable of displacing this temperature has been found.* This insensitivity of $B_f$ to prior treatment represents a distinct difference between the characteristics of stabilization of the bainite and martensite reactions. Once again, another point of departure in the behavior of bainite and martensite is observed.

* A treatment capable of raising this temperature would afford considerable advantage in commercial heat-treating practice.

The amount of austenite stabilized at $T_r$ will also depend upon the holding time at $T_a$. The upper part of Fig. 15 illustrates the effect of holding time at 935°F on the total amount of transformation after reaction at 800°F. There is very little change in the total amount of transformation until the time of interruption at 935°F exceeds 500 to 600 sec. The reaction curve at 935°F, presented in the lower part of Fig. 15, demonstrates that the bainite reaction has proceeded to within 90 pct of the total during this time, so that it is again the last few percentages of the bainite reaction at $T_a$ which are most effective in producing stabilization at $T_r$. Although the amount of stabilized austenite appears to reach a plateau value after approximately 2500 sec, initiation of the pearlite reaction re-establishes the stabilization process.

*Practical Significance of the Retardation Phenomenon:* The retardation of the bainite reaction resulting from partial decomposition at high temperatures in the bainite range suggests that it may be possible to increase appreciably the hardenability of these and similar steels with only a slight sacrifice in maximum hardness. Troiano[24] has conducted end-quench tests employing prior retardation treatments on a steel intermediate in analysis between that of the 4340 and K steels of the present investigation. Hardenability test bars were quenched in salt for 20 min at 935° and 950°F, respectively, prior to the normal end-quench test. Fig. 16 illustrates the effect of the prior retardation treatment on the hardenability characteristics. Transformation at the holding temperature (935° or 950°F) has reduced slightly the hardness at the water-quenched end of the bar. The sample treated at 935°F exhibited a lower hardness than the one treated at 950°F because of the larger amount of bainite formed at the lower temperature. Although the maximum hardness has been reduced, the position along the bar at which the hardness deviates from this value has been increased considerably. In fact, the specimen held at 935°F essentially retained its maximum hardness along the entire length of the end-quenched bar. It is clear that an appreciable improvement in hardenability has resulted from each of these interrupted quenching treatments.

The difference in behavior between the tests conducted at 950° and 935°F is in qualitative agreement

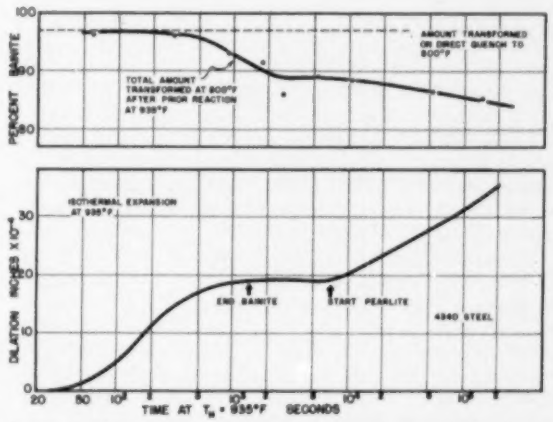
PERCENT BAINITE
AMOUNT TRANSFORMED ON DIRECT QUENCH TO 800°F
TOTAL AMOUNT TRANSFORMED AT 800°F AFTER PRIOR REACTION AT 935°F
ISOTHERMAL EXPANSION AT 935°F
DILATION INCHES X 10⁻⁴
END BAINITE
START PEARLITE
4340 STEEL
TIME AT $T_a$ = 935°F SECONDS

Fig. 15—Effect of time at 935°F on amount of austenite transformed at 800°F.

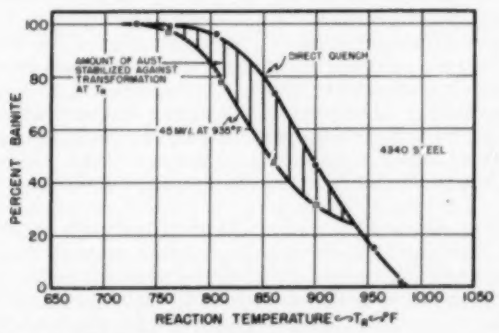
PERCENT BAINITE
AMOUNT OF AUST. STABILIZED AGAINST TRANSFORMATION AT $T_a$
DIRECT QUENCH
45 MIN. AT 935°F
4340 STEEL
REACTION TEMPERATURE ⟷ $T_a$ ⟷ °F

Fig. 14—Effect of reaction temperature ($T_r$) on amount of austenite stabilized by 45 min at $T_a$ = 935°F.

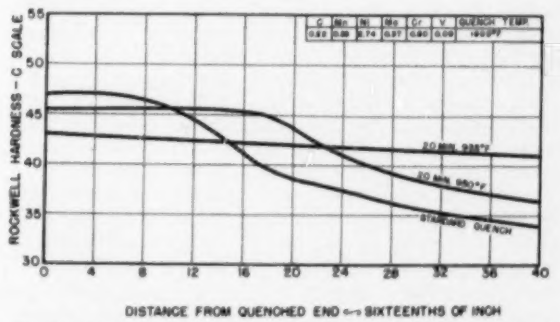
ROCKWELL HARDNESS - C SCALE
C | Mn | Ni | Mo | Cr | V | QUENCH TEMP
0.62 | 0.69 | 3.74 | 0.27 | 0.80 | 0.09 | 1550°F
20 MIN. 935°F
20 MIN. 950°F
STANDARD QUENCH
DISTANCE FROM QUENCHED END ⟷ SIXTEENTHS OF INCH

Fig. 16—Influence of prior transformation on the end-quench hardenability response. From patent application dated Nov. 1, 1947.

with the retardation picture developed previously. Fig. 10 demonstrates that, for constant holding time, the retardation becomes greater as the holding temperature is lowered. This is revealed in Fig. 16 by the fact that the specimen treated at 935°F did not decrease appreciably in hardness along the entire length of the bar, whereas the specimen held at 950°F did exhibit some loss in hardness away from the quenched end.

This retardation phenomenon may have even more far reaching significance in explaining the hardenability response of medium carbon alloy steels. In general, appropriate alloy combinations produce a significant reduction in the rate of the reactions which occur in the pearlite range, whereas their effect on the rate of the bainite reaction is considerably less. In spite of the short induction period for the isothermal bainite reaction, such steels frequently exhibit excellent hardenability in the end-quench test. Apparently, some stabilization of the bainite transformation occurs during continuous cooling through the bainite range.

### Rationalization of Reaction Kinetics

*The Isothermal Reaction:* The major kinetic features of the bainite reaction have not been adequately explained by any of the existing hypotheses for the reaction mechanism. It now seems certain that a nucleation and limited-growth process is involved.[17] Unlike other nucleation and growth processes, the amount of austenite consumed by the bainite reaction is a function of the transformation temperature. This signifies that both nucleation and growth of the transformation product stop prior to the disappearance of all austenite.

Morphological studies indicate that bainite forms as plates (probably coherent with austenite) in which the lateral growth is much more rapid and extensive than the growth in thickness. The growth of a bainite plate may be limited by loss of coherency resulting from excessive matrix and precipitate strains or by impingement with grain boundaries, inclusions, or other plates. This limitation on the growth of bainite plates signifies that each nucleus transforms only a small fraction of the available austenite before its growth is terminated.

Two conditions may be visualized which could interrupt the nucleation process: 1—Compositional changes in the austenite may lower the free-energy change associated with the transformation, so that a quasi-equilibrium state is attained. 2—Nuclei may appear only at certain high energy regions in the austenite. Once these have been consumed, transformation would virtually cease in the absence of growth.

The currently available experimental evidence points to the fact that no gross compositional changes accompany the transformation. Therefore, the former supposition must be discarded. Although a formal treatment is not yet possible, the concept involving nucleation from a limited number of high energy regions appears to offer the greatest promise of providing a means for rationalizing the kinetic characteristics of the bainite reaction.

Although the concept of homogeneous nucleation requires that nuclei form at random throughout a parent phase, a variety of theoretical and experimental evidence indicates that they actually appear at certain preferred locations.[18] Such nucleation has been termed "heterogeneous."[19] These nucleation sites may be grain boundaries, inclusions, embryos retained from the austenitizing treatment, or other crystal imperfections. Statistical fluctuations which occur at the austenitizing temperature create two types of regions capable of functioning as embryos for the bainite reaction. They may be low carbon regions with an austenitic structure or they may be regions with a ferritic structure. In the former case, the low carbon austenitic region may actually become ferritic on quenching to the reaction temperature. For the present purpose, the embryos will be viewed as regions with the ferritic structure and a carbon and alloy content which corresponds to the average composition of the austenite. The number of regions of a specific size is restricted to a distribution inherited from the austenitizing treatment. These embryos, which are retained at the transformation temperature, are initially subcritical in size and consequently will not become larger until there is an appropriate modification in their composition. This implies that the activation of embryos solely by configurational fluctuations does not occur at a detectable rate.

The activation of a particular embryo is accomplished by a process which lowers the critical size to that of the embryo. As illustrated schematically in Fig. 17, the critical size of a ferritic region becomes smaller (at constant temperature) as its carbon content is reduced. In this figure, the original composition of the embryo is represented by $C$ and the size of the region by $R$. At temperature $T_2$, this region is subcritical so that stable growth cannot occur. When the carbon content has been reduced to $C_1$, the critical size corresponds to that of the embryo and stable growth becomes possible. It is suggested that the reduction of carbon content required for activation of the embryo is accomplished by precipitation of carbide particles within the ferrite. Since the bainite plate must advance into austenite of average carbon content, its growth rate is controlled by diffusion of carbon from the surrounding austenite to the carbide particles precipitated within the ferritic phase.

As illustrated in Fig. 17, the critical size for a given carbon content increases as the transformation temperature is raised. If $R$ represents the largest embryo retained from the austenitizing treatment, bainite will not form at temperature $T_3$. The $B_s$ temperature thus represents that temperature above which the largest embryo retained from the austenitizing treatment is smaller than the critical size for carbon-free ferrite.

The course of the $B$-$T$ curve also can be visualized in terms of this model. At a given reaction temperature ($T_2$ in Fig. 17, for example), only those embryos will be activated which are larger than the critical size for carbon-free ferrite. This would include embryos in the size range $R$ to $R_1$. Once these have been activated, nucleation would stop. The transformation product associated with all of the activated embryos provides the rapid, incomplete reaction at temperature $T_2$. At a lower reaction temperature, $T_1$, the minimum embryo size capable of activation decreases to $R_1$. Activation of these smaller nuclei increases the extent of decomposition which is in qualitative agreement with experimental observations.

*The Retarded Reaction:* Qualitatively, the ability of partial transformation at one temperature to retard transformation at a lower temperature is also consistent with the embryo size-concentration model of the reaction mechanism. When some transformation takes place at a high temperature in the bainite range, the embryo distribution upon

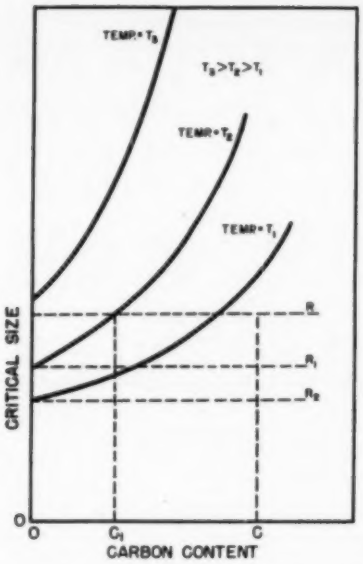


Fig. 17—Schematic illustration of the variation of critical size as a function of carbon content at several isotherms.

quenching to some lower temperature is different from that which exists after a direct quench. Transformation at the higher temperature has removed the larger embryos retained from the austenitizing temperature; however, others have been prepared for activation by precipitation of the carbide phase. In the early stages of reaction at $T_h$, this preparation process plays the controlling role. When the specimen is quenched to a lower temperature, the transformation initiated at $T_h$ is arrested, and further transformation at $T_r$ will require a new induction period. To be sure, this induction period actually is somewhat shorter than it would have been in the absence of the treatment at $T_h$ because of the preparation process which occurred at $T_h$.

As transformation at $T_h$ approaches the end of the rapid reaction, embryos larger than the minimum capable of activation at this temperature are rapidly consumed. Retardation of transformation at $T_r$, therefore, becomes more pronounced (see Figs. 10 and 12). The fact that the amount of retardation at $T_r$ (for a constant time at $T_h$) becomes less as $T_r$ is lowered (Figs. 7 and 8) may be attributed to the decrease in critical size at $T_r$ as this temperature is lowered.

Although this size-concentration model is able to explain the retardation behavior described above, it provides no clue as to why the retardation treatment should lower the total extent of decomposition at the second reaction temperature, that is, the observed stabilization of the bainite transformation. Unless the total number of embryos activated in the stepped quenching treatment is different from the number activated during direct reaction at $T_r$, it would appear that prior transformation should not affect the total amount of decomposition. Therefore it seems likely that some process is operative as a result of the treatment at $T_h$ which effectively reduces the total number of embryos capable of activation at $T_r$. This process undoubtedly is closely allied to the process which produces stabilization of the austenite to martensite transformation.

## Summary and Conclusions

Reaction at a low temperature in the bainite range may be retarded by partial transformation at a higher temperature. This retardation process can be characterized by the influence of prior transformation on the induction period at the lower temperature.

1—After partial reaction at a high temperature in the bainite range, a new induction period precedes transformation at the lower temperature.

2—Short times at the holding temperature will shorten the normal induction period at the reaction temperature.

3—As reaction at the holding temperature approaches the end, the induction period at the lower temperature becomes longer.

4—This retardation at the lower temperature continues even after transformation at the holding temperature has stopped.

5—For a specific treatment (holding time and temperature), the amount of retardation becomes less as the reaction temperature is lowered.

6—At a fixed reaction temperature, greater retardation is associated with lower values of the holding temperature.

The retardation phenomenon observed in these stepped quenching experiments is revealed in the end-quenched test as an appreciable increase in hardenability. This increase can be achieved with only a slight sacrifice in maximum hardness of the heat-treated steel.

Partial transformation at a high temperature in the bainite range does not eliminate the characteristic inability of the bainite reaction to consume all the austenite. In fact, the extent of austenite decomposition at the lower temperature can be reduced from its normal value by the high temperature treatment. This suggests that a stabilization process similar to that observed in the austenite-martensite reaction is also operative in the bainite range. The completion ($B_f$) temperature is essentially unaffected by the prior transformation.

## References


[1] T. Lyman and A. R. Troiano: Isothermal Transformation of Austenite in One Percent Carbon, High-Chromium Steels. *Trans.* AIME (1945) **162**, p. 196.

[2] T. Lyman and A. R. Troiano: Influence of Carbon Content Upon the Transformation in 3 Percent Chromium Steels. *Trans.* ASM (1946) **37**, p. 402.

[3] R. A. Flinn, E. Cook, and J. A. Fellows: Quantitative Study of Austenite Transformation. *Trans.* ASM (1943) **31**, p. 41.

[4] W. T. Griffiths, L. B. Pfeil, and N. P. Allen: The Intermediate Transformation in Alloy Steels. *Second Report.* Alloy Steels Research Committee, Iron and Steel Institute (1939) p. 343.

[5] E. P. Klier and T. Lyman: The Bainite Reaction in Hypoeutectoid Steels. *Trans.* AIME (1944) **158**, p. 394.

[6] J. P. Sheehan, C. A. Julien, and A. R. Troiano: The Transformation Characteristics of Ten Selected Nickel Steels. *Trans.* ASM (1949) **41**, p. 1165.

[7] A. R. Troiano and J. E. DeMoss: Transformations in Krupp-Type Carburizing Steels. *Trans.* ASM (1947) **39**, p. 788.

[8] A. Hultgren: *Jernkontorets Annaler* (1951) **135**, p. 403.

[9] A. Hultgren: Isothermal Transformation of Austenite. *Trans.* ASM (1947) **39**, p. 915.

[10] F. Wever, A. Rose, and W. Peter: On the Transformation Behavior and Tempering Stability of Steel with Special Carbide-Forming Alloying Elements, Represented in an Example of a Vanadium Steel. *Arch. Eisenhuttenwesen* (1950) **21**, p. 367.

[11] R. I. Entin: On the Intermediate Transformation of Austenite. *Doklady Akademii Nauk SSSR* (1951) **79**, p. 973.

[12] F. Wever et al.: A series of papers in *Mitteilungen.* Kaiser-Wilhelm-Institut Eisenforschung (1930 to 1940).

Summarized by F. Wever: On Transformation Kinetics. *Stahl und Eisen* (1949) **69**, p. 664.

[13] C. Zener: Kinetics of the Decomposition of Austenite. *Trans.* AIME (1946) **167**, p. 550; METALS TECHNOLOGY (January 1946).

[14] W. Jellinghaus: Stimulation of the Bainite Transformation in Steels by Small Amounts of α-Iron. *Arch. Eisenhuttenwesen* (1952) **12**, p. 459.

[15] A. B. Greninger and A. R. Troiano: Crystallography of Austenite Decomposition. *Trans.* AIME (1940) **140**, p. 307.

[16] A. Rose and W. Peter: *Stahl und Eisen* (1952) **72**, p. 1063.

[17] J. A. Cameron: Application of the Isothermal Transformation Diagram to the Normalizing of EN 40C Steel. *Journal* Iron and Steel Institute (1952) **170**, p. 313.

[18] L. M. Pevzner, G. M. Rovenski, and T. D. Kubyshkina: Redistribution of Carbon During Transformation in Bainite Range. *Doklady Akademii Nauk SSSR* (1952) **85**, p. 811.

[19] A. R. Troiano: Discussion of ref. 13.

[20] A. B. Greninger and A. R. Troiano: The Martensite Transformation. *Metals Handbook* (1948) p. 263. Cleveland. ASM.

[21] W. J. Harris, Jr. and M. Cohen: Stabilization of the Austenite-Martensite Transformation. *Trans.* AIME (1949) **185**, p. 447; JOURNAL OF METALS (August 1949).

[22] E. S. Machlin and M. Cohen: Isothermal Mode of the Martensite Transformation. *Trans.* AIME (1952) **194**, p. 489; JOURNAL OF METALS (May 1952).

[23] R. T. Howard and M. Cohen: Quantitative Metallography by Point-Counting and Lineal Analysis. *Trans.* AIME (1947) **172**, p. 413; METALS TECHNOLOGY (August 1947).

[24] A. R. Troiano: Unpublished research.

[25] M. Avrami: Kinetics of Phase Change, I. *Journal of Chemical Physics* (1939) **7**, p. 1103.

[26] D. Turnbull: Kinetics of Heterogeneous Nucleation. *Journal of Chemical Physics* (1950) **18**, p. 198.

[27] T. Ko and S. A. Cottrell: The Formation of Bainite. *Journal* Iron & Steel Institute (1952) **172**, p. 307.

---

**Technical Note**

# Data for One of the Martensitic Transformations in An 11 Pct Mo-Ti Alloy

by S. Weinig and E. S. Machlin

THE mechanism of the martensitic transformation has been the subject of a remarkable number of papers in recent years.[1] Because the task of evaluating all the available theories is a formidable one, the authors will confine themselves merely to the presentation of results of an experimental investigation of the habit orientation, lattice relations, magnitude and direction of average transformation shear strain, and orientation of subband markings for a single variant of the possible habit systems in an 11 pct Mo-Ti alloy. It is hoped that these data will assist in the establishment of a rigorous theory for the mechanism of the martensitic transformation.

## Experimental Procedure

*Specimen Preparation:* A sample, approximately ½ x ¼ x ¼ in., was cut from a double arc-melted ingot composed of commercial-process A titanium and high purity molybdenum (nominally, 11 pct Mo). It was capsuled in evacuated Vycor at $10^{-5}$ mm Hg subsequent to a double argon wash and homogenized for 48 hr at 1100°C. After a direct quench into $H_2O$ at room temperature, a large-grained specimen resulted, which, by X-ray diffraction and metallographic means, was subsequently shown to be in the body-centered-cubic phase, β. Two adjacent, approximately perpendicular faces were polished and the ends of the specimen were ground parallel in a *V*-block. Fiducial lines were inscribed at 45° to the common edge of the polished surfaces in order that they would be perpendicular to the habit traces of the subsequently formed α′ plates.[2] The specimen was then compressed between the ground ends in a Buehler press to stress induce the transformation β to α′.

*Experimental Measurements:* The habit-plane orientation, the orientation of subband markings, the orientation relation between the parent β and the product α′, and the transformation strain for the same plate were determined. To further establish the nature of the subbands, one surface was repolished and etched. The bands in the α′ were still visible and were found to be optically anisotropic under polarized light.

Back-reflection Laue patterns were obtained from the β matrix and from a region comprising both α′ plates and adjacent β matrix (a Cu target was used). By superposition of the two X-ray diffraction patterns, it was possible to obtain a tentative orientation relationship between the two phases. This result was confirmed by a pattern taken after the specimen was rotated to make the basal-plane pole of the hexagonal α′ phase strike the film. This necessitated cutting the specimen to expose the α′ plate in the new position relative to the X-ray beam.

## Analysis of Experimental Measurements

On the basis of the aforementioned X-ray patterns, the orientation between parent and product

Table I. Summary of Experimental Results

| Mode of Formation | Compression |
|---|---|
| Habit plane | 4° from (8, 9, 12) β |
| Crystallographic orientation | 4° from $(\bar{3}44)$ β<br>[111] β // [11.0] α′<br>$(10\bar{1})$ β // (00.1) α′ |
| Average transformation shear strain | 0.28 ± 0.05 |
| Direction of shear strain<br>Indices of subbands | Within 10° of $(14\bar{7})$ β<br>(01.2) α′ |

S. WEINIG, Student Associate AIME, and E. S. MACHLIN, Member AIME, are Graduate Student and Assistant Professor of Metallurgy, respectively, School of Mines, Columbia University, New York.

TN 232E. Manuscript, June 23, 1954.

Table II. Lattice-Parameter Data for 11 Pct Mo-Ti*

| | $\alpha'$ | $\beta$ |
|---|---|---|
| | | $a = 3.262$ |
| First martensite: {334} | $c = 4.65$<br>$a = 2.99$ | |
| Second martensite: {344} | $c = 4.40$<br>$a = 2.96$ | |

* Data compiled from ref. 3 and authors' measurements extrapolated to the 11 pct Mo level.

phase was determined to be:

$$(10\bar{1})\ \beta\ //\ (00.1)\ \alpha'$$
$$[111]\ \beta\ //\ [11.0]\ \alpha'.$$

A two-surface analysis of the habit plane and subinterfaces was made with the appropriate corrections for the included angle between polished reference surfaces. These results were referred stereographically to the $\beta$ and $\alpha'$ matrix to yield a habit plane 4° from $(\bar{3}44)$ $\beta$ and corresponding subinterfaces along (01.2) $\alpha'$.

The average transformation strain was obtained by analysis of the angular shifts of two fiducial lines normal to the habit-plane traces on the two reference surfaces. In this analysis, because the volume change associated with the phase transformation ($\beta$—$\alpha'$) is too small to be measured, the average strain was assumed to be a homogeneous shear and the shear plane was assumed to be the habit plane. The resultant magnitude of this average strain is a homogeneous shear equal to $0.28 \pm 0.05$. The direction of this shear was determined by a stereographic plot relative to the $\beta$ matrix. It was found to be within 10° of $(14\bar{7})$ $\beta$. All experimental results are plotted stereographically relative to the $\beta$ and $\alpha'$ matrix in Fig. 1 and are summarized in Table I. An example of the subband markings is presented in Fig. 2. As mentioned previously, these subbands reappear after polishing and etching and are optically anisotropic under polarized light. Because the subband interfaces are parallel to the $\alpha'$ twin interface (01.2), it has been concluded that these subbands are $\alpha'$ twins.

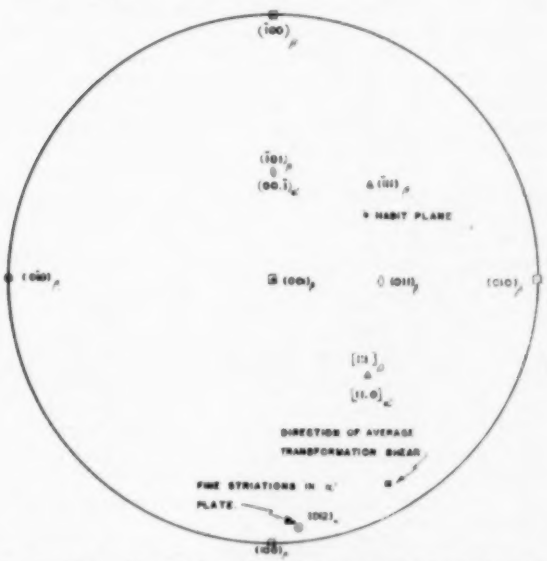


Fig. 1—Martensitic-transformation relations of a single $\alpha'$ plate in a $\beta$ matrix. 11 Pct Mo-Ti alloy.

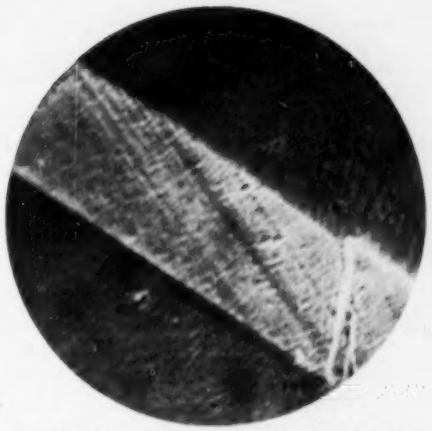

Fig. 2—Twin markings in an $\alpha'$ plate formed in compression. Etched in 2 parts HF (48 pct), 2 parts glycerine, and 1 part $HNO_3$. Polaroid light. X1400.

To facilitate theoretical use of this data, the authors have included in Table II lattice-parameter data compiled from ref. 3 and their own measurements extrapolated to the 11 pct Mo level.

## Discussion of Results

Two systems of habit planes have been found in titanium-base alloys, namely, {334} and {344}.[4] Although the authors have not examined the {334} type habit experimentally, they have investigated them theoretically. It appears that the {334} habit can be predicted by a number of the theories because the transformation matrix, which involves the smallest possible homogeneous strain (the motion of alternate dodecahedral planes is neglected in this matrix), has an invariant plane, the {334} plane. The matrix in question relates the transformation of coordinates from the orthogonal axes $[10\bar{1}]$, [101], and $[0\bar{1}0]$ of the cubic lattice to the orthogonal axes [001], [120], and $[\bar{1}00]$ of the hexagonal lattice, respectively, and is:

$$\begin{bmatrix} 1.00 & 0 & 0 \\ 0 & 1.12 & 0 \\ 0 & 0 & 0.915 \end{bmatrix}.$$

The lattice parameters corresponding to the $\alpha'$ having the {334} habit were used to calculate this matrix. The {344} type habit, however, is not obtained *simply* from any theory yet presented.


## Acknowledgment

The authors wish to thank Mr. G. Pincus for his valuable assistance. They wish to further acknowledge the financial support of the Watertown Arsenal, United States Army Ordnance Corps, under Contract DA-30-069-ORD-547.


## References


[1] J. S. Bowles and J. L. Mackenzie: The Crystallography of Martensite Transformations I, II. *Acta Metallurgica* (1954) **2**, p. 129.

[2] E. S. Machlin and S. Weinig: Le Chatelier's Principle and Stress-Induced Displacive Transformations. *Acta Metallurgica* (1953) **1**, p. 480.

[3] R. R. Elliott and W. Rostoker: Studies of Phase Relationships and Transformation Processes of Titanium Alloy Systems. *Progress Report No. 22* AF 33(038)-8708.

[4] Y. C. Liu and H. Margolin: *Trans.* AIME (1953) **197**, p. 529; JOURNAL OF METALS (April 1953).

# Mechanical Properties of Alpha Titanium as Affected By Structure and Composition

by R. I. Jaffee, F. C. Holden, and H. R. Ogden

**The effects of grain size and shape on alloys of titanium with nitrogen and aluminum have been determined. Increasing α grain size decreases strength and hardness and increases impact resistance. Quenching from the β field produces subgrain markings delineating α plates in Ti-N alloys but not in Ti-Al alloys. This suggests a precipitation from the high nitrogen alloys.**

ALPHA titanium alloys are single-phase alloys with the hexagonal-close-packed structure of α titanium. If these alloys are worked and annealed within the α field, equiaxed structures result in which strength is derived from the solid solution of the alloying elements present. Strain hardening can be used to increase further the strength of α titanium alloys. This is the only other mode of strengthening the α type of alloy.

Quenching from the β field has been noted by many investigators to have little effect on the strength of iodide titanium and on commercial titanium. Ti-Al alloys were found to be little different in hardness, whether annealed in the α field or quenched from the β field.[1] These facts illustrate a characteristic of α titanium alloys: they are insensitive to heat treatments from the β field. Underlying this heat-treatment insensitivity are the facts that the α-β field is generally narrow in α titanium alloys, the transformation-temperature range increases with α-stabilizing content, and the α solubilities of the alloying elements are greater than the β solubilities. When quenching is done from the β field, there is no supersaturation of the alloying elements in the acicular transformation structure produced. Welds in α titanium alloys generally are ductile, because no transformation hardening occurs during cooling.[1, 2] Other desirable features of α alloys are: no thermal-stability problem, excellent toughness, and retention of strength at elevated temperatures better than α-β or β alloys of comparable room-temperature strength.

The prime factors governing the properties of α titanium alloys are the amount and kind of solute present. This can change the α phase from a soft, tough material into a hard, brittle material with no apparent change in microstructure. Moreover, brittleness can exist over a wider alloy-content range, without change of phase, than in most other metals.

R. I. JAFFEE, F. C. HOLDEN, and H. R. OGDEN, Members AIME, are Chief, Principal Metallurgist, and Assistant Chief, respectively, Nonferrous Physical Metallurgy Div., Battelle Memorial Institute, Columbus, Ohio.

Discussion on this paper, TP 3858E, may be sent, 2 copies, to AIME by Jan. 1, 1955. Manuscript, Apr. 15, 1954. Chicago Meeting, November 1954.

The solutes for α titanium may be divided into interstitial and substitutional types. Oxygen and nitrogen dissolve interstitially in rather large amounts, extending well through the brittle range, and the transformation-temperature ranges are raised in the process.[3, 4] Carbon has a maximum interstitial solubility of about 0.5 pct at the peritectoid temperature, while at lower temperatures the solubility decreases to about 0.2 pct.[5, 6] Substitutional α solutes include aluminum and tin. Aluminum has a high α solubility of 25 pct Al, and increases the transformation-temperature range markedly.[6, 7] Tin has a high α solubility of about 20 pct, but has a relatively innocuous effect on the transformation-temperature range.[8]

The choice between interstitial and substitutional solutes generally has been conceded to the substitutional solutes because of a belief that they do not have as adverse an effect on ductility and notch toughness. However, a recent investigation[9] on the effect of hydrogen on titanium has shown that this element, which is not under compositional control, has a powerful detrimental effect on notch toughness. Hydrogen was shown to form a hydride which is practically insoluble (about 0.002 pct) in α titanium at room temperature, although the solubility at the eutectoid temperature of about 300°C is relatively high, about 0.16 pct. Limited data were presented on the effect of hydrogen on α alloys, where the same impairment of toughness as in unalloyed titanium is found.

The work reported here describes the effects of interstitial and substitutional solutes on 1—the mechanical properties of high purity titanium free of titanium hydride and 2—the influence of structural variables on these properties. Nitrogen was selected as an example of an interstitial solute with high solubility and aluminum as a substitutional solute with high solubility. All compositions were well within the ductile range, since it was not intended to study the brittleness problem here, but to study only the factors influencing optimum mechanical properties.

## Procedures

The alloys were prepared from iodide titanium as ½ lb ingots double melted to insure homogeneity.

The alloying additions were either 99.99+ pct Al or Ti-N master alloys containing 5 to 6 pct N prepared by arc melting iodide titanium in an argon-nitrogen atmosphere. Compositions prepared are listed in Table I. Generally, there was some loss of nitrogen, possibly caused by spattering, during arc melting, and 40 pct excess N was used in preparing TM-61. The analyzed value of 0.29 pct N, which was checked three times by Kjeldahl analysis, indicates that quantitative nitrogen recovery was secured in preparing this alloy. Three preliminary ingots, TM-10, TM-11, and TM-12, are also listed. These will be referred to primarily in discussion of microstructure.

The ingots were hot forged to ¾ in. rounds, and, to remove hydrogen, were vacuum annealed at 900°C for 5 to 16 hr, sufficient for a low final vacuum of less than $1 \times 10^{-4}$ mm Hg. The unalloyed bar was cold swaged to ½ in. round and annealed ½ hr at 850°C, then cold swaged to ¼ in. round. The $\alpha$ alloys were hot swaged to ¼ in. round at 750°C, except for TM-60 (5 pct Al) which was hot swaged at 850°C.

All heat treatments were conducted in argon-filled Vycor capsules. In quenching, the capsules were rapidly withdrawn from the furnace and broken under water.

Methods used for testing were described in a previous publication.[5] The tensile tests were made on ⅛ in. diam specimens with ½ in. gage length at a uniform strain rate of 0.005 in. per min throughout the test. Micro impact tests were made on subsize round Izod specimens broken as a cantilever in a Tinius Olsen testing machine. The impact values in in.-lb have been shown to correlate with Charpy ft-lb by multiplying the numerical values in in.-lb by a conversion factor of 0.8.

Approximate grain sizes were obtained by measuring the diameters of a series of representative adjacent grains with a calibrated micrometer eyepiece and averaging the values. The average grain diameters obtained are considered accurate to about 10 pct.

## Constitution and Microstructure

Metallographic preparation of the alloys involved polishing on wool laps with aluminum oxide. The surface was alternately polished and etched with 1½ pct HF—3½ pct $HNO_3$ until a clean scratch-free structure was obtained. It was imperative to examine and photograph the structures soon after final etching in order to avoid pickup of titanium hydride on the surface after standing for a few days. This surface-hydride effect is found with $\alpha$ titanium alloys and makes metallographic interpretation particularly troublesome.

Table I. Compositions of Experimental Alloys

| Alloy | Intended Composition | Analyzed Composition, Pct | | | | |
|---|---|---|---|---|---|---|
| | | C | O | N | H | Al |
| TM-31 | Unalloyed | 0.02 | 0.025 | — | 0.0010 | — |
| TM-45 | Ti-2.5 pct Al | 0.02 | 0.055 | 0.008 | 0.0015 | 2.55 |
| TM-60 | Ti-5 pct Al | 0.03 | 0.020 | 0.007 | 0.0030 | 5.12 |
| TM-62 | Ti-0.1 pct N | 0.02 | 0.028 | 0.070 | 0.0018 | — |
| TM-61 | Ti-0.2 pct N | 0.02 | 0.046 | 0.29 | 0.0028 | — |
| TM-10 | Ti-0.1 pct N | — | — | 0.064 | 0.0133 | — |
| TM-11 | Ti-0.2 pct N | — | — | 0.174 | 0.0127 | — |
| TM-12 | Ti-2.5 pct Al | — | — | — | 0.0129 | 2.55 |

*Equiaxed Structures:* There are two basic types of structures found with $\alpha$ titanium, equiaxed, and acicular. The equiaxed $\alpha$ structures are indistinguishable from each other, irrespective of the nature of the composition. Fig. 1 shows two such structures for unalloyed titanium and titanium with 0.29 pct N. Except for relative grain size, they could serve equally well for any of the all-$\alpha$ structures in this study. The mixed grain sizes apparent are typical of $\alpha$ titanium, as is the relatively slow rate of grain growth. Table II lists the ranges of equiaxed-$\alpha$ grain sizes covered for the various materials studied. A fifty times longer annealing treatment is required to increase the grain size of high purity titanium from 0.1 mm to 0.2 mm at 875°C, just below the transition temperature. Extensive annealing treatments similarly are required to increase the equiaxed-grain sizes of the $\alpha$ alloys. A fine grain size could not be produced in the Ti-0.07 pct N alloy, apparently because it has an initial grain size of about 0.05 mm in the hot-swaged condition.

*Transformation Structures:* In contrast to the fine $\alpha$ grain sizes, $\beta$ grains typically grow very coarse and result in coarse transformed-$\beta$ structures. The $\beta$ grain sizes for the Ti-Al alloys heat treated at 1000°C were considerably larger than those for the Ti-N alloys, indicating that their grain growth was much greater. The grain size of the $\alpha$-$\beta$ quenched alloys were relatively fine, about the same as for $\alpha$-annealed material. The presence of $\alpha$ is an effective grain-growth inhibitor for the $\beta$ grains.

A fundamental characteristic of $\alpha$ alloys is that the transformation from $\beta$ to $\alpha$ is complete despite the rapidity of the cooling rate employed. The microstructure developed in the transformed-$\beta$ structures of $\alpha$ titanium depends to a considerable

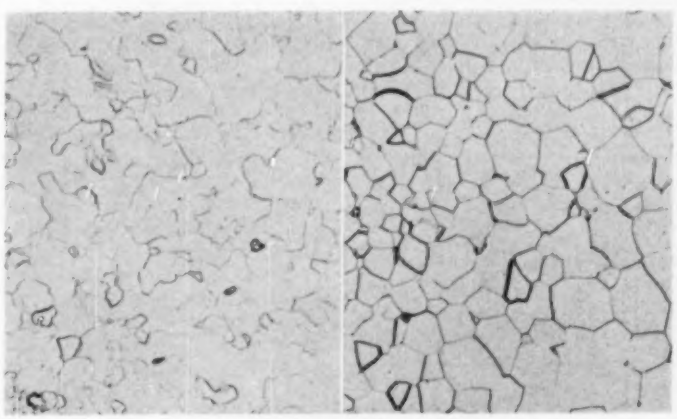

a — Titanium (TM-31) annealed for 2 hr at 875°C and quenched. X250. Area reduced approximately 20 pct for reproduction.

b—Ti-0.29 pct N alloy (TM-61) annealed for 1 hr at 750°C and quenched. X100. Area reduced approximately 20 pct for reproduction.

Fig. 1—Typical equiaxed-$\alpha$ structures.

a—Quenched from 1000°C.

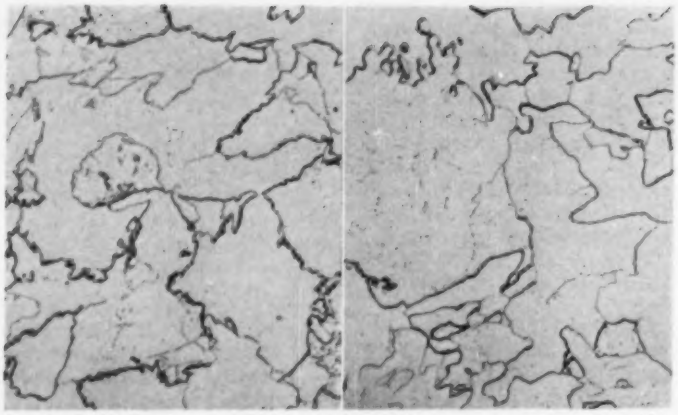

b — Furnace-cooled from 1000°C.

Fig. 2—Transformation structures of high purity hydrogen-free titanium. X100. Area reduced approximately 20 pct for reproduction.

extent on the alloy content and the cooling rate, as described in subsequent sections.

High purity hydrogen-free titanium, held in the $\beta$ field for 1 hr at 1000°C and quenched or furnace cooled, shows the serrated structures in Fig. 2. The $\alpha$ grain boundaries of the quenched material show a heavily serrated outline delineating the edges of $\alpha$ platelets formed from the $\beta$ phase during the quench. When the metal has been slowly cooled, sufficient grain-boundary movement takes place through diffusion processes so that the serrations become smoothed out. Some grains are only slightly different in orientation and their outlines, also serrated, may be seen faintly. The grains are made up of colonies of $\alpha$ platelets of like orientation transforming from the original $\beta$ grain. The serrated grain size is about 0.25 mm, but no reliable estimate could be made as to the original $\beta$ grain size.

Substitutional solutes of the type of aluminum cause some changes in the transformation structures compared to unalloyed titanium. The transformation ranges for the two Ti-Al alloys studied are shown in Fig. 3. It is difficult to distinguish the transformed $\beta$ from the equiaxed $\alpha$ in alloys quenched from the $\alpha$-$\beta$ field. Fig. 4a shows an $\alpha$-$\beta$ quenched structure for the Ti-2.55 pct Al alloy. The $\beta$ phase originally was present at the grain boundaries of the equiaxed-$\alpha$ grains. On quenching, the $\beta$ phase transformed to $\alpha$ phase without developing acicularity. The result is the indefinite structure shown. When the Ti-2.55 pct Al alloy is quenched from the $\beta$ field, the serrated-$\alpha$ structure shown in Fig. 4b is obtained. This is very similar to the equivalent

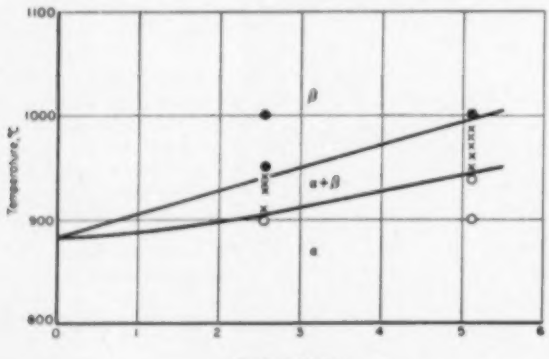


Fig. 3—Transformation range for high purity Ti-Al alloys studied.

structure for unalloyed titanium. Furnace cooling from the $\beta$ field produces the structure in Fig. 4c, made up of slightly serrated grain boundaries with the $\alpha$ platelets clearly shown as a subgrain structure.

The transformation ranges for the Ti-N alloys studied are shown in Fig. 5. The $\beta$ field was not bracketed for the Ti-0.29 pct N alloy, but as quenched from 1010°C, the structure was estimated to be over 95 pct $\beta$.

When the hydrogen-free Ti-N alloys are quenched from the $\beta$ field, the serrated $\alpha$ structure is obtained, but generally it is more interleaved and acicular than that for titanium and the Ti-Al alloys. Structures are shown for the Ti-0.07 pct N alloy in Fig. 6a and for the Ti-0.29 pct N alloy in Fig. 6b. Comparable structures for Ti-N alloys containing about 0.0125 pct H are shown in Figs. 6c and d. The structures are of the basket-weave type popularly associated with $\beta$-treated titanium. It is apparent that subgrain markings of titanium hydride between the $\alpha$ platelets are what accentuate the acicularity.

Table II. Equiaxed-$\alpha$ and Prior $\beta$ Grain Sizes in Ti, Ti-Al, and Ti-N Alloys

| Material | Initial Condition | Desired Grain Size | Annealing Treatment* Time, Hr | Annealing Treatment* Temperature, °C | Average Grain Size, Mm |
|---|---|---|---|---|---|
| Ti | Cold-swaged, 75 pct reduction in area | Fine $\alpha$ | 1 | 600 | 0.01 |
| | | Medium $\alpha$ | 1 | 800 | 0.06 |
| | | Coarse $\alpha$ | 2 | 875 | 0.10 |
| | | Very large $\alpha$ | 100 | 875 | 0.20 |
| | | $\beta$ quench | 1 | 1000 | — |
| | | $\beta$ furnace cool | 1 | 1000 | — |
| Ti-2.55 pct Al | 750°C, swaged | Fine $\alpha$ | 1 | 750 | 0.035 |
| | | Medium $\alpha$ | 1 | 900 | 0.07 |
| | | Coarse $\alpha$ | 16 | 900 | 0.16 |
| | | $\beta$ quench | 1 | 1000 | 0.6† |
| | | $\beta$ furnace cool | 1 | 1000 | 0.8† |
| Ti-5.12 pct Al | 850°C, swaged | Fine $\alpha$ | 1 | 750 | 0.02 |
| | | Medium $\alpha$ | 1 | 900 | 0.05 |
| | | Coarse $\alpha$ | 16 | 900 | 0.10 |
| | | $\beta$ quench | 1 | 1000 | 0.6† |
| | | $\beta$ furnace cool | 1 | 1000 | 1.0† |
| Ti-0.07 pct N | 750°C, swaged | Fine $\alpha$ | 1 | 750 | 0.05 |
| | | Medium $\alpha$ | 1 | 865 | 0.04 |
| | | Coarse $\alpha$ | 16 | 865 | 0.10 |
| | | $\beta$ quench | 1 | 960 | 0.35† |
| | | $\beta$ furnace cool | 1 | 960 | 0.35† |
| Ti-0.29 pct N | 750°C, swaged | Fine $\alpha$ | 1 | 600 | 0.035 |
| | | Medium $\alpha$ | 1 | 750 | 0.07 |
| | | Coarse $\alpha$ | 16 | 875 | 0.17 |
| | | $\beta$ quench | 1 | 1010 | 0.2† |
| | | $\beta$ furnace cool | 1 | 1010 | 0.2† |

* Quenched from temperature, except where noted.
† Prior $\beta$ grain size shown.

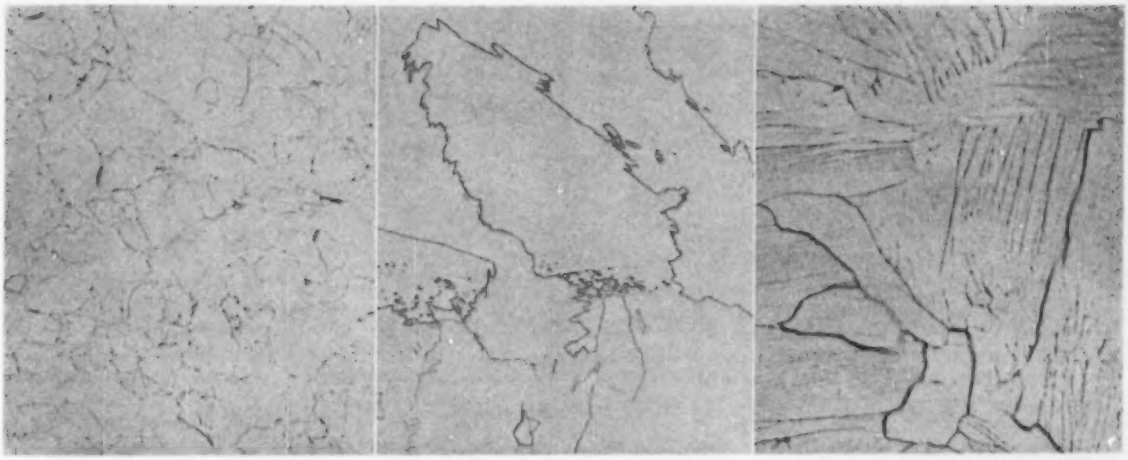

a—Quenched from $\alpha$-$\beta$ field at 935°C. b—Quenched from $\beta$ field at 1000°C. c—Furnace-cooled from $\beta$ field at 1000°C.

Fig. 4—Transformation structures for a high purity Ti-2.55 pct Al alloy. X250. Area reduced approximately 10 pct for reproduction.

The hydrogen-free material is seen to have much different structure.

Furnace cooling Ti-N alloys from the $\beta$ field produces a surprising result. The transformed $\beta$ grains become progressively more equiaxed as the nitrogen content increases. Also there is little or no subgrain structure developed. Fig. 7a shows a Ti-0.064 pct N alloy vacuum annealed to reduce the hydrogen content to 0.0014 pct, held 1 hr at 1000°C, and furnace-cooled. The structure is clear with a very slight serrated $\alpha$ plate structure. With a similarly treated Ti-0.174 pct N-0.0018 pct H alloy, the structure is shown in Fig. 7b and is practically equiaxed, except for a waviness of the grain boundaries. Also a curious mottling, suggestive of the original $\alpha$ platelets, may be discerned. Fig. 7c shows the Ti-0.174 pct N alloy, before vacuum annealing and containing 0.0127 pct H, as-furnace-cooled from 1000°C. The hydride has collected at the subgrain boundaries between the $\alpha$ platelets and at the grain boundaries. Fig. 7d shows the Ti-0.29 pct N alloy furnace-cooled from 1010°C. The grain structure is practically equiaxed and the mottled background is the subgrain structure of the original $\alpha$ platelets. This structure suggests recrystallization of the $\alpha$ platelets and grain refinement after $\beta$ heat treatment. It is the first case of titanium grain refinement by $\beta$ heat treatment to the authors' knowledge.

## Mechanical Properties

Data on hardness and tensile properties for unalloyed titanium are given in Table III, for the Ti-Al alloys in Table IV, and for the Ti-N alloys in Table V. The impact properties of these materials are presented in Figs. 8 to 10.

## Effect of Equiaxed-α Grain Size

Increased grain size was obtained by subjecting the materials to progressively more extensive annealing treatments. In the case of titanium and titanium alloys, this means that, as the grain size increases, the possibility for contamination also increases despite the care taken to avoid contamination by the use of Vycor encapsulation. Contamination would cause an effect on properties opposing that of grain size. This possibility must be kept in mind in a rigorous consideration of the data.

*Tensile Properties and Hardness:* Fig. 11 presents the tensile and hardness properties of the alloys plotted against average grain diameter.

Generally, ultimate strength decreases as the grain size increases. It will be noted that titanium and the Ti-2.55 pct Al alloy became somewhat stronger at the largest grain size. This is believed to be the result of slight contamination as a result of the extensive annealing treatment required to produce the large grain sizes.

The decreasing trend of yield strength with increasing grain size is the same as for ultimate strength.

Unalloyed titanium shows little or no effect of grain size on reduction of area. If anything, the percentage of reduction in area increases with increasing grain size. The alloys show the opposite effect. The decrease in reduction in area with grain size is particularly noted with the stronger alloys.

There is an increase in elongation in unalloyed titanium on going from fine to medium, or larger, grain size. The elongations of the alloys generally are insensitive to grain-size variations, except for the Ti-0.29 pct N alloy which has progressively lower elongations with increasing grain size.

Hardness generally follows the same trends as the strength values.

Taken as a whole, large grain size is definitely detrimental to the tensile properties of the $\alpha$ alloys because both strength and ductility tend to decrease with increasing grain size.

*Impact Properties:* Fig. 12 shows the micro impact values at −196°, −40°, 25°, and 150°C plotted for the various materials against average grain diameter. There is a beneficial effect of increasing grain size on unalloyed titanium and the substitutional

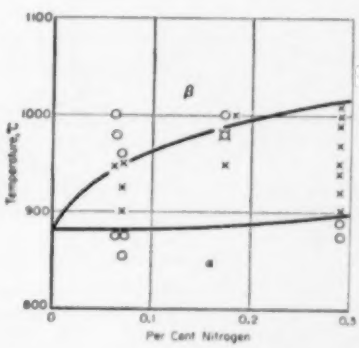


Fig. 5—Transformation range for high purity Ti-N alloys studied.

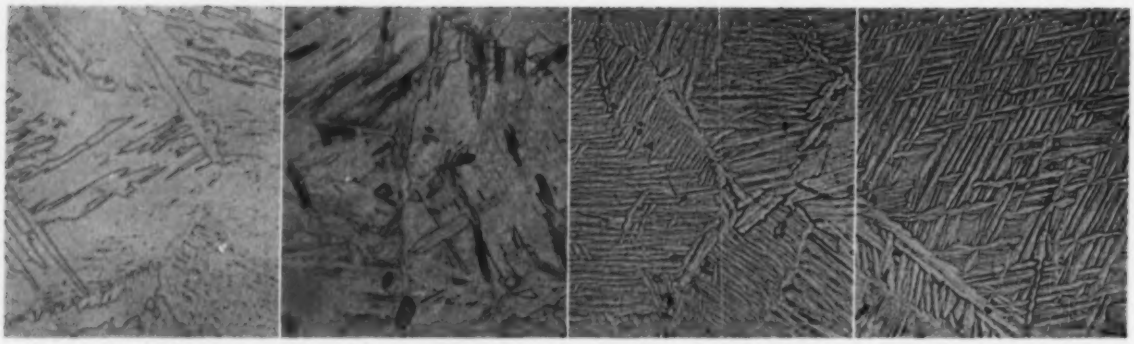

a—Ti-0.07 pct N-0.0018 pct H alloy quenched from 960°C. b—Ti-0.29 pct N-0.0028 pct H alloy quenched from 1010°C. c—Ti-0.064 pct N-0.0133 pct H alloy quenched from 1000°C. d—Ti-0.174 pct N-0.0127 pct H alloy quenched from 1000°C.

Fig. 6—$\beta$-quenched Ti-N alloys. X250. Area reduced approximately 33 pct for reproduction.

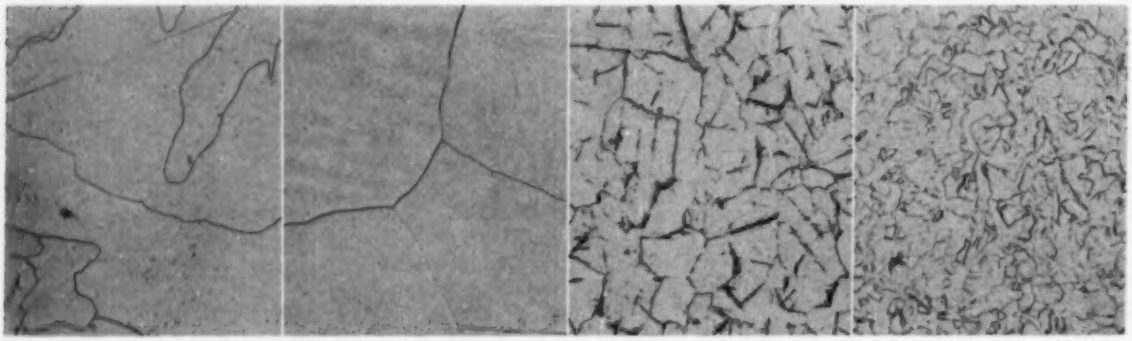

a—Ti-0.064 pct N-0.0014 pct H alloy furnace-cooled from 1000°C. b—Ti-0.174 pct N-0.0018 pct H alloy furnace-cooled from 1000°C. c—Ti-0.174 pct N-0.0127 pct H alloy furnace-cooled from 1000°C. d—Ti-0.29 pct N alloy furnace-cooled from 1010°C.

Fig. 7—Furnace-cooled Ti-N alloys. *a*, *b*, and *c* at X250. *d* at X100. Area reduced approximately 33 pct for reproduction.

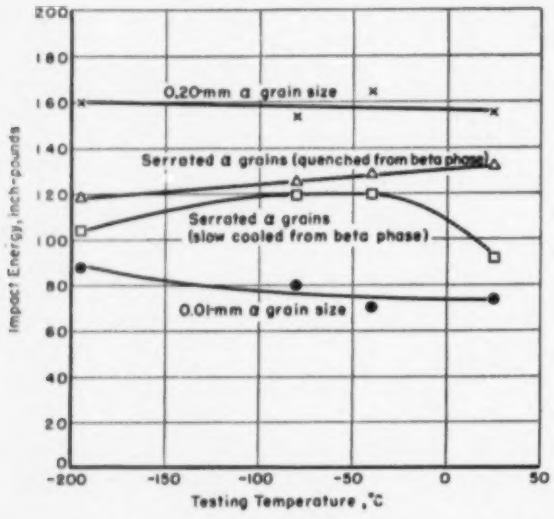


Fig. 8—Effect of temperature on the impact properties of high purity titanium in several conditions.

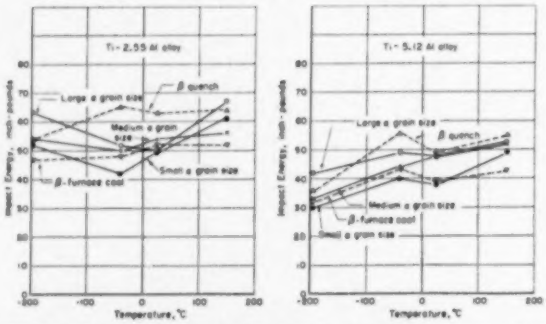


Fig. 9—Effect of testing temperature on the impact-energy values for high purity Ti-Al alloys in various microstructural conditions.

Ti-Al $\alpha$ alloys. The impact properties for the interstitial Ti-N alloys are insensitive to grain-size variations.

## Effect of $\alpha$-$\beta$ Transformation

Figs. 13 to 15 present the mechanical properties of the alloys in the four basic conditions: equiaxed $\alpha$, $\alpha$-$\beta$ quench, $\beta$ quench, and $\beta$ furnace-cool. The equiaxed-$\alpha$ condition is shown as the range of properties found from fine to large grain size.

Unalloyed titanium shows a distinct increase in yield strength over the equiaxed condition when quenched from the $\beta$ field. This increase most probably can be associated with the heavily serrated $\alpha$ structure in this condition. Furnace-cooled, the serrations are largely ironed out through diffusion, but there still is a slight increase to the yield strength in this condition over the equiaxed. Ultimate strength, hardness, elongation, and reduction in area are relatively unaffected by $\beta$ heat treatments. Toughness in the $\beta$-furnace-cooled condition is lower than in the $\beta$-quenched condition, but both conditions are within the range of toughness spanned by the range of equiaxed-$\alpha$ grain sizes.

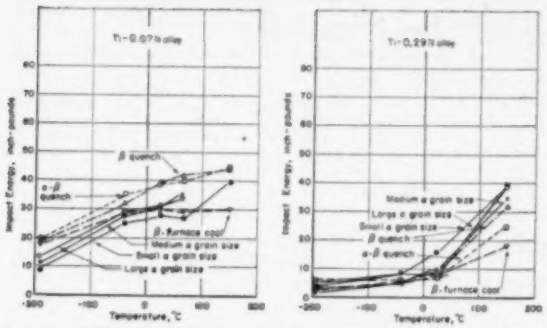


Fig. 10—Effect of testing temperature on the impact-energy values of high purity Ti-N alloys.

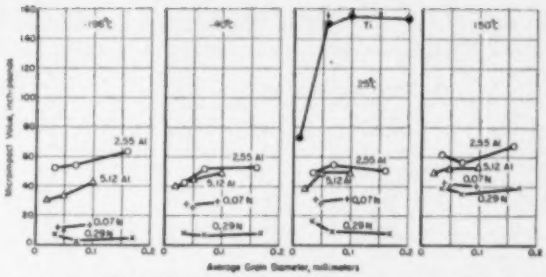


Fig. 12—Effect of equiaxed-α grain size on impact properties.

The properties of the Ti-Al alloys in the α-β-quenched condition are about the same as the properties in the equiaxed-α condition, except possibly for improved toughness. Quenching from the β field increases the yield strength, but not the ultimate strength of the softer Ti-2.55 pct Al alloy compared to the equiaxed condition, just as it did for unalloyed titanium. This effect is not carried over to the Ti-5.12 pct Al alloy, perhaps because of its higher strength level. Reduction in area for both alloys is lower as a result of the β heat treatments. This must be considered to be an effect of increased grain size, since, apart from grain-boundary serrations, the transformed-β structure is basically a large-grained α structure. Previously, it was shown that increased equiaxed-α grain size lowers reduction in area for α alloys (Fig. 11). β furnace cooling has a detrimental effect on toughness compared to β quenching for both alloys.

The most notable features of the effect of β heat treatment on the Ti-N alloys is the decrease in strength, particularly yield strength, when quenching is done from the α-β field. A reasonable explanation for this is that the α-β anneal separates the structure into two phases, one (the β phase), being the matrix, is lean in alloy content, and the other (the α phase), rich in alloy content. The low alloy matrix would tend to govern the flow characteristics and thus lower the yield strength. However, this explanation is insufficient, since, after a full β quench, the yield strength of the Ti-0.29 pct N alloy does not come back up to its equiaxed-α level, although the tensile strength and hardness do return.

The actual stress-strain curves for the Ti-N alloys, shown in Fig. 16, illustrate why the yield strengths do not return to the α annealed level. Yield points are found in the equiaxed-α condition, especially with the higher nitrogen alloy. The yield point disappears when the alloy has been heated to the α-β or β field and cooled either by quenching or furnace cooling. Yield points were found only with the nitrogen alloys, and not with the aluminum alloys (see Fig. 17). Other tests on Ti-0.064 pct N and Ti-0.174 pct N alloys showed yield points with and without hydrogen present, and both for α-furnace-cooled and quenched conditions. The only conditions always associated with yield points are that the material contain high nitrogen and that it be annealed in the α field.

Yield-point phenomena usually indicate strain aging, which is thought to be a diffusion of atoms to preferred sites under conditions of strain accompanied by precipitation and stress relaxation. The yield point has been observed by the authors[10] in α-annealed Ti-C alloys where carbon can precipitate from solid solution. Rosi and Perkins[11] have observed yield points in commercial titanium (0.08 pct N and 0.05 pct C) at elevated temperature.

If β heat treatments do not show the yield point, it follows that whatever was causing strain aging has already precipitated. One structural difference always present in this condition is the faint subgrain markings or veining between the α platelets. This could well be the precipitate involved. Another observation that ties in with the suggestion that β-treated Ti-N alloys have a precipitate present is the fact that β-grain growth was much less than for titanium or the Ti-Al alloys.

## Effect of Composition on Properties

The properties of the Ti-Al alloys in various structural conditions plotted against aluminum content are shown in Fig. 18. The strength and hardness vs composition curves are concave upward, which means that, in the same condition, strength and hardness increase more for higher aluminum contents than for lower aluminum contents. Conversely, the ductility and toughness vs composition curves show that the higher aluminum alloy is practically as ductile and tough as the lower alumi-

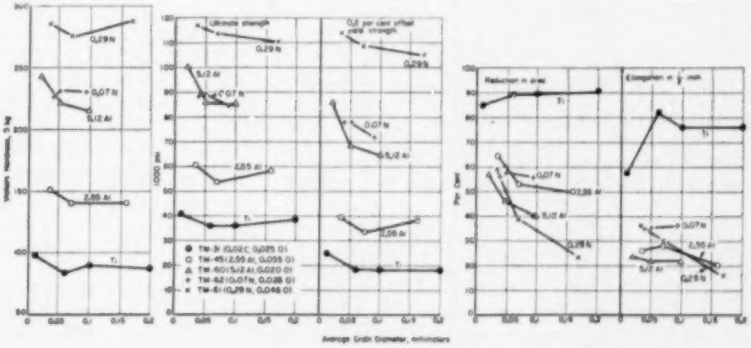


Fig. 11—Effect of equiaxed-α grain size on tensile properties and hardness of α-Ti alloys.

## Table III. Hardness and Tensile Properties of High Purity Titanium

| Heat Treatment | | | Vhn, 5 Kg Load* | Yield Strength at Offset (Pct) Shown, 1000 Psi | | | Ultimate Strength, 1000 Psi | Elongation, Pct in ½ In. | Reduction in Area, Pct |
|---|---|---|---|---|---|---|---|---|---|
| Time, Hr | Temperature, °C | Cooling† | | 0.01 Pct | 0.1 Pct | 0.2 Pct | | | |
| **TM-31, Titanium** | | | | | | | | | |
| 1 | 600 | WQ | 98 | 18.1 | 24.3 | 24.8 | 40.6 | 58 | 85 |
| 1 | 800 | WQ | 84 | 6.9 | 15.4 | 18.3 | 35.5 | 62 | 89 |
| 2 | 875 | WQ | 90 | 7.6 | 14.7 | 18.4 | 35.9 | 76 | 89 |
| 100 | 875 | WQ | 87 | 7.6 | 15.1 | 18.4 | 38.4 | 76 | 91 |
| 1 | 1000 | WQ | 99 | 22.1 | 30.5 | 33.1 | 41.6 | 64 | 87 |
| 1 | 1000 | FC | 89 | 12.7 | 22.3 | 24.4 | 38.3 | 66 | 85 |

* Hardness taken on cross-section.
† WQ stands for water-quenched; FC, for furnace-cooled.

## Table IV. Hardness and Tensile Properties of Ti-Al Alloys

| Heat Treatment | | | Vhn, 5 Kg Load* | Yield Strength at Offset (Pct) Shown, 1000 Psi | | | Ultimate Strength, 1000 Psi | Elongation, Pct in ½ In. | Reduction in Area, Pct |
|---|---|---|---|---|---|---|---|---|---|
| Time, Hr | Temperature, °C | Cooling† | | 0.01 Pct | 0.1 Pct | 0.2 Pct | | | |
| **TM-45, Ti-2.55 Pct Al** | | | | | | | | | |
| 1 | 750 | WQ | 151 | 27.4 | 37.2 | 39.3 | 60.2 | 26 | 64 |
| 1 | 900 | WQ | 140 | 17.0 | 29.2 | 33.2 | 53.7 | 28 | 53 |
| 16 | 900 | WQ | 140 | 20.6** | 32.6** | 38.0** | 57.3 | 20 | 50 |
| 1 | 935 | WQ | 158 | 27.3 | 32.1 | 35.0 | 55.4 | 36 | 62 |
| 1 | 1000 | WQ | 154 | 30.8 | 38.8 | 42.1 | 56.0 | 35 | 52 |
| 1 | 1000 | FC | 153 | 31.8 | 40.0 | 43.2 | 56.1 | 27 | 49 |
| **TM-60, Ti-5.13 Pct Al** | | | | | | | | | |
| 1 | 750 | WQ | 243 | 76.8 | 84.0 | 85.9 | 101.0 | 24 | 57 |
| 1 | 900 | WQ | 221 | 59.6 | 64.3 | 67.2 | 86.2 | 22 | 46 |
| 16 | 900 | WQ | 215 | 55.5 | 61.3 | 64.5 | 85.0 | 22 | 40 |
| 1 | 985 | WQ | 234 | 57.1 | 66.7 | 70.0 | 85.7 | 23 | 50 |
| 1 | 1000 | WQ | 222 | 51.6 | 62.8 | 67.4 | 80.4 | 22 | 27 |
| 1 | 1000 | FC | 232 | 66.2 | 74.1 | 77.0 | 83.0 | 14 | 27 |

* Hardness taken on cross-section.
† WQ stands for water-quenched; FC for furnace-cooled.
** Strength value obtained from defective SR-4 strain gage. Values are approximate.

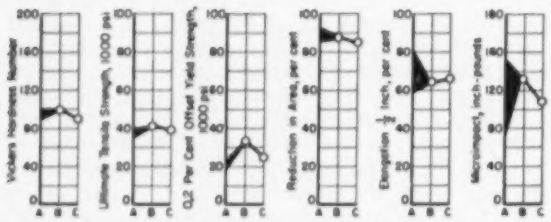
Vickers Hardness Number
Ultimate Tensile Strength, 1000 psi
0.2 Per Cent Offset Yield Strength, 1000 psi
Reduction in Area, per cent
Elongation in 1/2 inch, per cent
Micrompact, inch-pounds
A B C

Fig. 13—Effect of $\alpha$-$\beta$ transition on titanium. A—Shows range of properties in equiaxed-$\alpha$ condition. B—Property as-quenched from $\beta$ field. C—Property as-furnace-cooled from $\beta$ field.

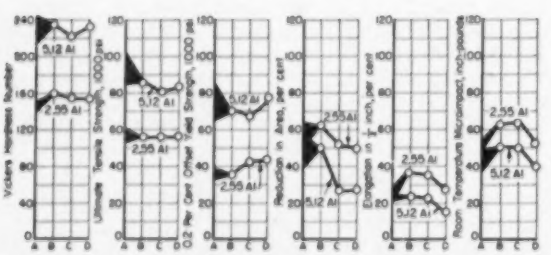
Vickers Hardness Number
Ultimate Tensile Strength, 1000 psi
0.2 Per Cent Offset Yield Strength, 1000 psi
Reduction in Area, per cent
Elongation in 1/2 inch, per cent
Room Temperature Micrompact, inch-pounds
5.12 Al
2.55 Al
A B C D

Fig. 14—Effect of $\alpha$-$\beta$ transformation on mechanical properties of Ti-Al alloys. A—Shows range of properties in equiaxed-$\alpha$ condition. B—Property as-quenched from $\alpha$-$\beta$ field. C—Property as-quenched from $\beta$ field. D—Property as-furnace-cooled from $\beta$ field.

num alloy. This effect has been shown previously by Ogden et al. for tensile properties of high purity Ti-Al alloys.[1] Thus, to obtain the most benefit from aluminum as an alloying element, the highest possible alloying content should be used. The limiting

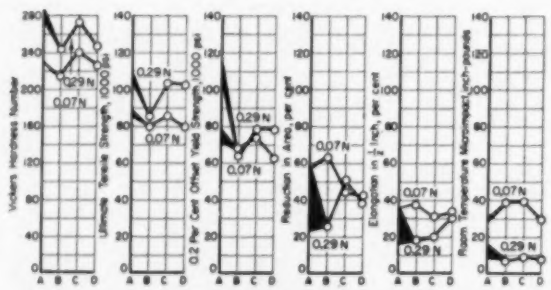
Vickers Hardness Number
Ultimate Tensile Strength, 1000 psi
0.2 Per Cent Offset Yield Strength, 1000 psi
Reduction in Area, per cent
Elongation in 1/2 inch, per cent
Room Temperature Micrompact, inch-pounds
0.29 N
0.07 N
A B C D

Fig. 15—Effect of $\alpha$-$\beta$ transformation on mechanical properties of Ti-N alloys. A—Shows range of properties in equiaxed-$\alpha$ condition. B—Property as-quenched from $\alpha$-$\beta$ field. C—Property as-quenched from $\beta$ field. D—Property as-furnace-cooled from $\beta$ field.

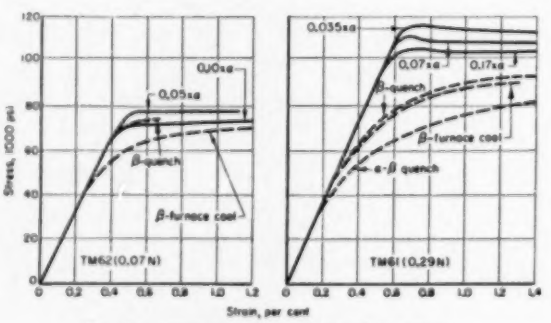


Fig. 16—Stress-strain curves for Ti-N alloys.

factor in this respect appears to be fabricability. Finlay et al.[2] report that 5 to 6 pct Al is the highest content commensurate with satisfactory commercial

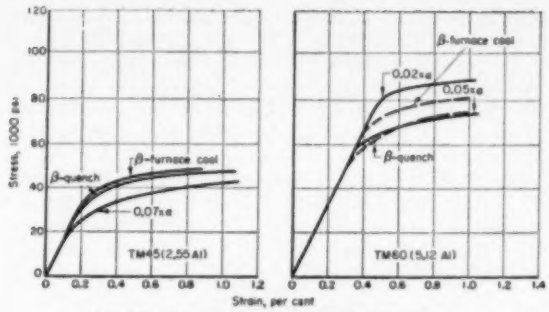


Fig. 17—Stress-strain curves for Ti-Al alloys.

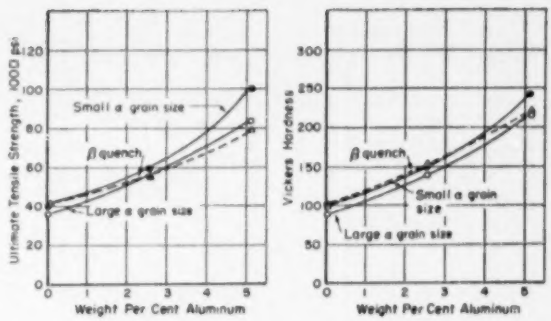


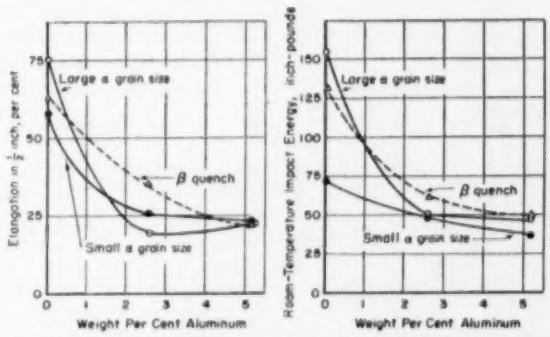


Fig. 18—Effect of composition on the mechanical properties of high purity Ti-Al alloys.

fabrication practice and that tin additions at the 5 pct Al level permit a further gain in strength without adversely affecting fabrication.

Fig. 19 presents the properties of the Ti-N alloys in various structural conditions plotted against nitrogen content. The interstitial addition of nitrogen has an effect opposite to that of aluminum, namely that the higher additions are less effective in strengthening and hardening than the initial additions. The ductilities and toughness values decrease progressively as the nitrogen increases and the greatest drop is for the initial addition, just as in the Ti-Al alloys. However, the degree of leveling off in ductility is not as pronounced as with the Ti-Al alloys.

Generally, since strength and ductility are inversely related, the best comparison of one alloying element with another is on the basis of ductilities and the same strength level. In Fig. 20, the tensile strengths of the materials studied are plotted against tensile ductility and toughness. Also shown are data from Lenning et al.[5] for hydrogen-free alloys prepared and evaluated identically to those in the present study. It is apparent that, as far as strength vs tensile-ductility is concerned, there is no reason to prefer aluminum over nitrogen or vice versa. In fact, the Ti-N alloys have slightly better tensile ductilities. The significant difference is in the strength vs toughness correlation. It is seen that for the strength level of about 80,000 psi, the substitutionally strengthened alloys are about 20 in.-lb tougher in the micro impact test. This would correspond to about 16 Charpy ft-lb difference. At 100,000 psi, the indication is that the substitutional alloys are 30 in.-lb tougher in the micro impact test.

The nature of the alloying element also has a strong influence on the impact vs temperature characteristics. The energy absorbed in breaking high purity titanium as a notched bar in impact is relatively independent of testing temperature, as shown in Fig. 7. The same characteristic holds for the Ti-Al alloys, except that the stronger Ti-5.12 pct Al alloy decreases slightly more in impact energy absorbed with decreasing temperature (see Fig. 8). The impact vs temperature curves for the nitrogen alloys, shown in Fig. 9, illustrate that there is a pronounced decrease in energy absorbed with lower testing temperature for the Ti-0.07 pct N alloy, while the Ti-0.29 pct N alloy exhibits a true brittle-to-ductile transition between 25° and 150°C. The indications, therefore, are that alloying of high purity titanium increases the temperature dependence of impact-energy absorption, and that, even

## Table V. Hardness and Tensile Properties of Ti-N Alloys

| Heat Treatment | | | Vhn, 5 Kg Load* | Yield Strength at Offset (Pct) Shown, 1000 Psi | | | Ultimate Strength, 1000 Psi | Elongation, Pct in ½ In. | Reduction in Area, Pct |
|---|---|---|---|---|---|---|---|---|---|
| Time, Hr | Temperature, °C | Cooling† | | 0.01 Pct | 0.1 Pct | 0.2 Pct | | | |
| **TM-62, Ti-0.07 Pct N** | | | | | | | | | |
| 1 | 750 | WQ | 226 | 73.9 | 78.1 | 78.1 | 88.5 | 35†† | 58 |
| 1 | 865 | WQ | 231 | 69.5 | 77.2 | 77.7 | 87.9 | 35 | 56 |
| 16 | 865 | WQ | 230 | 66.2 | 70.7 | 71.4 | 84.5 | 36 | 56 |
| 1 | 900 | WQ | 214 | 60.4 | 67.0** | 69.7** | 80.0 | 38 | 63 |
| 1 | 960 | WQ | 240 | 64.9 | 72.4 | 74.1 | 85.5 | 31 | 44 |
| 1 | 960 | FC | 226 | 40.7 | 57.2 | 62.3 | 79.6 | 33†† | 42 |
| **TM-61, Ti-0.29 Pct N** | | | | | | | | | |
| 1 | 600 | WQ | 285 | 109.0 | 114.1‡ | | 117.5 | 36 | 59 |
| 1 | 750 | WQ | 275 | 107.0 | 109.0‡ | | 113.9 | 30 | 39 |
| 16 | 875 | WQ | 287 | 99.9 | 105.3‡ | | 110.2 | 16 | 23 |
| 1 | 920 | WQ | 244 | 37.5 | 56.2 | 63.0 | 84.3 | 18 | 25 |
| 1 | 960 | WQ | 274 | 49.7 | 69.3 | 78.2 | 103.8 | 20 | 31 |
| 1 | 960 | FC | 246 | 50.5 | 69.8 | 78.0 | 102.4 | 32 | 38 |

* Hardness taken on cross-section.
† WQ stands for water-quenched; FC, for furnace-cooled.
** Strain gage defective. Values are approximate.
†† Specimen broke outside gage length. Elongation value estimated from extension between shoulders of tensile specimen.
‡ Yield point noted.

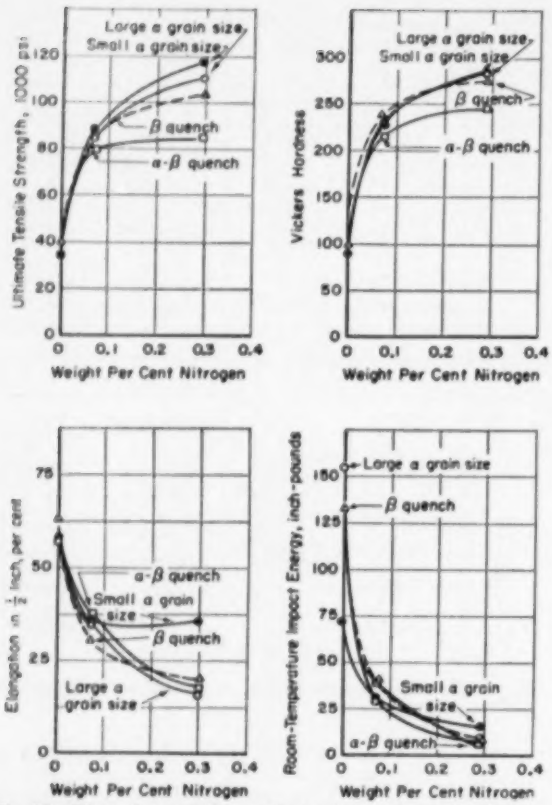


Fig. 19—Effect of composition on the mechanical properties of high purity Ti-N alloys.

taking strength level into account, the interstitial alloying-element nitrogen is more detrimental to toughness than the substitutional alloying-element aluminum.

## Summary


1—No basic difference was found in the equiaxed-$\alpha$ structures of titanium, Ti-N, and Ti-Al alloys.

2—After quenching from the $\beta$ field, serrated $\alpha$ structures without much subgrain marking were found for titanium and Ti-Al alloys. For the Ti-N alloys, subgrain markings delineating the $\alpha$ platelets were found. This and other facts suggest a precipitation from the high nitrogen alloys.

3—Furnace cooling from the $\beta$ field produces subgrain markings delineating the $\alpha$ platelets both for the Ti-Al and Ti-N alloys.

4—Increasing equiaxed-$\alpha$ grain size generally decreases strength and hardness and causes little reduction in the ductility of titanium but reduces the tensile ductility of the alloys. Increased grain size generally is beneficial to impact properties.

5—Heat treatment from the $\beta$ field increases the yield strength of titanium but is without effect on the strong Ti-Al alloy. It causes a disappearance in yield points found in Ti-N alloys and results in a marked lowering in yield strength.

6—Quenching from the $\alpha$-$\beta$ field has little effect on Ti-Al alloys, but decreases the yield and tensile strength of Ti-N alloys by a combination of partition of nitrogen between the two phases, resulting in a softer matrix, and elimination of strain aging.


## Acknowledgment


This work is part of a systematic investigation for the Army Ordnance Corps interrelating the various types of titanium alloys prepared from high purity materials. The authors are grateful to Watertown Arsenal for permission to publish this work done under their sponsorship under Contract No. DA-33-019-ORD-280.


## References


[1] H. R. Ogden, D. J. Maykuth, W. L. Finlay, and R. I. Jaffee: Mechanical Properties of High Purity Ti-Al Alloys. *Trans.* AIME (1953) **197**, pp. 267-272; JOURNAL OF METALS (February 1953).

[2] W. L. Finlay, R. I. Jaffee, R. W. Parcel, and R. C. Durstein: Tin Increases Strength of Ti-Al Alloys without Loss in Fabricability. JOURNAL OF METALS (January (1954) **6**, pp. 25-29.

[3] R. I. Jaffee, H. R. Ogden, and D. J. Maykuth: Alloys of Titanium with Carbon, Oxygen, and Nitrogen. *Trans.* AIME (1950) **188**, pp. 1261-1266; JOURNAL OF METALS (October 1950).

[4] E. S. Bumps, H. D. Kessler, and M. Hansen: The Titanium-Oxygen System. *Trans.* ASM (1953) **45**, pp. 1008-1025.

[5] I. Cadoff and J. P. Nielsen: Titanium-Carbon System. *Trans.* AIME (1953) **197**, pp. 248-252; JOURNAL OF METALS (February 1953).

[6] H. R. Ogden, D. J. Maykuth, W. L. Finlay, and R. I. Jaffee: Constitution of Ti-Al Alloys. *Trans.* AIME (1951) **191**, pp. 1150-1155; JOURNAL OF METALS (December 1951).

[7] E. S. Bumps, H. D. Kessler, and M. Hansen: The Ti-Al System. *Trans.* AIME (1952) **194**, pp. 609-614; JOURNAL OF METALS (June 1952).

[8] G. A. Lenning, C. M. Craighead, and R. I. Jaffee: Constitution and Mechanical Properties of Titanium-Hydrogen Alloys. *Trans.* AIME (1954) **200**, pp. 367-376; JOURNAL OF METALS (March 1954).

[9] F. C. Holden, H. R. Ogden, and R. I. Jaffee: Microstructure and Mechanical Properties of Iodide Titanium. *Trans.* AIME (1953) **197**, pp. 238-242; JOURNAL OF METALS (February 1953).

[10] H. R. Ogden, R. I. Jaffee, and F. C. Holden: *Properties of Titanium-Carbon Alloys.* Unpublished.

[11] F. D. Rosi and F. C. Perkins: Mechanical Properties and Strain Aging Effects in Titanium. *Trans.* ASM (1953) **45**, pp. 792-991.


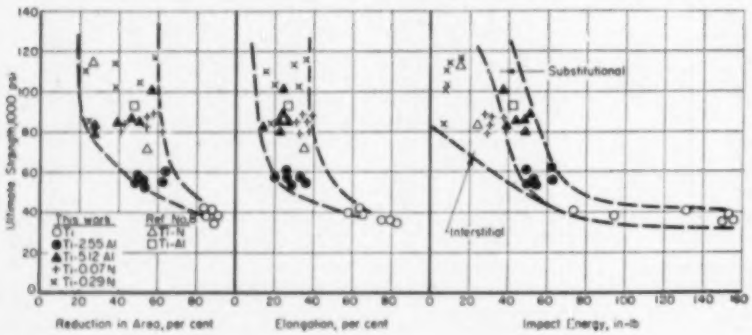


Fig. 20—Comparison of substitutional and interstitial solutions with respect to combinations of strength and ductility and toughness.

# Some Observations on the Tertiary Stage of Creep Of High Purity Aluminum

by G. R. Wilms

**A study has been made of the structural changes in polycrystalline high purity aluminum during the tertiary stage of creep under conditions of constant tensile load. It appears that there is no basic modification in the particular mechanism of deformation that characterized the preceding secondary stage of creep, but that the changes in crystalline structure produced during the tertiary stage are only a consequence and not a cause of the accelerated strain. Intercrystalline fissures were observed on entry into the tertiary stage, and these might supplement the accelerated rate of strain owing to local stress concentrations. There is evidence that the formation of these fissures may be associated with the presence of surface imperfections, and it is suggested that a more generalized treatment of the results may explain certain creep characteristics of commercial alloys.**

IN previous work[1-4] a study was made of the changes produced when specimens of annealed aluminum were deformed at various temperatures and rates of strain, especially under conditions leading to creep under constant tensile load. It was shown that, as the temperature was increased or as the rate of strain was decreased, elements of the substructure produced within the grains became coarser, and with the strain rate constant at a given temperature, their size tended to an equilibrium value. The preliminary process of the breaking down of the grains into a substructure was identified with primary creep.[1] The subsequent equilibrium condition was associated with secondary creep. The question then arose whether the tertiary stage corresponded to any further significant change in the substructure.

The question is also of interest in view of the opinion, expressed for instance by Andrade,[5] that the tertiary stage is merely an accelerated rate of strain due to the reduced area of section of a specimen under continuous tensile load, and the other opinion, as suggested by the observation by Sully, Cale, and Willoughby[6] of a tertiary stage in compressive loading, that this third stage is a real effect in its own right.

The object of this paper is to record some observations on the tertiary stage of high purity aluminum.

G. R. WILMS is associated with the Commonwealth of Australia Defense Standards Laboratories, Melbourne, Australia.

Discussion on this paper, TP 3837E, may be sent, 2 copies, to AIME by Jan. 1, 1955. Manuscript, Nov. 19, 1952.

## Experimental Procedure

The material was aluminum of 99.98 pct purity as previously used. The specimens had a rectangular section of ⅛x½ in., and extensions were measured over a 1 in. gage length. After machining to shape, the specimens were annealed to give a standard grain size of 0.2 mm and then electropolished.

The general procedure involved metallographic and X-ray diffraction examination at progressive stages of elongation (marked by arrows on the curves shown in Figs. 1 and 2), the specimen being extended to fracture under constant load at a given temperature. The X-ray tests were made by the back-reflection method from a stationary specimen, using CoK radiation. The longer edge of the micrographs in the paper corresponds to the direction of applied stress.

## Results

The previous work showed that, in the secondary stage of creep in aluminum, three basic types of structure could be developed according to the temperature and rate of strain. These were: 1—slip, which predominated at the lower temperatures and higher rates of strain and produced the finest and least perfect substructure; 2—cell structure, which superseded slip as the temperature was raised and the rate of strain decreased and which was characterized by a coarser and more perfect structure and an absence of slip lines; and 3—a stage termed "boundary microflow," which predominated at still higher temperatures and lower rates of strain when the cell size had increased and become comparable

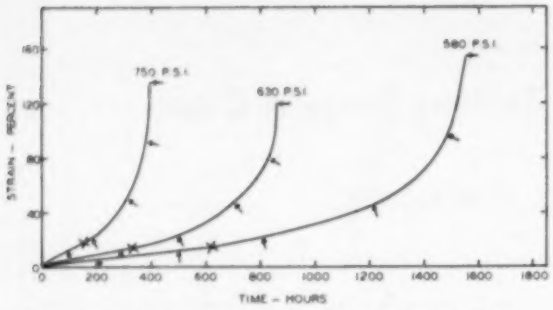


Fig. 1—Creep of aluminum under different loads at 250°C.

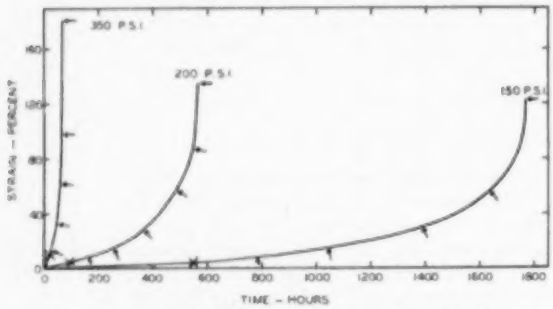


Fig. 2—Creep of aluminum under different loads at 350°C.

with the grain size. In considering the transition from the secondary to the tertiary stage, it was logical therefore to take typical examples of each stage.

The working temperatures chosen with the last object in view were 250° and 350°C. The range of secondary creep rates required to establish the different structures were given in practice by loads corresponding to the ranges of 580 to 750 psi at 250°C and 150 to 350 psi at 350°C. These gave the families of creep curves shown in Figs. 1 and 2, the last point recorded on each curve being the fracture. The beginning of the tertiary stage, defined as the point of departure from the linearity of the secondary stage, is marked by a cross on each curve.

*Tertiary Stage in Relation to Structural Changes:* After examination of a large number of specimens, the general result can be stated at once: the basic mechanism of deformation established in the secondary stage showed no significant alteration on entry to, or during, the tertiary stage. Therefore, as the rate of strain increased in the final stages of the tertiary creep, there was a tendency for the grains to form a finer substruture in accordance with the principles referred to earlier.

In order to limit the number of photographs for reproduction, the observations will refer to one typical specimen. This is a specimen extended under a constant load of 630 psi at 250°C.

Reference is made first to the changes shown by the X-ray examination. The initial annealed condition is indicated in Fig. 15. The condition after 12 pct extension in 287 hr is shown in Fig. 3; this photograph also serves to represent the equilibrium condition of the secondary stage. The initial X-ray reflections have broken up into numerous secondary reflection spots, and these are associated with the discrete elements of the coarser substructure formed in the grains when the cell structure is produced. Fig. 5 shows the condition of the specimen after 80 pct extension in 815 hr, when, according to the creep curve shown in Fig. 1, it has entered the tertiary stage. It will be evident at once that no appreciable change in the nature of the photograph has occurred. After some 60 pct extension, however, the specimen commenced to neck, and fracture finally occurred after 120 pct extension in 855 hr. Photographs taken in the region of necking (Fig. 6) then showed the local effects of accelerated strain, most marked at the fracture itself (Fig. 9). The latter shows a considerable break-up of the X-ray reflections; they have changed in the same manner as they would in a specimen strained at a considerably higher rate at this temperature than the average rate of strain for the specimen as a whole. No marked change in the structure occurred, however, in regions away from the point of fracture, as shown in Fig. 7. This confirms the point that the changes at fracture are most probably merely the secondary effects of the locally enhanced rate of strain and not the cause of it.

Reference will be made next to the micrographs corresponding to the X-ray photographs described. The first, Fig. 4, shows grain-boundary movements and an absence of slip lines, typical of the cell structure. The second, Fig. 8, obtained 1 in. from fracture, indicates no obvious change despite the greater rumpling of the specimen surface. The third, Fig. 10, taken near the fracture, shows a marked disturbance; but evidently this is a local effect due to necking.

The same general results were obtained on specimens for which the equilibrium condition of the secondary stage was characterized either by boundary microflow, or by the transition between slip and cell structures.

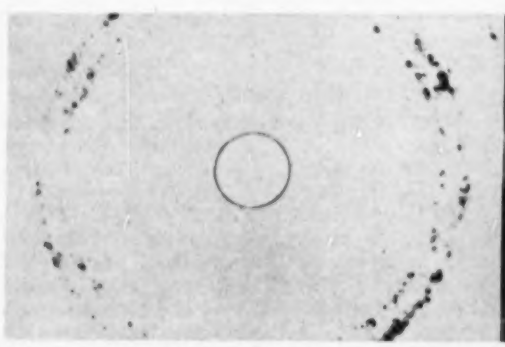

Fig. 3—Specimen of high purity aluminum extended under a constant load of 630 psi at 250°C. X-ray pattern after creep of 12 pct in 287 hr shows the equilibrium condition of the secondary stage of creep.

Fig. 4—Same specimen as in Fig. 3. Microstructure shows features typical of the cell structure. X100.

*Elongations to Fracture:* Specimens strained at room temperature (20°C) fractured after extensions of about 65 pct.

Specimens extended at 250°C under constant load, including those giving creep curves shown in Fig. 1, fractured only after much larger extensions within the range 115 to 160 pct. There was an appreciable variation in the extensions to fracture, and it was not possible to make any generalizations relating them to the load (strain rate).

Specimens extended at 350°C under constant load gave still greater extensions, between 120 to 180 pct. There was a general tendency for specimens which were extended under lower loads to give lower values of elongation.

There was also a tendency in all cases for the necking of the specimens to be more local and more pronounced, the less the overall elongation. In all cases the fractures appeared to be transcrystalline. The large elongations at 350°C, for example, were marked by a very gradual diminution of section along the entire length of the specimen, and the specimens ultimately drew out to a knife-edge type of (transcrystalline) fracture.

*Observation of Fissures in the Tertiary Stage:* The main difference between the secondary and the so-called tertiary stage appears to be the formation of fissures in localized areas during the latter stage.

In the tests at 250°C, fissures, usually intercrystalline, generally could be observed on entry into the tertiary stage. These then tended to increase in size and number on further elongation, concentrating especially in the region where necking occurred. An example of a fissure observed during the early stages

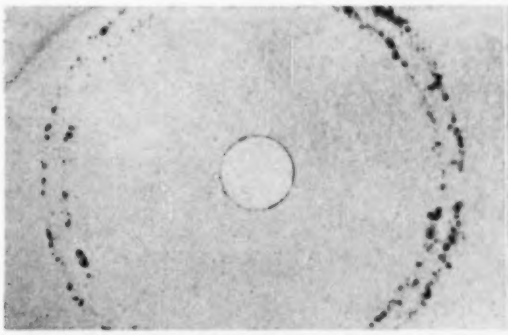

Fig. 5—Same specimen as in Fig. 3. X-ray pattern after creep of 80 pct in 815 hr shows no appreciable change in structure.

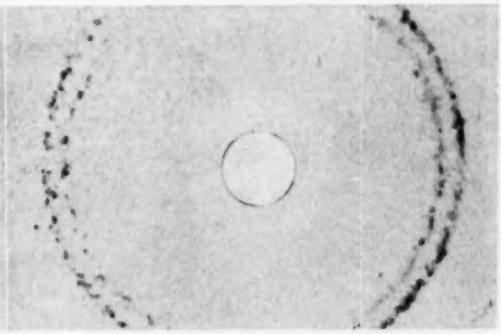

Fig. 6—Same specimen as in Fig. 5. X-ray pattern, taken in region of necking, shows a change in structure due to the local accelerated strain.

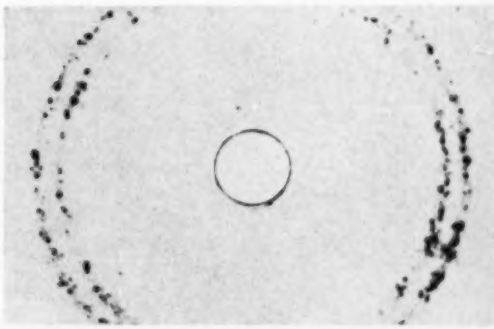

Fig. 7—Same specimen as in Fig. 3. X-ray pattern after creep of 120 pct (fracture) in 855 hr shows no marked change in structure in regions away from the point of fracture.

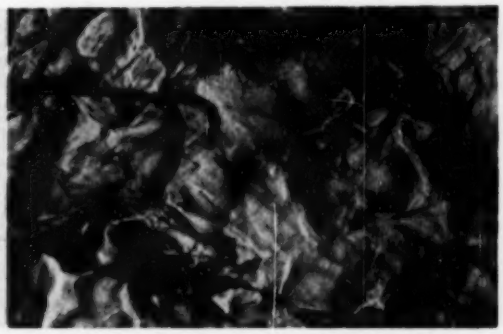

Fig. 8—Same specimen as in Fig. 7. Microstructure shows features still typical of the cell structure. X100.

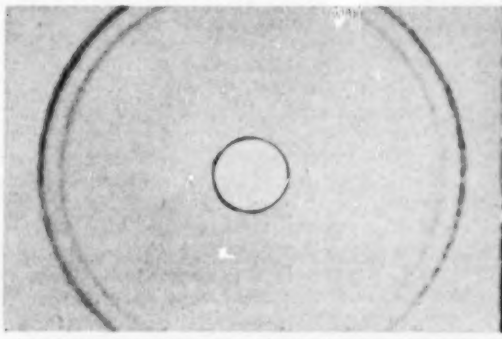

Fig. 9—Same specimen as in Fig. 7. X-ray pattern taken near the fracture shows a considerable breakdown of the structure due to the accelerated rate of strain.

Fig. 10—Same specimen as in Fig. 7. Microstructure near fracture shows a marked disturbance of the surface due to necking. X100.

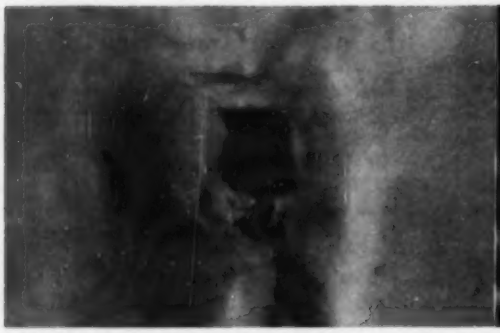

Fig. 11—Micrograph shows a typical intercrystalline fissure at an early stage of tertiary creep. After creep of 23 pct in 810 hr under a constant load of 580 psi at 250°C. X1000.

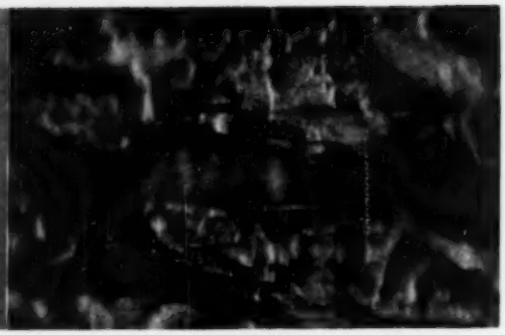

Fig. 12—Micrograph shows a fissure which has become elongated due to necking at fracture. After creep of 155 pct (fracture) in 1550 hr under a constant load of 580 psi at 250°C. X250.

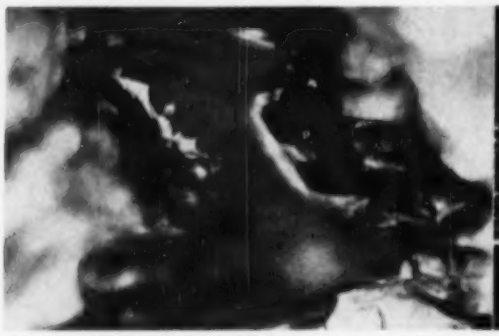

Fig. 13—Micrograph of pitted specimen (*B*) showing parting at grain boundaries near point of fracture. After creep of 95 pct (fracture) in 1420 hr under a constant load of 580 psi at 250°C. X250.

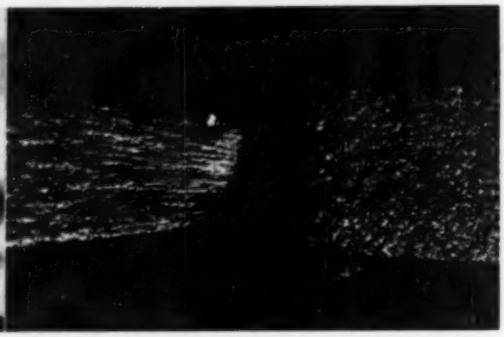

Fig. 14—Photograph of fractures of specimens *A* and *B*. Specimen *A* (left) shows considerable necking and a transcrystalline type of fracture; *B* (right) shows no appreciable necking and an intercrystalline type of fracture. X3.5.

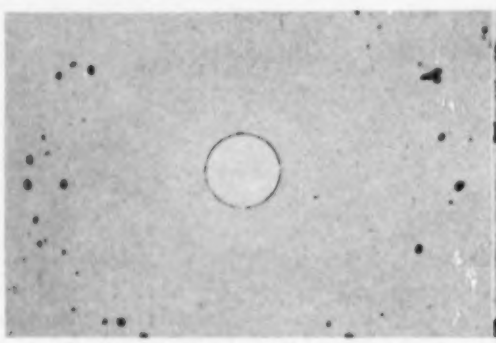

Fig. 15—X-ray photograph of initial annealed state.

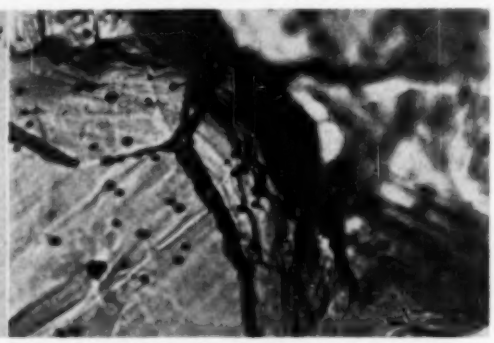

Fig. 16—Micrograph shows how parts of the grain boundary continually lag behind at the pits during creep deformation. After creep of 25 pct in 761 hr under a constant load of 600 psi at 250°C. X250.

is shown in Fig. 11; it will be noted that the fissure appears to have started at the junction of three grain boundaries. These fissures may have formed earlier during the secondary stage, but they were not detected. The development of a fissure after further extension is shown in Fig. 12, when it has become elongated due to the necking at fracture. There did not appear to be any appreciable difference in the number or size of fissures with variation of load (strain rate).

In tests at the higher temperature of 350°C, the fissures were much fewer and less pronounced at all rates of strain.

It would appear from the foregoing that, when fissures formed, abnormal macroscopic condition of the metal is produced which might tend to cause an accelerated rate of strain owing to local stress concentrations. But this condition is not essential for the accelerated strain, as shown by the observations at the higher temperatures.

It should be added also that no fissures were observed in specimens strained in such a manner as to result in a slip structure.

*Influence of Surface Imperfections on the Formation of Fissures:* There appears to be evidence in the present work that the formation of fissures may be connected with the presence of pits on the polished surface of the material. To illustrate this, two identical specimens were polished electrolytically, and the polishing conditions were so arranged that one

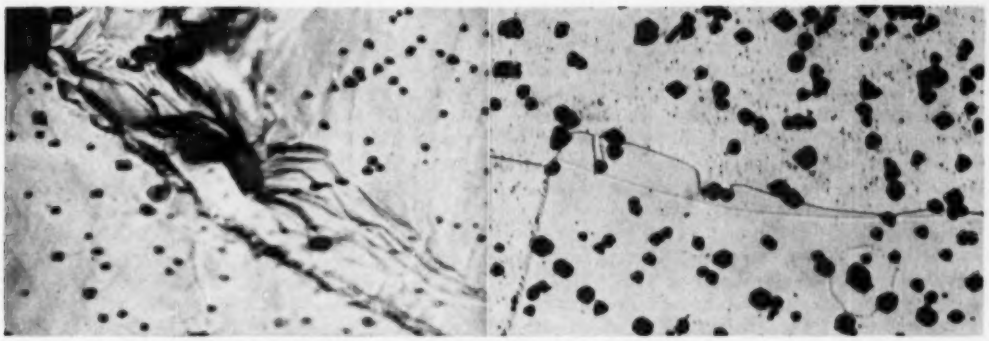

Fig. 17—Micrograph shows the formation of a fissure at retarded part of grain boundary. Same specimen as in Fig. 16. X250.

Fig. 18—Micrograph shows how pits retard the grain-boundary migration in an annealed specimen, heated 1½ hr at 350°C. Re-etched. X250.

(specimen *A*) had a reasonably good surface, similar to that shown in Fig. 4, and the other (specimen *B*) had a large number of polishing pits distributed over the surface. These two specimens were then subjected to a constant tensile load of 580 psi at 250°C. On entry into the tertiary stage, fissures were observed over the entire length of specimen *B*. Compared to specimen *A*, these fissures became considerably greater in number and size with continued extension, so that ultimately they led to a parting of the grains at fracture, as shown in Fig 13. Correspondingly, there were differences in the fractures of the two specimens, Fig. 14. Specimen *A* showed considerable necking to fracture. The final elongation was 155 pct reached in 1550 hr, resulting in a transcrystalline type of fracture. On the other hand, specimen *B* showed no appreciable necking to fracture. The final elongation was 95 pct reached in 1420 hr, and the fracture appeared to be intercrystalline. These results indicate that the fissures can penetrate quite deeply into the thickness of the specimen.

With reference to these results, it was also observed that both polishing and etch pits had some influence on the grain-boundary movements, which were associated with the deformation of the specimens considered. Fig. 16 shows how parts of the grain boundary continually lag behind at the pits during the migration process, in similar fashion to that recently reported by Chang and Grant.[7] Merely heating annealed metal produced the same effect (see Fig. 18), and it was only after prolonged heating that the arrested parts of the boundary caught up with the rest. It was of further interest to observe that when specimens were deformed, fissures frequently appeared at those very regions where the movement of the grain boundaries was retarded, as shown in Fig. 17.

## Discussion

In connection with the objects of the investigation, the results bring out the following points:

1—In the tertiary stage there appears to be no radical change in the particular mechanism of deformation that characterized the secondary stage. The subgranular structural condition associated with the equilibrium state of the secondary stage, whether that be characterized by slip, cell, or boundary microflow, is virtually preserved almost until fracture. It is considered that those changes which do occur are subsidiary changes due rather to the accelerated rate of strain, which is confined to the region of necking; this produces, in accordance with the general relation between substructure and strain rate, a finer substructure. This conclusion is of interest in relation to the suggestion made by some investigators[8] that the tertiary stage in some cases might be associated with recrystallization. In none of the aluminum specimens deformed under the conditions employed in the present research was recrystallization observed.

2—There are changes in microstructure with deformation extending into the tertiary stage. In particular, there is the formation of intercrystalline fissures, as described also in the early work of Hanson and Wheeler.[9] The formation of fissures was observed to be more pronounced at intermediate temperatures, 250°C, and less marked at higher temperatures, 350°C, when the stage of boundary microflow predominates.

3—There is the further point, however, that pits on the surface of the metal seem to promote the formation of fissures and intercrystalline fracture. In this connection, it is now generally thought that movements of grains and of grain boundaries are an integral part of the creep process when the cell structure or the stage of boundary microflow is predominant. Thus it may be expected that these boundary movements would tend to relieve the stresses built up in the regions of the grain boundaries due to the "interlocking" of the grains, thereby reducing the possibility of the formation of cracks or fissures. Alternatively, if it is assumed that microcracks are activated at some stage of the deformation, the mobility of the micromovements would tend to fill them in as fast as they formed; this is suggested by the observation mentioned, that the formation of fissures is less marked at 350°C compared to those observed at 250°C. Accordingly, as illustrated by the results of the present investigation, when parts of the grain boundary are inhibited from moving in accordance with the requirements of the deformation process, such as at a polishing pit, it would be expected that in some cases a fissure can be activated and grow to macroscopic size before the barrier can be overcome. In addition, there will be variations in the stress system at the grain boundaries arising from stress concentrations at the pits, with subsequent variations due to the formation of fissures. Evidently it would be of interest to determine whether fissures are formed in specimens entirely free from pits, with deformation over the range of temperatures and rates of strain considered.

4—It is generally accepted that commercial alloys very often exhibit intercrystalline cracking during creep at elevated temperatures, with a correspond-

ingly lower overall extension than the more usual transcrystalline fractures obtained in tensile tests at room temperatures. On the other hand, the results obtained with high purity aluminum show the elongations to be least with deformation at room temperature where the specimens exhibit the slip structure only, and greatest during creep at elevated temperatures where the specimens exhibit the cell structure or boundary microflow. The observations, however, show that the presence of pits on the aluminum tends to reduce the elongations to fracture at elevated temperatures, and it is possible that, as the number of pits is increased, the elongations will likewise continually decrease. Again considering the behavior of commercial alloys, it is known that they are rather complex in structure, and usually consist of more than one phase including intermetallic compounds and inclusions. In this connection, it is of considerable interest that other workers have found that, when a metal is heated, inclusions[10] and dispersed phases[11] can interfere severely with the migration of the grain boundaries. Therefore, providing the deformation characteristics of the alloys are similar to those observed on aluminum, the presence of these phases may possibly interfere with boundary movements during creep deformation, and so lead to the formation of intercrystalline cracks or fissures and subsequent intercrystalline fractures with correspondingly low overall extensions.


### Acknowledgments

Part of this work was carried out at the Baillieu Laboratory, University of Melbourne, and the author wishes to thank Professor J. N. Greenwood and Dr. W. A. Wood for much useful advice. Thanks are also due to Dr. R. I. Garrod for his continued encouragement. The paper is published by permission of the Chief Scientist, Dept. of Supply, Australia.


### References


[1] W. A. Wood and R. F. Scrutton: *Journal* Institute of Metals, London (1950) **77**, p. 423.
[2] G. R. Wilms and W. A. Wood: *Journal* Institute of Metals, London (1949) **75**, p. 693.
[3] W. A. Wood and W. A. Rachinger: *Journal* Institute of Metals, London (1949) **76**, p. 237.
[4] W. A. Wood, G. R. Wilms, and W. A. Rachinger: *Journal* Institute of Metals, London (1951) **79**, p. 159.
[5] E. N. daC. Andrade: *Proc.* Royal Society, London (1910) **84A**, p. 1; (1914) **90A**, p. 329.
[6] A. H. Sully, G. N. Cale, and G. Willoughby: *Nature* (1948) **162**, p. 411.
[7] H. C. Chang and N. J. Grant: *Trans.* AIME (1952) **194**, p. 619; JOURNAL OF METALS (June 1952).
[8] E. N. daC. Andrade: *Nature* (1948) **162**, p. 410.
[9] D. Hanson and M. A. Wheeler: *Journal* Institute of Metals, London (1931) **45**, p. 229.
[10] J. E. Burke: *Atom Movements.* (1951) p. 221. Cleveland. ASM.
[11] P. A. Beck, M. L. Holzworth, and P. R. Sperry: *Trans.* AIME (1948) **180**, p. 163; METALS TECHNOLOGY (September 1948).


# Discussion — Iron and Steel Division*


*No Meeting*

Silicon-Oxygen Equilibrium in Liquid Iron—A Revision (paper by John Chipman and Nev A. Gokcen. JOURNAL OF METALS, August 1953, p. 1017) ..... 1296

*New York Meeting, February 1954*

Regenerator Efficiency and Air Preheat in the Open Hearth (paper by B. M. Larsen. JOURNAL OF METALS, February 1954, p. 129) ..... 1298
Examination of a High Sulphur Free-Machining Ingot, Bloom and Billet Sections (paper by D. J. Carney and E. C. Rudolphy. JOURNAL OF METALS, August 1953, p. 999) ..... 1302
Development of Oxygen Steelmaking (paper by Otwin Cuscoleca. JOURNAL OF METALS, July 1954, p. 817) 1304
On the Basic Bessemer Process (paper by Pierre Coheur and Hans Kosmider. JOURNAL OF METALS, July 1954, p. 829) ..... 1305
Solid Phase Identification in Partially Reduced Iron Ore (paper by Gust Bitsianes and T. L. Joseph. JOURNAL OF METALS, December 1953, p. 1641) ..... 1305
Further Studies of the Tuyere Zone of the Blast Furnace (paper by J. B. Wagstaff. JOURNAL OF METALS, July 1953, p. 895) ..... 1307


*TP 3902C.

## Silicon-Oxygen Equilibrium in Liquid Iron—A Revision

by John Chipman and Nev A. Gokcen

**E. T. Turkdogan** *(British Iron & Steel Research Assoc., London, England)*—I would like to suggest a different method for the treatment of the authors' data on the Si-O equilibrium in liquid iron.

Because the activity coefficient of silicon dissolved in iron is influenced by the concentration of silicon as well as that of oxygen, the equilibrium constant $K_2'$ of reaction 2 becomes a function of metal composition, and, as shown in Fig. 1, a plot of log $K_2'$ at 1600°C against the weight percent of silicon gives a smooth curve. A similar curve is obtained when log $K_2'$ is plotted against the oxygen content of iron. Before

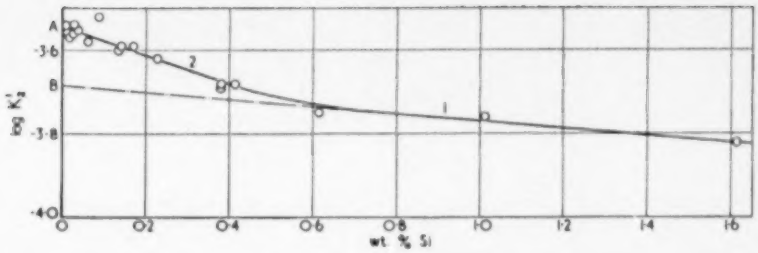


Fig. 1—Variation of log $K_2^1$ with concentration of silicon in iron at 1600°C.

extrapolating the curve to 0 Si concentration, the following consideration should be taken into account:

When silicon concentration in iron is high and, consequently, the oxygen concentration is low, the measurable effect on the activity coefficient of silicon is solely that brought out by the silicon concentration; and, as pointed out by the authors, the activity coefficient is greater than unity. On the other hand, as silicon in iron decreases and oxygen increases, the activity coefficient becomes progressively less and beyond a certain composition it becomes less than unity. When silicon in iron approaches infinite dilution, the oxygen concentration therein increases appreciably when the system is in equilibrium with cristobalite, and, therefore, the equilibrium constant $K_2^1$ increases very materially.

In view of these arguments, it follows that, at an intermediate composition, the log $K_2^1$ vs pct Si curve should have an inflexion. In fact, at about 0.65 pct Si, the curve deviates from the straight line 1 (Fig. 1), and the slope gradually decreases as the silicon content of iron decreases, but below about 0.4 pct Si, the points fall on a straight line 2.

As shown by the authors in their original paper, the value of log $f_{Si}^{O}$ is very nearly zero (—0.003) at 0.009 and 0.6 pct O and Si, respectively. Consequently, the extrapolation of the straight line 1 to 0 Si concentration at $B$ gives the true equilibrium constant because along this curve the $f_{Si}^{O}$ term has been eliminated.

The activity coefficient of silicon in the Fe-Si liquid system can be calculated from

$$\log f_{Si}^{Si} = \log K_2 - \log K_2^1 \qquad [12]$$

where log $K_2$ = —3.685 (point $B$) at 1600°C, and log $K_2^1$ is the value when silicon in iron is greater than 0.6 pct. In Fig. 2, log $f_{Si}^{Si}$ is plotted against the silicon content of iron. Up to about 4 pct Si, the relationship is linear. The error involved in this calculation, i.e., due to the omission of very small percentages of oxygen, the term $f_{Si}^{O}$ is negligible compared with the values of $f_{Si}^{Si}$.

When Eq. 12 is applied below 0.6 pct Si, the term $f_{Si}^{O}$

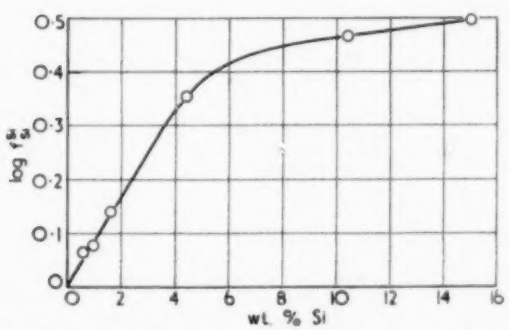


Fig. 2—Log $f_{Si}^{Si}$ related to concentration of silicon dissolved in iron at 1600°C.

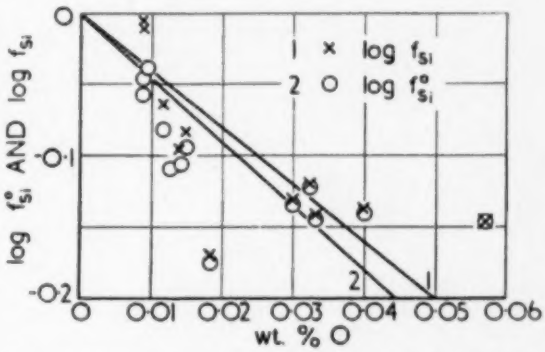


Fig. 3—Log $f_{Si}$ and log $f_{Si}^{O}$ related to concentration of oxygen dissolved in iron at 1600°C.

becomes progressively significant, and therefore

$$\log f_{Si} = \log f_{Si}^{Si} + \log f_{Si}^{O} = \log K_2 - \log K_2^1. \qquad [13]$$

Moreover, because the log $f_{Si}^{Si}$ vs [pct S] relationship is known from Fig. 2, the value of log $f_{Si}^{O}$ can be calculated from Eq. 13.

In Fig. 3, log $f_{Si}^{O}$ and log $f_{Si}$ are plotted against the oxygen content of iron.

Incidentally, in the calculations, melts series I: 104, 65, 69, and 105, and series II: 127 are omitted because of the authors' statement of the unreliability of their silicon contents.

Considering the experimental difficulties, the scatter of the points about the lines drawn is not excessive. Line 1 in Fig. 3 may be represented by

$$\epsilon_{Si}^{O} = \frac{\partial \log f_{Si}}{\partial [0\ \text{pct}]} = 4.0. \qquad [14]$$

From Eq. 14 and the method employed by the authors in their original paper, it follows that

$$\log f_O = \log f_O^{Si} = -2.29\ [\text{pct Si}] \qquad [15]$$

where $f_O$ is the activity coefficient of oxygen in the Fe-Si-O liquid system and $f_O^{Si}$ is a factor which indicates the magnitude of the interaction between silicon and oxygen dissolved in iron. $f_O = f_O^{Si}$ because, in the molten Fe-O binary system, Henry's law is obeyed up to oxygen saturation, i.e., $f_O^{O} = 1.0$.

Employing —3.635 as the value for log $K_2$ of Eq. 2 at 1600°C, together with the other appropriate reactions given in the paper, the free-energy change of reaction 7 becomes —41,754 cal per mol, and the free-energy changes of the following reactions are

$$Si(l) = \underline{Si} \quad \Delta G^\circ_T = -28{,}500 - 0.77T \qquad [16]$$

$$\underline{Si} + \underline{2O} = SiO_2(\text{crist}) \quad \Delta G^\circ_T = -133{,}340 + 48.91T. \qquad [17]$$

By using Eq. 16, $\gamma^\circ$ for silicon in very dilute solution in liquid iron becomes 0.016 at 1600°C.

**N. A. Gokcen** and **J. Chipman** (authors' reply)—The

authors wish to thank Dr. Turkdogan for his interest in the interpretation of the equilibrium results. They were aware of the alternative treatment presented by Dr. Turkdogan and of the fact that it leads to a slightly different value for the free energy of solution of silicon in liquid iron. The experimental data are not sufficiently detailed to permit a clear-cut decision between these interpretations. Observed values of the product [pct Si] [pct O]$^2$ agreed rather well with the earlier results of Körber and Oelsen and of Hilty and Crafts, and therefore appeared more firmly established than the equilibrium used in Dr. Turkdogan's calculations.

---

## Regenerator Efficiency and Air Preheat in the Open Hearth

by B. M. Larsen

*DISCUSSION, D. L. McBride and George Burrier, Chairmen*

**J. E. Eberhardt** *(Bethlehem Steel Corp., Bethlehem, Pa.)*—Mr. Larsen's paper is a logical and comprehensive description of a method of attack on the problem of getting the maximum possible flame-radiation intensity from a given fuel in an existing open-hearth furnace. His paper is so complete and so fundamentally sound that little can be added in the form of either further discussion or criticism. However, a brief summary of some of Mr. Larsen's points will serve to bring out a slightly different way of expressing his results which, it is believed, will aid in a further understanding of the art of operating open-hearth furnaces.

He first reiterates the well-known principle that flame-radiation intensity with a given fuel increases with increasing air-preheat temperature. He then makes a good case for the view that as much as possible of the oxygen required for the bath reactions should be supplied as oxygen-from-air rather than oxygen-from-ore. One may picture, then, two kinds of combustion air, fuel-combustion air (to burn the fuel) and charge-combustion air (to burn the metalloids of the charge). From the point of view of flame-radiation intensity, and hence furnace productivity, it is important to get the fuel-combustion air as hot as possible. From the viewpoint of thermal efficiency, it is important also to get the charge-combustion air as hot as possible. Many existing furnaces, however, have checkers that are simply too small to heat this much air. Mr. Larsen's answer to that is his description of the practice of furnace A where, by "controlled leakage," the operators supply a large excess of cold charge-combustion air directly into the melting chamber in order to keep the checkers hot enough to furnish hot fuel-combustion air.

Mr. Larsen's table of data descriptive of furnace A shows percentages based on the percentage of theoretical air, which he defines as total air required for combustion of fuel plus carbon monoxide from the bath. The writer believes that one's thinking is helped by referring "preheated air ingoing through checker" to fuel-combustion air. With the conditions as given, the hot air from the checker was approximately 103 pct of theoretical fuel-combustion air which, with reasonably good port and burner design, will allow good flame development. One may picture, then, a core of hot fuel-combustion air surrounding the flame and moving with it through the furnace and in turn more or less surrounded by a cooler mass of inleaking air which is heated by burning the bath gases and by convection from the hot surfaces in the melting chamber. This latter mass substantially is transparent to radiation and hence slows down the furnace very little.

Mr. Larsen has, in effect, given us a rule for determining if a checker is too small. Practically any checker can be operated at the maximum safe temperature of the top course of bricks by using the "controlled-leakage" technique. If that checker will then heat the fuel-combustion air for the maximum fuel to a good high temperature, it is big enough for maximum tons per hour from that furnace; any increase in size will save fuel but will not appreciably increase tons per hour.

These statements may be somewhat oversimplified but do come close to expressing the practical operating philosophy obtainable from this excellent paper.

**R. A. Lambert** *(Jones & Laughlin Steel Corp., Pittsburgh)*—The contribution that Mr. Larsen has offered to the Steel Institute and now to AIME is a most excellent presentation of "Regenerator Efficiency and Air Preheat in the Open Hearth" and will continue the emphasis, for operators, on the appreciable gains which can be obtained from high heat recovery through more efficient regeneration, gains not only in fuel savings as such, but in increased productivity. This is especially so in curtailed-production periods like the present when we seek optimum furnace operation primarily for overall lower ingot-manufacturing costs rather than high production rates only.

The paper by John Marsh[1] and referred to in Mr. Larsen's presentation is closely allied to the latter's paper in ultimate objective. The extent of agreement of the two papers certainly indicates that high air preheat is unquestionably a very important contributor to high furnace-production rates. The extent of divergence of the papers serves to stimulate mentally those fuel engineers associated with open-hearth practice in case they have become too complacent and assured in their analysis and interpretation of combustion phenomena and its related influencing factors.

An obvious first step in any comment on Mr. Larsen's data was to check the charts he presented in Figs. 1 and 6. The furnace A referred to in the paper bears some resemblance to our Pittsburgh Works Div. No. 31 furnace. Physical data on this furnace is as follows:

Forty-two net-ton stationary 100 pct cold-metal furnaces are used for foundry castings. The production rate is low due to time delays in meeting molding schedules. The regenerators are small, 12x9x6 ft in depth. Bath area is 188 sq ft, while the heating surface of checkers is only 2858 sq ft. Several tests in past years on this furnace have indicated that, with high draft (about 0.09 in. water draft at the foreplate level of the exit-end door), we cannot burn more than 155 gal of oil per hr and maintain more than 15 pct excess air in outgoing gases. There is no forced-draft combustion-air fan for the furnace and neither is there any waste-heat boiler to require us to burn fuel through the furnace for steam generation.

Since no combustion-air measurement through the regenerators is provided, we had to measure as closely as possible, through the square-type plate valve, the air entering the inlet flue to the regenerator chambers. These admittedly rough measurements indicated that 135,000 cu ft per hr or about 61 pct of the theoretical air was through regenerators and preheated as compared to the 87 pct in the furnace A of Larsen's paper and with an average of 1700°F preheat or 140°F less than furnace A. While undoubtedly some additional leakage occurred, the system appeared fairly tight and is relatively small. No tests were made of air pickup

within the regenerator. Calculations and complete data for the furnace are shown in Table IX. Since temperature spreads were relatively close to those in furnace A of the paper and to avoid cumbersome calculations, the same values for $S_g$ and $S_a$ specific heats were used. It was noted, incidentally, that $H_2O$ vapor has a decided influence on the specific-heat value. Results of tests and calculations indicate an $E_L$ value of 43.2 pct, which is the limiting efficiency under the conditions of furnace operation and which Mr. Larsen has termed "drift ratio." The $E_R$ value indicates at 29.8 pct, which is the actual regenerator efficiency as fuel engineers understand it. Note that the air flow per 1000 sq ft of heating surface is 3650 lb per hr.

Fig. 9 was prepared on which was copied the Fig. 1 of Mr. Larsen's paper and on which was plotted, by extrapolation, a curve to represent the $E_L$ value from the Jones & Laughlin No. 31 Furnace of our Pittsburgh plant. From the calculations previously shown, the pounds of air per hour per 1000 sq ft heated surface in this J&L furnace was 3650, which is much higher than the 2860 in the furnace A of Larsen's paper. However, reading from these two values, $E_L$ and air flow, the chart $E_R$ value is indicated at 27 pct. This comes close to the 29.8 pct as calculated. Larsen's "Electric Analogue," to derive an $E_L$ curve for variable loading conditions, obviously is a very worthwhile device. Absolute efficiency, in this instance, is 69 pct as compared to that for Larsen's furnace A of 72 pct, yet with the J&L furnace at 140°F less preheat-air temperature. While the two regenerators are probably different in physical design, it is not doubted that, if on the J&L furnace draft could be further increased to permit additional infiltration above sill level at the outgoing end and more fuel fired, a corresponding increase in top checker temperature and air preheat would result. Under such conditions of higher air preheat and consequent higher flame temperatures, it is believed that higher production rates would result. However, top-brick checker work would be more sensitive to high temperature and an excessive rebuild maintenance could result with higher fuel consumption. Mr. Larsen recognizes this also. The Fig. 6 of his paper indicates about 70 pct of the total air heating is done in the top third of the regenerator chamber. Under such conditions, I concur with Mr. Larsen's statement: "It strongly indicates how air-preheat temperature, measured in uptakes, has no necessary relation to *adequacy* of regenerator size and design and that high flame intensities should be obtainable in almost any commercial open hearth if properly managed. Also, it shows that such a result, if regenerators are too small, too inefficient, or too heavily overloaded, is obtained at the cost of excess fuel, partly wasted in the form of an excessive volume and temperature in the combustion gases flowing to the stack or waste-heat boiler."

At this point, I should like to refer to Mr. Marsh's original paper, since Mr. Larsen has done so. Mr. Marsh states: "Proponents of large flow of excess air are evidently in a difficult position. Although almost too obvious to justify mention, furnace pressure is surely a controller of infiltration, hence, air temperature." As

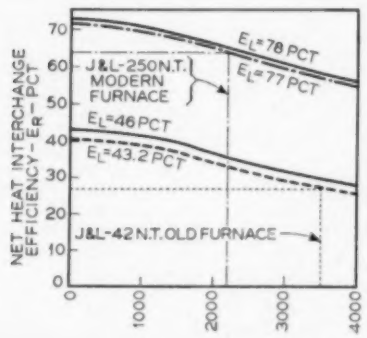


Fig. 9—Air-flow load on regenerator in lb per hr per 1000 sq ft of wiped surface.

**Table IX. Regenerator Efficiency. Data and Calculations for No. 31 Furnace***

| | |
|---|---|
| **Test Data** | |
| 155 gal oil per hr at 143,000 Btu per gal = | $22.17 \times 10^6$ Btu per hr fuel input |
| Orsat analysis | 15 pct excess air |
| Temperature of air entering regenerator, 270°F (calculated) = | $Ta_1$ |
| Preheat air, 1550° to 1850°F, or mean 1700°F = | $Ta_2$ |
| Temperature of waste gases entering regenerator, 2360°F (taken with optical) = | $Tg_2$ |
| Temperature of waste gases leaving regenerator, 1680°F (mean) = | $Tg_1$ |
| Air entering regenerator | 135,000 cu ft per hr |
| **Calculations: Weight of Waste Gases Entering Regenerator** | |
| 155 gal fuel oil x 8.238 lb oil per gal = | 1277 lb fuel oil per hr |
| Theoretical air = | 222,000 cu ft per hr |
| Then 222,000x1.15x0.07655 lb air per cu ft = | 19,545 lb air per hr |
| Total weight of gases entering regenerator = | 20,882 lb per hr = $Wg$ |
| **Calculations: Weight of Air Entering Regenerator** | |
| 135,000 cu ft per hr x 0.07655 lb air per cu ft = | 10,435 lb per hr = $Wa$ |

$$E_L = \frac{Wa\,Sa\,(Tg_2 - Ta_1)}{Wg\,Sg\,(Tg_2 - Ta_1)} \times 100 = \frac{10{,}435 \times 0.263\,(2360 - 270)}{20{,}882 \times 0.305\,(2360 - 270)} \times 100 = 43.2 \text{ pct}$$

$$E_R = \frac{Wa\,Sa\,(Ta_2 - Ta_1)}{Wg\,Sg\,(Tg_2 - Ta_1)} \times 100 = \frac{10{,}435 \times 0.263\,(1700 - 270)}{20{,}882 \times 0.305\,(2360 - 270)} \times 100 = 29.8 \text{ pct}$$

$$\text{Lb air per hr per 1000 sq ft regenerator surface} = \frac{10{,}435}{2.856} = 3650$$

* No appreciable bath reactions were noted during the test; such effects were ignored. Rated capacity: 42 net tons, 100 pct cold-metal furnace. Bath at fore plate: length, 22 ft 10 in.; width, 8 ft 3 in.; depth, 2 ft; area, 188 sq ft. Checkers: length, 12 ft; width, 9 ft; depth, 6 ft. Flues: chimney, 5½x5½ in. Exposed heating surface: 2858 sq. ft.

to just how much is "large flows," Mr. Marsh is not specific. I take Mr. Larsen's position that regenerator size and design and field-performance efficiency dictates, to very appreciable extent in the older furnaces, the excess-air needs, dependent upon production demands and the ingot-cost situation. It seems apparent that Larsen would not recommend that his furnace B (double-pass checkers) be carried with high draft and large flows of excess air above sill level. Furnace B passed 106 pct of theoretical air through regenerator chamber with a 23 pct excess air in waste gases at the outgoing end (I don't think 23 pct is too much for modern furnaces) and indicates an $E_A$ (absolute efficiency) of 88 pct. Further, it is questionable if any open-hearth furnace should be operated with a near-reducing atmosphere at the outgoing ends. Any sampling means for determination of atmosphere constituents at these high temperatures and with combustible and oxygen molecules at proximity at sampling-tube entry will always tend to indicate more complete combustion than actually exists in the gas stream due to a secondary combustion at the immediate sampling-tube entry. Therefore, from gas-analysis indications to set furnace atmospheres to about 1 pct $O_2$, which we hear is being practiced in some shops, in my opinion, will result in reducing atmospheres in the downtakes. For silica brick, this is said to be injurious; for basic brick this is reported to be more injurious.

For furnace C operation with the large single-pass regenerators, wherein large quantities of infiltrated air were existent in the upper regenerative zones (about 90 pct of the total infiltration into the chambers), subsequent illustrations and remarks by Mr. Larsen confirm Marsh's data relative to the importance of keeping such portions tight. It would be interesting to see com-

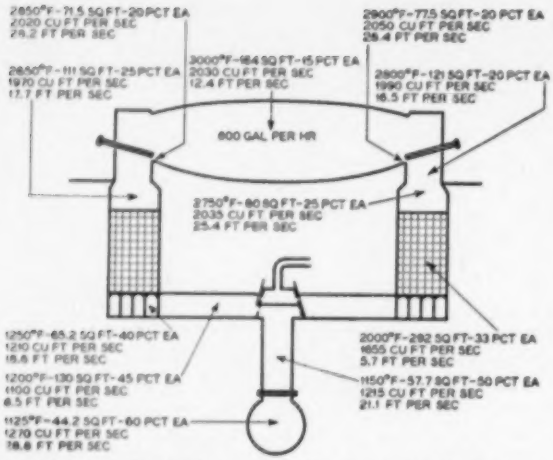
2850°F-71.5 SQ FT-20 PCT EA
2020 CU FT PER SEC
29.2 FT PER SEC
2900°F-77.5 SQ FT-20 PCT EA
2050 CU FT PER SEC
29.4 FT PER SEC
2850°F-111 SQ FT-25 PCT EA
1970 CU FT PER SEC
17.7 FT PER SEC
3000°F-184 SQ FT-15 PCT EA
2030 CU FT PER SEC
12.4 FT PER SEC
2800°F-121 SQ FT-20 PCT EA
1990 CU FT PER SEC
16.5 FT PER SEC
600 GAL PER HR
2750°F-80 SQ FT-25 PCT EA
2035 CU FT PER SEC
25.4 FT PER SEC
1250°F-65.2 SQ FT-40 PCT EA
1210 CU FT PER SEC
18.6 FT PER SEC
2000°F-282 SQ FT-33 PCT EA
1655 CU FT PER SEC
5.7 FT PER SEC
1200°F-130 SQ FT-45 PCT EA
1100 CU FT PER SEC
8.5 FT PER SEC
1150°F-57.7 SQ FT-50 PCT EA
1215 CU FT PER SEC
21.1 FT PER SEC
1125°F-44.2 SQ FT-60 PCT EA
1270 CU FT PER SEC
28.8 FT PER SEC

**Fig. 10—Theoretical performance of No. 4 open-hearth furnaces. *EA* represents excess air. All values represent performance during waste-gas travel.**

parisons of furnaces B and C with the minimum air leakage into regenerator chamber proper in both such designs. An attempt has been made to illustrate this by comparison of Larsen's furnace B with our recently installed furnaces having single-pass checkers. Fig. 10 indicates the performance anticipated before these J&L furnaces were built. Note that with a 25 pct excess air in the ingoing waste gases, there is a further anticipated pickup of 15 pct, totalling 40 pct at the end of the regenerator travel. We are now operating these 250 net-ton furnaces at about 15 to 20 pct excess-air setting at the downtakes (floorlevel) during the meltdown period. The furnaces are equipped with fuel-air-ratio controls which hold very well. To attempt a correction for combustible gases given off during reaction periods, we have advised a manual fuel cutback and a manual fuel-air-ratio reset to compensate. We are satisfied that fuel-air ratio is an aid, particularly with relatively inexperienced personnel on the furnaces. It is realized, as Mr. Larsen points out in his paper, that a sizable amount of oxygen is consumed in combustibles from bath reaction and in scrap oxidation, although frankly the latter has not been considered as appreciable. Fuel-air ratio does not compensate automatically for these bath combustibles.

We are seriously considering the installation of direct continuous oxygen analysis of the outgoing gases at the operating-floor level with such analysis tied into the reversal systems. Should the difficulties of sampling lines be satisfactorily resolved, we shall then proceed with having this oxygen-measurement function control the combustion air to the furnace. This should put under control the present unknown variable in oxygen demand due to bath reactions and scrap oxidation.

The furnace B of Larsen's paper with the double-pass checker design enjoys a high limiting efficiency $E_L$ of 73.2 pct with an absolute efficiency of 88 pct. The J&L single-pass checkers with regenerators 30 ft long by 18 ft 6 in. wide and a depth of 16 ft 6 in. setup, with 7½x7½ in. chimney flues for residual-tar fuel, has a total exposed heating surface of 36,500 sq ft compared to the 56,000 sq ft of Larsen's furnace B. Our Table X tabulates the comparison of incidental data. In both cases regenerators are well sealed. Calculations in the J&L furnace may not be quite as accurate, so I took the liberty of using Larsen's specific-heat values rather than calculate by the tedious process, inasmuch as water vapor affects the net value and Larsen's temperature ranges were within comparative limits.

The outstanding indications here again illustrate the accuracy of Larsen's Fig. 1. Fig. 9 indicates that the $E_L$ of 77 pct for the J&L furnace and the air flow of 2200 lbs per hr per 1000 sq ft of heated surface obtains an $E_s$ value of 64.0 pct, whereas the average of the air and gas $E_s$ values as calculated indicates at 59 pct. Note also that Larsen's double-pass checker had an absolute efficiency of 88 pct, while the J&L furnace was 77 pct, which probably indicates the J&L furnace regenerators can be somewhat improved to raise efficiency. Also, the double-pass regenerator efficiency averaged 64.5 pct with the J&L furnace at 59 pct, or 9 pct greater in fuel recovery, which confirms Larsen's remarks relative to the heat-recovery advantages of double-pass systems.

Some discussion is made in the paper about furnace control by checker-radiation units. Mr. Larsen remarks that such measurements aid the first helpers in giving a continuous indication of top-checker temperatures and would start reversing the furnaces on shorter cycles to give protection against excessive temperatures and serve as a warning to first helpers to either decrease fuel rate or increase air rate through checkers. Emphasis is made that a knowledge of high temperatures in this region would also indicate if the furnace was at maximum speed by actually reaching the maximum set point and so reversing the furnace ahead of the temperature-difference setting. While it is admitted, and rightly so, that this in itself is not the whole answer to the open-hearth complex control problem anymore than it is the frequent or continuous measurement of preheat air, such instrumentation poses to the reader's mind some question as to possible accuracy of measurements and maintenance involved.

Can we depend on this type of installation to render accurate measurement? Can these total radiation units be correctly calibrated by use of the optical pyrometer with its inherent measurement of a single wave length of light? Do such locals, where the unit is sighting on relatively large areas, simulate sufficiently accurate

**Table X. Comparison of Jones & Laughlin Furnace with Larsen Furnaces B and C**

| | Larsen's Furnace B | Larsen's Furnace C | J&L Furnace |
|---|---|---|---|
| Furnace capacity, designed for | 240 | — | 250 |
| Fuel input | 550 gal oil per hr | — | $95 \times 10^6$ Btu per hr { Oil & Gas |
| Checker data: | Double pass | Single pass | Single pass |
| Sq ft of wiped surface | 56,000 | 39,700 | 36,500 |
| Checker depth, ft | — | 14 | 16.5 |
| Checker length, ft | — | 30 | 30 |
| Checker width, ft | — | — | 19.5 |
| Condition of regenerator | Tight | Leaky | Fairly tight |
| Lb of air per hr per 1000 sq ft wiped surface | 1,100 | 1,800 | 2,200 |
| Lb of waste gases per hr per 1000 sq ft wiped surface | 1,410 | 3,820 | 2,670 |
| Total air in combustion gases, pct theoretical | 123 | 168 | 118 |
| Total air entering regenerator, pct theoretical | 106 | 86 | 110 |
| $Wa$: lb combustion air entering checkers | 61,810 | 71,820 | 80,375 |
| $Wg$: lb combustion gases into checkers | 78,960 | 151,030 | 97,390 |
| $Tg_1$: °F, waste gases leaving checkers | 1,110 | 1,420 | 1,270 |
| $Tg_2$: °F, waste gases entering checkers | 2,550 | 2,350 | 2,600 |
| $Ta_1$: °F, air entering checkers | 210 | 190 | 220 (calc) |
| $Ta_2$: °F, air leaving checkers | 2,240 | 1,680 | 2,040, 2150°F average air preheat into furnace |
| Pct $E_{Sg}$: efficiency of heat removal from waste gases | 66 | 46 | 60 |
| Pct $E_{Sa}$: Efficiency of heat storage in combustion air | 63 | 30 | 58 |
| Pct $E_L$: (drift ratio) limiting efficiency | 73 | 44 | 77 |
| Pct $E_A$: absolute efficiency | 88 | — | 77 |

black-body condition which is necessary to get correct calibration, particularly when checker or wall deposits can change so as to radiate changing temperatures? Tables set forth in Rhodes' *Industrial Instruments for Measurement and Control* indicate deviations from true temperature for coatings of iron oxide. Fig. 11 illustrates the extent of deviations. Note that, as the temperatures increase, the deviations from true temperature become greater. If this data is being interpreted correctly, at average top-checker conditions the error can be about 100°F on the low side, and if an estimated adjustment was not made, a low reading could be more damaging than a high reading.

When instrumentation and controls were being selected for the new open hearths at Pittsburgh J&L three years ago, we had considerable discussion about selection of either radiation units or flue thermocouples. It came to our attention from several sources that service maintenance on these radiation units was high and optical checks unreliable. We had had previous experience in our own shops with back-wall roof-temperature control, which was highly unsatisfactory from a maintenance standpoint. Of course, the latter is admittedly a more severe service. We decided on thermocouple installation in the flues and incorporated into the instrument as many similar features comparable to the radiation units as we could.

Fig. 12 illustrates what type of performance and record is obtained from this six-point circular-chart record. Stack temperature and atomizing-steam superheat is shown by the circular curves. The upper butterfly pattern is the familiar flue-temperature record. The lower radial lines indicate the temperature difference of the opposite end couples. There is also a maximum predetermined temperature setting to guard against excessive high temperature. If this is reached, the furnace will reverse. Early in the furnace-operating program, a platinum couple was inserted in the fantail arch and readings indicated that a maximum setting on the recording instrument of 1450°F would protect the top-checker brick to 2700°F. We realize that this reversal method has some shortcomings over any successfully operated radiation unit; however, the maintenance is negligible and the couples last several years, requiring cleaning only during flue cleaning.

A few months ago we abandoned a single-point roof-temperature control and experimented with a three-point control, with the fuel-air control throttled whenever any of the three points reached the predetermined control set-point. One location was in the roof center and the other two at the outgoing ends in the roof. It became evident that the center point was not necessary, and since then, three furnaces have been equipped with two-point control. An insufficient trial time does not permit any evaluations at this time; however, we are getting some very interesting results and they certainly reflect conditions which we believe will tie in with preheat-air temperatures and top-checker temperature. Recently we received a radiation unit which will be tried on one furnace with the two-point roof control and possibly the continuous oxygen recording

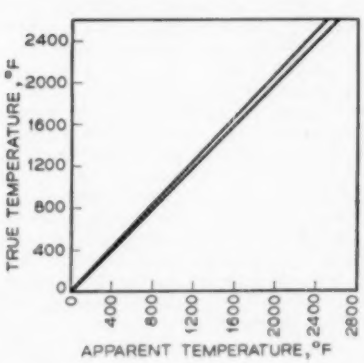


**Fig. 11—True vs apparent temperatures of radiation from iron-oxide coatings. From Rhodes' *Industrial Instruments for Measurement and Control*.**

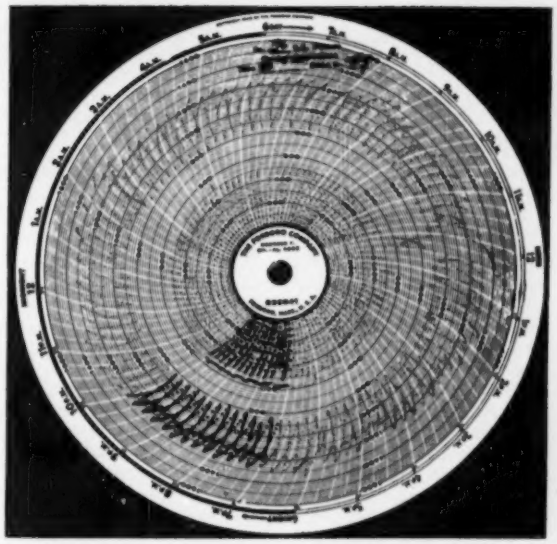

**Fig. 12—Type of performance and record obtained from J & L six-point circular-chart record.**

tied into fuel-air ratio. We shall certainly also take preheat-air temperature and perhaps we can place the open-hearth heat system under closer control.

Summarizing briefly, it is apparent that both Larsen and Marsh are in agreement on maintaining tight checkerwork below the sill level. It is questionable if we want to maintain a too low excess air in outgoing gases. I believe that, in most instances of modern furnace operation, 15 to 20 pct excess air is not too excessive. It is also recognized there are undercheckered furnaces that can be operated with high excess air to increase productivity at the expense of higher fuel costs, higher maintenance costs, and lower furnace availability. While there is not agreement here with Larsen's minimizing of preheat measurements, yet there is also no agreement with Marsh's position in the original paper that air-preheat influence is powerful enough to nullify other factors to the extent that, on the average, heat time is inversely proportional to air temperature. What about charging time, carbon at half lime-up, timing of hot-metal additions, tapping carbons, undesirable residuals, slag conditions and analysis, and a host of other variables? A qualifying statement that, were all other factors relatively equal, air preheat has large influence on furnace speed would be an acceptable premise.

Before concluding, I should like to ask Mr. Larsen to clarify the following:

1—On page 136,[12] Mr. Larsen states that the $E_L$ of 78 pct represents results to be expected on an ideal furnace. What are the limiting factors that do not permit higher efficiencies?

2—In the same paragraph,[12] it is stated that the maximum possible net efficiency is about 70 pct with non-preheated fuels. Does this refer to absolute efficiency $E_A$ or the $E_L$ value and why?

3—In actual practice, what, in Mr. Larsen's opinion, is the minimum air infiltration to expect through regenerator system on the waste-gas cycle? Would the same hold for the combustion-air cycle?

4—What merit would there be in a continuous oxygen analysis of waste gases at operating-floor level? Could such data be put to useful practical purpose?

5—Under what conditions would Mr. Larsen suggest higher excess air than that used on his furnace B? Would he recommend a lower excess air?

Mr. Larsen has performed a most commendable and outstanding service to the AIME and to the open-hearth section of the steel industry in development and

presentation of this paper. The many years of data collecting and painstaking work in this accumulation is a splendid example to all of us in our service to the industry. His work contributes to the standards of performance evaluation in open-hearth practices to gain what we are always seeking, high productivity with lower manufacturing costs.

[19] Paper under discussion: *Trans.* AIME (1954) **200**, pp. 129-144; JOURNAL OF METALS (February 1954).

**B. M. Larsen** (author's reply)—Mr. Lambert's checks on net efficiency in two very different furnaces are close enough to the curves of Fig. 1 to be very encouraging. In fact, the deviation from agreement for his larger new furnace is probably of equal significance. The limiting efficiency ($E_L$) here was 77 pct and the air-flow load 2200 lb per hr per 1000 sq ft which should have given an $E_n$ value of nearly 65 pct, whereas his indicated actual $E_n$ was only 59 pct. This brings out a point which was not very specifically developed in the paper, namely, that Fig. 1 is a simplification based on the assumption that the air-flow velocity and, therefore, the coefficients of heat transfer per unit surface are roughly constant over the load range. In Lambert's new furnace with long single-pass chambers, these levels are very probably much lower than for our A and B-furnace cases, so his net efficiency should be low relative to Fig. 1, as he finds. Since the paper was written, we have made another test on a similar single-pass system and find a very similar deviation. This, in brief, tends to prove the point that the double-pass design has an added advantage caused by the much higher flow velocity which gives increased coefficients of heat transfer per unit of wiped-surface area. The gains in efficiency, of the order of 5 to 8 pct in $E_n$, are more important than might appear because they are at the high and where further gain (see Fig. 6) is hard to obtain, but which also is "all gravy" in terms of hotter air or higher capacity for excess preheated air supply.

Our own experiences with total radiation measurement of top-checker temperature have on the whole been encouraging despite some practical difficulties. Optical-pyrometer checks are most accurate on the air-flow period of the reversal cycle, toward the end of which the rate of change in apparent brick temperature is slow enough to favor a fairly accurate comparison with recorder values from the total radiation receiver. Surface emmissivities are moderately high, coupled with a condition not too far from black-body conditions, so that errors are not really serious.

In regard to Mr. Lambert's concluding questions:

1—$E_L$ values for the common fuels can be higher than around 78 pct only if there is considerable excess air, which tends to give a small decrease of overall furnace efficiency. Thus, we considered this as an approximate limit for an "ideal furnace."

2—The 70 pct limit for nonpreheated fuels refers to net efficiency ($E_n$) and is based simply on the fact that products of combustion are 20 to 25 pct higher in heat capacity than the air required, plus the practical limits of deep-checker design.

3—The question about air leakage is a tough one. We have encountered apparent total leakages down as low as 3 to 7 pct, and I think it is possible to have leakage, in regenerator zones only, of less than this range on "waste-gas cycle." It is, of course, extremely difficult to *maintain* such low leakage levels. I think that air leakage tends to be less during the combustion-air period.

4—Certainly continuous oxygen analysis somewhere in the outgoing stream has a highly potential practical value. Just where it is best to sample, I do not think we know as yet.

5—I suspect that around 5 to 10 pct excess air *above the total for both fuel and bath gases* might be high enough. The difficulty lies in the uncertainty of how much is needed for bath requirements.

The writer finds himself in essential agreement with Mr. Eberhardt's remarks and would like to express his very sincere appreciation for both of these discussions.

---

## Examination of a High Sulphur Free-Machining Ingot, Bloom and Billet

by D. J. Carney and E. C. Rudolphy

*DISCUSSION, H. B. Emerick and W. O. Philbrook, Chairmen*

**D. C. Hilty** *(Electro Metallurgical Co., Niagara Falls, N. Y.)*—Dissection of a six-ton ingot with sufficient thoroughness to permit an evaluation of segregation and inclusion distribution is a formidable undertaking and the authors are to be commended for accomplishing such a task. This work adds materially to our store of factual information on ingot structure and inclusion formation.

It is considered, however, that further explanation of the observations relating to the distribution of oxides and sulphides is desirable. As the authors suggest, consideration of the liquidus surface of the Fe-Si-Mn-S-O system may be helpful in this respect. In the portion of the Fe-Mn-S-O system of greatest interest, metal-oxide and metal-sulphide miscibility gaps combine to form a continuous region of liquid immiscibility separating the metallic and nonmetallic liquids. Metal-sulphide and metal-oxide eutectics originate near the metal corner, cross the miscibility gap, and join with a sulphide-oxide eutectic to form a ternary eutectic located near the sulphide-oxide side, somewhat closer to the sulphide than to the oxide corner.

The introduction of a small but significant amount of silicon, such as that contained in the ingot examined by the authors, into the Fe-Mn-S-O system is known to lower the melting point of the oxide phase below that of the metal, presumably without greatly affecting the sulphide phase. As a result, the origin of the metal-oxide eutectic is shifted to the oxide side of the miscibility gap, and this eutectic no longer intersects the gap. Moreover, the oxide-sulphide eutectic and the metal-oxide-sulphide eutectic are shifted toward the oxide corner of the system.

The initial stage in the solidification of steel in this system, therefore, would be the rejection of an oxide-rich liquid, subsequently accompanied by the freezing of metal. It seems reasonable to expect that a substantial amount of this liquid would be trapped in the form of droplets in the portions of the metal that solidified first, thus accounting for the segregation of oxygen (and silicon) in the bottom of the ingot described by the authors. These droplets solidify as individual systems and may appear as duplex inclusions of oxide and sulphide when their solidification paths reach the metal-oxide-sulphide eutectic.

As solidification progresses, the immiscible liquid

becomes richer in sulphide, and during the later stages there is simultaneous freezing of metal and sulphide. In the last liquid to solidify, oxide will again appear with the sulphide at the ternary and higher eutectics which probably exist in this complex system, a condition that produces the duplex inclusions observed by the authors in the center of the top half of the ingot.

It is emphasized that the above rationalization is based mainly on inference from such of the side diagrams of the Fe-Si-Mn-S-O system as are known and, on inverse reasoning from the appearance of the inclusions. This system is quite complex, especially at higher silicon contents where silica appears as a separate phase and an additional miscibility gap between oxide and sulphide-rich liquids is probably in evidence. Experimental clarification is greatly to be desired.

**S. J. Beckman** *(Jones & Laughlin Steel Corp., Pittsburgh)*—The segregation characteristics of high sulphur-free machining steels have received some study at Jones & Laughlin. Our 1213 grade is made in 25x27x80 in. bottle-top molds. An investigation of the billet product of 13 ingots from three heats has shown the existence of maximum positive and negative segregation within the top 15 pct of the ingot below the crop. The ingots were bloomed to 5x5 in. billets, billet sections taken from the top and bottom of the top cut, and the bottom of successive cuts. The billets were rolled to 1⅜ in. rounds and tests obtained corresponding to the billet tests. Check analysis for carbon and sulphur on the bars from the top and bottom of the top cut is summarized in Table IV.

**Table IV. Check Analysis for Carbon and Sulphur from Top and Bottom of Top Cut**

| Variation in Chemistry from Middle Cut | | | |
|---|---|---|---|
| Pct C | Pct S | | |
| −0.01 | −0.06 | Maximum | Top of 1st cut |
| 0 | 0 | Minimum | |
| 0 | −0.03 | Average | |
| +0.02 | +0.06 | Maximum | Bottom of 1st cut |
| 0 | +0.01 | Minimum | |
| +0.015 | +0.03 | Average | |
| 0.02 | 0.06 | Average difference top to bottom of billet | |

Sulphur prints on these billet sections reflect the difference by a pronounced center segregation in the bottom of the first cut. Center, mid-radius, and edge drillings were made on the billet sections and checked for sulphur and carbon. Superimposed sulphur checks are shown on the reproduced sulphur prints for some typical patterns obtained. The sulphur prints are identical to comparison etch tests made on the same billets.

**F. W. Boulger** and **H. L. Shaw** *(Battelle Memorial Institute, Columbus, Ohio)*—The authors are to be congratulated on their thorough study of the segregation and inclusion characteristics of mechanically capped B1113 steel. The information is timely and important because of the current interest in resulphurized steels. This is probably the first article to describe the changes in inclusion shape and size during rolling of such steels. This part of the paper is of particular interest because the correlation between inclusion characteristics and machinability is becoming widely recognized.

Fig. 16 summarizes the authors' observations that the inclusions increased in *L/W* ratio and number and decreased in size during hot working. Some of this information warrants further discussion. Although the percentage reduction from ingot to bloom approximated that from bloom to billet, the changes in inclusion characteristics were not the same for both stages. Despite the variation in the ingot, the inclusion size was fairly constant after blooming. During this rolling operation, the change in inclusion size was directly proportional to the original size and inversely proportional to Mn/S ratio. Neither relationship held as well for the size changes in rolling the bloom to the billet. The data also show that inclusions in the billets had *L/W* ratios ranging from about 3.5 to 5.0. The range was greater in samples from blooms. This suggests that inclusions which did not receive much extension during blooming were elongated the largest amounts while rolling billets. Neither the changes in *L/W* ratios from ingot to billet nor the ratios in the billets seem to be influenced by either silicon content or Mn/S ratio at various locations.

Some of these observations differ from those made by Van Vlack[8] on bars of mechanically capped B1112 steel. In the bars he examined, both the number and the *L/W* ratios of the inclusions increased with silicon content. Furthermore, Van Vlack found that, in three of four cases, inclusions in bars from butt cuts had larger *L/W* ratios than those from middle cuts. His data showed that bars from butt cuts always exhibited poorer machinability in turning tests. Van Vlack's conclusions on the influence of size and shape of inclusions suggest that billet 18B (bottom) from the authors' ingot would have the best machinability. Therefore, it would be interesting to know whether this billet was better or worse in machining tests than billet 2T from the top of the ingot. The authors' opinion, or data, concerning the changes in size and shape of the inclusions when these billets were rolled to bars would also be appreciated.

There are reasons for suspecting that the composition and shape of sulphide inclusions change with heat treatment after solidification. Such changes might alter their deformation characteristics and the shapes measured after different stages of rolling. The discrepancies noted in Fig. 16 and in comparisons with Van Vlack's observations might result from such effects. Therefore, several questions seem pertinent. Was the ingot cooled below 1000°F before blooming? What were the initial and final rolling temperatures for the blooms and billets? Were the blooms cooled and then reheated before rolling to billets?

Foundrymen have shown that inclusion size depends principally on solidification time and that silicates and sulphides are globular in weakly deoxidized steels. The authors found that these observations held for their large ingot. Their quantitative data are very welcome and much more convincing than deductions which might be made from experiments on smaller castings.

**D. J. Carney** and **E. C. Rudolphy** (authors' reply)—The authors wish to thank the discussers for their kind comments and additional information.

We were pleased to have Mr. Hilty's discussion of our observations relating to the distribution of oxide and sulphide inclusions. The interesting discussion of the liquidus surface of the Fe-Si-Mn-S-O system aids in the explanation of the separation of the silicate and sulphide inclusions.

Mr. Beckman's observations on C1213 at Jones & Laughlin were quite interesting, particularly his notation of the maximum positive and negative segregation within the top 15 pct of the ingot below the crop. This result was not obtained in our study.

In reply to the discussion by Messrs. Boulger and Shaw concerning apparent differences in the authors' observations and those of Van Vlack,[8] certain facts should be borne in mind. Van Vlack's studies were made on bars, and significant differences in inclusion characteristics can exist on comparison of bar sections and billet sections. It should also be noted that the values for the *L/W* ratios of inclusions varied from center to surface. Other important factors to be considered are the billet and bar size and the rolling and finishing temperatures when rolling from billets to bars.

No data were obtained in the present study on the effects of rolling the billets studied to bars. However, data has been obtained on rolling bottom cuts similar to 15T and 18B from other heats of this grade to bars. These data show the following: 1—The inclusion size decreased from 10 to 50 pct. 2—The *L/W* ratio increased from 10 to 25 pct. 3—The number of inclusions

increased from 10 to 30 pct. Thus, significant changes in inclusion morphology can take place in rolling the billets to bars.

In answer to the other questions posed by the discussers, the ingot was not cooled below 1000°F prior to rolling. The ingot was heated and drawn at 2375°F for rolling to blooms and billets. The finishing rolling temperatures for blooms and billets of this grade are 1900° to 2000°F and 1600° to 1700°F, respectively. The ingot was rolled directly to billets, with no intermediate reheating of the blooms.

Machining tests were not run on steel from this examination so that machinability/inclusion-characteristics relationships were not made in this study.

In Fig. 8, the schematic diagram of the bottle-top ingot was drawn with an unnoticed error. This diagram should show a big-end-down bottle-top ingot as described in the text.

---

## Development of Oxygen Steelmaking

by Otwin Cuscoleca

*DISCUSSION, H. B. Emerick and W. O. Philbrook, Chairmen*

**H. B. Emerick** *(Jones & Laughlin Steel Corp., Pittsburgh)*—"It is true that in the practical realization of new ideas one's fantasy should not be allowed to go unchecked; but it is still not right to bring the conceivable difficulties too much into the foreground at the outset. Many an idea that was in itself good, has had to wait a long time for its realization because too much attention to its difficulties obscured its advantages, and because too much hesitation has for too long prevented the taking of bold steps forward." These statements are quoted from the concluding portion of a technical article by the eminent Swiss metallurgist Robert Durrer.[∞] Professor Durrer, of course, was referring to the fact of Henry Bessemer's recognition almost 100 years ago that the use of oxygen instead of compressed air for converter blowing was metallurgically desirable.

Acting upon his own advice, Dr. Durrer in 1947 instigated successful experiments with pure oxygen top blowing on a two-ton converter at Gerlafingen, Switzerland. Following this work, further pilot-plant development of the idea took place at Linz and Donawitz in Austria. The ultimate result was an entirely new concept of converter steelmaking which is now presented as a mature commercial process.

We in America are indeed grateful to Mr. Cuscoleca, and to the federated Austrian steel industry which he represents, for this comprehensive presentation of the economic, technical, and operating aspects of the oxygen steelmaking process.

There are a number of problems surrounding adaptation of the oxygen-steelmaking process to American practice and Mr. Cuscoleca's extensive experience with the process in Europe should make his opinions on these questions take on special significance. One of the foremost obstacles, of course, is the air-pollution problem to which Mr. Cuscoleca referred. Good chemical-analysis control and reproducibility must be assured if uniform acceptance over a wide range of products is to be obtained. Finally, operating costs and process yields must be at least equal to those available alternative processes.

In the matter of vessel linings, for example, Mr. Cuscoleca has stated that in Austria the converters are lined with unburned bricks pressed from a mixture of sintered magnesite and tar. This description, I believe, applies to the inner or working lining of the vessel, behind which there is a rammed layer of tar-bonded high magnesia refractory. According to Mr. Cuscoleca, the lining must be patched or replaced after approximately 250 heats, or roughly after one week of operations. Although the unit consumption of refractories (24 lb per ton of steel) appears to be lower than for the open hearth, obviously the "down time" for vessel relining is relatively great and improved lining life would be highly desirable in order to increase "availability" of converter equipment. This leads to two questions on which the author's comments will be appreciated:

1—What are the prospects for attaining substantially increased lining life, either by improvements in refractories or by modified operating techniques to counteract the damaging effects of siliceous slags formed early in the blowing cycle?

2—What type of refractory construction is used in the detachable bottom and what is its life in relation to that of the vessel-body lining?

Two other questions, not related to refractories, are:

3—In the case of plants desiring to utilize available scrap in other directions, what metallurgical effects might be anticipated from substituting lump ore or sinter as coolants?

4—Fig. 10 indicates that approximately 60 pct of the oxygen-steel heats finished over 0.015 pct phosphorus, though Donawitz pig iron contains only 0.2 pct Si and 0.075 pct P. Many applications in this country require phosphorus content below 0.015 pct. Assuming 1.25 pct Si and 0.10 pct P hot metal, is it considered feasible to operate the process, by manipulation of lime additions, to consistently produce 0.015 pct maximum phosphorus content?

**Otwin Cuscoleca** (author's reply)—The attack of the acid slag, with a high silicon content in the hot metal, on the lining of a converter can be prevented to a great extent by the use of small-sized lime which will result in the formation of a quick-combination lime silicate. By this method, we should be able to expect a lining life of 200 to 300 heats even with 1.25 pct Si in the hot metal.

The converter bottom is made of burned-magnesite blocks. After approximately 250 heats, the lining thickness will be decreased 200 cm in the bottom and approximately 500 to 600 cm in the lower part of the converter walls. The life of the converter lining at the present time is 250 heats, and it is expected that the lining life will be increased further.

The necessary cooling of the bath is achieved by the use of lump ore, or still better, by sinter or limestone. The addition of lump ore and sinter can be limited for metallurgical reasons on account of a possible violent reaction. Sufficient cooling can be achieved by an addition of solid pig iron and limestone.

With the content of 0.10 pct P in the hot metal, it will be possible, even with 1.25 pct Si in the hot metal, to produce 80 to 90 pct of the heats with a maximum phosphorus content of 0.015 by adding corresponding volumes of lime.

[∞] R. Durrer: Oxygen as an Aid in Metallurgical Processes. *Stahl und Eisen* (1937) 57.

## On the Basic Bessemer Process

by Pierre Coheur and Hans Kosmider

*DISCUSSION, H. B. Emerick and W. O. Philbrook, Chairmen*

**A. B. Wilder** *(National Tube Div., United States Steel Corp., Pittsburgh)*—Drs. Coheur and Kosmider are well qualified to discuss the basic-bessemer process and therefore have presented a very interesting paper. There are several questions which may develop information of further interest:

1—In blowing with oxygen/steam, does the presence of hydrogen gas affect the properties of the finished steel with respect to embrittlement or flaking tendencies?

2—Is it practical to use air during the first half of the blow and oxygen/steam during the second half and produce steel with 0.004 pct N? This would reduce the cost of oxygen.

3—Can steel be produced from iron containing 0.25 pct P rather than 1.75 pct P with oxygen/steam?

4—To what extent does the use of steam cool the bath?

5—What effect does oxygen/steam blowing have on tuyere life?

6—Table III shows that 1755 cu ft of oxygen are required per ton of steel. This value appears to be low, and a question is raised regarding the conversion of metric into English units.

7—May oxygen with 50 or 75 pct purity be used for oxygen/steam blowing to produce steel with 0.004 pct N?

8—In Figs. 17 through 19 concerning work hardening, were the steels heat treated and what was the nitrogen content of the open hearth steel?

**Pierre Coheur** and **Hans Kosmider** (authors' reply)—First, as we reported, we are using the oxygen/steam mixtures in order to decrease the nitrogen content of our *rimmed* steel. In this case, we have never noticed any embrittlement or flaking tendency of the finished steel. Moreover, we have checked the $H_2$ content of the liquid steel at the casting pit. The time lapse from the moment the sample was taken from the ladle to the moment we placed it in the dry ice was 30 sec.

Our latest figures are: 0.24 to 0.37 cu in. (4 to 6 cu cm) of $H_2$ per 3.5 oz (100 g) when blowing with oxygen/steam vs 0.24 to 0.31 cu in. (4 to 5 cu cm) when blowing with enriched air.

2—Blowing in two phases certainly reduces the cost of oxygen, but from a theoretical point of view it is not recommended, since the two kinds of blast passing through the bottom do not have the same volume. In order to smooth the blow, it is always advisable to adapt the blowing surface of the bottom to the composition of the blast. Nevertheless, we have blown many charges in two phases and produced a steel with an $N_2$ content below 0.004 pct. The oxygen consumption was of the order of 1412.40 cu ft (40 cu meter) per ton of iron, i.e., 30 pct less than when blowing with oxygen/steam only.

3—The answer is yes.

I should like to mention the results obtained by E. Eichkoltz, Behrendt, and Th. Kootz.[1] In the course of one week, blowing with atmospheric air, they converted in a basic converter more than 6613.8 short tons (6000 metric tons) of pig iron containing 2.5 to 3.2 pct Mn, 0.50 to 0.85 pct Si, 0.10 to 0.25 pct P, and 0.02 to 0.04 pct S. The temperature of the pig iron, when charged, was between 1240° and 1260°C, except for a special lot in which the temperature ranged from 1190° to 1200°C. The total blowing time was practically the same as that for the standard practice and was related to the composition of the pig iron. However, the time consumed before pouring the steel was shorter because of smaller quantities of slag and the lighter addition of Fe-Mn. A great number of blows might be poured in the ladle without adding Fe-Mn. The loss of Fe is more than 1 pct below that of the basic-bessemer blows, but the yield is about the same. Lining wear was about 10 pct higher, while bottom life was improved.

Dr. Kosmider recently had the opportunity of successfully blowing numerous charges of steel, containing traces of iron ("Stahl Eisen"), the composition of which was: 4.2 pct C, 2.1 pct Mn, 0.50 pct P, and 0.65 pct Si. He used either an enriched air or the mixture of oxygen/steam. His results were recently discussed in Düsseldorf and will be published shortly.[2]

4—A mixture of oxygen/steam containing between 60 and 65 wt pct oxygen and 40 to 35 wt pct steam has the same thermogenic power as atmospheric air for a 15 ton converter. In other words, for a given liquid iron and when other circumstances are equal, we add the same quantity of scrap to cool the bath when blowing with either atmospheric air or with oxygen/steam. If we want to increase (or decrease) the quantity of the metallic addition, we have to increase (or decrease) the oxygen content of the blast. For example, with 56 pct of oxygen in the mixture, the quantity of scrap added into the converter is 3 to 4 pct of the iron. With 63 pct of oxygen in the mixture, the amount of scrap is 6 to 9 pct.

5—When the steam condenses on the refractories, the life of the tuyeres is indeed very short. That is one of the reasons why we superheat the steam or the oxygen/steam mixture. By doing so, the bottom life is almost the same as when blowing with atmospheric air.

6—A figure of 63 cu meters of oxygen per metric ton of iron, or 2000 cu ft per short ton of iron, is correct when blowing with oxygen/steam.

7—The purity of the oxygen we used is between 95 and 99 pct. We have had no experience with blows of 50 or 75 pct pure oxygen.

8—The nitrogen content of the open hearth steel was between 0.004 and 0.006 pct. In Figs. 18 and 19, the steels were not heat treated. The steels in Fig. 17 were normalized.

Details of our physical results can be found in refs. 3 through 5.

[1] E. Eichkoltz, G. Behrendt, and Th. Kootz: *Stahl und Eisen* (1940) **60**, pp. 61-72.
[2] H. Kosmider: To be published in *Stahl und Eisen*.
[3] *Revue de Métallurgie* (1951) pp. 17-46.
[4] *Revue Universelle des Mines* (April, November 1952).
[5] *Ossature Métallique* (April 1954).

---

## Solid Phase Indentification in Partially Reduced Iron Ore

by Gust Bitsianes and T. L. Joseph

*DISCUSSION, Gerhard Derge and John F. Elliott, Chairmen*

**R. Wild** *(Imperial College of Science & Technology, London, England)*—Messrs. Bitsianes and Joseph have made a most interesting and valuable contribution to our knowledge of the behavior of iron ores during

reduction. I would, however, like to make a few criticisms and comments on certain details of their investigation.

The authors' decision to use hydrogen rather than carbon monoxide as the reducing gas is, I feel, to be regretted, since, as they themselves admit, there are appreciable differences in the behavior of these two gases toward iron oxides. Certainly carbon deposition interferes to some extent with reduction, especially at lower temperatures; but this does not affect the identification of the solid phases within the partially reduced specimen. The use of hydrogen for quenching, rather than pure nitrogen, seems surprising, since reduction will be continuing during the quenching process.

The rate of flow of hydrogen used would appear to be adequate but it would have been advantageous to have checked this by carrying out preliminary experiments at varying rates of flow. A flow-rate could then have been chosen which was known to have no limiting effect upon the reduction.

The reasons which the authors give for their choice of the ore used for this work seem to be unnecessarily limiting. Although those ores which break up on heating or which, because of their chemical or physical structure, do not reduce evenly must be avoided; porous hematites or limonites may be used providing that they are reasonably homogeneous in structure. The reason given for avoiding magnetites seems surprising, since the dense Swedish magnetites, which are commonly used in Great Britian, have considerable similarity in structure and in behavior during reduction.

The use of blocks of ore seems hard to justify other than by the simplicity of their preparation. Cylindrical specimens, which can be prepared from any ore with reasonable ease, placed coaxially within the furnace would eliminate the complicating effect of corners and edges. While this may not be serious with the dense ore used, it would be much more so with porous ores.

The use of X-ray diffraction photography for the identification of the oxide phases present within partially reduced ores clearly has many advantages. The fact that only very small amounts are needed allows the nature of the reduced material at any point to be determined; it also permits any change in the composition of the wüstite phase to be noted. Any local abnormality, revealed by visual examination, may be investigated in detail by this means.

The writer has been carrying out a somewhat similar investigation on the reduction of lump ores, the results of which will be published at a later date.

**A. E. El-Mehairy** *(St. John Cass College, London, England)*—In an investigation[28] of the reduction progress through lumps of a haematite ore from the Asswan district in Egypt, it was found that the reduction proceeds in a "topochemical" fashion in the sense used by the authors. Emphasis was laid only on the first and final phases of the reduction.

The ore is of oolithic nature with a rather uniform texture. The total porosity of the specimens used was

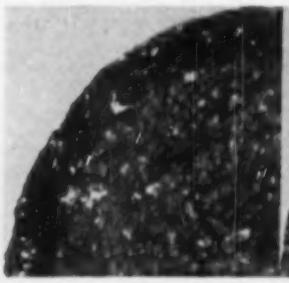

Fig. 9—A quarter central-plane fracture of a 25 mm diam ore sphere partially reduced with $H_2$ at 800°C for 3 min.

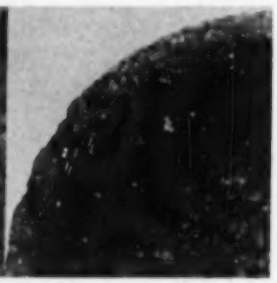

Fig. 10—A quarter central-plane fracture of a 25 mm diam ore sphere partially reduced with $H_2$ at 800°C for 14 min.

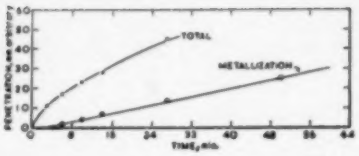


Fig. 11—Recession of the unreduced core and advance of the metallization zone.

42 pct with a pore diameter of 2.0 microns. The chemical analysis of the fairly large lump used for the investigation was: 80.12 pct $Fe_2O_3$, 8.01 pct $SiO_2$, 2.60 pct $Al_2O_3$, 3.99 pct CaO, 0.86 pct Mgo, 0.16 pct MnO, 0.01 pct $TiO_2$, 2.62 pct $P_2O_5$, 0.03 pct S, and a loss on ignition of 1.46 pct. The ore resisted thermal spalling and showed no appreciable change in volume on reduction.

Partial reduction of ore spheres was carried out, with $H_2$ at 800°C, in an apparatus of a type commonly used for such experiments. The $H_2$ flow was maintained at 4 liters per min (measured at room temperature and atmospheric pressure [244.1 cu in. per min]), which appeared to eliminate any effect due to variations in the linear flow of $H_2$ for the range of sphere diameters used (15 to 42 mm). The spheres were held in the reduction tubes in a nearly coaxial position by the use of nichrome-wire spiral cages.

The cooled partially reduced spheres showed a considerable mechanical strength. These were fractured at a central plane. The advance of the visible phase boundaries with time was followed by simple linear measurements from macrographs similar to those shown in Figs. 9 and 10, the linear degree of enlargement being standardized as 120 mm = 25 mm. No attempt was made to study the intermediate stage (magnetite-wüstite interface).

Fig. 11 shows the course of recession of the unreduced core and the course of advance of the metallization zone. These were found to be independent of lump size, thus apparently a characteristic of the ore under certain experimental conditions. The scale of the penetration in Fig. 11 is arbitrarily based on direct measurements from the macrographs.

There appears, as shown by Figs. 9 and 11, the existence of a certain lag in the first appearance of a metallization zone, which is in this case about 3.5 min. A similar behavior was mentioned by Diepschlag, Zillgen, and Poetter[26] and emphasized by Wetherill and Furnas,[27] who claim that for all small particles no ferric iron is present when metallization begins.

The recession of the unreduced core is parabolic and is proportional to $(\text{time})^{0.5}$, whereas the advance of metallization, which is apparently much slower, follows a linear curve. If this straight line is extrapolated to a thickness = 60 mm, which on the arbitrary scale corresponds to complete metallization of a 25 mm diam sphere, the time required would be about 120 min. This compares well with 125 min required for almost complete reduction of a sphere of the same size cut from the same lump.[25]

The behavior of the recession of the unreduced core supports the supposition that the process is a diffusion controlled one (in this case diffusion of $H_2O$ vapor outward), in which case the power factor of the time should be 0.5.[29] Barrett,[29] working on the burning out of combustibles from refractory-clay cubes, found a similar type of behavior: $(\text{recession})^2$ = constant x time.

The advance of metallization being much slower than the first stage is in fact the general belief as pointed out by Stälhane and Malmberg and expressed by several authors as being the one which determines the overall rate of reduction.

While the linear radial advance of metallization, independent of size, explains well why the time for 90 pct reduction is nearly directly proportional to the diameter of the lump,[25] it seemingly fails to conform to simple diffusion laws.

The search for an explanation leads to the supposition that the advance of metallization is slowed down, in effect, by the diffusion of the water vapor, from the

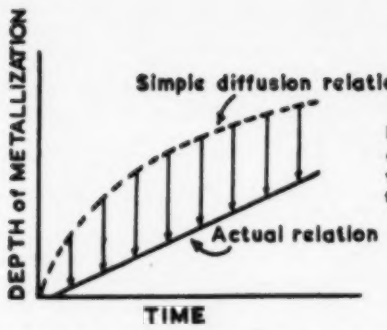


Fig. 12—Slowing down of the advance of metallization.

other stages of reduction, from the interior of the lump outward, thus passing by the scene of the last controlling stage (metallization boundary). Such a supposition might explain as well, from a purely physical (diffusion) standpoint, why the last stage of the reduction has the slowest rate. (Fig. 12.) Peretti[30] has also shown, for the last stage of a multistage reaction, roasting of CuS, that the thickness of the outer layer of CuO is directly proportional with time.

Finally, it is necessary to point out that no attempt has been made to theorize on such a linear advance of metallization and the foregoing explanation is advanced as a suggestion accounting for some experimentally discovered facts from the standpoint of a diffusion-controlled reaction.

**G. Bitsianes** and **T. L. Joseph** (authors' reply)—Dr. Wild's comments on some of the experimental details of the investigation are appreciated. Most of these experimental factors were thoroughly investigated but could not be elaborated upon because of restrictions imposed by publication. The investigation originally started out as a study of the kinetics of the reduction process, but it soon became evident that the present knowledge of the mechanisms involved was too limited for rigorous treatment. Accordingly, this and succeeding papers have, as a major purpose, the presentation of a broad picture of the gas-solid type of reaction which is characteristic of iron-ore reduction. The kinetic studies of the process will be presented at a later date on the basis of this clarification. In this connection, Dr. El-Mehairy's work is very interesting and checks many of our own findings in the study of interfacial movements within a solid ore particle.

[25] A. E. El-Mehairy: *Ph. D Thesis* (1953) University of London.
[26] E. Diepschlag, M. Zillgen, and H. Poetter: *Stahl und Eisen* (1932) 52, p. 1134.
[27] W. H. Wetherill and C. C. Furnas: *Industrial and Engineering Chemistry* (1934) 26, p. 983.
[28] H. Herne: *Discussions* Faraday Society (1948) No. 4, p. 233.
[29] L. R. Barrett: *Discussions* Faraday Society (1948) No. 4, p. 234.
[30] E. A. Peretti: *Discussions* Faraday Society (1948) No. 4, p. 174.

## Further Studies of the Tuyere Zone of the Blast Furnace

by J. B. Wagstaff

*DISCUSSION, Gerhard Derge and John F. Elliott, Chairmen*

**G. C. Gardner** *(National Smelting Co. Ltd., Avonmouth, England)*—I recently performed experiments similar to Mr. Wagstaff's on the "raceway" size with a model somewhat larger in size, 1 ft square in plan, but otherwise identical. The principal difference between the respective experiments was that Mr. Wagstaff confined himself to the use of air as a driving fluid while most of my work was done with water.

My results do not agree with Mr. Wagstaff's correlation and I believe this to be due to his inclusion of the total pressure on the system in his dimensional analysis. According to the correlation, if we choose an incompressible fluid as a driving fluid and increase the total pressure $x^2$ times, the fluid volume will have to be increased $x$ times to maintain the same raceway size. This is ridiculous. There is no reason why the pressure should alter the bubble size if the fluidity remains constant.

Before presenting a new correlation, new observations on the physical nature of the raceway are required. In the stable raceway, a fluid jet travels from the tuyere with little diminution of velocity to the opposing wall where some of its energy is destroyed. Part of the fluid passes through the wall into the bulk of the charge but the majority divides and circulates round the walls of the raceway. That fluid which does not leave the raceway by the time the stream has returned to the tuyere tip is entrained by the jet and the cycle is repeated.

The recirculating fluid also contains large quantities of the particles constituting the charge; and the weight of this material, which is dependent on the particle size and shape as well as on the jet velocity, probably has a modifying influence on the magnitude and distribution of the forces on the raceway surface.

If attention is concentrated on the walls of the raceway, it is seen that that opposing the tuyere is held in a compact mass by the impact of the jet and by the passage of fluid being vented at this point. On the other hand, the upper surface is constituted of particles with a relatively great freedom of movement which are held in a state of suspension chiefly by the outgoing fluid stream. The lower surface is scooped out by the circulating fluid, the depth being maintained by rolling particles away from this face.

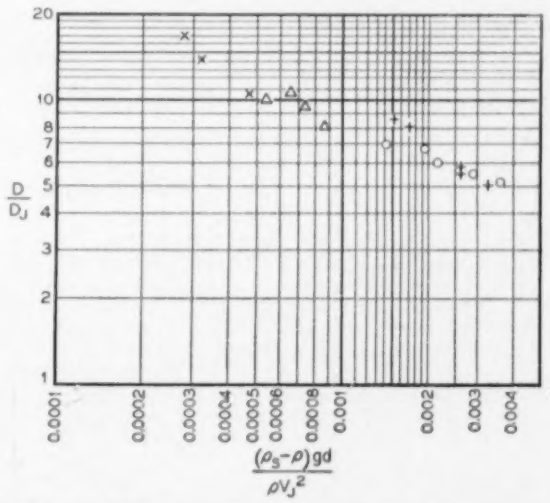


Fig. 8—Correlation of raceway size. + represents ½ in. coke and air ($\rho_s - \rho$) = 68 lb per cu ft, $D_j$ = ¾ in. Triangle represents ½ in. coke and water ($\rho_s - \rho$) = 9.1 lb per cu ft, $D_j$ = ½ in. × represents ½ in. coke and water ($\rho_s - \rho$) = 9.1 lb per cu ft, $D_j$ = ¾ in. Circle represents ⅜ in. gravel and water ($\rho_s - \rho$) = 94 lb per cu ft, $D_j$ = ¾ in.

It is obvious that the forces employed are so varied that a separate correlation for each major direction is required. The simplest case is that of the equivalent diameter in the upward direction where, as a first approximation, it can be assumed that each particle is individually supported by the passage of the fluid round it into the bulk of the charge. This condition introduces the drag coefficient $\left(\frac{\rho V_j^2}{(\rho_s - \rho) gd}\right)$, where jet velocity, $V_j$, must be modified for change of the exit velocity with the surface area of the raceway and for the proportion of the total volume leaving the raceway through the particular area in question. This is done by introducing two length ratios $\left(\frac{D_T}{D_j}\right)$ and $\left(\frac{d}{D_j}\right)$ to form a correlation

$$\left(\frac{D_T}{D_j}\right) = fT\left(\frac{\rho V_j^2}{(\rho_s - \rho) gd}\right), \left(\frac{d}{D_j}\right).$$

The bottom surface affords a similar correlation as the lifting force due to the circulating volume is opposed by the weight of individual particles. We may write

$$\left(\frac{D_B}{D_j}\right) = fB\left(\frac{\rho V_j^2}{(\rho_s - \rho) gd}\right), \left(\frac{d}{D_j}\right).$$

The correlation for the face opposing the jet is more complex, since here the reaction due to jet impact is of major importance. The impact force, together with that due to passage of fluid through the wall, is opposed by a dead weight of charge which, above a certain charge depth, will be independent of charge depth and will vary as the area of the surface to the 3/2 power, or as $D_o^3$. The jet impact in terms of the tuyere velocity will depend upon the distance $D_o$ travelled by the jet and upon the amount of charge circulated in the raceway. When all these factors are considered, it is still found possible to make a correlation in the form

$$\left(\frac{D_o}{D_j}\right) = fo\left(\frac{\rho V_j^2}{(\rho_s - \rho) gd}\right), \left(\frac{d}{D_j}\right).$$

Mr. Wagstaff's presentation of his results obviates any attempt to fit them to this type of correlation. My own results are meager and do not justify any attempt to include the ratio $\left(\frac{d}{D_j}\right)$ in their correlation, but Fig. 8 shows that a plot of $\left(\frac{D}{D_j}\right)$ vs $\left(\frac{\rho V^2}{(\rho_s - \rho) gd}\right)$ fits them very well. The value $D$ is the average of $D_o$ and $D_T$ whose magnitudes were similar and both of which varied in the same direction. Within the limitations of the small ranges of some variables, the correlation is justified. In particular, it will be noted that the value of $(\rho_s - \rho)$ was varied from 9.1 to 94 lb per cu ft, and owing to this, it would be impossible to correlate the results so well according to Mr. Wagstaff's dimensionless groups.

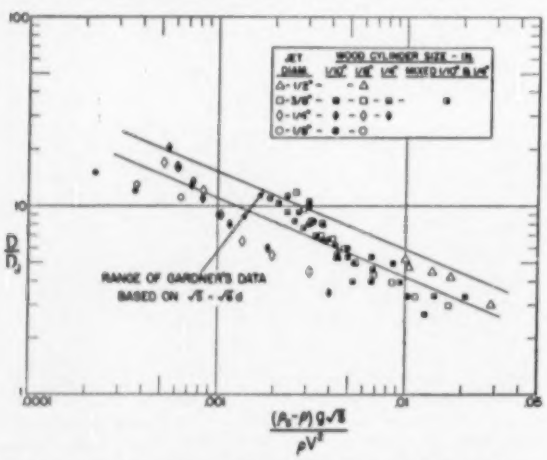


Fig. 9—Curve of the raceway diameter in the form $D/D_j$ as a function of Gardener's term $\rho V^2/(\rho_s - \rho) g\sqrt{s}$.

The experimental values shown for air at higher values of $\left(\frac{D}{D_j}\right)$ are probably in some error due to the extremely rapid pulverization of the coke which occurred at the higher air flows. I am curious to know whether Mr. Wagstaff encountered the same difficulty, since it must influence the combustion zone of a blast furnace.

In conclusion, I would like to point out the value of performing experiments with water. Since $(\rho_s - \rho)$ for coke was decreased seven times and $\rho$ was increased 830 times in changing from air to water, the fluid velocities required to produce a bubble of the same size were reduced 76 fold, which greatly simplified visual observations of raceway formation and of the nature of the stable raceway.*

* Nomenclature: d is charge-particle diameter, $D_B$ is the equivalent raceway diameter to bottom surface, $D_o$ is the equivalent raceway diameter to wall opposing the tuyere, $D_T$ is the equivalent raceway diameter to top surface, $D_j$ is the jet diameter, $g$ is the gravitational constant, $V_j$ is the jet velocity at the tuyere, $\rho$ is fluid density, $\rho_s$ is solid-particle apparent density, and $f$ is function of. Subscripts $B$, $0$, and $T$ refer to correlations for the bottom face, the face opposing the tuyere, and the top face of the raceway, respectively.

**J. B. Wagstaff** (author's reply)—I would like to thank Mr. Gardner for his contribution to the subject, which is all the more interesting because I agree only with some of his statements. I think he has made a valuable contribution in showing the effect of the density of the solid, which we had not investigated.

Mr. Gardner's theoretical discussion of the cause of the raceway may well be incomplete. It is known that a jet of fluid entering a large enclosure always tends to recirculate; also, we have found that the raceway size is not independent of the packing of the granular solids in the bed. Both these points are omitted by Mr. Gardner. It seems to me that this subject is too complex to yield to any analysis based on first principles. So little is known about the distribution of forces in a granular bed even when no fluid is flowing that any argument must surely be empirical at this stage, particularly when we are discussing the more complex case where fluid flow is present.

The packing-density effect itself must be quite complex. We have found that the bed as a whole expands to a negligible extent when the raceway is formed. Since the raceway is nearly void of particles by comparison with the rest of the bed, obviously the packing density of other parts of the bed must increase. This makes discussion of packing density difficult, as I know of no way of measuring it in a nonhomogeneous bed.

In an attempt to check Mr. Gardner's proposed method of correlation, I have drawn a curve of the raceway diameter in the form $D/D_j$ as a function of his term $\rho V_j^2(\rho_s - \rho) g\sqrt{S}$ where $\rho_s$ is the density of the solid and the other symbols have the meaning given in the body of the paper. It can be seen from Fig. 9 that the points on this graph are separated by jet size but not by particle size. Now Mr. Gardner's suggestion that the appropriate correction for jet size might be some function of $\frac{\sqrt{S}}{D_j}$ cannot apply, since there is adequate compensation for the effect of particle size in the use of the previous dimensionless ratio.

Since this paper was written, a considerable amount of work on this subject has been carried out which will be reported in due course. It can now be said, however, that the size of the model has an effect probably due to the "lubricating" effect of the fluid moving through the packed bed.

# Discussion — Extractive Metallurgy Division*

*New York Meeting, February 1952*
Constitution of the $FeO$-$Fe_2O_3$-$SiO_2$ System at Slagmaking Temperatures (paper by R. Schuhmann, Jr., R. G. Powell, and E. J. Michal. JOURNAL OF METALS, September 1953, p. 1097) ..... 1309
*Los Angeles Meeting, February 1953*
Reaction of Silver with Aqueous Solutions of Cyanide and Oxygen (paper by G. A. Deitz and J. Halpern. JOURNAL OF METALS, September 1953, p. 1109) ..... 1309
Copper Converting Practice at American Smelting and Refining Company Plants (paper by F. W. Archibald. JOURNAL OF METALS, March 1954, p. 358) ..... 1310
Thermodynamic Properties of Molybdenum Dioxide (paper by Nev A. Gokcen. JOURNAL OF METALS, August 1953, p. 1019) ..... 1311
Preparation of Metallic Iron of High Purity (paper by George A. Moore. JOURNAL OF METALS, November 1953, p. 1443) ..... 1311

*TP 3903D.

## Constitution of the $FeO$-$Fe_2O_3$-$SiO_2$ System at Slagmaking Temperatures

by R. Schuhmann, Jr., R. G. Powell, and E. J. Michal

*DISCUSSION, H. H. Kellogg and A. J. Phillips, Chairmen*

**Lawrence H. Van Vlack** *(University of Michigan, Ann Arbor, Mich.)*—It is gratifying to see this work concerning the $SiO_2$-$FeO$-$Fe_2O_3$ system published. While its initial application was intended to aid the slag technologist, those concerned with refractory behavior and with iron-ore benefication, will find the quantitative information presented very helpful.

For sometime the refractory engineer has known that a reducing atmosphere in the open-hearth furnace would promote rapid wear on a silica roof. It made no difference whether the oxygen pressure in the atmosphere in contact with the roof was low because of the air-fuel ratio or because of a heterogeneous flow pattern of the gases within the furnace. This paper indicates why a roof can be melted quickly with the lower oxygen supply even though the furnace temperature is not changed. By reducing the oxygen supply, the liquid absorbed by the brick's surface may have its silica solubility increased quickly from 25 to 35 pct. Not only does this permit the fluxing of the solid-silica phases with the increase in liquid content, but also evidence may be presented indicating that such a composition change permits a change in the microstructure of the brick so that there is markedly less solid-to-solid contact of the silica grains. That being the case, the effect of the change in the $FeO$-$Fe_2O_3$ ratio upon the brick's performance would become relatively more significant.

Another technical application of the foregoing paper is to be found in the sintering of iron-ore fines for blast-furnace consumption. It may be pointed out from Fig. 9 that the process of sintering and partial fusion of the ores is dependent not only upon the temperature of sintering but also upon the amount of oxygen available to the sinter bed. Further, sinters which required a relatively high temperature for agglomeration on the sinter bed because the oxygen level was kept high may have their microconstituents and microstructure altered appreciably within the blast furnace where the oxygen pressure is low. With that in mind, the paper should serve to insert some caution in attempts at predicting the behavior of sinter in a blast furnace solely on the basis of its physical properties under normal atmospheric conditions.

## Reaction of Silver with Aqueous Solutions of Cyanide and Oxygen

by G. A. Deitz and J. Halpern

*DISCUSSION, O. C. Ralston and R. Schuhmann, Chairmen*

**E. A. Peretti** *(University of Notre Dame, Notre Dame, Ind.)*—Mr. Deitz and Professor Halpern are to be congratulated on a fine piece of work which adds to our knowledge of precious metal—cyanide-solution reactions.

I should like to offer the following comments: The authors state, "the rate plots were always linear, indicating a zero order reaction rate." This appears to conflict with the data of Fig. 6 which clearly show the rate to vary with the NaCN concentration.

It seems to me that the rate curves are linear because of the experimental setup. The volume of solution is so large that over a three-hour period the change in NaCN concentration is very small. A rough calculation for the experiments of Table I where the initial NaCN strength was 0.0096 mol per liter show a *change* of NaCN concentration of about 0.0009 mol per liter at the end of three hours. In short, over the period of time that the experiment was in progress, the NaCN strength was practically constant; hence the rate of dissolution remained practically constant.

Eq. 10, as written, specifies that 1 mol of $H_2O_2$ and 2 mol of hydroxyl ion are formed when 2 mol of silver react. Is this true?

The effect of $H_2O_2$ on the rate was made in solutions having an oxygen pressure of 4.8 atm. Were any tests made in solutions containing hydrogen peroxide, but no oxygen?

**G. M. Willis** *(University of Melbourne, Melbourne, Australia)*—The authors have shown that, under their experimental conditions of high $O_2$ concentrations, the rate of solution of silver in aqueous cyanide solutions is controlled by diffusion of $O_2$ or $CN^-$ to the metal surface. With diffusion control, it is generally not possible to obtain further information about the mechanism of a process.

However, Dr. T. Mills and the writer have found that the dissolution of silver and gold in cyanide, like most corrosion processes, occurs as an electrochemical reaction. By measurements of loss in weight and electrode potential, with cathodic and anodic polarization of the metal, it has been found possible to determine the polarization curves for the anodic solution of the metal, and the cathodic reduction of $O_2$, and so separate the two processes. In general, our conclusions are in agreement with those of the authors. In our solutions (saturated with air or $O_2$ at 1 atm and mostly of lower cyanide concentrations) mixed control may occur, but, depending on the relative concentrations of $CN^-$ and $O_2$, the rate may be controlled by diffusion of one or the other. For example, in 0.0108 N KCN, saturated with air, the rate of solution of silver is substantially controlled by the diffusion of $O_2$ to the metal surface. Reducing the cyanide concentration to 0.0043 N lowers the rate which then is under mixed control. Saturation with $O_2$ increases the rate to a stage where anodic polarization becomes the limiting factor for low cyanide concentrations. Our results confirm the necessity of maintaining dissolved $O_2$ as high as possible in practice in order to obtain maximum rates of solution.

The authors suggest that under their conditions reduction of $O_2$ is predominantly to $H_2O_2$. However, this conclusion should not be taken to be necessarily true under all conditions. The cathodic reduction of $O_2$ is a complex process, and the literature indicates the need for further work on this important reaction. On silver, Laitinen and Kolthoff[20] find reduction to $H_2O_2$; Delahay[21] shows that the electrode potential determines the extent to which reduction is to $H_2O_2$ or to $OH^-$. Lund[22] found that the reduction to $H_2O_2$ could be followed by catalytic decomposition of $H_2O_2$. This depends on the state of the silver surface, and is apparently inhibited by the presence of $CN^-$ ions above a certain concentration. We have found that the cathodic reduction of $O_2$ depends greatly on the experimental conditions; under our conditions, reduction is predominantly to $OH^-$. It appears that, on the whole, more negative electrode potentials favor the 4-electron step, as Delahay found. This will be the case in solutions of high $CN^-$ and low $O_2$ concentrations: high $O_2$ concentrations raise the electrode potential and lead to the presence of substantial amounts of peroxide in the solution, in agreement with the authors' observations. For these reasons, care should be taken in applying the authors' conclusions to conditions other than those to which they refer.

**G. A. Deitz** and **J. Halpern** (authors' reply)—Professor Peretti's observations regarding the significance of our "zero order reaction rate" are valid. Our use of the term "zero order" refers to the linear shape of the rate plots and implies that the rate of reaction remained constant during any given experiment. As Professor Peretti points out, this apparent zero order behavior resulted from the fact that the reactants which influence the rate, such as $O_2$ and NaCN, were always present in constant concentration or in large excess.

No experiments were made in which $H_2O_2$, but not $O_2$, was present. While the results of such experiments would be of interest, they do not affect our conclusions relating to the ordinary cyanidation process which depends on the presence of dissolved oxygen.

We are grateful to Dr. Willis for quoting results of his electrochemical experiments and advancing conclusions similar to ours regarding two regions of diffusion controls for the dissolution of silver. Under these circumstances however, there appears to us to be some danger in concluding on the basis of polarization measurements that the normal dissolution of the metal in the absence of an external current is an electrochemical process, in the sense that it involves separated anodic and cathodic reactions.

In our experiments, reduction of $O_2$ appeared to occur largely through the 2-electron mechanism leading to the formation of $H_2O_2$ in accordance with Eq. 10. However, we recognize that under different conditions alternative reactions, such as the 4-electron reduction of $O_2$ to $OH^-$ or the catalytic decomposition of $H_2O_2$, might become important and we therefore would emphasize with Dr. Willis the danger of extending our conclusions to conditions widely different from those which we used.

[20] H. A. Laitinen and I. M. Kolthoff: *Journal of Physical Chemistry* (1941) 45, p. 1079.
[21] P. Delahay: *Journal* Electrochemical Society (1950) 97, p. 205.
[22] V. Lund: *Acta Chemica Scaninavica* (1951) 5, p. 555.

## Copper Converting Practice at American Smelting and Refining Company Plants

by F. W. Archibald

*DISCUSSION, L. L. McDaniel and J. C. Kinnear, Jr., Chairmen*

**Anton Gronningsater** *(Falconbridge Nickel Mines Ltd., Sudbury, Ont., Canada, Falconbridge Nikkelverk, Kristiansand, Norway)*—Mr. Archibald's paper, although excellent, concentrates mainly on mechanical details and on means for prolonging lining life, and pays little attention to the chemical efficiency of the operation. My feeling is that not enough attention is paid to the possibility of using the converter as a smelting machine, an opinion which has been elaborated upon by Anton Gronningsater and Peter R. Drummond.[1] Of course, there are good reasons why we hear little about this feature. One reason may be that, with the high copper content of the mattes now obtained at most smelters, converting is not an important economic feature of the operations. The grade of matte used does not leave much FeS as fuel, while the combination with reverberatory smelting calls for a converter slag of a composition unfavorable for the smelting of ore. In order to lessen magnetite trouble, a high silica converter slag is desired and a high silica content is also of advantage in the reverberatory slags proper.

However, there have been and still are cases where large amounts of low grade matte have to be converted and where the amount of ore used as flux represents an appreciable saving. We are still confronted with such conditions in the nickel industry. When smelting green ore, we have operated with a matte containing only 7 pct Ni plus copper. Some months, under such conditions, we were able to smelt one-third of our ore in the converter. All our efforts were directed toward smelting as much ore as possible in that way, and that meant running the converter hot enough to get maximum air efficiency. The present aim is for less than 1 pct O in the gases from the reverberatories, and a similar oxygen content is also desirable in the converter gases. To obtain that, however, it is necessary to maintain the required high bath temperature, and that, I am afraid, is not very often done where there is a continuous struggle to prolong the life of the lining. When converting the 7 pct matte, we were satisfied with 100 days between repairs, and we developed a practice of completing the repairs in 3 to 4 days.

I appreciate the importance of long lining life and the advantage of as few shut-downs as possible, particularly when, as is often the case, full spare equipment is not available. However, it is possible that the

efforts to prolong lining life are sometimes carried too far, beyond what is economical. Perhaps the mechanical maintenance crew and the foremen have more to say in directing operations than the chemists and metallurgists.

With the high working temperatures in smelters, research and effective control present many difficulties not encountered at lower temperatures and in wet metallurgy. This is perhaps the main reason the statement has been made that the pyrometallurgist may be replaced more and more by the chemical engineer. Today increasing attention is being paid to the chemical extraction processes so frequently discussed about 40 years ago before flotation appeared and changed the metallurgical picture.

[1] A. Gronningsater and P. R. Drummond: Notes on the Operation of the Basic Copper (And Copper Nickel) Converter. *Trans.* Canadian Mining & Metallurgy Bulletin (1942) 45, pp. 99-139.

## Thermodynamic Properties of Molybdenum Dioxide

by Nev A. Gokcen

*DISCUSSION, N. C. Fick and B. W. Gonser, Chairmen*

**T. G. Perry** *(The APV Co. Ltd., London, England)*—Professor Gokcen's interesting paper shows a large discrepancy between his results and those of Collins. An extension of Collins' work carried out at Massachusetts Institute of Technology has suggested a reason for this discrepancy. Fig. 3 shows calculated and experimental results for the vapor pressure of $MoO_3$ over $MoO_2$ and over $MoO_3$; it can be seen that $MoO_3$ vapor should be formed at an appreciable rate under the dynamic conditions of Gokcen's experiments. Thus, the condition of no loss in weight of the molybdenum specimen is brought about by a loss in weight due to vaporization of $MoO_3$ and a gain due to surface oxidation to $MoO_2$. A correction of Gokcen's experimental results for this factor would bring them more in line with those of Collins.

**Nev A. Gokcen** (author's reply)—According to Mr. Perry's interesting results, the vapor pressure of $MoO_3$ over $MoO_2$ is of the order of $10^{-6}$ atm at the highest temperature in this investigation. The maximum error in $P_{H_2O}/P_{H_2}$, introduced by the vaporization, hence by the side reaction $H_2O(g) + MoO_2(s) = H_2(g) + MoO_3(g)$, is much less than the experimental errors. Further, experimental observations indicated that the weight loss after the formation of $MoO_2$ was extremely small.

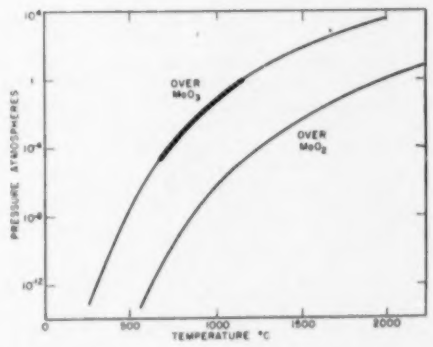


Fig. 3—Vapor pressure of $MoO_3$.

## Preparation of Metallic Iron of High Purity

by George A. Moore

*DISCUSSION, N. C. Fick and B. W. Gonser, Chairmen*

**J. Talbot, Ph. Albert,** and **G. Chaudron** *(Centre d'Etudes de Chimie Métallurgique, Vitry-sur-Seine, France)*—We have also prepared different samples of iron of very high purity.[16] The raw material used is, for example, ferrous ammonium sulphate, purified by fractional crystallization, either from Armco iron, or from certain preparations of carbonyl iron. In all cases, one has as a result a solution of ferrous chloride which undergoes a double electrolysis. Thus a pure iron cathode which is annealed in pure dry hydrogen is prepared. Then the plate of metal can be rolled or drawn, without which operation it would be necessary to pass through a fusion operation. This point is very important because it is known that the fusion of high purity iron is a very delicate problem; the best refractories are always introducing impurities into the metal.

The determination of metalloid impurities, such as oxygen or carbon, has been made by microanalytical methods[17] and that of metallic impurities by the radioactive tracer method. When one starts from ferrous ammonium sulphate or from certain carbonyl irons, metallic plates of very high purity are obtained.

These samples of iron have been studied and show very interesting properties,[18] particularly from the viewpoint of recrystallization.

**G. A. Moore** (author's reply)—We are glad to know that the experiments of M. Talbot and his associates have been successful, and regret that their reports did not appear in time to be mentioned in the paper.

We have avoided use of ferrous ammonium sulphate, although amenable to recrystallization, on the presumption that sulphate, unlike sulphide, cannot be entirely eliminated, and might introduce sulphur into the cathodes. We did not attempt to make coherent cathode plates because it was felt that the conditions necessary to make such cathodes might not be the same as those necessary to obtain highest purity.

We have received a little information on NBS iron from radioactive experiments, showing that very small traces of some elements can be detected, but do not feel that these methods have as yet been sufficiently standardized to give a reliable analysis for all the impurities which might be present.

The writer is in complete agreement with the statement of the inevitability of contamination in any established fusion method and the necessity of compacting the cathodes by working, but hopes that one of the potential methods of melting without crucibles will soon be proved practical. It is agreed that recrystallization and grain growth are quite different in high purity iron than in iron still containing traces of nonmetallic phases.

[16] J. Talbot, Ph. Albert, M. Caron, and G. Chaudron: Congress of Metallurgy, Paris (October 1952) *Revue de Métallurgie* (1953) 50, p. 818.

[17] L. Moreau, J. Talbot, and J. Bourrat: *Revue de Métallurgie* (1953) 50, p. 775.

[18] J. Talbot, Ch. de Beaulieu, and G. Chaudron: *Comptes Rendus* (1953) 236, p. 818.

# Discussion — Institute of Metals Division*

*Cleveland Meeting, October 1953*


Heat Treatment, Structures, and Mechanical Properties of Ti-Mn Alloys (paper by F. C. Holden, H. R. Ogden, and R. I. Jaffee. JOURNAL OF METALS, February 1954, p. 169) ..... 1312


*New York Meeting, February 1954*


Annealing of a Cold Rolled Aluminum Single Crystal (paper by A. H. Lutts and P. A. Beck. JOURNAL OF METALS, February 1954, p. 257) ..... 1313

Torsional After-Effect Measurement and Applications to Aluminum (paper by C. S. Barrett, P. M. Aziz, and I. Markson. JOURNAL OF METALS, December 1953, p. 1655) ..... 1315

Mechanism of Plastic Flow in Titanium: Manifestations and Dynamics of Glide (paper by F. D. Rosi. JOURNAL OF METALS, January 1954, p. 58) ..... 1316

Uranium-Titanium Alloy System (paper by M. C. Udy and F. W. Boulger. JOURNAL OF METALS, February 1954, p. 207) ..... 1317

Creep Correlations of Metals at Elevated Temperatures (paper by O. D. Sherby, R. L. Orr, and J. E. Dorn. JOURNAL OF METALS, January 1954, p. 71) ..... 1318

Aging Characteristics of Nickel-Chromium Alloys Hardened with Titanium (paper by R. Nordheim and N. J. Grant. JOURNAL OF METALS, February 1954, p. 211) ..... 1322

Solidification of Aluminum-Rich Aluminum-Copper Alloys (paper by A. B. Michael and M. B. Bever. JOURNAL OF METALS, January 1954, p. 47) ..... 1323

Constitution and Properties of Ag-Cu-Zn Brazing Alloys (paper by K. M. Weigert. JOURNAL OF METALS, February 1954, p. 233) ..... 1325

Investigation of the Heat Treatment of Commercial Titanium-Base Alloy (paper by L. Luini and E. Lee. JOURNAL OF METALS, May 1954, p. 581) ..... 1326

Hydrogen Embrittlement of Steels (paper by J. T. Brown and W. M. Baldwin, Jr. JOURNAL OF METALS, February 1954, p. 298) ..... 1327

A Study of the Effect of Carbon Content on the Structure and Properties of Sintered WC-Co Alloys (paper by J. Gurland. JOURNAL OF METALS, February 1954, p. 285) ..... 1327

Solid State Bonding of Aluminum to Nickel (paper by S. Storchheim, J. L. Zambrow, and H. H. Hausner. JOURNAL OF METALS, February 1954, p. 269) ..... 1330

High Temperature Strength of Wrought Aluminum Powder Products (paper by E. Gregory and N. J. Grant. JOURNAL OF METALS, February 1954, p. 247) ..... 1334


* TP 3904E.

---

## Heat Treatment, Structure, and Mechanical Properties of Ti-Mn Alloys

by F. C. Holden, H. R. Ogden, and R. I. Jaffee

*DISCUSSION, M. A. Hunter and J. H. Jackson, Chairmen*

**C. M. Bishop** *(Aircraft Div., A. V. Roe Canada Ltd., Toronto)*—Reference is made to the coherency hardening of $\beta$ due to $\beta'$ and also to the hardening of $\beta$ due to a coherent precipitation of the $\alpha$ phase. What is meant by the term "$\beta'$?" Would not the coherency hardening of $\beta$ during cooling be due to precipitation of a submicroscopic dispersion of $\alpha$, as is the case during reheating a $\beta$-quenched alloy? I feel that these two phenomena are essentially the same mechanism, i.e., precipitation of $\alpha$ from unstable or supersaturated $\beta$.

From the text, it would appear that Tables III and IV are intended to show the effect of the martensite transformation on the properties of Ti-Mn alloys. Referring to Table III, the $\beta$-quenched alloys would contain a greater proportion of retained $\beta$ than would the equilibrated alloy. Could not the increase in properties be attributed to this, along with possible coherency hardening of the $\beta$? In the same way, the structures referred to in Table IV contain $\beta$ from which they could derive their hardness. It would appear to be difficult, if not impossible, to assess the role of the martensite transformation from the data contained in these tables.

**F. C. Holden, H. R. Ogden,** and **R. I. Jaffee** (authors' reply)—In reply to the first question raised by Mr. Bishop, the term "$\beta'''$" designates an apparent retained-$\beta$ structure which is harder than it is after the most rapid cooling from the $\beta$ field. It is thought to be the result of a coherent precipitation of $\alpha$. The mechanism by which hardening takes place is undoubtedly the same as that involved in the early stages of aging of a retained-$\beta$ structure, and we are in agreement with Mr. Bishop on this point. The term "$\beta'''$" to designate the anomalously hard retained-$\beta$ structure was agreed upon at a symposium in 1953.[a]

The authors do not agree that the quantity of retained $\beta$ and/or $\beta'$ in the $\beta$-quenched specimens of Table III is necessarily greater than that of the 600°C equilibrated specimens. The $\beta$-quenched specimen has a structure which appears to be completely $\alpha'$ formed by the martensite reaction. It is recognized that there could be some retained $\beta$ (or $\beta'$) between the $\alpha$ plates if the $M_f$ temperature is below room temperature. This is unlikely for the 3.4 pct Mn alloy where the $M_s$ is known to be at about 640°C. Therefore, the increase in strength cannot be attributed to the presence of a greater quantity of coherency-hardened $\beta$, but, rather, the increase in strength must be attributed to the transformation products formed, e.g., $\alpha'$ (martensitically formed $\alpha$).

Concerning the data in Table IV, we agree that it is difficult to estimate the role of the martensite reaction, since the 6.4 pct Mn alloy was retained $\beta$ in the quenched condition.

[a] Symposium sponsored by the Ordnance Metallurgical Advisory Committee on Titanium. Pittsburgh, June 9 and 10, 1953.

# Annealing of a Cold Rolled Aluminum Single Crystal

by A. H. Lutts and P. A. Beck

*DISCUSSION, F. D. Rosi and M. A. Steinberg, Chairmen*

**J. P. Nielsen** *(New York University, New York)*—In Fig. 1 the slope of the softening-with-time curve is not monotonic in that it increases mildly up to 1000 sec and after this it decreases rapidly. This suggests that both a softening and a hardening component contributed to the resultant values plotted. I am wondering if this may be evidence of a hardening due to the "budding" stage of recrystallization grains. Recrystallization has been greatly delayed here, and the hardening component would also appear to be delayed.

The hardening due to the budding of recrystallization grains has been worked on recently in our laboratory, and we have submitted our analysis for publication.[15] We use the term "budding" because we believe that the grains to serve as recrystallization grains are present immediately after cold work but that their stimulation to extensive growth requires a special mechanism which we call "geometrical coalescence." This mechanism requires a time interval or induction period to take effect.

A minor item that also may be worthy of mentioning is that annealing is not the reverse of work hardening. Metals with the same hardness level arrived at by draw tempering and by direct work hardening do not have the same properties in general. Hence, the third conclusion should be restated so that is implies that the internal crystallographic mechanisms which account for line sharpening are not the same as the mechanisms for softening during annealing. In other words, the authors did not show that line broadening is inconsistent with work hardening, but rather that line sharpening is inconsistent with softening on recovery anneal.

**C. G. Dunn** and **F. W. Daniel** *(General Electric Co., Pittsfield, Mass., General Electric Co., Brackenridge, Pa., respectively)*—The authors present an interesting curve of isothermal softening of cold-rolled aluminum crystals. In an explanation of their result, they assume that the cold work produces a subgrain structure with internal imperfections and that annealing alters these two features at different rates. Thus, annealing at 350°C quickly removes imperfections within individual subgrains, restoring sharpness to diffracted $K\alpha$ lines but producing little, if any, softening. Softening occurs through subgrain growth which proceeds more slowly.

If subgrain growth alone produces 100 pct softening and if subgrain growth slows down with increasing subgrain size as observed for large subgrain sizes, how do the authors account for the rapid drop in hardness above 1200 sec at temperature?

These remarks are not made to imply that near 100 pct softening (as indicated by microhardness) is unreasonable. In fact, when no primary recrystallization or large-angle phenomena occurs, our own tests made on deformed silicon-iron crystal (3.3 pct Si) have shown complete softening.[9, 10]

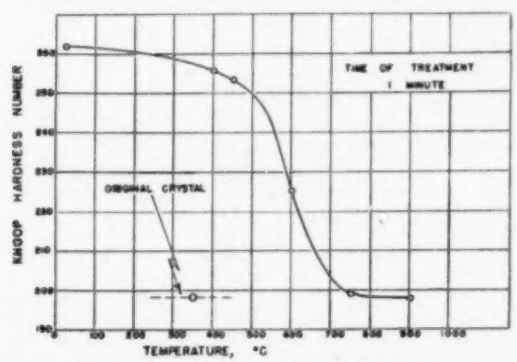


Fig. 7—Effect of temperature on the hardness of a deformed single crystal annealed for 1 min. No recrystallization.

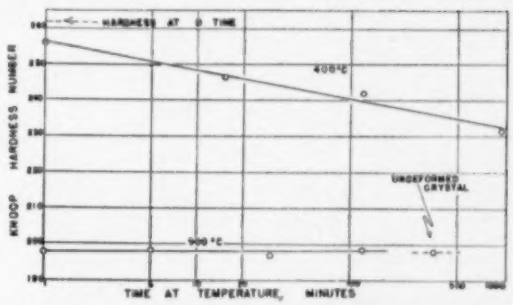


Fig. 8—Curves of Knoop hardness vs time showing the effect of temperature on rate and amount of softening as measured by the change in Knoop hardness. No recrystallization of the deformed single crystals.

In our unpublished work[16] two phenomena regarding hardness were considered: namely, the removal of work hardening by annealing and the relationship of hardness to primary recrystallization. The results pertain to the present paper.

Briefly, the first experiment involved a large single crystal sheet specimen cold rolled from 0.024 to 0.020 in. thickness. Initial and final orientations were (112) <110>. Small samples were prepared with lightly etched surfaces and heavily etched edges. Some samples were annealed to temperatures of 1100°C and no primary recrystallization occurred. Other samples were annealed for various lengths of time at 900°C, sectioned to expose {110} surfaces, prepared for Knoop hardness measurements,[17] and tested with the long axis of the Knoop indenter parallel with a <110> direction. In comparison with the hardness of the undeformed crystal, the results showed complete softening for all the anneals given, the shortest time being one minute. X-ray tests prior to Knoop measurements and metallographic examination of the tested surfaces disclosed that no primary recrystallization had occurred in any samples.

Keeping the time of anneal constant at one minute, a temperature series for still other samples gave the results shown in Fig. 7. Again, no primary recrystallization occurred. Clearly, all the work hardening could be removed without primary recrystallization in 1 min anneals at temperatures above 750°C.

Another set of samples were annealed for various lengths of time at 400°C. Fig. 8 shows these results and also those of the 900°C series. On a linear time scale, it can be seen that the hardness falls off rapidly at first, then more slowly with increasing time at 400°C. In this respect, it is similar to recovery phenomena reported in the literature and somewhat different from the curve of Lutts and Beck. Unfortunately, we obtained no isothermal data showing the rate characteristics of softening near 100 pct softening; according to the form of the curve in Fig. 7, however, a rapid drop in hardness near 100 pct softening would appear unexpected.

At the time of this work, we were unaware of subgrain growth. It appeared to us that imperfections such as dislocations were being removed in the way Burgers has described[18] (see also ref. 19). Subsequent work[20] disclosed subgrains and their growth above 750°C. For example, it was possible to observe the formation of short subboundaries 90° to slip-line markings that persisted even after 15 min at 775°C. Without fur-

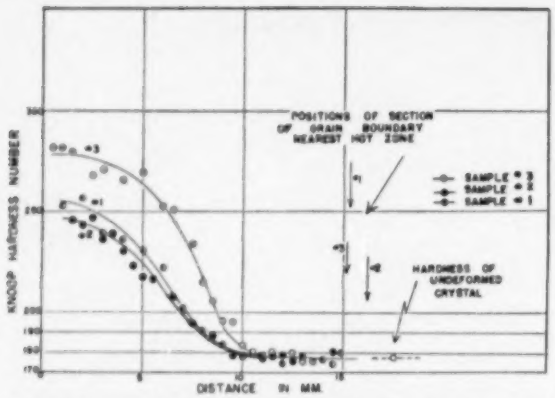
KNOOP HARDNESS NUMBER
POSITIONS OF SECTION OF GRAIN BOUNDARY NEAREST HOT ZONE
SAMPLE # 3
SAMPLE # 2
SAMPLE # 1
HARDNESS OF UNDEFORMED CRYSTAL
DISTANCE IN MM.

*Fig. 9—Curves showing Knoop hardness along deformed single crystals annealed in a temperature zone varying from room temperature (0 mm) to over 900°C (15 mm or the positions of the recrystallization grain boundaries).*

ther data in subgrain phenomena below 775°C, we cannot say just what role subgrain growth may have played in the softening process.

In the second experiment, which involved recrystallization, the picture is clearer. Three crystals in the (110) [1$\bar{1}$0] orientation were cold rolled lightly (enough to produce primary recrystallization on annealing). The crystals were moved into a high temperature gradient furnace far enough to produce recrystallization in one end and no softening in the other end (gradient parallel to the [1$\bar{1}$0] direction). Hardness tests were made on a {100} section with the indenter parallel to a <110> direction. Fig. 9 gives the plot of hardness vs distance into the furnace, with recrystallization occurring at about 900°C. Positions of the boundaries of the new grains are indicated. Clearly, these new grains are growing at the expense of completely soft unrecrystallized material (confirmed by X-ray and metallographic examination). According to later information,[20] which includes documented evidence of this kind, the energy for growth in the above samples no doubt resides in subboundaries that are well formed at these temperatures. From an energy point of view, therefore, 100 pct softening does not imply 100 pct removal of the energy introduced by work. The amount of energy left, however, would be small just as it would be if the single crystal recrystallized to a fine-grained structure involving large-angle boundaries.

When a heavily cold-rolled crystal of silicon iron recrystallizes to a fine-grained structure near 500°C, it is quite possible that softening prior to primary recrystallization does not proceed as far as in the examples cited above. In other words, 100 pct softening is a possibility and not a requirement according to our point of view. (Clarebrough, Hargreaves, and West[21] have shown that, in deformed polycrystalline nickel of commercial purity, most of the softening and the removal of energy occurs during primary recrystallization.) Also, the energy introduced by straining a crystal (strain energy) takes a number of forms, particularly during annealing. All of it is removed when the final state is another crystal of equivalent perfection of the starting crystal.

**E. C. W. Perryman** *(Aluminum Laboratories Ltd., Kingston, Ontario, Canada)*—Although this work refers to a very special case, namely, a heavily rolled single crystal which did not change its orientation after cold working, it might be interesting to compare these results with similar measurements carried out on polycrystalline superpurity aluminum cold rolled 20 and 80 pct. We have investigated the recovery process by measuring electrical resistance, X-ray line breadth, and hardness as a function of time at constant temperature. In agreement with the authors, we find that line breadth anneals out before hardness and, furthermore, electrical resistance anneals out before line breadth. The isothermal-recovery curves all show the same shape, a rapid rate initially which decreases with time. In agreement with other workers, we find that the recovered values of the various properties measured are much higher than the fully recrystallized values; in fact, only 30 to 40 pct hardness, 50 pct line breadth, and 30 pct electrical resistivity are lost during recovery before sufficient recrystallized grains are formed to affect these properties. It is interesting to note that the final recovered hardness value is greater for high, than for small, amounts of cold work, whereas the recovered value of line breadth is independent of cold work. Furthermore, the final hardness value decreases slightly with increasing annealing temperature, whereas the final value of line breadth is independent of temperature. These results suggest that the recovery of line breadth is due to a redistribution of dislocations, these diffusing and becoming blocked at the subgrain boundaries. Microstructural evidence for this has been given by Perryman.[22] Later work, besides confirming the original microstructural observations, has shown that the activation energy for recovery of line breadth is independent of cold work, which also supports the above conclusion.

The variation of the final recovered hardness value with cold work and annealing temperature can be explained by the fact that the subgrain size increased with decreasing cold work and increasing temperature so that a low hardness value was obtained with a larger subgrain size. The authors suggest that softening is produced by subgrain growth after the subgrains have become perfect. Our results indicate that subgrain growth must take place in the very early stages of annealing for, although the subgrain size directly after cold working is independent of cold work, after annealing it increases with decreasing cold work and increasing annealing temperature. Furthermore, no indication of subgrain growth has been obtained once the subgrains have become perfect. From this work, it seems that during recovery, although the dislocations are redistributed, the dislocation density is not changed very markedly which is in keeping with the very small amount of stored energy released during this process.[23] It is hoped that a full account of this work will be published shortly.

**A. H. Lutts** and **P. A. Beck** (authors' reply)—Since the hardness drop on annealing was found to be monotonous, our data appear to provide no direct justification for Dr. Nielsen's assumption that a hardening component is involved in the annealing process. We did detect recrystallization without noticeable hardness change, but in no case did we encounter recrystallization (budding or otherwise) causing an increase in hardness. The third paragraph of Dr. Nielsen's discussion is apparently based on a misunderstanding. We did not wish to imply that annealing contributes to X-ray line broadening. We did find, however, as stated in our third conclusion, that the crystal imperfections resulting from plastic deformation, which account for line broadening, show a distinctly different annealing behavior from that of the imperfections responsible for the major part of work hardening.

We would like to thank Drs. Dunn and Daniels for contributing to the discussion their own excellent, previously unpublished results. We are, of course, gratified to see that their softening data for rolled silicon-iron single crystals show so many similarities with the data for aluminum single crystals. In particular, the occurrence of complete softening without recrystallization may now be considered confirmed by Dunn and Daniels. The apparent differences in the isothermal kinetics of softening are probably not real. Fig. 1 of the paper shows that initially, up to about 700 sec, the rate of softening of the rolled aluminum single crystal is actually decreasing at 350°C, in accordance with the observations on silicon-iron. This recovery-type softening kinetics is much more conspicuously

evident in the isothermal softening curves at lower temperatures obtained since the present paper was written. On the other hand, the apparent absence in silicon-iron of the accelerated phase of softening, observed in aluminum after more prolonged annealing, may be due to the fact that the isothermal annealing experiment with the silicon-iron crystal has not been carried to completion. The question of the mechanism of softening is undoubtedly still not definitely answered. Judging by the kinetics, the initial part of softening may well be a recovery-type process, not involving any boundary migration, although this conclusion is by no means certain. The work hardening remaining after complete recovery of line broadening would be difficult to associate with any imperfection other than subboundaries. The subsequent softening should then be ascribed to subgrain growth. However, again, no direct confirmation of this interpretation has been obtained as yet. It is hoped that the experimental investigation of this question will be accomplished within the next few months.

Dr. Perryman's account of his results on the recovery of hardness, line broadening, and electrical resistivity in rolled polycrystalline aluminum is most welcome. Our preliminary experiments with 80 pct rolled polycrystalline aluminum suggested that the separation between recovery and recrystallization in this case was quite difficult to carry out, since the two processes took place largely concurrently. We did note, however, that simultaneously with the first 50 pct of softening (probably largely by recrystallization), about 75 pct of the line broadening was lost on annealing. This indicates, in accordance with Dr. Perryman, that, even in heavily cold-worked polycrystalline aluminum, the recovery of line broadening runs somewhat ahead of recrystallization.

[15] J. P. Nielsen: Mechanism for the Origin of Recrystallization Nuclei. *Trans.* AIME (1954) **200**, p. 1084; JOURNAL OF METALS (September 1954).
[16] F. W. Daniels and C. G. Dunn: *Report No. 52698.* (September 1948) General Electric Co.
[17] F. W. Daniels and C. G. Dunn: The Effect of Orientation on Knoop Hardness of Single Crystals of Zinc and Silicon Ferrite. *Trans.* ASM (1949) **41**, p. 419.
[18] W. G. Burgers: Recovery and Recrystallization Viewed as Processes of Solution and Movement of Dislocations. *Proceedings* Koninkl. Nederland. Akad. Wentenschap. (1947) **50**, p. 452.
[19] C. G. Dunn: Some Aspects of Crystal Recovery in Silicon Ferrite Following Plastic Strains. *Trans.* AIME (1946) **167**, p. 373; METALS TECHNOLOGY (August 1946).
[20] C. G. Dunn and F. W. Daniels: Formation and Behavior of Subboundaries in Silicon Iron Crystals. *Trans.* AIME (1951) **191**, p. 147; JOURNAL OF METALS (February 1951).
[21] L. M. Clarebrough, M. E. Hargreaves, and G. W. West: The Release of Energy Stored in Deformed Nickel. *Phil. Mag.* (August 1953) Series 7, **44**. No. 355.
[22] E. C. W. Perryman: *Acta Metallurgica* (1954) **2**, p. 26.
[23] G. Borelius, S. Berglund, and S. Sjöberg: *Arkiv for Fysik* (1953) **6**, p. 143.

## Torsional After-Effect Measurement and Applications to Aluminum

by C. S. Barrett, P. M. Aziz, and I. Markson

*DISCUSSION, F. D. Rosi and M. A. Steinberg, Chairmen*

**N. K. Chen** *(Johns Hopkins University, Baltimore)*—Since the abnormal after-effect observed here and by Dr. Barrett in previous investigations[1, 2] is attributed to the release of residual stresses by the escape of piled-up dislocations, it may be asked whether such an escape of dislocations could be studied directly under the microscope. In order to check this, an experiment was conducted in the following manner: a single crystal of high purity aluminum, ⅛ in. square in cross-section and 1⅜ in. long in gage length, was grown from the melt, homogenized, etched, and then chemically polished using the "R-5 Bright-Dip" process. The specimen was anodized in a 20 pct solution of sulphuric acid at 5.5 v for 60 min (temperature of the solution was maintained at 69°F), immediately immersed in cold water, and dried with alcohol. It was deformed in tension by means of the technique previously described.[5] After an extension of about 1 pct, the surface of the specimen exhibited markings, shown in Fig. 12a. These markings are not slip lines but are actually oxide-film cracks which do not correspond to any {111} planes in the specimen. They assume the normal features of film cracks upon careful examination, particularly near the specimen edges. It will be shown later as a further confirmation of the identity of these markings that they were made to diminish when the thickness of the film was carefully reduced by etching. Little evidence of slip markings can be witnessed in Fig. 12a at this magnification or any higher magnification up to X1000.

a—After an extension of about 1 pct.

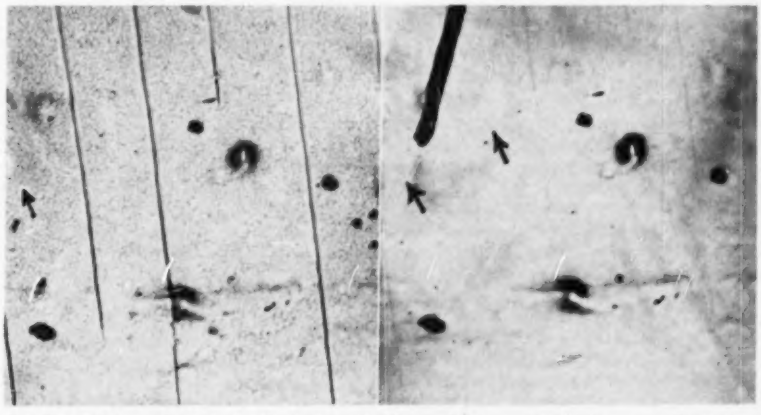

b—Immediately etched after the extension with a 3 pct NaOH solution for 4 min. Same area as a.

Fig. 12—Oxide cracks and slip lines of an aluminum single crystal which was anodized in a 20 pct aluminum solution of sulphuric acid at 5.5 v for 60 min. X250. Area reduced approximately 40 pct for reproduction.

The arrow in Fig. 12a marks the only trace of slip which was detected.

The load was released after this extension and the specimen was immediately etched with a 3 pct solution of NaOH for 4 min. The etch was done by continuously dropping the solution through a hypodermic syringe on the specimen surfaces while the specimen was maintained at its original position under the microscope. After etching, the specimen was rinsed with water and then with alcohol, again by means of syringes. The markings on the specimen surface are shown in Fig. 12b. The etch has removed the coating to a considerable extent and, as a consequence, the oxide-film cracks seen in Fig. 12a have almost vanished. Since there is no widening or undercutting of the cracks and no evidence of etch pits (the thick, dark line on the upper left-hand corner is probably a piece of lens tissue used for absorbing unwanted solution), direct attack of the reagent on the aluminum itself (as distinct from the oxide) does not seem to have occurred. Therefore, any evidence of slip found after this etch could be regarded as a confirmation of the theory that the oxide-metal interface is a barrier to dislocations and that piled-up dislocations can be relieved by elastic and plastic process during etching.

Indeed, slip lines, though very faint, were observed after the removal of the oxide film. Two such lines are present in Fig. 12b (marked by arrows) and are confirmed by stereographic analysis to be slip lines on the primary slip plane of the specimen. One of these lines corresponds to the trace marked with an arrow in Fig. 12a but is now more pronounced. The other slip line was not visible at all before etching.

It should be mentioned that, prior to this experiment, observations were made of slip lines on five aluminum single crystals that have been kept in air for more than a month after being electropolished in a solution of 2:1 methyl alcohol and nitric acid. In all these cases where only a natural oxide film was present, no noticeable change of the character and/or the number of slip lines was detected at areas observed before and after etching.

**C. S. Barrett** (authors' reply)—We wish to thank Dr. Chen for his contribution of metallographic evidence for plastic flow initiated by the removal of an oxide film. On the basis that the abnormal after-effect caused by this removal is of the order of one thousandth the original strain, we had presumed that it would be extremely difficult to find such evidence and had not attempted such experiments.

A controversial point in the explanation of the abnormal after-effect is the possible role played by dislocation generators, such as the Frank-Read type, springing into action upon removal of a surface film. A. H. Cottrell has remarked to me that a Frank-Read source, even if located so that one end was at the surface, should extend to depths that are large compared with the depth in which many dislocations would be piled up; consequently, the plastic flow accompanying the release of the piled-up dislocations should occur more quickly than flow due to the source springing into operation.

We had anticipated someone's questioning whether torsional yield strengths might not be comparable in sensitivity to the torsional after-effect measurements of the current series of papers; this is being investigated.

[6] N. K. Chen and R. B. Pond: *Trans.* AIME (1952) 194, p. 1085; JOURNAL OF METALS (October 1952).

---

## Mechanism of Plastic Flow in Titanium: Manifestations and Dynamics of Glide

by F. D. Rosi

*DISCUSSION, J. S. Smart, Jr. and Bruce Chalmers, Chairmen*

**N. K. Chen** *(Johns Hopkins University, Baltimore)*—The author described the nature of slip bands in titanium under "Experimental Results" as being orientation dependent: For orientations with the stress axes near the [0001] [11$\bar{2}$0] zone, the slip-band formation is of the coarse, widely spaced type, and for orientations approaching the [0001] [10$\bar{1}$0] symmetry position, the slip bands are finer and closely spaced. Thus, it was concluded (4) that "the slip-band density varies inversely with the angle $\chi$, which the slip plane makes with the stress axis." It should be pointed out that this general conclusion, if correctly interpreted according to crystallography, implies that slip bands are most coarse for specimens with stress axes in the region around the pole [11$\bar{2}$0] and most fine around the pole [0001], as can be seen from a stereographic projection of orientations of equal $\chi$ values (Fig. 26). Furthermore, it implies that crystals having the same $\chi$ angle should have approximately the same slip-band density. I wonder if these derivations from the conclusion could be reconciled to the author's data and, after all, whether the value $\chi$ could be used without reservations as a single parameter to describe the nature of slip bands.

I was rather interested to note the author's second conclusion that "unpredictable cross slip occurs on the same crystallographic family of planes which define primary slip; i.e., {10$\bar{1}$0}." This observation on cross slip differs from those reported for face-centered-cubic metals[20] and for uranium[17] in that the primary and the cross-slip plane do not possess the same slip direction in the present case. However, since the author stated

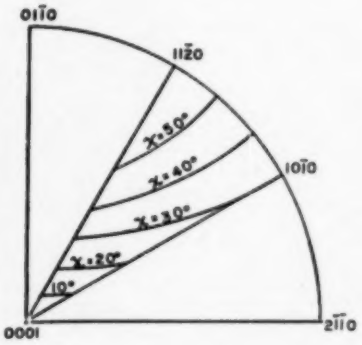


Fig. 26—Stereographic projection indicating orientations of equal $\chi$ values, assuming (01$\bar{1}$0) [2$\bar{1}$$\bar{1}$0] slip. $\chi$ is the angle between stress axis and the slip plane.

that "the appearance of unpredicted cross slip in its typical steplike character was observed in only one crystal" and since Anderson, Jillson, and Dunbar[20] have reported basal slip in titanium for crystals of certain orientations, I am tempted to suspect that the participation of the basal plane, gliding in the same direction as the primary prismatic slip, is highly probable and could account for a steplike appearance.

**F. D. Rosi** (author's reply)—In reply to Dr. Chen's objection to the use of the angle $\chi_0$ to describe the orientation dependence of slip-band development, it is important to emphasize that this dependence was concerned solely with orientations where extensive slip occurred on $\{10\bar{1}0\}$ planes. For those orientations in the region of the stereographic triangle approaching [0001], the deformation process becomes more complex. In the early stages of flow, additional slip systems occur, and frequently twinning replaces slip as the primary mode of deformation. Under such conditions of flow, it would not be possible to properly evaluate the effect of the $\chi_0$ value on $\{10\bar{1}0\}$ slip-band development. For this obvious reason, it was not intended to indicate that the value of $\chi_0$ was used without reservation as a parameter to describe the development of $\{10\bar{1}0\}$ slip bands.

A regards the cross-slip observed in titanium, it also occurred to the author that it would be most convenient if its crystallographic nature were similar to that observed in other metals. However, in the only crystal where the cross-slip was well defined, there was no possibility of attributing the stepped segments to cooperative slip on the basal plane or any other rational plane containing the same slip direction as the primary $\{10\bar{1}0\}$ plane.

[20] E. A. Anderson, D. C. Jillson, and S. R. Dunbar: Deformation Mechanism in Alpha Titanium. *Trans.* AIME (1953) 197, p. 1191; JOURNAL OF METALS (September 1953).

---

## Uranium-Titanium Alloy System

by Murray C. Udy and Francis W. Boulger

*DISCUSSION, B. D. Cullity and A. H. Geisler, Chairmen*

**R. W. Buzzard** *(National Bureau of Standards, Washington)*—There are numerous methods available for the collection of data to be used in the derivation of the constitution of an alloy system. The X-ray and microscopic techniques utilized by the authors represent two of the more popular approaches and constitute excellent sources of data, especially when verified by one of the various thermal-analysis techniques.

In the preliminary microscopic and X-ray work at the National Bureau of Standards, data similar to that presented by the authors were observed. As this could not be correlated with the thermal data, additional metallographic work was instigated. It was shown that, by proper preparation of the alloy surface, the X-ray and microscopic data would correlate with the thermal data. The experience of the writer with several uranium systems has shown that alloys of high uranium content are particularly susceptible to improper polishing and etching techniques, and it has been found that the results of thermal analyses serve as excellent guides in the selection of proper polishing and etching procedures. Similarly, it is the experience of the writer, in connection with the U-Ti system, that heat tinting and deep etching tend to obliterate the true microscopic structures in the high uranium alloys. This tendency of the metallographic technique to obscure microstructures is not peculiar to the uranium alloys but is common to other systems as exemplified by the fact that the $\chi$ phase of stainless steel was long confused with the $\sigma$ phase until adequate metallographic techniques were developed to differentiate between the two phases.

The writer has noted in the literature that many investigators are prone to use the temperature at which fusion is noted on visual examination as the liquidus temperature. There is a definite lack of agreement among investigators as to the exact interpretation of such fusion data. It is noted that Domagala and McPherson[3] in their study of the Zr-O system utilized a comparable technique to obtain a rough estimate of the solidus temperature, a conclusion with which the writer is in accord. Visual observations of the fusion point of quasi-pure metals give an approximation of the melting point of the element. On the other hand, in an alloy system, fusion temperatures more closely reflect a rough approximation of the solidus, depending on the fluidity of the mushy stage between the solidus and liquidus. Many compositions of alloys are sufficiently fluid in the mushy stage to permit pouring at temperatures below the liquidus. In the examination of several alloy systems, the writer has found it necessary to examine several compositions of alloys to determine questionable fields. Examination of the authors' liquidus data for the 90.8, 84.3, and 78.4 atomic pct uranium alloys hardly permits correlation with the previously reported thermal data. Assuming these determinations to be a rough estimate of the solidus, there is a very definite trend shown that tends to confirm the interpretation of a peritectic terminating in a rapidly rising solidus as previously reported. The $U_2Ti$ field conforms with the phase to be expected from the previous work. The thermal arrests depicting the decomposition of the $\delta$ phase, reported by the writer, were also observed and reported by Seybolt.[1] From the thermal data obtained on the U-Ti system, the sharpness of the recorded thermal arrests leaves little question as to the existence of a reaction horizontal characteristic of the eutectoid decomposition of the $\delta$ phase.

In the preparation of the microscopic specimens for the study of the U-Ti system at the National Bureau of Standards, certain factors were observed to be peculiar to the quenching technique which tended to mask the true microstructures of the quenched alloys. The writer would be interested in the authors' experience with the alloys in the composition range 0 to 30 atomic pct Ti in respect to the following: 1—Did the authors note any reaction between the alloys and the Vycor? 2—Did the authors determine the effects of rate of quenching on these alloys to assure themselves that the quenching rate was of sufficient rapidity to retain the true structure of the alloys?

**M. C. Udy** and **F. W. Boulger** (authors' reply)—The authors wish to thank Mr. Buzzard for his discussion of our paper. We agree with him that alloys of high uranium content are particularly susceptible to improper polishing and etching techniques. However, in the present work, care was taken to avoid the pitfalls. Specimens were examined under many conditions of polishing and etching until it was certain that the

structures reported were real. As was noted in the paper, we too used thermal analyses as a guide in our work. However, we are not as convinced of the infallibility of thermal analyses as Mr. Buzzard seems to be. In fact, failure to check, with small samples of the identical alloys, some of the preliminary liquidus and solidus data reported by Seybolt[1] and ourselves, led to the present careful recheck of the whole system.

For most alloys, both liquidus and solidus points were observed, and some are shown on the diagram. However, the solidus point was more difficult to determine accurately by optical readings. The liquidus point, on the other hand, was readily reproducible on duplicate samples.

We agree that it would be desirable to examine more compositions in the "questionable" range. However, we feel that the compositions we examined were sufficient to discredit some of the previous information, particularly the existence of a so-called "δ" phase. The alloys examined by Seybolt were prepared by us and examined independently. Seybolt concurs that no intermediate phase other than $U_2Ti$ was found.

In answer to the question about reaction between Vycor and alloys in the 0 to 30 atomic pct Ti range, very little reaction was noted except at points of contact when the tubes were suitably purged of possible carrier gases. Tubes were designed so that alloy bars rested on only two point contacts. These points were avoided in taking specimens for examination.

In regard to the effect of quenching rate, it was not claimed that all the alloy structures were retained on quenching. In fact, composition limits are presented beyond which it was impossible to retain the high temperature structure on water quenching. However, appearance of such things as Widmanstaetten patterns in the quenched structure is evidence of a change in structure on cooling.

Admittedly, further work on this system is desirable to pin point some of the established features. We feel that a high temperature X-ray study would be particularly fruitful.

[1] R. F. Domagala and D. J. McPherson: System Zirconium-Oxygen. Trans. AIME (1954) 200, p. 238; JOURNAL OF METALS (February 1954).

---

## Creep Correlations of Metals at Elevated Temperatures

by Oleg D. Sherby, Raymond L. Orr, and John E. Dorn

*DISCUSSION, D. N. Frey and G. V. Smith, Chairmen*

**I. S. Servi** and **E. M. Onitsch-Modl** *(Electro Metallurgical Co., Niagara Falls, N. Y.)*—The authors should be commended for their summarization of selected data on creep of metals and for their attempt to develop a novel theory. In this field, where the industrial progress is generally ahead of basic knowledge and where most of the data have been obtained following no logical patterns, any work aimed at the correlation of existing results is very welcome and worthy of praise. However, the authors' substantial contribution to the understanding of creep would be much more valuable after certain obscure and rather incongruous points are clarified.

The authors' conclusion, that $\Delta H$ is a constant independent of stress at temperatures above about 0.45 $Tm$, can be accepted only when an extensive range of stresses is considered, and other variables, such as structural instabilities, are removed from the analysis. It is fortunate that Alexander, Dawson, and Kling[18] obtained accurate data for creep of gold over a broad span of stresses. Such data, replotted in Fig. 13, show rather poor agreement with the postulation that $\Delta H$ is independent of stress. Perhaps this can be shown better by analyzing the five pairs of points at about 224, 120, 91, 67, and 43 psi for 1193° and 1293°K. The values of log $Z$, based on the assumption that $\Delta H$ is constant and equal to 50,000 cal per mol, are reported in Table III.

If computations are repeated in order to keep the variation in function $Z$ below 2 pct, the values of activation energies, shown in Table IV, must be used.

Table III. Computation of Function Z Based on Data[18] for Gold

| Approximate stress, psi | 224 | 120 | 91 | 67 | 43 |
|---|---|---|---|---|---|
| Log Z (1293°K) | 7.165 | 6.830 | 6.716 | 6.573 | 6.193 |
| Log Z (1193°K) | 7.335 | 6.841 | 6.540 | 6.381 | 5.727 |
| Log $Z_{1293}$ − log $Z_{1193}$ | −0.170 | −0.011 | +0.176 | +0.192 | +0.466 |
| Variation in Z, pct | 48 | 2.5 | 50 | 55 | 190 |

These results are in agreement with a previous suggestion[17] that $\Delta H$ decreases with increasing creep stress. The same conclusion can be reached using data by Servi and Grant[11] for high purity aluminum; however, the data for 866° and 755°K cannot be included in the analysis because they refer to a condition of excessive grain growth during creep testing.

It should also be mentioned that Sherby and Dorn[2] found a marked effect of annealing conditions on the activation energy of creep of 2S-O aluminum, thus indicating that the activation energy is a structurally sensitive parameter.

With regard to the boundary between "low temperature" and "high temperature" creep, experimentally established at about 0.45 $Tm$, the statement was made that, "Perhaps no special meaning can be ascribed to the number 0.45 $Tm$." The factor 0.45, known as Tamman's factor, is purely empirical, but is related to some physical phenomena. Hüttig,[20] studying the sintering process of powders, found that surface diffusion occurs at Tamman's factors 0.23 to 0.36, grain-boundary displacement at 0.33 to 0.45, lattice diffusion through the entire crystal section at 0.37 to 0.53, and formation of new crystallization centers at 0.48 to 0.80. Therefore, it appears that the number 0.45 $Tm$ may be related to the beginning of recrystallization rather than to self-diffusion.

The literature on self-diffusion experiments has indicated that the accuracies and reproducibilities of activation energies are generally rather poor. Therefore, the correlation of Fig. 16 does not appear to be sufficient ground for assuming that "the rate-controlling process for self-diffusion might also be the rate-controlling process for creep." Moreover, Hoffman and Turnbull[21]

Table IV. Computation of Values of $\Delta H$ for Variations in $Z = \dot{\epsilon} e^{\Delta H/RT}$ Below 2 Pct

| Approximate stress, psi | 224 | 120 | 91 | 67 | 43 |
|---|---|---|---|---|---|
| $\Delta H$, cal per mol | 39,000 | 49,000 | 62,000 | 63,000 | 83,000 |

found that the activation energy of self-diffusion of silver is 45,950 cal per mol for single crystals, and 26,400 for fine-grained polycrystalline specimens. Hoffman and Turnbull computed the absolute activation energy for grain-boundary self-diffusion, obtaining a value of 20,200 cal per mol for 99.97 pct Ag, and 21,500 for 99.999 pct Ag, thus indicating a marked effect of grain size and an appreciable effect of purity on the activation energy for self-diffusion. Therefore, if a close correlation exists between activation energies for creep and self-diffusion, it might be expected that grain size, and perhaps purity, should affect the activation energy for creep.

The hypothesis that "high temperature creep appears to occur due to removal of barriers to the motion of dislocation" would be of substantial value for the understanding of the mechanism of creep if the nature of such barriers is suggested. In fact, it appears quite difficult to explain all the complex phenomena associated with plastic deformation at elevated temperatures, such as slip, grain-boundary glide, polygonization, and, in some cases, twin formation, based on the removal of hypothetical and unidentified barriers.

**A. R. Chaudhuri, H. C. Chang,** and **N. J. Grant** *(Massachusetts Institute of Technology, Cambridge, Mass.)*—This interesting paper which is an effort to rationalize the creep process on the basis of pure diffusion phenomena, is bound to raise a large number of questions in a field of activity where many previous theories have been unsuccessfully presented. In view of the fact that the authors have utilized data communicated from our laboratory, particularly data which were interpreted quite differently, and in view of their efforts to rationalize creep on the basis of a heat of activation value which matches the coefficient of self-diffusion, a number of questions and doubts come to mind:

1—The equations used by the authors come back to the mechanical equation of state which was so effectively criticized by Orowan[28] and others during the past several years. How do the authors reconcile their equations with these arguments?

2—The values of creep rate predicted by interpolation from Eq. 4 of their paper, namely

$$\sigma_c = f\,(\dot{\epsilon}.e^{\Delta H/RT}) = f\,(Z)$$

show good agreement with experimental values. A check of data shows, however, that, whereas the experimental points are randomly scattered about the stress-minimum creep-rate curves for high purity aluminum,[11] the values obtained from the curves representing the correlation $\sigma_c = f\,(\dot{\epsilon}.e^{\Delta H/RT})$ show systematic deviations from the stress-minimum creep-rate plot. This fact indicates that the $ln\ (\dot{\epsilon}.e^{\Delta H/RT})$ isothermals do not form parts of the same curve except for a general over-lapping or quasi-parallelism. Do these departures, which are evident in several of the authors' curves (Figs. 6, 7, 12, and 13), show that the functional relationship suggested by the authors requires further modification of an empirical nature?

3—Is it not true that the functional relationship $\sigma_c = f\,(\dot{\epsilon}.e^{\Delta H/RT})$ cannot be used safely to predict data outside of the stress range of the experimental points used to prepare the curve representing the above relationship? For example, in the Servi and Grant data[11] on aluminum, the authors' equation could predict creep rates with reasonable accuracy at 600°F (a temperature at which no tests were carried out but which lies within the experimental stress range), but it cannot predict the creep rates at stresses of 6,500 psi or more at any temperature at which no tests were performed.

4—A point of very considerable interest is the question of the variation or constancy of the activation energy for creep with, for example, stress. The authors have stated that the value of this quantity can be determined from the equation

$$\Delta H = R\,\frac{ln\dot{\epsilon}_2/\dot{\epsilon}_1}{1/T_1 - 1/T_2}$$

where $\dot{\epsilon}_1$ and $\dot{\epsilon}_2$ are two values of the minimum creep rate (equivalent to their term "secondary-creep rate") at temperatures $T_1$ and $T_2$, respectively, corresponding to a given stress. This procedure was carried out with the Servi-Grant aluminum data[11] within a stress range of 100 to 3,500 psi. It was found that the activation energy was most definitely dependent on the stress. Without placing unduly great significance on the activation energy for creep, Servi and Grant had also determined the value for $\Delta H$ for creep from their data by a method different from that of the authors, namely by plotting the creep rate vs the reciprocal of the absolute temperature for a constant stress,[11] and in that instance, had also shown the same variation of the activation energy with the stress. Analysis of the data on annealed monel (Grant and Bucklin[29]) also showed a variation of the activation energy with stress.

Since both methods, that of Servi and Grant and that in the present analysis, show a variation of the activation energy with stress, what is the basis of the authors' statement that $\Delta H$ for creep is not a function of stress, or that it can be called a "universal constant?"

5—In addition to this disagreement of the calculated $\Delta H$ values from the same data, there are a number of other measured and calculated values which are worth noting. Buffington and Cohen[30] found that the coefficient of self-diffusion for $\alpha$-iron is remarkably influenced by strain-rate changes by a factor of about 15. Rhines,[20] in measuring the activation energy for grain-boundary displacement in the creep of high purity aluminum at low stresses, based on a large number of tests, obtained a value of about 10,000 cal per mol, a figure considerably different from the 36,000 cal per mol value which was claimed by the authors to be the activation energy for the overall creep process in aluminum.

In view of these highly divergent activation-energy results, and the experimental evidence of variations in

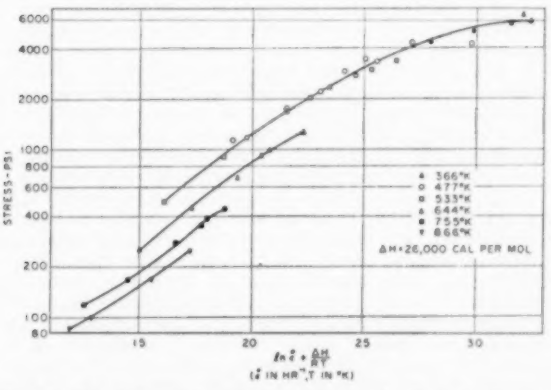


Fig. 19—Correlation of Servi-Grant data[11] for aluminum by the relation $\sigma = f(\dot{\epsilon}e^{\Delta H/RT})$. $\Delta H = 26{,}000$ cal per mol.

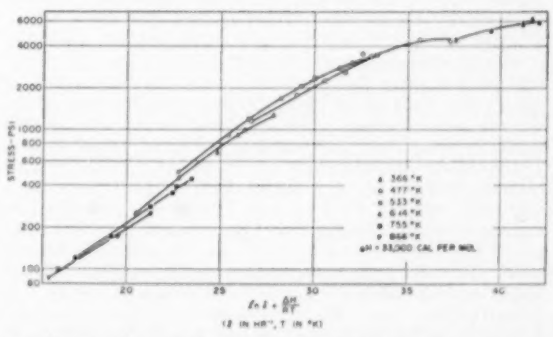


Fig. 20—Correlation of Servi-Grant data[11] for aluminum by the relation $\sigma = f(\dot{\epsilon}e^{\Delta H/RT})$. $\Delta H = 33{,}000$ cal per mol.

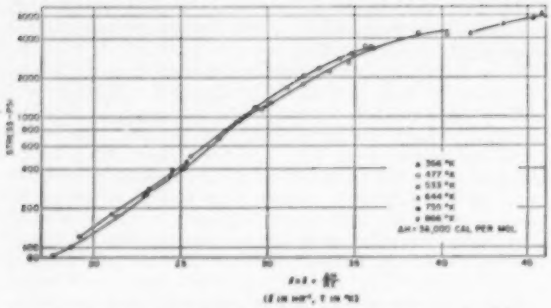

Fig. 21—Correlation of Servi-Grant data[11] for aluminum by the relation $\sigma = f(\dot{\epsilon}e^{\Delta H/RT})$. $\Delta H = 36{,}000$ cal per mol.

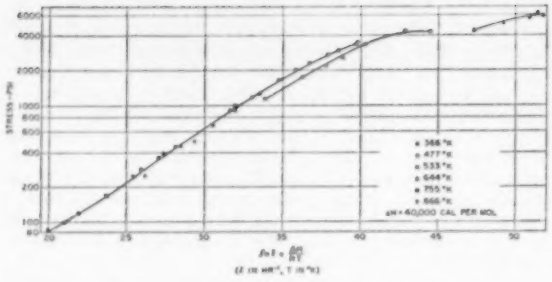

Fig. 22—Correlation of Servi-Grant data[11] for aluminum by the relation $\sigma = f(\dot{\epsilon}e^{\Delta H/RT})$. $\Delta H = 40{,}000$ cal per mol.

$\Delta H$ for self-diffusion with stress, can the authors reconcile the data? Furthermore, would the authors state their criteria for the selection of an unique value of the activation energy for creep, a value which is being endowed with the privileges of a universal constant?

6—For the functional relationship postulated by the authors to be true, it is necessary that the $ln\ (\dot{\epsilon}e^{\Delta H/RT})$ values for every temperature lie on a single curve for each alloy. However, in most cases it was found that the $ln\ (\dot{\epsilon}e^{\Delta H/RT})$ values for each temperature fall along obviously separate lines, though these lines lie about a selected mean line. The selected value of the activation energy determines the degree of fit of the various isothermals about the mean line. This is demonstrated in Figs. 19 to 22, which present the Servi-Grant aluminum data.[11] Values of $ln\ (\dot{\epsilon}e^{\Delta H/RT})$ have been determined for four values of $\Delta H$. $\Delta H = 26{,}000$ cal per mol, and 40,000 cal per mol represent the limits of the $\Delta H$ values obtained by Servi and Grant as well as by the authors' method in the present analysis. $\Delta H = 33{,}000$ represents the activation energy of self-diffusion for aluminum as given by the authors, and $\Delta H = 36{,}000$ cal per mol is the value of the activation energy for creep obtained by them for aluminum. The authors limit the applicability of their equation to temperatures above 0.45 $Tm$, presumably a temperature above which active recovery occurs. As a test of the usefulness of the $Tm$ value, we have included the 200°F (366°K) test values from the original aluminum data[11] to emphasize an important point. In Fig. 19 it is seen that if only the 200°, 400°, and the 500°F (366°, 477°, and 533°K) data are considered (these points would correspond to high stress values at these lower temperatures) along with the low $\Delta H$ value of 26,000 cal, the authors' equation is applicable at temperatures below 0.45 $Tm$. The fit at high temperatures is not as good. At the highest measured values of $\Delta H$ (40,000 cal), the high temperature isothermals show a much smaller deviation and even the low temperature points (including 200°F) fit well except for one or two points (see Fig. 22). Thus, high $\Delta H$ values show a good fit of the data at all temperatures, Figs. 20 and 21. ($\Delta H =$ 33,000 and 36,000 cal per mol) still show the distinct separation of each of the isothermals but with better average fit in the temperature range above 0.45 $Tm$. It would appear, therefore, that the limiting temperature depends on the particular value of $\Delta H$ which is used. Our data show that $\Delta H$ varies with stress; thus we are not surprised that a different selection of this limiting temperature permits a different value of $\Delta H$. Thus, lower temperatures, which go hand in hand with higher stresses, show a better fit in Fig. 19 for lower values of $\Delta H$. In view of this systematic relationship, the use of data over narrow temperature ranges of not more than 200°C (Figs. 7, 9, 12, 13, and 15) leaves much to be desired in selecting a $\Delta H$ value which would apply equally well over wider temperature ranges. It appears that the authors' equation is not especially sensitive to the value of $\Delta H$ and can be corrected by adjustments with $Tm$ fraction.

Our concern is not so much with the utilization of the equations proposed by the authors. Interpolation and even a limited amount of extrapolation may be possible through their use. Our concern is 1—with the statement that $\Delta H$ does not vary with stress, since our measurements show it does; and 2—with the statement that the $\Delta H$ value for creep is a universal constant and that it is equal to the self-diffusion coefficient.

**R. W. Guard** *(General Electric Co., Schenectady)*—The authors have done an excellent job of correlating the available data on the creep of metals. Work is going on in our laboratory to check these and similar correlations on a number of other materials. Our results can be interpreted with the same order of agreement as presented in the paper, but several points have arisen as follows, and we would be interested in the authors' comments concerning them:

1—Our tests are constant-stress tests conducted on wires. In most cases, we find difficulty in determining any "secondary creep rate." When there is a minimum rate, it rarely occurs at anything like a constant strain for different tests. Might it not be better to use the creep rate at constant values of strain?

2—We have found deviations on plots of $\epsilon$ vs $\theta$ among tests made at different temperatures often to be greater than the experimental error in duplicate tests. This variation suggests that there are other factors involved and that the correlation is only approximate.

**Oleg D. Sherby, Raymond L. Orr,** and **John E. Dorn** (authors' reply)—The authors must agree with the various discussers of their paper relative to the numerous factors involved in high temperature creep and to the inherent complexity of the processes that take place. Not all of the data in the literature correlate in the manner suggested by the authors but much of it does reasonably well within appropriate limits of materials and temperature. The authors believe that it is unreasonable to expect any law of nature (vis., Newton's laws of motion or the ideal gas laws) to be universally valid. Consequently, exceptions to newly proposed idealized creep laws are expected. And the question then arises as to whether any new law should be completely and irrevocably discarded because some deviations from it have been noted or whether the alternative position of more complete testing of the proposed law should be attempted in order to more fully evaluate its ranges of validity and the ranges where it deviates from the experimental facts. Whereas some discussers appear to prefer abandoning the law because of exceptions, the authors of this paper believe more rapid progress might be made by more complete examination of the law. Of course, the conditions of such examinations should be limited to the realm wherein the law might be correct. For example, the ideal gas laws could neither be verified nor rejected when tested only in the realm of high pressures and low temperatures. The greater complexity of the creep process and the added complications of strain-history dependency of creep, however, have thus far impeded attempts to clearly reveal the range of validity of the proposed idealized laws.

Table V. Computation of Values $\Delta H$ for Gold Based on 1243° and 1293°K Data (Data of Alexander, Dawson, and Kling[16])

| Stress, psi | 200 | 150 | 100 | 50 |
|---|---|---|---|---|
| $\Delta H$, cal per mol | 52,0000 | 52,000 | 57,000 | 56,000 |

The major question proposed by Drs. Servi and Onitsch-Modl appears to be concerned with the possible dependence of the activation energy for creep on the stress. For analysis they selected only the 1293° and the 1193°K data of Fig. 13 for gold which appear to indicate that the activation energy for creep decreases with increasing stress. But, as shown in Table V, if they had made their comparison between the 1293° and the 1243°K data, the calculated activation energy would have been found to be rather insensitive to the stress. Therefore, these data on gold are not definitive due to internal inconsistencies of unknown origin. And consequently, it appears justifiable to give greatest weight to the trends that appear to follow the observations made on sets of internally consistent data for the purpose of evaluating an activation energy. The excellent and more self-consistent data of Smith[10] (Fig. 15) on lead, Carreker[17] (Figs. 10 and 11) on platinum, Tapsell and Clenshaw[12] (Fig. 3) on iron, Sherby and Dorn[3, 4] (Fig. 2) on aluminum, and numerous other investigations[20, 21] suggest that the activation energy for high temperature creep is insensitive to the stress.

Additional verification of the insensitivity of $\Delta H$ to the stress is given by the data[22] supporting Eq. 5. If $\Delta H$ depended on the stress, $B$ should have been found proportional to the reciprocal of the absolute temperature. The fact that $B$ was insensitive to temperature reveals that $\Delta H$ is insensitive to the stress.

The above-mentioned creep laws are not valid for 24S-T alloys and would be expected to fail for any precipitation-hardened alloys or other thermally unstable system. But as mentioned by Drs. Servi and Onitsch-Modl, and as demonstrated by the present authors, the laws occasionally appear to fail for such simple systems as 2S-O. This is perturbing but scarcely devastating because the exact limitations of the law are not fully established. Actually a few metals (e.g., iron) obey the law much below 0.45 $Tm$, whereas in others the law is invalid somewhat above 0.45 $Tm$. This suggests that the number 0.45 $Tm$ has little significance and that the limitation might be ascribed to some fundamental thermal property. Contrary to the suggestion of Drs. Servi and Onitsch-Modl, this property cannot be recrystallization because recrystallization in the common sense seldom occurs during creep of annealed metals. The singular example of recrystallization during creep is that found during creep of lead uncovered by Greenwood and Worner[23] and later confirmed by Andrade,[24] where it was shown that, over each recrystallization period, the creep rate accelerated giving a stepped creep curve. Most creep curves are relatively smooth and X-ray and metallographic analyses have shown that recovery leading to subgrain formation, and not classical recrystallization, occurs during creep. Since recovery is so sensitive to impurities, it is quite possible that some metals like 2S-O only exhibit high temperature creep at very high temperatures. But at present, no method of predicting the range of conditions over which the law will be valid is known. Consequently, it is currently necessary to rely on experimental verification in each case.

We thank Messrs. Chaudhuri, Chang, and Grant for their interesting discussion. The functional relationships presented in our paper, namely, $\epsilon = f(\theta, \sigma_c)$ and $\sigma_c = f(\dot{\epsilon}_c e^{\Delta H/RT})$ were not intended to indicate the existence of a mechanical equation of state. As mentioned in the paper, Eq. 2 is applicable only for constant-stress or constant-load tests. The validity of the equation arises from the fact that the creep structure developed during constant-load (or stress) creep testing is dependent only on $\epsilon$ or $\theta$, independent of the temperature history. This has been clearly proved in earlier investigations on aluminum by means of tensile and X-ray investigations.[4] The cyclic temperature results on nickel shown in Fig. 5 suggest the same conclusion. It has been shown,[4] however, that at different stresses different creep structures are developed and no individual structure developed at one stress appears to be correlatable with any other structure developed at another stress. Therefore, a series of $\epsilon$-$\theta$ curves obtained under constant stresses or loads cannot be utilized for the prediction of the creep curve under alternating stress conditions. The same arguments are valid for Eq. 4.

Points 2, 4, and 6 in Messrs. Chaudhuri, Chang, and Grant's discussion are identical arguments referring to the question on whether $\Delta H$ for creep of high purity aluminum (data of Servi and Grant) is constant as a function of stress. The original analysis of the data for obtaining activation energies by Servi and Grant[11] were not carried out in the stress range 3500 to 100 psi, but in the stress range 5000 to 400 psi. If they had extended their analysis down to 100 psi and left out the low temperature (366°K) data, the activation energy would have varied much less with stress than suggested by the Servi and Grant analysis. Our interpretation of Chaudhuri, Chang, and Grant's Figs. 19 through 22 is that the activation energy for creep of high purity aluminum is about a constant equal to 36000 cal per mol, within ±10 pct, if the 366°K data are excluded. Incidentally, the highest stress test at 477°K should have been plotted at 5000 psi instead of 4200 psi; if this point is corrected, a sharper break is indicated between the 366°K data (low temperature creep), and the other temperature data (high temperature creep), see Fig. 21. The same rather sharp break is clearly seen in Carreker's[17] platinum data (Fig. 10) and was shown earlier for pure aluminum.[4]

We are in agreement with Chaudhuri, Chang, and Grant's point 3 in that the function $\sigma_c = f(\dot{\epsilon}_c e^{\Delta H/RT})$ is useful for predicting creep rates at stresses where data already are available but that extrapolation of the curve much beyond the actual $\sigma - \dot{\epsilon}_c e^{\Delta H/RT}$ data might be dangerous. The arguments presented in point 5 are not clear to the authors. First, it is agreed that Buffington and Cohen showed that the superposition of an applied stress increased the rate of self-diffusion in $\alpha$-iron, but they did not show whether or not the activation energy was changed, which is the issue in question. This is similar to the situation where the effect of cold work is to change the creep rate of a metal but not necessarily the activation energy of the creep process.[21] The second point is with regard to Rhines' work. We are not familiar with the NACA conference on creep held in 1953. Rhines and Cochardt, however, in an excellent paper on the creep of aluminum bicrystals,[25] studied grain-boundary shearing as a function of temperature under a stress of 100 psi. These authors plotted the logarithm of the boundary displacement at a given time vs the reciprocal of the absolute temperature; the slope of the resulting straight line was assumed equal to the activation energy divided by the gas constant times 2.3. They obtained 9800 cal per mol for the activation energy. Their method of

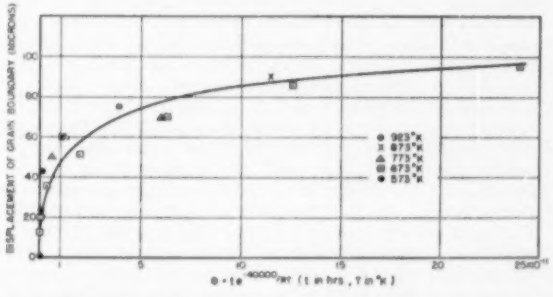


Fig. 23—Grain-boundary displacement as a function of $\theta$ for high purity aluminum under a stress of 100 psi. Data of Rhines and Cochardt.[25]

analysis utilizes an entirely different principle from the $\epsilon$-$\theta$ correlation. Rhines and Cochardt's data were analyzed in a recent paper[46] by means of Eq. 2, and Fig. 23 illustrates such a correlation where the best average value for the activation energy was equal to 40,000 cal per mol. Furthermore, results in the same paper on the creep of aluminum at 250 psi indicate that $\Delta H$ for grain-boundary shearing was equal to 37,000 cal per mol. This approximate equality between $\Delta H$ for grain-boundary shearing and $\Delta H$ for slip is not unexpected, since it is believed that crystallographic slip[46, 47] is prominently responsible for grain-boundary shearing.

Mott[48] has recently suggested that high temperature creep might occur by a dislocation-climb process for which the activation energy is that for volume self-diffusion. Inasmuch as the barriers to dislocations are probably other dislocations as well as precipitates, etc., the Mott process is not greatly dissimilar from a recovery process. In fact, Kuhlmann[49] and also Mott[48] have treated recovery as a dislocation-climb process. Thus, the suspected correlation between the activation energy for creep and that for volume self-diffusion can be rationalized. Of course, much of the reported activation energies for self-diffusion are suspect in view of abnormal scatter in the reported values. And in some cases, grain-size effects have been noted, but in other cases they appear to be absent. In fact, the activation energies for high temperature creep appear to be more reliable than those for self-diffusion because the realm of reliability of the creep law can be established experimentally, whereas some sources of scatter of $\Delta H$ for self-diffusion are unknown and the reliability of $\Delta H$ for self-diffusion cannot yet be established experimentally.

We are pleased to see that Mr. Guard has been able to correlate creep data on other materials by means of the equations presented in the paper. Our correlations and experiments have indicated to us that the secondary creep rate is obtained at the same strain, independent of temperature, for a given stress. However, the strain at the initiation of secondary creep is definitely a function of the stress. As a rule, the higher the stress used, the higher the creep-strain value for initiation of the constant rate of creep. In the case of constant-stress creep tests where frequently the second stage is very small or absent, it would be better to use the creep rate at constant values of strain for correlation attempts with the Zener-Hollomon parameter, Eq. 4.

[45] G. F. Hüttig: *Die theoretischen Grundlagen der Sintervorgänge innerhalb von Pulvern.* (1948) Graz. Internationale Pulvermetallurgische.
[46] C. G. Goetzel: *Treatise on Powder Metallurgy.* (1950) Vol. 2, p. 811. New York. Interscience Publications.
[47] R. E. Hoffman and D. Turnbull: *Journal of Applied Physics* (1951) 22, pp. 634-639.
[48] E. Orowan: *Journal* West Scotland Iron and Steel Institute (1946) 54, pp. 45-82.
[49] N. J. Grant and A. G. Bucklin: *Trans.* ASM (1953) 45, pp. 151-170.
[50] F. S. Buffington and M. Cohen: *Trans.* AIME (1952) 194, p. 859; JOURNAL OF METALS (August 1952).
[51] F. N. Rhines: *NACA Report on Conference of Creep of Metals* (June 1953) p. 28.
[52] R. L. Orr, O. D. Sherby, and J. E. Dorn: Correlations of Rupture Data for Metals at Elevated Temperatures. *Trans.* ASM (1954) 46, pp. 113-128.
[53] R. E. Frenkel, O. D. Sherby, and J. E. Dorn: Effect of Cold Work on the High Temperature Creep Properties of Dilute Aluminum Alloys. To be published in *Trans.* ASM (1955) 47.
[54] O. D. Sherby, R. Frenkel, J. Nadeau, and J. E. Dorn: Effect of Stress on the Creep Rate of Polycrystalline Aluminum Alloys under Constant Structures. *Trans.* AIME (1954) 200, pp. 275-279; JOURNAL OF METALS (February 1954).
[55] J. N. Greenwood and H. W. Worner: Types of Creep Curves Obtained with Lead and Its Alloys. *Journal* Institute of Metals (1939) 64, pp. 135-167.
[56] E. N. da C. Andrade: Creep of Metals and Recrystallization. *Nature*, London (1948) 162, p. 410.
[57] F. N. Rhines and A. W. Cochardt: Preview of Behavior of Grain Boundaries in Creep of Aluminum Bicrystals. *NACA TN 2746* (July 1952).
[58] B. Fazan, O. D. Sherby, and J. E. Dorn: Some Observations on Grain Boundary Shearing during Creep. *Trans.* AIME (1954) 200, p. 919; JOURNAL OF METALS (August 1954).
[59] F. N. Rhines: Research in Progress. JOURNAL OF METALS (1953) 5, p. 1081.
[60] N. F. Mott: The Mechanical Properties of Metals. *Proceedings* Physical Society (1951) 64, pp. 729-741.
[61] D. Kuhlmann: On the Theory of Plastic Deformation. *Proceedings* Physical Society (1951) 64A, pp. 140-155.
[62] N. F. Mott: A Theory of Work Hardening of Metals, II: Flow without Slip Lines, Recovery, and Creep. *Philosophical Magazine* (1953) 44, Series 7, pp. 742-765.

## Aging Characteristics of Nickel-Chromium Alloys Hardened with Titanium and Aluminum

by Rolf Nordheim and Nicholas J. Grant

*DISCUSSION, D. N. Frey and G. V. Smith, Chairmen*

**F. N. Darmara** and **E. S. Machlin** *(Utica Drop Forge & Tool Corp., Utica, N. Y., Columbia University, New York)*—Drs. Nordheim and Grant have undertaken a study of an important mode of providing high temperature strength and are to be congratulated for the fine job they have done. The discussers are convinced, as a result of research and experience in vacuum melting and fabricating such alloys on a production basis, that the key to stronger and better super alloys for high temperature application lies in the intelligent use of precipitation hardening systems. Already, a Waspalloy composition, which makes use of the same precipitation hardening system, has, through the means of vacuum melting in our production furnaces, far exceeded the strength of available forgeable or cast alloys at 1500°F. We have also developed, again through the ability to control melting variables provided through the lack of oxygen and nitrogen in the vacuum-melting technique, a precipitation hardening alloy that extends such strength to higher temperatures. Consequently, the importance of studies such as that undertaken by the authors is not to be overlooked.

With respect to the apparent discrepancy in the solubilities of titanium and aluminum in the 80 pct Ni-20 pct Cr solution between the authors' results and those of Taylor and Floyd, the discussers wonder whether there might be a larger uncertainty in the amount of titanium and aluminum in the alloy. We note that there is a relatively large variation from the 4:1 ratio sought for titanium and aluminum. Could this be due to lack of recovery of these elements or to uncertainty in the chemical composition? As part of the answer to this question, we would appreciate a statement as to the method of chemical analysis for these elements, i.e., wet (if so, how) or spectrographic.

We are in agreement in general with the conclusion that $\gamma'$ is the prevailing precipitate over most of the quaternary field (at least for the aging times used). This same precipitate appears in Waspalloy as shown in the electron micrograph, Fig. 16. As shown in the figure, for production aging cycles, the distribution and size of the cubic $\gamma'$ is extremely fine even after a stress-rupture cycle at 1500°F. There is no doubt that this optically "invisible" precipitate is basically responsible for the high temperature strength of Waspalloy. However, it is by no means the only factor that affects the

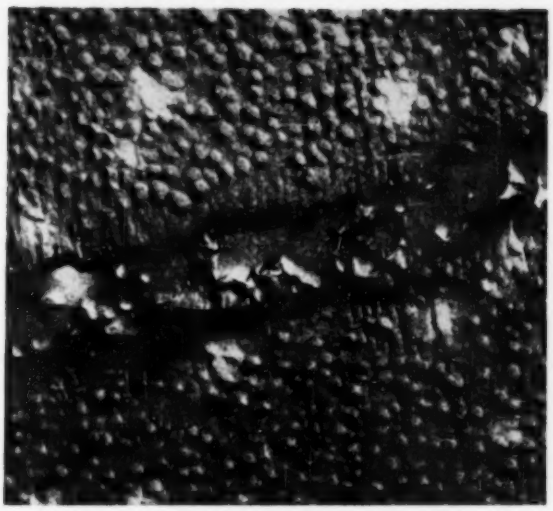

Fig. 16—$\gamma'$ precipitate and grain boundary in Waspalloy. Replica torn at grain boundary. Shadowed with palladium at 30°. X43,500. Area reduced approximately 60 pct for reproduction.

rupture life of these alloys. Indeed, the potential that can be reached with this means is generally not approached with such alloys melted in air. It appears from our results that the grain-boundary regions are much weaker in air-melted Ni-Cr alloys containing titanium and aluminum than in vacuum-melted alloys of the same composition. Of course, one unknown parameter in air-melted alloys is the amount of titanium *in solution* (uncombined with oxygen or nitrogen). Another factor is melting practice. Melting under vacuum is no cure at all if performed without foresight and knowledge of the factors involved. Unintelligent melting practice can lead to botched alloys even without a change in the apparent chemistry or microstructure. Other factors such as trace elements which reduce grain-boundary strength can be called upon. Whenever intercrystalline failure occurs, we believe that one effect of alloying elements may be indirect, as, for example, through the redistribution of elements that decrease the resistance of the grain boundaries to stress-relaxation and migration. The authors' observation that titanium decreases the rate of growth of $\gamma'$ is most significant. Have the authors any information as to the effect of titanium on the relative rate of grain-boundary depletion, or some approximate quantitative data on the effect of titanium at a given aluminum level on the rate of growth of $\gamma'$?

Again, the authors are to be congratulated for a significant contribution to the literature on high temperature alloys.

**Rolf Nordheim** and **Nicholas J. Grant** (authors' reply)—We thank Messrs. Darmara and Machlin for their comments and contributions to this subject. Answers to some of their questions are as follows:

1—Chemical analysis was by wet means, a method whereby the sample is dissolved and chromium is removed by distillation as chromyl chloride. Nickel is removed by a mercury cathode. Aluminum and titanium are precipitated together, ignited, and weighed. Titanium determined colorimetrically or gravimetrically by cupferron, and aluminum is taken by difference.

We agree that important errors can be made in interpretation of data if the titanium and aluminum in solution are not correctly measured. Titanium used up by carbon, oxygen, nitrogen, and other elements is lost from the important function of precipitation. We are sorry that there is not a safer or more sure analytical method known for the analysis of these two elements. Deviations from desired analysis did result from unexpected losses of both titanium and aluminum.

2—Vacuum melting, as such, literally guarantees a higher more reproducible alloy recovery on melting than can ever be hoped for by air melting. The absence or decrease of carbides, nitrides, and oxides is also a welcome gain and should be important in forging practice as well as in creep-rupture performance.

3—The influence of trace elements on the creep-rupture properties and on hot forgeability is a very important subject which has not yet been properly investigated. It is to be expected that some trace elements capable of being harmful can survive even vacuum melting. The role of these trace elements should be thoroughly examined.

4—We do not yet have any measure of the effect of titanium on the relative rate of grain-boundary depletion but have work underway to measure it.

The same answer holds for the effect of titanium at a given aluminum content on the rate of growth of the $\gamma'$. Unfortunately, it may be difficult to make these measurements because of the fineness of the precipitate, as noted in the election micrograph submitted by Dr. Machlin. Our electron micrographs show similar structures, but unfortunately we feel that the size of the $\gamma'$ precipitate is smaller than that shown in the figure, the size shown being a function of the etching technique which causes a pitting attack.

---

## Solidification of Aluminum-Rich Aluminum-Copper Alloys

by Arthur B. Michael and Michael B. Bever

*DISCUSSION, J. H. Frye and B. Lement, Chairmen*

**R. Hultgren** *(University of California, Berkeley, Calif.)*—The authors are to be congratulated on a really basic study of casting of alloys. Such studies obviously should have important practical applications in the foundry and in the casting of ingots.

The statement is made, "The liquid alloy was stirred immediately before pouring . . . Without this precaution, segregation occurred . . ." Does this imply that the liquid will segregate itself on quiet standing, presumably by the heavier copper atoms concentrating toward the bottom? If so, what is the magnitude of the effect? Or does the sentence merely refer to a stirring operation which could be carried through at any time after melting?

**F. N. Rhines** *(Carnegie Institute of Technology, Pittsburgh)*—The authors' interpretation of the finding of a variation in the degree of microsegregation from dendrite arm to dendrite arm is subject to an alternative explanation. In passing a plane of observation through a dendrite, it is improbable that the plane

will cut the center lines of a succession of dendrite arms because 1—polished surfaces are only approximately plane, 2—dendrites are imperfect in their spacing and the direction of their arms, and 3—it is rather improbable that a random plane would lie *exactly* parallel to the main axis of any of the dendrites cut by it. Thus it is to be expected that the plane of measurement will cut successive dendrite arms off-center by varying amounts. This would give the impression of varying degrees of microsegregation from arm to arm and varying concentration gradients as well. Strong evidence in favor of this hypothesis may be derived from the "C-values" given in Table IV. There it will be observed that $C_{max}$ and $C_{min}$ always bracket completely the values of $C'_{max}$ and $C'_{min}$. This would occur if successive dendrite arms were identical, composition-wise, but were cut at varying distances from their central axes, the "*C* max and min." corresponding to the most nearly diametral traverse and the "*C'* max and min." corresponding to a traverse along a cord.

It is interesting to note also in Table IV that the $C_{max}$ values not only vary with the copper content but that they never attain the maximum solid solubility value of 5.65 pct Cu. If an instantaneous equilibrium exists between the eutectic liquid and the surface of the solid phase, the latter should, of course, be saturated with copper no matter what the gross composition of the alloy. Does this mean that the assumption of instantaneous equilibrium is not valid, or is the diffusion velocity in the solid, subsequent to freezing, adequate to reduce the maximum copper concentration from 5.65 to the values shown in Table IV?

At the opposite end of the scale, the authors suggest that the reason for the absence of expected low values of copper content is to be associated with the diffusion effect and with the smallness of the volume of the material of minimum copper content. It may be added that undercooling would tend also to increase the value of the minimum copper content.

Finally, it may be worthy of note that the present, as well as older, findings provide a clear demonstration that diffusion in the liquid state is far from being "effectively infinitely fast." Were such the case, normal segregation would achieve a maximum of 35 pct Cu, instead of the 8 pct found.

**W. G. Pfann** *(Bell Telephone Laboratories Inc., Murray Hill, N. J.)*—I wish to compliment the authors for their very interesting paper and to make the following minor comments:

It is stated that Eq. 2 is true if the liquidus and solidus are straight lines. However, I should like to point out that this is unnecessarily restricted. It is only necessary that the distribution coefficient, $k$, defined as the ratio of the solute concentration in the freezing solid to that in the liquid, be constant. Both liquidus and solidus might be curved and yet meet this requirement.

Assumption 2 concerning conditions of freezing, namely, that diffusion in the liquid is complete, has today, judging from the remarks of Dr. Rhines and in the past in my own work, for example, been a bit misleading. It implies that solidification occurs under a condition in which diffusion is the only transport process in the liquid. However, convection or mechanical or inductive stirring may be present, leading to more rapid mixing than could be achieved by diffusion. Hence, solidification may occur at a rate greater than that which would permit diffusion in the liquid to remove essentially all excess solute from the advancing solid, without seriously invalidating the assumption of complete *mixing* in the liquid.

**Simon A. Prussin** *(Austenal Laboratories, New York)*—The application of the autoradiographic technique to the study of nonequilibrium freezing certainly will aid in increasing our knowledge of this subject. In addition to providing an accurate method for determining the variation in solute concentration on a microscale, as shown by the authors, this technique

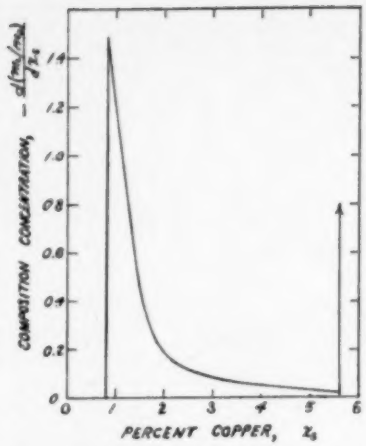


Fig. 10—Calculated concentration distribution for sample *p*.

appears to yield an equally accurate determination of the gross concentration distribution.

The writer would like to point out that the gross concentration distribution also can be calculated on the basis of the same three assumptions used for deriving the authors' Eq. 1. Comparing the experimentally measured concentration distribution with this calculated distribution will indicate how close actual nonequilibrium freezing conditions are approximated by the three assumptions.

The expression for the calculated concentration distribution is a byproduct of any of the analyses of nonequilibrium freezing based on the three assumptions. The writer is choosing the analysis of Hayes and Chipman,[5] as it entails the minimum number of substitutions. Hayes and Chipman's Eq. 7, using the symbols of the present authors, is

$$\frac{dx_s}{x_s\,(1-k)} = \frac{dm_s}{m_o - m_s}$$

where $k = x_s/x_L$. Substituting $m_s = m_o - m_L$, $dm_s = -dm_L$, dividing through by $m_o$, and rearranging, we obtain

$$-\frac{d(m_L/m_o)}{dx_s} = \frac{m_L/m_o}{x_s\,(1-k)}.$$

If $k$ is a constant, an expression for $m_L/m_o$ is given by the present authors' Eq. 2.

When the liquid metal cools through an infinitesimal temperature interval, it deposits solid of composition $x_s$. The fraction of original melt frozen in producing this solid is $-d(m_L/m_o)/dx_s$.

Since one of the three assumptions in the analysis is the complete suppression of solid diffusion, we would expect the quantity of solid of composition $x_s$ existing after complete solidification to be equal to the quantity

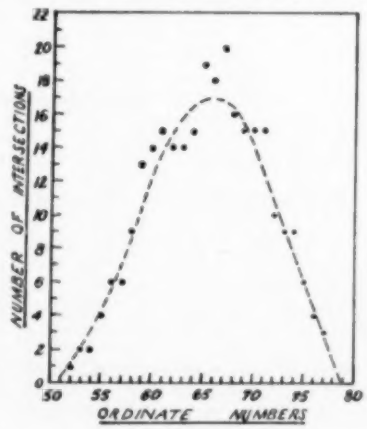


Fig. 11—Measured concentration distribution obtained from authors' Fig. 8.

originally deposited. Plotting values of $-d(m_L/m_o)/dx_s$ vs $x_s$ will give the concentration distribution calculated on the basis of the three assumptions.

Fig. 10 is a calculated concentration distribution for the same composition as the authors' sample p. Since the measured amount of eutectic for this sample equals, within the experimental error, the amount calculated for maximum segregation, it is reasonable to assume that the freezing conditions were closely approximated by the three assumptions. Fig. 10 therefore could be expected to closely represent the measured concentration distribution of sample p.

A measured concentration distribution can be obtained from a series of random microphotometer traces of the autoradiograph of a particular sample. Using the authors' Fig. 8 as an example, we note that the vertical distance from the base line is correlated with the copper concentration in the solid solution. Thus every horizontal line corresponds to a given copper concentration. The relative number of intersections by a particular horizontal line with the trace should be proportional to the quantity of that concentration in the solid solution. The writer's Fig. 11 contains a plot of intersections vs the ordinate units taken from the authors' Fig. 8.

**Arthur B. Michael** and **Michael B. Bever** (authors' reply)—The authors wish to express their appreciation of the interest shown by the discussers. In reply to Professor Hultgren's question, the melt had to be stirred immediately before pouring into the mold or solidification in the crucible in order to assure uniform composition. The magnitude of the segregation which the stirring operation prevented is illustrated by the example of a 4.5 pct Cu alloy solidified in the crucible without prior stirring: the top layer of the ingot analyzed 2 pct and the bottom layer 8 pct Cu. The authors agree with Professor Hultgren's suggestion that this effect is due to gravity segregation.

Professor Rhines gives three reasons why a plane need not necessarily cut the center lines of successive dendrite arms. 1—Polished surfaces are only approximately plane, but because of the thickness of the dendrite arms (100 microns or more) the variation in depth across a series of dendrite arms due to a "wavy" polished surface would probably be small compared to the width of the arms. 2—The variation in the direction of the arms in a dendrite is the most obvious cause of difficulty in this work. 3—Only prominent dendrite systems with maximum arm spacings were chosen for measuring microsegregation and these dendrite arms were likely to be most nearly parallel to the plane of polish. However, as stated in the paper, the observations are speculative, since the orientation of the dendrite system in relation to the plane of polish is an important factor.

Diffusion subsequent to freezing probably tended to reduce all copper concentrations shown in Table IV, since samples *w*, *v*, *u*, and *s* solidified at a slow rate. The last primary solid solution to form should contain 5.65 pct Cu, but its amount would probably be too small for detection. Moreover, the densitometric evaluation of the autoradiographs was made only on areas which did not include $\theta$ particles (or eutectic); in these areas saturated primary solid solutions are not to be expected. The assumption of instantaneous equilibrium between liquid and solid, therefore, is not invalidated by the data in Table IV.

The authors agree with Professor Rhines that the observed undercooling tended to increase the value of the minimum copper content of the primary solid solution. The degree of undercooling measured, however, was too small to account for the difference between the theoretical and measured minimum copper content.

The liquidus and solidus in the Al-Cu system are nearly straight lines, but Mr. Pfann is correct in pointing out that Eq. 2 only requires a constant distribution coefficient *k*; this condition can be met by special combinations of curved liquidus and solidus lines. Regarding the assumption of "complete diffusion" in the liquid, the authors agree with Mr. Pfann that only complete "mixing" must be assumed; possible transport processes, in addition to diffusion, are natural convection and mechanical or inductive stirring. The role of natural and forced convection in the solidification of alloys has recently been analyzed and reference is made to this paper for a quantitative treatment of the problem.[20]

In reply to Mr. Prussin's comments, we would like to point out that all reported measurements of excess phase and microsegregation were made in the central area of a section through each sample, where the average chemical composition and rate of solidification (solidification index) were also determined. Measurements of the degree of macrosegregation in each small ingot were not made and a comparison with Mr. Prussin's analysis, therefore, is not possible. The evaluation of a sufficient number of densitometer traces taken over a large distance would give a measure of the degree of macrosegregation and might serve as a check on the autoradiographic method.

[20] Carl Wagner: Theoretical Analysis of Diffusion of Solutes During the Solidification of Alloys. *Trans.* AIME (1954) **200**, p. 154; JOURNAL OF METALS (February 1954).

---

## Constitution and Properties of Ag-Cu-Zn Brazing Alloys

by Karl M. Weigert

*DISCUSSION, L. A. Carapella and W. D. Robertson, Chairmen*

**J. L. Christie** *(Handy & Harman, Bridgeport, Conn.)*—The data presented, in general, are a refinement of the results of others.

It is interesting to see where alloys adopted years ago without the benefit of profound metallurgical knowledge fit into the vertical sections of the constitutional diagram.

The compositions of brazing alloys must be such that the alloys will join together what the user wants them to join; they must be such that they can be made efficiently into the forms, sizes, and shapes the user wants them in; and, silver being so much more costly than the other component metals, the silver content must be as low as possible.

In the author's presentation, he answered a logical question: he stated that there was no important diffusion of his brass blocks into the brazing-alloys samples.

Some confusion may result from the means for identifying the commercial alloys referred to. The alloys are referred to as ASTM No. 1, ASTM No. 2, ASTM No. 11, etc.; and ref. 3 is to ASTM Spec. B260-52T (1952) and B73-29 (1929). Actually the alloy numbers and compositions referred to are those in the article on

brazing in *Metals Handbook*.[7] From 1 to 8, the alloys are the same in both Spec. B73-29 and *Metals Handbook*; but there are only 8 alloys listed in B73-29. In B260-52T quite a different system of numbering is used.

The author refers to a narrow melting range for the alloys he designates as grades 1, 2, 4, 5, 11, and 12. The spread between liquidus and solidus of some of these alloys is upwards of 150°F, hardly a narrow range compared with a spread of 15° to 30°F available in other brazing alloys.

**Karl M. Weigert** (author's reply)—Mr. Christie's practical considerations for useful brazing alloys, e.g., joint strength and workability, have been discussed in another article.[8] The diagrams were intended to aid the understanding of the physical properties rather than recommend any particular alloys for brazing purposes. We are looking forward to discussing these questions in the AWS Subcommittee VIII for Brazing Filler Materials.

The interest demonstrated in the question of the amount and nature of a diffusion between the brass block and the solder samples lead to further studies of the mechanism of crystallization, segregation, and erosion in the boundary lines. The colored photographs have been favorably accepted as an aid to the identification of phases and their transformations.

Mr. Christie untangled the confusion in the nomenclature of ASTM alloys correctly, and recognized them as the grades listed in the *Metals Handbook*.[7] The old ASTM Spec. B73-29 was abandoned last year with the understanding that some of its alloys might eventually be incorporated into the new ASTM Spec. B260-52 Tentative.

Alloys near the peritectic point *P* have narrow melting ranges, Table II.

Table II. Melting Ranges of Alloys Near the Peritectic Point *P*

| Pct Ag | Melting Range °F Approximate at Peritectic Point *P* |
|---|---|
| 10 | 40 |
| 20 | 40 |
| 30 | 60 |
| 40 | 35 |
| 50 | 15 |
| 60 | 15 |

It can be seen from the diagram that these alloys consist of rather brittle $\beta$ phases and are not likely to be recommended for the use of as brazing alloys. The ASTM grades have been chosen as a practical compromise solution. Some of the considerations involved were: sacrificing the lowest liquidus temperatures and narrow melting ranges for maintaining primary copper crystallization with its high strength and ductility, a minimum silver content, and last, but not least, good workability for economical manufacturing.

[7] *Metals Handbook* (1948) p. 80. Cleveland. ASM.
[8] *Welding Engineer* (March 1954) p. 33.

## Investigation of the Heat Treatment of Commercial Titanium-Base Alloy

by L. Luini and E. Lee

*DISCUSSION, O. T. Marzke and W. Finlay, Chairmen*

**William W. Wentz** *(Rem-Cru Titanium Inc., Midland, Pa.)*—The authors are to be congratulated for their fine contribution to the field of titanium-alloy heat treatment. As shown in the comparison given in Table VII, Rem-Cru's experiences with RC-130B (now known as C-130AM) are in general agreement with those presented by the authors.

Our results indicate, however, that slightly better strength-ductility combinations than those shown by the authors may be obtained by employing 1-lower $\alpha$-betatizing temperatures and 2-longer aging times, a combination which has been publicized by Frost and his coworkers during the past year.

Just recently, a group of specimens from ten production ingots of C-130AM were chosen at random and heat treated as follows: 2 hr at 1450°F, water-quenched and 8 hr at 900°F, water-quenched. The net result of this heat treatment was an average (for ten heats) increase in tensile ultimate of 13,000 psi with a sacrifice of 2 pct elongation (as compared with the annealed condition). The tensile results obtained on the heat-treated material are given in Table VIII.

Table VII. Comparison of Titanium Alloys, Authors and Rem-Cru

| Heat Treatment | Authors | | Rem-Cru | |
|---|---|---|---|---|
| | Ultimate, 1000 Psi | Elongation, 2 In. | Ultimate, 1000 Psi | Elongation, 1 In. |
| 1550°F, 2 hr, air-cooled | 158.0 | 10.0 pct | 157.0 | 17.0 pct |
| 1550°F, 2 hr, water-quenched and 4 hr at 700°F | Brittle | | Brittle | |
| 1650°F, 2 hr, water-quenched and 6 hr at 700°F | Brittle | | Brittle | |

Table VIII. Results Obtained from Heat Treatments on C-130AM

| | Ultimate, Psi | 0.2 Pct Yield Strength, Psi | Elongation, Pct | Reduction in Area, Pct |
|---|---|---|---|---|
| Average | 173,000 | 159,000 | 14.5 | 28.0 |
| $\sigma$ | 5,700 | 8,000 | 1.1 | 4.8 |

The uniformity is seen to be quite good: 80 pct of the ultimates fall within $\pm$5,700 psi and 80 pct of the elongations within $\pm$1.1 pct.

**L. Luini** and **E. Lee** (authors' reply)—The authors wish to thank Mr. Wentz for his corroborating comments on the heat treatment of RC-130B alloy.

We recognize and quite agree with Mr. Wentz that the better strength-ductility combinations are obtained at the lower $\alpha$-betatizing temperatures. The structural basis for our heat treatment is the $\beta$ continuous phase. As indicated in our discussion of the solution temperature, 1550°F is the lower temperature limit for a $\beta$

matrix. It must be recognized, however, that this temperature is by no means a fixed value and depends on the distribution of the $\alpha$ and $\beta$ phases resulting from the fabrication procedure. Solution temperatures below 1550°F generally produce an $\alpha$ continuous phase structure which would be expected to provide better ductility. Recent tests in our laboratory and Mr. Wentz's results indicate that the $\alpha$ continuous phase structure will exhibit better ductility for a particular tensile strength than a $\beta$ continuous phase structure.

---

## Hydrogen Embrittlement of Steels

by Jack T. Brown and William M. Baldwin, Jr.

*DISCUSSION, W. J. Harris, Jr. and L. D. Jaffe, Chairmen*

**F. de Kazinczy** *(Swedish Institute for Metal Research, Stockholm, Sweden)*—Comparatively few quantitative studies have been carried out earlier on the effect of deformation rate on hydrogen embrittlement; the contribution of the authors to this problem therefore is very valuable. Their results on this point give valuable support to the current theories.

The authors have also shown that the fracture strain of hydrogen-charged steel may increase with increasing temperature in a certain temperature range. To this usually no sufficient attention has been given, and, as the authors point out, no direct attempt was made to explain this effect theoretically.

It is generally accepted that embrittlement is in some way caused by molecular hydrogen of high pressure, which is included in "voids" or "cracks" of the steel. It is obvious that the higher the pressure of the included gas, the more embrittlement will be caused. The hydrogen pressure is under equilibrium conditions determined by the activity of hydrogen dissolved in the lattice. This was calculated on thermodynamic basis by Phragmén[13] as a function of temperature and amount of hydrogen dissolved. An attempt to estimate the equilibrium pressure at different temperatures as a function of the total hydrogen content of a sample has also been carried out.[14]

At the rather high hydrogen contents to which the samples in this investigation probably were charged, the equilibrium hydrogen pressure is decreasing with temperature. Thus, assuming constant hydrogen content, the fracture strain will increase with temperature in a range in which the decrease in equilibrium pressure with temperature exerts a larger influence than the increase of hydrogen diffusivity with temperature.

It is important to note that the minimums of the authors' curves in Fig. 6 probably should disappear if the experiments could have been carried out, not at constant hydrogen content, but at constant hydrogen activity. Correspondingly, hydrogen embrittlement could be characterised by a surface of type *a* only in the three-dimensional system described by the authors, or rather by a series of *a* surfaces, each representing a certain hydrogen activity. Whereas the *c* and *d* surfaces have no true physical meaning, the *b* surface, which represents losses of hydrogen from the test bar by diffusion, does not represent a fundamental material property, and is different for test bars of different shapes.

By these considerations, the authors' experimental results can be brought into full accord with current theories of hydrogen embrittlement.

**Jack T. Brown** and **William M. Baldwin, Jr.** (authors' reply)—We interpret Mr. de Kazinczy's suggested explanation of our data as follows: The Zapffe-Sims-Petch type of rationalization for hydrogen is valid and explains the "*a*" surface. Solubility of the hydrogen increases with increasing temperature to a point where it dissolves the hydrogen charge in the steel, leaving none in the voids to cause brittleness. We agree that this hypothesis is in accord with the "*d*" surface. We had considered this possibility ourselves (it being commonly associated with the upper arm of a *c*-type reaction-rate curve such as we found in Fig. 9), to the extent that we set up a series of critical experiments to test its validity. These are virtually finished and will be published this fall. They consist in determining *c*-curves of the type shown in Fig. 9 of the paper for a mild steel charged for various times. As Mr. de Kazinczy knows, while ductility drops with charging time to a saturation value as shown in Fig. 4 of our paper, the hydrogen content of the steel continues to rise with charging time even after saturation brittleness has been reached. The criticality of our experiments shall rest in the behavior of the upper arm of the *c*-curves. If hydrogen dissolves in the steel as temperature is raised to such an extent, it can no longer do damage in the voids; then the upper arm of the *c*-curves should move up with temperature as charging time is increased, irrespective of whether or not the steel is a state of "saturation brittleness."

[13] G. Phragmen: *Jernkontorets Annaler* (1944) 128, pp. 537-552.
[14] F. de Kazinczy: *Journal* Iron & Steel Institute (May 1954).

---

## A Study of the Effect of Carbon Content on the Structure and Properties of Sintered WC-Co Alloys

by Joseph Gurland

*DISCUSSION, F. N. Rhines and A. J. Shaler, Chairmen*

**John W. Graham** and **John C. Redmond** *(Kennametal Inc., Latrobe, Pa.)*—In studying two interrelated phenomena which occur in the equilibrium system, WC-Co, Dr. Gurland and his associates have carried out a most painstaking study of a fundamental nature in an attempt to further locate the specific reaction points in this ternary system.

This work points out again the exactness required in the preparation of production quantities of cemented

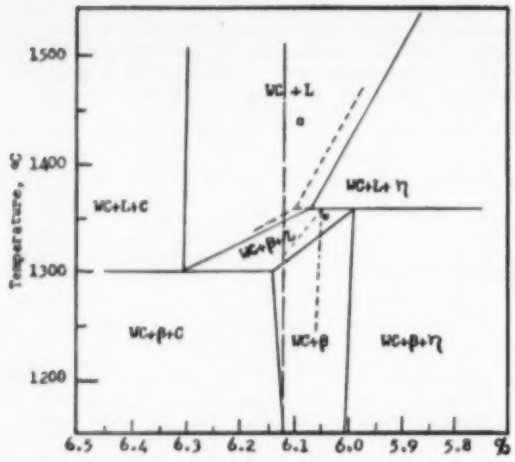


Fig. 20—Carbon content of WC. Solid lines are Dr. Gurland's vertical section at 16 pct Co in W-C-Co; dashed lines, possible shift at 4 pct Co.

tungsten carbides where slight changes in constituent content brought about by incomplete reactions, oxidation, etc., can produce inferior carbides.

The complexity of the problem can only be realized by a study of the works of those authorities listed by the author. Rautala and Norton[5] have made the latest and most comprehensive study of the three-component system.

Dr. Gurland has studied a narrow but important area within this system, using 16 pct Co with tungsten carbide. Commercial grades contain as little as 3 pct Co. A complete evaluation of this wide area would be a tremendous task but without doubt, very constructive. Every carbide manufacturer has probably produced this brittle η phase which they first observed when specimens had an unnaturally high hardness with low transverse-rupture strength. This phase has been observed at Kennametal in compositions that were well within the combined carbon tolerance of 97.5 pct of theoretical (C = 97.5x6.12 pct = 5.96 pct) as described by Sanford and Trent.[6] This is, as Dr. Gurland pointed out, somewhat below the limit where the η phase is produced, viz., 6.06 pct, when optimum equilibrium conditions are maintained. It is believed from some work in the Kennametal laboratory that the η phase can be obtained when the carbon content is as high as 6.09 pct or within 99.5 pct of theoretical especially when the cobalt content is low.

A composition containing about 4 pct Co content made with tungsten carbide having 6.05 pct C content produced the η phase after being held at 1343°C which is 14°C below the η decomposition invariant temperature, for ½ hr in vacuum. These examples would indicate that the η invariant plane could extend closer to the theoretical carbon content as the cobalt content decreases such as is shown on the reproduction of Dr. Gurland's vertical section, Fig. 20. These examples should not be construed as a formal evaluation but rather should indicate that much more work is necessary before we completely understand exact phase relationship through the commercial cobalt-tungsten carbide composition ranges.

It is known that tungsten carbides can be significantly decarburized by hydrogen even at 1800°F, so it is suggested that carbon analysis of the sintered compacts might locate more exact phase relationship especially when hydrogen atmospheres are used for sintering.

The author should also be complimented on the tedious task that was attacked to show the influence of carburization and decarburization on grain growth. His statement that large grains are formed upon recarburization of the $W_3Co_3C$ is borne out by experiences that marginal tungsten carbide compositions having slightly deficient carbon content (½ to 1 pct low) invariably have numerous large grains. This can reasonably occur when cooling rates allow sufficient time for the η phase to decompose and reform the phases WC and the *B* phase (cobalt with WC in solid solution) even without recarburization. (Fig. 21.)

This paper represents a significant contribution toward solving some practical and fundamental questions about cemented tungsten carbides. The answers have created new questions that can only be worked out by further studies of this kind.

**E. Lardner** *(Hard Metal Tools Ltd., Coventry, England)*—All who are interested in the manufacture of cemented carbides will have read this paper by Dr. Gurland with great interest. Much of the information which it contains has been appreciated, in a rather vague manner for many years, by those in the carbide industry, but the quantitative and detailed way in which the results have now been presented make them of the greatest value. In particular, the work emphasizes the need for the extremely close control of carbon content which is absolutely vital in the production of consistently high quality hard metals.

However, there are some points connected with grain growth in sintered WC-Co alloys that deserve a more detailed consideration because carbon content appears

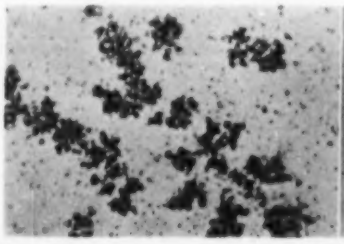

Fig. 21a—4 pct Co, 6.05 pct C in WC. As-sintered, η rosette. X200. Area reduced approximately 35 pct for reproduction.

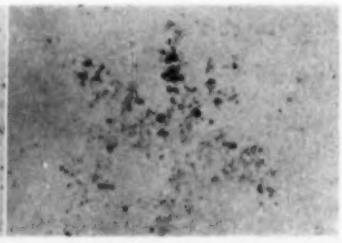

Fig. 21b—4 pct C, 6.05 pct C in WC. Reheated 1343°C for ½ hr. WC-Co not completely recovered from $W_3Co_3C$ η phase. X200. Area reduced approximately 35 pct for reproduction.

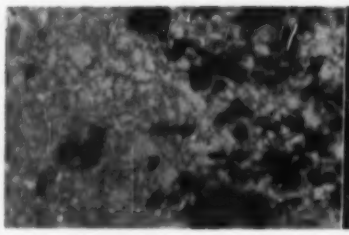

Fig. 21c—4 pct Co. As-sintered, η phase areas. X1500. Area reduced approximately 35 pct for reproduction.

Fig. 21d—4 pct Co. Reheated at 1343°C for ½ hr. Wc-Co recovered from η phase. Note the large grain formation. X1500. Area reduced approximately 35 pct for reproduction.

to be only a minor influence where grain growth is concerned.

Sintered carbides may show both continuous grain growth, in which there is a more or less uniform increase in the size of all the tungsten carbide grains, or discontinuous grain growth, in which only a few grains grow to a very large size while the remainder show little or no increase in size.

The former type of grain growth is of little trouble to the carbide manufacturer, since its magnitude is generally small and the factors by which it is influenced are readily controlled. Some of these factors, of which temperature is undoubtedly the most important, are temperature, time, carbon and cobalt contents, and initial grain size. The effect of all these factors are shown quantitatively in Dr. Gurland's paper. However, it would appear that these results must not be regarded as being quantitatively correct for carbides from any other source and containing different trace impurities, although they would be expected to show the same trends. Thus, with our normal production material one would find a similar grain size-temperature relationship to that given in Fig. 9, but the effect of variation in cobalt content would be less marked. Close agreement with the results of Fig. 10 showing the influence of initial grain size would be expected, and there would be fairly good agreement with Fig. 13 although the effect of carbon content would be less.

Discontinuous grain growth, however, can be very troublesome and with some powders excessively large grains of the order of 25 to 50 microns may be produced at, or even below, normal sintering temperatures. Dr. Gurland describes at length a mechanism whereby this type of grain growth might be produced by the recarburization of $\eta$ phase grains during sintering, but he only mentions that other factors, such as impurities, trace elements, local temperature variations, and initial grain-size distribution, may also have some effect. Some of these factors, however, are probably vastly more important than the recarburization of $\eta$ phase, and there is a distinct possibility that a one-sided view of the problem is likely to arise.

Severe discontinuous grain growth may occur in a sintered WC-Co alloy with normal (6.12 pct C) or high carbon content under conditions where the predominating factors appear to be the grain size and grain-size distribution of the original powder and the purity of the alloy. Thus, in very fine grain-size carbides, especially those with an average grain size of about 0.8 micron, or below, exaggerated grain growth of this discontinuous type can be very common over any normal range of carbon content. With such materials, it is common practice to add small amounts of some grain-growth inhibitor, such as vanadium carbide, to prevent the effect.

Discontinuous grain growth due to recarburization of $\eta$ phase is something that we have not encountered although the possibility has been suggested and looked for. Probably the most convincing fact is our normal production experience. In order to control the carbon content of sintered material, we use sintering furnaces in which the atmosphere is slightly carburizing. The compacts prior to final sintering almost always have a carbon content in the range corresponding to 6.00 to 6.05 pct on the WC, the stoichiometric carbon content being obtained by carburization during sintering. Thus the initial alloy composition will be in the three-phase field WC + $\eta$ + $L$, and yet we rarely find instances of nonuniform grain growth. On the other hand, when discontinuous grain-growth troubles are experienced, they generally can be traced back and related to either one particular batch of tungsten metal or ammonium paratungstate.

Dr. Gurland states, "The grain size of the tungsten-carbide constituent of sintered alloys is controlled in practice by the adjustment of a number of process variables extending back to the ore, but it is finally determined by the extent of grain growth taking place during the sintering operation." This is perfectly correct but, by the time the sintering stage is reached, the influence of all these variables has not been wiped out and may have considerably more effect on the response of the alloy to sintering than a variation in carbon content.

When discontinuous grain-growth troubles do arise, it is found that the compacts are exceptionally sensitive to sintering temperature, especially as regards the size attained by the very large grains. In fact, it is a matter of great difficulty to sinter two test pieces on separate occasions and obtain large grains of similar size. This is especially true at temperatures of 1400°C and below. Also, with such structures, where the average grain size of the matrix may be one-tenth to one-twentieth of the grain size of the abnormally coarse grains, it becomes very difficult to obtain micrographs which are simultaneously able to show the grain structure of the matrix and yet be fully representative of the extent of discontinuous grain growth. Such troubles as this may account for the results shown in the micrographs, Figs. 14 through 19.

**E. M. Trent** *(Hard Metal Tools Ltd., Coventry, England)*—There are two points I would like to raise in connection with Dr. Gurland's valuable paper. The first of these concerns the formation of the $\eta$ phase. The author mentions one of the formations in which this appears in sintered carbides, i.e., in the form of relatively large, sharply angular crystals. We have noted that this phase occurs in four or five different formations depending on the carbon content and the sintering temperature of the alloy, and the diagram, Fig. 1, published by the author, may help to explain some of these.

If the carbon content is only slightly deficient, the most usual formation is that of the sharply angular crystals such as those in Fig. 7, which often show rectangles, triangles, and sometimes "needles" in the polished section. If the sintering temperature is very high, e.g., 1500°C, the $\eta$ phase may occur in a dendritic formation, the dendrites being of approximately the same size as the crystals at lower sintering temperatures. When the carbon deficiency is greater, for example, where the carbon content of the WC is below 5.95 pct, the formation is entirely different and takes the form of an even dispersal of fine particles of $\eta$ phase throughout the section, the particles being of the same size or only slightly larger than the WC grains.

Often the atmosphere during sintering is slightly carburizing and in this case two formations of $\eta$ phase often occur in a low carbon alloy: a core containing the finely dispersed particles sharply separated from an outer zone where the carbon content is slightly higher and where the $\eta$ phase occurs as the large crystals or as dendrites depending on the sintering temperature. Such a structure is shown in Fig. 8 in a previous paper by Drs. Sandford and Trent.[4]

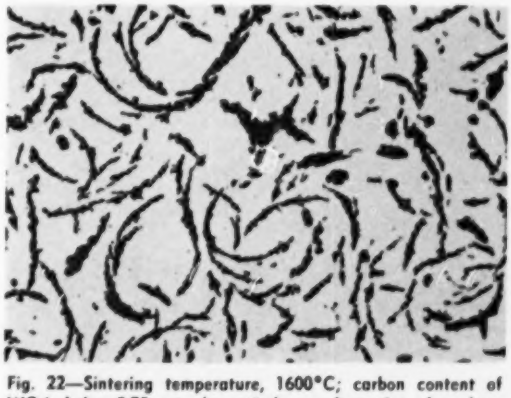

**Fig. 22—Sintering temperature, 1600°C; carbon content of WC is below 5.75 pct. An entirely new formation of $\eta$ phase occurs; very large curved flakes of $\eta$ replace the other forms. Etched in alkaline ferricyanide. X200. Area reduced approximately 25 pct for reproduction.**

If the sintering temperature is raised still further to 1600°C, an entirely new formation of $\eta$ phase occurs in alloys where carbon content of the WC is below 5.75 pct. Very large curved flakes of $\eta$ replace the other forms, as shown in Fig. 22.

Referring to Fig. 1 of the paper, it would appear likely that when the sintering temperature and carbon content are such that the alloy is in the WC + *L* field at the maximum temperature, the $\eta$ phase is precipitated on cooling and adopts one or other of the coarsely crystalline formations, depending on the carbon content. If the carbon deficiency is only slight (e.g., 5.95 pct C on the WC), the formation is generally that of the sharply angular crystals. When the carbon content is lower, the temperature must be higher to keep the alloy in the two-phase field and either the dendrites or the large curved scrolls are formed on cooling. When the carbon content is such that the alloy is in the three-phase field WC + *L* + $\eta$ at the sintering temperature, the $\eta$ appears to adopt the form of evenly dispersed fine particles.

The other point which I would like to raise concerns the form of the WC grains. The author states that "with increased sintering times, the carbide grains tend to form rectangular parallelepipeds." It seems unlikely that hexagonal crystals would adopt this form and in our experience the most common form produced with large crystals of WC is that of thin hexagonal prisms where the ratio of the length of the edge of the triangle to the thickness is 10:1 or greater. This is shown most readily by heating the carbides in molten zinc when the carbide particles are dispersed and can be extracted by treatment with hydrochloric acid. Large crystals up to 1 mm across have been separated in this way and these are nearly always more or less perfect triangular prisms. Only occasionally have smaller grains been seen approximating to a rectangular formation. Is it not possible that the most frequently occurring angle between the sides of sections through such flat triangular prisms would be near 90°?

**J. Gurland** (author's reply)—The author wishes to thank the discussers for their valuable supplements to this paper. Some limited experimental evidence at Firth Sterling supports the conclusion of Mr. Redmond that the two-phase field, WC + *L*, becomes narrower as the cobalt content decreases.

Although the recarburization of the $\eta$ phase is only one of many possible factors which may cause discontinuous grain growth, it was found possible to reproduce this phenomenon at will. The reason that Mr. Lardner has not encountered it may be due to a rapid rate of carburization, or a different temperature range, or a possible shift of the phase boundaries by certain impurities.

No difficulties were encountered in photographing alloys showing discontinuous grain growth. Figs. 14 through 19 were selected to show structures which are representative of each compact.

The description of the various formations of the $\eta$ phase by Mr. Trent is most useful. The results of the angular measurements of Fig. 12 have been duplicated recently on samples of 16 and 25 pct Co sintered for only 45 min. It is true that the 90° angles can be accounted for, not only by rectangular parallelepipeds, but also by rectangular prisms.

---

## Solid State Bonding of Aluminum to Nickel

by S. Storchheim, J. L. Zambrow, and H. H. Hausner

*DISCUSSION, F. N. Rhines and A. J. Shaler, Chairmen*

**Dr. W. Seith** *(University of Münster, Münster, Germany)*—I am not in a position to give an explanation of the Storchheim effect. However, some observations in the same direction were made in our Institute which may be helpful for further experiments. Dr. Heumann of our Institute studied various problems of diffusion between metals which form intermetallic phases and among others he investigated the Ni-Al system. For these latter studies, a slight conical hole was drilled into a cylindrical piece of nickel and an aluminum core was driven into this hole. After several days of heating at 600°C in vacuum, a surprisingly low, hardly observable degree of diffusion took place. During a repetition of this experiment, a power failure took place and cooling of the specimen occurred; the experiment was continued after reheating. During the time of reheating, a small amount of air entered the equipment. In this case only one distinct diffusion zone was observed, as shown in Fig. 13.

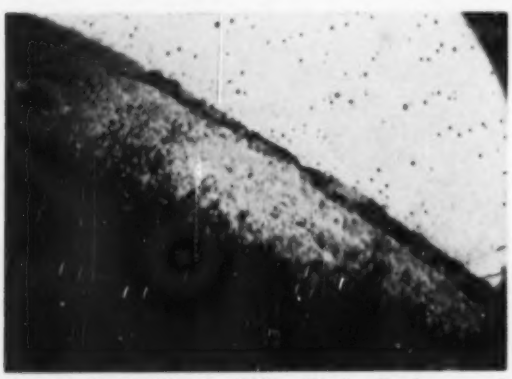

**Fig. 13—Al-Ni diffusion, 600°C, 280 hr. Break occurred during cooling. Light area (top right) is Ni; dark area (bottom left) is $Al_3Ni$. X400. Area reduced approximately 35 pct for reproduction.**

According to Messrs. Storchheim, Zambrow, and Hausner, the explanation would be that in the first case high pressure between the two metals affected the diffusion, whereas in the second case a certain pressure release occurred during cooling and reheating. I am not in a position to say whether the traces of oxygen promoted diffusion or not. According to some observations by Seith and Loepmann, such a possibility exists.

**Dr. Cyril Stanley Smith** *(Institute for the Study of Metals, University of Chicago, Chicago)*—Your findings are not only of considerable practical importance but are also most interesting theoretically The effect could simply be one of decreased diffusion rate in one or the other of the intermediate phases or it could actually be a result of the elimination of one of the phases from the equilibrium constitution diagram in a more condensed system. I wonder if you have done any experiments in which you formed a thin inter-

metallic layer at low pressure and then increased the pressure to the point where it would not form? This should answer very quickly the question of stability vs diffusion rate. The phase approximating NiAl must have many vacancies (the amount being a very sensitive function of composition) and therefore its behavior would be expected to be strongly pressure dependent.

**M. Cohen** *(Massachusetts Institute of Technology, Cambridge, Mass.)*—The possibility that pressure may inhibit the formation of intermetallic layers during diffusion or sintering has considerable scientific and practical significance. From a scientific standpoint, it is desirable to know just why pressure should have a pronounced effect; and from a practical standpoint, the avoidance of brittle intermediate phases may improve the properties of bonded layers and powder-metallurgy products.

At the present time, it is not clear whether pressure alters the relative stability of the phases involved or modifies the interdiffusion rates. The latter alternative seems to offer a reasonable working hypothesis. The $\delta$ phase (NiAl) has a defect structure and presumably the vacancy concentration could be reduced by pressure, thus lowering the diffusion rate. However, the authors have found no evidence for the presence of this phase. They have tentatively identified the $\beta$ phase ($NiAl_3$) and the $\gamma$ phase ($Ni_2Al_3$) as comprising the two observed diffusion layers, but further work on the nature of these diffusion zones would seem essential for a thorough understanding of the pressure effect. The $\beta$ phase has such a limited range of homogeneity that its presence as a diffusion zone seems surprising in the light of the fact that the very stable $\delta$ phase (NiAl) with a substantial range of homogeneity is not found.

If the influence of pressure in inhibiting the formation of intermetallic layers during diffusion depends upon defect structures, then the practical utilization of this phenomenon will be limited to relatively few systems. On the other hand, the possibility should not be ruled out that the aluminum and nickel undergo plastic deformation during these compressive runs, and the attendant increase in diffusion rate[1] in the terminal phases may be a contributing factor. If the diffusion rate through the intermetallic layers is naturally slow and if the diffusion rates in the terminal phases are increased by virtue of plastic deformation,[1] the resulting concentration gradients will tend to reduce the thickness of the intermediate phases. Because of this possibility, the investigators should insure that the compression is substantially hydrostatic during the diffusion runs. If plastic deformation of the terminal phases plays an important role in the phenomena described by the authors, the technique may have wide application because it would not then be limited to those systems in which the intermediate phases are sensitive to pressure.

With regard to the mechanical properties attained, the authors have placed emphasis on the maximum strength values instead of the average values for correlation purposes. This procedure seems reasonable because the tensile specimens are so short that slight misalignment in the grips may cause premature breaking and apparently low strength. Hence, the maximum values may be assumed to correspond to those tests in which the alignment was good.

**Professor Norman H. Nachtrieb** *(Institute for the Study of Metals, University of Chicago, Chicago)*—I read with great interest your paper on bonding of aluminum to nickel. It shows clearly that pressure can alter the free energy of formation of certain alloys very markedly.

In the Al-Ni system which you studied, I believe there is a density anomaly in the region of the stoichiometric composition AlNi, which has been interpreted in terms of a lattice-defect structure with several percentage of vacancies. G. Raynor has studied the conductivity of either this system or the Al-Co system, and F. Nix reported several years ago that diffusion coefficients for nickel are anomalously high in the 1:1 range of composition. All of this makes sense in terms of a high vacancy density, and your findings that pressure eliminates one of the phases (presumably the same one which is responsible for the high diffusion rate) seem to be consistent. I think one might profitably discuss the facts you observe in terms of the volume of formation of the phase in question:

$$\Delta V = \left( \frac{\partial \Delta F}{\partial P} \right)_T$$

$aNi + bAl \rightarrow Ni_aAl_b$ (containing vacancy volume $\Delta V$). One would expect the effects you observe to be most pronounced for systems in which $\Delta V$ is large; i.e., for systems in which there is an unusually large vacancy density.

**J. W. Butler, Jr.** *(Johnson Bronze Co., New Castle, Pa.)*—We clad aluminum on nickel-plated steel bimetallic stock for sleeve-bearing purposes by preheating the metals and rolling. It was very interesting to learn that the optimum bonding conditions for aluminum and nickel, as determined by your static method, were a corroboration of the conditions we found necessary in joining the two metals by rolling.

Your paper is very clear and concise and, to the best of our knowledge, the data seems to be correct. In our application, the time for optimum strength of bond is necessarily limited due to the type of pressure application (rolling); therefore, we try to exert higher pressures to gain the resultant higher tensile strength. Our tensile strengths are in the range of 10,000 to 12,000 psi, and the separation is normally in the aluminum alloy.

**Harunbou Swada** *(Mining & Metallurgical Research Laboratory, Mitsubishi Metal Mining Co. Ltd., Saitama Pref., Japan)*—It seems to me that your calculation of "penetration" based upon the parabolic law of diffusion cannot be applied adequately to this case where two zones are formed under relatively low pressure. The formation mechanism of $Ni_2Al_3$ and $NiAl_3$ layer is the most interesting problem in the research. Fig. 10 in your report shows that too high an applied pressure prohibits the formation of the intermetallic-compound zone. Can we understand this phenomenon as the result of squeeze out of molten compound by the applied pressure?

All specimens tested have been broken at the Ni-Al interfaces and never within the aluminum or the nickel. What kind of relation can be expected between the tensile strength of this specimen and that of pure $Ni_2Al_3$ or $NiAl_3$ near the interface? Because the problem of tensile strength is very complicated and is not yet completely clarified. I wish to hear your ideas on this phenomenon.

We are interested in the X-ray techniques you applied to the determination of structures of interface materials. What do you think about the application of electron diffraction to the structural determination?

Did you investigate the Kirkendall effect with your penetration couples?

I look forward to your reply and the further development of your splendid work.

**J. B. Clark** *(The Dow Chemical Co., Midland, Mich.)*—The effect of pressure on the weld strength of Al-Ni couples is demonstrated very nicely. The penetration studies of the diffusion layers as a function of pressure suggest some interesting possibilities for further research.

The authors report a series of curves of the *ln* penetration vs $1/T$ for a series of pressures. The slopes of these curves are reported as activation energies. I question the use of the term "activation energy" from these data alone. Activation energies should be reported only in conjunction with a detailed mechanism of the rate-controlling reaction of the penetration process. Such a mechanism is not reported in this paper. The diffusion system in this study is very complex. Diffusion is proceeding in four phases and across

three interfaces. In such a complex system in which several types of reactions are occurring simultaneously, it is difficult to see how such a gross measurement as the depth of penetration with time can yield the activation energy of the rate-controlling process. Without a detailed model of the rate-controlling process in this complex diffusion system, the slopes of these penetration curves should not be interpreted as true activation energies.

The second point that I want to mention concerns the effect of pressure on the number and thickness of the diffusion layers. If the Ni-Al phase diagram is correct, at atmospheric pressure, diffusion of an Ni-Al couple should generate four diffusion layers. However, in the case of high pressures, the authors report the generation of only two diffusion layers and the decrease in number and thickness of these layers as pressure is increased. The effect of pressure may be explained in either of two ways:

1—The external pressure may decrease the rate of diffusion in the system, possibly by reducing the number of vacancies available for diffusion. As the external pressure is increased, the slower diffusion rates would increase the time required for the system to approach equilibrium. Thus, for a fixed diffusion time as the external pressure is increased, the number of layers generated and their depth of penetration would be smaller. Note that the higher melting point layer of $Ni_2Al_3$ or roughly, the slower diffusion layer, disappears first as the pressure is increased.

The authors may have shown qualitatively the effect of pressure on the diffusion process in a complex system. If a simple one-phase system (e.g., Cu-Ni) were substituted for the complex system studied in this paper and the diffusion times greatly extended, classical methods of studying diffusion could be applied and quantitative determinations of the effect of pressure on the rates of diffusion could be made with their apparatus.

2—The effect of pressure on the number and thickness of the diffusion layers may be explained on the basis that the applied pressure may change the normally reported equilibrium relationships between nickel and aluminum. The pressure effects shown in this paper may be a demonstration of a *P-T-X* diagram in the solid state. If this is the case, the effect of pressure could be shown quantitatively by making diffusion couples of the terminal metals of a simple eutectic system and diffusing the couples for long times at various pressures. At the interface, the concentration-penetration curves of such couples will show a sharp discontinuity corresponding to the concentration difference between the solvus lines of the terminal solid solutions at the diffusion temperature. If the applied pressure affects the position of the solvus lines, the concentration difference across the couple interface will vary with applied pressure.

In this paper, the effect of pressure on either the diffusion rates in Al-Ni couples or the normally reported Al-Ni phase diagram has been shown qualitatively. With the selection of simpler metal systems, the authors with their apparatus could demonstrate quantitatively the effects of pressure on either the rate of diffusion or equilibrium relationships in the solid state.

**H. T. Sumsion** (*Knolls Atomic Power Laboratory,* Schenectady*)—The authors are to be congratulated on their presentation of data of great value and interest. They have stated that maximum values rather than average values of bond-strength determinations are presented because the lower values result from nonoptimum bonding conditions. It would be of interest to know the spread of values observed in multiplicate samples, especially how the spread compares with the observed differences in maximum values attributed solely to changes in experimental conditions.

Tensile data for bond strengths obtained at 2 tsi are given in Figs. 4 and 5. However, in Figs. 7, 9, and 10 no diffusion data are included for pressures of less than 5 tsi. An investigation at the Knolls Atomic Power Laboratory of another binary system of aluminum, one in which the primary reaction product exhibits a pronounced volume expansion over the individual components, has shown a marked effect of pressure on diffusion. It was found that a minimum pressure at least in excess of the yield strength of one of the components was necessary to obtain consistent diffusion data. It would be of interest to know whether the Al/Ni diffusion data at low pressures indicate a similar effect.

Hot-press bonding of Al-Ni also has been investigated at the Knolls Atomic Power Laboratory. The hot-pressing was done in air rather than a vacuum, but oxidation of the bonding surfaces was prevented by applying pressure before heating the specimens. In our study, we used a specimen with considerably smaller area to test bond strengths than the one described in this paper. We investigated the effect of pressure on bond strength over the range of 1 to 12 tsi.

We found as did the authors that at 600°C there was only slight increase in strength with increasing pressures. At temperatures of 550° and 600°C tensile values were increased from 8,000 to 11,000 psi as the pressure was increased from 1 to 12 tsi. These values are approximately double comparative data given by the authors. At 500°C, tensile strength fell away to about half that obtained at 550° and 600°C. Below 500°C insufficient bonding occurred to permit machining of tensile specimens, irrespective of bonding pressure.

Within the 1 to 12 tsi range investigated, pressure was not observed to have a marked effect upon the extent of diffusion. Approximately equal amounts were observed at 1 as at 12 tsi.

I should like to know if there has been subsequent verification of the tentative identification of the two phases. In our work a third phase was thought to have appeared in the reaction product at 600°C. Have the authors observed more than the two phases at any time?

In solid-state bonding of aluminum to nickel, the effect of high pressures in suppressing formation of intermetallics and increasing diffusion bond strengths has been shown by data presented by the authors. The paper should prove a stimulant to further investigation of the problem.

**S. Storchheim, J. L. Zambrow,** and **H. H. Hausner** (authors' correction)—In the course of further metallographic investigation of Ni-Al interfaces after solid-state reaction, we have observed that a couple reacted at 500°C at 34 tsi for 2 min *in vacuo* did exhibit a slight amount of reaction product. That is, we originally reported,[2] that the reaction products, tentatively identified as $\beta$ and $\gamma$ phases, had been completely inhibited from forming by the high pressure used. However, by improving our metallographic technique, some $\beta$ alloy was detected at the interface.

The indication is that increasing reaction pressure does eliminate the $\gamma$ phase and does inhibit the $\beta$ alloy formation. However, the suppression of the $\beta$ phase is not a straight line plot of decreasing penetration rate with increasing pressure. It is rather a parabolic decrease which asymptotically approaches zero rate at some very high pressure.

A tensile bar, made under the above conditions, ruptured within the parent aluminum metal of the couple rather than at the interface. This was in contrast to the fact that all other tensile bars reacted such that the intermetallics at the interface were thicker than for the specimen mentioned, ruptured at the bond interface. Again the observation of increasing strength with decreasing alloy zone thickness was verified. This, however, was the first time that we found the bond strength of the couple to be greater than one of its parent metals.

**S. Storchheim, J. L. Zambrow,** and **H. H. Hausner** (authors' reply)—In response to Dr. Smith's question

* Operated by the General Electric Co. for the United States Atomic Energy Commission on Contract W-31-109 Eng-52

as to whether or not we had done any experiments concerning the question of stability vs diffusion rate, we wish to say that we have. We made up another penetration couple and heated it to 500°C and pressed it at 11 tsi for 2 min. Fig. 14 shows a sketch of the alloy layers as observed. The same sample was then heated again to 500°C and pressed 34 tsi for 5 min. The effect of repressing is shown schematically in Fig. 15. The nickel-rich diffusion zone decreased in width, whereas the aluminum-rich diffusion zone increased in width. The total width of the two diffusion zones was not affected by repressing. If the nickel-rich phase had disappeared, then the indication from this information would be that the phenomenon is based primarily upon equilibrium relationships in the solid state. This, of course, requires more detailed investigation for confirmation.

We agree with Dr. Cohen that further work on the nature of the diffusion zones, we have observed, would be essential for a more thorough investigation of the pressure effect. The statement that the $\beta$ phase being present is a surprise because it has such a limited range of homogeneity is of interest. Perhaps this can be rationalized in that pressure could have affected the homogeneity range of the $\beta$ phase to such an extent that its existence was possible.

Based on the chapter in the book *Surface Treatment of Metals* by F. N. Rhines,[5] we felt that the penetration calculations we made were applicable contrary to Mr. Sawada's views. From the chapter, "The rate of growth at constant temperature of diffusion layers of any degree of complexity usually follows a parabolic law, $x^2 = kt$, where the thickness is represented by $x$, time of reaction by $t$, and $k$ is a constant involving the diffusion coefficient as well as several other quantities. This expression may be applied to all, or any group of layers of a diffusion system taken together, or to any one, or part of one, layer."

We do not believe that the inhibition to formation of the intermetallic compound zones is caused by the "squeeze-out of molten compound by applied pressure." We do not feel that any melting is occurring during the type of reaction described in our paper.

We do not know, at present, the tensile strength of either pure $Ni_2Al_3$ or $NiAl_3$. Because of this fact, we are not able to describe the relationship between the tensile strength of our specimens and that of the pure intermetallics.

The X-ray diffraction method we used to determine the structure of the interface materials was the Debye-Scherrer technique. What we did was to take a specimen and rupture it at the interface by putting the reacted couple in tension. The interface was then scraped to remove the intermetallic as a powder. The powder so obtained was then subjected to X-ray diffraction using a copper target and a nickel filter. The results obtained, we felt, were not conclusive, and were only indicative. The suggestion for the application of electron diffraction to determine the intermetallics formed is certainly worthwhile.

We did not specifically investigate the Kirkendall effect mentioned by Mr. Swaba; however, the effect was observed. We found that the thin molybdenum pieces of foils used both to prevent Al-Ni interaction

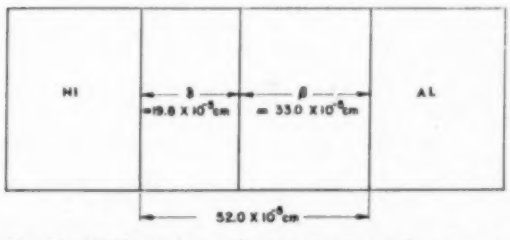


Fig. 14—Ni-Al couple interface after reaction *in vacuo* at 500°C at 11 tsi held 2 min.

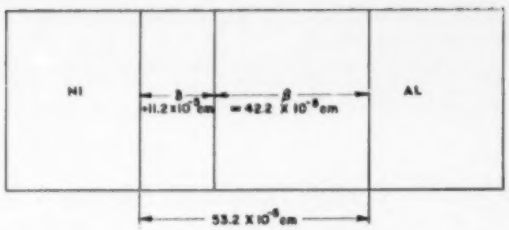


Fig. 15—Same specimen as in Fig. 14 reacted again *in vacuo* at 500°C but at 34 tsi held 5 min. Note that the total zone thicknesses in both cases are the same.

and to subsequently define the original interface were effected by the atom flow during reaction. More specifically, we observed that the edges of these molybdenum strips were bent into the aluminum portions of the couples. This effect did not extend along the entire length of the molybdenum strip.

Dr. Clark brings up a point of interest with regard to the term "activation energy." His attention is called to the paper by B. Lustman and R. F. Mehl.[4] The authors used the same Arrhenius equation we used and referred to $Q$ as the heat of activation. Based upon this reference, we calculated activation energies for the processes we studied.

The experiment that Dr. Clark suggests we use to determine the effect of pressure on either rate of diffusion or equilibrium relationships in the solid state is interesting. He is referred to our answer of Dr. Smith's query about the same point.

In reply to Dr. Sumsion's questions, we state the following: The maximum spread observed in multiplicate samples was 50 pct. The observed differences attributed to changes in experimental conditions was 1½ pct.

We also observed that at low pressures, or a combination of a fairly high pressure, 5 tsi, at low temperatures, 500° to 550°C, that our penetration data were not consistent. This was not attributed to the yield strength of either of the components making up our couples. We believe that the oxide existing at the interface is the controlling factor. In other words, a certain minimum amount of oxide rupture is required in order to have consistent penetration data.

It has been our experience that the size of the specimens have considerable effect upon the tensile strength ultimately developed. We found this true for changes in both the length and diameter of the tensile couples.

The fact that Dr. Sumsion did not find the same marked effect of pressure upon the extent of penetration is probably explained in that the technique he used to react specimens was considerably different than ours. It is pointed out that his specimens were in intimate contact during the whole heating period. This was not true for our experiments. Only after application of pressure did we get penetration. This we verified by examining couples which had been heated to 600°C but were not subjected to pressure. Interface examination showed that no penetration had occurred. Thus, his time for penetration was approximately the length of time the specimen was being heated, and in addition, his temperature of reaction was not a constant but a continually changing value. It is our belief that the effect we observed was masked in his experiments.

The reason Dr. Sumsion was not able to eliminate $\alpha$ phase was that a high enough pressure was not applied. The maximum pressure used in his experiments was 12 tsi. We did not find phase elimination until a pressure of 20 tsi was used.

In answer to his last questions, we wish to state that no subsequent verification of the two phases has been made. We have seen more than two phases but only when we worked with nickel plated from an electroless bath. This type of material contains a considerable

percentage of phosphorous and therefore probably effects diffusion rates.

[1] F. S. Buffington and M. Cohen: Self-Diffusion in Alpha Iron Under Uniaxial Compressive Stress. *Trans.* AIME (1952) 194, p. 859; JOURNAL OF METALS (August 1952).
[2] S. Storchheim, J. L. Zambrow, and H. Hausner: Solid State Bonding of Aluminum to Nickel (paper under discussion). *Trans.* AIME (1954) 200, p. 269; JOURNAL OF METALS (February 1954).
[3] F. N. Rhines: Diffusion Coatings on Metals. *Surface Treatment of Metals* (1940) pp. 135-136. Cleveland. ASM.
[4] B. Lustman and R. F. Mehl: Rate of Growth of Intermediate Alloy Layers in Structurally Analogous Systems. *Trans.* AIME (1942) 147, p. 369.

## High Temperature Strength of Wrought Aluminum Powder Products

by Eric Gregory and Nicholas J. Grant

*DISCUSSION, F. N. Rhines and A. J. Shaler, Chairmen*

**C. Dean Starr** *(Wilbur B. Driver Co., Newark, N. J.)*—The authors are to be congratulated for this interesting paper concerning the effect of dispersed oxides on the mechanical properties of metals. The results of previous investigations[17] on the effect of oxides have not been suitable for correlating the distance between oxide particles with mechanical properties, since the oxides were present primarily in the grain-boundary region of polycrystalline aggregates. For example, oxidized samples of silver containing small quantities of molybdenum and aluminum, copper containing manganese, and nickel containing aluminum revealed that the presence of oxides in polycrystalline specimens increased the tensile strength but decreased the elongation. Oxidized single crystals of the same composition, however, showed the crystals to be quite ductile. From these observations, it is inferred that the oxides were located primarily in the grain boundary in the polycrystalline specimens and that equivalent amounts of oxides distributed in the matrix of an alloy would not appreciably alter the properties of a metal.

The present investigation reveals that oxides, which are more or less uniformly distributed in the matrix of polycrystalline aggregates, increase the flow stress of metals in the same manner that intermetallic compounds increase the flow stress of alloys. But as the authors have pointed out, their data do not permit an unequivocal choice to be made for the most appropriate relationship between stress and the distance between the oxide particles. The authors have shown in Fig. 16 that their relationship is valid for all the data plotted. With the exception of the tensile data for material M255, the data are also in agreement with the form of relationship proposed by Gensamer et al.[12] and by Shaw et al.,[10] as shown in Figs. 17 and 18, respectively. It should be recalled, however, that the stresses used by Gensamer and Shaw were true stresses and not engineering stresses as used by the authors. If the yield stresses recorded were determined by the conventional offset method for nonferrous materials, it would be more appropriate to compare the yield strength against spacing between oxide particles, since the yield strength would be directly proportional to the true stress at a strain of $\epsilon = 0.2$ pct. Such a plot does indicate, within a reasonable amount of scatter, that the authors' relationship is valid but closer examination of the yield strengths of material M255 and M293 in Table I indicates the yield strength is essentially independent of particle spacing. Since the stress-rupture data indicate that alloy M255 is appreciably weaker than the other four alloys, it is possible that the tensile data recorded are not representative for this material. Were the tensile values recorded in Table I averages of a number of lists or the results of a single test?

It is hoped that the authors will be able to continue their investigations with alloys containing yet larger mean free paths to determine the appropriate relationship for oxides in metals.

The stress-rupture data indicate that the effect of the mean free path on the creep resistance diminishes with increasing temperature until at approximately 900°F the rupture time is approximately independent of particle spacing. During an investigation on the elevated-temperature tensile properties of Al-Cu alloy,[18] a similar trend was noted. Whereas a fine dispersion was stronger than a coarse one at room temperature, both dispersed alloys exhibited equal strength characteristics at 420°K. At intermediate temperatures (420° to 650°K) an inversion occurred and the coarse dispersion was stronger than the finely dispersed alloy. But at elevated temperatures (above 650°K) the fine dispersion again exhibited the superior strength properties.

Since the stress-rupture data correlated in the present paper is for very short rupture times, it would be anticipated that the results would correspond closely to those obtained in a tensile test. Somewhat similiar effects would also be expected in an investigation on the creep properties of dispersed alloys. But since it is known that strain rate is analogous to temperature, the correlation between stress and structure is not as simple as in the tensile test wherein the strain rate is maintained constant. Thus for the longer-time creep tests, it might be more appropriate to compare the stress in an isothermal test that is necessary to produce a given secondary creep rate for a series of dispersed alloys against the structure (mean free path). Utilizing this criteria, Giedt et al.[19] found that the data on the creep behavior of biphase alloys of $CuAl_2$ in Al-Cu solid solutions could be reasonably well correlated. They showed that a log-log cross-plot of $\sigma\dot{\epsilon}$'s vs the mean free path gave a straight line for any given secondary creep rate. This correlation was shown to be valid for a variation in the creep rate of 1000 and a 15 fold difference in the mean free path of dispersed alloys. It would be interesting, if the data are available, to see if the same generalizations are applicable to the alloys under consideration here.

**Eric Gregory** and **Nicholas J. Grant** (authors' reply)—Unfortunately, the room-temperature tensile data were supplied by Alcoa. We did not make those particular measurements ourselves. It is entirely likely, especially with experimental products of this type, that there is an error for the yield value for either M255 or M293. It is to be noted that the room-temperature ductility values are also not as would be expected for these two alloys. Since our tests were from independent bar stock, our results need not be subject to the same error which resulted in the room-temperature tensile data for these two alloys.

If the strengthening benefits at 100 or 1000 hr rupture life were compared instead of at 0.1 hr at high temperatures, in effect the role of strain rate or time could be measured. On this basis there is a large contribution to the strength of the fine oxide dispersion. At the time we had no basis for comparison and therefore utilized the short-time data, instead, to check against previously suggested structure-strength relationships. Our work is continuing and we plan to try other relationships including that of Giedt et al.[19] as suggested by Mr. Starr.

Our current work includes studies of copper powders as well as the Ni-5 pct Al and Ni-10 pct Al alloys.

[17] J. L. Meijering and M. S. Druyvesteyn: Hardening of Metals by Internal Oxidation. *Philips Research Reports* (1947) 2, No. 2, Parts I, II, p. 81.
[18] C. D. Starr, R. B. Shaw, and J. E. Dorn: Effect of Dispersions of Cu $Al_2$ on the Elevated Temperature Tensile Properties of Al-Cu Alloys. *Trans.* ASM (1953) Preprint No. 16W.
[19] W. H. Giedt, O. D. Sherby, and J. E. Dorn: The Effect of Dispersions on the Creep Properties of Aluminum-Copper Alloys. *Research Report* University of California (December 1, 1952) Issue No. 22.